UNIVERSITY of BRADFORD Library

University of Bradford eThesis

This thesis is hosted in Bradford Scholars – The University of Bradford Open Access repository. Visit the repository for full metadata or to contact the repository team

© University of Bradford. This work is licenced for reuse under a Creative Commons Licence.

INVESTIGATION OF MECHANISMS OF DRUG RESISTANCE IN COLORECTAL CANCER: A PROTEOMIC AND PHARMACOLOGICAL STUDY USING NEWLY DEVELOPED DRUG-RESISTANT HUMAN CELL LINE SUBCLONES

M. ORTEGA DURAN

PhD

2017

Investigation of mechanisms of drug resistance in colorectal cancer: a proteomic and pharmacological study using newly developed drug-resistant human cell line subclones

Mario Ortega Duran

Submitted for the Degree of

Doctor of Philosophy

Faculty of Life Sciences

University of Bradford

2017

Abstract

Mario Ortega Duran

Investigation of mechanisms of drug resistance in colorectal cancer: a proteomic and pharmacological study using newly developed drug-resistant human cell line subclones

Keywords: Colorectal cancer, 5-Fluorouracil, Oxaliplatin, Irinotecan, Drug resistance, Proteomics, SILAC, chemotherapy, protein interactions, chemosensitivity assays

Despite therapeutic advances, colorectal cancer still has a 45% mortality rate, and one of the most crucial problems is the development of acquired resistance to treatment with anticancer drugs.

Thus the aims of this project are to develop drug-resistant colon cancer cell lines in order to identify mechanisms of resistance for the most commonly drugs used in colorectal cancer: 5-fluorouracil, oxaliplatin, and irinotecan.

Following evaluation of drug sensitivity to these agents in an initial panel of eight colorectal cancer cell lines, 3 lines (DLD-1, KM-12 and HT-29) were selected for the development of 5-FU (3 lines), oxaliplatin (2) and irinotecan (1) resistant sublines by continuous drug exposure, with resistance confirmed using the MTT assay. Consistently resistant sublines were subject to a ‘stable isotope labelling with amino acids in cell culture’ (SILAC) approach and a MudPIT proteomics strategy, employing 2D LC and Orbitrap Fusion mass spectrometric analysis, to identify novel predictive biomarkers for resistance. An average of 3622 proteins was quantified for each resistant and parent cell line pair, with on average 60-70 proteins up-regulated and 60-70 down-regulated in the drug resistant sublines. The validity of this approach was further confirmed using immunodetection techniques.

These studies have provided candidate proteins which can be assessed for their value as predictive biomarkers, or as therapeutic targets for the modulation of acquired drug resistance in colorectal cancer.

Acknowledgements

I would like to express my deepest gratitude to my two Ph.D. supervisors: Dr. Steve Shnyder and Dr. Chris Sutton. Without their knowledge, support, guidance, and mentorship, I would never have become the scientist that I am today, and I will be grateful to them forever for that.

I wish firstly to thank my main supervisor Dr. Steve Shnyder, for trusting me from the first moment. Thanks for his kindly welcome, and his weekly and constant supporting, patience, advising, and understanding of my professional and personal life. It was a pleasure to share all these issues during three years and a half with you.

I am also thankful to Dr. Chris Sutton for his closeness, his support and for all the confidence placed in me. You have been always there whenever I needed advice to discuss any issue.

Really, it has been a great pleasure to work with both of you, great professionals and wonderful people.

I would like to thank my new in life-brother, Sadr-ul-shaheed for his invaluable spiritual and professional aid and the most important issue, he did always all of that with a smile on his face.

I wish to offer my sincerest thanks to The University of Bradford and all ILSR scholarship and postgraduate program members (Dr. Anne Graham, Mrs. Shamim Haider) for their time and guidance. Thanks to all the staff and members at the Institute of Cancer Therapeutics for sharing three very pleasant years.

Finally, I would like to express my deepest gratitude to all my beloved family. You have believed in me and offered your unconditional support. Thank you all.

To my parents, you have been the mirror of my soul and the main source of all values I have received. Thank you for all you have done and especially for the love with which you have done it. You are the reference in my life. You have also been an example of love and constancy in the midst of difficulties. Thank you for the bountiful knowledge and experiences I gained with you, because is something that I will use during the rest of my life. You are the pride of my life, an example of fight, sacrifice, and perseverance. Thank you for showing me that all things in life must be done with love and at its necessary time.

To my brother, I always feel you with me, as if you were by my side. Thank you for growing up with me. Thanks for taking part in so many adventures and new discoveries throughout our lives. Together we will share the dreams of the future.

A special dedication to the soul of my beloved grandmother, all time invested in this work is the time that I will never share with any of my family members and friends anymore.

Thanks to my homeland, my past history and all special people who entered our lives to enrich ourselves.

Finally, this is a work is dedicated to all people around the world who are directly or indirectly affected by any form of cancer and which help us to learn more about life than death.

To my family, I could never have been writing this today, without your love and support.

Thank you.

Table of Contents

List of Figures

List of Tables

List of Abbreviations

5-FU	5-fluorouracil
9-AC	9 Amino Camptothecin
ABC	ATP-Binding Cassette Transporters Family
ACADVL	Very Long-Chain Specific Acyl-CoA Dehydrogenase
ACSF3	Acyl-CoA Synthetase Family Member 3
AGO	Argonaute protein
AMACR	α-Methylacyl-CoA Racemase
APP	Amyloid Precursor Protein
AR	Androgen Receptor
ARF3	ADP-Ribosylation Factor 3
ATCC	American Type Culture Collection
BAIAP2	Brain-Specific Angiogenesis Inhibitor 1-Associated Protein 2
BCRP	Breast Cancer Resistance Protein
BER	Base Excision Repair
BLOC	Lysosome-Related Organelles Complex
BSA	Albumin from Bovine Serum
CAN	Acetonitrile
CE	Carboxylesterase
CHMP	Charged Multivesicular Body Protein
CRC	Colorectal Cancer
CSC	Cancer Stem Cell
CYCS	Cytochrome C
DHFU	Dihydrofluorouracil
DPD	Dihydropyrimidine Dehydrogenase
DSB	Double-Strand Break
DTT	Dithiothreitol
EGF	Epidermal Growth Factor

EHBP1L	EH Domain–Binding Protein 1–Like 1
ER	Endoplasmic Reticulum
ERMP	Endoplasmic Reticulum Metallopeptidase
ESCRT	Endosomal Sorting Complex Required for Transport
ESI	Electrospray Ionization
FADD	FAS-associated death domain
FDA	Food and Drug Administration
FSCN	Fascin
FUdR	Fluorodeoxyuridine
FUMP	5-Fluorouridine Monophosphate
FUTP	5-Fluorouridine Triphosphate
GCS	Glucosylceramide Synthase
GGT1	Gamma-Glutamyltranspeptidase 1
GOLPH3	Golgi Phosphoprotein 3
HCCS	Cytochrome c-type Heme Lyase
HDACIs	Histone Deacetylase Inhibitors
HGP	Human Genome Project
hNSC	Human Neural Stem Cell
HPLC	High-Performance Liquid Chromatography
HSP	Heat Shock Protein
HUPO	Human Proteome Organization
HUVECs	Human Umbilical Vein Endothelial Cells
HYOU1	Hypoxia Up-Regulated Protein 1
IAA	Iodoacetamide
IC	Inhibitory Concentration
ICLAC	International Cell Line Authentication Committee
IGF2BP3	Insulin-like Growth Factor 2 mRNA-Binding Protein 3
IRI	Irinotecan
iTRAQ	Isobaric Tags for Relative and Absolute Quantitation

LAMP	Lysosomal-Associated Membrane Protein
LB	Loading Buffer
LC-MS/MS	Liquid Chromatography Tandem-Mass Spectrometry
LGALS3BP	Galectin-3-Binding Protein
LGMN	Legumain
Log	Logarithmic
LOQ	Limit Of Quantification
LRP	Lung Resistance-Related Protein
m/z	Mass/Charge
MALDI	Matrix Assisted Laser Desorption/Ionization
MDR	Multi-Drug Resistance
MMR	DNA Mismatch Repair Protein
MRM	Multiple Reaction Monitoring
MRP	Multidrug Resistance-related Protein
MSI	Microsatellite Instability
MSS	Microsatellite Stability
MUC	Mucin
MVB	Multivesicular Bodies
NCBI	National Center for Biotechnology Information
NOL3	Nucleolar protein 3
NT5C3A	Cytosolic 5'-Nucleotidase 3A
OPRT	Orotate Phosphoribosyltransferase
OXA	Oxaliplatin
PA	Phosphatidic Acid
PAGE	Polyacrylamide Gel Electrophoresis
PARP2	Poly [ADP-Ribose] Polymerase 2
PBS	Phosphate-Buffered Saline
PDCD	Programmed Cell Death Protein
Pgp	P-Glycoprotein

PSMs	Peptide-Spectrum Matches
PPIA	Peptidyl-Prolyl Cis-Trans Isomerase A
PPIs	Protein–Protein Interaction
PRKCD	Protein Kinase C δ Type
PRM	Parallel Reaction Monitoring
PSMB10	Subunit β Type-10 of the Proteasome
PTMs	Post-Translational Modifications
RNA Pol II	RNA-Polymerase II
ROS	Reactive Oxygen Species
RR	Ribonucleotide Reductasa
SCID	Severe Combined Immunodeficiency
SCX	Strong Cationic Exchange Chromatography
SILAC	Stable Isotope Labelling with Amino acids in Cell Culture
SLC	Solute Carriers
SRC	Proto-Oncogene Tyrosine-Protein kinase Src
STIM	Stromal Interaction Molecule
SYTL	Synaptotagmin-Like Protein
TAD	Transactivation Binding Domain
TAOK1	Serine/Threonine-Protein Kinase
TAP1	Antigen Peptide Transporter 1
TC	Ternary Complex
TEP1	Telomerase-Associated Protein 1
TFRC	Transferrin Receptor Protein 1
TFs	Transcription Factors
TIMP	Metalloproteinase Inhibitor
TK	Thymidine Kinase
TMED	Transmembrane Emp24 Domain-Containing Protein
TNF	Tumour Necrosis Factor
TNFRSF	Tumour Necrosis Factor Receptor Superfamily

TOFMS	Time-Of-Flight Mass Spectrometry
Topo I	Topoisomerase I
TP	Thymidine Phosphorylase
TRAIL	TNF-Related Apoptosis-Inducing Ligand
TS	Thymidylate Synthase
UMPS	Uridine Monophosphate Synthase
UP	Uridine Phosphorylase
VEGF	Vascular Endothelial Growth Factor
VPS	Vacuolar Protein Sorting-Associated Protein
WB	Western Blotting
WRAP53	Telomerase Cajal Body Protein 1

- Chapter one -

General introduction

1 General Introduction

1.1 Colorectal Cancer

Cancer is defined as the abnormal cell proliferation and the uncontrolled growth of cells due to a malignant process called neoplasia. Neoplasm is derived from the Greek words "neo" meaning new and "plasma" that means “formation” (Schwab 2008). When a malignant neoplasia occurs in the large intestine, it is called colon cancer, and when the malignant neoplasm occurs 16 cm or less distance from the anocutaneous line it is called rectal cancer (Schwab 2008).

1.1.1 Colorectal Cancer Epidemiology

Colorectal cancer (CRC) is the third most common cancer in the world after lung and breast cancer and the fourth most common cancer in the UK after breast, lung, and prostate cancer respectively (Kufe, Pollock et al. 2003). In the most recently available global figures from 2012, according to the GLOBOCAN 2012 project, new CRC cases were estimated to be 1,361,000 (746,000 in men and 614,000 in women) (Ferlay, Soerjomataram et al. 2015). Almost 55% of the cases occur in developed regions. However, mortality is lower in developed regions (694,000 deaths, 8.5% of the total) than in the underdeveloped regions of the world with poor sanitary conditions, lack of access to treatments, and worst life expectancy (52% of the total deaths) (Ferlay, Soerjomataram et al. 2015). Age is an important factor in CRC incidence, being the highest incidence rates in older men and women. Around 45% of CRC cancer cases are diagnosed in people aged 75 years and over, and 95% were diagnosed in people aged 50 and over (Kufe, Pollock et al. 2003). Data also shows differences according to sex, with around 75 and 58 new CRC cases for every 100,000 males and females in the UK, respectively (Coley 2004).

1.1.2 Stages of CRC

Cell turnover constantly occurs in normal cells of the colon under healthy conditions (Rando 2006). During this renewal process of colorectal cells, hyperproliferation may occur on the surface of the colon wall, this abnormal growth of cells can form a mass of cells known as polyp (Kufe, Pollock et al. 2003). There are two kinds of polyps: benign or malignant. A benign polyp does

not contain any tumour cells inside, can be removed by surgery, and it cannot spread to other parts of the body. Malignant polyps do have tumour cells inside and they have an abnormal genomic stability, so they can proliferate uncontrollably.

The intestinal glands in the colon are often referred to as colonic crypts. Colon crypts are formed from different types of cells. Colorectal cells show specific colon crypt location that is related with their features and their differentiation level (Fig. 1.1). A crypt contains multiple types of cells: enterocytes that absorb water and electrolytes, goblet cells which secrete mucus, enteroendocrine cells that secrete hormones, and stem cells at the base of the gland.

Hence tumour features depends on the biological origin of the cells from where the tumour is derived. Most of the heterogeneity at a genetic and transcriptional levels found in patients may be observed among the individual CRC cell lines used in research (Fig. 1.1). Different CRC cell lines classification are discussed in detail below in Chapter 2, section 2.2. Anguraj Sadanandam *et al.*, developed a sorting system to classified CRC in five subtypes according to their gene profiling (Sadanandam, Lyssiotis et al. 2013). These five subtypes of CRC tumours and cell lines are shown below.

1) Goblet-like: CRC cells defined by high mRNA expression of goblet-specific MUC2 and TFF3. This cell subtype has a high differentiated phenotype.

2) Enterocyte: CRC cells defined by high mRNA expression of enterocyte-specific genes.

3) Stem-like: CRC cells defined by high expression of Wnt signalling targets plus stem cell, myoepithelial and mesenchymal genes and low expression of differentiation marker.

4) Inflammatory: CRC cells marked by comparatively high expression of chemokines and interferon related genes. CRC samples classified in this group normally are associated with MSI status.

5)Transit-amplifying: CRC cells with variable expression of stem cell and Wnt-target genes.

Once the malignant tumour appears, independently of the CRC tumour subtype, CRC is classified depending on the level of spread and proliferation, which are crucial factors to the success of the invasion process. There are four stages of CRC classification, which depend on the survival prognosis for the patient and they are described below. Moreover, there is an additional "Stage 0", also called carcinoma *in situ*, which has the best prognosis (Fig. 1.1).

Stage I – Tumoural mass is localized on the surface of the colon or on the surface of the rectum (Fig. 1.1). The cancer is located in the innermost lining of the colon or rectum or slightly growing into the muscle layer.

Stage II –Tumoural mass is entering into the wall of the colon or it has grown through the muscle layer of the rectum (Fig. 1.1).

Stage III - Cancer has penetrated through the wall and it has spread to at least one lymph gland in the area close to the colon (Fig. 1.1).

Stage IV - Cancer has overflowed the lymph glands and it has spread to somewhere else in the body, usually into the liver or lung (Fig. 1.1). It is also known as advanced CRC.

For 90% of cases, the survival rate of patients who have been diagnosed with stage I is 5 years. However, survival rate decreases to 35-60% if the diagnostic stage is III and to 5% in stage IV if there is metastatic disease (Kufe, Pollock et al. 2003).

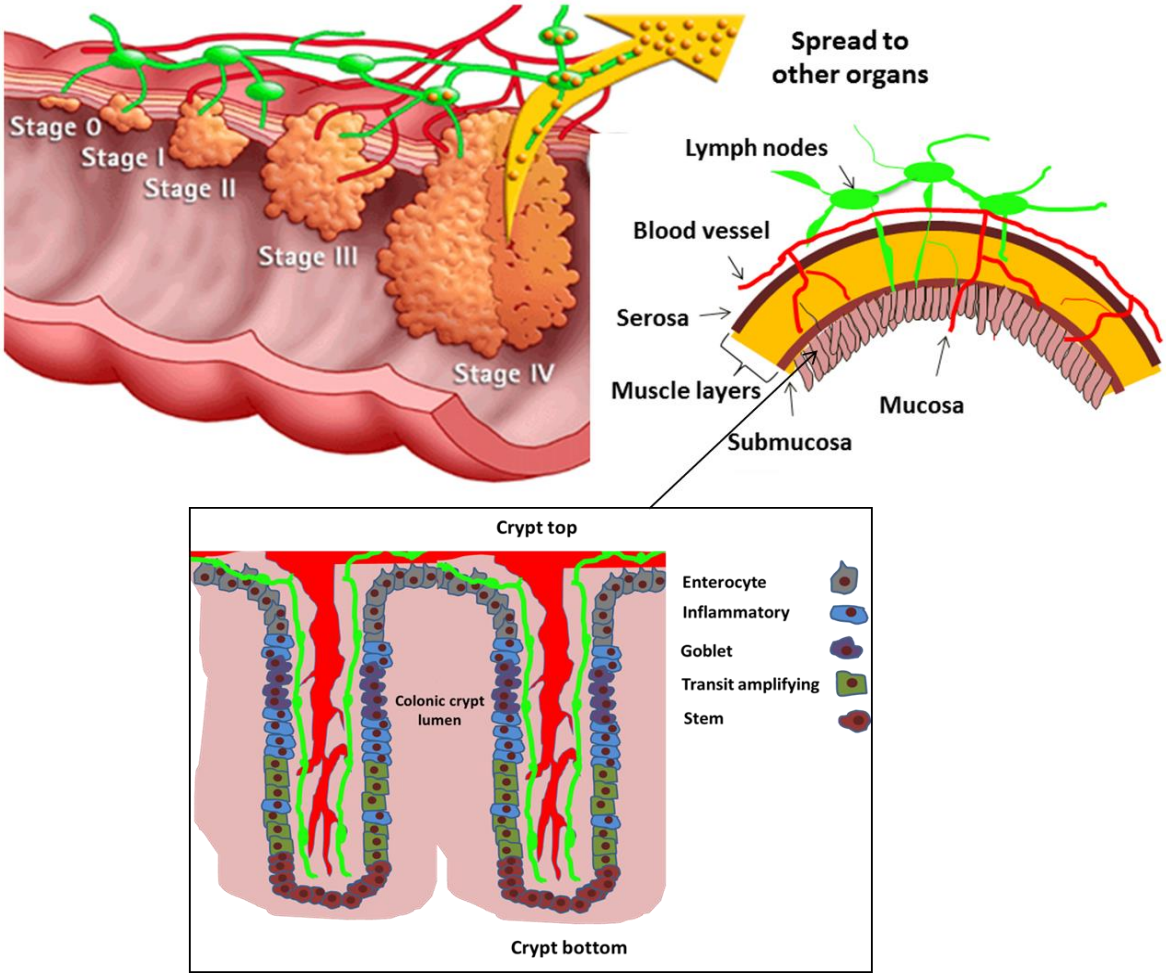

Figure 1.1: Different CRC staging. The number of the stage depends on both cancer location and cancer spreading. Figure adapted from (Medico, Russo et al. 2015) and from (Terese Winslow LLC, U.S.Govt. 2011).

1.2 Treatments for CRC: Surgery, radiotherapy, and chemotherapy

Once a patient has been diagnosed with CRC there are three main treatments: surgery, radiotherapy, and chemotherapy. In most cases, a combinational treatment of surgery with both radiotherapy or/and chemotherapy is used in CRC patients.

1.2.1 Surgery

Surgery is always the essential primary treatment for CRC patients. Surgery is relatively straightforward in the early stages of CRC and tumours can be removed using a colonoscope for guidance (Lacy, Garcia-Valdecasas et al. 2002). A colonoscope is a long thin flexible tube with a light and a video camera attached to its end. The camera transmits the image to a monitor, where

doctors can see the inside of the colon. Once the tumour is located, it will be removed by surgeons. However, if the tumour has spread into the muscle area close to the wall of the colon, a bigger piece of the colon region needs to be removed. So, advanced cases require a partial colectomy (Lacy, Garcia-Valdecasas et al. 2002). After removal of the section of the colon affected by cancer, the two remaining portions of the colon are connected and this is called anastomosis. Even though surgery is the main treatment for CRC patients, this treatment does not always get rid of all the tumour completely (Rodriguez-Bigas MA 2003). This is because surgery leaves small clusters of tumour cells that cannot be removed or cannot be detected on scans or other tests. Some months after surgery, these cancer cells can grow up and proliferate again. If the time taken to reappearance of the related cancer symptoms is three months or less, the regrowth is referred to as cancer progression by doctors (Kufe, Pollock et al. 2003). However, if a patient shows absence of symptoms for at least a year before the new regrowth of tumours, the regrowth is referred to as cancer recurrence. Therefore, to prevent recurrence and progression of CRC after surgery, there are two additional treatments which are normally used to complement surgery: radiotherapy and chemotherapy (Kufe, Pollock et al. 2003, Rodriguez-Bigas MA 2003, Schwab 2008).

1.2.2 Radiotherapy

X-Rays and gamma rays emit ionising radiation energy that is enough to ionise atoms, molecules and cause double-strand breaks of DNA. It is called ionising radiation because it forms ions by removing electrons from atoms and molecules of the cells it passes through. Ionising radiation removes an electron from the water inside the cells and free radicals are created. During ionising processes, large amounts of damaging free radicals are released. Free radicals are unstable molecules and highly reactive due to the presence of an unpaired electron that allows them to donate an electron to or accept an electron from other molecules, increasing cell damage (Olive 1998, Kufe, Pollock et al. 2003). The value of radiotherapy as a cancer treatment lies in the fact that tumours often have defective radiation repair pathways, whereas normal cells and normal tissues keep a higher capacity to recover from radiation damage (Lliakis 1991, Olive 1998, Kufe, Pollock et al. 2003). Improvements in radiotherapy

applied to CRC patients are taking place over the last decade. There are three main types of radiotherapy used in CRC patients- (1) External-beam radiation therapy: the radiation is focused on the CRC cancer from an external machine and it last from few days to weeks. (2) Internal radiation therapy (brachytherapy): a radioactive source is put inside rectum in rectal cancer patients, hence adverse effects of radiotherapy in other parts of the body is decreased. (3) Systemic radiation therapy: a radioactive substance is injected into blood system to travel through the blood to locate and destroy tumoural cells. Radiotherapy may be used either before or after an operation to improve the success of the surgery or in some cases to alleviate specific symptoms caused by cancer (Ismaili 2011, van Gijn, Marijnen et al. 2011). X-ray radiation can be used before surgery to damage the tumour tissue, which would make easier to remove the tumour during surgery (van Gijn, Marijnen et al. 2011), but also it can be used after surgery in order to decrease the recurrence of cancer (van der Meij, Rombouts et al. 2016).

1.2.3 Chemotherapy

Chemotherapy is a treatment based on the use of chemical compounds in order to damage cancer cells to avoid their spreading and proliferation. Although there are different types of chemotherapy, most drugs act during specific phases of the cell cycle to stop cells dividing or to cause cell death (Kufe, Pollock et al. 2003, Schwab 2008). Normally, chemotherapy is used after surgery to avoid the recurrence of cancer (Schrag, Cramer et al. 2001). But, chemotherapy can be used before both radiotherapy to make tumour cells more sensitive to radiation and before surgery by debulking of tumour, decreasing tumour size as much as possible (Nordlinger, Sorbye et al. 2008). Despite the broad range of chemotherapies developed to treat CRC patients. There is a lack of knowledge in how CRC patient responses differ from patients and tumours (Schwab 2008, Group 2012). Chemotherapy has different effects on cancer cells with different genomic backgrounds and drug response prediction is one of the main issues that need to be answered. Main widespread most used chemotherapy agents in CRC patients are discussed and classified below.

1) Alkylating agents that act by attaching an alkyl group to DNA by crosslinking guanine nucleobases in DNA double-helix strands forming strands unable to separate. These drugs are cell-cycle non-specific and normally act during the resting phase of cells (Fu, Calvo et al. 2012), for example, cisplatin and oxaliplatin (OXA). Cisplatin cytotoxic effect occurs by its hydrolysis generating a highly reactive charged platinum complex $[Pt(NH_3)2ClH_2O]^+$ which binds to genomic and mitochondrial DNA and produces inhibition of replication and transcription processes leading to cell death (Fuertes, Alonso et al. 2003). OXA undergoes non enzymatic conversion in physiological solutions resulting into reactive species such as dichloro (1,2-diaminocyclohexane) platinum (II) (DACHPt), which covalently binds with DNA and macromolecules. Forming monoadducts guanine initially, but eventually, OXA attaches simultaneously to two nucleotide bases resulting in DNA cross-links between adjacent adenine and guanines which cause inhibition of both DNA replication and transcription (Kweekel, Gelderblom et al. 2005).

2) Cell-cycle specific inhibitors as irinotecan (IRI) (Shi, Hui et al. 2014), doxorubicin, and paclitaxel. IRI and doxorubicin, are topoisomerase I (Topo I) and topoisomerase II (Topo II) inhibitors, respectively.

3) Antimetabolites are molecules very similar to natural substances which are normally presented within the cell and that are required for cellular metabolism. Antimetabolites have a cell-cycle specific effect (Tiwari 2012) such as 5-fluorouracil (5-FU) that acts as cell-cycle specific by inhibition of Thymidylate synthase (TS), a key enzyme in the creation of thymine required for synthesis of DNA and RNA.

Additionally, there are targeted molecules cancer therapies. Targeted therapies act on specific molecular targets that are associated with cancer, whereas previous chemotherapies mentioned above, act on all rapidly dividing normal and cancerous cells. Targeted therapies are designed to block tumour cell proliferation (cytostatic) through a specific target (Perez-Herrero and Fernandez-Medarde 2015). Two new molecularly-targeted agents are Cetuximab (Erbitux) and Panitumumab (Vectibix) that target Epidermal growth factor receptor (EGFR). EGFR is a receptor protein with three domains, one

external domain, a second domain in the cellular membrane and an internal domain. EGFR presents a ligand-induced internalization response with EGF and this process mediates signal pathways involved in cell differentiation and cell overgrowth (Pettigrew, Kavan et al. 2016).

To understand how chemotherapy works, it is essential to know what kind of mechanisms can turn a normal cell into a tumour cell. Chemotherapy normally works by targeting the fast growth of tumour cells.

During normal health conditions, the turnover of colon epithelial occurs every five days. Normally, intestinal epithelial cells are self-renewed by stem cells that grow under microenvironment influence (Mathonnet, Perraud et al. 2014). In 2000, Hanahan and Weinberg published the six Hallmarks of Cancer (Hanahan and Weinberg 2000). These authors tried to summarize the complexity of cancer in six crucial features of any tumour cell. They thought that these six basics hallmarks could explain how a normal cell can be transformed into a protumoural cell. In 2011 a newly revised paper was published by Hanahan and Weinberg with four additional new hallmarks described (Hanahan and Weinberg 2011). So, there are ten hallmarks in cancer that are: self-sufficiency in growth signals, evading growth suppressors, evading apoptosis signals, evading the immune system, alterations in cellular metabolism, genomic instability, sustained angiogenesis, activating tissue invasion and metastasis, promoting inflammation (Hanahan and Weinberg 2000, Kufe, Pollock et al. 2003, Hanahan and Weinberg 2011). The transformation of normal cells to cancer cells normally is mediated by some of these hallmarks shown above.

Normal epithelial cells die by apoptosis and new cells replace them during normal cell cycle process. This process is regulated by extracellular and intracellular signals that allow the body to renew its cells when they have died (Schwab 2008). Colon homeostasis is carried out under this carefully regulated process. The loss of homeostatic balance can change into a malignant environment that affects growth inhibition, apoptosis, and carcinogenesis processes. Carcinogenesis requires the accumulation of different epigenetic and genetic alterations that converge in the abnormal growing of colorectal cells (Schumacher, Nehmann et al. 2012, Mathonnet, Perraud et al. 2014).

Angiogenesis and stem cell characteristic of limitless replicative potential are the two major hallmarks of carcinogenesis in CRC and therefore they have been the two main targets during the development of novel therapeutic treatments (Mathonnet, Perraud et al. 2014). Mutations and alterations in these hallmark areas can converge in ineffective therapies and chemotherapy resistance (Hanahan and Weinberg 2011).

Chemotherapy treatment used with each patient depends very much on individual's specific circumstances and on the type and the stage of cancer (Hanahan and Weinberg 2000). Chemotherapy can be administered by different routes depending on the place where the tumour area is found and depending on the nature of the chemical compound used. Some chemotherapeutic agents are contained in capsules and pills, so the chemotherapy can be administered orally. A benefit of oral chemotherapy is that it can be ingested by the patient at home as another conventional treatment. Chemotherapy can be administered in liquids orally, tablets, by intramuscular injections, by intravenous injections (IV) or using cannulas (Kufe, Pollock et al. 2003). Duration of chemotherapy treatments can take weeks or months. In most of the cases, the patient is treated with different chemotherapy drugs in order to improve treatment effectiveness (Kufe, Pollock et al. 2003).

1.2.3.1 Common chemotherapeutics used in CRC

For more than 60 years, several chemical agents have been extensively used in the fight against CRC (Kufe, Pollock et al. 2003). However, this thesis has been focused on the most widely used drugs in CRC patients that are: 5-FU, OXA and IRI. The mechanism of action and known mechanisms of resistance to these three agents will be explained further in detail in their respective Chapters 3-5, dedicated specifically for each drug.

1.2.3.1.1 5-FU

The use of chemotherapy in CRC started in the 1950s when 5-FU was first used for advanced CRC patients (Fig. 1.2) (Watson 1964, Ferlay, Soerjomataram et al. 2015). 5-FU is an analogue of uracil that once is incorporated into DNA and RNA causes cell death by cytotoxicity (Longey

2003). Mechanism of action of 5-FU and mechanisms of resistance to 5-FU are discussed in greater detail in Chapter 3, section 3.1.1 and 3.1.2. Treatment with 5-FU consists of a 5-FU dose of 444 mg/m^2 injected once daily for 4 successive days. Then, a single dose of 370 to 555 mg/m^2 is injected per week (Jung, Jeung et al. 2007, 2016). Normally, 5-FU is used with folinic acid (leucovorin). Leucovorin 20 mg/m^2 is administered by injections followed by 5-FU at 425 mg/m^2 in 5 days treatments repeated at 4-week intervals, this chemotherapy treatment was approved by the U.S (2016) Food and Drug Administration (FDA) in 1991 (Fig. 1.2) (Jung, Jeung et al. 2007). In 2005, a new prodrug of 5-FU called capecitabine (Xeloda® Tablets, made by Hoffman-LaRoche Inc.) was approved by the FDA in combination with OXA (Hoff, Ansari et al. 2001, Van Cutsem, Twelves et al. 2001) as a single treatment for stage III CRC patients (Fig. 1.2), showing a higher effectiveness than 5-FU (Van Cutsem, Hoff et al. 2004). The recommended dose of capecitabine is 1250 mg/m^2 administered orally twice daily for 2 weeks followed by a 1 week rest period given as 3-week cycles during 6 months (Pentheroudakis and Twelves 2002, 2016).

1.2.3.1.2 OXA

Another conventional drug used in CRC patients is OXA. OXA is a platinum-based drug, which damages the tumour cell by covalent and irreversible binding to the negative charges of the DNA (Alcindor and Beauger 2011). Mechanism of action of OXA and mechanisms of resistance to OXA are discussed in greater detail in Chapter 5, section 5.4.3 and 5.4.4. OXA was approved in 2004 by FDA to be used in combination with 5-FU and leucovorin for adjuvant treatment for stage III CRC patients (Fig. 1.2) (Jung, Jeung et al. 2007, 2016).

1.2.3.1.3 IRI

Another standard treatment for CRC patients is IRI. It is a camptothecin derivative. IRI is hydrolyzed by carboxylesterase to an active metabolite, SN-38 (7-ethyl-10-hydroxycamptothecin) which is conjugated by hepatic uridine diphosphate glucuronosyl transferase to SN-38 glucuronide (SN-38G) a Topo I inhibitor that causes cell death by apoptosis and it was approved in 1996 for advanced CRC patients (Fig. 1.2) (Liu, Desai et al. 2000). Mechanism of action

of IRI and mechanisms of resistance to IRI are discussed in greater detail in Chapter 4, section 4.4.3 and 4.4.4. Folfox (folinic acid, 5-FU, and OXA) was approved in 2004 (Fig. 1.2) for stage III CRC patients. Treatment is a combination of OXA, 5-FU and leucovorin.

In 2011, Capox (Xelox) (Capecitabine and OXA) was approved to be used in stage III and advanced CRC patients (Fig. 1.2) (Diaz-Rubio, Evans et al. 2002). Treatment is administered every 21 days, usually for up to 8 cycles as follows: Day 1) OXA 130 mg/m^2. Followed by 1-14 days of Capecitabine 1,000 mg/m^2 twice daily (Diaz-Rubio, Evans et al. 2002, 2016).

Finally, FOLFIRI (folinic acid, 5-FU, and IRI) was approved in 2012 (Fig. 1.2). It is a combinational treatment of IRI (180 mg/m² injected over 90 min) with folinic acid (400 mg/m² [or 2 x 250 mg/m²] over 120 min), followed by 5-FU (400–500 mg/m²) then 5-FU (2400–3000 mg/m² over 46 h (Klingbiel, Saridaki et al. 2015). This cycle is typically repeated every 2 weeks (2016).

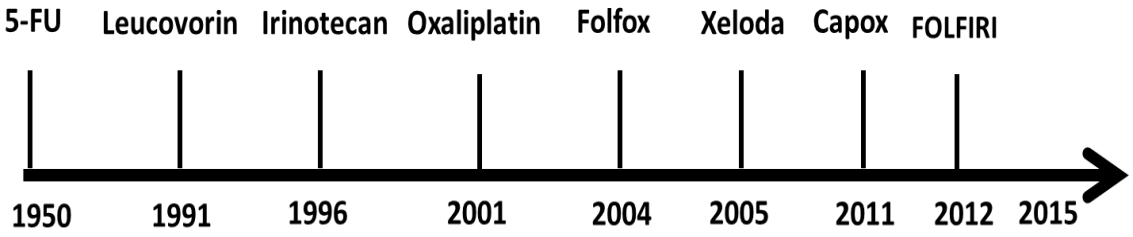

Figure 1.2: Drug-approval timeline for chemotherapy treatments in CRC patients.

1.3 A review of the known mechanisms of resistance in CRC chemotherapy

CRC has a 45% mortality rate due to failings in CRC therapies and one of the main barriers to therapeutic success is the development of acquired resistance to anticancer drugs (Kufe, Pollock et al. 2003). Chemotherapy resistance is the acquired ability of cancer cells to evade the effects of chemotherapeutics agents. Most chemotherapy drugs are targeted to specific proteins, so mutations or changes in these proteins could result in a reduction in the

effectiveness of the drug (Zahreddine and Borden 2013, Housman, Byler et al. 2014). These changes can be inherently presented in tumours before any chemotherapy treatment is administered, or they can be acquired during treatment. The main mechanisms that can converge in drug resistance in human tumours are: drug efflux, cell epigenetics changes, cell death inhibition, DNA repair system failures, drug target alterations and drug inactivation (Zahreddine and Borden 2013, Housman, Byler et al. 2014). Tumour's predisposition to develop these mechanisms differs according to their diverse genomic and proteomic features. Therefore, it is necessary to select the best drug treatment to use for each patient according to the molecular differences of the tumour.

It is important to know about the genetic profile of the tumour because the expression of some specific proteins can play an essential role in sensitivity and prognosis during drug treatment, and expression of a specific group of genes can be correlated with patient survival as it has been observed in CRC (Housman, Byler et al. 2014). Additionally, cross-resistance must be borne in mind before the selection of a drug. Cross-resistance can occur when a mechanism of resistance for a particular drug converges with resistance for another different drug (Zahreddine and Borden 2013). For example, cross-resistance to gemcitabine (Gem) occurs in HCT116 cell line with acquired resistance to decitabine (DAC) by decreasing of Deoxycytidine kinase (dCK), an enzyme that phosphorylates deoxyribonucleosides deoxycytidine (Hosokawa, Saito et al. 2015).

The complex mechanisms of resistance in CRC cell lines are not completely understood and this lack of knowledge is still an issue in cancer research. However, as stated above, some mechanisms of resistance are known. These known mechanisms of resistance can be considered in two different groups:

1) Mechanisms of multi-drug resistance (MDR) that are reviewed below.
2) Specific mechanisms of resistance for specific drugs that are reviewed in Chapters 3-5.

1.3.1 Known mechanisms of MDR

MDR is a broad term that includes a high number of molecular strategies that tumour cells use to avoid the effects of cytostatic drugs. There exists a high number of different cellular mechanisms able to develop MDR. These mechanisms include: changes in membrane transporters (Gottesman and Pastan 1993, Scotto 2003), deregulation in autophagy or alteration in survival process (Kumar, Zhang et al. 2012), and changes in chromosomal instability that can converge in polyploidy (Coward and Harding 2007, Erenpreisa, Salmina et al. 2015). These known mechanisms of resistance are described in more detail below.

1.3.1.1 Mechanisms of MDR mediated by membrane transporters

Under normal extracellular and intracellular environment conditions in cell physiology, membrane transporters such as solute carriers (SLC) and ATP-binding cassette (ABC) transporters can transport and pass solutes, macromolecules, and ions into and out of cells. In some unusual environments, for example under chemotherapy treatment conditions, extracellular matrix microenvironment may be remodelled and some transporters can pump drugs outside the cell too (Gottesman and Pastan 1993, Scotto 2003). SLC is a group of membrane proteins which includes 43 families and 298 transporter genes that mediate the transporter and control uptake and efflux processes of crucial compounds such as inorganic ions, nucleotides and amino acids (Hediger, Romero et al. 2004). Further, ABC transporters which include 8 subfamilies and 49 *ABC* genes can mediate transport of different substances such as lipids, carbohydrates, ions and xenobiotics compounds (Hediger, Romero et al. 2004). To achieve this aim, membrane transporters use energy from the hydrolysis of ATP (Li and Shu 2014). This transport generates and maintains electrochemical ion gradients across membranes of the cell and it also can act by itself as a self-defence mechanism of the cell by actively transporting toxic substances. Drugs can be pumped out from the cell to the extracellular space by these transporter proteins (Hediger, Romero et al. 2004). So, the cytotoxic agent inside the cell tends to decrease due to the efflux by itself and the decrease in both the influx

process of the agent into the cell and the cell permeability (Gottesman and Pastan 1993).

Frequently, MDR is identified by a high increase in the expression of ABC transmembrane transporters like P-glycoprotein (Pgp) (MDR1) and the overexpression of the multidrug resistance-related protein (MRP1) (Gottesman and Pastan 1993, Scotto 2003, Schumacher, Nehmann et al. 2012). MDR1 is a 170 kDa transmembrane glycoprotein. It is one of the best characterized proteins involved in avoiding the cytotoxic effects of multiple drugs on tumour cells (Mechetner, Kyshtoobayeva et al. 1998, Perez-Herrero and Fernandez-Medarde 2015). It is overexpressed in malignant cells in order to remove chemotherapeutic drugs such as IRI from the cells by an active pathway (Xu and Villalona-Calero 2002). However, the specific role that transmembrane transporters play during the development of drug resistance mechanisms is still unknown. Focusing on MDR1, CRC cell lines with low levels of MDR1 protein were more sensitive to drugs and high levels of MDR1 was an important factor during establishment of resistant sublines (Kramer, Weber et al. 1993).

Other studies have shown that MDR1 positive HT 29 CRC cells proliferate much slower than MDR1 negative cells and metastasize less frequently in severe combined immunodeficiency (SCID) mice models (Schumacher, Nehmann et al. 2012). A deceleration of cell growth could be a mechanism of resistance against any drug whose target was the proliferation process. In addition, HT 29 CRC cell line with high expression of MDR1 would have more time to repair damages in DNA, because MDR1 cells proliferate slower than MDR1 negative cell lines.

Whilst the MDR1 transporter accepts amphipathic cationic compounds and neutral compounds as substrates (Chu, Suzuki et al. 1999), the MRP1 transporter family are organic anion transporters that transport anionic drugs and neutral drugs. Normally, MRP1 mediates glutathione S-conjugate export pump, playing its main role in the glutathione S-conjugates transporting and in the transport of glutathione disulfide to the extracellular space, taking a very important part in detoxification and defence against oxidative stress (Chu, Suzuki et al. 1999). Moreover, it has been shown that ABC proteins can play an

important role in camptothecins efflux. It has been demonstrated that both MDR1 and MRP1 overexpression are involved in the active efflux of IRI and its activated form SN-38 (Chu, Suzuki et al. 1999). Some tumour suppressor proteins such as p53 can repress the expression MDR1 and MRP1 proteins (Xu and Villalona-Calero 2002, Cai, Miao et al. 2013). Furthermore, decreasing p53 expression is correlated with MRP1 expression in CRC cancer (Scotto 2003) and some *p53* mutations can activate *MDR1* promotor (Scotto 2003). Another gene involved in drug transporter regulation is *c-MYC*. *c-MYC* is a gene that encodes a transcription factor involved in cell cycle progression, apoptosis and cellular transformation (Kugimiya, Nishimoto et al. 2015). Besides, p53 regulates ABCB5 (MRP5) expression, another transmembrane transport protein which is involved in development of resistance to 5-FU in CRC cell lines (Kugimiya, Nishimoto et al. 2015).

Finally, MDR1 and MRP1 are not the unique members of the ABC family that can act like transporters and mediate resistance to cytotoxic agents used in CRC therapy, like camptothecins and CPT-11 (IRI) (Chu, Suzuki et al. 1999). An additional identified ATP-binding cassette transporter is the breast cancer resistance protein (BCRP), that is overexpressed in colon, breast, gastric, and ovarian cancer cell lines (Maliepaard, van Gastelen et al. 2001). BCRP recognizes and transports a large number of anticancer agents (IRI, SN-38, 9 amino camptothecin (9-AC) and topotecan) and increases MDR expression that mediates efflux of toxic chemical compounds (Ismaili 2011). BCRP is involved in camptothecins resistance and its inhibition by GF120918 (a BCRP inhibitor) overcomes the resistant phenotype in human ovarian tumours (Maliepaard, van Gastelen et al. 2001). BCRP has been described also as a stem cell marker (Nakanishi and Ross 2012).

To sum up, overexpression of certain family ABC transporter proteins such as MRP1, MDR1, and BCRP play crucial roles in the active excretion and efflux of chemical agents involved in CRC therapy and consequently, they are potential targets for modulation of pharmaceutical therapy (Gottesman and Pastan 1993).

1.3.1.2 Mechanisms of MDR mediated by autophagy

In addition to ABC transporter proteins, autophagy has been implicated in MDR (Kumar, Zhang et al. 2012). Autophagy is a normal physiological process in the cells that maintains cellular homeostasis. Autophagy regulates protein and organelle degradation which may be necessary for generate energy to enable continuous cell survival and promote the turnover process of the cells. So, baseline levels of autophagy maintain cellular homeostasis and genomic integrity (Ryter, Cloonan et al. 2013). Furthermore, autophagy can mediate apoptosis and cell death. Autophagy is activated by cells, mainly in response to homeostatic stress but also in cellular stress conditions when cells require increases in metabolic demand (White 2008). Autophagy promotes progression of tumours by stimulation of cell survival process (Ryter, Cloonan et al. 2013). Therefore, autophagy can be considered as a pro-survival mechanism and can be used by cancer cells to develop chemotherapy and radiotherapy resistance (Lu and Harrison-Findik 2013). In 2010, Jie Li *et al.,* showed that the use of 5-FU can stimulate resistance by autophagy in CRC cell lines *in vitro* and *in vivo* (Li, Hou et al. 2010). Consequently, autophagy must be studied as an alternative new target for CRC therapy.

1.3.1.3 Mechanisms of MDR mediated by polyploidy

Polyploidy is a 2-fold increment or more in the number of the normal set of paired (homologous) chromosomes of a cell. Cancer cells can develop polyploidization after treatment with some drugs that act by damaging DNA and mitotic checkpoints (Cortés, Mateos et al. 2004). Polyploid cells can have alterations in the p53 pro-apoptotic pathway, and p53 stimulates p21 protein that plays a crucial role avoiding cell division. Besides, p53 regulates mechanisms of senescence and its alteration can converge into cancer stem cells (CSCs) phenotypes involved in mechanism of resistance to different drugs as 5-FU (Coward and Harding 2007, Paschall, Yang et al. 2016). Hence, polyploidy is a potential mechanism of resistance to cytotoxic chemotherapy.

1.3.1.4 Mechanisms of MDR mediated by cancer stem cells

Cancer stem cells (CSCs) are a very small proportion of the tumour mass and can increase their own population by self-renewal (Schwab 2008). CSCs have

the capacity to differentiate into heterogeneous lineages of cancer cells. Furthermore, CRC stem cells secret a large number of growth factors that encourage angiogenesis, which play an important role in tumour microenvironment that is involved in CRC progression and metastasis (Mathonnet, Perraud et al. 2014). Colorectal CSCs have been shown to take part in resistance to chemotherapeutic treatments. Mainly, the resistance of CSCs is due to the fact that CSCs have self-renew capacity and show overexpression of multidrug transporters involved in resistance to drugs used in CRC. Additionally, CSCs show a high level of anti-apoptotic proteins, so they have the capacity to deregulate signalling pathways targeted by chemotherapy drugs (Housman, Byler et al. 2014, Mathonnet, Perraud et al. 2014, Vidal, Rodriguez-Bravo et al. 2014). Finally, there is evidence that colorectal CSCs can develop resistance to drugs by autocrine IL-4 expression. IL-4 is a cytokine that inhibits apoptotic signalling. Hence, colon CSCs with high levels of IL-4 can avoid the apoptosis caused by 5-FU and OXA (Rich and Bao 2007, Todaro, Perez Alea et al. 2008).

1.4 Experimental approaches for identification of novel mechanisms of resistance in CRC

1.4.1 Understanding of cancer resistance through genomics

CRC is caused by mutations in multiple genes. Development of resistance to chemotherapy agents is also derived from new mutations at the genetic level. A global project known as The Human Genome Project (HGP) started in 1990 to identify genes that are involved in cancer and abnormal cell development (Collins and Mansoura 2001). DNA models with the most frequent variants were established using blood samples from healthy people and used to build DNA "libraries". After this achievement, during the last ten years, researchers have focused on the analysis and comparison of DNA sequencing of healthy samples and many different types of cancer cells (Sjöblom, Jones et al. 2006, Consortium 2012). The main idea was to find which mutations are common for most of the cancers or those that are more frequently detected in specific cancers, such as CRC and breast cancer (Sjöblom, Jones et al. 2006). The next step is to know what functions the mutated genes have in CRC. With these

approaches, the idea is to build a network map to identify the genetic mutations involved in each cancer (Collins and Barker 2007, Hudson, Anderson et al. 2010) in order to develop the best chemotherapy for each type of tumour (McLeod and Evans 2001, Efferth and Volm 2005, Nelson, Wegmann et al. 2012).

The main features of CRC cells are genomic instability and accumulation of genetic alterations in comparison with normal colorectal cells (Lengauer, Kinzler et al. 1998, Fodde, Smits et al. 2001, Grady 2004, Pino and Chung 2010). Therefore the most crucial goal of genomics is to identify which of these changes are relevant to study (Greenman, Stephens et al. 2007). Tumours are formed by cells whose genetics is constantly changing and that respond to a microenvironmental stimulus such as chemotherapy (Kreso, O'Brien et al. 2013). This ongoing change makes possible for a sensitive CRC cell line to evolve into in a resistant subline (Kreso, O'Brien et al. 2013). Mutations that cause incapacity of the cell to repair mutations contribute to spreading genomic instability and genetic variability of new mutations that may result in chemotherapy treatment failures (Pino and Chung 2010). Hence, these mutations in regulatory genes such as *BCL2* or *KRAS* and tumour suppressor genes such as *TP53* play a crucial role in drug resistance development during chemotherapy treatment (Scherf, Ross et al. 2000, Violette, Poulain et al. 2002, Loupakis, Ruzzo et al. 2009).

It is known that the total length of the human genome is over 3 billion base pairs with around 20,000 to 25,000 encoding genes expressing protein (Fig. 1.3) (Consortium 2004). The entire set of proteins in an organism or a cellular system is called the proteome. Proteomics is the study of the proteins in a biological system, through their identification, modification, quantification and localization (Yarmush and Jayaraman 2002). Human proteome is integrated by around 18,097 different proteins according to Bernhard Küster from The Technical University of Munich (Wilhelm, Schlegl et al. 2014). Similar results from Akhilesh Pandey from Johns Hopkins University established that around 17,294 different proteins are present in the human body (Mathivanan, Ahmed et al. 2008). However, this number may be higher as there are protein pathways

from the extensive use of alternative pre-mRNA splicing in humans that provides the ability to build a very large number of modular proteins (Fig. 1.3) (Seo and Lee 2004). Mutations and splicing variants play a crucial role increasing the functional diversity of the proteome over time and across the tissues that generate variants of the basic protein form (Nilsen and Graveley 2010). As a consequence, the Human Proteome Organization (HUPO) estimates there are around 500,000 different proteins in the human body (Fig. 1.3) (Collins and Mansoura 2001).

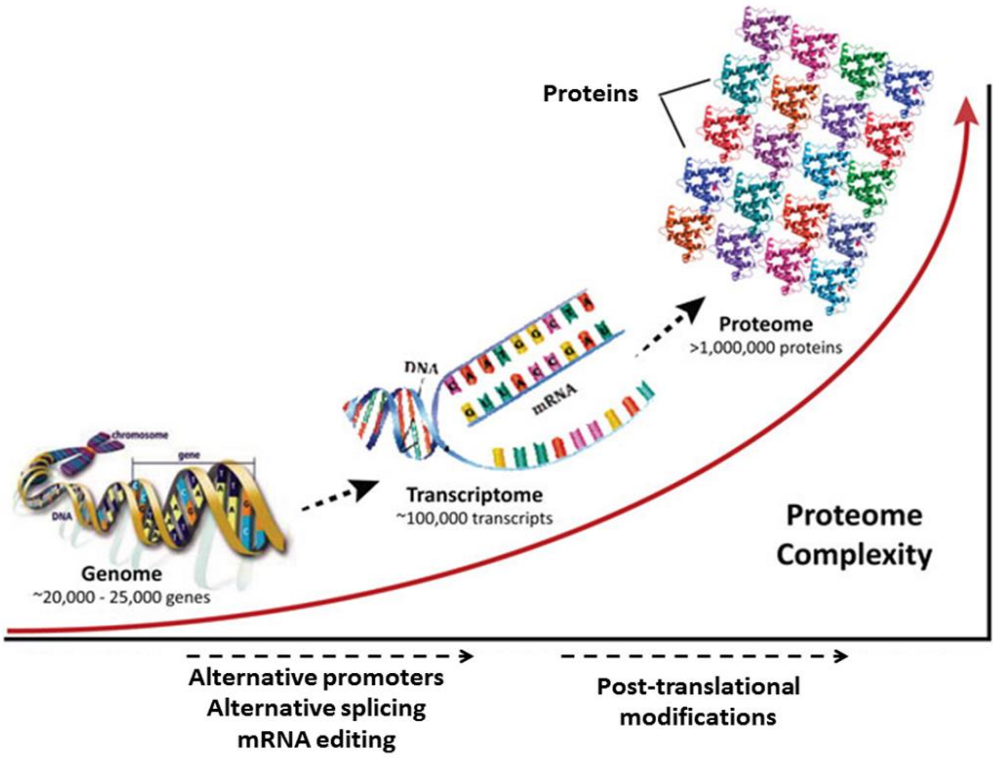

Figure 1.3: Proteome Complexity. The increasing complexity of the human proteome compared with the simplicity of the human genome. Figure adapted from Science.energy.gov/ber/

1.4.2 Understanding genomics through proteomics

As discussed above, genomics is complemented and expanded in complexity by proteomics (Fig. 1.3). Despite the fact that all human cells contain the information for the whole human genome, only a small number of these genes are expressed in each type of cell according to its functionality. There is no eukaryotic cell that expresses all its genome simultaneously and not all genes

are expressed in all cells. It depends on the type of cell and the external or intracellular signal pathways that the cell receives. Depending on these signals, cells will express a proportion of its genome. Post-translational modifications (PTMs) of the proteins may affect their structure, localization, and functionality. So, most of proteins are found as multiple forms and this information can be investigated through proteomics. There is only one genome for each cell line, however, each cell line exhibits different proteomes which change with time (Cohen, Geva-Zatorsky et al. 2008, Ly, Ahmad et al. 2014). Genomics helps to map the human genome to determine risk factor from a disease, while proteomics determines information about the proteins and the current state of a disease (Ly, Ahmad et al. 2014).

For the last sixty years, most of the approaches used to study proteins have focused on the study of specific target proteins. So, studying multiple proteins has been taken a high costs in time and money resources. However, during the last twenty years, proteomics approaches have enabled a global, simultaneous overview of multiple proteins. This advance has been possible thanks to the interaction of various scientific disciplines as molecular biology, biochemistry, physics and bioinformatics (Tyers and Mann 2003).

1.4.3 Understanding of cancer resistance through proteomics

Cancer resistance is a complex problem derived from alterations of normal cellular proteins functions and these alterations may occur as consequence of different molecular biology processes.

1.4.3.1 Mutational processes

DNA sequence can suffer from a permanent change that is known as a mutation. One type of mutation is the point mutation that results from a change of one or two nucleotides at a single location in the DNA sequence. There are two types of point mutations: the base substitution, which happens when a nucleotide base is switched out with another base, and secondly the frameshift mutation, which occurs when a nucleotide base is added (insertion) or removed (deletion) from the DNA sequence. During insertion mutations one or few nitrogenous bases are added to the DNA sequence, so making DNA sequence

longer and altering codon sequences. In deletion mutations, one or a few bases are removed resulting in a shortening in the DNA sequence and these also can affect to codons. Mutations can affect coding region of DNA sequence, which is translated to form proteins and may lead to important changes at protein level. These changes in DNA coding sequences affect proteins at different levels such as spatial expression, temporal expression, protein–protein interaction (PPIs), PTMs, protein turnover process and at the protein expression level.

1.4.3.2 Transcriptional and Post-transcriptional processes

Additionally, there are different issues that affect protein levels and are not a consequence of mutational processes. These multiple and different regulation steps that can affect protein levels are shown below.

i) Transcriptional regulation process: it is regulated by transcription factors (TFs), proteins synthesized in cytoplasm that migrate into the nucleus and interact with specific sequence of genes in the DNA and activate transcription. Hence, any potential change in a transcription factor protein can affect its regulated genes. (e.g., transcription factor p38 blocks the ability of Ras or Raf to activate the transcription function of NF-κB, altering protein kinase signalling pathways (Baldwin 2001)).

ii) Post-transcriptional regulation process: after gene transcription, its regulation can still occur affecting its protein product through different post-transcriptional processes which are summarised below (e.g., alternative splicing of UMPS can mediate acquired 5-FU resistance in CRC cell lines (Griffith, Mwenifumbo et al. 2013)).

- RNA processing: Alternative splicing.

- RNA stability: Exclusion or inclusion of regulatory elements that play a role in RNA stability; Premature stop codon.

- Translational: General translation; Regulatory elements in 5' UTR (e.g., upstream open reading frame, internal ribosome entry site); Depletion of ternary complex.

- Protein turnover/modification: Differential half-lives of the same protein isoforms under different conditions (e.g., ubiquitination directing target proteins for proteasomal degradation (Ciechanover 1998)).

1.4.3.3 Protein alterations modelling chemotherapy resistance

As described above, some changes caused by mutations in DNA coding sequences affect spatial expression of proteins. Changes in spatial expression of proteins play an important role in chemotherapy resistance. For example, some resistant cancer cells show abnormal patterns of surface receptors such as CD95 and TRAIL (Johnstone, Ruefli et al. 2002). Frequently, these receptors may receive signals from neighbouring cells or from the microenvironment. These signals may be related to activation of apoptotic pathways or activation of the immune system. For example the absence of tumour necrosis factor related apoptosis-inducing ligand (TRAIL), a member of the tumour necrosis factor (TNF) superfamily, correlated to resistance to the inhibitor imatinib mesylate in melanoma and resistance to antibodies that target death receptors in breast cancer (Mahalingam, Szegezdi et al. 2009, Twomey, Kim et al. 2015). Therefore, lack of these apoptotic receptors may result in an interruption of pro-apoptotic signalling pathways (Twomey, Kim et al. 2015). Furthermore, TRAIL-receptor endocytosis or up-regulation of apoptosis inhibitors may inhibit the signalling of caspase cascade, converging in a resistance phenotype (Mahalingam, Szegezdi et al. 2009).

Other protein changes involved in chemotherapy resistance are related to protein-protein interactions (PPIs). PPIs are defined as the physical interactions or molecular relationships that two or more proteins have between each other in a living system (De Las Rivas and Fontanillo 2010). The whole map of PPIs in a live organism is called the interactome (Stumpf, Thorne et al. 2008). It has been estimated that the human interactome contains around 650,000 PPIs involved in biological human body processes (Stumpf, Thorne et al. 2008, De Las Rivas and Fontanillo 2010). There are many different groups of proteins involved in PPIs pathways. However, the main role in these routes is played by TFs.

TFs are molecules and proteins that take part in the regulation process of gene expression by DNA-Protein interaction and PPIs with other proteins. One of the best known TFs involved in cancer is the tumour protein p53 (TP53) (Petitjean, Mathe et al. 2007). p53 is a tetrameric complex. Each subunit of the complex consists of four domains: C-terminal domain, DNA binding domain, tetramerization domain and N-terminal domain (Muller and Vousden 2013). The tetrameric p53 complex binds to p53 consensus DNA sequences by the binding domain (Muller and Vousden 2013) and mediates the transcription of specific genes by RNA Polymerase II. It is known that p53 mutations are presented with high frequency in most cancers: 50% in colorectal (Li, Zhou et al. 2015), ovarian, oesophageal, lung, larynx, head and neck cancers and around 5% in cervical cancer, sarcoma, testicular cancer, malignant melanoma, and primary leukaemia (Petitjean, Mathe et al. 2007). These mutations in *p53*, cause changes in the expression of p53 dependant genes and at PPI level as occurs with the complexes p53/p21, MDM2/p53 and hDM2/p53 (Petitjean, Mathe et al. 2007).

TFs as p53 are especially relevant due to the PPI networks and DNA-binding regions where they are involved. DNA-binding proteins such as p53 play a key role in repression and stimulation of transcription of a broad range of genes involved in multiple biological processes that can be potentially involved in drug resistance. Some p53 target genes are involved in cell cycle control, such as *p21$^{WAF1/CIP1}$*, *GADD45*, *WIP1*, *MDM-2*, *EGFR*, *PCNA*, *CyclinD1*, *CyclinG*, *TGF-α* and *14-3-3 sigma* (Muller and Vousden 2013). Other p53 dependent genes are involved in DNA repair like *GADD45*, *PCNA*, and *p21$^{WAF1/CIP1}$* (Muller and Vousden 2013). Another group of p53 regulated genes involved in apoptosis are: *BAX, Bcl-L, FAS1, FASL, IGF-BP3, PAG608*, *DR5/KILLER, GML*, *P2XM*, *TSP-1* and BAI1 (Muller and Vousden 2013). Finally, some p53 dependent genes are involved in cellular stress response like *TP53TG1*, *CSR,* and *PIG3* that also can act as a mediator of drug resistance (Muller and Vousden 2013). Alterations in the expression of these proteins, which are involved in crucial biology functions of a healthy cell, may result in an uncontrolled growth of the cell that will increase tumoural features like aggressive growth, invasion, proliferation, development of cancer stages or development of resistant

phenotypes and survival pathways (Muller and Vousden 2013). Due to the large number of genes regulated by p53 activity, mutations in *p53* can play a variable role in tumour sensitivity responses to chemotherapy (Breen, Heenan et al. 2007).

Other somatic changes that alter proteins involved in drug resistance occur at PTMs level. Once the polypeptides chain is synthesised by ribosomes to form the protein, but before becoming the mature protein, it may undergo modifications. These PTMs include, amongst others, glycosylation, phosphorylation, lipidation, methylation, acetylation, and proteolysis and are shown below.

i) Glycosylation consists of the addition of sugar groups that alter the folding and conformation of proteins (Shental-Bechor and Levy 2008). Glycosylation is a frequent modification in membrane proteins involved in drug transporters and membrane surface receptors proteins. Glucosylceramide synthase (GCS) has been found to be overexpressed in doxorubicin- and cisplatin-resistant breast cancer, CRC, and leukaemia cells (Liu and Li 2013). GCS is an enzyme that catalyzes ceramide glycosylation (Liu and Li 2013). Drug treatments increase of ceramide that initiates processes of proliferation arrest, apoptosis, and autophagy. Overexpression of GCS is a cellular response that by ceramide glycosylation can arrest these cellular processes, and thereby protect cancer cells from apoptosis. Ceramide glycosylation has been observed in development of resistance to doxorubicin, anthracyclines, Vinca alkaloids, and taxanes drugs in breast cancer (Liu, Han et al. 2001). In CRC cell lines, increasing of GCS expression has been found during drug resistance acquisition, in SW-620 colon cell line with 121 fold resistance to doxorubicin and 1.33 fold GCS expression in HCT-8/VCR cell line with 4.5 fold resistance to cisplatin (Liu and Li 2013).

ii) Phosphorylation consists of binding of phosphate to proteins, as occurs with Src protein, which can be switched from an inactive to an active state through control of its phosphorylation state. Normally GCS overexpression is correlated with MDR1 levels in cell lines and tumours resistance to drugs (Liu, Gupta et al. 2010). MDR1 up-regulation by GSC occurs via Src kinase and β-catenin

signalling pathways. But up-regulation of MDR1 only occurs under both GSC overexpression and phosphorylated Src state conditions. However, the complete understanding of this mechanism is unknown, and the unique evidence is that blocking of GSC decreases MDR1 expression (Liu, Gupta et al. 2010).

iii) Lipidation is adding a lipid component into amino acids. This modification is normally present in proteins involved in interactions in mitochondrial, lysosomal, and plasma membranes. Lipidation modifications enhance the hydrophobic character of the proteins and are crucial during autophagosome formation. An increase in the number of autophagosomes have been observed in HT 29 and HCT116 CRC resistant sublines to 5-FU (Kumar, Zhang et al. 2012, Sui, Kong et al. 2014). Additionally, activation of autophagosome biogenesis promotes CRC cells survival and this fact has been demonstrated by using autophagy inhibitors that may reverse the resistant phenotype in CRC cells (Li, Hou et al. 2010, Sui, Kong et al. 2014, Zhang, Kumano et al. 2014).

iv) Methylation consists of the addition of a methyl group ($-CH_3$) into the amino acids by methyltransferase enzyme. This PTM is involved in gene expression regulation. So, DNA methylation patterns of unregulated cell lines may be found with hypomethylation and hypermethylation changes. In gastric cancer patients, DNA hypomethylation of some multidrug transporter proteins such as MDR1 was observed, while DNA hypermethylation was found in genes related to apoptosis pathways (Baker and El-Osta 2003, Hervouet, Cheray et al. 2013). But the most important methylation occurs in histones. Histone methylation causes modification of enzymes associated with tumourigenesis and drug resistance. Increases of H2A/H4R3me2 and the two associated enzymes PRMT1, PRMT5, have been associated with poor prognosis in prostate cancer patients (Seligson, Horvath et al. 2005). Furthermore, expression of H3K9me2/3, KMT1, KMT8, KDM1, KDM3, KDM4 have been found increased in lymphoma (Braig, Lee et al. 2005) and H3K9me3 with increasing of KMT1, KMT8, KDM3, KDM4 in treatment with 5-aza-2′deoxycytidine (5-Aza-CdR) in bladder cancer cells (Nguyen, Weisenberger et al. 2002). Also, the use of

histone methyltransferase inhibitors is starting to be used to reverse epigenetic mechanisms that drive into drug resistance (Lachner, O'Sullivan et al. 2003).

v) Acetylation process consists of adding an acetyl functional group onto specific amino acids. Main acetylation process involved in cancer is related to acetylation of histones. Histones are responsible for maintaining chromatin shape and structure. Histone acetylation occurs at the amino-terminal tale of the histone and it plays a key role in regulation of gene expression. Histone acetylation is controlled by the balance of two families of enzymes: Histone acetyl transferases (HATs) and histone deacetylases (HDACs). Under histone acetyl transferase activity, histones are acetylated and the chromatin structure is opened giving access to TFs to stimulate gene expression. There are two main types of acetylation in histones. On the one hand, lysine acetylation is a reversible PTM of proteins and plays a key role in regulating gene expression but with unknown role in cancer resistance. On the other hand, N-acetylation consists of the substitution of N-terminal methionine by an acetyl group during transcriptional process. Methionine aminopeptidase enzyme cleavages the N-terminal methionine and the acetyl group replacement is mediated by N-acetyltransferase enzymes (Marks, Rifkind et al. 2001). Regarding cancer resistance, there are histone deacetylase inhibitors (HDACIs), like PCI-24781 which targets HDAC enzyme of colon carcinoma cells changing the global histone acetylation pattern (Marks, Rifkind et al. 2001, Banuelos, Banáth et al. 2007). HDACIs have been studied for use in MDR in CRC as a novel class of anti-tumour drug (Wang, Huang et al. 2016).

vi) Proteolysis is the process by which a protease enzyme breaks an inactivated protein (zymogen form of a protein) to activate the protein. However, the role of proteolysis in cancer resistance is unknown.

1.4.3.4 Proteomics approaches to identify mechanisms of resistance in cancer

Emergence of high-throughput proteomics technology has shed light on the complex picture of the mechanisms of drug resistance in cancer. Proteomics can be applied to characterizing the mechanisms of drug resistance and to identify biomarkers for predicting drug response to chemotherapy. A brief

summary of main methods for protein separation and quantification are described below. Some of the proteomics approaches which have previously been used in identification of mechanisms of resistance in cancer are summarized in Table 1.1.

Proteomics approach	**Drug**	**Type of Cancer**	**Mechanism of resistance**	**Author & Publication**
SDS-PAGE TOFMS	Camptothecin	Prostate	Up-regulation of ANXA1, GAL3, GST	Urol Int. 2006 (Hasegawa, Mizutani et al. 2006)
SDS-PAGE LC-MS/MS	Carboplatin and paclitaxel	Ovarian	Up-regulation of ENOA, EFTU, GRP75, APOA1, RDX2	Proteomics 2017 (CRUZ, COLEY et al. 2017)
TOFMS	Paclitaxel	Non-small-cell lung	Up-regulation of MET, DPP4, PTPRF	Expert Rev Proteomics (Cho 2016)
SILAC	Doxorubicin	Breast	Up-regulation of TKs family	Mol Cell Proteomics (Stebbing, Zhang et al. 2015)
SDS-PAGE ESI-Q-TOFMS	Docetaxel	Naso-pharyngeal	Up-regulation of ENO1, CNE-2R	Anticancer Drugs (Peng, Gong et al. 2016)
SDS-PAGE LCQ XP Ion Trap LC-MS	Oxaliplatin	Colorectal	Down-regulation of PK-M2	Molecular Cancer Therapeutics (Ginés, Bystrup et al. 2015)
SDS-PAGE Label-free LC-MS/MS	5-FU	Colorectal	Up-regulation of NQO1, PRDX, and Down-regulation of CTNNB, RhoA	Proteomics (Bauer, Lambert et al. 2012)

Table 1.1: Proteomics approaches previously used in discovery of mechanisms of resistance in cancer. Key: Time-of-flight mass spectrometry (TOFMS), Electrospray ionization (ESI), Sodium dodecyl sulphate polyacrylamide gel electrophoresis (SDS-PAGE), Liquid chromatography tandem-mass spectrometry (LC-MS/MS).

Most proteomics approaches are used to separate, identified and quantified proteins. A brief summary of main methods for protein separation and quantification are described below.

1.4.3.4.1 Proteomics separation approaches

Proteins exhibit different biophysical and electrostatic properties based on the sequence of constituent amino acids. These properties can be exploited to separate proteins for subsequent analysis. The traditional proteomics strategy to identify proteins is based on protein separation of a sample by one and two-dimensional polyacrylamide gel electrophoresis which enable proteins to be isolated in a band or spot for identification by mass spectrometry.

One dimensional gel electrophoresis is used to separate proteins based on their molecular weights, after unfolding and linearisation of proteins by using of chaotropes such as urea and thiourea, and an anionic detergent as sodium dodecyl sulphate (SDS). Proteins with lower molecular weights migrate faster than proteins with high molecular weights through the polyacrylamide gel (Brunelle and Green 2014) (Shi and Jackowski 1998).

Two-dimensional gel-based separation (2D-PAGE) approach can be used to separate proteins through the Isoelectric point (pI) of proteins (O'Farrell 1975). pI is the pH at which the peptide or protein have a net charge of zero. Using an immobilised pH gradient in an isoelectric focusing (IEF) gel it is possible to separate proteins based on their pI, when an electric current is passed across the gel. Initially, all proteins are anions with negative charge but when they achieve their pI, proteins acquire neutral charge and they stop their movement through the electric field. The IEF gel than then be transferred to an SDS-PAGE gel for separation based on molecular weight, separating proteins in two dimensions. However, in this thesis a proteome screening method is required to identify as many proteins as possible, to identify novel biomarkers of drug-response.

Hence, Shotgun or Mudpit proteomics was the main approach used in this research to obtain an overview of proteome expression in resistant and sensitive cell lines. Shotgun proteomics is an indirect measurement method to

identify and quantify proteins through peptides derived from proteolytic digestion of intact proteins. This global proteomics approach was used to identify and quantify as many proteins as possible in resistant and sensitive cell lines. This approach required the use of multidimensional chromatographic separation to reduce complexity of protein lysates. In this work, columns of strong cation exchange (SCX) were utilised as separation technique. The different protein lysate fractions obtained by SCX separation contain different groups of proteins which are subsequently identified by mass spectrometric analysis in a database search.

1.5 Mass spectrometry

A mass spectrometer is an instrument to measure the mass and charge of molecules to determine their structures. Mass spectrometer ionises molecules and then transfer them to an analyser which separates them based on mass and/or charge and then detects the separated ions. Proteins and peptides are polar, non-volatile, and thermally unstable species that require an ionisation approach to transfer them into a gas phase without a high degradation of the molecule. To positively ionise a molecule consist of adding a proton or removing an electron from the molecule. Protein and peptides form a protonated molecule $[M + H]^+$ which produces a peak at an m/z value of M + 1, where M is the mass of the analyte.

The transformation from protein and peptide ions in solution to ions in the gas phase is mostly commonly achieved by electrospray ionisation (ESI) in combination with heated auxiliary gas. ESI can analyse the mass of polar compounds in excess of 100,000 Da (Ashton, Beddell et al. 1994).

An electrospray needle creates droplets that are electrically charged at their surface as a liquid emerges from an interface connected to an High-performance liquid chromatography (HPLC) system. In electrospray, charge density at the surface of the droplets increases as solvent evaporates, while an auxiliary gas helps solvent evaporation from the droplets. The electrical charge density at the surface of the droplets increases until reaching a critical point known as the Rayleigh stability limit. At this point, the droplets divide into

smaller droplets because the electrostatic repulsion is greater than the surface tension. Finally, electrostatic repulsion ejects sample ions from the very small, highly charged droplets into the gas phase. The sample ions enter the mass spectrometer through the ion transfer tube where they are analysed according to their mass-to-charge (m/z) ratio.

There are two main types of mass spectrometers used for proteomics, primarily depending on how the samples are prepared (gel electrophoresis or liquid chromatography): Time-of-Flight Mass Spectrometer and Quadrupole-Orbitrap Mass Spectrometer.

a) Time-of-Flight Mass Spectrometer

In the ToF Mass Spectrometer, which most frequently employs matrix-associated laser desorption ionisation (MALDI), ions are formed by firing a pulse of laser-generated photons at the samples. Singly charged ions of same kinetic energy, but different m/z ratio, are separated by time of flight over an identical path between the ion source and the detector. Heavy particles travel more slowly and arrive at the detector later than light particles.

b) Quadrupole-Orbitrap Mass Spectrometer

The Quadrupole-Orbitrap Mass Spectrometer was used for data presented in the thesis. Once the ionised analytes have entered into the mass spectrometer, they pass through an ion accelerator and a mass filtering quadrupole that consists of four parallel metal rods forming an electric passage. The trajectory of flight of ions during travelling between the four rods is affected by the applied voltages from the rods. The mass spectrum is obtained by monitoring ions' movement through the quadrupole filter voltages and that depends on the ions m/z ratios.

After the ionised sample has crossed the linear ion accelerator and the mass filter, parent ions will enter the Orbitrap analyser via the C-trap. Before starting the analysis of any sample, an initial injection of a fixed number of ions of a known compound is analysed for a robust internal calibration of each spectrum. Finally, specific parent ions are ejected through a lenses system from the C-Trap to the Orbitrap (Fig. 1.4).

Once parent ions have entered the Orbitrap, the central electrode of the Orbitrap is charged by voltage. Due to the electrode voltage, parent ions are forced to oscillate with different frequencies of the trapped ions as they move across the trap spindle and drawing different orbits around the Orbitrap. Each peptide has different harmonic oscillation frequencies which are derived from their particular m/z values. After ions with different m/z ratio have entered into the Orbitrap and move far enough from the outer electrodes, the voltage on the central electrode is stabilised and the detection can occur. According to the parent ion intensity, a parallel quantification of peptide abundance may be carried out to quantify peptide abundance in the sample.

After parent ion isolation, they are fragmented by collision-induced dissociation in a neutral gas phase, normally helium, nitrogen or argon. During the collision, some of the kinetic energy is converted into internal energy which results in bond breakage and the fragmentation of the molecular ion into smaller fragments. These fragment ions are detected at the ion trap (Fig. 1.4). Comparisons of m/z fragment ion spectra are used in an algorithm that allows performing database searches which lead to peptide identification. The data acquired by the Orbitrap, is transferred to a database search engine, such as Mascot to compare the experiment spectra with an *in silico* database of all protein sequences and identify the protein in the sample.

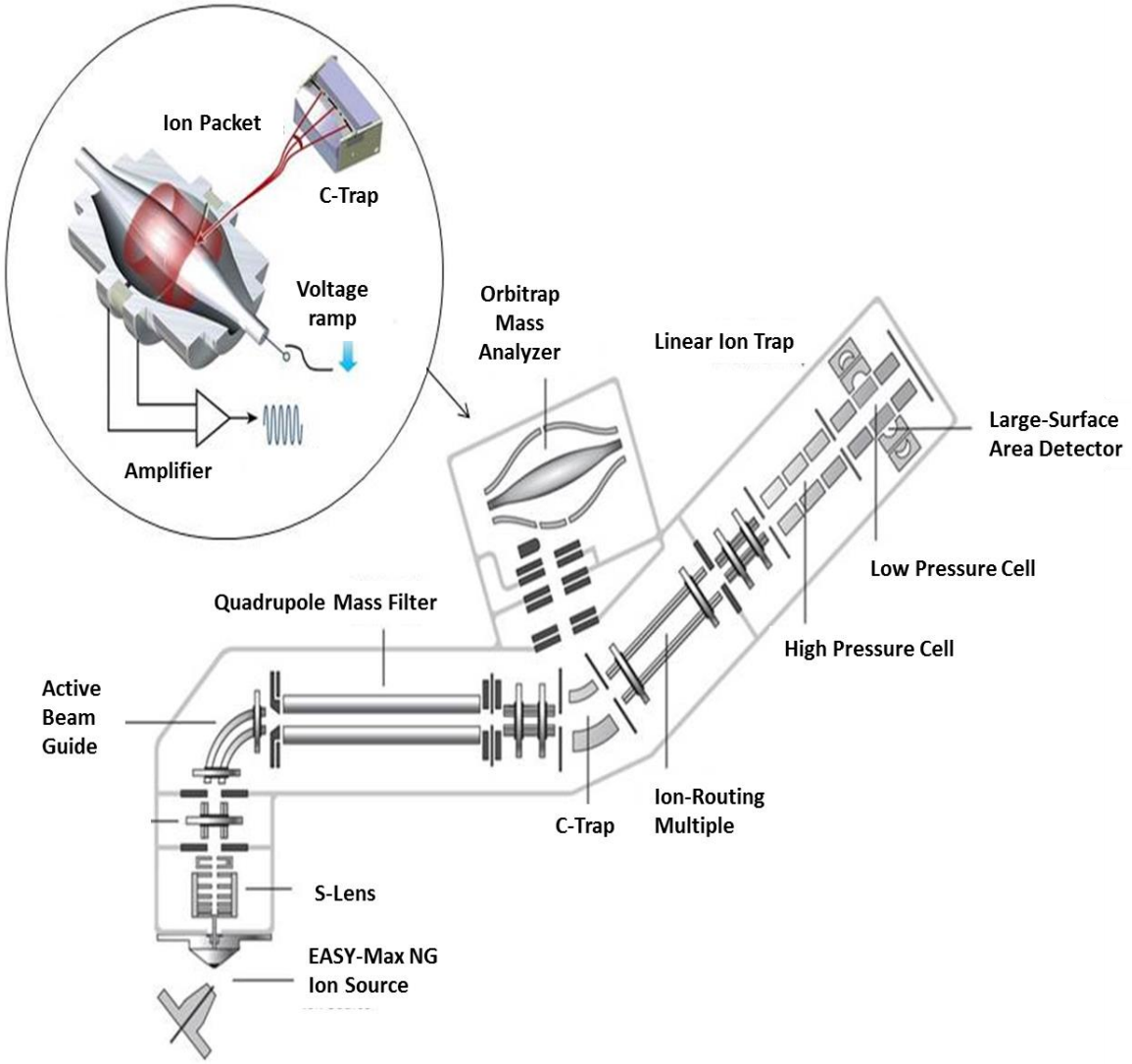

Figure 1.4: Schematic diagram of an Orbitrap mass spectrometer and Orbitrap Analyser. Figure adapted from © Thermo Fisher Scientific.

1.5.1 Approaches in quantitative proteomics

Three main approaches are Multiple Reaction monitoring (MRM) / Parallel reaction monitoring (PRM), Isobaric Tags for Relative and Absolute Quantitation (iTRAQ) and Stable Isotope Labelling by Amino acids in Cell culture (SILAC), and their main advantages and disadvantages are summarised in Table 1.2 below.

Gel-Free approach		
Proteomics approach	**Advantages**	**Disadvantages**
SILAC	High yield, Robust, Sensitive and simple	Available for cell/tissue culture only, Expensive reagents, Not available for tissue samples
iTRAQ	Available to different type of samples, Good quantitation	Required high amount of protein, Incomplete labelling, Expensive reagents
Label-free (MRM/PRM)	Required low amount of protein, High proteome coverage, Low cost (avoid labelling)	High instrumentation quality, High abundance of proteins required, Incomplete digestion introduce error, More than one experiment required for multiple analysis

Table 1.2: Main advantages and disadvantages of main Gel-Free proteomics approaches.

1.5.2 Multiple reaction monitoring (MRM) and Parallel reaction monitoring (PRM)

MRM has high sensitivity, high selectivity, and robust quantification to identify a target peptide with a high confidence. MRM is a label-free method that makes possible to quantify hundreds of proteins by analysis of fragments from specific proteotypic peptides ionized (Fig. 1.7) (Rauniyar 2015). Fragmentation of ions is carried out in the gas phase by Higher-energy collisional dissociation (HCD) (Rauniyar 2015). Ions are accelerated by electrical potential to high kinetic energy until hitting against neutral molecules as helium, nitrogen or argon. Ions are fragmented and distributed in different clusters according to their masses to eliminate background and interferences. In MRM method, samples are processed independently, and once mass spectrum analysis has been done on

a single product ion selected, results of relative abundance of specific peptides will be compared between two or more samples (Fig. 1.7) (Rauniyar 2015). However, PRM method is a variant of tandem mass spectrometry (MS/MS), where detection of all product ions occurs in parallel, in a single analysis using a high resolution mass spectrometer, known as Orbitrap mass analyser (Zhou and Yin 2016). The method required adding of synthetic peptide standards to prepare calibration curves for relative quantification, alternatively, stable isotope labelled standard peptides can be added to the sample for absolute quantification as occurs with the SILAC approach used in the thesis.

It is the main method to quantify protein relative abundances in mammalian cells (e.g., MCF-7 breast and SW480 CRC cell lines have been investigated by PRM to identify altered proteins involved in metabolic processes (Drabovich, Pavlou et al. 2012, Kim, Lin et al. 2015, Rauniyar 2015).

1.5.3 Isobaric Tags for Relative and Absolute Quantitation (iTRAQ)

iTRAQ is proteomics relative quantification technique based on the labelling of peptides with a compound that produces isobaric fragments, or reporter ions, that are detected only under MS/MS or MS^3 conditions. Isobaric reagents used for chemical labelling contain an amino-reacting group, a balance group and a reporter group (Fig. 1.5) (Seligson, Horvath et al. 2005). Firstly, isobaric reagents are used to label the amino groups of the peptides. These isobaric reagents are an N-methyl reporter group with different masses and an N-hydroxysuccinimide ester group that reacts with the amines of the peptides to be attached (Seligson, Horvath et al. 2005). Each isobaric reagent has an additional balance group giving the same final mass to all peptides, independently of the N-methyl reporter group attached to the peptide. All peptides are labelled according to their specific masses (Seligson, Horvath et al. 2005). iTRAQ labelled samples are analysed by mass spectrometry in MS/MS mode to generate (a) fragments from the peptide and (b) fragments from the reporter ions, the intensities of which enable relative quantification (Seligson, Horvath et al. 2005) (Fig. 1.7). iTRAQ has been successfully used to find that low expression level of β-catenin combined with the up-regulation of Calcyclin binding protein (CacyBP) promote metastatic processes in CRC: 1140

unique proteins were identified in SW480 and SW-620 CRC cell lines and, 147 of those proteins showed significant changes in expression between healthy and metastatic cells (Ghosh, Yu et al. 2011).

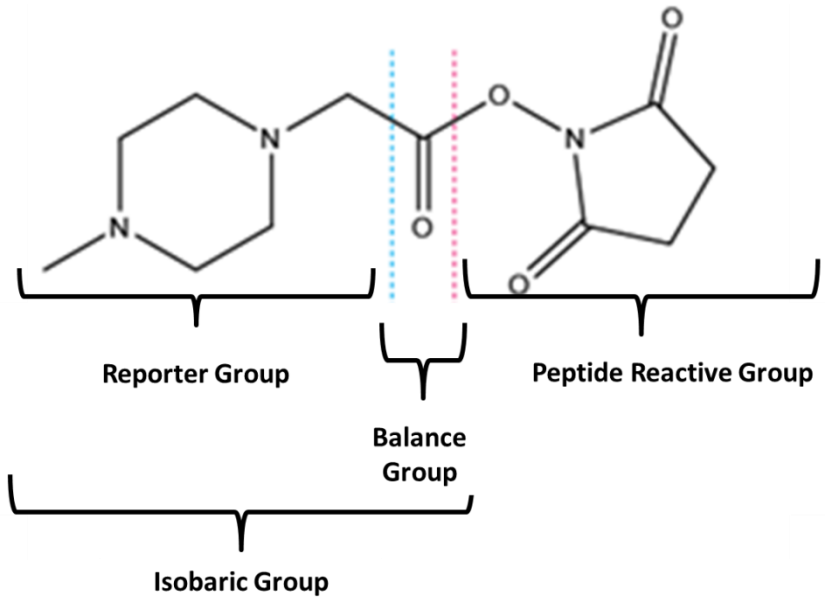

Figure 1.5: Isobaric reagent used in iTRAQ methodology. Figure adapted from © Ross PL, Huang YN, *et al*., (2004).

1.5.4 Stable Isotope Labelling by Amino acids in Cell culture (SILAC)

This proteomics study has been carried out using stable isotope labelling by amino acids in cell culture (Seligson, Horvath et al. 2005, Zhang, Xu et al. 2014) (SILAC), a relative quantification and label method. SILAC was described initially by Pratt *et al.,* in 2002 (Pratt, Robertson et al. 2002). The principle of SILAC is based on replacement of the natural (light isotopes) amino acids with (Seligson, Horvath et al. 2005) isotopes with higher mass number than the original atom called heavy isotope- amino acids. An isotope is an atom of an element with higher or lower number of neutrons than the original chemical element, but with the same number of protons and electrons than original element. The physicochemical properties and features of light and heavy isotopes are equal. Hence, the only difference between the original atom and its isotope is related to mass number that can be detected by a mass spectrometer (Seligson, Horvath et al. 2005).

To make possible the replacement of light amino acids with heavy amino acids that contain heavy isotopes, cells need to take the heavy amino acids from their medium (Fig. 1.6) (Zhang, Xu et al. 2014). To be sure that cells take heavy (labelling) amino acids from the medium, just essential amino acids are selected for labelling in SILAC experiments (Seligson, Horvath et al. 2005). An essential amino acid is an indispensable amino acid that cannot be synthesized by cells and is limited by special pathophysiological conditions. There are nine amino acids that humans cannot synthesize: phenylalanine, valine, threonine, tryptophan, methionine, leucine, isoleucine, lysine, and histidine. Arginine is also used during labelling process because it is a semiessential or conditionally essential amino acid that is used by cells during proteins biosynthesis. Normally, to carry out SILAC experiments, the ^{12}C and the ^{14}N element are chosen to produce the stable isotopes ^{13}C and ^{15}N by adding an extra neutron into the atoms of the element (Fig 1.6). Stable isotopes will form part of the heavy amino acids (Fig. 1.6).

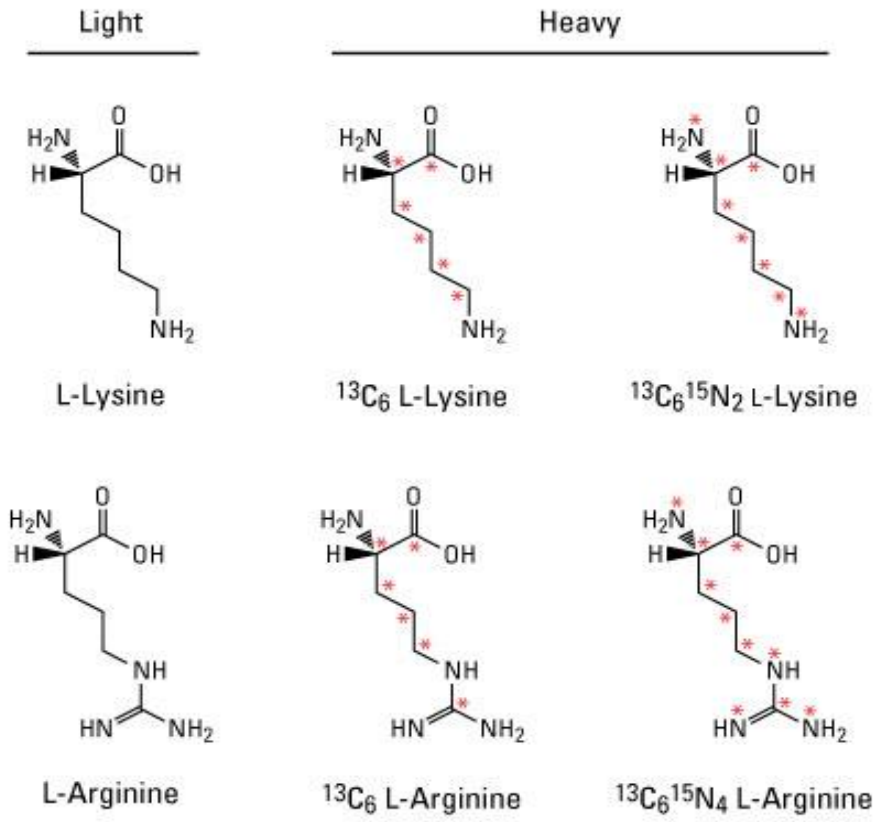

Figure 1.6: Light / Heavy lysine and arginine amino acids for SILAC approach. © Thermo Fisher Scientific.

Labelled amino acids presented in SILAC media can be metabolically incorporated by cells, which will use them during peptide biosynthesis. Maintaining cells in media with heavy amino acids (heavy medium) during more than six doublings will lead to the incorporation of heavy peptides into most of the proteins of the cells that will show the isotope labelling (Fig. 1.7) (Seligson, Horvath et al. 2005, Zhang, Xu et al. 2014). Finally, proteomics study of the cells starts with the lysis of the cells and the extraction of the proteins (Fig. 1.7) (Zhang, Xu et al. 2014). Later, proteins will be digested into peptides and a mass spectrometer will make possible to discern peptides from cells growth in a heavy amino acids medium from cells growth in a normal light medium (Fig. 1.7) (Seligson, Horvath et al. 2005). The relative abundance of the labelled and non-labelled peptides will correspond to the amount of protein present in the cells of the study. SILAC approach has been used to quantify and analyse different proteome expression in normal bladder cells and bladder cancer cells, 3721

proteins were identified and 110 proteins were found with different expression levels (Zhang, Xu et al. 2014, Yang, Xu et al. 2015). SILAC in CRC has been used to study secretome in CRC metastatic cells (Barderas, Mendes et al. 2013, Zeng, Yang et al. 2013) and combined with microarray analysis to study changes of mRNA expression (Kaller, Liffers et al. 2011, Zhang, Xu et al. 2014). Advantages of SILAC over iTRAQ and label-free approaches have been shown above in Table 1.2.

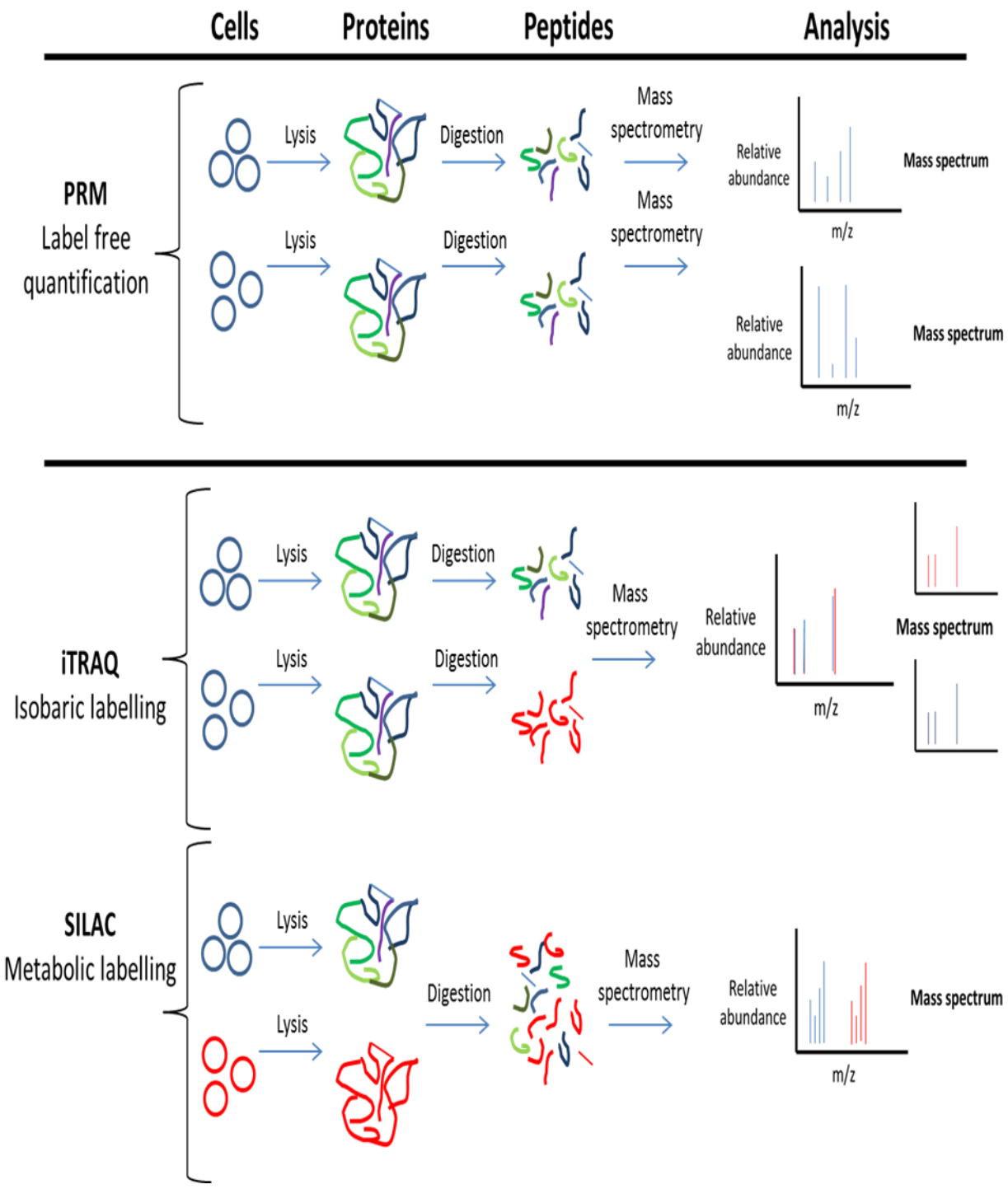

Figure 1.7: Summary scheme of main quantitative proteomics approaches used to identify mechanisms of resistance in cancer. Graphic adapted from © Thermo Fisher Scientific "Quantitative Proteomics". Key: red colour shows samples labelled.

1.6 Aims & Objectives

As has been reviewed in this introduction (see section 1.3), and it will be see in Chapters 3-5, CRC acquired resistance depends on the drug's mechanism of action and the capacity of the cells to reduce the pathway-targeted anticancer effect of drugs. So, most of the molecular mechanisms of resistance that are known are based on the biochemistry and metabolism of these drugs. However, overall five-year survival rate for CRC (stage II-III) is 45%. Hence, it is probable that there exist unknown mechanisms of acquired resistance to therapy. Therefore, the main aim of this Ph.D. project is focused on developing new drug-resistant human subclones which can be used to identify these novel mechanisms of resistance in CRC, and also as experimental models for evaluation of novel therapies which may overcome drug resistance that would explain the lack of success in the current chemotherapies strategies in CRC.

To achieve this aim, the objectives of this research will be as follows:

1) Selection of suitable cell lines for development of resistant sublines from a CRC cell line panel.

2) Establishment of drug resistant sublines of the CRC lines for one of the three most common CRC chemotherapeutics, 5-FU, IRI, OXA and characterise cell lines for cross-reactivity with other anti-cancer agents.

3) Identification of novel mechanisms of drug resistance using a proteomic approach.

4) Validation of the proteomics results using immunodetection techniques to analyse candidate proteins.

- Chapter two -

Selection of CRC cell lines

for use in resistance studies

2 Selection of CRC cell lines for use in resistance studies

One of the leading causes of high mortality rate in advanced CRC is acquired resistance to therapeutic treatment. 5-FU, IRI and OXA are the main postoperative treatments for CRC patients. In order to identify new mechanisms of resistance, three different CRC cell lines were chosen to establish more than three resistant sublines by continuous exposure to 5-FU, IRI and OXA.

2.1 Heterogeneity of CRC cell lines

To choose the three most relevant CRC cell lines to be used during development of resistant sublines by long-term drug exposure, it is necessary to know what differences in growth rate, attachment features, shape, size and genetic background are presented in different CRC cell lines. One of the main advantages of working in cell culture is maintaining homogeneity of cell lines. Knowing cell lines growth features allows synchronizing cells at different stages of the cell cycle in a culture, bringing to the same phase different types of cell lines which differ in term of growth rates. This makes possible to compare chemical compounds or drugs on specific cell lines at a specific stage of the cell cycle, increasing consistency and reproducibility of results.

Molecular heterogeneity observed in patients is maintained in CRC cell lines and it may be observed when CRC cell lines are classified in different subtypes according to their gene expressions and transcriptional features. There are five different classifiers which differ from algorithms used to establish different subtypes of CRC cell lines. However, the CRC-assigner (CRCA) classification system established by Sadananman *et al.*, showed the highest overlap with all other classifiers (Sadanandam, Lyssiotis et al. 2013). Enzo Medico *et al.* also found that main mutations in oncogenes (*KRAS, NRAS, BRAF, PIK3CA, PTEN*) found in the clinic, were represented in the same proportion in a sample collection of 103 CRC cell lines (Medico, Russo et al. 2015). Genetic background and mutation landscape of four commonly altered oncogenes in the clinic are shown in Table 2.1. Molecular heterogeneity between the eight CRC cell lines analysed, may partially explain differences among the anti-proliferative effects of 5-FU, IRI and OXA, in each of the eight CRC cell lines studied in this chapter.

2.2 Criteria for selection of a cell line for resistance studies

There are many drugs that are used to treat CRC patients (see Chapter 1, Fig. 1.2). Usually, combinations of several of these drugs are used in order to enhance the effects of the chemotherapy. Most of these chemotherapies are based on the combination of the three most used drugs in CRC patients that are: IRI, 5-FU, and OXA (Kufe, Pollock et al. 2003, Ismaili 2011) (Fig. 2.1) and their chemical structures are shown below (Bandrés, Zárate et al. 2007).

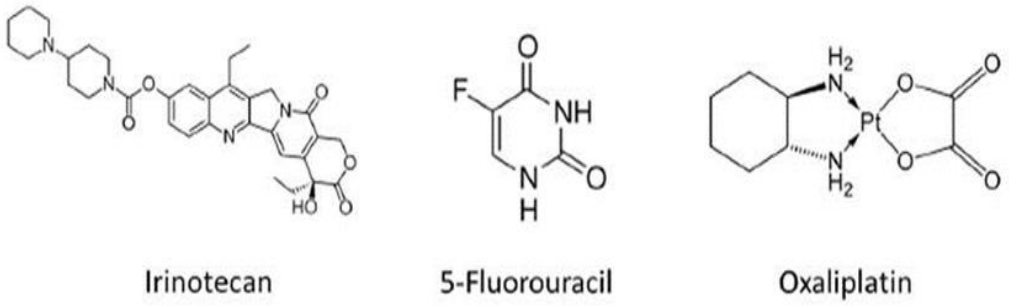

Figure 2.1: Chemical structures of three conventional drugs used in CRC chemotherapy.

Whilst the principal mechanisms of resistance for these three conventional drugs are known and explained in three dedicated chapters for each one of the drugs studied: 5-FU, IRI and OXA (see Chapters 3-5), there is still a lack of knowledge on how CRC tumours develop resistance to chemotherapy as is observed, in part, from the high mortality rate of the disease in advanced CRC patients (Hammond, Swaika et al. 2016).

To make possible the measurement and comparisons of the anti-proliferative effect of three different drugs on eight different CRC cell lines, characterization of growth curves rate during cell culture were carried out for all CRC cell lines used.

Initially, cell culture requires to authenticate that the eight CRC used in the present thesis show the specific features expected from the database online sources as National Center for Biotechnology Information (NCBI), The American Type Culture Collection (ATCC), and The International Cell Line Authentication Committee (ICLAC). A summary background information on the

eight CRC cell lines used is displayed in Table 2.1. This step is crucial to avoid misidentification and cross-contamination problems. To avoid common mistakes during cells passaging in cell culture, each time a new flask or tube with cells was used it was labelled with three marks: cell line name, date and researcher initials.

Cell Line	Disease		Cell subtype Sadanandam *et al.* classification	Age / Gender	*TP53* Status	MSI Status	*KRAS* AA change	*BRAF* AA change	*PIK3CA* AA change
COLO 205	Stage IV	CR adenocarcinoma	Goblet	70 years, Male	WT	MSS	WT	p.V600E	WT
DLD-1	Stage III	CR adenocarcinoma	Stem	45 years, Male	p.S241F	MSI	p.G13D	WT	p.E545K
HT 29	-	CR adenocarcinoma	Goblet	44 years, Female	p.R273H	MSS	WT	p.V600E	WT
SW-620	Stage III	CR adenocarcinoma	Transit amplifying	51 years, Female	p.R273H	MSS	p.G12V	WT	WT
LS 174T	Stage II	CR adenocarcinoma	Goblet	58 years, Female	WT	MSI	p.G12D	WT	p.H1047R
KM 12	Stage II	CR adenocarcinoma	Goblet	-	-	MSI	WT	WT	WT
HCC 2998	-	CR adenocarcinoma	Goblet	-	p.R213F	MSS	p.A146T	WT	WT
HCT 116	-	CR adenocarcinoma	Stem	48 years, Male	WT	MSI	p.G13D	WT	p.H1047R

Table 2.1: Background information about eight CRC cell lines used in MTT assays. Abbreviations: MSI microsatellite instability, MSS microsatellite stable (Woerner, Yuan et al. 2010, Ahmed, Eide et al. 2013). WT wild type, AA amino acid, - Unavailable data

2.3 Material and Methods

Selection of CRC cell lines to be used in development of cancer resistant sublines by continuous exposure to 5-FU, IRI, and OXA requires different material and methodologies, as described below.

2.3.1 Drugs

IRI and OXA were purchased from Selleckchem (Houston, USA) and stored at -20°C, whilst 5-FU was obtained from Sigma-Aldrich (Poole, UK) and stored at room temperature (RT). For cellular analyses, compounds were prepared as stock solutions in dimethyl sulfoxide (DMSO) obtained from Sigma-Aldrich (Poole, UK). Approximately 3 mg of IRI, 3 mg of 5-FU and 4 mg of OXA were accurately weighed out and dissolved in 100 µl of DMSO to give a stock solution (Table 2.2). After ensuring compounds were completely dissolved in the DMSO by vortexing, they were aliquoted into 50 µl aliquots which were stored at -20°C until use. Then, aliquots were used to make up 1 ml and or 100 µl of a 3 mM DMSO solutions to be used in Thiazolyl Blue Tetrazolium Bromide (MTT) cell proliferation or cytotoxicity assays, or for developing drug-resistant cell lines. MTT was obtained from Sigma-Aldrich (Poole, UK). 1000 µl of 300 µM solutions of all compounds were made up and are shown in Table 2.2. Dilutions were vortexed thoroughly to ensure that the compound was fully dissolved. Later, 50 µl of each solution were aliquoted into labelled sterile 0.5 ml Eppendorf tubes that were stored at -20°C until be used during MTT assay. For MTT working solutions, 100 mg of MTT stock was dissolved in 20 ml of Maxima water, passed through a 0.2 µm filter and stored at 4°C.

Compound name	Mol. Wt.	Amount (mg)	x mM	DMSO used (DMSO concentration)
5-FU	130.08	3.42	26.29	100 µl (DMSO 0.114%)
IRI	586.68	2.98	50.79	100 µl (DMSO 0.006%)
OXA	397.29	4.44	111.76	100 µl (DMSO 0.003%)

Table 2.2: Initial stock solutions of the drugs used during MTT assays.

2.3.2 Cell lines

All human colon adenocarcinoma cell lines COLO 205, DLD-1, HT 29, SW-620, LS 174T, KM 12, HCC 2998, and HCT 116 were provided by European Collection of Cell Cultures (Salisbury, UK) and American Type Culture Collection (ATCC) (Manassas, Virginia, USA) (see Table 2.1 for details of the cell lines).

2.3.3 Cell culture media

The cells were maintained in RPMI 1640 culture medium supplemented with 10% (v/v) fetal bovine serum (FBS), 1 mmol/L sodium pyruvate, 2 mmol/L of L-glutamine and incubated at 37°C in 5% CO_2. Dulbecco's phosphate-buffered saline (PBS) obtained from Severn Biotech Ltd. (Kidderminster, UK) was used for washing during passaging. All products were provided from Sigma-Aldrich (Poole, UK).

2.3.4 Characterisation of cell growth and cell seeding density optimisation by MTT assay

Growth curve profiles of eight CRC cell lines studied were plotted. Different cell lines have different doubling times, and they were calculated to maintain cell lines between 30-85% confluency in logarithmic (Log) phase under drug exposure conditions for as long as possible during 4 days of treatment. Growth curve profiles were determined using the 3-(4,5-Dimethylthiazol-2-yl)-2,5-Diphenyltetrazolium Bromide (MTT) salt which is soluble in water and it was added to each assay well (Barderas, Mendes et al. 2013). After an incubation time of 4 h, MTT was reduced into formazan by mitochondrial dehydrogenase enzyme that is found activated only in living cells. Formazan is an insoluble crystal with a purple colour. Formazan can be solubilized in DMSO and quantified by spectrophotometric reader using the absorbance of its purple coloured solution (van Meerloo, Kaspers et al. 2011, Barderas, Mendes et al. 2013) at 540nm wavelength. So, the reaction of dehydrogenase enzyme reflects the number of viable cells and it can be used as measure of the number of viable cells present and to test the anti-proliferative effect of a drug.

Serial dilutions of each one of the eight different CRC cell lines were prepared and tested using the MTT assay during 6 days. Cells were seeded at nine different initial seeding density concentrations into 96-well plates containing 200 µl of complete RPMI 1640 medium and placed under standard incubator conditions. Plates were removed for analysis of cell growth at different times over the 6 days incubation period. Supernatants were removed and 200 µl of the MTT solution [2 ml MTT stock solution to 18 ml of complete RPMI 1640 medium] were added to each well. Plates were incubated at RT, 5% CO_2, for 4 h. Finally, MTT supernatant was removed and 150 µl of the DMSO was added to solubilise the crystals of formazan. Absorbance values for the resulting solutions were read at 540 nm on a Thermo Scientific Multiskan EX from Thermo Scientific (Loughborough, UK). Graphs were plotting using GraphPad Prism 5.0 (GraphPad Software, Inc., San Diego, USA) and Microsoft Office Excel Ver. 3. 2013 (Chicago, USA).

2.3.5 CRC cell lines chemosensitivity panel using the MTT assay

To characterise the anti-proliferative effect of 5-FU, OXA, and IRI compounds commonly used in the clinic for treatment of CRC in a panel of eight CRC cell lines, MTT assays were carried out. *In vitro* evaluation of the response profile of eight human CRC cell lines to these three chemotherapeutic agents were established for 96 h of continuous exposure. For an initial seeding concentration of $1x10^4$ cells/ml in a cell doubling time rate about 20-24 h, 96 h is a time long enough to duplicate the cells population 3-fold and achieve the Log phase in the culture at the 4^{th} day. Cell lines used were DLD-1; HT 29; SW-620; COLO 205; LS 174T; KM 12; HCC 2998 and HCT 116.

Based on growth curve profile results to reach Log phase at day 4^{th}, adjusted cell seeding density optimised concentrations in 180 µl of growth medium suspension were inoculated into each test well of a 96-well plate and incubated overnight (O/N) at 37 °C (Table 2.3). Cell attachment occurs within 24 h of initial seeding, and so the drug was added after 24 h. A range of drug concentrations was made up in cell culture medium and 20 µl of test chemotherapeutic agents and control solutions were added into each well. Additionally, the maximum final

DMSO concentration during drug dilution was not greater than 0.25% solution that causes toxicity to the cells (Barderas, Mendes et al. 2013).

Following addition of drugs, the plates were incubated for a further 96 h under standard conditions and then analysed by MTT as described in the previous section (Fig. 2.2).

The chemosensitivity of each cell line to each drug was measured by determining three different inhibitory concentrations (IC_s). The IC_{50}, IC_{75}, IC_{90}, values are defined as the drug concentration that inhibits cell growth by 50%, 75%, and 90% compared with the growth of untreated control cells, respectively. So, percentages of survival of drug-treated cells were evaluated using absorbance values of untreated cells as control and absorbance of treated cells using the following equation:

$$\%\ Survival = \frac{\bar{X}\ Treated\ absorbance - \bar{X}\ Blank\ absorbance}{\bar{X}\ Control\ absorbance - \bar{X}\ Blank\ absorbance} * 100$$

Three independent experiments of 4 replicates were carried out for each drug concentration, with each one of the eight CRC cell lines studied. Graph plotting and IC_s were calculated using GraphPad Prism 5.0 (GraphPad Software, Inc., San Diego, CA). In all tests, $p<0.05$ was considered to indicate a statistically significant difference.

	Blank	0.1 µM	1 µM	3 µM	10 µM	30 µM	0.1 µM	1 µM	3 µM	10 µM	30 µM	Control
	1	**2**	**3**	**4**	**5**	**6**	**7**	**8**	**9**	**10**	**11**	**12**
A		#1	#1	#1	#1	#1	-	-	-	-	-	
B		#1	#1	#1	#1	#1	-	-	-	-	-	
C		#1	#1	#1	#1	#1	-	-	-	-	-	
D		#1	#1	#1	#1	#1	-	-	-	-	-	
E		#2	#2	#2	#2	#2	#3	#3	#3	#3	#3	
F		#2	#2	#2	#2	#2	#3	#3	#3	#3	#3	
G		#2	#2	#2	#2	#2	#3	#3	#3	#3	#3	
H		#2	#2	#2	#2	#2	#3	#3	#3	#3	#3	

Table 2.3: Dimensional scheme of the 96-well plates. Distribution of drugs concentrations, control and blanks used during the evaluation of CRC cell lines to IRI (#1), OXA (#2), and 5-FU (#3) using MTT assay.

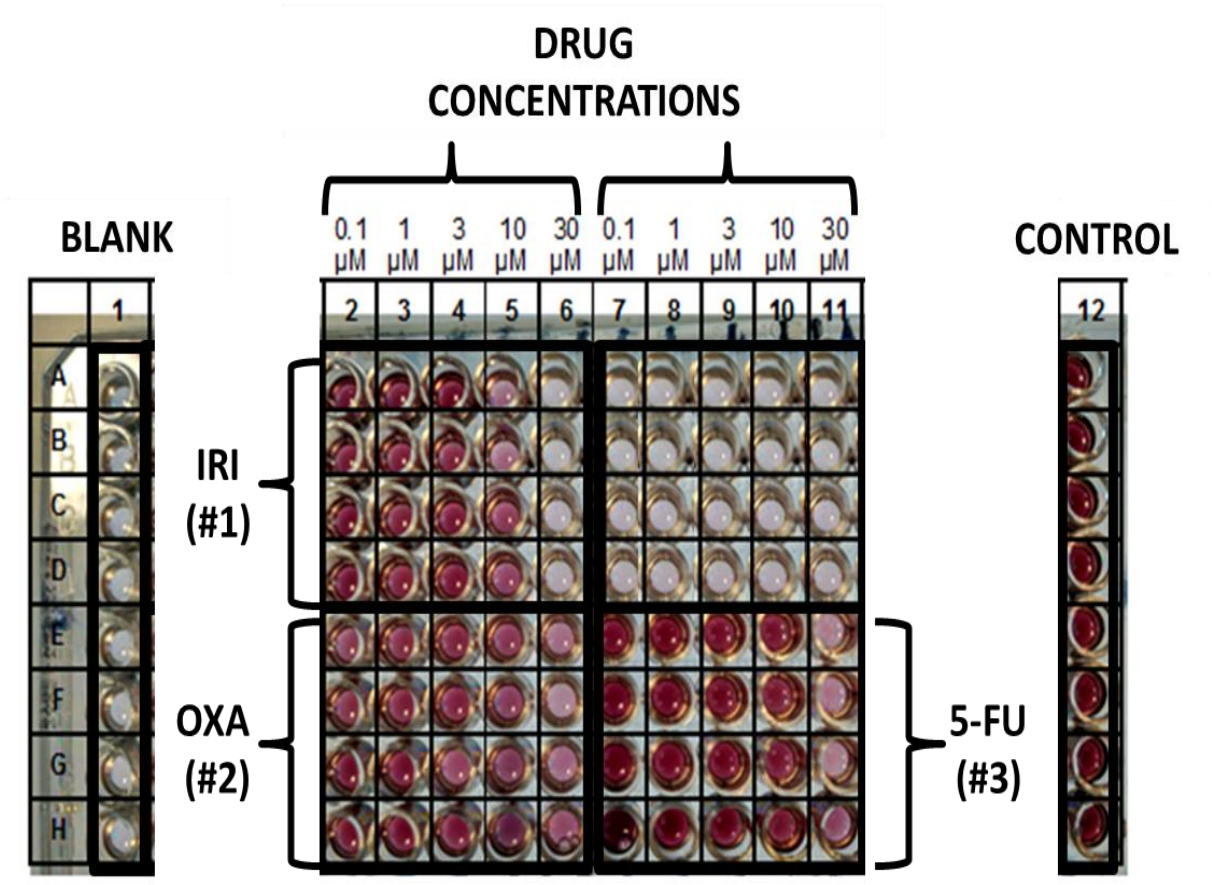

Figure 2.2: Fragmented picture of a 96-well plate. Example of MTT assay used for evaluation of the chemosensitivity to IRI (#1), OXA (#2), and 5-FU (#3) by in DLD-1 cell line, as it has been described in Table 2.3.

2.3.6 Statistical analysis of MTT assay

Effect of each drug on the viability of CRC cell lines was measured by MTT assay. Cells in Log phase were exposed to indicated concentrations of different drugs and after 4 days cell survival was determined by MTT assay. Results are expressed as the means ± SD of 3 independently repeated experiments. Statistical analyses Student's t-test: * $p \leq 0.05$, ** $p \leq 0.01$, *** $p \leq 0.001$, **** $p \leq 0.0001$ was selected to compare the sensitivity for IC_{50} value among sensitive-parent cell line and resistant subline. If necessary, data were logarithmically converted into a normal distribution of variables to remove heterogeneity of variance before analysis.

2.4 Results

2.4.1 Cell seeding density optimisation by MTT assay

To be confident with cell density concentration seeded, linear regression growth curves for day 0 for the eight CRC cell lines studied were done. A highly significant linear relationship between number of cells seeded and MTT absorbance signal is clearly seen for all cell lines used during Day 0 (Fig. 2.3). After confirmation of MTT values for initial cell density concentrations, growth curves profiles allow choosing the best cell concentration to reach the Log phase at day 4^{th} for chemosensitivity assays using MTT (Fig. 2.4).

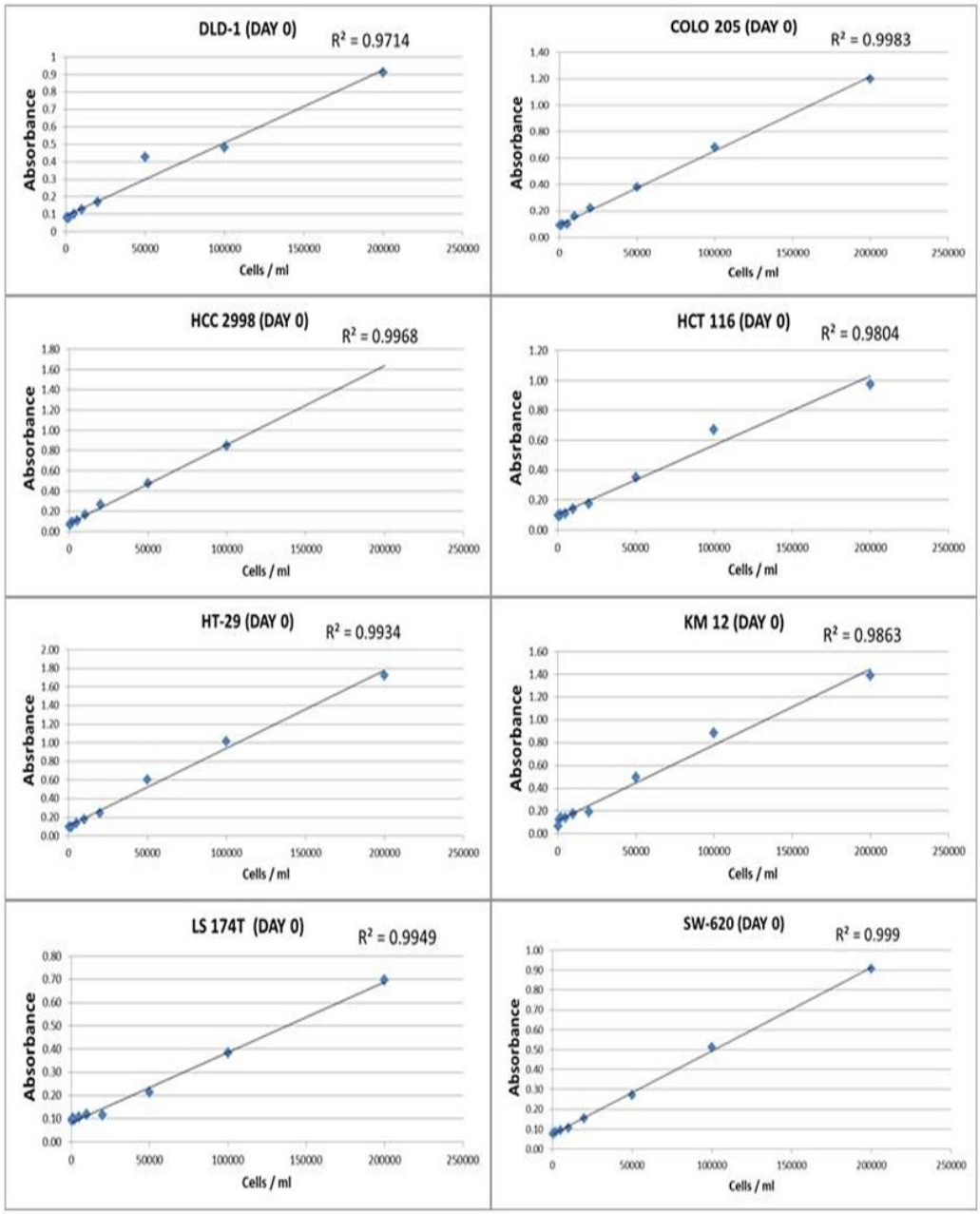

Figure 2.3: Linear regression growth curves for day 0 for the eight CRC cell lines studied. A highly significant linear relationship between number of cells seeded and MTT absorbance signal is clearly seen for all cell lines used during Day 0.

Based on growth curve profile results to reach Log phase at day 4th, (Figure 2.4) adjusted cell seeding density optimised concentrations of 1x10^4 cells/ml (DLD-1, HT 29, SW-620, LS 174T), 2x10^4 cells/ml (COLO 205, KM 12, HCC 2998) and 5x10^3 cells/ml (HCT 116) were used as optimal cell seeded concentrations during chemosensitivity curve profiles by MTT assay.

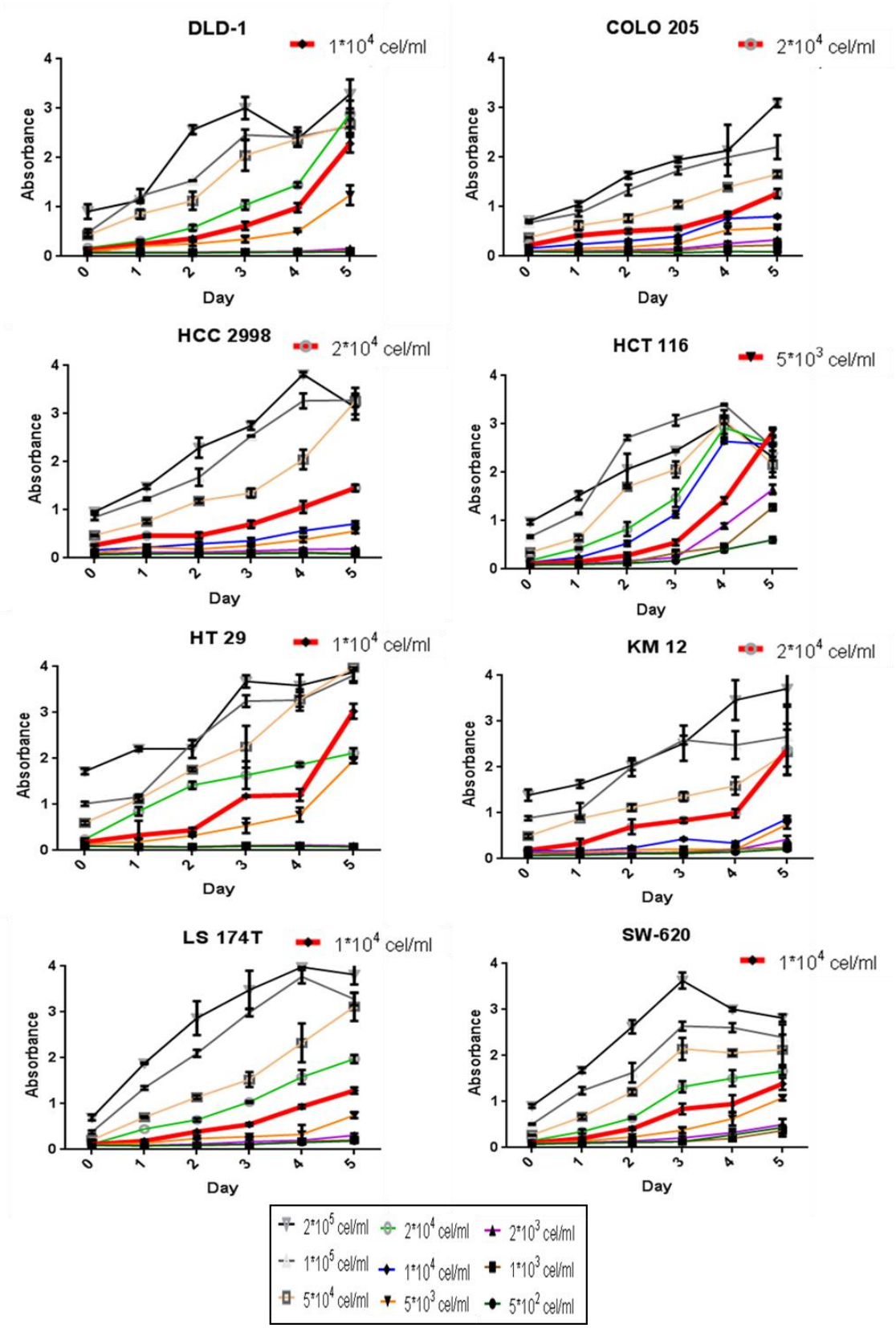

Figure 2.4: MTT Growth curve profiles for eight CRC cell lines. Coloured in red, optimal cell seeded concentrations for each CRC cell line to reach Log phase at day 4th and that was used during chemosensitivity MTT assays.

2.4.2 Chemosensitivity curve profile of eight CRC cell lines

Three screening panels to study cytotoxicity effect of 5-FU, IRI and OXA on eight different CRC cell lines were done. To make this possible, the eight CRC cell lines were evaluated using five different drug exposure concentrations. After four days under drugs conditions, percentage of cell survival was measured by MTT assay (Fig. 2.5). Results were expressed in terms of survival and IC_{50}, IC_{75}, and IC_{90} values. The IC_s values were obtained by straight-line projection from y-axis coordinates where cell survival was 50%, 25% and 10% to the x-axis. Interpolation with x-axis shows the respective concentrations of drug to achieve IC_{50}, $IC_{75,}$ and IC_{90} values, respectively, for each CRC cell line.

2.4.2.1 Chemosensitivity curve profile to 5-FU

Calculation of IC_s values of the eight CRC cancer cell lines to 5-FU after 96 h exposure to the 5-FU compound by growth inhibition assay.

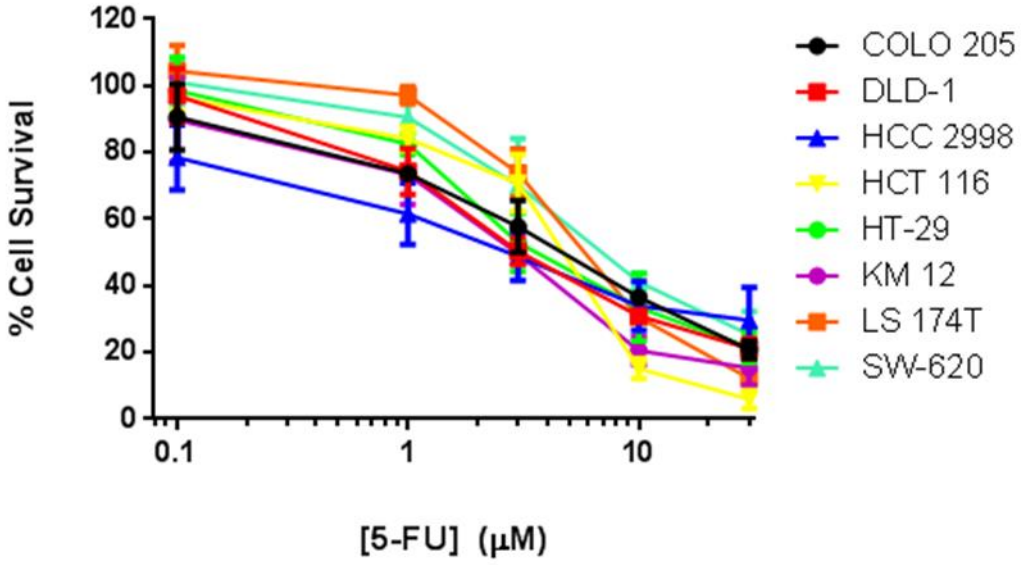

Figure 2.5: Graphs of Growth Inhibition Assays Results for eight CRC cell lines to 5-FU. All values are averages of at least four independent experiments performed in triplicate.

Cell line	5-FU		
	IC_{50} (µM)	IC_{75} (µM)	IC_{90} (µM)
COLO 205	4.6 ± 1.0	22.39 ± 0.5	>30
DLD-1	3.7 ± 0.5	15.0 ± 3.5	>30
HCC 2998	2.66 ± 0.5	> 30.0	>30
HCT 116	4.78 ± 1.2	7.94 ± 0.1	14.13 ± 0.1
HT 29	2.99 ± 1.1	18.62 ± 0.7	>30
KM 12	2.79 ± 0.2	7.59 ± 0.1	30 ± 0.1
LS 174T	5.62 ± 0.2	12.88 ± 1.0	30 ± 0.2
SW-620	6.37 ± 1.1	30.0 ± 1.1	>30

Table 2.4: Results for ICs values of eight CRC cell lines to 5-FU. Means ± SD are summarized. The highest sensitivity to 5-FU is showed in red colour [5-FU] ≤ 5 µM; intermediate sensitivity to 5-FU is showed in grey colour 5 µM < [5-FU] < 30 µM and lowest sensitivity to 5-FU is showed in green colour [5-FU] ≥ 30 µM.

2.4.2.2 Chemosensitivity curve profile to IRI

Calculation of IC_s values of the eight CRC cancer cell lines to IRI after 96 h exposure to the compound by growth inhibition assay is shown in Figure 2.6 below. Additionally, results were summarised in Table 2.5.

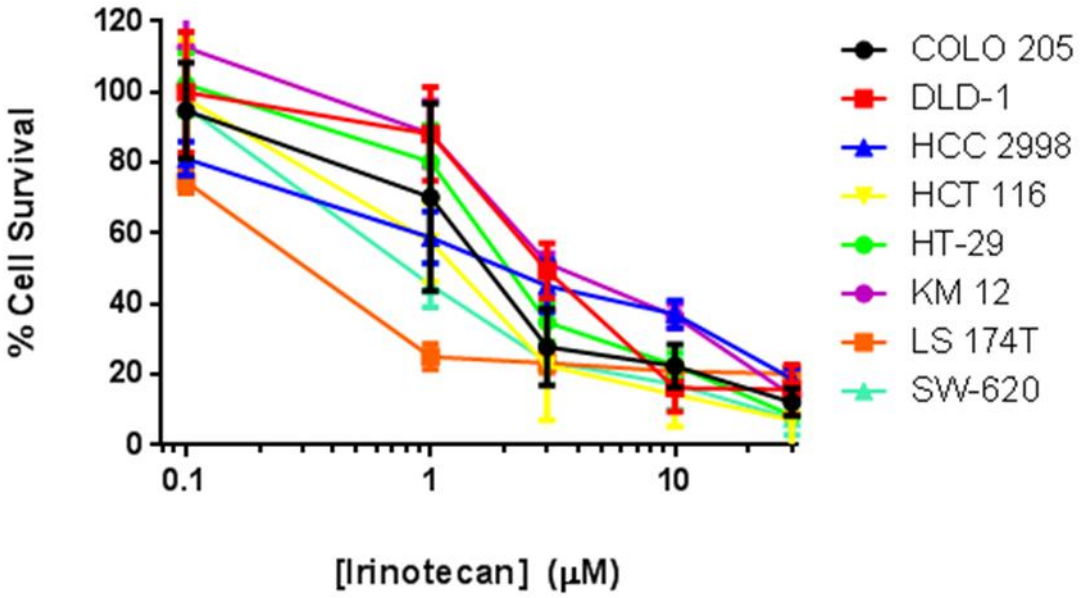

Figure 2.6: Graphs of Growth Inhibition Assays Results for eight CRC cell lines to IRI. All values are averages of at least four independent experiments performed in triplicate.

Cell line	IRI		
	IC_{50} (µM)	IC_{75} (µM)	IC_{90} (µM)
COLO 205	1.79 ± 0.7	2.99 ± 0.8	30 ± 0.0
DLD-1	3.3 ± 0.7	8.0 ± 0.0	30 ± 0.0
HCC 2998	2.07 ± 0.2	21.88 ± 0.2	>30
HCT 116	1.28 ± 0.5	2.79 ± 0.0	15.85 ± 0.2
HT 29	2.06 ± 0.1	6.89 ± 1.1	25.70 ± 2.6
KM 12	3.37 ± 0.0	16.60 ± 0.0	30 ± 0.1
LS 174T	0.32 ± 0.0	1 ± 0.5	>30
SW-620	0.78 ± 0.1	2.18 ± 0.2	26.3 ± 4

Table 2.5: Results for ICs values of eight CRC cell lines to IRI. Means ± SD are shown. The highest sensitivity to IRI is showed in red colour [IRI] ≤ 5 µM; intermediate sensitivity to IRI is showed in grey colour 5 µM < [IRI] < 30 µM and lowest sensitivity to IRI is showed in green colour [IRI] ≥ 30 µM.

2.4.2.3 Chemosensitivity curve profile to OXA

Calculation of IC_s values of the eight CRC cancer cell lines to OXA after 96 h exposure to the compound by growth inhibition assay. The calculation of IC_s values by interpolation was complicated, specifically for HCC 2998, HCT 116

and LS 174T to OXA due to the high anti-proliferative effect of this drug on these cell lines for the initial range of concentration (0.1 µM – 30 µM) (Fig. 2.7a). Hence, the growth inhibition assay was repeated using a lower range concentration of OXA, specifically among 0.001 µM – 10 µM range of concentration, instead of 0.1 µM – 30 µM (Fig. 2.7b). Results were summarised in Table 2.6.

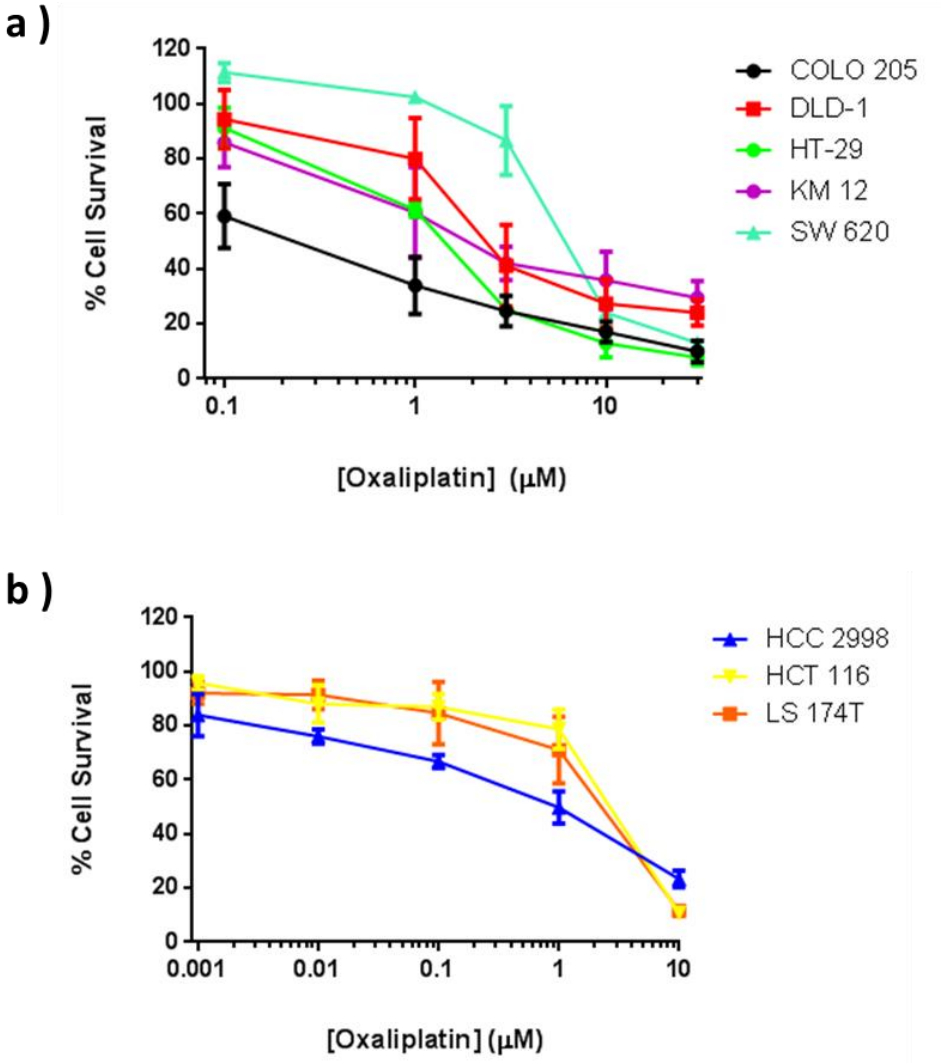

Figure 2.7: Graphs of Growth Inhibition Assays Results for eight CRC cell lines to OXA. (a) Initially, the range concentration used of OXA was from 0.1 µM to 30 µM. (b) New OXA doses from 0.001 to 10 µM were diluted to achieve the IC_{50}, IC_{75} and IC_{90} values of HCC 2998, HCT 116 and LS 174T. All values are averages of at least four independent experiments performed in triplicate.

Cell line	OXA		
	IC_{50} (µM)	IC_{75} (µM)	IC_{90} (µM)
COLO 205	0.22 ± 0.1	2.01 ± 0.5	22.88 ± 0.0
DLD-1	2.7 ± 0.3	28.0 ± 1.7	>30
HCC 2998	0.72 ± 0.4	7.3 ± 1.0	>10
HCT 116	2.1± 0.2	5.57 ± 0.1	10 ± 0.0
HT 29	1.46 ± 0.2	3.02 ± 0.7	16.98 ± 0.1
KM 12	1.79 ± 0.6	30 ± 0.0	>30
LS 174T	2.4 ± 0.1	5.72 ± 0.1	10 ± 0.0
SW-620	6.68 ± 0.2	9.62 ± 0.8	30 ± 0.0

Table 2.6: Results for ICs values of eight CRC cell lines to OXA. Means ± SD are displayed. The highest sensitivity to OXA is showed in red colour [OXA] ≤ 5 µM; intermediate sensitivity to OXA is showed in grey colour 5 µM < [OXA] < 30 µM and lowest sensitivity to OXA is showed in green colour [OXA] ≥ 30 µM.

2.5 Discussion

2.5.1 Discussion of CRC cell lines growth and cell seeding density optimisation by MTT assay

Evaluation of linearity for formazan crystal formation for the eight CRC cell lines was carried out. At day 0 each specific cell line shows a linear relationship between cell density and absorbance and hence the assay can be used with confidence with each specific cell line (Fig. 2.3). A good linear relationship was seen with R^2 values greater than 0.95 for all cell lines tested (Fig. 2.3).

All growth curves obtained from eight CRC cell lines by MTT assay shown three clearly differentiated phases during cells growth. First phase known as "Lag" phase where cells start recovering from the passaging effect. A second phase, the "Log" phase were cells growth exponentially and a final "Plateau" phase where the confluence of cells limit the expansion of cells within the flask.

All CRC cell lines used grew attached to the flask surface forming monolayer cultures. Except for COLO 205 cell line, as it was expected from ATCC database source. COLO 205 cell line grew to form aggregates in suspension with clusters of rounded cells floating in the medium and only a few groups of cells grew weakly attached to the plastic surface from the flask.

MTT readings for Day 1, Day 2, Day 3, Day 4 and Day 5 were carried out. The eight CRC cells showed similar growth rates achieving 1 unit of absorbance during the fourth day when the initial concentration of cells seeded was close to $1x10^4$cells/ml in each well. Despite the similarities in the growing rates, three different subgroups were seen: firstly, HCT 116 showed the fastest growth rate, following by DLD-1, HT 29, LS 174T, SW-620 and finally, COLO 205, HCC 2998, KM 12, which showed the slowest growth rates (Fig. 2.4). Hence, different optimal initial cell seeded concentrations to achieve a 1.000 unit on absorbance during optical density reading at 540nm wavelength after 4 days of growing were selected to be used during cellular chemosensitivity assays (Fig. 2.4).

2.5.2 Discussion of chemosensitivity curve profiles

The aim of this project is to clarify the knowledge about unknown molecular mechanisms involved in CRC resistance to conventional chemotherapy. To achieve this aim, the establishment of drug resistant CRC sublines is required. New drug resistant sublines can be used both *in vitro* and *in vivo* for screening novel therapeutics and to identify predictive biomarkers of drug response in CRC. Initially, a chemosensitivity screen was carried out using a panel of eight CRC cell lines.

Evaluation of the response curve profile of eight CRC cell lines to three conventional chemotherapeutic drugs showed appreciable differences both among the eight cell lines studied and among the three drugs used. However, there are some considerations that must be borne in mind to interpret the information related to IC_{50}, IC_{75}, IC_{90}. Researching cancer by *in vitro* cell culture experiments lets researcher control experimental factors. These factors included physicochemical microenvironment elements in the culture such as pH, temperature, humidity, oxygen levels, osmolarity, and nutrients concentration. Additionally, homogeneity of cells is easily maintained and cells can be stored in liquid nitrogen with cryopreservation medium such as DMSO. Hence, cell samples with both different number of passages and different fold-change in resistance may be stored to be used in future studies during the development of resistant sublines. Nevertheless, technical factors such as cell culture conditions, number of cell passages, solvent used to make up drug dilutions may interfere with the final experiment results.

Different results in values for IC_s among drugs in the same cell line could depend on the mechanism of action of the drug. For example, OXA is a platinum drug that damages DNA by the induction of DNA lesions, forming interstrand cross-links with the binding of two guanine, or less frequently, a guanine-adenine base pair as it will be described in Chapter 5, section 5.1.1. Consequently, a cytotoxic effect occurs and inhibition of the proliferation of cancer cells happens (Alcindor and Beauger 2011). The prevention of cell proliferation has a so strong effect that can be lethal for all kind of tumour cells,

so the high sensitivity of the eight cell lines to this drug could be due to the OXA mechanism of action by binding to DNA, leading to guanine-guanine or adenine-guanine intra-strand crosslinks. Its consequence is blocking DNA synthesis and escaping recognition by the mismatch repair enzyme complex. This mechanism of action could be involved in chemotherapy side effect as healthy human cells could die by OXA cytotoxic effect too (Rabik and Dolan 2007).

The epigenetic and genetic background of a cell line may play key roles in chemosensitivity and resistance to different drugs. Drug chemosensitivity may be affected by specific gene mutations that can confer resistance to mutated cell lines. Experts disagree regarding a specific methodology to use for CRC cell line classification (Ahmed, Eide et al. 2013, Sadanandam, Lyssiotis et al. 2013). There exist some classifications based on genetic origin, MSI, CpG island methylator phenotype (CIMP) and hotspots mutations in oncogenes. Concerning oncogenes and genes associated with chemoresistance a key protein is p53. *TP53* gene is the most frequently mutated gene in CRC cells this issue is observed in Table 2.1. Among the eight CRC cell lines studied in the present project: HCT 116 and LS 174T are known to present *TP53* wild type and a higher sensitive to OXA, while DLD-1, HT 29 and SW-620 have mutations at *TP53* gene and they are less sensitive to OXA (Table 2.1) (Martinez-Cardús, Martinez-Balibrea et al. 2009). This difference in response can be due to the main function of TP53, which induces apoptosis when DNA damage caused by OXA cannot be repair. DLD-1, HT 29 and SW-620 cell lines would avoid activation of pro-apoptotic pathways by *TP53*. Other frequently mutated genes in CRC are *KRAS*, *PIK3CA*, *BRAF*, and *PTEN* (Ahmed, Eide et al. 2013).

Different molecular and genomic backgrounds of the eight CRC cell lines studied could be involved in the chemosensitivity response to the drugs. For example, DLD-1, HCT 116 and LS 174T cell lines showed some of the lowest sensitivities to 5-FU (Table 2.4), although all CRC cell lines showed the lowest sensitivity to this drug, it is known that these three cell lines show the MSI phenotype (Ahmed, Eide et al. 2013) (see Table 2.1) and consequently, their

DNA mismatch repair system is not working normally. MSI is presented in 15% of CRC tumours and it has been related to 5-FU resistance in CRC (Sinicrope and Sargent 2012). So, it could be interesting to know if the low sensitivity of DLD-1, HCT 116 and LS 174T to 5-FU is due to the failure in DNA mismatch repair (MMR) system. Moreover, SW-620, HCT 116 and LS 174T have a low sensitivity to 5-FU, but they present a high sensitivity to IRI and OXA drugs. Previously published results of drug sensitivity in CRC, showed that COLO 205 was more sensitive to 5-FU than DLD-1 or HCT 116 (Jung, Jeung et al. 2007). However, in the present study, it is seen that COLO 205 shows lower sensitivity to 5-FU than DLD-1 and HCT 116 (Table 2.4). Differences with previous results may be the result of differences in cell culture conditions such as exposure times, cell concentrations and drug dose used. Result shown in this thesis makes sense if it is kept in mind that COLO 205 was isolated in 1975 by T.U. Semple, *et al*. from a patient who had been treated with 5-FU for 4-6 weeks (Semple, Quinn et al. 1978, Paillas, Causse et al. 2012). Cells of the patient were exposed to 5-FU during the chemotherapeutic period. So, tumour cells were growing in a 5-FU environment over treatment time. It is possible that during this time, patient's COLO 205 CRC cells started to develop some mechanisms of resistance to the 5-FU drug that may be noticed in the final patient-derived cell line. So, it is important to know the background of both cell line and patient as far as possible, in order to keep in mind how different variations can affect to the experimental design.

Another fact that shows the importance of knowledge of the nature of the cell line used in the experiment can be extracted from HCT 116 MTT results. During growth curves profiles assays, HCT 116 showed the highest growth in normal conditions (Fig. 2.4). Besides, HCT 116 cell line shows the highest sensitivity to 5-FU and OXA, among the eight CRC cell lines studied (Table 2.4) (Table 2.6). Both agents damage DNA, affecting stabilisation and activation of p53 that can activate genes involved in apoptosis pathways. In this way, the more a cell proliferates, the more its DNA suffers from a drug effect. Studies have shown that cells during S-phase are 1000-fold more susceptible to camptothecins as

OXA (Shah and Schwartz 2001). Hence, the time taken for cells to complete a cycle can be an important factor to keep in mind.

Finally, a possible toxicity effect of DMSO was studied. A 0.4% concentration of DMSO was necessary for making up 1000 µl of a 300 µM solution for IRI. No cytotoxic effect of DMSO (0.4% concentration) was found.

Finally, based on chemosensitivity curve profiles of the eight CRC cell lines and discussion here displayed, cell lines DLD-1, KM 12 and HT 29 were selected to generate resistant sublines to 5-FU, OXA and IRI. These three cell lines showed the lowest sensitivity among all three drugs, hence development of high drug resistance phenotypes from these three parent cell lines may be possible. They also showed the best correlation in increasing of cell survival with increasing drug concentration (IC_{50}, IC_{75}, and IC_{90}) (Table 2.4-6). Hence, these three cell lines are expected to file a progressive response within the ten months that cells are expected to be growing under drug conditions.

- Chapter three -

Identification of new mechanisms of resistance to 5-FU

3 Identification of new mechanisms of resistance to 5-FU

3.1 Introduction

5-FU is a heterocyclic aromatic organic compound analogue of uracil, which is used before or after surgery at any stage of CRC patients (Longey 2003). The structural study of 5-FU showed that this drug crystallises adopting a hydrogen-bonded sheet structure with four molecules in its asymmetric unit (Hulme, Price et al. 2005). The specific structure of the 5-FU, which is similar to the uracil, makes possible the incorporation of 5-FU into DNA and RNA during nucleoside metabolism and converges into cytotoxicity and cell death (Zhang, Yin et al. 2008).

3.1.1 Mechanisms of action of 5-FU

5-FU is converted by two main different routes into several active metabolites in mammalian cells. A scheme of mechanism of action of 5-FU is shown below.

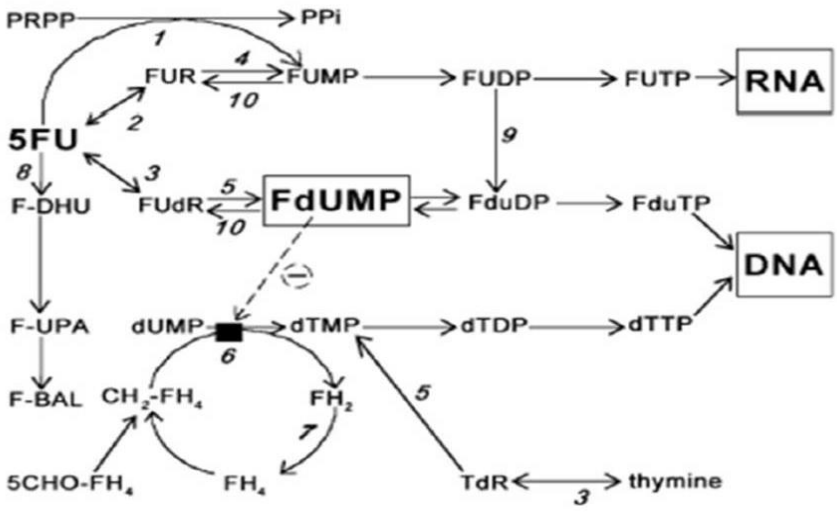

Figure 3.1: Metabolic conversions and mechanisms of action of 5-FU. The enzymes involved in these reactions are: (1) orotate phosphoribosyltransferase (OPRT); (2) uridine phosphorylase (UP); (3) thymidine phosphorylase (TP); (4) uridine kinase (UK); (5) thymidine kinase 1 (TK1); (6) thymidylate synthase (TS); (7) dihydrofolate reductase; (8) dihydropyrimidine dehydrogenase (DPD); (9) ribonucleotide reductase (RR); (10) 5'-nucleotidases and phosphatases. Metabolic pathways are depicted as solid lines. The inhibition of TS by FdUMP is depicted as a broken line with a minus sign (Peters, Backus et al. 2002).

The main activation route for 5-FU activation is the conversion in fluorodeoxyuridine (FUdR), which is then phosphorylated to fluorodeoxyuridine monophosphate (FdUMP) by thymidine kinase (TK1) (Fig. 3.1) (Peters, Backus et al. 2002) or converted to FdUDP by ribonucleotide reductase (RR). A second alternative route is the conversion of FdUMP directly from 5-FU by uridine phosphorylase (UP) and uridine kinase (UK). The stable 5-FdUMP forms a complex by its union with the enzyme thymidylate synthase (TS) (Fig. 3.1) (Peters, Backus et al. 2002). Consequently, the inhibition of deoxythymidine monophosphate (dTMP) production occurs. dTMP is an essential element for DNA repair and replication processes. So, a decreasing of dTMP level causes cytotoxicity and cell death (Fig. 3.1) (Peters, Backus et al. 2002, Longey 2003). Alternatively, dihydropyrimidine dehydrogenase (DPD) mediates conversion of 5-FU to dihydrofluorouracil (DHFU) which is a rate-limiting step of 5-FU catabolism in normal and tumour cells.

From Figure 3.1, it may be interpreted that some anticancer drugs such as 5-FU require metabolic activation, and thus cancer cells can develop resistance through decreased drug activation. Additionally, active metabolites of drugs which target multiple enzymes and that cause damage to multiple molecular pathways may be more useful to carry out the cytotoxic function. However, they may also be more susceptible to different mechanisms of resistance that can appear to decrease drug effects.

3.1.2 Known mechanisms of resistance to 5-FU

3.1.2.1 Mechanisms of resistance to 5-FU related to thymidylate synthase

One of the best known mechanisms of resistance to 5-FU is related to the TS enzyme. After binding of FdUMP to TS protein, a new stable complex is formed. The new stable ternary complex blocks access of dUMP to the nucleotide-binding site and inhibiting dTMP synthesis. So, an increase in the expression of TS can be by itself a potential mechanism of resistance to 5-FU. There exist multiple elements which can play a role in TS induction: target-associated resistance, pharmacokinetic resistance or decreased accumulation of activated metabolites (Peters, Backus et al. 2002).

It is unclear if the mRNA-mediated induction of TS occurs at the postranscriptional level. Nevertheless, it is known that TS mRNA-bound enzyme is an autoregulatory translation model and that ligand-bound enzyme is more stable than TS ligand-free enzyme (Forsthoefel, Peña et al. 2004). The binding of TS mRNA to the enzyme produces conformational changes, normally in the C-terminal domain in the TS molecule. These changes increase the stabilisation and half-life of the enzyme. An increase in TS levels could affect the dose of the drug that is needed to induce cell death by TS inhibition and consequently, 5-FU may lose its effectiveness. Therefore, ligand binding can be a possible mechanism of resistance to TS-directed drugs (Forsthoefel, Peña et al. 2004).

Another possible mechanism of resistance related to TS could be TS over-expression, which has been found in CRC drug-resistant sublines, but not in the drug-sensitive parent lines (Wang, McLeod et al. 2007). TS overexpression could be described as an additional molecular mechanism responsible for 5-FU resistance, with an increase in TS expression resulting in an increase in the target protein of 5-FU. So, higher doses of the drug would be required to kill cells with overexpression of TS (Wang, McLeod et al. 2007).

Concerning 5-FU resistance mediated by TS, it is thought that interferon gamma (IFNγ) can act as a suppressor for TS resistance. IFNs are a glycoprotein family known as cytokines. IFNs are classified into three types: type I (IFNα, IFNβ), type II (IFNγ) and type III (IFNλ). They have different peptide sequences and contribute to the protective defences of the immune system (Rando 2006). During the activation of IFNγ, the mechanism of resistance to 5-FU mediated by TS induction can be avoided. New data suggest that the antitumour effect of 5-FU can be enhanced by IFNγ, due to its suppressing effect against the overexpression of TS. It was found that a combinational chemotherapy of 5-FU and IFNγ showed better results in stopping tumour growth than 5-FU alone (Chu, Zinn et al. 1990).

3.1.2.2 Mechanisms of resistance to 5-FU related to dihydropyrimidine dehydrogenase

Another mechanism involved in 5-FU resistance is due to an increase in dihydropyrimidine dehydrogenase (DPD) activity and the corresponding catabolism of 5-FU (Fig. 3.1). DPD metabolises the nucleobases uracil and thymine, but also some chemotherapy drugs such as 5-FU that are similar to these pyrimidines may be metabolised by DPD activity too (Zhang, Yin et al. 2008). Studies in mice using an HT 29 human CRC xenograft model have shown that following treatment of mice with 5-FU, the tumours that showed the highest levels of DPD expression had the fastest growth rate (Zeng, Yang et al. 2013). Therefore, a possible mechanism of resistance to 5-FU could be mediated by DPD upregulation (Zeng, Yang et al. 2013). In the same way, it has been shown that tumours with low DPD expression are sensitive to 5-FU and an increase in DPD mRNA expression is directly related to the resistance capacity of the cells against the 5-FU drug in CRC tumours (Milano, Etienne et al. 1999, Zeng, Yang et al. 2013).

3.1.2.3 Mechanisms of resistance to 5-FU related to microsatellite instability

Apart from TS and DPD, there are other proteins not directly involved in 5-FU metabolism that play a role in the resistance to 5-FU. For example, tumour cells with microsatellite instability (MSI) caused by defective MMR system have been related to less sensitivity to 5-FU *in vitro* in contrast to non-MSI cells, despite the availability to misincorporate similar amounts of 5-FU into the DNA of the cells (Tajima, Hess et al. 2004, Sinicrope and Sargent 2012). One of the proteins involved in 5-FU resistance via DNA repair, it is the protein Smug1 that repairs single- and double-stranded DNA by removing uracil from DNA and base excision. Qian An *et al.* (An, Robins et al. 2007) suggested that Smug1 could mediate a protective mechanism or cell survival strategy by excision of 5-FU that had previously been incorporated into DNA (Wang, McLeod et al. 2007). So, high Smug1 levels is a potential mechanism of resistance to 5-FU in tumours and Smug1 may be used as a predictive biomarker for poor 5-FU

response and it will allow selecting a better treatment for these patients (Wang, McLeod et al. 2007).

3.1.2.4 Mechanisms of resistance to 5-FU related to cell cycle

Moreover, cell cycle perturbations may be implicated in development of 5-FU resistance. The cell cycle can decelerate, delaying the incorporation of cytotoxic molecules into DNA (Moore, Houghton et al. 2011). This process is mediated by proteins such as CDK2, Cyclin D3 or Cyclin A that were reduced in both resistant H630 CRC cell lines and resistant T47D breast cancer cell lines (Guo, Goessl et al. 2008). These proteins are mediators of the delay in G1 and G1/S cell cycle phase and can affect DNA synthesis time (Guo, Goessl et al. 2008). The prevention of incorporation of 5-FU metabolites into DNA can give enough time to allow the cells to repair the misincorporated nucleotides (Moore, Houghton et al. 2011). Guo and his colleagues (Guo, Goessl et al. 2008) studied cell cycle alterations in colon and breast resistant sublines to 5-FU. They found that cells remained in G1 for a longer time, and they took more time to change between G1/S phases (Guo, Goessl et al. 2008).

3.1.2.5 Mechanisms of resistance to 5-FU related to ATP synthase

The main mechanism of action of 5-FU is inhibition of TS that reduces dTMP production causing changes at ATP/dTTP ratio levels which are required for DNA synthesis and repair, resulting in lethal DNA damage (Danenberg 1977).

At the ATP synthase level, down-regulation may lead to cellular events responsible for 5-FU resistance. A study carried out by Shin YK *et al*. (Shin, Yoo et al. 2005) showed that a decrease in the expression levels of the α subunit of mitochondrial F1F0-ATP synthase and the reduction in the expression of other ATP synthase complex subunits happened in resistant cell lines that showed to be less sensitive to 5-FU (Shin, Yoo et al. 2005). Consequently, when ATP synthase activity is decreased, the intracellular ATP content is reduced. Moreover, these results were confirmed using an inhibitor of the ATP synthase called oligomycin A, which inhibits suppression of cell proliferation mediated by 5-FU (Shin, Yoo et al. 2005).

3.1.2.6 Mechanisms of resistance to 5-FU related to reactive oxygen species

Finally, another mechanism of resistance to 5-FU is the cellular adaptive response to reactive oxygen species (ROS). Oxidative stress is one of the causes that can produce necrosis or apoptosis in cells. Apoptosis occurs after acute but persistent oxidative stress conditions leading to genomic instability, tumour progression and drug resistance (Hwang, Chung et al. 2007). Some tumour cells increase specific gene expression such as manganese superoxide dismutase (*MnSOD*), *Bcl-2* and *Prx* I in oxidative stress conditions. Research carried out by Tae Hwang *et al*., (Hwang, Chung et al. 2007) showed that ROS plays an important role in human lung cancer progression and can induce drug resistance to a variety of anticancer agents such as 5-FU (Hwang, Chung et al. 2007). Another recent CRC study demonstrated that the use of a double treatment of both 5-FU and antioxidants can be harmful due to the inhibitor effect that antioxidants have on Src protein (Fu, Yang et al. 2014). Src is a kinase that drives the apoptotic action of 5-FU via caspase-7 through its phosphorylation (Fu, Yang et al. 2014). 5-FU can induce ROS-dependent Src activation in CRC cells, so a failure of apoptosis via 5-FU could be a potential mechanism of resistance contributing to tumour development (Fu, Yang et al. 2014). Additionally, in-depth studies have shown that reactive oxygen species modulator 1 (*Romo1*) siRNA treatment had positive results and high efficiency against 5-FU-induced ROS generation. *Romo1* is a gene that encodes a mitochondrial membrane protein responsible for ROS production. At the same time, 5-FU induces an increase in mRNA levels of *Romo1*. So the use of a *Romo1* siRNA to block Romo1 expression directly contributes to decrease ROS generation by 5-FU (Hwang, Chung et al. 2007).

3.1.3 Aims & Objectives for 5-FU

The main aims and objectives of this study were focused on developing new resistant sublines to 5-FU which could be used to explore novel mechanisms of resistance in CRC. This was achieved by the following objectives:

1) Establish and characterise 5-FU resistant sublines for DLD-1, HT 29 and KM 12 cell lines in terms of sensitivity to 5-FU both *in vitro* and *in vivo*.

2) Identify novel mechanisms of 5-FU resistance using a proteomic approach.

3) Validate the proteomics approach using immunodetection techniques.

3.2 Material & Methods

All materials used and methods were applied as described in Chapter 2 to study chemosensitivity curve profiles by MTT assay. Additionally, new methods used during development of resistant sublines and validation of proteomics approach by immunodetection techniques are detailed below.

3.2.1 Establishment of resistant CRC cell lines

CRC sublines with resistance to conventional drugs were established and derived from DLD-1, KM 12 and HT 29 parent cell lines by continuous exposure to increasing concentrations of 5-FU, IRI and OXA. Drug concentrations were increased at each step of resistance over a period of ten months. IC_{75} values were used as initial starting doses for DLD-1, KM 12 and HT 29 cell lines. As an example of the establishment of resistant cell line process, development of DLD-1 resistant subline to 5-FU is explained below (see figure 3.2).

Firstly, DLD-1 parent cell line was split into a T25 flask (surface area 25 cm^2) with RPMI 1640 complete medium plus the corresponding doses of the drug. Initial concentrations used for each drug was the IC_{75} (drug concentration that inhibits cell growth by 75%) and it was doubled each time. The drug exposure dose was increased until 250 µM was reached.

For instance, in 5-FU case, the initial dose concentration of the drug in the flask was 15 µM (Fig. 3.2). (e.g., [15 µM] 5-FU initial dose was increased in successive concentrations of 2 x IC_{75}, 3 x IC_{75} each 4-7 days. Passages were done once the confluence in the T25 flask was around 80%. In this way, after the first 2 weeks, the drug dose was increased from 15 µM to 60 µM (Fig. 3.2). Simultaneously, jointly at the same time with each new passage of DLD-1, an extra passage was done into a T25 flask with no drugs added, apart from the regular T25 flask with DLD-1 cell line in presence of 5-FU (Fig. 3.2). This parallel T25 untreated flask with cells with the same number of passage that treated cells was based on the idea to be able to assess the effects that the

passage number has on MTT assay and proteomics results. Development of resistant sublines by higher exposure dose to the drug is a procedure that takes time and it is known that passage number has effect in cells (Chang-Liu and Woloschak 1997, Pronsato, La Colla et al. 2013). After a long period of time (10 months) with DLD-1 growing under drug conditions, changes in IC_{50} value are expected. The IC_{50} of resistant sublines are expected to be higher than the IC_{50} value of the DLD-1 parent cell line that has been maintained in drug-free medium. So, the drug sensitivity was examined by the MTT assay as described in Chapter 2, section 2.3.5 (Table 3.2) each time that parent DLD-1 cell line was exposed to a higher dose of the drug. Further, at each step of resistance to 5-FU, a T75 flask (surface area 75 cm^2) was split with no drug added in order to freeze down for cryovials and cell freezing (Fig. 3.2). Cells were stored at different stages of resistance development process by freezing the cells in medium containing 10% DMSO, using cryovials and storing them in liquid nitrogen at -196°C.The reason for this was to avoid a loss of samples due to unexpected events such as contamination of cell cultures and power cuts in the facilities.

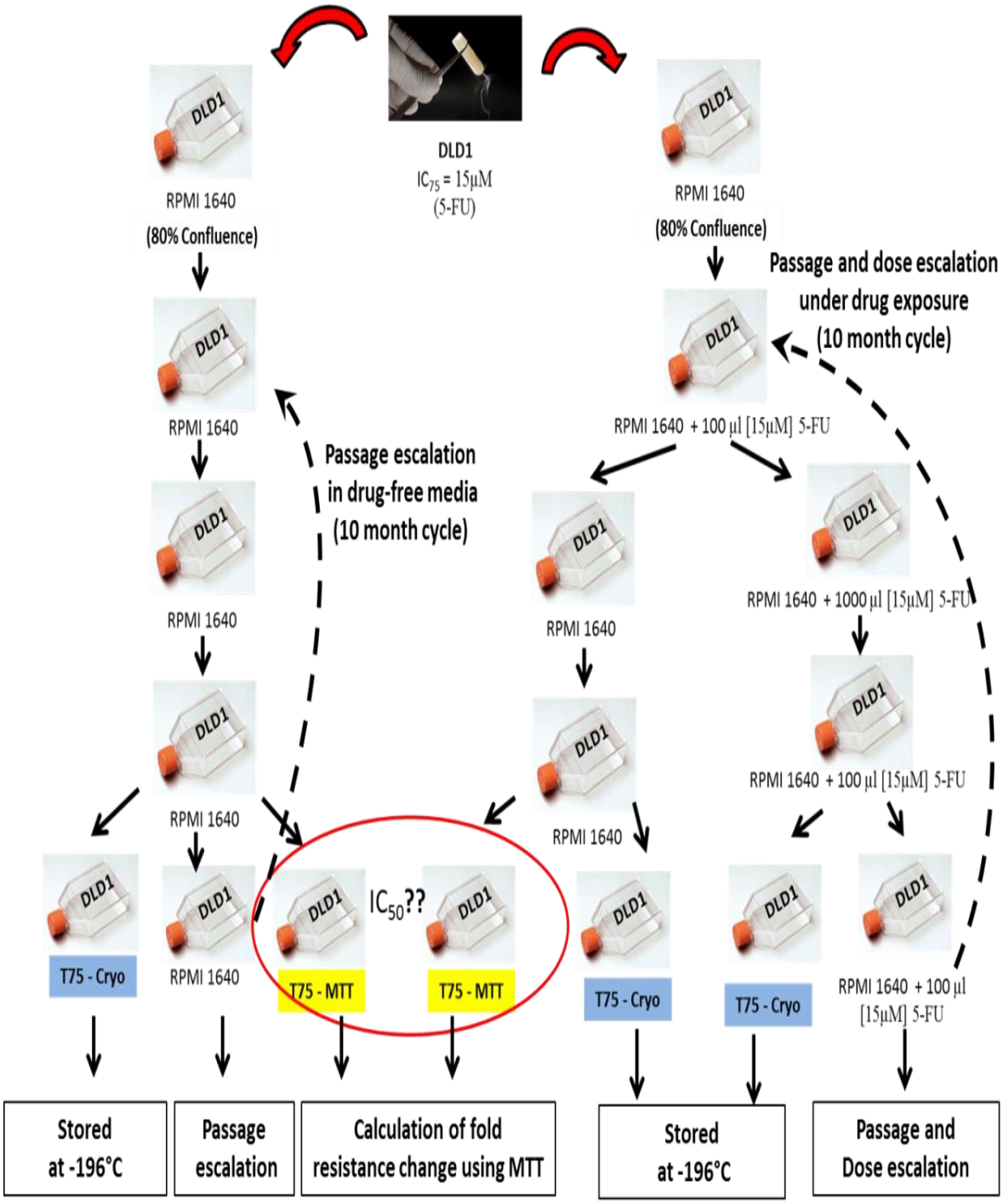

Figure 3.2: Scheme showing the protocol used to establish DLD-1 resistant cell line to 5-FU from the parent DLD-1 CRC cell line. On the left, a parallel passaging of initial parent cell line was done in free-conditions media to detect potential changes caused by passaging effect during development of resistant sublines (right side).

3.2.2 Microscopy studies

Resistant and parent-sensitive cell lines were examined using x40 objective magnification under Light-Olympus CK2 Inverted Microscope (Tokyo, Japan) and pictures were taken using Lumascope 488 Series obtained from Etaluma Inc. (Carlsbad, USA).

3.2.3 Development of drug-resistant xenograft CRC models in nude mice to confirm stability of DLD-1 5-FU subline

10 week old male athymic nude mice (Envigo Ltd. Balackthom, UK) were used to develop subcutaneous xenograft models. Mice were maintained under pathogen-free conditions throughout-in facilities approved by the Home Office to meet all current regulations and standards of the United Kingdom. All procedures were carried out under a United Kingdom Home Project License, following UK National Cancer Research Institute Guidelines for the Welfare of Animals.

$1x10^6$ cells in a volume of 100 µl of DLD-1 5-FU [250] resistant subline and DLD-1 parent cell line were injected subcutaneously in both right and left flanks of 12 nude mice. Once tumours were palpable, then therapy commenced (designed day 0). 5-FU was administered to the treatments groups as a single intraperitoneal injection at 100 mg/Kg on day 0. For comparison, a control group was left untreated. Tumour volume using callipers and animal body weight were recorded frequently, and normalised to the respective volume on the initial day of treatment. Mann-Whitney U tests were conducted to determine the statistical significance of any differences in growth rate (based on tumour volume doubling time) between control and treated groups.

3.2.4 SILAC and Cell culture media

Cell culture was carried out as described in Chapter 2, section 2.3.3, but also a new cell culture technique was applied four quantitative proteomics characterization. Characterisation of resistant cell lines was carried out using a stable isotope labelling amino acids in cell culture (SILAC) based approach as follows: DLD-1, KM 12 and HT 29 CRC parent cell lines were SILAC-labelled with 50 mg of L-Arginine-HCl ($^{13}C_6$, $^{15}N_4$) and 50 mg of L-Lysine-2HCl

($^{13}C_6$, $^{15}N_2$) by culturing them for 8 passages in 500 ml of RPMI media for SILAC with 10% (v/v) dialyzed FBS and incubated at 37°C in 5% CO_2. This number of passages was done to ensure incorporation of isotope label was as close to 100% as possible. 115 mg of L-Proline was added to prevent the metabolic conversion of heavy arginine to heavy proline, causing inaccuracy during comparison between the light and heavy peptides ion signal (Van Hoof, Pinkse et al. 2007). All products were obtained from Thermo Fisher Scientific (Loughborough, UK).

Cells were split into T25 flasks using $1x10^4$ cells/ml during first 5 passages. Last 3 passages were done using T75 flasks. The medium was replaced every 4 days, until cells reached 65–75% confluency, when cells were passaged. So cells were maintained in Log phase growing (between 30-80% confluency) for as long as possible during all passaging. Finally, cells were collected from an 80% confluent T75 flask by trypsinisation. Long and low generation controls plus the resistant subline were compared with the SILAC-labelled samples collected.

3.2.5 General quantitative proteomics approach

The approach proposed to identify proteomic changes in CRC resistant sublines using mass spectrometry by SILAC approach was divided in three main stages which are summarized in three schemes below. After that, a detailed section of general material and methods used is described.

1st Stage - Preparation of proteomics samples -

A two-stage stable isotope labelling by amino acids in cell culture (SILAC) protocol was used to identify protein changes in CRC resistant sublines established *in vitro* (Fig. 3.3).

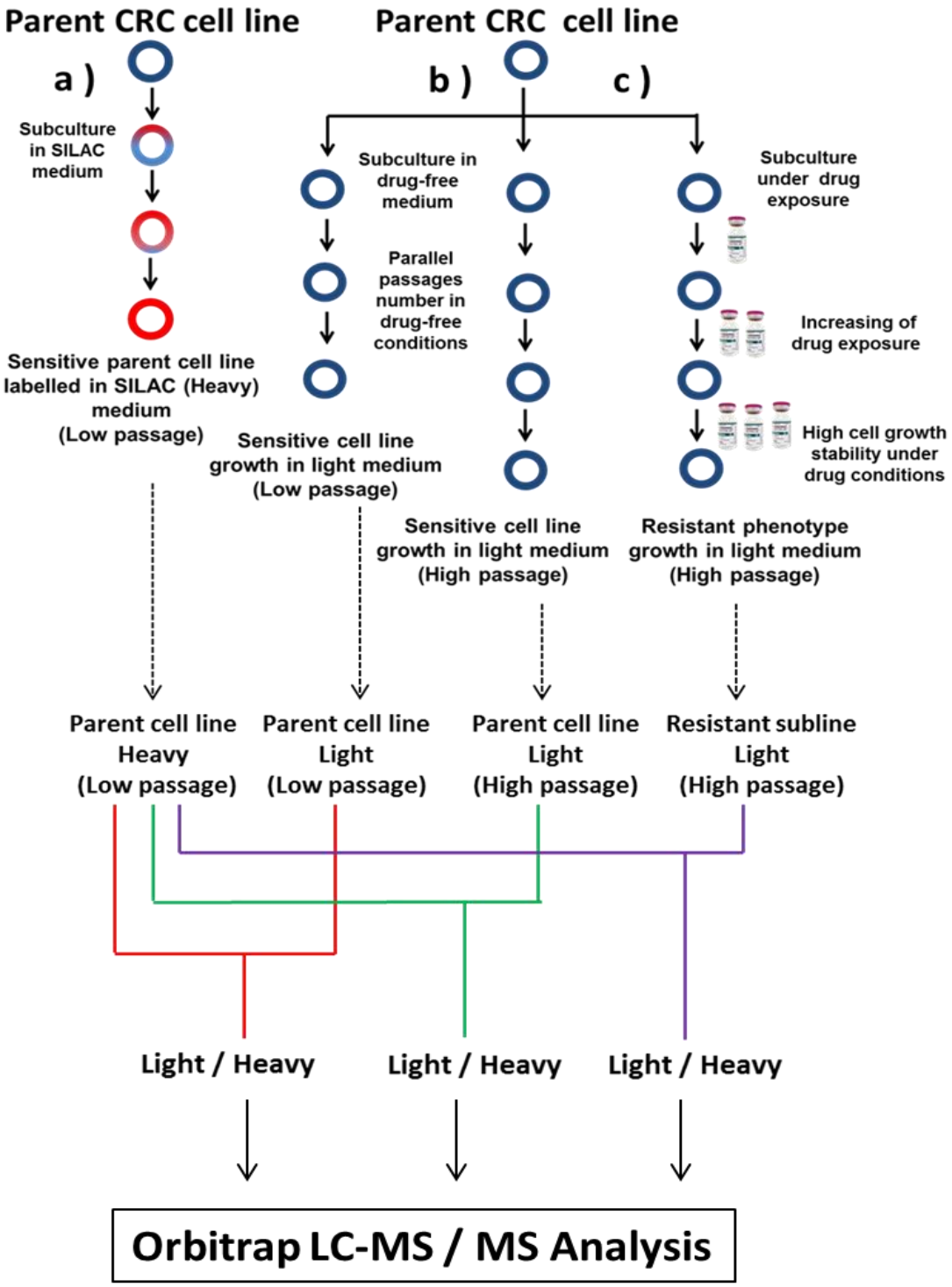

Figure 3.3: Diagram of experimental protocols and general strategy design. (a) Flowchart of SILAC approach showing the parent cell line growth in SILAC medium. (b) Parent cell line growth in drug-free medium to be used as low and long generation control during protein quantification. (c) Parent cell line growth under drug exposure conditions during establishment of CRC resistant sublines process.

2nd Stage – Protein extraction and Strong Cation Exchange Chromatography (SCX) -

The flow chart shows the protocol used for cell lysis, protein extraction and proteins separation by SCX to be used in mass spectrometry analysis (Fig. 3.4). See sections 3.2.5.1 to 3.2.5.5 for details.

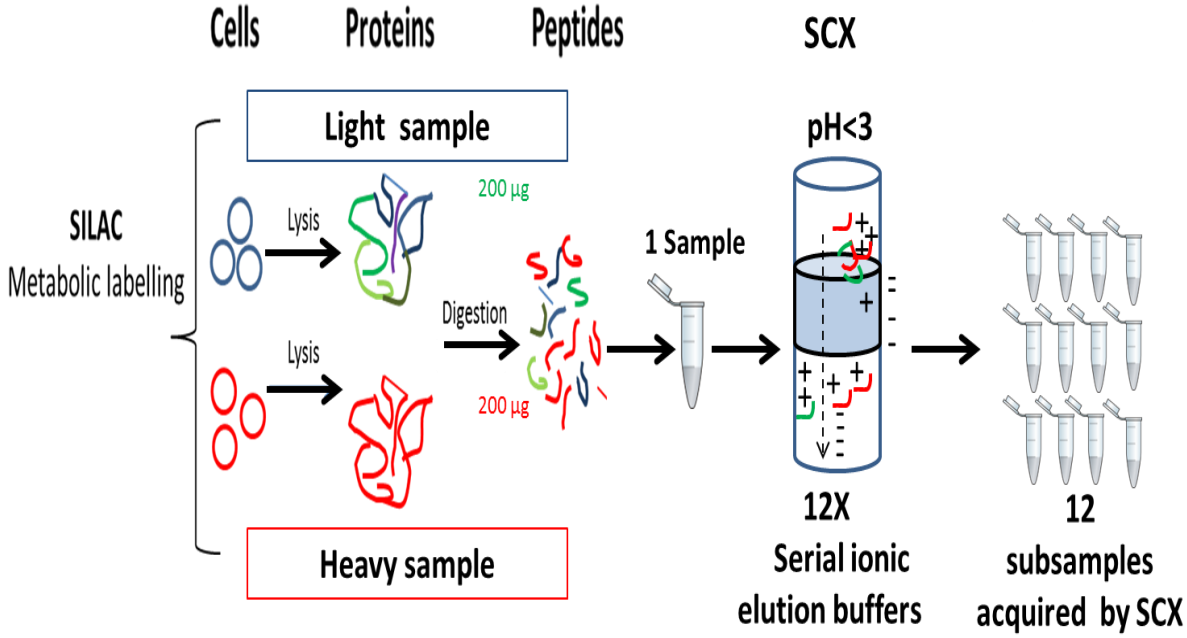

Figure 3.4: Flowchart describing samples preparation before MS analysis. Initially, 200 µg of light sample and 200 µg of heavy sample were combined to get 400 µg of L/H combined sample prior to protein digestion. L/H digested sample was separated in 12 subsamples by SCX to be analysed in triplicate in Orbitrap Mass Spectrometer.

3rd Stage – Protein quantification and data analysis -

The flow chart shows the protocol used for data processing, filters, statistics and interpretation of proteomics data (Fig. 3.5). Each eluted subsample by SCX was analysed by Orbitrap Mass Spectrometer in triplicate and all identified peptides were used for protein identification. From all peptides detected during MS analysis, only the three best unique peptides were used for protein quantification. After protein quantification three filters were applied:

(1) only proteins quantified from unique peptides with 2 or more PSMs were used, (2) only master proteins were considered and (3) mascot score applied for $p<0.05$. Proteins only quantified in light or heavy sample were removed. Finally, Log_2 transformation of raw data was done after normalized each single SILAC experiment. Multi SILAC datasets were formed by three single SILAC experiments (resistant subline, low generation control, long generation control) and Multi SILAC datasets were analysed under LIMMA and the 5^{th} percentile criteria. See sections 3.2.5.6 to 3.2.5.8 for details.

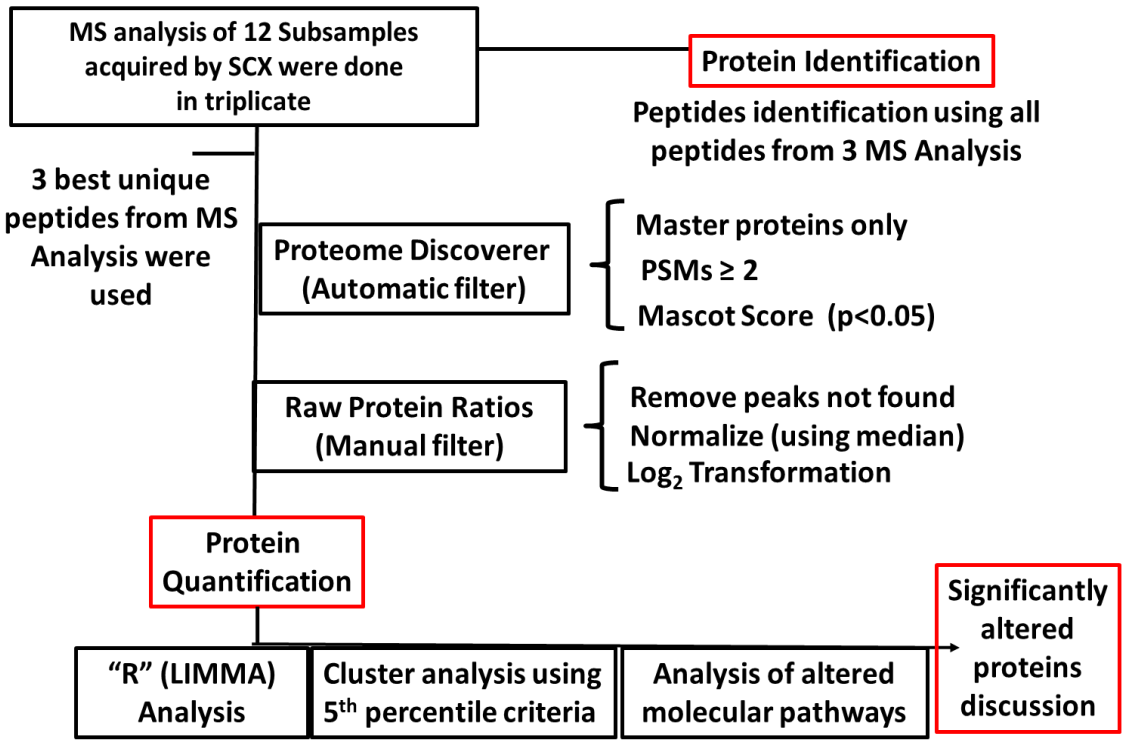

Figure 3.5: Flowchart describing quantification and proteomics analysis process. Unique peptides were used during protein quantification to avoid misidentifications of proteins. Automatic and manual filters were applied before data normalisation and transformation.

3.2.5.1 Cell lysis and protein extraction

Proteins for analysis were extracted from the cells using a Complete™, Mini Protease Inhibitor Cocktail with EDTA and containing 7M urea, 2M thiourea, 0.4% CHAPS, 0.1% sodium dodecyl sulphate (SDS), 0.05% sodium deoxycholate in PBS (Severn Biotech Ltd., Kidderminster, UK) at 4˚C and homogenized by sonication with a SH70G Sonicator from Philip Harris Scientific

(Lichfield, UK). Samples were centrifuged at 13,000 rpm for 25 min at 4˚C. All materials for protein extraction buffer were provided from Sigma-Aldrich (Poole, UK).

3.2.5.2 Bradford Protein Assay

Concentration of protein extracts was measured using Bradford protein assay kit (ThermoFisher, Loughborough, UK) (Bradford 1976). To carry out the Bradford assay, firstly five serial dilutions of 1 mg/ml, 0.5 mg/ml, 0.25 mg/ml, 0.125 mg/ml and 0.06 mg/ml were done from an initial concentration of 2 mg/ml albumin from bovine serum (BSA) and a 40 fold dilution was done for each cell line lysate sample. Secondly, 1.5 ml of Bradford assay reagent was added to 50 µl of standards (BSA dilutions), blank and cell lysate and vortex following by incubation at RT for 15 min. Select SkanIt™ Software from Thermo Fisher (Loughborough, UK) was used to read absorbance at 595 nm wavelength using 1ml of samples in plastic cuvettes on the Thermo Scientific Multiskan spectrophotometer. BSA reading values were used to yield a linear calibration curve over the entire BSA protein concentration range. Sample protein concentration was calculated by Y-axis intercept and its projection over X-axis. Graphs were generated using GraphPad Prism 5.0 (GraphPad Software, Inc., San Diego, CA).

3.2.5.3 Protein digestion

After the Bradford assay, 200 µg of light and 200 µg of heavy samples combinations were mixed prior to digestion. These 12 different samples were defined as 12 single SILAC experiments are summarised below.

	SILAC control	Passaging effect control	Resistance
DLD-1 5-FU	DLD-1 P=9 – Light (200 µg) DLD-1 P=9 – Heavy (200 µg)	DLD-1 P=65 - Light (200 µg) DLD-1 P=9 - Heavy (200 µg)	DLD-1 5-FU – Light (200 µg) DLD-1 P=9 - Heavy (200 µg)
DLD-1 OXA	DLD-1 P=9 - Light (200 µg) DLD-1 P=9 - Heavy (200 µg)	DLD-1 P=65 - Light (200 µg) DLD-1 P=9 - Heavy (200 µg)	DLD-1 OXA – Light (200 µg) DLD-1 P=9 - Heavy (200 µg)
DLD-1 IRI	DLD-1 P=9 - Light (200 µg) DLD-1 P=9 - Heavy (200 µg)	DLD-1 P=65 - Light (200 µg) DLD-1 P=9 - Heavy (200 µg)	DLD-1 IRI – Light (200 µg) DLD-1 P=9 - Heavy (200 µg)
KM 12 5-FU	KM 12 P=9 - Light (200 µg) KM 12 P=9 - Heavy (200 µg)	KM 12 P=55 - Light (200 µg) KM 12P=9 - Heavy (200 µg)	KM 12 5-FU – Light (200 µg) KM 12 P=9 - Heavy (200 µg)
KM 12 OXA	KM 12 P=9 - Light (200 µg) KM 12 P=9 - Heavy (200 µg)	KM 12 P=55 - Light (200 µg) KM 12 P=9 - Heavy (200 µg)	KM 12 OXA – Light (200 µg) KM 12 P=9 - Heavy (200 µg)
HT 29 5-FU	HT 29 P=9 - Light (200 µg) HT 29 P=9 - Heavy (200 µg)	HT29 P=57 - Light (200 µg) HT29 P=9 - Heavy (200 µg)	HT29 5-FU – Light (200 µg) HT29 P=9 - Heavy (200 µg)

.

Figure 3.6: Combinations of cell lines extracts to make up 12 different single SILAC experiments. A mix of 200 µg protein of light sample / 200 µg protein of heavy sample were used during mass spectrometry analysis.

To the combined extracts, 1 ml of chilled acetone was added and stored O/N at -20ºC. The precipitates were then centrifuged at 13,400 rpm for 20 min at 4ºC, the supernatant decanted and the protein pellet lyophilised. Protein pellets were re-solubilised in 40 µl of 8 M urea. 1 µl of Dithiothreitol (DTT) 50mM, a reducing agent to disrupt disulfide bonds between cysteine residues and 1 µl of iodoacetamide (IAA) 100mM an alkylating agent to avoid sulfhydryl groups reforming. DTT and IAA were obtained from Sigma-Aldrich (Poole, UK). Digestion using 20 µl of Pierce™ trypsin protease (20 mg/ml) from Thermo Scientific (Loughborough, UK) was carried out O/N at 37˚C.

3.2.5.4 MALDI mass spectrometry

Before applying digests to SCX chromatography and desalting, protein digestion was confirmed as follows. 1 µl of Bruker matrix CHCA (LC MALDI) made up in 1 ml of 30% CH_3CN and 0.01% TFA was deposited on the MALDI

plate. An aliquot of 1 µl sample was diluted 10 fold in 10% acetonitrile (ACN) from Sigma-Aldrich (Poole UK) and added on the matrix. Secondly, 1 µl of matrix was deposited on the sample to be analysed using Ultraflex Matrix Assisted Laser Desorption/Ionization (MALDI) tandem Mass Spectrometer from Bruker Daltonics (Bremen, Germany). Data was acquired in reflector mode using 1000 shots for MS and 2000 shots for MS/MS.

3.2.5.5 SCX chromatography and desalting

Digested samples were collect as 12 fractions from SCX chromatography. The ISOLUTE® SCX column from Biotage (Hengoed, UK) was equilibrated with loading buffer (LB). The column was equilibrated with LB of 10mM potassium di-hydrogen phosphate (KH_2PO_4) (pH=3) in 25% acetonitrile (ACN) from Sigma-Aldrich (Poole, UK) was used for SCX. The sample (400 µg of digested mix) was applied and washed initially with LB followed by washing with 11 LB gradient to remove non-binding components, which was retained as a flow through fraction. Peptides were eluted sequentially with incremental increases in KCl (in LB) (Table 3.1). The flow through and eluted samples were diluted 4-fold with 2% acetonitrile, 0.1% formic acid desalted using C_{18} columns from Kinesis (Cambridgeshire, UK) before lyophilisation as follow. Initially, ZipTip columns were equilibrated using three times 20 ul of 100% methanol and three times 20 ul of Buffer A (2% ACN, 0.1% formic acid). These steps act as a gradient for the mini-column, which wets the resin and conditions it to be ready to bind peptides prior to sample loading. Load the sample was done by pipetting the protein digest up and down (discarding it back into its tube) 10 fold diluted (1 ul Sample + 9 ul of Buffer A). ZipTip were washed three times using Buffer A and finally, sample was eluted using Buffer B (100% ACN, 0.1% formic acid). Lyophilisation was done at 45ºC aqueous mode of Genevac Centrifugal Evaporator EZ-2 SP from Fisher Scientific (Loughborough, UK).

Buffer LB + KCl (mg)	mM	Volume	Fraction
LB+30 mg	30.0	22.4	E1
LB+60 mg	60.0	44.7	E2
LB+90 mg	90.0	67.1	E3
LB+120 mg	120.0	89.5	E4
LB+150 mg	150.0	111.8	E5
LB+180 mg	180.0	134.2	E6
LB+250 mg	250.0	186.4	E7
LB+300 mg	300.0	223.7	E8
LB+500 mg	500.0	372.8	E9
LB+700 mg	700.0	521.9	E10
LB+1000 mg	1000.0	745.5	E11

Table 3.1: Making up of 11 elution buffers used during SCX chromatography for protein separation.

3.2.5.6 Data acquisition

A preliminary quality control step to check SILAC labelling efficiency prior to SCX chromatography and SCX fractionated samples were analysed on an Orbitrap Fusion™ Tribrid™ Mass Spectrometer connected with Ultimate 3000 HPLC. Each SCX fraction was resuspended in 30 µl of 0.1% formic acid (FA), sonicated for 5 min in a Ultrawave 50 ultrasonic bath (Wolf Laboratories, York, UK), and centrifuged at 14,500 rpm, for 1 min. An aliquot (10 µl) of the fraction was used during Mass spectrometer analysis. Each SCX fraction was run in triplicate on the LC-MS as shown below (Fig. 3.7).

Digested peptides were washed on a C_{18} Trap-column (300 µm x 5 mm, 100 A), at a flow rate 300 nl/min for 4 min then transferred C_{18} Analytical-Column (75 µm x 50 cm, 2 µm, 100 A) at temperature 40˚C. C_{18} columns were provided by Thermo Scientific (Loughborough, UK). Peptides were eluted by using

Solvent A (2% ACN, 0.1% FA) and Solvent B (100% ACN, 0.1% FA). Total run time was 120 min using a gradient of solvent B: 0 min at 5%, 5 min at 7%, 65 min at 25%, 80 min at 45% and 85 min at 85%. Column cleaning was performed during 20 min with 85% solvent B and equilibration of column was performed during 15 min with 5% solvent B. Eluted peptides were subject to a Spray voltage at 2000 V and heated capillary Full MS scan in the Orbitrap was followed by the MS/MS scans of the ions selected from the MS spectrum in the Orbitrap (HPLC-MS).

MS analysis of eluted peptides was conducted through Xcalibur™ 4.0 Software with Foundation 3.1 SP1 (Thermo Scientific) package with Chromeleon™ 7.2 Chromatography Data System software on Orbitrap Fusion™ from Thermo Fisher Scientific (Loughborough, UK). Mass resolution was 120,000 between 350 and 1,500 m/z with the maximum injection time was 100 ms. All MS/MS acquisition was performed on the Ion-trap, in top speed mode with 3 s cycle time, a dynamic exclusion (±5 ppm) of 50-60 s, intensity threshold 5,000, with parent charge states 2+ to 7+ were sequentially fragmented by collision-induced dissociation with a normalised collision energy of 35%. A maximum of 200 ms ion injection time was allowed.

3.2.5.7 Protein identification and quantification

MS spectra generated were analysed in the Mascot 2.4 Database Manager search algorithm (Matrix Science, London, United Kingdom) using the human database from UniProt (SwissProt) 2016 with records of 551,705 functional proteins.

All proteins were classified based on the protein Mascot scores of each single SILAC experiment analysis. Mascot software uses a probability-based scoring, where a "high" score is a "low" probability for false protein identification. Scores are given in -10 x Log10 (p) and p is the value of absolute probability. A probability of 10-20 thus becomes a score of 200.The protein identified with the most accuracy based on matches using mass values and peptide mass fingerprinting receives the highest score. Finally, a confidence threshold is selected for the rest of proteins identified. For a 95% confidence, the software shows the lowest score to establish the confidence threshold at $p<0.05$.

For example, selecting proteins with Mascot scores higher than “x” and 95% confidence ($p<0.05$), a wrong protein identification of a protein with a mascot score higher than “x”, it is expected to occur at random with a frequency of less than 5%. Consequently, the lower the expectation value for a wrong identification is, the higher the mascot score attached to the protein is.

The peptide and protein SILAC ratios were determined using fixed modifications for SILAC peptide pairs searches with fixed L-Arginine-HCl ($^{13}C_6$, $^{15}N_4$) and L-Lysine-2HCl ($^{13}C_6$, $^{15}N_2$) modifications. Modifications from the quantitative method was SILAC (2 Lysine (K) + 8 Arginine (R)) = + 10 [Mass-shift]. Search parameters included; up to 2 missed trypsin cleavage, MS mass tolerance of 10 ppm and MS/MS mass tolerance of 0.6 Da were selected. Dynamic modifications included were Oxidation (M) and Deamidated (NQ). Carbamidomethyl (C) was established such as static modification. Confidence threshold was established for $p<0.05$ and all proteins identified with $p\geq0.05$ were excluded from analysis and not included in the list of quantified proteins.

Identified proteins were quantified by tracking pairs of peptides signals (light and heavy) in the ion chromatogram using Proteome Discoverer™ 2.1 software from Thermo Fisher Scientific (Loughborough, UK). The Proteome Discoverer™ Protein quantitation was carried out by the SILAC approach. Master proteins were defined as those with two or more unique peptide identification and two or more peptide SILAC ratios from the total triplicate analyses for all SCX fractions (i.e. 36 LC-MS profiles). Software determined the SILAC ratios from the signal intensities of the light SILAC peptide (containing $^{12}C_6{}^{14}N_4$-Arg) and the paired heavy SILAC peptide (containing $^{13}C_6{}^{15}N_4$-Arg). Master proteins were defined as those with two or more unique peptide identification and two or more peptide SILAC ratios from the total triplicate analyses for all SCX fractions (i.e. 36 LC-MS profiles).

$$\text{Expression ratio} = \frac{Abundance\ of\ Light\ peptide\ \ in\ 200\ \mu g\ of\ Light\ sample}{Abundance\ of\ Heavy\ peptide\ in\ 200\ \mu g\ of\ Heavy\ sample}$$

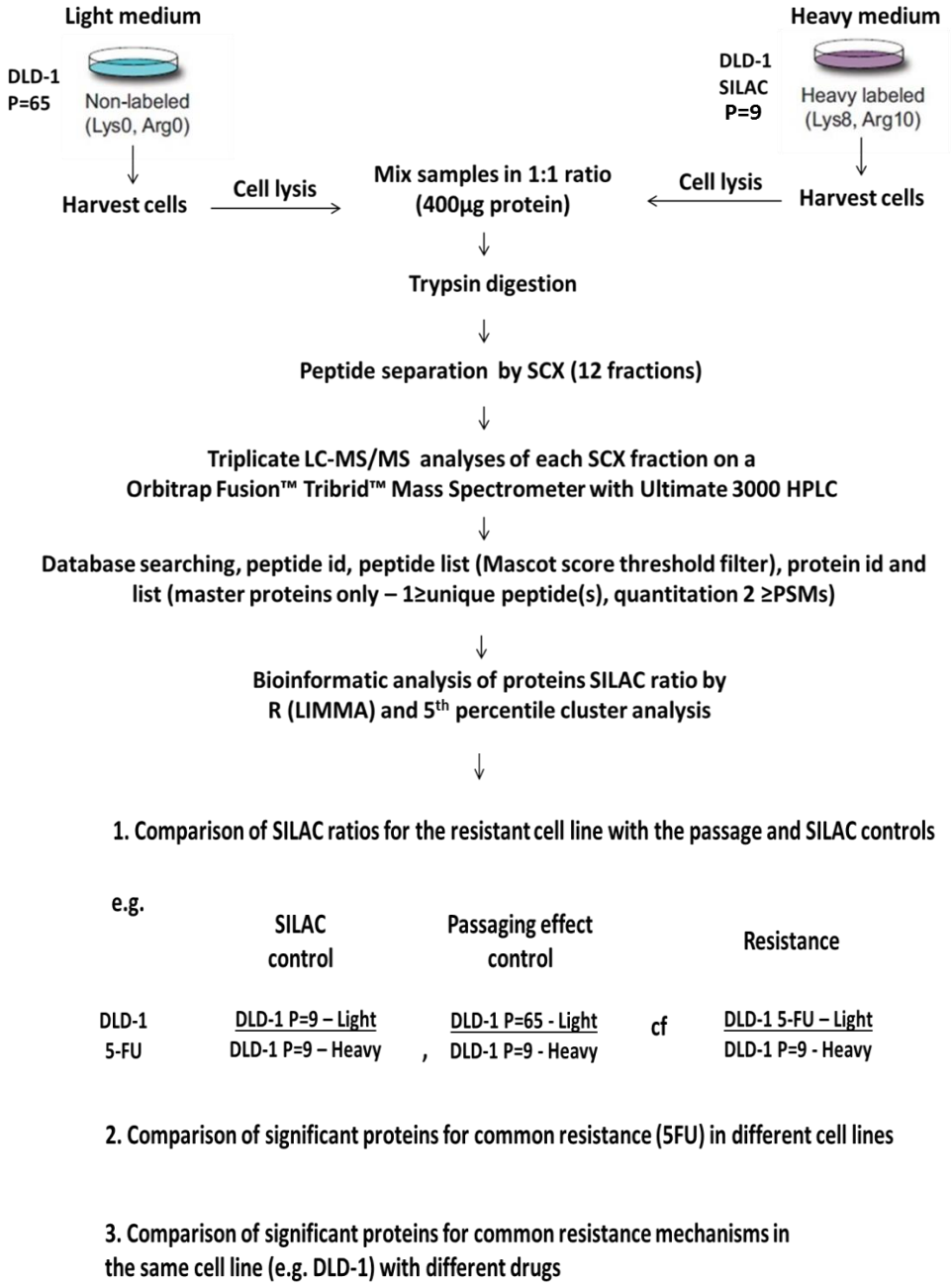

Figure 3.7: Diagram with a brief description of the SILAC-approach protocol applied for protein quantitation. After combination of 200 µg of light and heavy samples, mixed sample was digested and separated in 12 subsamples by SCX. Each single SILAC experiment was analysed in triplicate by MS. After filtering, results from single SILAC sample for each resistant subline and results from single SILAC samples for its two controls (low and high passage) were grouped to form a multi SILAC dataset. A total of 6 multi SILAC dataset were generated to be analysed under "R" and "Cluster analysis".

Single SILAC experiment ratios were determined from the average of the three best peptide ratios. Three examples of MS spectrum and MS/MS spectrum of peptides are illustrated below.

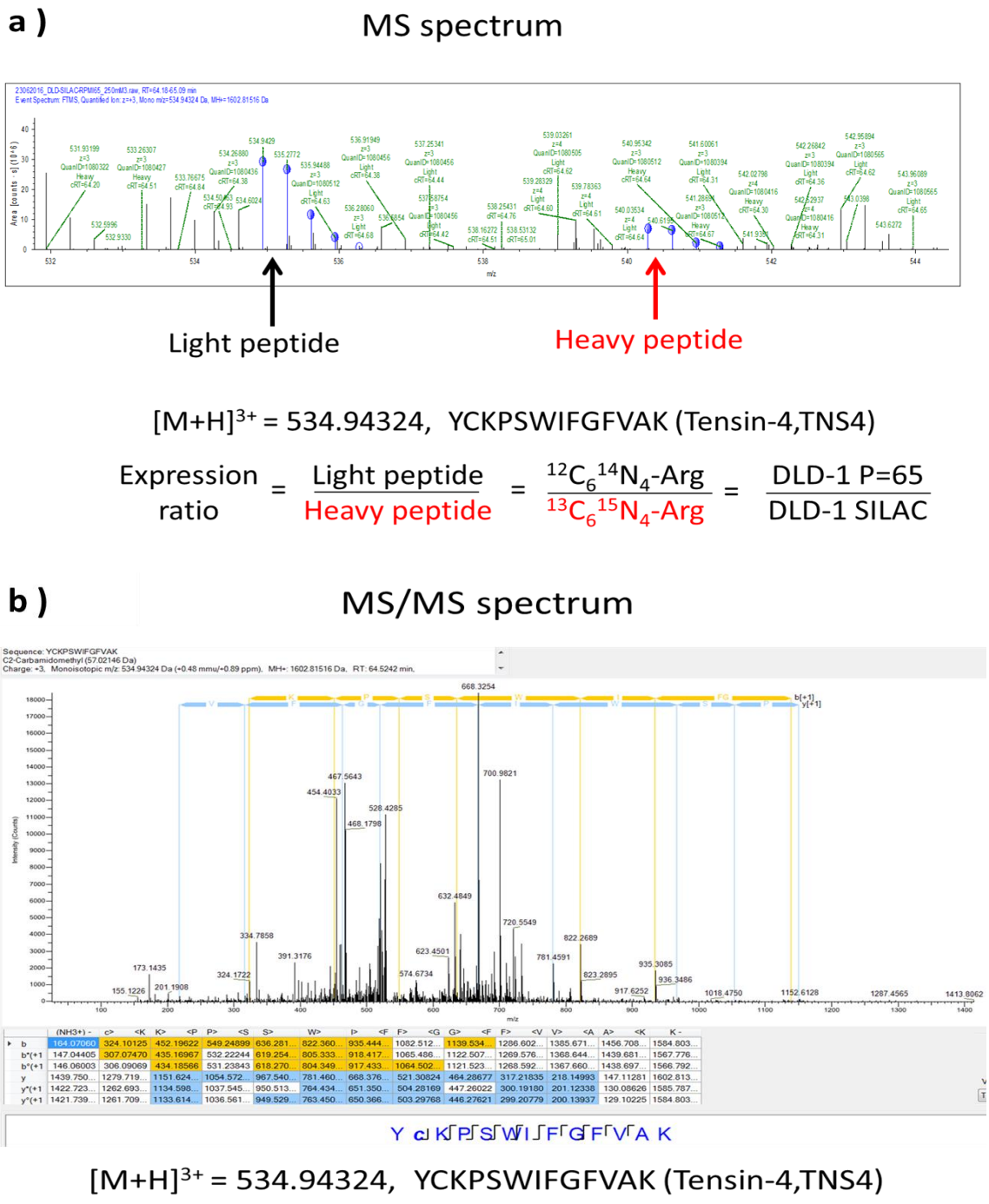

Figure 3.8: Increased expression in resistance. (a) MS spectrum showing more intense light than heavy mass signals of the peptide YCKPSWIFGFVAK from the Tensin-4 (TNS4) and (b) MS/MS spectrum used to identify YCKPSWIFGFVAK and the fragment matching sequence (highlighted in yellow and blue).

a) MS spectrum

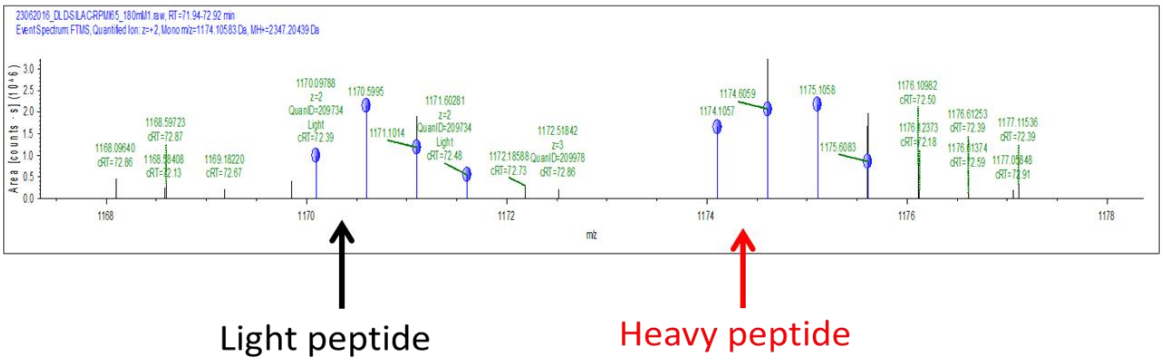

$[M+H]^{3+}$ = 1174.10583, IDQLEGDHQLIQEALIFDNK (α actin-1,ACTN1)

$$\text{Expression ratio} = \frac{\text{Light peptide}}{\text{Heavy peptide}} = \frac{^{12}C_6{}^{14}N_4\text{-Arg}}{^{13}C_6{}^{15}N_4\text{-Arg}} = \frac{\text{DLD-1 P=65}}{\text{DLD-1 SILAC}}$$

b) MS/MS spectrum

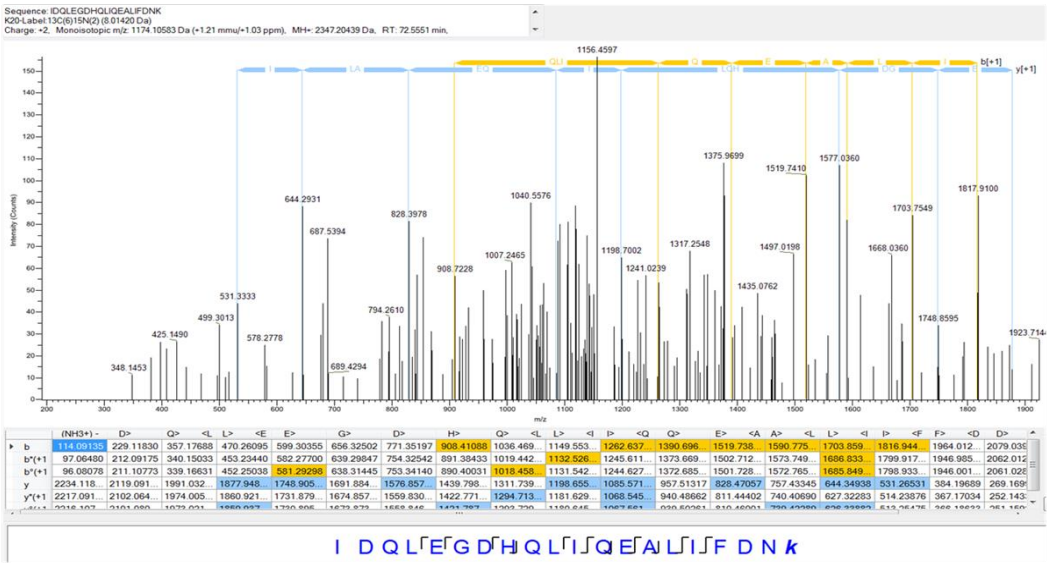

$[M+H]^{3+}$ = 1174.10583, IDQLEGDHQLIQEALIFDNK (α actin-1,ACTN1)

Figure 3.9: No change in expression. (a) MS spectrum showing similar intense light and heavy mass signals of the peptide IDQLEGDHQLIQEALIFDNK from the protein α actin-1(ACTN1) and (b) MS/MS spectrum used to identify IDQLEGDHQLIQEALIFDNK and the fragment matching sequence (highlighted in yellow and blue).

a) MS spectrum

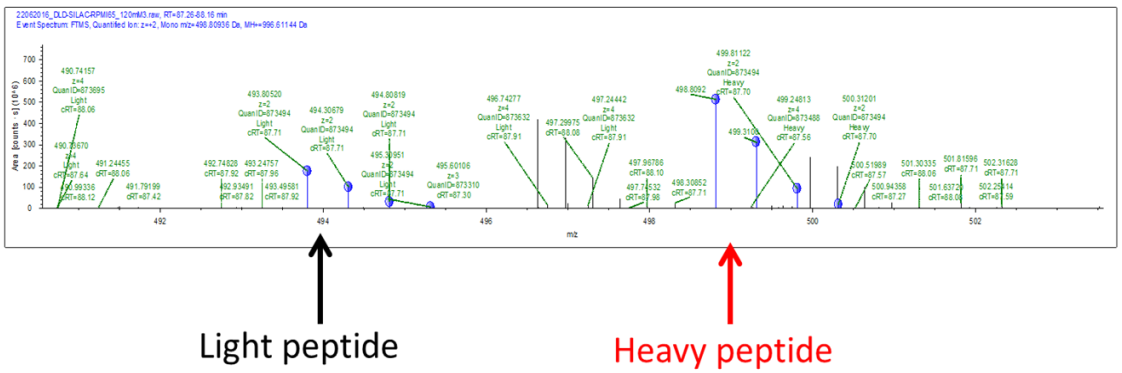

$[M+H]^{3+} = 498.80936$

DLPLLFR (D-3-Phosphoglycerate Dehydrogenase , PHGDH)

$$\text{Expression ratio} = \frac{\text{Light peptide}}{\text{Heavy peptide}} = \frac{^{12}C_6{}^{14}N_4\text{-Arg}}{^{13}C_6{}^{15}N_4\text{-Arg}} = \frac{\text{DLD-1 P=65}}{\text{DLD-1 SILAC}}$$

b) MS/MS spectrum

$[M+H]^{3+} = 498.80936$

DLPLLFR (D-3-Phosphoglycerate Dehydrogenase , PHGDH)

Figure 3.10: Decreased expression in resistance. (a) MS spectrum showing lower intense light than heavy mass signals of the peptide DLPLLFR from the protein D-3-Phosphoglycerate Dehydrogenase (PHGDH) and (b) MS/MS spectrum used to identify DLPLLFR and the fragment matching sequence (highlighted in yellow and blue).

3.2.5.8 Bioinformatics and statistical analysis of quantitative proteomics data

Raw single SILAC results were subjected to median normalisation and Log_2 transformation to enable cross-experiment comparison during multi SILAC datasets study. Three single SILAC experiments (resistant cell line, low and long generation controls) were used to generate multi SILAC datasets in Venn diagrams. Venn diagrams were created with web tool provided by the University of Pretoria through Bioinformatics and Evolutionary Genomics department following website http://bioinformatics.psb.ugent.be/ and retrieved from November, 2016. All commonly quantified proteins in resistant and parent cell lines (multi SILAC dataset) were classified into three groups in terms of expression relative between single SILAC experiments. Three groups defined were “Not altered proteins” (N), “up-regulated proteins” (U) and “down-regulated proteins” (D) using two different statistical methods.

1. The first method was based on multi SILAC datasets analysis by R, using linear models and differential expression for microarray data studies (LIMMA) (Ritchie, Phipson et al. 2015) (Fig. 3.11). LIMMA was introduced as an empirical Bayes approach that specifically allowed developing a realistic distribution of biological variances. LIMMA statistical is based on the use of the full data to shrink the observed sample variances towards a pooled estimate. Results of LIMMA are more stable with a higher and powerful inference compared to ordinary t-tests particularly when the number of samples is small (Kammers, Cole et al. 2015). LIMMA has been used in more than 6000 citations in the last ten years and in hundreds of proteomic experiments (Brusniak, Bodenmiller et al. 2008, Margolin, Ong et al. 2009, Ting, Cowley et al. 2009, Jankova, Chan et al. 2011, Zhao, Li et al. 2013). A fold change and its associated p-value were calculated for each protein according to their significant different ratio expressions between the resistant subline and its two related control cell lines with a high and a low number of passages. This information was summarized in a Volcano plot of LIMMA-modelled proteomics data. The data for all proteins are plotted as Log_2 fold change versus the $-Log_{10}$ of the adjusted p-value.

2. Proteins from multi SILAC datasets were clustered using the 5th percentile criteria of Log_2 normalized ratios distribution to classify all proteins in the three different responses defined above. Hence, 10% of the most altered proteins of each sample (5% up-regulated (U) and 5% down-regulated (D) proteins) were considered changed, whilst the remaining 90% were considered unaltered. Cluster analysis was performed for sets of experiments to define groups of like-responding proteins (e.g., Fig. 3.23).

Those proteins classified as altered using the 5th percentile cluster analysis and with a significant p-value ($p<0.05$) obtained from LIMMA analysis were selected for further bioinformatics analysis.

R Script for LIMMA test

```
1.  library(Biobase)
2.  library(limma)
3.  getOption("max.print")
4.  options(max.print = 99999999)
5.  #calling data file
6.  mydata
7.  mydata <- read.table(file = "Proteome.txt", sep = "\t", header = T,row.names=1,
    as.is=TRUE,check.names = F)
8.  #How to summarise data
9.  head(mydata)
10. sml <- c("G0","G1","G1","G1","G1","G1","G1")
11. table(sml)
12. # set up the data and proceed with analysis
13. fl <- as.factor(sml)
14. fl
15. design<-model.matrix(~0+fl)
16. design
17. colnames(design)=levels(fl)
18. design
19. #boxplot(mydata)
20. #differetial expression
21. fit <- lmFit(mydata, design)
22. cont.matrix <- makeContrasts(G1-G0, levels=design)
23. cont.matrix
24. fit2 <- contrasts.fit(fit, cont.matrix)
25. fit2 <- eBayes(fit2, 0.01)
26. # dim means dimension of data
27. dim(fit2)
28. tT <- topTable(fit2, adjust="fdr", sort.by="p", number=nrow(fit2))
29. head(tT)
30. #how to select all those proteins which have p < 0.05
31. #tT <-tT[tT$P.Value <0.05,]
32. dim(tT)
33. write.table(tT, file="Proteome.txt", sep="\t")
34. ############################################################
```

Figure 3.11: R script to perfom multi SILAC dataset analyses.

3.2.5.9 Data analysis of altered proteins expression in resistant sublines

Initially, STRING was used to predict functional interactions of up-regulated and down-regulated proteins in resistant sublines. Links between proteins were defined as "Known interactions, experimentally determined" (pink colour), "Known interactions, database" (blue colour), "Protein neighbourhood" (green colour), "Proteins frequently mentioned together" (yellow colour) and "Co-expression" (grey colour) (Von Mering, Huynen et al. 2003).

Secondly, protein networks from STRING were modified based on EnrichNet (Network-based gene and protein set enrichment analysis) and GO (Biological Process ontology) results (Tsui, Chari et al. 2007, Liu and Ruan 2013). Proteins were classified into 5 different biological processes groups that contain proteins that may mediate drug response and drug resistance. These 5 biological processes were: (1) apoptotic and anti-apoptotic pathways, (2) DNA repair process, (3) drug and small molecules metabolism, (4) intracellular protein transport, (5) cellular membrane transporters and membrane organization (Tsui, Chari et al. 2007, Liu and Ruan 2013). Finally, significantly altered proteins were used to build up the Venn diagrams that show common up-regulated and significantly down-regulated protein in sublines resistant to the same drug.

3.2.6 Validation of relative protein expression levels identified by proteomics

Protein extract quality control was performed by SDS-PAGE and validation of proteomic results was performed by Western blotting (WB).

3.2.6.1 SDS-PAGE

Whole cell lysate from each single SILAC experiment (20 µg) was separated by SDS-PAGE electrophoresis, with the gels made up according to table 3.2, below.

5 ml Solution Components	Stacking gel 6%	Separating gel 12%
H_2O	1.95 ml	0.75 ml
30% Acrylamide mix	1 ml	2 ml
10% SDS	0.05 ml	0.05 ml
10% ammonium persulfate	0.05 ml	0.05 ml
TEMED	0.004 ml	0.002 ml
Tris	0.5 M Tris/HCl (pH 6.8) 1.95 ml	1.5 M Tris (pH 8.8) 1.95ml

Table 3.2: Composition of the SDS-PAGE gels used in these studies.

Mini-gels (100mm x50mm x1mm) were used, with a 6% stacking gel, 12% separating gel and 10-well comb. PageRuler™ Plus Prestained Protein Ladder (5-250kDa MW range) from Thermo Scientific (Loughborough, UK) was used as a guide during protein separation in electrophoresis (SDS-PAGE) and WB for all proteins validated. Protein Ladder was loaded in the first well in all gels followed by all remaining cell lysate samples. An initial voltage of 50 mV was applied to the tank with the gel and the buffer for 15 min and then increased to 150 mV for 1 h. Running buffer (25 mM Tris, 192 mM glycine, 0.1% SDS, pH 8.3) was stored at RT and diluted to 1x before use.

Gel transferring was done by Wet electroblotting (Tank transfer). The gel was placed in a "transfer sandwich" (filter paper-gel-membrane-filter paper), cushioned by pads and pressed together by a support grid after air-bubbles removing. Transfer was performed with an ice pack and at 4°C to mitigate the heat produced. Proteins were transferred from the gel matrix to a Hybond-P nitrocellulose blotting membrane (0.45 μm) (Sciences, Germany) using constant Amperage of 300 mA for 2 h. Protein presence in membrane after blotting was confirmed by Ponceau S solution provided by Sigma-Aldrich (Poole, UK). Stock

transfer buffer (39 mM glycine, 48 mM Tris base, 0.04% SDS, pH 8.3) prepared by adding 29.275 g of glycine, 58.147 g of Tris and 4 g of SDS into 1000 ml of distilled water. Stock transfer buffer was stored at 4˚C and was used to prepare working transfer buffer by adding 100ml of stock transfer buffer and 200 ml of methanol into 700 ml of distilled water.

3.2.6.2 Western blotting

Antibody labelling was carried out after blocking for 1 h at RT using blocking buffer (0.416% mM Tris (pH 7.6), 10% Tween-20, 5% (w/w) skimmed milk (Marvel, Premier Food, UK). Details of the primary antibodies used in the studies are detailed below in Table 3.3. A monoclonal Anti-β-Actin (A2228) (mouse IgG2a isotype) at 1:7000 dilution from Sigma-Aldrich (Poole, UK) was used as a protein identification control.

Supplier	Antibody Primary/ Secondary	Clonality	Isotype (Ig)	Host	Protein recognition amino acids (Aa)	Antigen species	Dilution factor	Reference
Abcam®	ab157107 Primary	Polyclonal	IgG	Rabbit	Aa 692-742 of Human CD44	Mouse, Rat, Human	1:2000	Has not yet been referenced
GeneTex®	GTX114872 Primary	Polyclonal	IgG	Rabbit	Centre region of Human UMPS	Human, Rat, Mouse	1:2000	Has not yet been referenced
Abcam®	EPR14545 Primary	Polyclonal	IgG	Rabbit	Aa 176-403 of Human VPS4	Human, Mouse, Rat,	1:2000	(Shtanko, Nikitina et al. 2014)
Abcam®	TS63 Primary	Monoclonal	IgG1	Mouse	Human CD63 protein	Human	1:500	(Nakase, Kobayashi et al. 2015)
Sigma-Aldrich®	A2228 Primary	Monoclonal	IgG2a	Mouse	N-terminal end of the β-isoform of actin	Human, pig, rabbit, mouse, dog,	1:7000	(Jalilian, Heu et al. 2015)
Abcam®	ab6721 (HRP) Secondary	Polyclonal	IgG	Goat	Rabbit IgG	Rabbit	1:5000	(Oh, Na et al. 2016)
Abcam®	ab6728 (HRP) Secondary	Polyclonal	IgG	Rabbit	Mouse IgG	Mouse	1:5000	(White, Jansen et al. 2015)

Table 3.3: List of antibodies and their features used in WB and IF experiments.

After primary antibody incubation O/N, the membrane was washed three times for 10 min each using TBS wash buffer after adjusting pH at 7.6. After the membrane was washed, it was incubated for 1 h in 2 ml of the secondary antibody in blocking at 1:5000 dilution (Table 3.3). After secondary antibody incubation, a further three washes for 10 min each using TBS wash buffer were performed before protein revelation.

For protein labelling development, the ECL™ Prime WB System (GERPN2232) kit from Sigma-Aldrich (Poole, UK) was used. Briefly, the blot was exposed to ECL reagents (A and B) for two minutes at RT before being enveloped in a hard plastic sheet. After removing excess reagent, the membrane was covered in a transparent plastic wrap. Then, in the dark room, the blot was exposed to hyper film ECL for a variable time ranging from 10 seconds to 15 min depending on the antibody. Hyperfilm was developed using Multi-grade rapid developer solution (ILFORD) for up to 3 min, followed by distilled water to remove the excess developer solution and at the end, the blot was fixed using the Rapid film fixer for 5 min.

3.3 Results

3.3.1 Establishment of DLD-1, HT 29 and KM 12 drug resistant cell lines to 5-FU

After ten months of episodic drug exposure, DLD-1 5-FU [250μM] resistant subline, KM 12 5-FU [60μM] resistant subline and HT 29 5-FU [60μM] resistant subline were established. An example of the progressive development of resistance is shown for DLD-1 5-FU (Fig. 3.12a).

Resistance indices were evaluated according to the relative resistance for pretreated cell lines with 5-FU in comparison with parent cell lines, defined by the ratio of IC_{50} of the resistant subline to the IC_{50} of the sensitive parent cell lines. Several criteria were set for successful establishment of a resistant line: the 5-FU resistant subline had to show stable growth and proliferation in culture medium with a drug concentration higher than the IC_{50} of the parent cell line: the sublines must maintain 5-FU resistance following the cell freezing and

defrosting process, and a new resistant subline must retain resistance phenotype after growth during at least one month in a drug-free medium. Under these conditions

After ten months of episodic drug exposure, DLD-1 5-FU [250µM] resistant subline, KM 12 5-FU [60µM] resistant subline, and HT 29 5-FU [60µM] resistant subline were successfully established. Three independent chemosensitivity curve profiles for DLD-1 parent and DLD-1 pretreated with 5-FU cell lines were carry out to measure progressiveness of resistance phenotype development process. An example of the progressive development of resistance is shown for DLD-1 5-FU (Fig. 3.12a).

IC_{50} values were calculated and are shown in figure 3.12b for DLD-1 5-FU, in figure 3.13a for KM 12 5-FU, and in figure 3.13b for HT 29 5-FU resistant sublines. Important differences of IC_{50} values were observed between the original parent cell lines and the 5-FU resistant sublines which have been growing under 5-FU. DLD-1 5-FU [250µM] resistant subline was around 130.2 fold change resistant to 5-FU than DLD-1 parent cell line (Fig. 3.12b). Whilst, KM 12 5-FU, and HT 29 5-FU is 3.2-fold change (Fig. 3.13a) and 3.5-fold change in resistance (Fig. 3.13b) in comparison to KM 12 and HT 29 parent cell lines respectively.

Visual comparison of resistant sublines and parent-sensitive cell lines under microscope at 40x magnification showed both an increase in size and in number of cells with irregular shapes around the monolayer clusters formed by 5-FU resistant sublines on the flasks surface (Fig. 3.14-3.15). 5-FU resistant sublines showed colonies more tightly packed than for parent cell lines. Additionally, DLD-1 5-FU resistant subline showed higher size on average and more irregular shapes than initial parent DLD-1 cell lines.

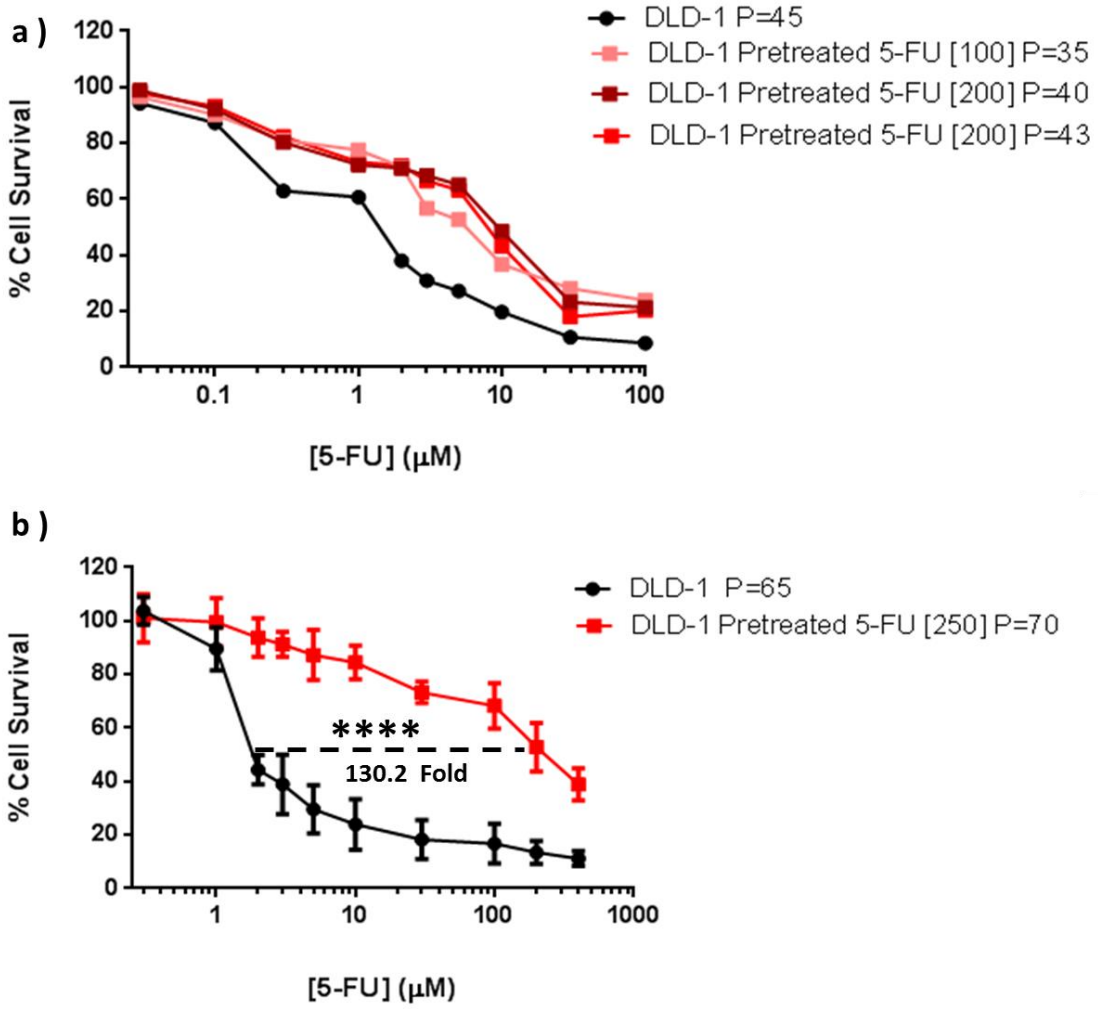

Figure 3.12: Chemosensitivity curve profiles for DLD-1. (a) Three independent chemosensitivity curve profiles for DLD-1 parent and DLD-1 pretreated with 5-FU cell line during establishment of DLD1 5-FU resistant subline (b) DLD-1 no pretreated cell lines and DLD-1 5-FU resistant subline with 5-FU during 70 generations were exposed to 5-FU [0.3-400 µM] doses during 96 h. MTT assays were performed in three independent experiments. Graphs show the cell survival of DLD-1 5-FU resistant subline against different 5-FU concentrations. The difference in IC_{50} among DLD-1 parent cell line and DLD-1 5-FU resistant subline was highly significant with 130.2-fold change (**** $p \leq 0.0001$). Error bars showing standard deviations between replicates are displayed too.

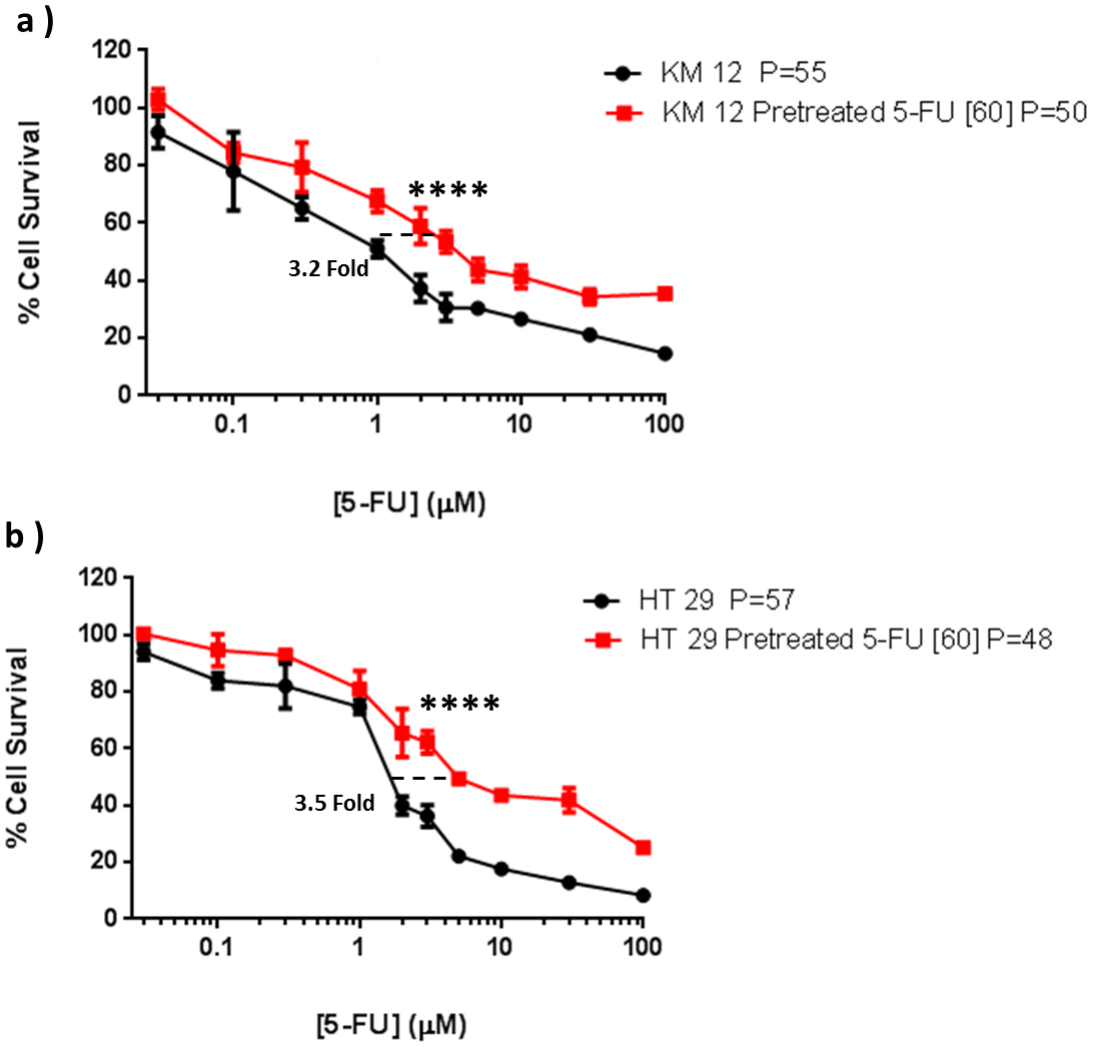

Figure 3.13: Chemosensitivity curve profiles for KM12 and HT 29. (a) KM 12 parent cell line and KM 12 5-FU resistant subline during 50 generations and (b) HT 29 parent cell line and HT 29 5-FU resistant subline with 5-FU during 48 generations were exposed to 5-FU [0.03-100 µM] doses during 96 h. MTT assays were performed in three independent experiments. Graphs show the cell survival of KM 12 and HT 29 pretreated and non-pretreated cell lines against different 5-FU concentrations. The difference in IC_{50} among parent cell line and resistant 5-FU sublines is highly significant in both experiments ($p \leq 0.0001$). A 3.2-fold change and a 3.5-fold change difference in IC_{50} were found in the KM 12 5-FU [60] and HT 29 5-FU [60] resistant sublines respectively (**** $p \leq 0.0001$). Error bars showing standard deviations between replicates are displayed too.

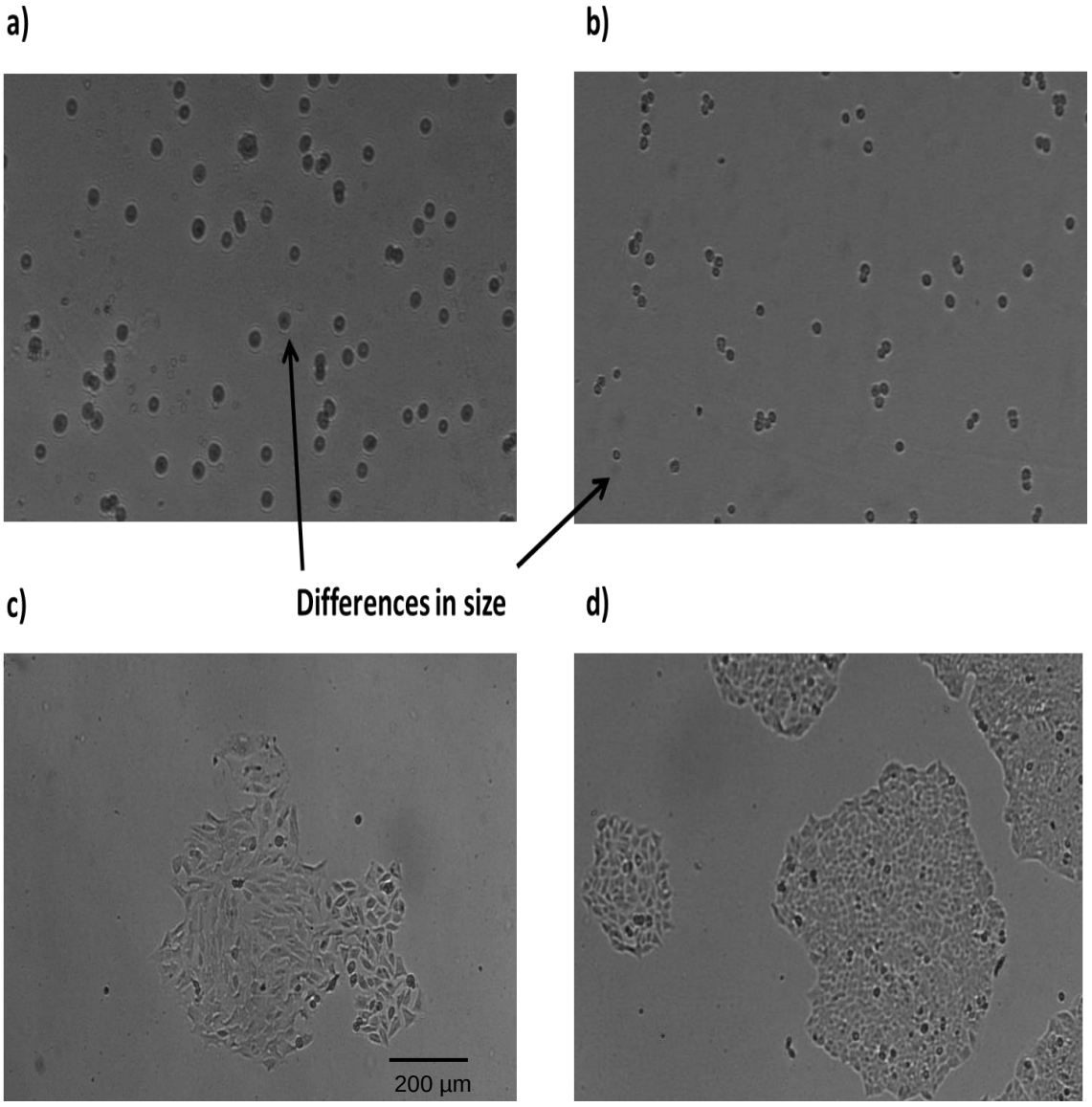

Figure 3.14: DLD-1 cells growth in normal media. In the upper part, freshly isolated cells from (a) DLD-1 5-FU resistant subline and (b) DLD-1 parent-control cell line. Difference in cells size is clear under the microscope. In the lower part, confluent monolayer clusters of (c) DLD-1 5-FU resistant subline cells showed colonies more tightly packed than for (d) DLD-1 parent-control cells growing in RPMI medium. Several colonies of CRC cells have attached and started to spread on the T25 flasks after four days. Scale Bar size = 200 µm.

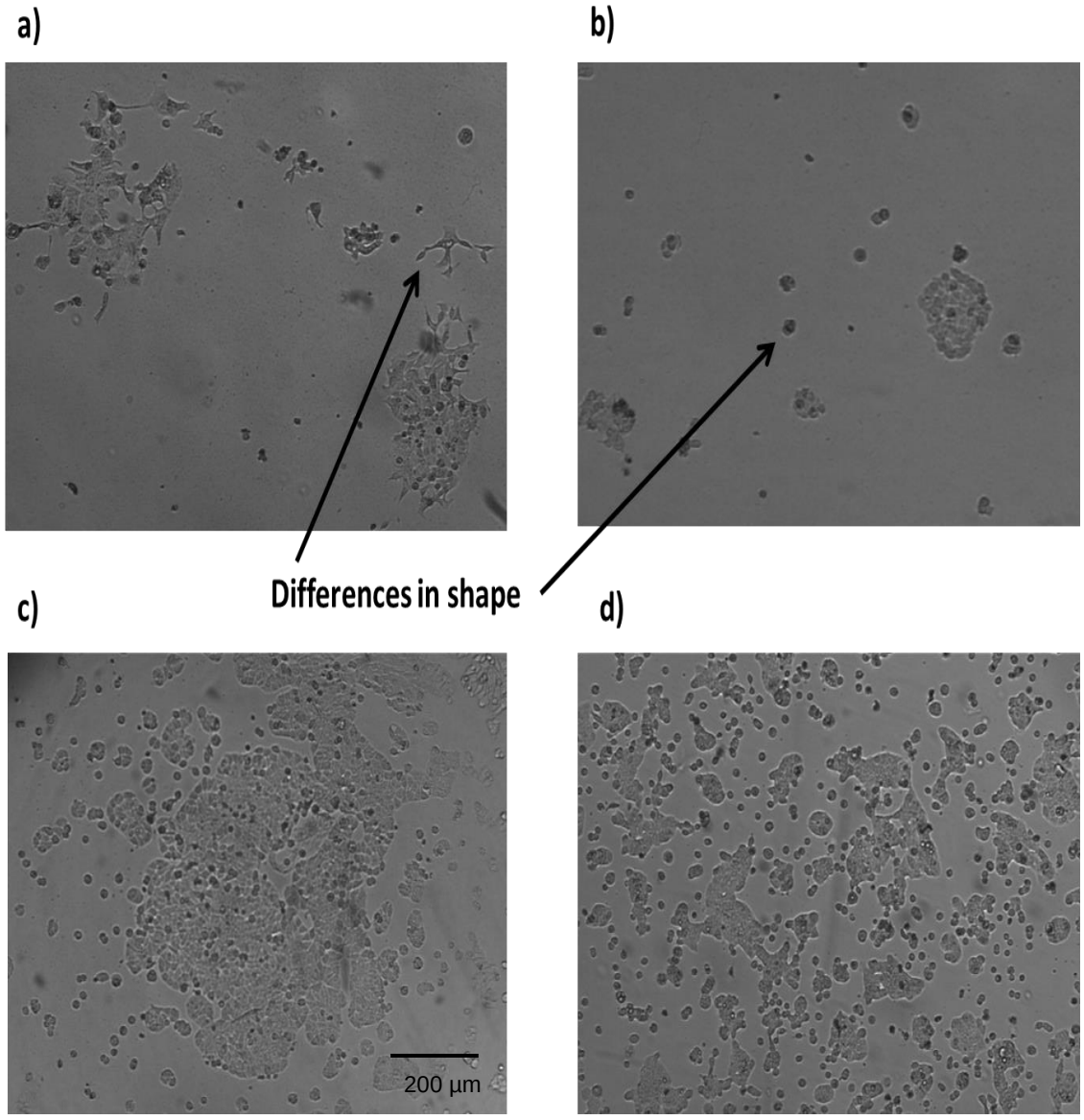

Figure 3.15: KM 12 and HT 29 cells growth in normal media. In the upper part, freshly isolated cells from (a) KM 12 5-FU resistant subline and (b) KM 12 parent cell line. Difference in cells shape is clear under the microscope. In the lower part, confluent monolayer clusters of (c) HT 29 5-FU resistant subline cells and (d) HT 29 control parent cells growing in RPMI medium on the T25 flasks after four days. Scale Bar size = 200 µm

3.3.2 Characterisation of cell growth for DLD-1, KM 12 and HT 29 resistant sublines to 5-FU

To confirm results obtained by MTT and to test if the number of passage of the flask could have some effect on the MTT assay, a growth curve analysis was

done for all resistant sublines to 5-FU established. Growth rate and capacity to proliferate was measured for resistant sublines (Fig. 3.16). Growth curves were done using an initial concentration of $1x10^4$ cells/ml. No significant differences in growth curve were found during the study of three resistant sublines to 5-FU.

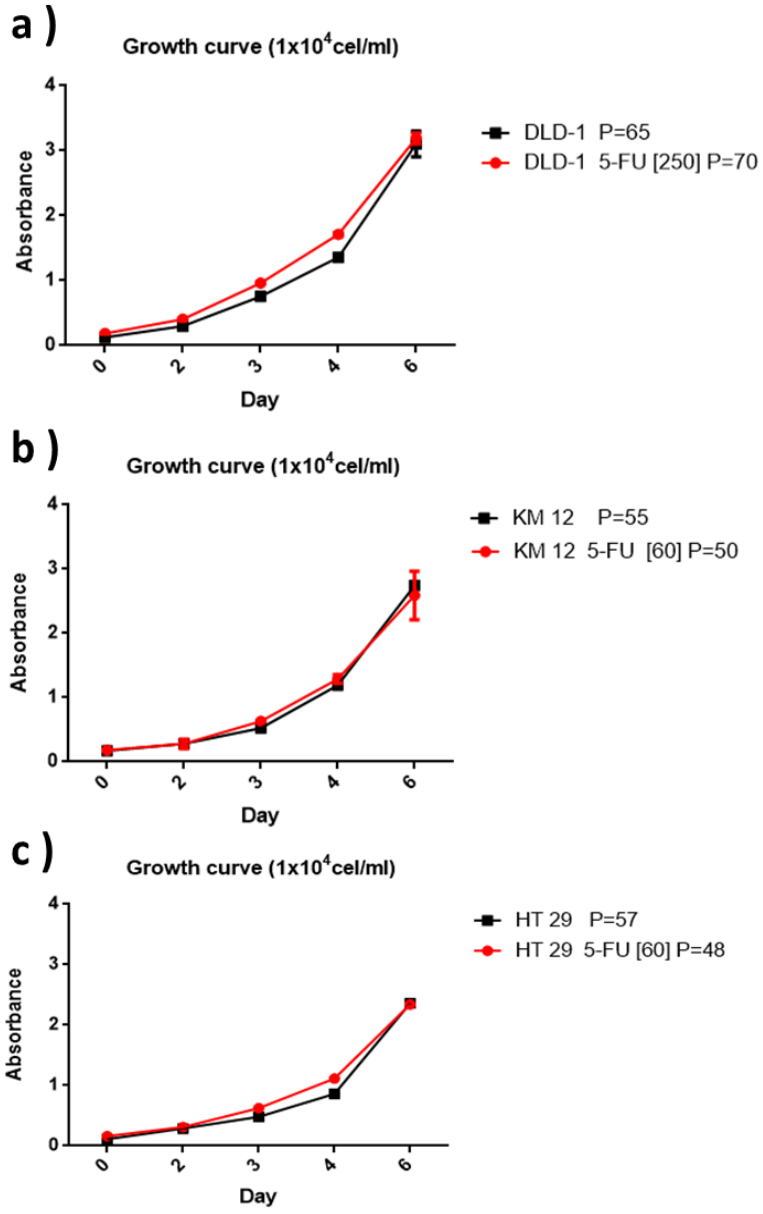

Figure 3.16: MTT Growth curve profiles. During 5 days of $1x10^4$ cells/ml concentrations seeded for (a) DLD-1 parent cell lines and DLD-1 5-FU resistant subline; (b) KM 12 parent cell lines and KM 12 5-FU resistant subline; (c) HT 29 parent cell lines and HT 29 5-FU resistant subline. No significant differences ($p>0.05$) were found in growth curve profiles between parent and resistant sublines during 5 days after.

3.3.3 Evaluation of cross-resistance in the DLD-1 5-FU subline by MTT

Cross-resistance is the capacity of cancer cells to withstand different drugs by one or more mechanisms of action like the increasing of ABC transporters, polyploidy, autophagy (see Chapter 1; section 1.3). Due to the lack of knowledge related to cross-resistance mechanisms in chemotherapy, a further study of collateral loss of sensitivity to eight chemotherapy agents used in CRC was carried out.

During the cross-resistance study, eight different standard agents were used covering a wide range of mechanisms of action and probably different mechanisms of resistance. The eight drugs were: 5-FU, OXA, IRI, carmustine, cisplatin, colchicine, doxorubicin, and paclitaxel. According to their different mechanisms of action, these drugs can be classified into three groups described in Chapter 1, section 1.2.3.

- Antimetabolites like 5-FU that acts as cell-cycle specific by interfering with synthesis of DNA and RNA (Tiwari 2012).

- Alkylating agents such as carmustine, cisplatin, and OXA that act during rest phase of the cell causing cross-links in DNA. So, they are cell cycle non-specific (Fu, Calvo et al. 2012).

- Plant alkaloids like colchicine, IRI, doxorubicin and paclitaxel that act at cell-cycle specific points. Colchicine and paclitaxel inhibit microtubule assembly (Bombuwala, Kinstle et al. 2006), whilst doxorubicin, and IRI are topoisomerase II and topoisomerase I inhibitors, respectively, that act during phases of cell division (Biondi, Fusco et al. 2013, Shi, Hui et al. 2014).

Evaluation of cross-resistance in DLD-1 5-FU and DLD-1 parent cell line was carried out by a chemosensitivity study using MTT assay as it has been described in Chapter 2, in sections 2.3.5 and 2.3.6.

None of the eight compounds studied showed such as spectacular differences in resistance as 5-FU. However, some fold changes in resistance were observed in some of the drugs tested. Without considering the resistance fold change to 5-FU, the highest fold change (2.6-fold) was found to OXA, but not to cisplatin, despite the fact that both agents have similar mechanisms of action (see Chapter 5, section 5.4.1). Additionally, a 2.3-fold change in resistance was observed to IRI and carmustine. A small 1.9-fold change was observed to Colchicine, whilst in doxorubicin, cisplatin, and paclitaxel no activity in resistance was found.

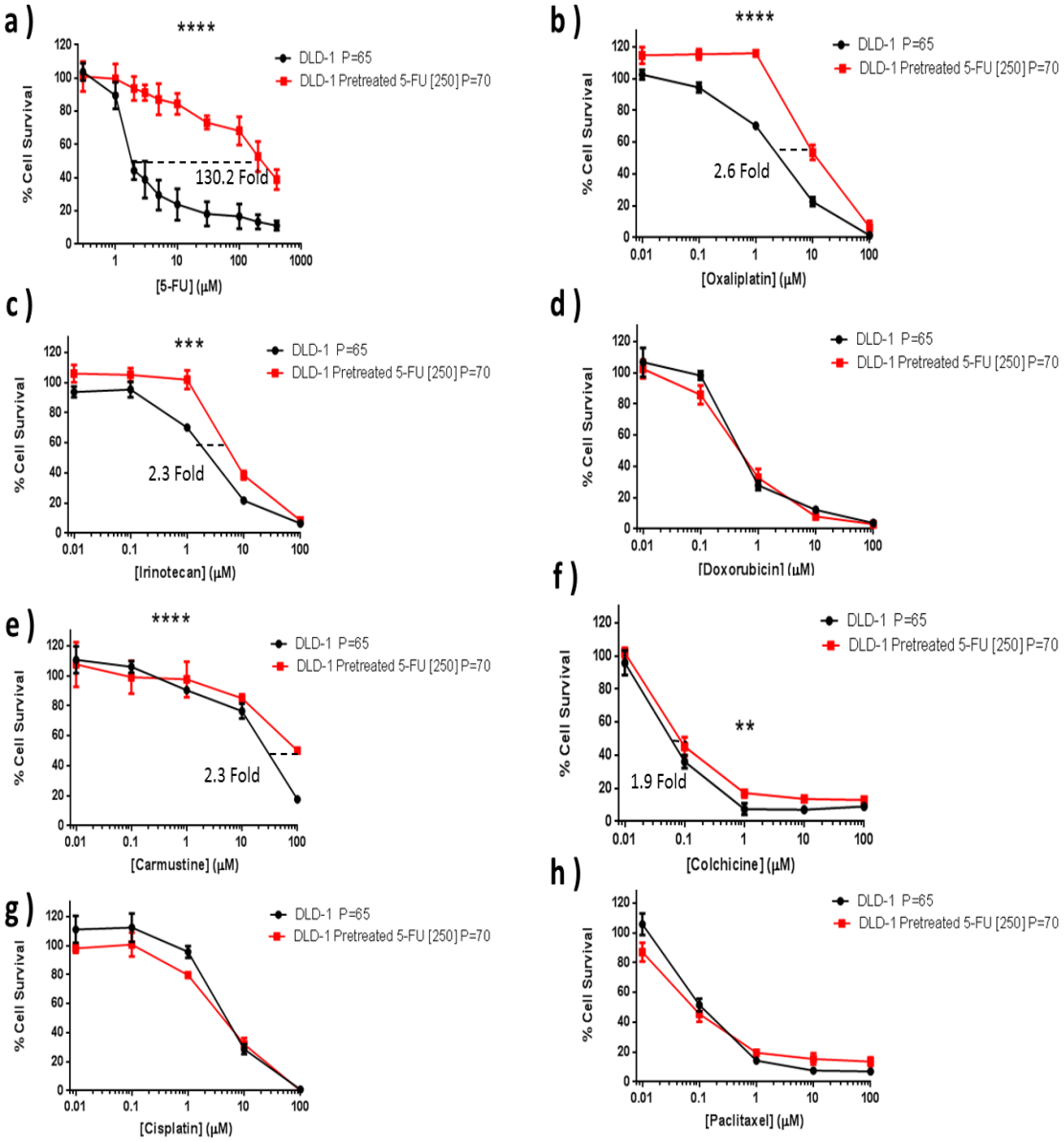

Figure 3.17: MDR profile conferred by DLD-1 5-FU resistant subline and DLD-1 parent cell line. The 96 h cytotoxicity assays were performed with eight different drugs: (a) 5-FU, (b) OXA, (c) IRI, (d) doxorubicin, (e) carmustine, (f) colchicine, (g) cisplatin and (h) paclitaxel. Curves are representative of separate experiments in triplicate. Relative resistance values were obtained by dividing the IC_{50} value of the resistant DLD-1 5-FU resistant subline by the IC_{50} value of the DLD-1 parent cell line. (*p≤0.05; ** p≤0.01; *** p≤0.001; ****p≤0.0001).

3.3.4 DLD-1 5-FU subline maintains tumourigenicity and drug resistant phenotype when grown *in vivo*

To further confirm the permanency of the acquired 5-FU drug resistance in the DLD-1 5-FU subline, the cells were implanted by subcutaneous injection in immunodeficient mice and treated with 5-FU.

It was observed that tumourigenicity was maintained in the DLD-1 5-FU [250] subline, although it appeared to grow slower than the DLD-1 parent cell line xenograft models (Figure 3.18 and Table 3.4), mirroring the *in vitro* findings.

In terms of response to 5-FU treatment, negligible toxicity was seen for both models with maximum bodyweight losses of 7% and 9% for DLD-1 parent cell line and DLD-1 5-FU resistant subline xenograft models respectively. For 5-FU treated groups, a significant ($p \leq 0.01$) delay of 4.6 days in tumour growth was seen for the DLD-1 parent line-derived xenografts, whilst DLD-1 5-FU resistant subline did not show any significant response ($p > 0.05$) (Fig. 3.18 and Table 3.4). This suggests that the resistant phenotype has been maintained *in vivo* and it can be used in future studies.

Cells injected	Treatment	Growth delay (days)	Significance	Maximun% weight loss
DLD-1 P=65	Untreated	-	-	3
DLD-1 P=65	5-FU	4.6	P<0.01	7 (day 3)
DLD-1 5-FU[250]	Untreated	-	-	1
DLD-1 5-FU[250]	5-FU	0	p>0.05 ns	9 (day 3)

Table 3.4: Results of xenograft mice models. Measures obtained for tumour growth and body weight in untreated mice and treated mice derived from DLD-1 5-FU and DLD-1 parent cell line. Development of xenograft models was done by Cooper PA under HO project licence number 40/3670.

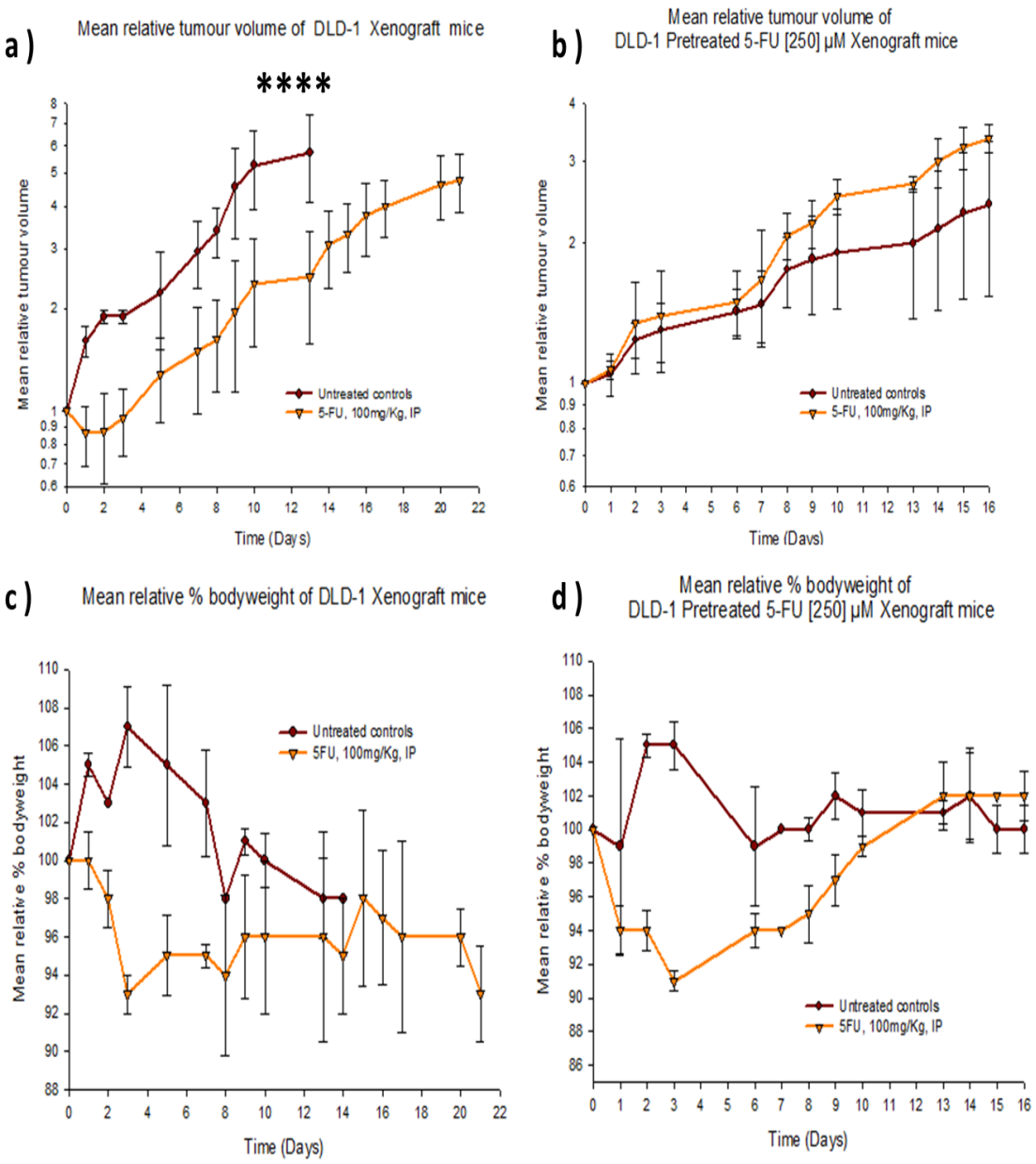

Figure 3.18: Relative tumour volume curves of xenograft mice were done with or without 5-FU treatment. (a) Significant differences were found in growth under treatment in xenograft models derived from DLD-1 parent cell line but (b) not in xenograft derived from DLD-1 5-FU, which showed resistance to the treatment. (c) Relative % bodyweight of mice bearing sensitive DLD-1 cells with or without 5-FU treatment and (d) relative % bodyweight of mice bearing resistant DLD-1 cells with or without 5-FU treatment. No significant differences were found in body weight.

3.3.5 Protein extraction and Bradford protein assays

Three independent Bradford assays were done for each cell lysate sample to calculate the volume required to obtain 200 μg of protein to be applied during proteomic analysis. Four examples of Bradford assays results are shown below (Fig. 2.8) and final protein amounts extracted from all samples is summarised in table 2.7.

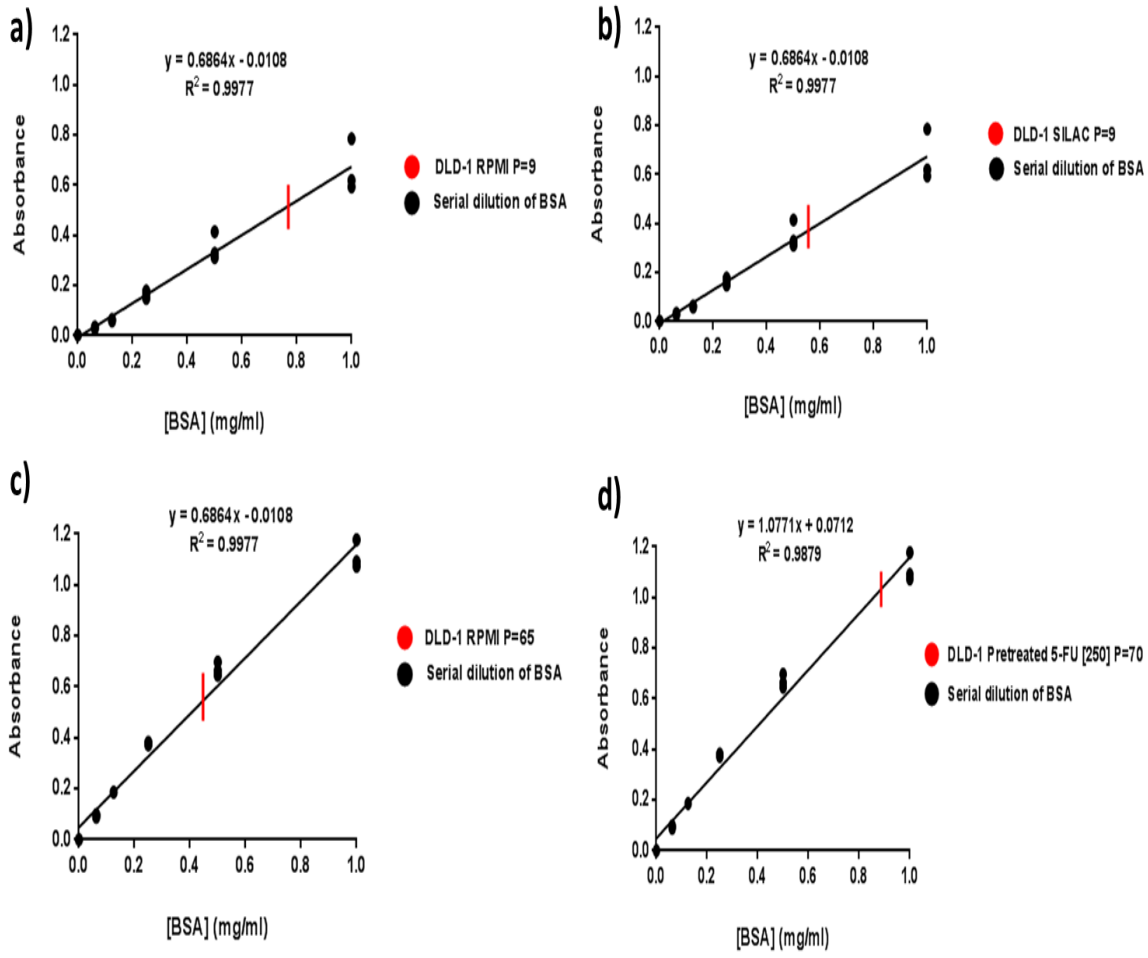

Figure 3.19: Examples of protein concentration measurements of 4 different cell lines. (a) DLD-1 RPMI P=9; (b) DLD-1 SILAC P=9; (c) DLD-1 RPMI P=65 and (d) DLD-1 5-FU [250] P=70 resistant subline by Bradford assay using BSA in a serial dilution (mg/ml). All samples were 40 fold diluted.

All initial samples were 40 fold diluted

Cell line Sample	Protein extracted µg	Volume required for Acetone ppt (200 µg of protein)
DLD-1 SILAC P=9 (Heavy sample)	4379.00	8.86 µl
DLD-1 RPMI P=9	5675.67	10.4 µl
DLD-1 RPMI P=65	1175.19	9.19 µl
DLD-1 5-FU [250] P=70	2790.00	6.74 µl
DLD-1 OXA [250] P=60	1720.17	10.92 µl
DLD-1 IRI [200] P=55	270.47	17.74 µl
KM 12 SILAC P=9 (Heavy sample)	5994.63	6.47 µl
KM 12 RPMI P=9	3756.26	7.66 µl
KM 12 RPMI P=55	3457.07	11.22 µl
KM 12 5-FU [60] P=50	2703.40	10.65 µl
KM 12 OXA [40] P=45	801.65	15.97 µl
HT 29 SILAC P=9 (Heavy sample)	7634.03	5.08 µl
HT 29 RPMI P=9	6590.00	5.89 µl
HT 29 RPMI P=57	3579.88	8.04 µl
HT 29 5-FU [60] P=48	3300.84	8.73 µl

Table 3.5: Summary table with the total amount of protein extracted from CRC cell lines. The volume required for 200 µg of protein that was used during proteomic analysis to combine in the single SILAC samples. P = passage number.

3.3.6 Identification of proteome changes in DLD-1, HT 29 and KM 12 resistant sublines to 5-FU using mass spectrometry by SILAC approach

Before starting the analysis of protein expression, the labelling incorporation efficiency was measured to avoid incomplete isotope labelling due to amino acid conversion problems that could affect quantification. After nine doublings, a small aliquot of proteins digested from SILAC cell lines was analysed to determine the efficiency of incorporation. In the three cases: DLD-1, KM 12 and HT 29 cell lines grown in SILAC achieved >98% incorporation of labelled amino acid into their proteins, as recommended in previous publications on this technique (Ong and Mann 2006, Waanders, Hanke et al. 2007). A figure with total number of labelled proteins identified in a small aliquot of SILAC sample is shown below.

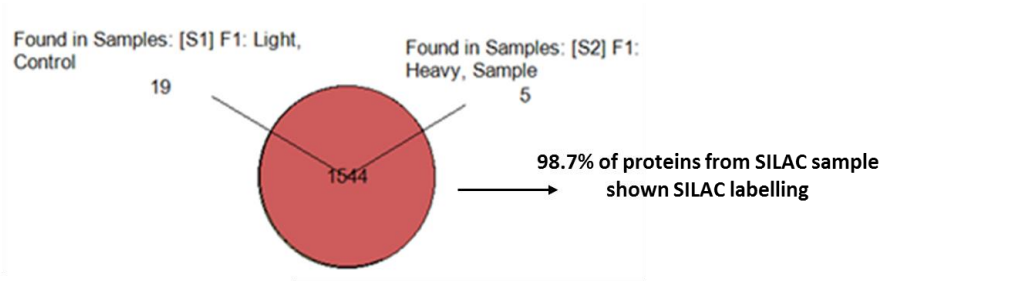

	Exclusive	Total	
	19	1563	Proteins identified containing light amino acids in SILAC sample
	5	1549	Proteins identified containing heavy amino acids in SILAC sample
	1544	1544	Proteins identified containing light and heavy amino acids in SILAC sample
Sum	1568		

Figure 3.20: Summary graph and table with labelling efficacy incorporation detected in a small aliquot of digested SILAC sample. SILAC achieved >98% incorporation of labelled amino acid into proteins.

Proteins from the complete 2DLC MS datasets were quantified as described in Chapter 3, section 3.2.5.6 and identified in at least two of three independent injections on the mass spectrometer in both heavy (labelled) and light (no labelled) samples. All proteins in each single SILAC experiment were quantified using the best three peptide-spectrum matches (PSMs) to define each master protein form. But if there were less than 3 PSMs identifying the protein, then the two best PSMs were used for quantification.

All proteins with a Mascot score less than 95% confidence were excluded from the list of identified proteins during single SILAC experiments. Lowest Mascot score used in single SILAC experiments was established by Mascot software for a 95 % confidence rate and these Mascot scores are summarized in Table 3.6.

Cell Line	DLD-1 P=9	DLD-1 P=65	DLD-1 5-FU	KM 12 P=9	KM 12 P=55	KM 12 5-FU	HT 29 P=9	HT 29 P=57	HT 29 5-FU
Mascot Score	>31	>30	>31	>28	>28	>28	>28	>28	>28

Table 3.6: Lowest Mascot scores used during proteomics analysis for single SILAC experiment samples during identification of altered proteins in 5-FU response.

From the full profiling of passage controls, SILAC controls and resistant cell lines a total of $3x10^7$ MS/MS (product ions), $6.5x10^6$ PSMs, $1.1x10^5$ peptides and 57450 proteins were obtained. Each single resistant cell line result was compared to its low and long generation control to form the multi SILAC dataset. Multi SILAC datasets were used to identify: (a) proteins commonly identified and (b) those proteins significantly changed due to resistance.

The total number of proteins quantified in three multi SILAC datasets for 5-FU were similar, with the total number of commonly quantified proteins shown in the centre (Fig. 3.21). For complete protein lists identities see Appendix Proteomics results in CD along with this thesis.

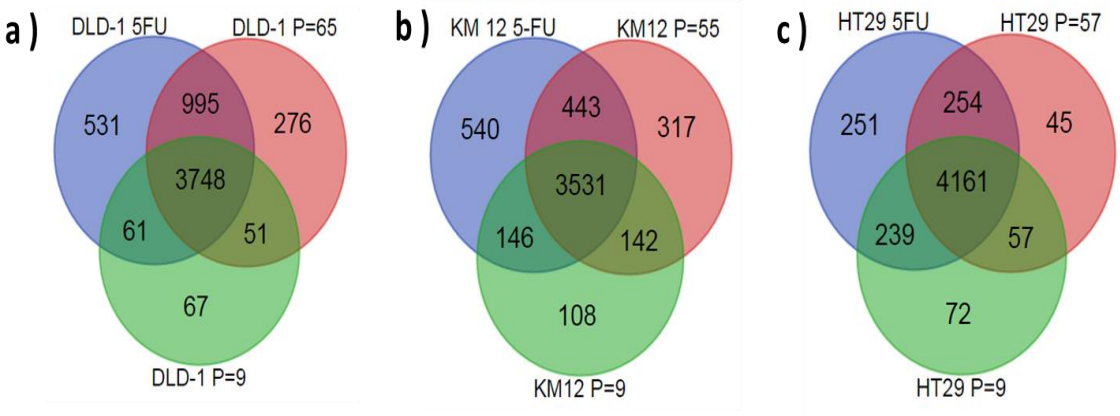

Figure 3.21:Venn diagrams results of multi SILAC datasets in 5-FU. The number of proteins commonly quantified between the two parent cell lines of (a) DLD-1; (b) KM 12; (c) HT 29 with a high and a low number of passages and in their respective drug-resistant sublines to 5-FU.

3.3.7 Protein quantification and results of the MS analysis

Analysis of proteomics data was performed as described in sections 3.2.5.7 and 3.2.5.8. This process requires normalization and transformation of single SILAC experiment raw data, followed by multi SILAC dataset (Fig 3.21) analyses using (a) a LIMMA algorithm in "R" software and (b) Cluster analysis. Finally, STRING, EnrichNet and GO data analysis platforms were used to identify the most significant altered proteins found in resistant sublines.

3.3.7.1 Raw data normalization and transformation

Initially, median normalization was performed to remove systematic biases from the data before statistical methods are applied (see Proteomic results included in CD Appendix). Normalization was followed by Log_2 transformation of the normalized SILAC-ratio data, to enable cross-experiment comparison between different SILAC experiments. Frequency distributions of commonly quantified proteins were plotted in Figure 3.22. Distribution of Log_2 SILAC-ratio proteins in resistant sublines exceeded parent cell lines proteins distribution. This difference in data distribution may be presumably caused by drug effects, these trends were observed in the multi SILAC datasets. Surprisingly, KM 12 5-FU multi SILAC dataset showed a more extended proteins distribution than DLD-1 5-FU dataset, which contrary showed a higher resistance fold change

during MTT assays (Fig. 3.12b and Fig. 3.13). This difference may be attributed to the type of altered proteins in different resistant sublines. Although DLD-1 5-FU subline shows a lower number of altered proteins than KM 12 5-FU, proteins altered in DLD-1 5-FU may be directly involved in 5-FU response, while altered proteins in KM 12 5-FU may not taking part in 5-FU response.

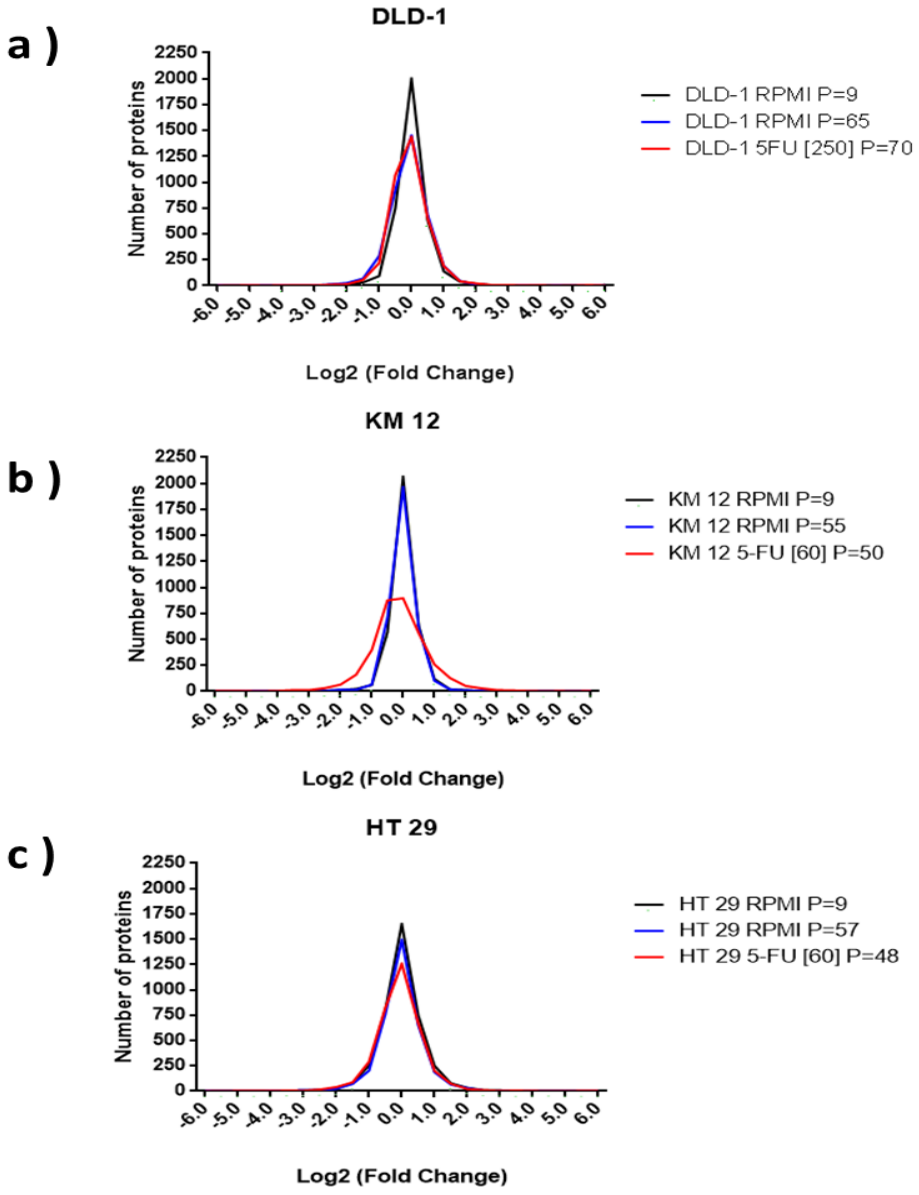

Figure 3.22: A histogram view of superimposed fold change distributions of the total number of proteins commonly quantified in resistant sublines to 5-FU. (a) DLD-1, (b) KM 12 and (c) HT 29 compared with their respective parent and sensitive cell lines after Log_2-transformation and normalisation of experimental SILAC-ratio data (L/H).

3.3.7.2 R-LIMMA analysis

5-FU Multi SILAC datasets were analysed by R, using LIMMA. A fold change and its associated p-value were calculated for each protein according to their significant difference in ratio expressions between the resistant subline and its two related control parent cell lines (with a high and a low number of passages).

This information was summarized in a Volcano plot of LIMMA-modelled proteomics data (Fig. 3.23). Volcano plots summarise all proteins commonly quantified in 5-FU resistant sublines compared to parent cell lines. The data for all proteins commonly quantified were plotted as normalized Log_2 fold change versus the $-Log_{10}$ of the adjusted p-value. Orange dot line is at p=0.05 and proteins above it represent significantly altered proteins in resistant sublines. Red and green dots represent up- and down-regulated proteins respectively, with FDR adjusted p<0.001. Vertical black dot lines are positioned at 1 and -1, corresponding to 2-fold change in up-regulated and down-regulated proteins respectively. A summary table containing significantly altered proteins from Volcano plots is shown below.

Resistant cell lines to 5-FU	Significant Up-regulated Proteins	Significant Down-regulated Proteins	Percentage of Significantly Altered proteins
DLD-1	105	112	5,79%
KM 12	301	419	20.39%
HT 29	32	89	3.42%

Table 3.7: Significantly up-regulated (Fold change ≥ 2) and down-regulated (Fold change ≤ 2) proteins in resistant cell lines to 5-FU.

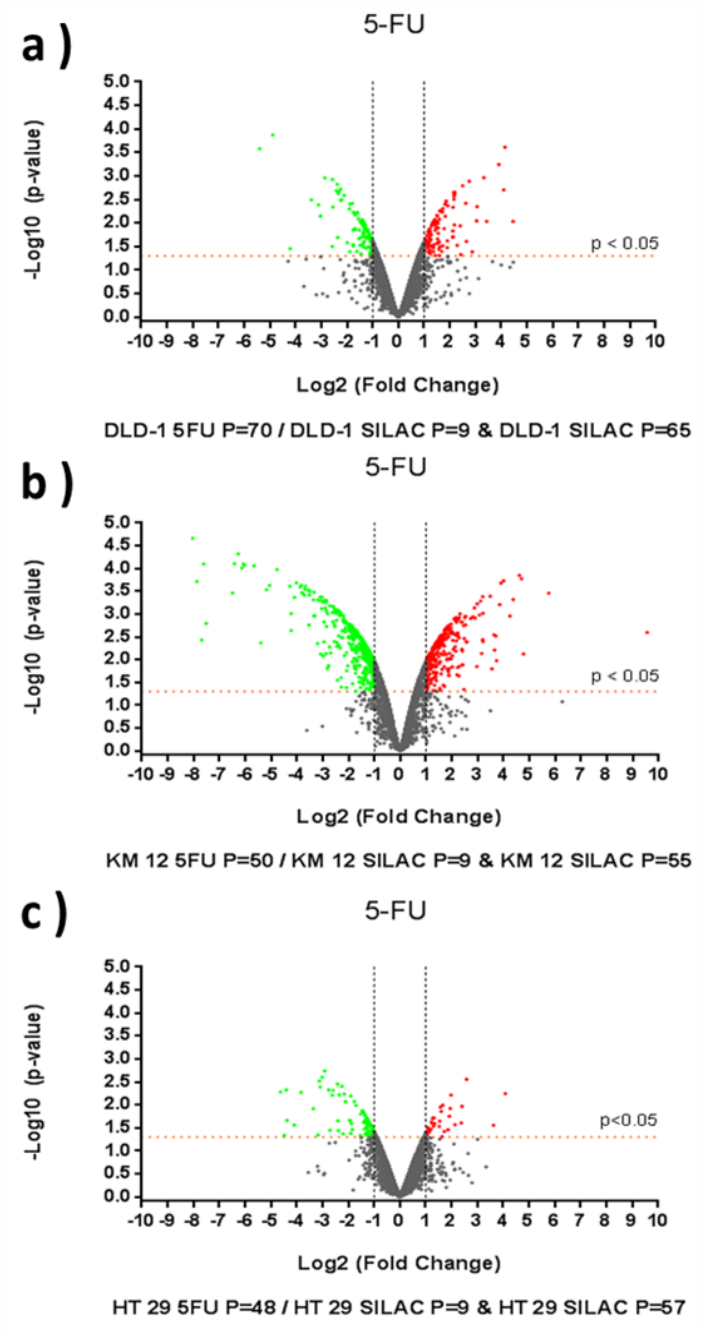

Figure 3.23: Volcano plots showing the distribution of significantly down- and up-regulated proteins following LIMMA modelling in 5-FU multi SILAC datasets. Criteria for significance are a 2-fold change for the (a) DLD-1 5-FU, (b) KM 12 5-FU, and (c) HT 29 5-FU sublines compared to the parent data, with $p<0.05$. Key: Red-Upregulated, Green – Downregulated proteins, Grey-Unaltered and non-significant proteins.

Log_2 fold changes and their respective p-value were calculated using LIMMA. However, fold change calculated is a measure of how much the abundance of commonly quantified proteins differs from initial parent cell lines to a final protein value in resistant sublines. This measure does not differentiate how significant the fold change is, estimated from a biological point of view. So, a further clustering classification was done based on the highest group of proteins altered just in resistant sublines but not in parent cell lines. Proteins of each sample were ordered from the highest to the lowest according all normalized Log_2 ratio data from SILAC results.

3.3.7.3 Cluster analysis

Cluster analysis using a 5^{th} percentile threshold was performed (as described in section 3.2.5.7), for 5-FU multi SILAC datasets (Table. 3.8). Of the 27 possible different response combinations, the largest group for each cell line was the group “NNN” containing unaltered proteins under any of the 3 conditions. Encouragingly the smallest groups of proteins were those exhibited apparent sporadic response combinations (for example group “ DNU”). Relevant proteins for discussion were obtained from clusters of proteins that only were increased or decreased in 5-FU resistant sublines with no change in SILAC and passage controls (NNU and NND). These proteins are shown in Figure 3.24, along with the unchanged NNN clusters.

The significantly altered proteins in DLD-1 5-FU, KM 12 5-FU and HT 29 5-FU resistant sublines are shown in Tables 3.9 - 3.14.

Status in Parent cell line with Low Passage	Status in Parent cell line with High Passage	Status in 5-FU Resistant Subline	Status Sum-up	Number of proteins in Set DLD-1	Number of proteins in Set KM 12	Number of proteins in Set HT 29
D	D	D	DDD	18	5	27
D	D	N	DDN	32	29	14
D	D	U	DDU	6	7	1
D	N	D	DND	9	12	23
D	N	N	DNN	99	107	98
D	N	U	DNU	12	7	1
D	U	D	DUD	1	1	1
D	U	N	DUN	8	6	6
D	U	U	DUU	2	3	6
N	D	D	NDD	30	8	37
N	D	N	NDN	92	107	94
N	D	U	NDU	7	10	2
N	N	D	NND	113	133	80
N	N	N	NNN	2930	2686	2797
N	N	U	NNU	91	113	68
N	U	D	NUD	3	9	3
N	U	N	NUN	81	94	61
N	U	U	NUU	27	17	38
U	D	D	UDD	1	1	2
U	D	N	UDN	1	7	0
U	D	U	UDU	0	3	0
U	N	D	UND	11	5	3
U	N	N	UNN	96	104	92
U	N	U	UNU	13	10	18
U	U	D	UUD	1	3	1
U	U	N	UUN	35	37	18
U	U	U	UUU	29	7	43
			TOTAL	3748	3531	3534

Table 3.8: Thresholds for protein status in 5-FU multi SILAC datasets were established using a 5th percentile criteria. From the column of "Status Sum-up" in the table, only the proteins which remain as unaltered (brown) in both parent cell lines and with an altered status (green or red) in the resistant subline were considered to be studied as altered proteins involved in drug-resistance.

DLD-1 5-FU

Cluster analysis for DLD-1 5-FU resistant subline showed similar results to those observed during “R” LIMMA analysis (see Fig. 3.23a). The highest number of proteins remain unaltered in both parent cells lines, whilst DLD-1 5-FU shows a high symmetry in (a) up- and (b) down-regulated proteins fold change dispersion.

Detailed results for significantly altered proteins in DLD-1 5-FU resistant subline are summarized in Tables 3.9 and 3.10. Log_2 SILAC results for DLD-1 5-FU / DLD-1 SILAC P=9 ratio and p-values from R analysis of resistant and control cell lines are included.

a)

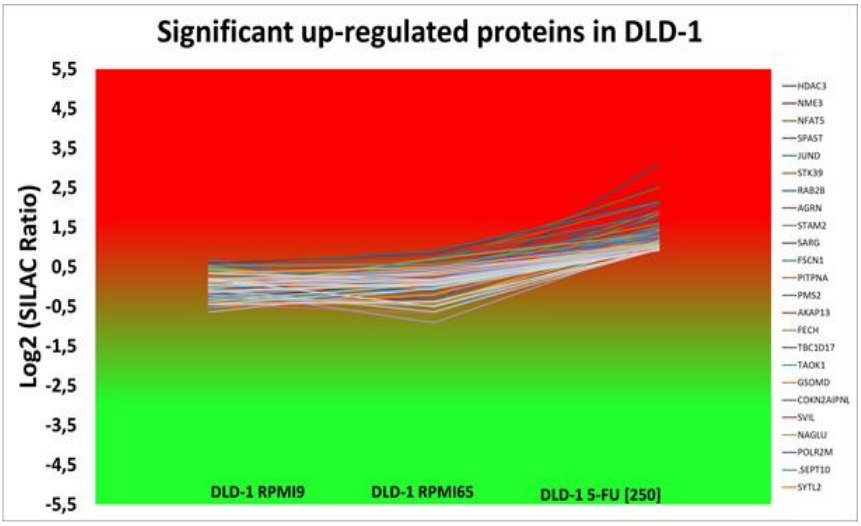

b)

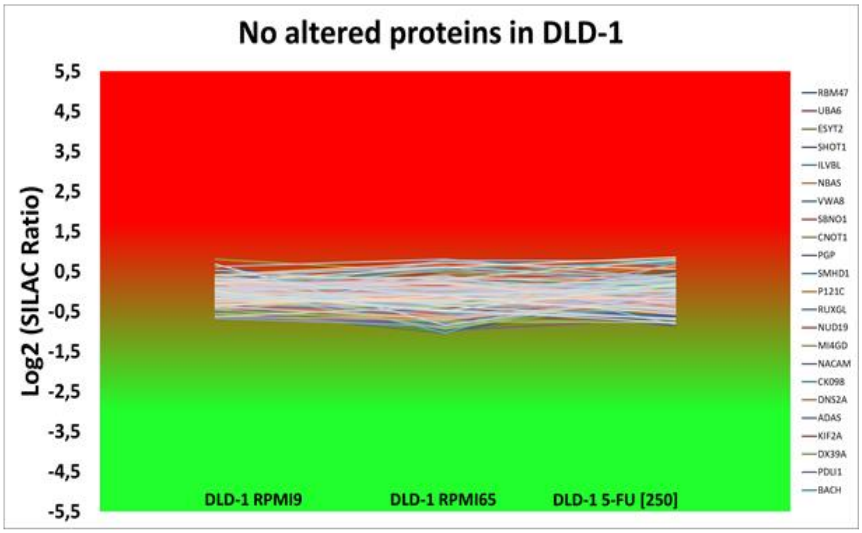

c)

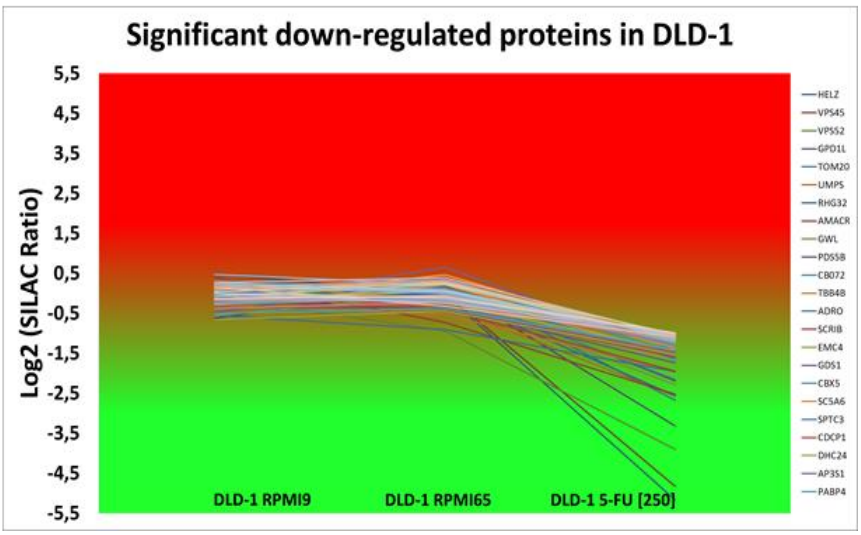

Figure 3.24: Cluster analysis for DLD-1. Proteins were classified using 5th percentile threshold for significantly (a) up-regulated proteins; (b) unaltered proteins; (c) down-regulated proteins in DLD-1 5-FU and unaltered in sensitive parent-control cell lines DLD-1 P=9 and DLD-1 P=65.

N	Protein name	AC. number	MW [kDa]	SC %	PSMs	Unique Peptides	Score Mascot	Normalized Log2 Ratio: L/H	p-value
1	HDAC3	O15379	48.8	12.6	4	3	54	3.11	0.001
2	NME3	Q13232	19.0	10.1	4	1	84	2.64	0.001
3	NFAT5	O94916	165.7	9.1	25	7	605	2.51	0.005
4	SPAST	Q9UBP0	67.2	11.9	26	4	266	2.18	0.010
5	JUND	P17535	35.2	24.2	8	4	217	2.15	0.014
6	STK39	Q9UEW8	59.4	26.8	58	6	758	2.13	0.008
7	RAB2B	Q8WUD1	24.2	43.1	92	2	1159	2.08	0.002
8	AGRN	O00468	217.1	19.3	92	20	1344	1.91	0.024
9	STAM2	O75886	58.1	13.3	19	4	250	1.90	0.003
10	C1orf116	Q9BW04	63.9	31.3	67	10	846	1.83	0.002
11	FSCN1	Q16658	54.5	55.2	235	20	3488	1.83	0.060
12	PITPNA	Q00169	31.8	35.9	52	6	685	1.82	0.003
13	LOC107984056	P54278	95.7	3.8	10	2	113	1.74	0.008
14	AKAP13	Q12802	307.4	22.1	109	30	1148	1.64	0.035
15	FECH	P22830	47.8	40.4	80	11	463	1.59	0.016
16	TBC1D17	Q9HA65	72.7	7.6	9	2	158	1.56	0.004
17	TAOK1	Q7L7X3	116.0	11.3	38	6	196	1.52	0.013
18	GSDMD	P57764	52.8	34.7	67	11	643	1.50	0.007
19	CDKN2AIPNL	Q96HQ2	13.2	31.0	8	2	163	1.48	0.084
20	SVIL	O95425	247.6	17.2	109	23	1035	1.47	0.025
21	NAGLU	P54802	82.2	26.9	61	12	561	1.45	0.038
22	POLR2M	Q6EEV4	15.1	25.0	21	2	417	1.44	0.089
23	SEPTIN10	Q9P0V9	52.6	55.1	189	19	2328	1.43	0.010
24	SYTL2	Q9HCH5	104.9	27.2	99	17	626	1.42	0.004
25	APP	P05067	86.9	24.8	103	14	1122	1.39	0.009
26	Hsp40	Q96KC8	63.8	13.7	31	5	512	1.39	0.004
27	EIF2AK4	Q9P2K8	186.8	7.4	22	7	340	1.34	0.091
28	ROMO1	P60602	8.2	21.5	26	1	674	1.34	0.021
29	GALK1	P51570	42.2	42.1	105	12	1801	1.30	0.053
30	RNF13	O43567	42.8	18.4	7	3	49	1.27	0.029
31	PIK3C2A	O00443	190.6	12.2	59	14	484	1.25	0.038
32	IGF2BP3	O00425	63.7	36.8	162	13	2216	1.24	0.016
33	MAN2B1	O00754	113.7	19.7	67	13	658	1.23	0.047
34	GGT1	P19440	61.4	16.9	42	7	524	1.23	0.076
35	DDAH2	O95865	29.6	36.5	32	6	405	1.18	0.022
36	UBE3C	Q15386	123.8	19.3	39	12	350	1.17	0.010
37	CNOT10	Q9H9A5	82.3	15.9	37	7	297	1.17	0.034
38	ITGA3	P26006	116.5	15.6	100	11	1338	1.16	0.006
39	RABL3	Q5HYI8	26.4	22.0	13	3	142	1.16	0.007
40	NOL3	O60936	22.6	60.6	42	7	781	1.12	0.029
41	GOPC	Q9HD26	50.5	34.6	67	10	619	1.11	0.058
42	PAWR	Q96IZ0	36.5	36.2	67	10	1184	1.11	0.072
43	PRKCD	Q05655	77.5	7.5	14	3	158	1.10	0.034
44	CORO7	P57737	100.5	28.6	64	12	864	1.09	0.028

45	AMDHD2	Q9Y303	43.7	37.4	46	8	324	1.09	0.047
46	TMED4	Q7Z7H5	25.9	25.1	48	3	428	1.09	0.036
47	ASPH	Q12797	85.8	30.7	156	15	1983	1.09	0.011
48	CCDC53	Q9Y3C0	21.2	26.3	13	3	264	1.07	0.024
49	LOC102724023	P30042	28.2	36.9	87	6	665	1.05	0.029
50	DCTN3	O75935	21.1	10.8	14	1	298	1.04	0.037
51	CHURC1	Q8WUH1	16.1	28.1	18	3	178	1.04	0.030
52	VPS16	Q9H269	94.6	17.5	45	8	266	1.00	0.050
53	SYNRG	Q9UMZ2	140.6	13.2	46	11	757	1.00	0.035
54	HIP1	O00291	116.1	21.2	88	16	1202	1.00	0.068
55	TRIP4	Q15650	66.1	22.0	27	6	201	0.98	0.089
56	MYADM	Q96S97	35.3	7.1	23	1	625	0.97	0.064
57	DOCK6	Q96HP0	229.4	8.7	38	10	489	0.95	0.066
58	INF2	Q27J81	135.5	41.3	366	35	5976	0.94	0.031
59	VPS36	Q86VN1	43.8	29.3	40	9	196	0.94	0.031
60	ACADVL	P49748	70.3	49.8	249	26	4775	0.93	0.010
61	SEC24D	O94855	112.9	24.4	59	14	450	0.93	0.026
62	ACSF3	Q4G176	64.1	17.9	25	6	260	0.93	0.077
63	DYNLT3	P51808	13.1	35.3	29	2	623	0.93	0.034
64	ARMCX3	Q9UH62	42.5	18.7	29	5	554	0.92	0.048

Table 3.9: Results of high SILAC-ratios for single SILAC DLD-1 5-FU experiment. p-value from multi SILAC dataset analysed by LIMMA is included.

N	Protein name	AC. number	MW [kDa]	SC %	PSMs	Unique Peptides	Score Mascot	Normalized Log2 Ratio: L/H	p-value
1	HELZ	P42694	218.8	7.2	16	7	166	-5.17	0.000
2	VPS45	Q9NRW7	65.0	11.9	30	6	377	-4.83	0.000
3	VPS52	Q8N1B4	82.2	16.7	25	7	264	-3.91	0.003
4	GPD1L	Q8N335	38.4	8.8	13	2	565	-3.32	0.004
5	TOMM20	Q15388	16.3	17.2	9	2	122	-2.68	0.001
6	UMPS	P11172	52.2	40.4	79	12	1367	-2.57	0.002
7	ARHGAP32	A7KAX9	230.4	19.5	76	19	956	-2.56	0.001
8	AMACR	Q9UHK6	42.4	26.7	47	6	600	-2.53	0.020
9	MASTL	Q96GX5	97.3	9.3	10	4	180	-2.29	0.002
10	PDS5B	Q9NTI5	164.6	8.6	26	6	226	-2.20	0.002
11	C2orf72	A6NCS6	30.5	11.9	11	2	85	-2.16	0.002
12	TUBB4B	P68371	49.8	73.0	4561	1	66661	-1.97	0.008
13	FDXR	P22570	53.8	38.9	75	12	770	-1.96	0.021
14	SCRIB	Q14160	174.8	20.5	99	17	817	-1.95	0.007
15	EMC4	Q5J8M3	20.1	22.4	15	4	202	-1.76	0.020
16	RAP1GDS1	P52306	66.3	23.9	50	9	1010	-1.75	0.009
17	CBX5	P45973	22.2	44.0	72	5	1668	-1.67	0.004

18	SLC5A6	Q9Y289	68.6	3.8	6	2	138	-1.65	0.013
19	SPTLC3	Q9NUV7	62.0	6.0	3	2	58	-1.63	0.006
20	CDCP1	Q9H5V8	92.9	13.5	53	10	278	-1.59	0.014
21	DHCR24	Q15392	60.1	22.1	98	10	849	-1.53	0.032
22	AP3S1	Q92572	21.7	7.8	18	1	239	-1.51	0.045
23	PABPC4	Q13310	70.7	36.2	385	10	7754	-1.51	0.006
24	HAS1	Q92839	64.8	1.4	12	1	281	-1.51	0.006
25	WDR18	Q9BV38	47.4	14.4	30	5	340	-1.50	0.014
26	SLC3A2	P08195	68.0	46.8	344	24	6878	-1.48	0.026
27	TEX10	Q9NXF1	105.6	8.4	45	5	367	-1.43	0.016
28	MYD88	Q99836	33.2	25.0	7	4	46	-1.43	0.040
29	CLPTM1	O96005	76.0	16.1	38	6	924	-1.41	0.028
30	H2AFY2	Q9P0M6	40.0	10.2	79	1	511	-1.37	0.025
31	HMGCS1	Q01581	57.3	53.5	247	18	3706	-1.32	0.009
32	SMARCD2	Q92925	58.9	24.7	34	7	280	-1.26	0.016
33	AP3B1	O00203	121.2	15.5	106	13	1119	-1.26	0.019
34	PELP1	Q8IZL8	119.6	19.6	121	13	1093	-1.25	0.020
35	CGN	Q9P2M7	136.3	11.6	53	8	495	-1.23	0.024
36	TAMM41	Q96BW9	51.0	19.5	29	6	177	-1.21	0.033
37	P4HA2	O15460	60.9	18.9	51	6	644	-1.21	0.019
38	ACSL4	O60488	79.1	19.1	33	7	435	-1.21	0.036
39	AGO1	Q9UL18	97.2	13.9	26	4	176	-1.20	0.019
40	AP3M1	Q9Y2T2	46.9	33.3	50	8	597	-1.18	0.026
41	RPL7L1	Q6DKI1	28.6	14.2	13	3	168	-1.18	0.013
42	MYBBP1A	Q9BQG0	148.8	24.5	174	27	1908	-1.15	0.012
43	NDUFAF3	Q9BU61	20.3	19.0	9	3	67	-1.15	0.009
44	LBP-1a	Q9NZI7	60.5	6.5	40	1	593	-1.14	0.010
45	TCTN3	Q6NUS6	66.1	1.3	2	1	37	-1.13	0.020
46	PTPN6	P29350	67.5	27.9	41	10	281	-1.12	0.029
47	LARP1	Q6PKG0	123.4	26.7	94	14	780	-1.10	0.013
48	EMC8	O43402	23.8	36.2	49	5	467	-1.10	0.049
49	TRIM28	Q13263	88.5	58.3	675	29	9525	-1.07	0.016
50	MINA	Q8IUF8	52.8	18.1	33	7	254	-1.06	0.010
51	AK6	Q9Y3D8	20.0	14.5	9	2	177	-1.02	0.019
52	PMPCA	Q10713	58.2	29.1	116	11	964	-1.01	0.044
53	TKT	P29401	67.8	47.0	659	20	10387	-1.01	0.031
54	ATP1B3	P54709	31.5	32.6	83	8	882	-0.99	0.035

Table 3.10: Results of low SILAC-ratios for single SILAC DLD-1 5-FU experiment. p-value from multi SILAC dataset analysed by LIMMA is included.

KM 12 5-FU

Cluster analysis results for KM 12 5-FU are shown in Figure 3.25. Detailed results for significantly altered proteins in KM 12 5-FU resistant subline are summarised in Tables 3.11 and Table 3.12. Log_2 SILAC results for KM 12 5-FU / KM 12 SILAC P=9 ratio and p-values from R analysis of resistant and control cell lines are included.

Cluster analysis for KM 12 5-FU resistant subline showed similar results to those observed during “R” LIMMA analysis (see Fig. 3.23b). The highest number of proteins remain unaltered in both parent cells lines, whilst KM 12 5-FU shows a higher number of down-regulated proteins than up-regulated proteins.

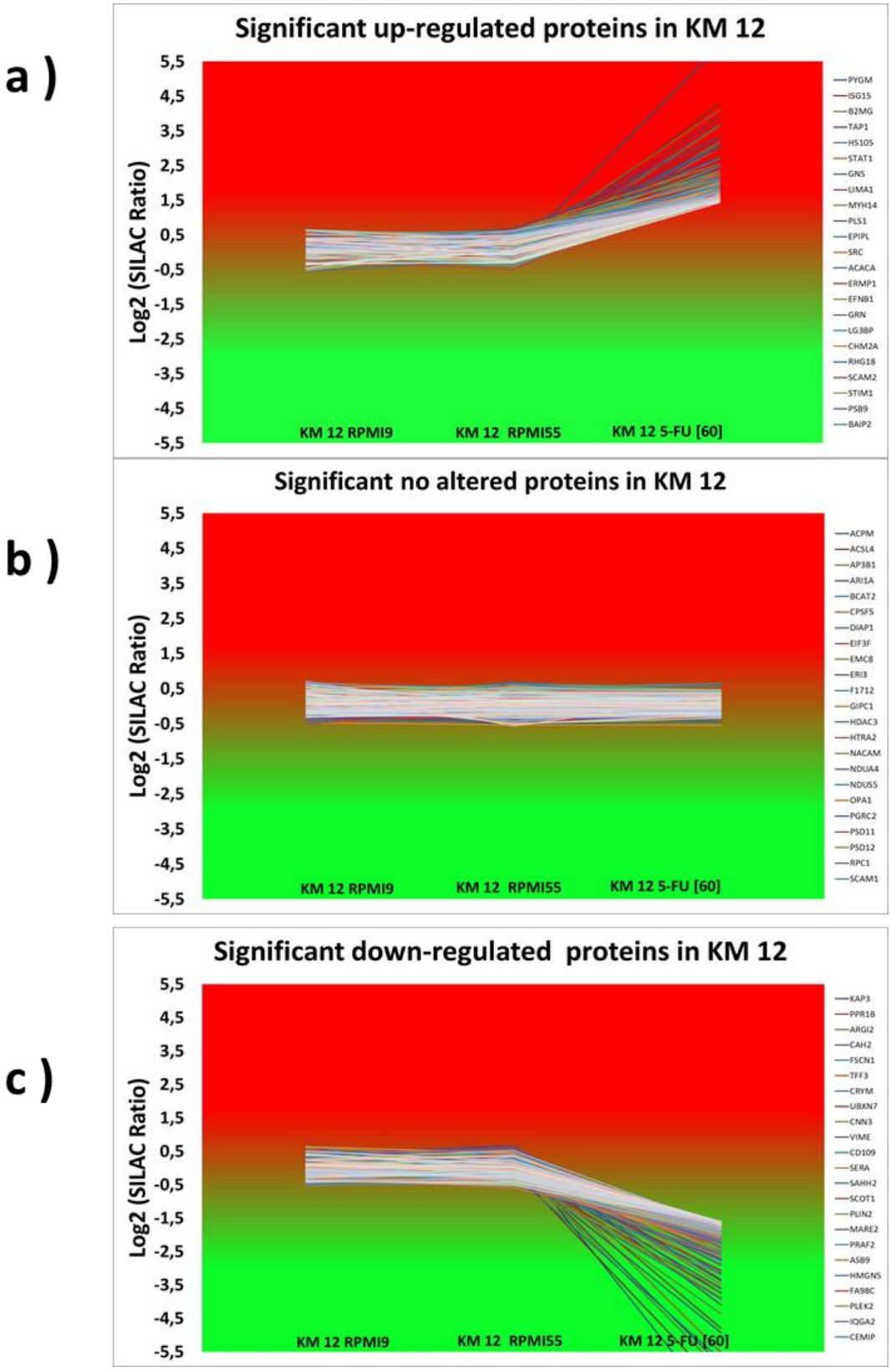

Figure 3.25: Cluster analysis for KM 12. Proteins were classified using 5th percentile threshold for significantly (a) up-regulated proteins; (b) unaltered proteins; (c) down-regulated proteins in KM 12 5-FU and unaltered in sensitive parent-control cell lines KM 12 P=9 and KM 12 P=55.

N	Protein name	AC. number	MW [kDa]	SC %	PSMs	Unique Peptides	Score Mascot	Normalized Log2 Ratio: L/H	p-value
1	PYGM	P11217	97.0	17.8	159	2	1686	5.95	-
2	ISG15	P05161	17.9	44.8	117	7	1764	4.30	0.006
3	B2M	P61769	13.7	47.1	46	4	526	4.11	0.003
4	TAP1	Q03518	87.2	24.8	65	10	1193	3.91	0.008
5	Hsp110	Q92598	96.8	47.7	261	33	4315	3.70	0.000
6	STAT1	P42224	87.3	47.9	448	29	7843	3.64	0.001
7	GNS	P15586	62.0	32.1	50	11	640	3.33	0.017
8	LIMA1	Q9UHB6	85.2	40.6	177	24	2043	3.25	0.000
9	MYH14	Q7Z406	227.7	43.9	873	75	14550	3.19	0.001
10	PLSCR1	O15162	35.0	21.7	45	4	968	3.12	0.089
11	EPPK1	P58107	555.3	54.3	436	63	5764	3.12	0.002
12	SRC	P12931	59.8	38.2	54	10	815	3.03	0.002
13	ACACA	Q13085	265.4	28.3	158	43	1875	3.03	0.001
14	ERMP1	Q7Z2K6	100.2	21.9	79	12	891	2.76	0.005
15	EFNB1	P98172	38.0	26.0	25	5	242	2.73	0.084
16	GRN	P28799	63.5	32.9	138	10	1591	2.72	0.018
17	LGALS3BP	Q08380	65.3	36.8	501	15	9580	2.69	0.021
18	CHMP2A	O43633	25.1	11.7	29	3	1212	2.55	0.001
19	ARHGAP18	Q8N392	74.9	18.4	42	10	671	2.53	0.004
20	SCAMP2	O15127	36.6	10.6	20	4	604	2.48	0.043
21	STIM1	Q13586	77.4	28.3	77	13	531	2.47	0.004
22	PSMB9	P28065	23.3	30.1	34	5	513	2.45	0.012
23	BAIAP2	Q9UQB8	60.8	42.2	72	14	967	2.36	0.012
24	ABCC3	O15438	169.2	12.9	65	13	713	2.35	0.001
25	ACAD9	Q9H845	68.7	25.3	75	13	1178	2.30	0.002
26	IPO7	O95373	119.4	19.9	127	16	1413	2.30	0.001
27	MGLL	Q99685	33.2	16.2	7	3	37	2.28	0.002
28	APLP2	Q06481	86.9	11.0	35	5	240	2.28	0.005
29	ST14	Q9Y5Y6	94.7	21.8	74	12	968	2.26	0.010
30	GPRC5A	Q8NFJ5	40.2	21.3	58	6	599	2.24	0.001
31	GNAI2	P04899	40.4	52.1	113	9	1099	2.19	0.004
32	HPCAL1	P37235	22.3	31.1	38	5	386	2.17	0.001
33	C1orf116	Q9BW04	63.9	29.6	46	9	475	2.16	0.159
34	CNPY3	Q9BT09	30.7	21.2	47	4	379	2.15	0.007
35	IGF2R	P11717	274.2	19.9	84	28	692	2.12	0.018
36	TMUB1	Q9BVT8	26.2	12.6	16	2	103	2.08	0.895
37	REPIN1	Q9BWE0	63.5	2.6	10	1	124	2.07	0.002
38	RAC1	O96013	64.0	26.4	56	7	375	2.07	0.007
39	CHCHD6	Q9BRQ6	26.4	23.8	27	3	224	2.06	0.002
40	GSTK1	Q9Y2Q3	25.5	61.1	190	10	1949	2.04	0.011
41	NEU1	Q99519	45.4	29.9	36	7	237	2.04	0.026
42	NSDHL	Q15738	41.9	49.3	104	15	1199	2.01	0.003
43	AGK	Q53H12	47.1	36.0	46	10	612	1.98	0.005

44	PSMB10	P40306	28.9	33.3	37	4	738	1.97	0.033
45	ASAP2	O43150	111.6	26.8	52	14	726	1.96	0.002
46	TRIM56	Q9BRZ2	81.4	13.1	21	7	198	1.94	0.021
47	NPC2	P61916	16.6	41.1	60	4	405	1.93	0.008
48	DDAH2	O95865	29.6	36.5	74	6	1572	1.90	0.006
49	ABHD12	Q8N2K0	45.1	39.4	68	9	676	1.89	0.017
50	MYADM	Q96S97	35.3	12.1	16	3	448	1.89	0.007
51	ACP2	P11117	48.3	8.5	20	3	91	1.86	-
52	CNDP2	Q96KP4	52.8	56.4	184	19	1927	1.86	0.003
53	ACOT13	Q9NPJ3	15.0	30.7	18	3	299	1.86	0.021
54	PCCB	P05166	58.2	28.0	34	10	307	1.84	0.034
55	CLN6	Q9NWW5	35.9	11.3	31	3	240	1.84	0.003
56	USP8	P40818	127.4	9.7	20	7	252	1.83	0.068
57	GALNS	P34059	58.0	16.3	19	7	150	1.82	0.071
58	CLPTM1L	Q96KA5	62.2	15.8	33	5	163	1.82	0.013
59	NT5C3A	Q9H0P0	37.9	50.9	74	15	1089	1.82	0.047
60	NUDT3	O95989	19.5	35.5	19	4	108	1.82	0.037
61	RAP2C	Q9Y3L5	20.7	42.6	15	3	402	1.81	0.003
62	SLC9A3R1	O14745	38.8	34.9	104	8	789	1.78	0.002
63	TNS4	Q8IZW8	76.7	19.3	23	7	229	1.75	0.051
64	PRKAR1A	P10644	43.0	17.3	27	5	452	1.75	0.030
65	SQSTM1	Q13501	47.7	57.3	228	15	3175	1.74	0.018
66	IVD	P26440	46.3	29.8	76	8	1111	1.74	0.005
67	CTSD	P07339	44.5	50.0	506	18	9602	1.73	0.433
68	TP53	P04637	43.6	36.1	44	6	465	1.72	0.008
69	RNMT	O43148	54.8	30.7	47	9	618	1.72	0.012
70	ABCF1	Q8NE71	95.9	19.5	70	14	1117	1.71	0.069
71	TFAM	Q00059	29.1	22.0	44	5	576	1.70	0.019
72	FAM49B	Q9NUQ9	36.7	40.7	206	11	3204	1.68	0.002
73	TEAD1	P28347	47.9	12.0	11	3	98	1.67	0.025
74	PSMB8	P28062	30.3	49.3	62	10	735	1.66	0.139
75	PARP4	Q9UKK3	192.5	13.0	48	14	716	1.66	0.002
76	SPTLC2	O15270	62.9	34.2	86	10	1194	1.65	0.032
77	NUDT4	Q9NZJ9	20.3	41.1	45	6	353	1.65	0.012
78	AHNAK	Q09666	628.7	73.6	2961	283	31255	1.65	0.003
79	SPOUT1	Q5T280	42.0	15.2	26	3	278	1.63	0.006
80	PDCD6	O75340	21.9	37.7	69	6	1188	1.63	0.004
81	VAPA	Q9P0L0	27.9	34.5	87	5	860	1.63	0.003
82	USP14	P54578	56.0	51.6	165	18	2267	1.63	0.003
83	TMEM43	Q9BTV4	44.8	42.5	52	9	508	1.62	0.001
84	PARVA	Q9NVD7	42.2	19.1	20	7	434	1.61	0.020
85	SGPL1	O95470	63.5	34.3	112	11	1478	1.58	0.458
86	CYB5A	P00167	15.3	42.5	50	5	245	1.58	0.006
87	RAD50	Q92878	153.8	23.2	104	22	701	1.58	0.021
88	LAMP2	P13473	44.9	4.9	28	2	213	1.57	0.029

89	PIP4K2C	Q8TBX8	47.3	24.7	34	8	803	1.57	0.085
90	COASY	Q13057	62.3	21.3	50	8	464	1.56	0.006
91	MRE11	P49959	80.5	34.9	102	18	1143	1.56	0.004
92	LIG3	P49916	112.8	19.2	60	14	871	1.56	0.003
93	ADAM10	O14672	84.1	32.9	110	15	1272	1.56	0.003
94	NNT	Q13423	113.8	24.3	73	17	1063	1.56	0.429
95	SDF2	Q99470	23.0	29.9	50	4	630	1.56	0.068
96	SAMHD1	Q9Y3Z3	72.2	56.1	213	29	3347	1.55	0.205
97	S100A13	Q99584	11.5	29.6	16	2	159	1.54	0.404
98	FAM129B	Q96TA1	84.1	49.7	323	22	3165	1.54	0.002
99	WASL	O00401	54.8	18.2	14	5	159	1.54	0.018
100	EIF2AK2	P19525	62.1	38.1	171	17	2809	1.53	0.147
101	MYO6	Q9UM54	149.6	37.3	199	39	2593	1.53	0.002
102	BCAP31	P51572	28.0	14.2	49	5	805	1.52	0.033
103	CORO1B	Q9BR76	54.2	39.1	192	12	2352	1.51	0.012
104	NUP153	P49790	153.8	28.3	69	21	681	1.51	0.005
105	CAPG	P40121	38.5	31.32	141	7	2300	1.50	0.003
106	PSAP	P07602	58.1	47.3	308	18	3773	1.50	0.165
107	ISOC2	Q96AB3	22.3	72.7	95	8	1383	1.49	0.066
108	EXOC4	Q96A65	110.4	18.8	46	12	466	1.49	0.023
109	GDF15	Q99988	34.1	18.2	12	3	118	1.49	0.417
110	TM9SF3	Q9HD45	67.8	11.9	37	6	255	1.49	0.018
111	SRPRA	P08240	69.8	35.1	74	15	850	1.47	0.007
112	ANXA4	P09525	35.9	67.4	338	22	6665	1.45	0.021
113	CD59	P13987	14.2	18.8	26	2	160	1.45	0.001

Table 3.11: Results of high SILAC-ratios for single SILAC KM 12 5-FU experiment. p-value from multi SILAC dataset analysed by LIMMA is included. *- Protein not quantified in at least one control sample.

N	Protein name	AC. number	MW [kDa]	SC %	PSMs	Unique Peptides	Score Mascot	Normalized Log2 Ratio: L/H	p-value
1	PRKAR2B	P31323	46.3	17.7	28	2	473	-7.33	-
2	PPP1R1B	Q9UD71	22.9	58.8	54	7	582	-6.57	0.000
3	ARG2	P78540	38.6	29.9	19	6	333	-6.07	0.000
4	CA2	P00918	29.2	48.8	87	11	963	-5.90	0.000
5	FSCN1	Q16658	54.5	47.5	115	16	1543	-5.75	0.000
6	TFF3	Q07654	8.6	22.5	6	1	101	-5.53	0.000
7	CRYM	Q14894	33.8	10.8	9	2	82	-4.93	0.000
8	UBXN7	O94888	54.8	20.4	31	6	300	-4.80	0.038
9	CNN3	Q15417	36.4	32.2	28	7	242	-4.37	0.000
10	VIM	P08670	53.6	29.4	37	10	467	-4.10	0.001
11	CD109	Q6YHK3	161.6	15.8	45	14	759	-3.93	0.001

12	PHGDH	O43175	56.6	54.0	417	27	7013	-3.89	0.000
13	AHCYL1	O43865	58.9	18.1	31	3	259	-3.75	0.071
14	OXCT1	P55809	56.1	37.3	119	12	2444	-3.74	0.000
15	PLIN2	Q99541	48.0	16.9	9	4	80	-3.63	0.001
16	MAPRE2	Q15555	37.0	17.7	17	4	203	-3.60	0.000
17	PRAF2	O60831	19.2	16.9	15	3	279	-3.49	0.000
18	ASB9	Q96DX5	31.8	19.0	8	3	108	-3.49	0.003
19	HMGN5	P82970	31.5	21.6	46	4	831	-3.39	0.000
20	FAM98C	Q17RN3	37.3	16.6	6	4	37	-3.34	-
21	PLEK2	Q9NYT0	39.9	24.1	23	4	136	-3.19	0.020
22	IQGAP2	Q13576	180.5	15.4	39	13	436	-3.18	0.001
23	CEMIP	Q8WUJ3	152.9	8.3	15	7	32	-3.16	0.057
24	BDH2	Q9BUT1	26.7	16.3	9	3	146	-3.12	0.000
25	BAZ1A	Q9NRL2	178.6	5.3	10	5	75	-3.08	0.017
26	S100A14	Q9HCY8	11.7	77.9	70	5	847	-3.06	0.000
27	RPL22L1	Q6P5R6	14.6	36.1	10	2	141	-2.94	-
28	KRR1	Q13601	43.6	12.6	17	4	236	-2.89	0.534
29	ALDH2	P05091	56.3	58.6	212	20	4848	-2.79	0.000
30	ALCAM	Q13740	65.1	33.1	87	12	1123	-2.75	0.001
31	BLMH	Q13867	52.5	26.4	21	7	202	-2.75	0.002
32	MUC5AC	P98088	585.2	15.2	113	30	1034	-2.72	0.000
33	SOD2	P04179	24.7	42.8	109	6	1729	-2.72	0.001
34	KIF2C	Q99661	81.3	30.6	60	13	836	-2.72	0.002
35	AGR2	O95994	20.0	57.1	371	8	5697	-2.69	0.001
36	EIF4EBP1	Q13541	12.6	63.6	24	4	198	-2.66	0.039
37	HLCS	P50747	80.7	6.3	4	3	38	-2.59	0.774
38	PARP2	Q9UGN5	66.2	8.7	11	3	71	-2.58	0.003
39	LYN	P07948	58.5	14.1	29	5	100	-2.58	0.001
40	ULBP2	Q9BZM5	27.4	11.8	4	2	83	-2.55	0.002
41	WRAP53	Q9BUR4	59.3	12.2	8	4	82	-2.54	0.003
42	TTC19	Q6DKK2	42.4	12.6	7	3	57	-2.50	-
43	MTA1	Q13330	80.7	15.4	19	5	250	-2.48	0.100
44	KIF20A	O95235	100.2	10.6	17	5	287	-2.47	0.002
45	PACSIN3	Q9UKS6	48.5	21.5	8	5	137	-2.45	0.001
46	TRIM2	Q9C040	81.5	12.5	18	5	115	-2.39	0.001
47	UBASH3B	Q8TF42	72.6	5.7	7	2	91	-2.36	0.662
48	FABP5	Q01469	15.2	70.4	426	12	5771	-2.34	0.003
49	MCRIP2	Q9BUT9	17.8	35.0	25	3	441	-2.34	0.075
50	ETFDH	Q16134	68.5	10.0	5	3	88	-2.33	0.022
51	GAA	P10253	105.3	12.5	32	8	353	-2.33	0.000
52	EYA3	Q99504	62.6	6.8	4	2	33	-2.28	-
53	PTER	Q96BW5	39.0	31.5	31	7	281	-2.28	0.001
54	MVD	P53602	43.4	29.5	40	7	353	-2.27	0.002
55	CDKN2AIP	Q9NXV6	61.1	10.7	25	4	388	-2.27	0.077
56	Hsp40	Q96KC8	63.8	7.2	8	2	57	-2.24	-

57	FBXO30	Q8TB52	82.3	6.3	6	3	58	-2.23	0.019
58	OAT	P04181	48.5	65.6	249	21	3799	-2.23	0.001
59	CDCA2	Q69YH5	112.6	4.6	11	3	102	-2.18	-
60	SNTB2	Q13425	57.9	4.3	11	2	215	-2.17	0.003
61	CORO1A	P31146	51.0	7.8	9	2	134	-2.16	0.082
62	DNA	P11388	174.3	32.0	242	30	3498	-2.15	0.003
63	CYCS	P99999	11.7	46.7	77	8	293	-2.13	0.002
64	RIDA	P52758	14.5	45.3	21	4	353	-2.13	0.001
65	TAMM41	Q96BW9	51.0	19.0	32	6	209	-2.11	0.002
66	MPC2	O95563	14.3	30.7	13	3	66	-2.11	0.008
67	MYO1E	Q12965	127.0	13.4	26	9	184	-2.10	0.001
68	COPS7A	Q9UBW8	30.3	20.7	13	3	222	-2.10	0.004
69	HCCS	P53701	30.6	20.5	18	5	153	-2.09	0.001
70	KIF15	Q9NS87	160.1	3.6	5	3	86	-2.09	-
71	PRKCI	P41743	68.2	20.1	26	6	103	-2.09	0.528
72	PLCD3	Q8N3E9	89.2	11.7	15	6	128	-2.09	-
73	FUT8	Q9BYC5	66.5	2.4	2	1	47	-2.08	0.001
74	HMGCS2	P54868	56.6	37.8	150	11	2623	-2.08	0.004
75	LUC7L	Q9NQ29	43.7	21.0	79	4	509	-2.07	0.003
76	DPP4	P27487	88.2	18.1	54	11	592	-2.07	0.003
77	DDT	P30046	12.7	83.1	226	9	2832	-2.05	0.002
78	KIF11	P52732	119.1	17.4	45	12	921	-2.05	0.012
79	C12orf43	Q96C57	28.2	26.3	15	4	68	-2.04	0.028
80	PRPS2	P11908	34.7	51.3	224	6	2879	-2.02	0.005
81	HSP90AA1	P07900	84.6	62.2	2383	35	39957	-1.99	0.006
82	ABHD17C	Q6PCB6	35.8	14.0	8	3	82	-1.97	-
83	SLC25A4	P12235	33.0	42.6	148	3	2147	-1.97	0.003
84	PPID	Q08752	40.7	41.6	56	10	810	-1.96	0.006
85	PBK	Q96KB5	36.1	26.7	36	5	577	-1.95	0.007
86	UTP20	O75691	318.2	8.5	67	16	666	-1.93	0.013
87	PRPSAP2	O60256	40.9	41.2	82	8	589	-1.92	0.007
88	GLS	O94925	73.4	37.7	143	17	1804	-1.91	0.007
89	GPD1L	Q8N335	38.4	13.1	15	3	461	-1.89	0.021
90	SLC25A11	Q02978	34.0	19.4	44	5	864	-1.87	0.001
91	COQ5	Q5HYK3	37.1	30.9	13	6	120	-1.87	0.006
92	LARS	Q9P2J5	134.4	42.4	337	39	4377	-1.86	0.159
93	GPHN	Q9NQX3	79.7	16.7	18	7	263	-1.84	0.002
94	DDI2	Q5TDH0	44.5	47.6	55	11	315	-1.84	0.004
95	CKAP4	Q07065	66.0	40.9	138	18	2625	-1.84	0.000
96	TXNL4B	Q9NX01	17.0	12.1	4	1	73	-1.83	0.027
97	TRUB1	Q8WWH5	37.2	22.6	8	4	30	-1.81	0.966

98	NCDN	Q9UBB6	78.8	3.2	4	2	48	-1.80	-
99	GTPBP3	Q969Y2	52.0	14.8	11	4	152	-1.79	0.008
100	OGFOD1	Q8N543	63.2	18.8	28	7	335	-1.77	0.112
101	TSEN15	Q8WW01	18.6	33.3	12	3	146	-1.76	0.630
102	MTO1	Q9Y2Z2	79.9	5.3	8	2	41	-1.75	0.007
103	APOO	Q9BUR5	22.3	23.2	22	3	291	-1.74	0.001
104	SMTN	P53814	99.0	9.8	9	5	123	-1.74	0.003
105	ASF1B	Q9NVP2	22.4	34.16	28	4	444	-1.74	0.016
106	PRMT5	O14744	72.6	22.0	88	11	816	-1.74	0.006
107	PYGL	P06737	97.1	50.5	308	28	2911	-1.74	0.001
108	KLC1	Q07866	65.3	27.6	66	10	632	-1.74	0.018
109	APPL1	Q9UKG1	79.6	22.3	66	9	536	-1.74	0.032
110	EPB41L2	O43491	112.5	42.1	211	25	3561	-1.74	0.176
111	CDCA3	Q99618	29.0	6.7	9	1	211	-1.73	0.092
112	DUSP12	Q9UNI6	37.7	35.3	21	7	237	-1.73	0.008
113	HEATR3	Q7Z4Q2	74.5	12.5	42	7	407	-1.72	0.007
114	WDR77	Q9BQA1	36.7	35.7	108	7	1481	-1.72	0.010
115	DECR1	Q16698	36.0	34.3	134	8	1563	-1.71	0.001
116	PSAT1	Q9Y617	40.4	50.5	176	15	2215	-1.71	0.047
117	GGA1	Q9UJY5	70.3	12.2	12	3	107	-1.70	0.004
118	SLC3A2	P08195	68.0	42.5	364	21	6392	-1.69	0.007
119	SLC4A7	Q9Y6M7	136.0	5.8	11	4	172	-1.69	0.005
120	TTC38	Q5R3I4	52.8	19.8	10	6	73	-1.68	0.004
121	PRKAR2A	P13861	45.5	44.1	119	12	2255	-1.68	0.004
122	CLASP2	O75122	141.0	8.7	39	5	362	-1.68	0.017
123	DFFA	O00273	36.5	27.8	62	7	1115	-1.67	0.014
124	IMPDH2	P12268	55.8	45.5	283	19	5200	-1.66	0.050
125	QRSL1	Q9H0R6	57.4	15.0	17	5	219	-1.66	0.011
126	GUF1	Q8N442	74.3	4.3	5	2	61	-1.65	0.005
127	PDE12	Q6L8Q7	67.3	36.3	93	14	1281	-1.63	0.011
128	NCKIPSD	Q9NZQ3	78.9	8.2	20	5	164	-1.63	0.004
129	BPNT1	O95861	33.4	42.2	103	11	1802	-1.62	0.001
130	MED4	Q9NPJ6	29.7	15.9	10	3	94	-1.61	0.008
131	COA6	Q5JTJ3	14.1	22.4	15	3	174	-1.61	0.008
132	HK2	P52789	102.3	21.4	41	12	388	-1.60	0.023
133	CIAPIN1	Q6FI81	33.6	39.7	88	9	676	-1.60	0.030

Table 3.12: Results of low SILAC-ratios for single SILAC KM 12 5-FU experiment. p-value from multi SILAC dataset analysed by LIMMA is included. *- Protein not quantified in at least one control sample.

HT 29 5-FU

Cluster analysis results for HT 29 5-FU are shown in Figure 3.26. Detailed results for significantly altered proteins in HT 29 5-FU resistant subline are summarized in Tables 3.13 and 3.14. Log_2 SILAC results for HT 29 5-FU / HT 29 SILAC P=9 ratio and p-values from R analysis of resistant and control cell lines are included.

Cluster analysis for HT 29 5-FU resistant subline showed similar results to those observed during “R” LIMMA analysis (see Fig. 3.23c). The highest number of proteins remain unaltered in both parent cells lines, whilst HT 29 5-FU shows a higher number of down-regulated proteins than up-regulated proteins.

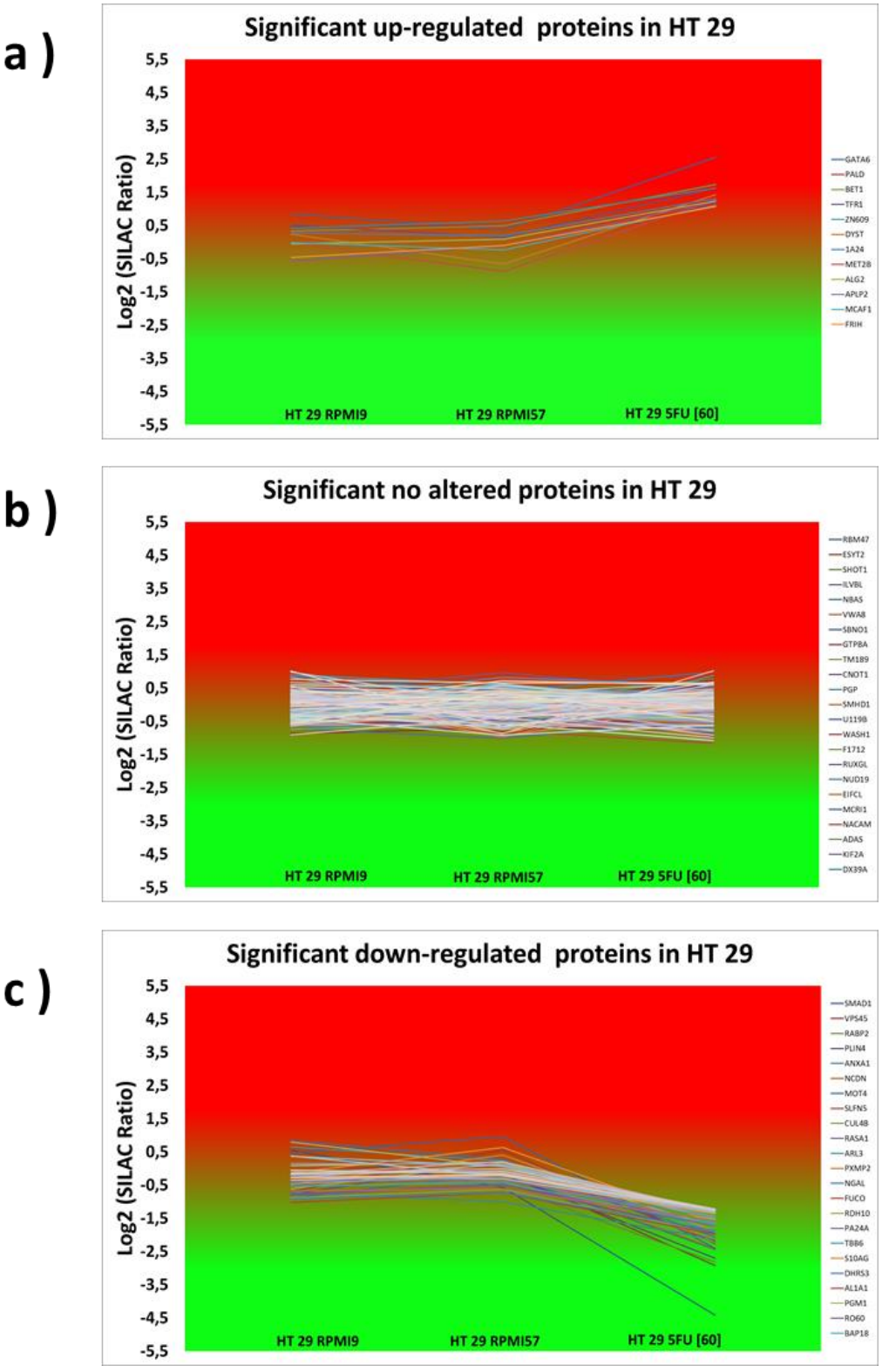

Figure 3.26: Cluster analysis for HT 29. Proteins were classified using 5th percentile threshold for significant (a) up-regulated proteins; (b) unaltered proteins; (c) down-regulated proteins in HT 29 5-FU resistant subline and unaltered in sensitive parent-control cell lines HT 29 P=9 and HT 29 P=57.

N	Protein name	AC. number	MW [kDa]	SC %	PSMs	Unique Peptides	Score Mascot	Normalized Log2 Ratio: L/H	p-value
1	GATA6	Q92908	60.0	2.4	3	1	228.03	3.13	0.012
2	PALD1	Q9ULE6	96.7	3.6	4	2	72.67	2.33	0.020
3	BET1	O15155	13.3	15.3	4	1	75.66	2.31	0.019
4	SQSTM1	Q13501	47.7	56.8	313	13	4032.1	2.26	0.085
5	OCLN	Q16625	59.1	26.4	49	9	351.14	2.24	0.094
6	TFRC	P02786	84.8	39.9	365	25	5250.2	2.21	0.029
7	ZNF609	O15014	151.1	5.2	15	3	37.317	2.21	0.034
8	TOR4A	Q9NXH8	46.9	25.1	42	7	697.98	2.18	0.061
9	FUT4	P22083	59.0	7.4	8	3	139.4	2.13	0.142
10	B2M	P61769	13.7	21.8	26	2	300.09	2.12	0.097
11	LDLR	P01130	95.3	13.5	51	7	324.21	2.10	0.120
12	MAN2A1	Q16706	131.1	20.7	58	14	456.84	2.10	0.122
13	EPCAM	P16422	34.9	33.8	280	7	4744.9	2.07	0.096
14	CHDH	Q8NE62	65.3	37.0	68	13	694.09	2.04	0.070
15	ALDH1B1	P30837	57.2	44.7	120	16	1638.9	2.02	0.132
16	DST	Q03001	860.1	1.5	12	6	35.05	2.01	0.049
17	NAGLU	P54802	82.2	11.7	12	5	91.11	2.01	0.159
18	PARP14	Q460N5	202.7	7.3	26	9	163.82	2.01	0.160
19	REEP4	Q9H6H4	29.4	12.8	10	2	32.97	1.98	0.094
20	NFU1	Q9UMS0	28.4	21.3	26	4	255.21	1.96	0.172
21	TPMT	P51580	28.2	33.5	35	6	465.85	1.95	0.119
22	SP100	P23497	100.4	14.9	48	7	579.91	1.95	0.125
23	TUBB3	Q13509	50.4	44.9	1366	3	20228	1.94	0.188
24	ADGRE5	P48960	91.8	10.5	41	5	369.95	1.92	0.067
25	HLA-A	P05534	40.7	43.6	204	2	3630.8	1.89	0.031
26	PLSCR1	O15162	35.0	15.4	31	3	438.82	1.88	0.077
27	MAP3K4	Q9Y6R4	181.6	3.7	15	4	328.27	1.88	0.179
28	ADPGK	Q9BRR6	54.1	25.6	82	7	535.46	1.88	0.275
29	TNFRSF21	O75509	71.8	8.2	19	4	461.38	1.87	0.262
30	METTL2B	Q6P1Q9	43.4	13.8	20	3	401.68	1.85	0.038
31	ATL2	Q8NHH9	66.2	9.3	42	3	622.95	1.85	0.085
32	SPINT1	O43278	58.4	16.8	56	7	444.45	1.84	0.125
33	TIMM8B	Q9Y5J9	9.3	13.3	11	1	259.49	1.83	0.140
34	ALG2	Q9H553	47.1	11.8	7	3	47.263	1.82	0.024
35	ERLIN1	O75477	38.9	33.8	37	6	623.78	1.82	0.219
36	HIBADH	P31937	35.3	47.3	179	13	2573.2	1.79	0.108
37	APLP2	Q06481	86.9	15.2	74	7	449.57	1.78	0.023
38	HACD3	Q9P035	43.1	22.7	63	6	536.41	1.78	0.166
39	CPD	O75976	152.8	22.8	122	19	1363.6	1.78	0.318
40	MYOF	Q9NZM1	234.6	34.4	399	52	3611.6	1.77	0.069
41	GCAT	O75600	45.3	29.6	24	7	419.49	1.77	0.091
42	GOLIM4	O00461	81.8	8.9	36	4	416.93	1.77	0.100
43	WBSCR22	O43709	31.9	20.6	28	3	258.82	1.77	0.222
44	AMDHD2	Q9Y303	43.7	30.6	38	8	186.7	1.76	0.076

45	CLN6	Q9NWW5	35.9	18.0	41	4	268.8	1.74	0.137
46	PLPP2	O43688	32.6	5.2	15	1	144.91	1.73	0.456
47	FDFT1	P37268	48.1	29.0	50	9	754.35	1.72	0.106
48	HK2	P52789	102.3	16.9	30	10	293.93	1.72	0.282
49	POLR1B	Q9H9Y6	128.1	2.5	7	2	135.91	1.72	0.434
50	WDR74	Q6RFH5	42.4	34.0	37	9	421.14	1.71	0.244
51	ZNF830	Q96NB3	42.0	31.5	29	7	242.24	1.70	0.180
52	ATF7IP	Q6VMQ6	136.3	7.6	18	5	40.115	1.69	0.025
53	SLC12A2	P55011	131.4	26.4	288	24	4031.3	1.68	0.259
54	CCDC51	Q96ER9	45.8	7.1	9	3	47.148	1.67	0.071
55	RRP7A	Q9Y3A4	32.3	13.2	8	2	74.19	1.67	0.397
56	EFL1	Q7Z2Z2	125.4	12.8	19	7	274.18	1.66	0.327
57	RRP8	O43159	50.7	16.4	17	5	217.16	1.66	0.568
58	UTP14A	Q9BVJ6	87.9	15.3	49	8	467.75	1.66	0.572
59	FTH1	P02794	21.2	39.9	31	5	253.34	1.65	0.026
60	NUDT1	P36639	22.5	16.2	8	3	131.42	1.65	0.299
61	SPOUT1	Q5T280	42.0	18.4	46	4	309.65	1.63	0.087
62	RNF114	Q9Y508	25.7	16.7	14	2	311.27	1.63	0.202
63	GALNT7	Q86SF2	75.3	21.2	49	8	908.11	1.63	0.298
64	RBBP5	Q15291	59.1	11.9	29	3	267.61	1.63	0.618
65	APP	P05067	86.9	20.6	87	10	764	1.62	0.208
66	QSOX2	Q6ZRP7	77.5	20.8	66	8	904.48	1.62	0.311
67	DSG2	Q14126	122.2	33.8	198	17	2976.5	1.62	0.607
68	NDUFAF4	Q9P032	20.3	17.1	27	2	40.428	1.61	0.158

Table 3.13: Results of high SILAC-ratios for single SILAC HT 29 5-FU experiment. p-value from multi SILAC dataset analysed by LIMMA is included.

N	Protein name	AC. number	MW [kDa]	SC %	PSMs	Unique Peptides	Score Mascot	Normalized Log2 Ratio: L/H	p-value
1	SMAD1	Q15797	52.2	5.8	11	1	144.4	-3.83	0.005
2	VPS45	Q9NRW7	65.0	14.0	38	5	397.99	-2.35	0.002
3	CRABP2	P29373	15.7	57.2	164	7	2285.9	-2.24	0.006
4	PLIN4	Q96Q06	134.3	9.2	13	5	85.675	-2.12	0.004
5	ANXA1	P04083	38.7	60.4	590	20	10910	-1.86	0.023
6	NCDN	Q9UBB6	78.8	6.6	10	3	161.68	-1.83	0.008
7	SLC16A3	O15427	49.4	4.3	3	2	29.25	-1.82	0.003
8	SLFN5	Q08AF3	101.0	6.4	7	3	48.11	-1.69	0.043
9	CUL4B	Q13620	103.9	13.8	56	6	515.33	-1.65	0.008
10	RASA1	P20936	116.3	11.9	46	8	410.58	-1.60	0.042

11	PXMP2	Q9NR77	22.2	6.2	7	1	29.4	-1.55	0.006
12	ARL3	P36405	20.4	68.1	60	10	357.66	-1.55	0.026
13	LCN2	P80188	22.6	38.9	48	5	726.45	-1.49	0.006
14	FUCA1	P04066	53.7	16.5	51	5	584.23	-1.40	0.039
15	RDH10	Q8IZV5	38.1	14.1	11	3	95.04	-1.37	0.029
16	PLA2G4A	P47712	85.2	4.8	10	2	119	-1.36	0.025
17	TUBB6	Q9BUF5	49.8	21.5	1448	1	13443	-1.33	0.006
18	S100A16	Q96FQ6	11.8	44.7	16	3	321.49	-1.30	0.034
19	DHRS3	O75911	33.5	13.6	3	2	59.24	-1.29	0.037
20	MBNL2	Q5VZF2	40.5	11.5	30	1	92.241	-1.23	0.062
21	CD55	P08174	41.4	21.3	65	5	695.28	-1.20	0.052
22	ALDH1A1	P00352	54.8	56.3	972	25	14234	-1.17	0.010
23	PGM1	P36871	61.4	28.1	50	11	872.09	-1.17	0.047
24	TROVE2	P10155	60.6	27.0	74	9	1148.6	-1.15	0.044
25	ZNFX1	Q9P2E3	220.1	2.2	4	2	40.88	-1.14	0.095
26	C17orf49	Q8IXM2	17.9	19.8	5	2	101.21	-1.11	0.024
27	RTF1	Q92541	80.3	9.0	15	5	315.09	-1.05	0.026
28	CSNK1D	P48730	47.3	13.5	21	4	235.1	-1.04	0.017
29	EPHX1	P07099	52.9	38.7	136	10	1002	-1.04	0.139
30	NME3	Q13232	19.0	20.1	14	2	119.83	-1.03	0.056
31	EPPK1	P58107	555.3	55.0	1072	74	16423	-1.02	0.074
32	LYPLA2	O95372	24.7	37.7	75	5	850.15	-1.00	0.045
33	TSEN15	Q8WW01	18.6	10.5	8	1	133.67	-1.00	0.074
34	BTF3L4	Q96K17	17.3	19.0	14	2	190.24	-0.98	0.053
35	CLPP	Q16740	30.2	23.1	45	4	1211.6	-0.97	0.064
36	ENO2	P09104	47.2	61.8	358	12	8367.2	-0.97	0.115
37	S100P	P25815	10.4	78.9	55	4	344.1	-0.95	0.022
38	BPNT1	O95861	33.4	30.2	46	7	765.77	-0.90	0.028
39	SERPINB8	P50452	42.7	22.2	48	4	232.91	-0.90	0.097
40	RAP1GDS1	P52306	66.3	19.4	44	7	523.94	-0.87	0.028
41	FTO	Q9C0B1	58.2	18.6	27	6	426.54	-0.85	0.193
42	NRDC	O43847	131.5	9.2	21	7	84.31	-0.83	0.143
43	TMSB4X	P62328	5.1	43.2	4	1	32.2	-0.83	0.144
44	QSOX1	O00391	82.5	8.8	25	5	132.78	-0.83	0.210
45	IQGAP3	Q86VI3	184.6	8.4	45	7	507.27	-0.81	0.052
46	SH3GLB1	Q9Y371	40.8	15.1	35	5	142.6	-0.80	0.053
47	TSTD1	Q8NFU3	12.5	12.2	10	1	63.65	-0.80	0.164
48	CAPZA1	P52907	32.9	62.2	406	10	3689.5	-0.78	0.031
49	OGFR	Q9NZT2	73.3	22.9	98	11	1260.1	-0.78	0.070
50	GNL1	P36915	68.6	16.1	59	7	641.52	-0.78	0.199
51	40787	Q9NVA2	49.4	33.3	97	5	802.4	-0.78	0.218
52	CTSD	P07339	44.5	42.2	493	12	8415.3	-0.77	0.153
53	GYS1	P13807	83.7	25.1	67	13	299.32	-0.77	0.220
54	PGD	P52209	53.1	42.7	256	13	4029.8	-0.75	0.014
55	RBM15B	Q8NDT2	97.1	6.4	4	3	31	-0.75	0.021

56	CAP1	Q01518	51.9	37.1	276	14	3910.4	-0.75	0.045
57	NDUFA11	Q86Y39	14.8	37.6	9	3	166.39	-0.74	0.013
58	GLRX	P35754	11.8	43.4	27	4	392.86	-0.74	0.240
59	SSU72	Q9NP77	22.6	31.4	13	5	36.1	-0.73	0.016
60	TAGLN3	Q9UI15	22.5	14.1	4	1	107.25	-0.73	0.132
61	UBA6	A0AVT1	117.9	26.8	124	19	1439	-0.72	0.038
62	PHPT1	Q9NRX4	13.8	44.0	113	6	702.09	-0.72	0.127
63	NAXD	Q8IW45	36.6	36.3	37	6	447.08	-0.72	0.372
64	PNPLA2	Q96AD5	55.3	8.5	16	2	147.82	-0.71	0.030
65	ASAH1	Q13510	44.6	18.5	18	5	251.82	-0.71	0.037
66	EFHD2	Q96C19	26.7	37.1	116	9	1798.9	-0.71	0.101
67	HERC4	Q5GLZ8	118.5	12.9	25	8	59.75	-0.70	0.025
68	TESC	Q96BS2	24.7	24.3	17	4	161.05	-0.70	0.069
69	WFS1	O76024	100.2	7.9	12	4	124.2	-0.69	0.037
70	DPYSL2	Q16555	62.3	61.2	224	20	3036.6	-0.69	0.043
71	RABGGTA	Q92696	65.0	2.6	13	1	103.48	-0.69	0.127
72	LRSAM1	Q6UWE0	83.5	11.2	15	5	73.86	-0.69	0.228
73	NECAP2	Q9NVZ3	28.3	22.4	22	3	226.84	-0.67	0.087
74	HP1BP3	Q5SSJ5	61.2	4.7	9	2	87.315	-0.66	0.030
75	RNPEP	Q9H4A4	72.5	39.2	250	19	2645.9	-0.66	0.037
76	TAGLN2	P37802	22.4	66.8	459	10	8778	-0.66	0.064
77	RHOC	P08134	22.0	43.0	189	1	2337.3	-0.66	0.076
78	LZIC	Q8WZA0	21.5	28.9	7	3	71.875	-0.65	0.071
79	SRSF4	Q08170	56.6	12.3	66	4	604.38	-0.64	0.028
80	WDR1	O75083	66.2	53.6	531	19	8712.8	-0.64	0.056

Table 3.14: Results of low SILAC-ratios for single SILAC HT 29 5-FU experiment. p-value from multi SILAC dataset analysed by LIMMA is included.

3.3.7.4 Bioinformatics analysis of proteins significantly changed due to resistance

Proteins classified as significantly altered by (a) 5th percentile cluster analysis and (b) p-values ($p \leq 0.05$) from LIMMA analysis were selected for network analysis by STRING (Protein-Protein Interaction Network) (see section 3.2.5.8). Initially, STRING analysis was applied to identify relationships between proteins significantly altered in resistant sublines. For each resistant subline set results, proteins were classified according to five biological processes which may mediate drug response and drug resistance 1) apoptotic process, 2) DNA repair process, 3) metabolism of drugs and small molecules, 4) intracellular protein transport and 5) cellular membrane transport and cell membrane organization

processes. This is based on molecular functions identified by GO and pathway analysis for selected proteins using EnrichNet (Fig. 3.28-3.30). Furthermore, significantly altered proteins were used to build up Venn diagrams to show common significantly up-regulated and significantly down-regulated protein in different resistant sublines to 5-FU (Fig. 3.27). Commonly up-regulated and down-regulated proteins are presented at the intersection of the Venn diagrams and they will be discussed in detail further in the section 3.4.3.2.

3.3.8 Cross-cell line related protein responses to 5-FU resistance

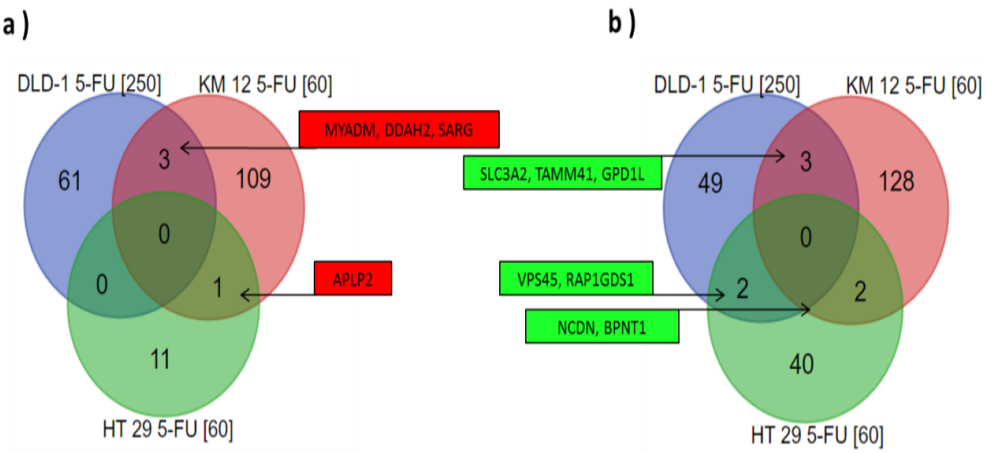

Figure 3.27: Venn diagrams showing common significantly altered proteins in 5-FU resistant sublines. (a) Up-regulated and (b) down-regulated proteins using 5th percentile threshold in three different resistant CRC sublines to 5-FU.

Common significantly altered proteins presented in at least two of the three resistant sublines to 5-FU are shown in the table 3.15. Additional information relating to two important proteins that may be playing a crucial role in 5-FU resistance (CD44, UMPS) which were significantly altered but unique to DLD-1 5-FU cell line have been included in the table too. Uniquely altered proteins from the three resistant sublines were used to develop three different protein network model of 5-FU resistance and they are shown below.

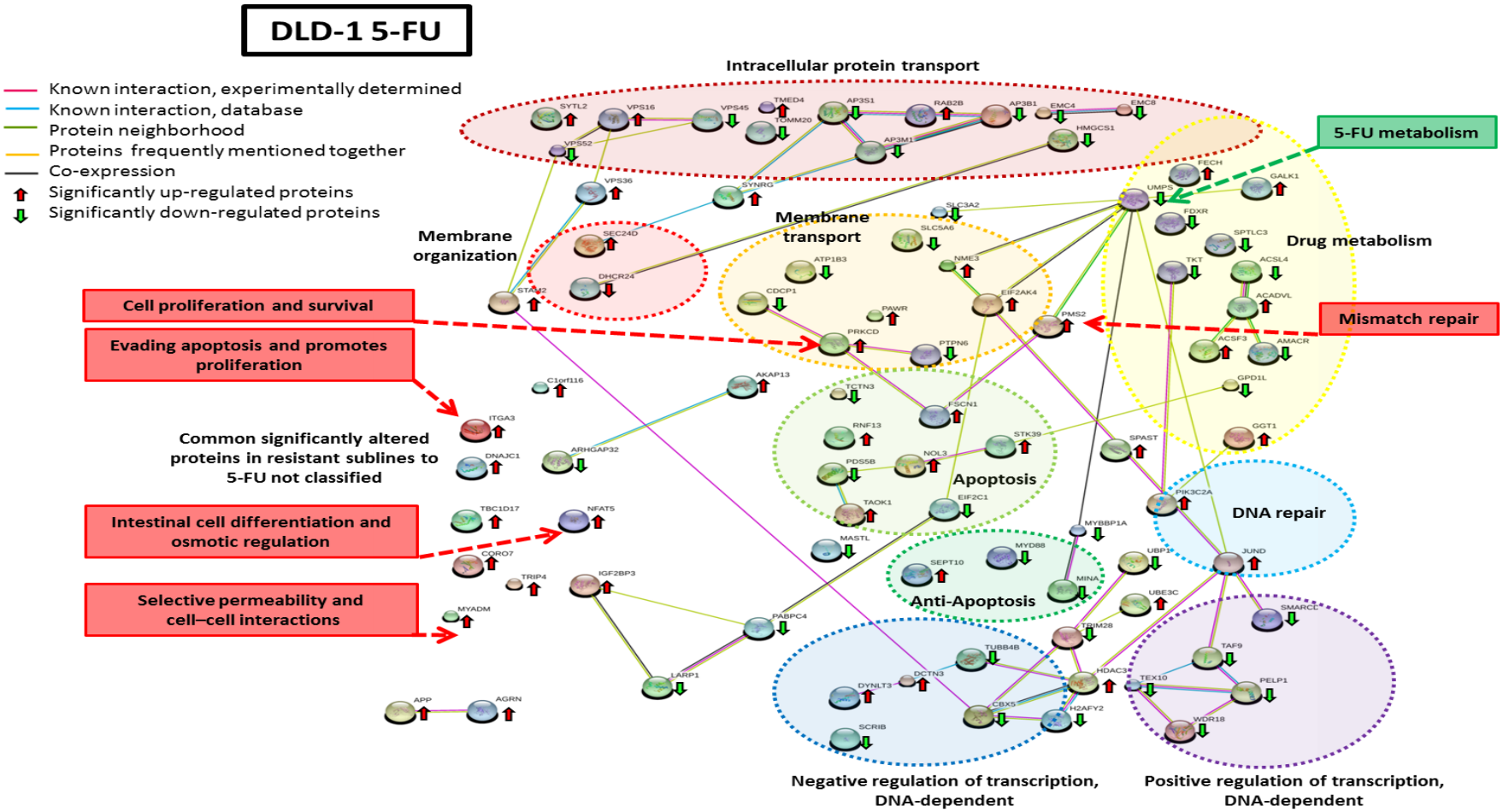

Figure 3.28: Proteomic network model for DLD-1 5-FU. Significantly altered proteins obtained by modification on EnrichNet and GO from the initial bubble map obtained in STRING. Coloured circles group proteins by functionality. Not grouping proteins are commonly altered proteins in at least other resistant 5-FU subline and not linking to other proteins. Dotted arrows indicate the most relevant proteins with known functions which may be involved in response to 5-FU. All significantly altered proteins not linked by STRING software with other altered proteins or presented altered just in one of the 5-FU resistant sublines, were removed from the model. Key: Green arrow: significantly down-regulated protein; Red arrow: significantly up-regulated protein.

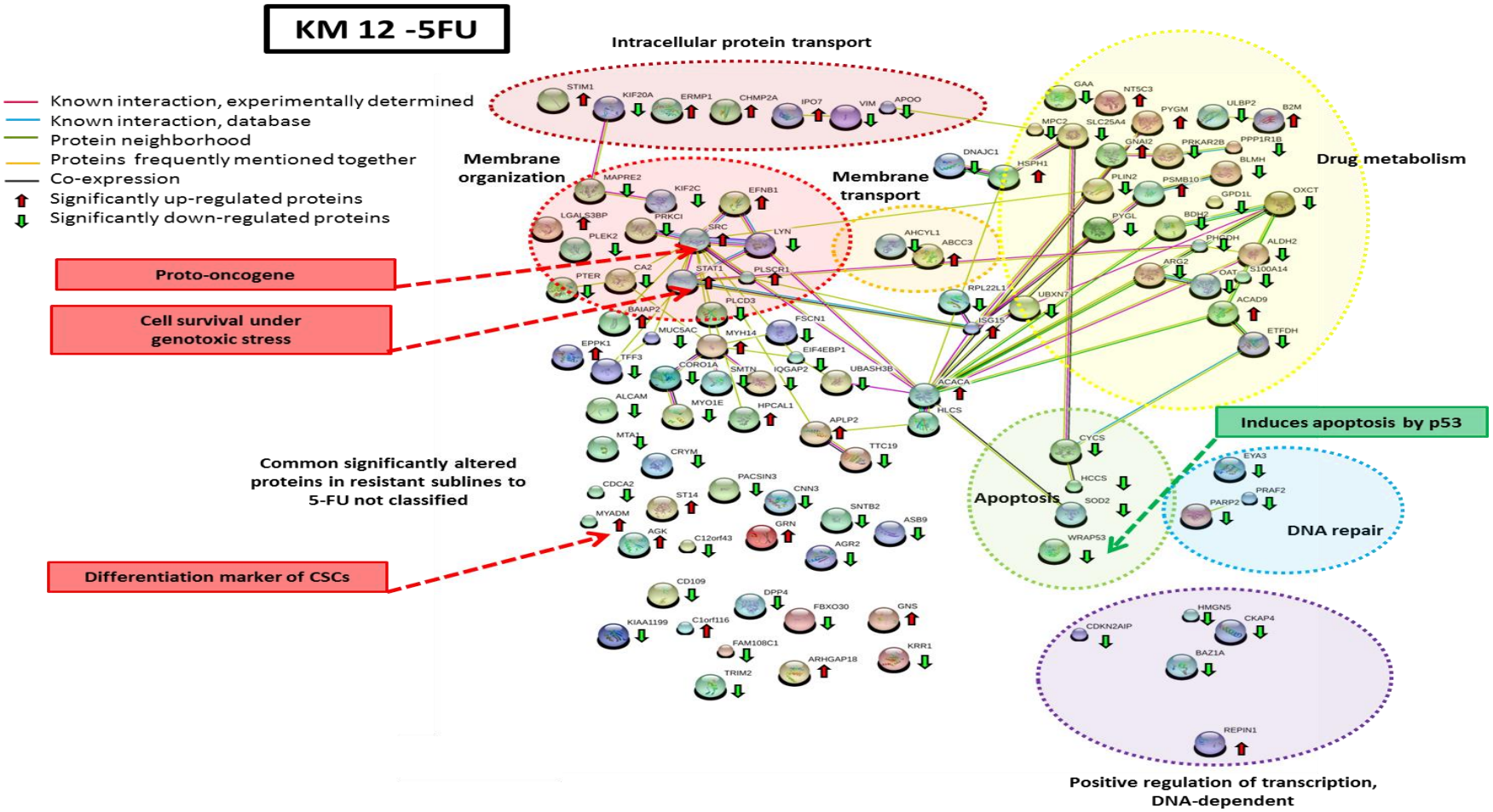

Figure 3.29: Proteomic network model for KM 12 5-FU. Significantly altered proteins obtained by modification on EnrichNet and GO from the initial bubble map obtained in STRING. Coloured circles group proteins by functionality. Not grouping proteins are commonly altered proteins in at least other resistant 5-FU subline and not linking to other proteins. Dotted arrows indicate the most relevant proteins with known functions which may be involved in response to 5-FU. All significantly altered proteins not linked by STRING software with other altered proteins or presented altered just in one of the 5-FU resistant sublines, were removed from the model. Key: Green arrow: significantly down-regulated protein; Red arrow: significantly up-regulated protein.

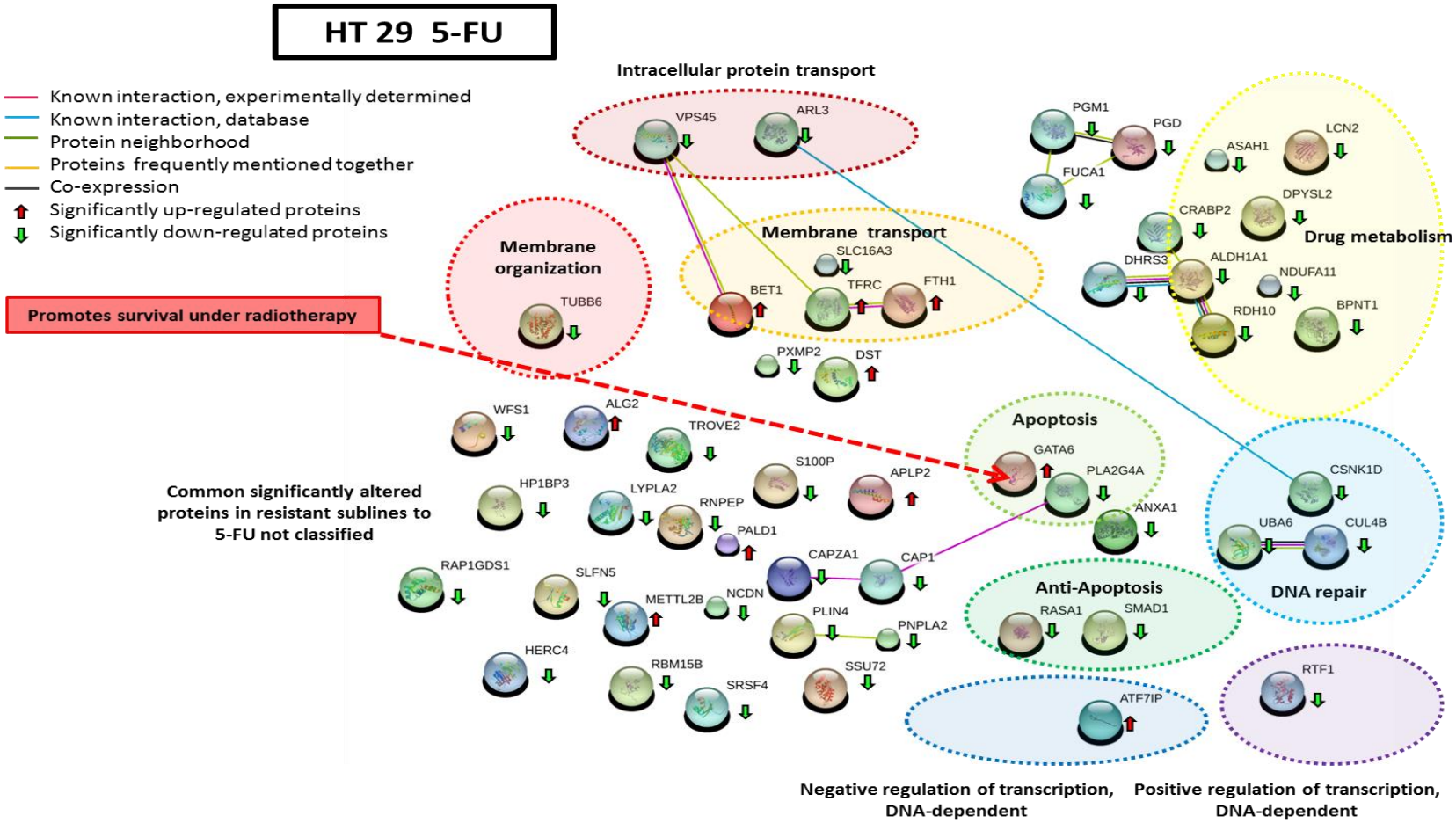

Figure 3.30: Proteomic network model for HT 29 5-FU. Significantly altered proteins obtained by modification on EnrichNet and GO from the initial bubble map obtained in STRING. Coloured circles group proteins by functionality. Not grouping proteins are commonly altered proteins in at least other resistant 5-FU subline and not linking to other proteins. Dotted arrows indicate the most relevant proteins with known functions which may be involved in response to 5-FU. All significantly altered proteins not linked by STRING software with other altered proteins or presented altered just in one of the 5-FU resistant sublines, were removed from the model. Key: Green arrow: significantly down-regulated protein; Red arrow: significantly up-regulated protein.

N	Protein name	Gene name	Abundance Ratio: L / H									Normalized Log2 Ratio: L / H									Log2 Fold-change			Significant differences p-value		
			DLD-1 RPMI P=9	DLD-1 RPMI P=65	DLD-1 5-FU [250] P=70	KM 12 RPMI P=9	KM 12 RPMI P=55	KM 12 5-FU [60] P=50	HT 29 RPMI P=9	HT 29 RPMI P=57	HT 29 5-FU [60] P=48	DLD-1 RPMI P=9	DLD-1 RPMI P=65	DLD-1 5-FU [250] P=70	KM 12 RPMI P=9	KM 12 RPMI P=55	KM 12 5-FU [60] P=50	HT 29 RPMI P=9	HT 29 RPMI P=57	HT 29 5-FU [60] P=48	DLD-1 5-FU	KM 12 5-FU	HT 29 5-FU	DLD-1 5-FU	KM 12 5-FU	HT 29 5-FU
1	Myeloid-associated differentiation marker	MYADM	1.54	2.74	4.79	1.21	1.18	5.99	0.78	0.94	1.50	0.20	0.31	0.97	-0.17	-0.50	1.89	-0.23	-0.25	0.00	0.71	2.22	0.25	0.06	0.00	0.45
2	N(G),N(G)-dimethylarginine dimethylaminohydrolase 2	DDAH2	1.31	1.42	5.57	1.52	1.88	6.00	0.64	0.55	0.79	-0.03	-0.64	1.18	0.15	0.17	1.90	-0.51	-1.02	-0.92	1.52	1.74	-0.15	0.02	0.00	0.71
3	Specifically androgen-regulated gene protein	SARG	0.97	1.87	8.74	0.95	2.25	7.19	0.39	0.74	0.40	-0.46	-0.25	1.83	-0.52	0.43	2.16	-1.23	-0.60	-1.91	2.19	2.20	-0.99	0.00	0.02	0.10
4	Amyloid-like protein 2	APLP2	#	1.79	2.80	1.60	1.56	7.83	0.61	1.04	3.44	#	-0.30	0.19	0.23	-0.10	2.28	-0.57	-0.10	1.20	#	2.21	1.54	#	0.00	0.02
5	CD44 antigen	CD44	0.44	1.24	4.79	0.93	0.84	1.02	2.80	0.42	2.14	-1.59	-0.83	0.97	-0.55	-0.99	-0.67	1.62	-1.43	2.23	2.18	0.10	2.14	0.01	0.75	0.25
6	4F2 cell-surface antigen heavy chain	SLC3A2	1.48	1.68	0.88	1.52	1.62	0.50	1.96	2.58	2.96	0.15	-0.40	-1.48	0.15	-0.05	-1.69	1.10	1.20	0.98	-1.35	-1.75	-0.17	0.03	0.00	0.61
7	Phosphatidate cytidylyltransferase, mitochondrial	TAMM41	1.19	3.05	1.06	1.09	1.27	0.37	0.83	#	0.61	-0.17	0.46	-1.21	-0.33	-0.40	-2.11	-0.14	#	-1.29	-1.35	-1.75	#	0.03	0.00	#
8	4F2 cell-surface antigen heavy chain	GPD1L	0.87	2.54	0.25	1.87	1.59	0.43	#	0.99	2.04	-0.62	0.20	-3.32	0.46	-0.08	-1.89	#	-0.18	0.45	-3.10	-2.09	#	0.00	0.01	#
9	Vacuolar protein sorting-associated protein 45	VPS45	1.45	2.22	0.09	1.25	0.06	0.59	0.95	1.06	0.20	0.11	0.01	-4.83	-0.12	-4.83	-1.45	0.06	-0.09	-2.93	-4.89	1.03	-2.91	0.00	0.69	0.00
10	Rap1 GTPase-GDP dissociation stimulator 1	RAP1GDS1	1.05	1.72	0.73	1.21	1.22	0.61	0.70	1.02	0.55	-0.35	-0.36	-1.75	-0.17	-0.46	-1.41	-0.38	-0.14	-1.46	-1.39	-1.10	-1.19	0.01	0.02	0.03
11	Neurochondrin	NCDN	1.40	2.86	1.74	1.32	1.57	0.47	0.62	1.06	0.28	0.07	0.37	-0.50	-0.05	-0.10	-1.80	-0.56	-0.09	-2.41	-0.71	-1.72	-2.11	0.08	0.00	0.01
12	3'(2'),5'-bisphosphate nucleotidase 1	BPNT1	1.19	2.12	1.49	1.44	1.53	0.53	0.70	0.89	0.54	-0.17	-0.06	-0.72	0.08	-0.13	-1.62	-0.38	-0.33	-1.49	-0.61	-1.59	-1.13	0.09	0.00	0.03
13	Uridine 5'-monophosphate synthase	UMPS	1.32	1.79	0.41	1.18	1.26	1.56	1.08	1.41	1.55	-0.03	-0.30	-2.57	-0.21	-0.41	-0.05	0.24	0.33	0.05	-2.41	0.26	-0.23	0.00	0.29	0.48

Table 3.15: Commonly significantly altered proteins in at least two of three 5-FU resistant sublines. Proteins were used to identify new mechanisms of resistance involved in resistance to 5-FU. Additionally, some relevant proteins as CD44 and UMPS with a potential role to develop resistance to 5-FU are included.

Key: Red - Significantly up-regulated protein, Green – Significantly down-regulated protein, # - protein not quantified.

3.3.9 Verification of experimental fold changes using housekeeping-control proteins

From clustering analysis, unsurprisingly the largest group of proteins was seen to be the group of proteins not changed in any of the three samples (SILAC control, passage control and resistant experiment) across the 3 different cell lines. A total of 1793 proteins were quantified commonly unchanged in all 9 samples studied (3 cell lines x 3 types of sample (low passage control, high passage control and resistant subline)). To verify the accuracy of any proteomics finding discussed, the fold change of some housekeeping proteins were analysed to ensure that significantly altered proteins changed expression only due to the drug effect. These housekeeping proteins were selected as control proteins whose expression should not to be influenced by the drug under study, and its functionality should be normal among all CRC samples used including both parent cell lines and resistant sublines. ß-actin, tubulin or GAPDH are housekeeping proteins frequently used in proteomics studies (Ferguson, Carroll et al. 2005), however were discarded due to lack of quantification during Mass spectrometer analysis. Information related to the seven housekeeping control proteins used is shown in the table 3.16 below.

Housekeeping proteins selected were:

1) Peptidyl-prolyl cis-trans isomerase A (PPIA) promotes folding of proteins and it catalyses the cis-trans isomerization of proline in oligopeptides (Camilloni, Sahakyan et al. 2014). PPIA participates in the cell-virus interaction (Hopkins and Gallay 2015). Cells-virus interaction is not expected to be presented during cell culture conditions for any sample.

2) ADP-ribosylation factor 3 (ARF3) is a GTP-binding protein that functions as an allosteric activator of the cholera toxin catalytic subunit, that it is not expected to affect this study (Kahn and Gilman 1986).

3) Hypoxia up-regulated protein 1 (HYOU1) is a protein involved in cytoprotective cellular mechanisms triggered by oxygen deprivation. Oxygen levels are not expected to be altered as cell culture conditions remain the same for all cell lines (Semenza 2002).

4) ATP synthase subunit d, mitochondrial (ATP5H) is a mitochondrial membrane ATP synthase which has been used in different previous publications as housekeeping protein (Leyva, Bianchet et al. 2003).

5) Osteoclast-stimulating factor 1 (OSTF1) activated during bone resorption processes and enhances osteoclast formation and activity. These processes are not expected to be altered in CRC cell lines under any drug effect (Roodman 1999)

6) Heme oxygenase 2 (HMOX2) is a heme oxygenase that plays its main role in the spleen, where senescent erythrocytes are sequestrated and destroyed. Any of these processes is expected to change in CRC under drug effects (Stocker and Perrella 2006).

7) Cytoskeleton-associated protein 5 (CKAP5) regulates microtubule dynamics and organization and it has been used in previous studies as housekeeping proteins (Li, Finley et al. 2002).

Once control proteins were selected, the summary Table 3.16 was done, containing SILAC-ratio raw data and normalised Log_2 SILAC-ratio data. Last two columns show the fold change for the protein obtained during LIMMA analysis where relative protein abundance in resistant subline was compared with the relative protein abundance in both parent control cell lines and the corresponding "p-value". A "p-value" lower than 0.05 means that no significant differences were found between the resistant subline and parent cell lines in relative abundance for the specific protein. No significant changes were found in any of the seven control proteins studied (Table. 3.16).

N	Protein name	Gene name	Abundance Ratio: L / H									Normalized Log2 Ratio: L / H									Log2 Fold-change			Significant differences p-value		
			DLD-1 RPMI P=9	DLD-1 RPMI P=65	DLD-1 5-FU [250] P=70	KM 12 RPMI P=9	KM 12 RPMI P=55	KM 12 5-FU [60] P=50	HT 29 RPMI P=9	HT 29 RPMI P=57	HT 29 5-FU [60] P=48	DLD-1 RPMI P=9	DLD-1 RPMI P=65	DLD-1 5-FU [250] P=70	KM 12 RPMI P=9	KM 12 RPMI P=55	KM 12 5-FU [60] P=50	HT 29 RPMI P=9	HT 29 RPMI P=57	HT 29 5-FU [60] P=48	DLD-1 5-FU	KM 12 5-FU	HT 29 5-FU	DLD-1 5-FU	KM 12 5-FU	HT 29 5-FU
1	Peptidyl-prolyl cis-trans isomerase A	PPIA	1.09	1.63	1.92	1.23	1.43	1.75	0.82	1.02	1.07	-0.30	-0.44	-0.35	-0.15	-0.23	0.12	-0.15	-0.14	-0.48	0.02	0.31	-0.33	0.95	0.19	0.33
2	ADP-ribosylation factor 3	ARF3	1.31	1.72	2.11	1.34	1.45	2.05	0.79	1.03	1.18	-0.03	-0.36	-0.21	-0.02	-0.21	0.34	-0.21	-0.12	-0.35	-0.02	0.45	-0.19	0.96	0.11	0.57
3	Hypoxia up-regulated protein 1	HYOU1	1.31	1.31	1.80	1.43	1.85	1.53	1.79	1.47	1.71	-0.03	-0.75	-0.43	0.07	0.14	-0.07	0.97	0.39	0.19	-0.04	-0.18	-0.49	0.92	0.40	0.31
4	ATP synthase subunit d, mitochondrial	ATP5H	1.58	2.07	2.64	1.36	2.07	1.64	0.97	1.18	1.86	0.24	-0.09	0.11	-0.01	0.30	0.02	0.08	0.08	0.32	0.04	-0.13	0.24	0.91	0.62	0.47
5	Osteoclast-stimulating factor 1	OSTF1	1.44	1.96	2.34	1.28	1.29	1.17	0.74	1.38	1.31	0.11	-0.18	-0.06	-0.10	-0.38	-0.47	-0.31	0.29	-0.19	-0.03	0.23	0.18	0.92	0.38	0.69
6	Heme oxygenase 2	HMOX2	1.00	1.61	1.79	1.40	1.94	1.52	1.11	1.74	2.68	-0.42	-0.46	-0.45	0.04	0.22	-0.09	0.29	0.63	0.84	-0.02	-0.22	0.38	0.95	0.36	0.33
7	Cytoskeleton-associated protein 5	CKAP5	1.12	1.73	1.99	1.38	1.34	1.31	1.04	1.21	2.04	-0.26	-0.35	-0.30	0.01	-0.32	-0.30	0.19	0.11	0.44	0.01	-0.14	0.31	0.98	0.60	0.36

Table 3.16: Control proteins that are unaltered by drug effects and which were used to evaluate the success of SILAC approach and statistical analysis applied to 5-FU resistant sublines. Log_2 fold change of all control proteins were found close to zero in the three 5-FU resistant sublines when they were compared to its respective parent-control cell lines. A Log_2 fold proximaly to 0, means that levels of the proteins quantified were similar in light and heavy samples.

3.3.10 Validation of proteomics findings using Western Blotting for 2 proteins with identified altered expression profiles, CD44 and UMPS

In order to validate the findings of the quantitative proteomics methodology, 2 proteins whose expressions were identified as being up-regulated in the 5-FU resistant sublines, were further investigated using immunodetection techniques. Expression of CD44 (Fig. 3.31) and UMPS (Fig. 3.32) selected proteins was further analysed using WB. Validation of quantitative proteomics results was necessary to support from SILAC-approach and LIMMA analysis. CD44 protein was selected due to its role in chemoresistance in different types of cancer, included CRC (Fanali, Lucchetti et al. 2014), whilst UMPS was selected because it mediates the initial step in the metabolism of the drug 5-FU and it has been related to 5-FU drug response (see section 3.1.2.1) (Griffith, Mwenifumbo et al. 2013).

CD44 Western blot analysis of DLD-1 parent and resistant subline showed a single band of 81 kDa molecular weight, which was most intense in the DLD-1 5-FU resistant subline sample. Band intensities were adjusted relative to ß-actin, which was analysed as a house-keeping protein. After correction for cross-experiment variations, the ratios for CD44, closely matched the SILAC data (Fig. 3.31b-c). Similar results were obtained for CD44 Western blot analysis of HT 29 parent and resistant sublines which showed the most intense single band of 81 kDa molecular weight in HT 29 5-FU and a second intense single band of 81 kDa molecular weight in HT 29 P=9. WB results for the CD44 ratios closely matched with previous SILAC data (Fig. 3.31h-i). However, different results were found for KM 12 analysis that showed the two most intense bands for CD44 in KM 12 parent cell lines but no band for CD44 was found in KM 12 5-FU which showed a poor matched with previous SILAC data results (Fig. 3.31e-f).

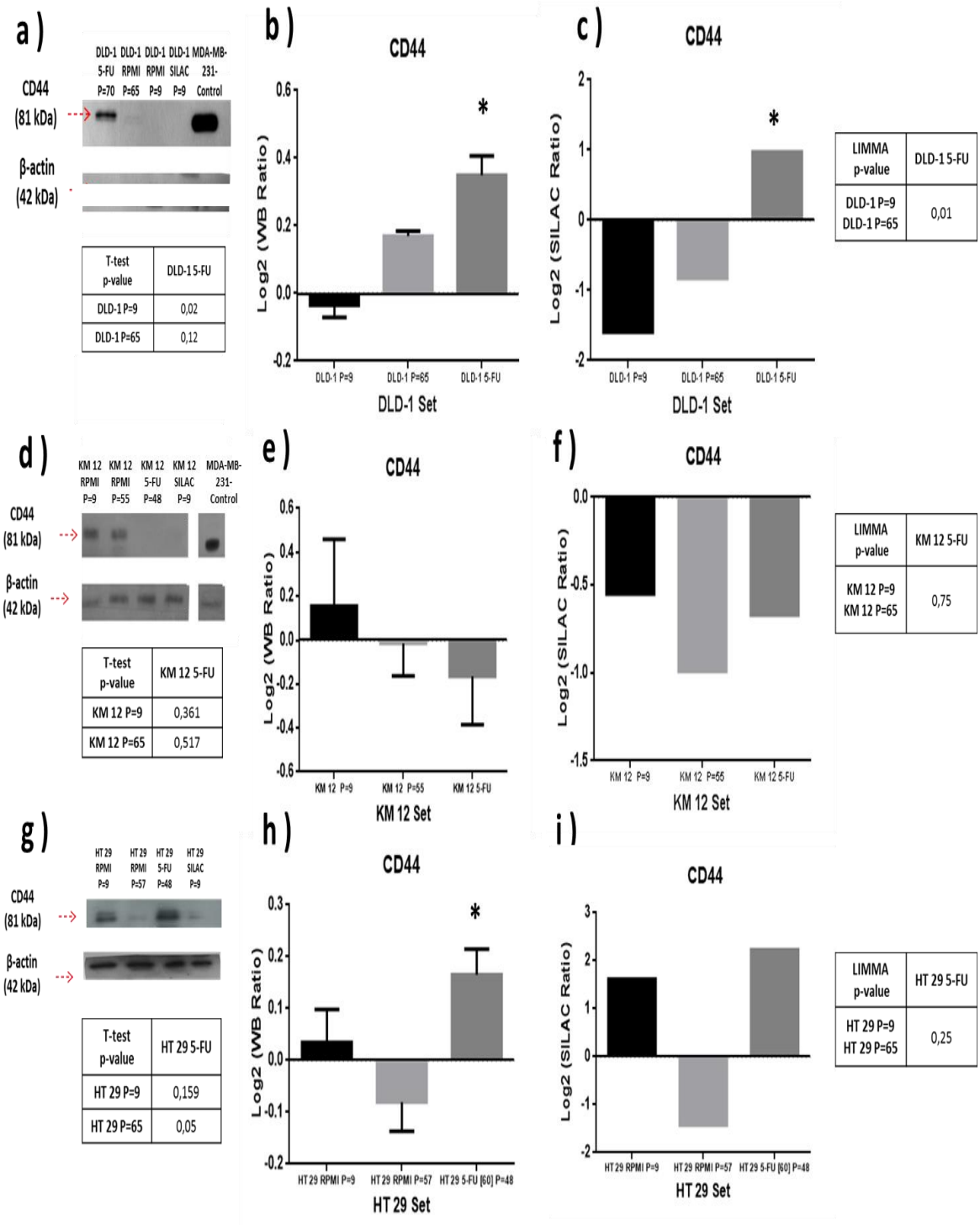

Figure 3.31: WB results for CD44. (a) (d) (g) WB analysis of the presence of CD44 was performed for resistant sublines DLD-1, KM 12 and HT 29 to 5-FU. A WB example used to estimate CD44 abundance containing both β-actin results and MDA-MB 231 cell line positive for CD44 which were used as control during WB. Table showing p-values obtained from WB by t-test statistics analysis. (b) (e) (h). Relative expression of CD44 abundance in the indicated samples was divided between CD44

abundance in SILAC sample, as it had been done during SILAC protocol to estimate SILAC-ratios (L/H). (c) (f) (i) Bar graphs obtained from SILAC approach with Log_2 (SILAC-ratios) data for each sample and a table showing p-values obtained from SILAC approach by LIMMA statistics analysis. Data are presented as mean; an asterisk represents significant differences ($p<0.05$).

UMPS Western blot analysis of DLD-1 parents and resistant subline showed two bands of 52 kDa and 33 kDa molecular weights in DLD-1 P=65 and DLD-1 5-FU. 33 kDa band was most intense in DLD-1 5-FU resistant subline than in DLD-1 P=65. While DLD-1 P=9 showed a single band of 52 kDa molecular weight. Band intensities were adjusted relative to ß-actin, which was analysed as a house-keeping protein. After correction for cross-experiment variations, the ratios for UMPS did not match with the SILAC data (Fig. 3.32a,b). A new WB analysis was carried out based on the Microarray study of the ratio between the two isoforms identified as it was done in the article published in The Pharmacogenomics Journal (January 2012) where authors demonstrated that the ratio of isoform A to B was 25.6 in MIP101 sensitive cells and 0.85 in MIP/5FU resistant sublines (Fig. 3.32c). This new results presented were similar in ratio abundance to previous results described by M. Griffith *et al.*: relative ratio abundance of UMPS isoform A / UMPS isoform B was close to 1 in DLD-1 5-FU resistant subline and the highest abundance of UMPS isoform A was found in long generation control obtained from WB in this thesis (Fig. 3.32d).

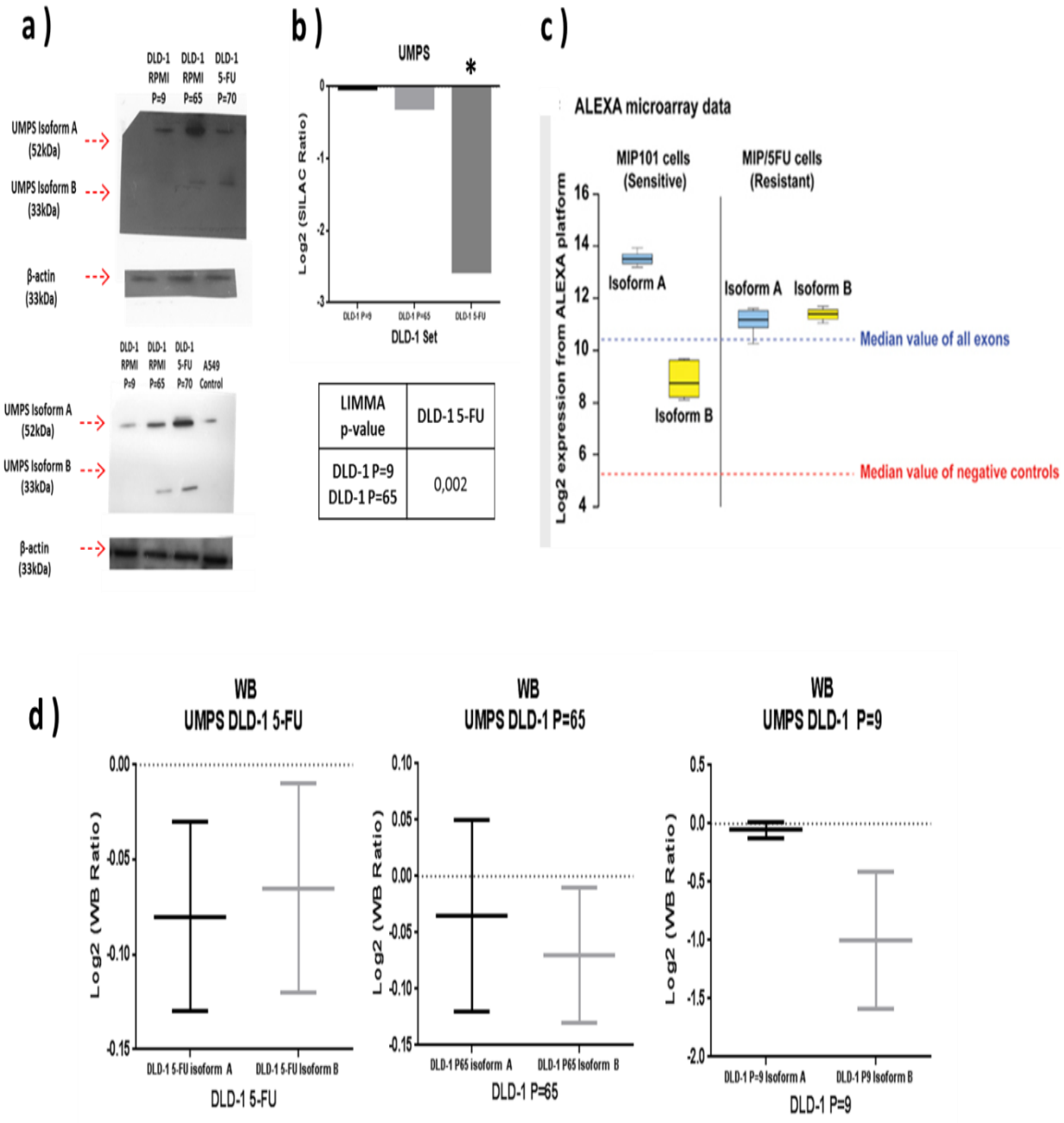

Figure 3.32: (a) WB analysis for UMPS in DLD-1 5-FU. Additionally, an immunoblot example used to estimate UMPS abundance containing both β-actin results and A549 cell line positive for UMPS which were used as control during immunoblotting. (b) Bar graph obtained from Log_2 SILAC-ratios data for each sample and table showing p-values obtained from SILAC approach by LIMMA statistics analysis. Data are presented as mean; an asterisk represents significant differences ($p<0.05$). (c) The ratio of isoform A to B was 25.6 in MIP101 cells and 0.85 in MIP/5-FU cells. Data obtained from microarray hybridization and analysis of microarray data

on the ALEXA splicing microarray platform by M. Griffith *et al*. (Griffith, Mwenifumbo et al. 2013). (d) New results presented in this thesis which are similar in ratio abundance to previous results described by M. Griffith *et al,*: Relative ratio abundance of UMPS isoform A / UMPS isoform B was close to 1 in DLD-1 5-FU resistant subline and the highest abundance of UMPS isoform A was found in both two DLD-1 parent cell lines obtained from WB in this thesis.

3.4 Discussion

Three different resistant cell lines to 5-FU models were established, and were used to increase our understanding of how CRC cells develop resistance to 5-FU. 5-FU resistant sublines for 3 cell lines, DLD-1, KM 12 and HT 29, were developed by continuous 5-FU exposure, and resistance fold changes of 130.2, 3.2 and 3.5 respectively were achieved. Differences in resistance fold change can be caused by genomic background of the initial parent cell lines and cellular sensitivity to 5-FU effects may differ between different cell lines. Additionally, establishment of resistant sublines is a long process (more than 10 months), so during this period of time new randomly and different mutations appear and these can have different roles in 5-FU response. Hence, new alterations in proteins expression will progressively lead the development of a resistant phenotype. Additionally, according with results here presented, the number of altered proteins is not representative of the total resistance fold change achieved by a resistant subline. Hence, the molecular functions of altered proteins and their potential roles in 5-FU response, appear to be most relevant than the total number of proteins during establishment of resistance sublines. This issue can be observed from results obtained for KM 12 5-FU which was the resistant subline with more altered proteins, although its resistance fold change was low. However, DLD-1 5-FU showed the highest resistance fold change even though the total number of altered proteins was not so high. Due to high differences in resistance fold change between DLD-1 5-FU and the other two sublines, DLD-1 5-FU was selected for development of xenograft models which will be used in future studies of mechanisms of resistance to 5-FU *in vivo*. Once 5-FU resistant sublines were developed they were analysed proteomically using a stable isotope labelling with amino acids in cell culture

(SILAC)-approach and Orbitrap Fusion™ Tribrid™ Mass Spectrometry analysis, to identify new biomarkers of drug resistance.

3.4.1 Evaluation of cross-resistance in the DLD-1 5-FU subline

Significant cross-resistant effects were observed for DLD-1 5-FU [250] resistant subline to OXA, IRI, carmustine and colchicine (Fig. 3.17b,c,e,f). Similar results for 5-FU and IRI cross-resistant effect were found in 2014 by John Boyer *et al*., with HCT 116 resistant cell line to 5-FU that showed a 2 fold resistant phenotype to IRI than parent HCT116 cell line [347]. Special attention requires the cross-resistance effect observed with DLD-1 5-FU resistant subline to OXA drug. These findings are similar to results obtained by Nikolaos A. Dallas *et al*., which showed cross-resistance to OXA in a HT 29 resistant subline to 5-FU [348]. Together, these findings suggest the presence of common mechanisms of resistance to 5-FU and OXA drugs that could be relevant for the clinical treatment of CRC patients. OXA and 5-FU combination therapy is normally used in advanced CRC patients and although initial outcomes for patients show benefits, appearing of resistance to combination therapy occurs later. So, studying of proteomics behind this cross-resistance process could help to prevent this clinical problem. Although it is important to highlight that these results are specific for a single resistant subline to 5-FU and it may not be extrapolated to general terms.

Results from DLD-1 resistant subline to 5-FU shows that the use of 5-FU in combination with any of the drugs that show cross-resistance as OXA, IRI, carmustine and colchicine could converge into the failure of the combinational therapy (Fig. 3.17b,c,e,f).

Researcher partnerships could create data platforms using CRC cell lines and cross-resistance studies *in vitro* and *in vivo*, that may help to understand the cross-resistance process. Establishment of cross-resistance guides of successful combinational therapies would avoid cross-resistance problems and it will promote working on personalized combinational therapies based on the presence of specific mechanisms of resistance in each patient.

3.4.2 Development of drug resistant xenograft models

Whilst *in vitro* models of acquired resistance are useful in exploring mechanisms of resistance, they do not take into account influence of other cells and factors in the tumour microenvironment. For this reason, it is useful to show that the resistance phenotype can be maintained in an *in vivo* situation, which more closely mimics the clinical situation. The subcutaneous xenograft model is the first step in this direction but still, further studies need to be done to solve few issues. The main issue is that high passage parent cell line phenotype from original cancer cells has not been studied. Hence, potential differences in high and low passaging are not shown during *in vivo* models.

Recently trend of the use of patient-derived xenograft model is increasing, as the use of xenograft model derived directly from the patient primary tumour isolated during surgery. But also issues are present during trying to establish drug resistant sublines due to limited passaging in animal models.

During the thesis here presented, clearly demonstrated maintenance of resistant phenotype *in vivo* for this particular cell line was found. Without 5-FU therapy the volume growth times for the sensitive or resistant tumours were similar. However, under 5-FU treatment, xenograft tumours from DLD-1 parent cell lines grew slower than xenograft tumours from DLD-1 5-FU (Fig. 3.18).

In vivo studies are important for understanding metastatic process where resistant phenotypes are maintained leading to failures during chemotherapy treatment in different regions of the body with resistant tumours, a high problem presented frequently in the metastatic breast cancer (Coley 2008) and metastatic colorectal carcinomas (Benhattar , Cerottini et al. 1996). So in conclusion, xenograft model may be used to validate novel mechanisms of resistance in a complete organism and as initial method of study new targets for new chemotherapy after *in vitro* resistant sublines development.

3.4.3 Mechanisms of resistance to 5-FU identified by proteomics

3.4.3.1 Bradford protein assays

After the establishment of resistant sublines, cell lysis and protein extraction were carried out for these new resistant cell sublines developed and for their long and low generation controls. Additionally, proteins were extracted from SILAC labelled parent cell lines for each cell line to be used during SILAC-approach. According to results previously shown in Table 3.6, amount of proteins extracted from each samples were similar and volumes were high enough to use the 200 µg of proteins required to build up the mixed SILAC-samples by combination of the Light/Heavy samples.

3.4.3.2 Significantly altered proteins seen in more than one 5-FU resistant subline

Due to the lack of commonly altered proteins in resistant sublines, a deeper study of uniquely altered proteins in each particular resistant subline to 5-FU was done and discussed in section 3.4.3.3.

3.4.3.2.1 Up-regulated proteins of DLD-1 5-FU and KM 12 5-FU (3)

High significantly up-regulation was found for Myeloid-associated differentiation marker (MYADM) in the resistant sublines: DLD-1 5-FU, DLD-1 OXA, KM 12 5-FU and KM 12 OXA. But no differences in MYADM expression was found neither in DLD-1 IRI, HT 29 5-FU resistant cell lines nor in any of the two parent control cell lines DLD-1, KM 12 and HT 29. MYADM is a protein that takes part in the organisation of endothelial cells surface and cell-cell junctions playing a role at the biological defense facing the vessel lumen. MYADM was described as a differentiation marker of stem cells and as an initial marker of CD34+ bone marrow myeloid cells derived from normal marrow cells. MYADM modulates selective permeability, such as mechanical forces, cytokine signalling, and cell–cell interactions (Aranda, Reglero-Real et al. 2013). MYADM-GFP is located at the plasma membrane and in cell–cell junctions in confluent endothelial cells. MYADM distribution overlaps with filamentous actin and junctional markers, such as vascular endothelial (VE)-cadherin (Aranda, Reglero-Real et al. 2013). Interestingly, DLD-1 5-FU and KM 12 5-FU resistant sublines showed

differences during cell culture in cells distribution at the edge of the colony. Cell distribution of these two resistant cell lines gives a rounder shape border in contrast with HT 29 5-FU and control samples that show an irregular colony border (Fig 3.15). It has been observed that MYADM reduction induced the appearance of intercellular gaps, increasing cell membrane permeability. Similar results indicate that MYADM knockdown causes endothelial barrier dysfunction (Aranda, Reglero-Real et al. 2013). So, an increase of cell-cell junctions may act as physical barrier decreasing penetration of the drugs into cells by decreasing of cell membrane permeability. In 2005, during a microarray analysis of 298 genes using human melanoma cell lines, the overexpression of MYADM was associated with melanoma aggressiveness and progression and MYADM were defined as a prognostic factor in melanoma (De Wit, Rijntjes et al. 2005). A possible use of MYADM as a biomarker for promyelocytic leukemia cells was described in 2001 by Cui W. *et al*. Suggesting a role of MYADM during myelocytic leukemia development (Cui, Yu et al. 2001).

MYADM regulates activation of the family proteins, ezrin, radixin, and moesin (ERM proteins) that are the best-known connectors between plasma membrane, transmembrane receptors, and the subcortical actin cytoskeleton. ERM proteins increase cell permeability and they have been observed phosphorylated and activated under MYADM silencing in Human Umbilical Vein Endothelial Cells (HUVEC), promoting the inflammatory response (Aranda, Reglero-Real et al. 2013). ERM proteins co-localize with CD44 at actin filament-plasma membrane interaction sites, associating with CD44 via their N-terminal domains and with actin filaments via their C-terminal domains.

Interestingly CD44 is a transmembrane receptor protein found overexpressed in DLD-1 5-FU and HT 29 5-FU resistant sublines and it has been related to poor prognosis, aggressiveness by EGFR modulation in breast cancer (Bellerby, Smith et al. 2016)**.** Additionally, CD44 is known to be a cell surface biomarker of cancer stem-like cells (CSLCs)**.** Tumour cells with CSCs properties have the potential to proliferate through self-renewal and they are able to survive chemotherapy. CD133 and CD24 are CSCs markers that normally are co-expressed with CD44 and that have been associated with CRC resistance.

However, CD133 and CD24 were not detected during proteomics screening in any sample (Sahlberg, Spiegelberg et al. 2014, Bonneau, Rouzier et al. 2015).

CD44 acts as a receptor for hyaluronic acid, which activates intracellular survival pathways and it is involved in proliferation, differentiation, and motility. CD44 has been associated with chemoresistance in different types of cancer, included CRC (Hiraga, Ito et al. 2013, PYLVÄS-EEROLA, Liakka et al. 2016, Xia and Xu 2016). CD44 protein was found up-regulated in DLD-1 5-FU and DLD-1 OXA resistant subline. Although no clear evidence about a differentiation role of CD44 in resistant sublines was found because CD44 ratios expressions were irregular along all subsamples, so no conclusions were established. However, the insulin-like growth factor 2 mRNA-binding protein 3 (IGF2BP3) was found significantly up-regulated in DLD-1 5-FU resistant subline. IGF2BP3 binds to the 5'-UTR of the insulin-like growth factor 2 (IGF2) mRNAs and to sequences in the 3'-UTR of CD44 mRNA. Significantly up-regulation of the androgen-regulated gene protein receptor (SARG) was also found in DLD-1 5-FU and KM 12 5-FU, than in DLD-1 and KM 12 parent cell lines (Steketee, Ziel-van der Made et al. 2004)**.** Despite the lack of knowledge about this specific androgen receptor, the relevance of androgen receptors (AR) has been one of the main targets of prostate cancer therapies during last years. Furthermore, AR overexpression and mutations have been studied as mechanisms of cancer resistance during anti-AR therapies. So, the potential role of SARG as CRC biomarker must be studied.

Other protein significantly up-regulated in 5-FU resistant samples was N(G), N(G)-dimethylarginine dimethylaminohydrolase 2 (DDAH2). DDAH2 is a protein that inhibits the nitric oxide synthase (NOS) enzyme. NOS mediates the production of nitric oxide from arginine. This conversion from arginine to NOS mainly occurs in vascular endothelium tissues that are rich in arginine like gastrointestinal tract, kidney, and urinary bladder (Uhlén, Fagerberg et al. 2015). It is known that levels of NOS enzyme are variable according to arginine availability within the cell microenvironment. Nitric oxide production by NOS may play a protector role in the vascular endothelium as a vasodilator and antiplatelet agent. It is known that under vascular endothelium damage

conditions, the level of nitric oxide decreases and the production of vasoconstrictor molecules increases. Colorectal cell lines were exposed to drug agents during resistant cell lines development and an increase in DDAH2 expression may be a response to decreasing nitric oxide levels by NOS enzyme inhibition. Nitric oxide has been proposed as an inhibitor of cell proliferation in endothelium so a decrease of nitric oxide levels in resistant cells by NOS inhibition through DDAH2 overexpression may have a proliferation effect. A complementary result of NO decreasing by NOS inhibition is the up-regulation of the enzyme ferrochelatase (FECH) in DLD-1 5-FU subline. The main role of FECH is to catalyse the ferrous insertion into protoporphyrin IX. FECH enzyme is inhibited by NO and the overexpression of FECH may be a consequence of a decreasing at the NO levels caused by inhibition of NOS by DDAH2 (Furukawa, Kohno et al. 1995). Studies about nitric oxide signalling pathways and NO production has been considered to be therapeutic beneficial too (Choudhari, Chaudhary et al. 2013, Vasudevan and Thomas 2014). Recently, DDAH2 overexpression has been considered as a poor prognosis factor for initial stages of lung adenocarcinoma and it has been related with angiogenesis and invasiveness (Shiozawa, Iyama et al. 2016)**.** Hasegawa *et al.* reported that DDAH2 stimulates expression of VEGF through the transcription factor Sp1 in vascular endothelial cells. VEGF was not identified during initial proteomics screening, whilst Sp1 do not show any expression change in resistant samples to 5-FU (Hasegawa, Wakino et al. 2006). DNA methylation of DDAH2 and its overexpression at gene level have been suggested as differentiation marker from neural stem cells to embryonic stem cells (Bäckdahl, Herberth et al. 2009). However, the role of DDAH2 overexpression in CRC is still unknown.

3.4.3.2.2 Up-regulated proteins of HT 29 5-FU and KM 12 5-FU (1)

The unique significantly up-regulated protein found in HT 29 5-FU and KM 12 5-FU samples was the amyloid β precursor-like protein (APLP2). However, APLP2 was not detected in DLD-1 5-FU subline, so a WB should be done to confirm if APLP2 may be an important marker of 5-FU in CRC. APLP2 is together with amyloid β A4 protein (APP) and the amyloid-like protein 1 (APLP1) part of the amyloid precursor protein (APP) family. APP was found up-regulated in DLD-1 5-FU, DLD-1 OXA, DLD-1 IRI and HT 29 5-FU resistant

sublines in contrast with the four DLD-1 and HT 29 generation controls. APLP1 was not detected in any sample during the proteomics analysis. Despite the high lack of knowledge about physiological functions of APLP2 and APLP1 proteins. It is known that APP family is expressed in gastrointestinal tumours. APP family members have been proposed to be transported to the cell membrane where they act in cell-cell interaction, cells adhesion, and metastatic processes. A high expression of APLP1 over APLP2 expression has been described as a feature of neuroendocrine tumours (Arvidsson, Andersson et al. 2008)**.** APLP2 have been described as crucial protein in many kinds of cancers: prostate, breast, colon, thyroid, lung, nasopharynx, and gastrointestinal cancer (Pandey, Sliker et al. 2016). APLP2 plays a role in synaptic plasticity, promoting neurite outgrowth and differentiation, neural cell motility and copper homeostasis, has also been shown to regulate development of the brain by regulating migration and differentiation of neural stem cells (Srivastava, Khurana et al. 2012)**.** APLP2 has been related with radioresistance in pediatric Ewing's sarcoma (EWS) and in human cervical carcinoma HeLa cell line. As APLP2 expression decreases the expression of MHC class I molecules in EWS cancer this may inhibit and interfere with cell lysis mediated by T-cell. EWS is a cancer presented in bones, cartilage or nerves. EWS is characterised by the presence of a high chromosomal translocation with high capacity to develop resistance to therapy (Peters, Yan et al. 2013).

3.4.3.2.3 Down-regulated proteins of DLD-1 5-FU and KM 12 5-FU (3)

Three different proteins were found significantly down-regulated in DLD-1 5-FU and KM 12 5-FU sublines. One of these proteins was 4F2 cell-surface antigen heavy chain (SLC3A2). SLC3A2 is a protein that plays a role in metal ion homeostasis and toxicity with a high activity during up-taking of methylmercury (MeHg). SLC3A2 transmembrane protein transporter regulates intracellular calcium levels and transports L-type amino acid, playing a role in nitric oxide synthesis in human umbilical vein endothelial cells (HUVECs) via transport of L-arginine. So, SLC3A2 down-regulation and DDAH2 up-regulation (previously described as NOS inhibitor) together could be involved in a mechanism of resistance against 5-FU by decreasing of nitric oxide levels in two different CRC cell lines DLD-1 5-FU and KM 12 5-FU. Previous literature supports the idea of

nitric oxide as chemotherapy resistance factor in neuroblastoma cell lines. This mechanism of resistance is has been proposed to be related to MYC inhibition and an enhancement of ABC transporters activity and overexpression (Porro, Chrochemore et al. 2010). Previous publications led by Weiming Xu and his team showed the relevance of NO levels for cell cytotoxicity. High levels of iNOS expression may be cytostatic or cytotoxic for tumour cells, whereas lower activity can have the opposite effect and promote tumour growth in MCF-7 and ZR75 breast cancer cell lines (Liu and Xu 2013).

Another significantly down-regulated protein in DLD-1 5-FU and KM 12 5-FU resistant cell lines is the phosphatidate cytidyltransferase mitochondrial (TAMM41). TAMM41 is an enzyme that catalyses the formation of CDP-diacylglycerol (CDP-DAG) from phosphatidic acid (PA) in the mitochondrial inner membrane. Required for the biosynthesis of the dimeric phospholipid cardiolipin that stabilises supercomplexes of the mitochondrial respiratory chain in the mitochondrial inner membrane (Swan, Maxwell et al. 2015).

The third significantly down-regulated protein involved in 5-FU resistance was the Glycerol-3-phosphate dehydrogenase 1-like protein (GPD1L). GPD1L plays a role in the regulation of cardiac sodium current and decreases enzymatic activity that results in an increase in glycerol 3-phosphate. Glycerol 3-phosphate activates the DPD1L-dependent SCN5A phosphorylation pathway, which may ultimately lead to decreased sodium current; cardiac sodium current may also be reduced due to alterations of NAD(H) balance induced by DPD1L (Valdivia, Ueda et al. 2009)**.** Apart from DLD-1 5-FU and KM 12 5-FU, GPD1L was found down-regulated in DLD-1 IRI resistant subline too.

3.4.3.2.4 Down-regulated proteins of DLD-1 5-FU and HT 29 5-FU (2)

Only two significantly down-regulated proteins were commonly found in DLD-1 5-FU and HT 29 5-FU.The first protein was Rap1 GTPase-GDP dissociation stimulator 1 (RAP1GDS1) factor that participates in activation of G proteins like Rap1a/Rap1b, RhoA, RhoB, and KRas. RAP1GDS1 promotes GDP/GTP exchange reaction by stimulating GDP dissociation from G-proteins (Kikuchi, Kaibuchi et al. 1992).

The second protein down-regulated was the vacuolar protein sorting-associated protein 45 (VPS45) (5) that plays a role in vesicle-mediated protein trafficking from the Golgi stack through the trans-Golgi network (Rajasekariah, Eyre et al. 1999). Some recent studies in yeast show that methylmercury toxicity depends directly on the activity of both the endosome transport and the vesicular trans-Golgi trafficking network. Increasing of trans-Golgi network factor as VPS45 increases sensitivity of yeast to methylmercury and down-regulation of endosome trans-Golgi transport increase the resistance phenotype in yeast model (Hwang, Murai et al. 2014). However, no evidence of VPS45 role has been described in cancer drug resistance or CRC.

3.4.3.2.5 Down-regulated proteins of KM 12 5-FU and HT 29 5-FU (3)

The enzyme 3'(2'), 5'-bisphosphate nucleotidase 1 (BPNT1) was found significantly down-regulated in both KM 12 5-FU and HT 29 5-FU resistant sublines. BPNT1 mediates conversion of adenosine 3'-phosphate 5'-phosphosulfate (PAPS) to adenosine 5'-phosphosulfate (APS) and 3'(2')-phospho- adenosine 5'- phosphate (PAP) to AMP (Spiegelberg, Xiong et al. 1999). However, the role of BPNT1 is unknown in cancer.

The other significantly down-regulated protein was the neurochondrin (NCDN) factor. NCDN is involved in nervous system development and its main function is to act as promotor of surface localization of GRM5 to increase neural signal transduction. It is important to regulate melanin concentration by its interaction with MCHR1 that interferes with G protein-coupled signal transduction pathways (Francke, Ward et al. 2006).

3.4.3.3 Significantly altered proteins unique to one of the 5-FU resistant sublines

Whilst some proteins were consistently altered across the cell lines (see Fig. 3.27), in the majority of cases the altered proteins were unique to one cell line. This confirms the heterogeneity seen in CRC, and why molecular characterisation of an individual patient´s tumour is important in developing therapeutic strategies. In this section, the findings for each one of the three cell lines are discussed. In considering potential novel mechanisms of resistance,

since this process is usually the outcome of longer-term processes involving a net of proteins and different biological pathways, and not a single protein or pathway, this will be focused on 5 biological processes: 1) apoptotic and anti-apoptotic pathways, 2) DNA repair process, 3) drug and small molecules metabolism, 4) intracellular protein transport, 5) cellular membrane transporters and membrane organization.

A summary table containing unique proteins altered in 5-FU resistant sublines derived from DLD-1, KM 12 and HT 29 is shown below (Table 3.17). Most relevant up-regulated proteins were classified based on the specific literature background of the protein in two groups:

1) Altered proteins by direct effect of 5-FU exposure: apoptotic mechanism, stress proteins…

2) Altered proteins by indirect effect of 5-FU exposure: DNA repair, drug transport, drug metabolism, exocytosis, vesicle formation…

	Indirect effect of 5-FU	**Direct effect of 5-FU**
DLD-1 5-FU	ACSF3, NOL3, LGMN, EHBP1L1, GAA, LAMP1, LAMP2, RAB2B, SEC24D, HID1, MUC5AC, ITGA3, CD44, MAC-2-BP, MDR1, ATP7B, FSCN1, SYTL2	FAS, FADD, NFAT5, TAOK1, PRKCD, PAR-4, PMS2, HSP27, UMPS, GGT1, TMED4,
KM 12 5-FU	ERMP1, CHMP2A, IPO7, LGALS3BP, EFNB1, SRC, STAT1	PYGM, NT5C3A, GNAI2, HSPH1, STIM1, PLSCR1
HT 29 5-FU	BET1, TFRC, FTH1	GATA6

Table 3.17: Up-regulated proteins identified in 5-FU resistant sublines.

3.4.3.3.1 DLD-1 5-FU

3.4.3.3.1.1 Apoptotic process (1)

Among the three resistant sublines, DLD-1 5-FU showed the highest number of proteins altered in pro-apoptotic and anti-apoptotic pathways.

From DLD-1 5-FU results, one of the most significantly up-regulated proteins was the nucleolar protein 3 (NOL3) (ARC). NOL3 has two isoforms. Whilst isoform 1 participates in the regulation of the splicing process of the arginine/serine-rich SRp30c protein, isoform 2 is a repressor of the apoptotic process that avoids cell death. Inhibition of apoptosis by NOL3 is mediated by blocking of tumour necrosis factor receptor superfamily (FAS) and its FAS-associated death domain (FADD) interaction protein. FAS and FADD proteins were found up-regulated in DLD-1 5-FU resistant subline as a possible consequence of the 5-FU cytotoxicity effect (Park, Yoon et al. 2002). NOL3 overexpression in CRC has previously been related to activation of DNA repair mechanisms and suppression of apoptotic pathways mediated by caspase activity (Tóth, Meinrath et al. 2016)**.**

Argonaute-1 (AGO1) (EIF2C1) is involved in mRNA silencing leading to down-regulation of different gene expression such as RNA Pol ll. Silencing of target genes is mediated by argonaute proteins by mRNA degradation and translational repression of mRNA. AGO1 binds to RNA Polymerase II (RNA Pol II) interfering with RNA Pol II transcription (Huang, Zheng et al. 2013) and hence down-regulation of AGO1 may unbalance gene expression of different proteins directly involved in cancer pathways such as BRCA2, RAD51, BCL-2, and p21 (Mondal, Pal et al. 2016). Genomic deregulation and increasing expression of genes as RNA Pol II would mediate drug resistance in DLD-1 5-FU subline. Interestingly, two mediators of RNA polymerase II, the transcription MED9 and MED31 were also found up-regulated in DLD-1 5-FU. Results presented here correlate with a similar previous study in CRC patients that showed how somatic mutations which involved repression and down-regulation of AGO2, may contribute to development of MSI state by increasing mutations and alterations that may lead to cancer development (Kim, Oh et al. 2010)**.** Another important finding related to RNA Pol II in DLD-1 5-FU was the up-

regulation of the nuclear factor of activated T-cells 5 (NFAT5). NFAT5 showed a positive regulation of transcription from RNA polymerase II promoter. NFAT5 is a protein involved in cell regulation under osmotic stress conditions (López-Rodríguez, Aramburu et al. 2001). Additionally, NFAT5 plays a crucial role during intestinal cells differentiation. It has been demonstrated that NFAT5 inhibition by siRNA blocks Caco-2 and HT 29 intestinal cells differentiation process and increasing of NFAT5 has been observed in intestinal mucosa with high differentiation (López-Rodríguez, Aramburu et al. 2001).

Significant up-regulation of serine/threonine-protein kinase (TAOK1), which is involved in the p38/MAPK14 stress-activated MAPK cascade, and the DNA damage response, was also observed in DLD-1 5-FU. TAOK1 mediates G2/M transition during DNA damage (Raman, Earnest et al. 2007) and activates p38, a protein also found overexpressed in the DLD-1 5-FU subline. Hence, TAOK1 overexpression would be expected in cells that have been grown under DNA damage conditions over a prolonged period. However, TAOK1 activity in CRC has not previously been studied.

Similar effects were found with protein kinase C δ type (PRKCD), which was found significantly up-regulated in DLD-1 5-FU. PRKCD is a pro-apoptotic protein that is activated during DNA damage-induced apoptosis. Under oxidative stress conditions which may be similar to drug treatment, PRKCD interacted with CHUK/IKKA proteins and promoted phosphorylation of p53/TP53. An alternative regulation of apoptosis by PRKCD is mediated by activation of MAPK11 or MAPK14.The treatment of HCT 116 CRC cell line with 5-FU caused up-regulation of PRKCD in line with our observations (Mhaidat, Bouklihacene et al. 2014)*.*

Serine/threonine-protein kinase PRKC (Par-4) (PAWR) is a pro-apoptotic regulator of WT1 protein, a transcription factor with proline/glutamine-rich DNA-binding domain and regulator of p53. Par-4 protein is inactivated in CRC cell lines under normal conditions however it is up-regulated in CRC cell lines after 5-FU treatment. Par-4 activity is also increased by Src inhibition using Src kinase inhibitors *in vitro* (Kline and Irby 2011). Therefore, an increasing of Par-4

expression may be a consequence of continuously 5-FU treatment that promotes apoptotic pathways in CRC cell lines.

3.4.3.3.1.2 DNA repair process (2)

Two related proteins to DNA repair process were found significantly up-regulated in DLD-1 5-FU subline, transcription factor jun-D (JUND) and AP-1 complex-associated regulatory protein (Berger and Shaul 1991). The role of AP-1 in CRC is to increase the expression of drug transporter proteins like MDR1 (Guan, Zhao et al. 2016), which was also up-regulated in DLD-1 5-FU subline.

Mismatch repair endonuclease PMS2 that forms part of the post-replicative DNA mismatch repair system (MMR) was also up-regulated. PMS2 causes single-strand breaks close to the mismatch point and thus creates new entry points for the exonuclease EXO1 which degrades the strand containing the mismatch. Therefore, PMS2 plays a crucial role in DNA damage signalling. PMS2 may arrest the cell cycle and this may derivate into apoptotic pathways in case of serious DNA damage occurring in CRC cell lines exposed to excess 5-FU (Adamsen, Kravik et al. 2011). The up-regulation of PMS2 may play a role in assisting MMR system to DNA damage caused by the 5-FU active metabolite. Additionally, it has been demonstrated that overexpression of PMS2 contributes to DNA damage toleration in mammalian cells causing MMR system deregulation (Gibson, Narayanan et al. 2006)***.***

3.4.3.3.1.3 Drug and small molecules metabolism (3)

Several proteins in metabolism showed a significantly change in expression under 5-FU conditions. One of these proteins significantly overexpressed in DLD-1 5-FU is the heat shock protein 27 (HSP27). HSPs proteins are evolutionarily conserved molecules synthesised by cells in response to heat or chemical stress, conditions equivalent to prolonged drug exposure. HSP27 shows a negatively regulation of apoptotic process, which is activated by anti-cancer drugs or under oxidative stress conditions (Heinrich, Donakonda et al. 2016). Previous multiple studies reflect an important protective effect by HSP27 on CRC cell lines when they were treated with 5-FU while HSP27 phosphorylation and down-regulation return the 5-FU sensitive phenotype in

CRC cells (Wong, Wong et al. 2008, Matsunaga, Ishii et al. 2014, Lu, Sun et al. 2016). Additionally, HSP27 has been described as a biomarker for resistance to cisplatin in ovarian cancer cell lines and HSP27 inhibition can reverse resistance *in vitro* (Wong, Wong et al. 2008).

Among all significantly down-regulated proteins in DLD-1 resistant subline to 5-FU, the uridine monophosphate synthase (UMPS) (OPRT) is involved directly in the conversion of 5-FU into active metabolites with anticancer properties. 5-FU can be metabolised into 5-fluorouridine monophosphate (FUMP) by UMPS. FUMP is essential for its metabolic conversion into deoxyuridine triphosphate (dUTP) and 5-fluorouridine triphosphate (FUTP). dUTP cytotoxicity effect occurs after its incorporation into DNA causes irreparable cell damage during DNA synthesis and DNA repair (Muhale, Wetmore et al. 2011). Additionally, FUTP misincorporation into different RNA structures causes cell death by alteration of cellular metabolism and homeostasis (Ghoshal and Jacob 1994). Recently, it has been discovered that UMPS isoforms A and B are crucial during the development of resistance to 5-FU. Expression of isoform B occurs in a high percentage of resistant tumours by splicing of exon 2, while, high levels of isoform A are predominant in 5-FU sensitive cell lines. Moreover, M Griffith *et al*. showed that protein relative expression levels of UMPS isoforms A and B might have an effect on 5-FU resistant outcomes (via an unknown molecular mechanism) (Griffith, Mwenifumbo et al. 2013). Similarly, expression levels of A and B isoforms were feature of the proteomics results for DLD-1 resistant sublines. WB results generated as part of our study showed a strong signal for two isoforms of UMPS in the resistant subline DLD-1 5-FU and a weak signal for one of the two isoforms in DLD-1 P=65 parent cell line. However, the second isoform was not detected in DLD-1 P=9 parent cell line. After analysis of UMPS isoforms levels in DLD-1 Set, it was observed that similar expression levels were presented in the resistant subline DLD-1 5-FU but no in the parent cell lines that were sensitive to 5-FU. So, similar results to M Griffith *et al*., studies were found.

Two enzymes involved in lipid metabolism were found significantly up-regulated in DLD-1 5-FU too. One was the acyl-CoA synthetase family member 3

(ACSF3) protein and the second was the enzyme known as the very long-chain specific acyl-CoA dehydrogenase (ACADVL). ACSF3 activates the synthesis of fatty acid in mitochondria by metabolising malonate and methylmalonate while ACADVL protein is involved in the β-oxidation of fatty acids in mitochondria.

A different and intriguing finding was the up-regulation of gamma-glutamyltranspeptidase 1 (GGT1). GGT1 is a protein involved in reduction of glutathione to cysteine, a stress marker (Fentiman 2012) and its up-regulation may be related to the 5-FU treatment as consequence of an increasing of oxidative stress in cells due to continuous drug treatment. GGT1 overexpression has been linked to risk of a poor prognosis in cervical cancer patients and associated with invasiveness features of melanoma cell lines and mouse xenograft models (Corti, Franzini et al. 2010)**.** Recently, GGT1 was identified as an important factor and potential marker of CRC progression from stage-III to stage-IV. Hence, the role of GGT1 in CRC resistance warrants further investigation (Palaniappan, Ramar et al. 2016).

3.4.3.3.1.4 Intracellular protein transport (11)

Some proteins significantly up-regulated proteins found in DLD-1 5-FU, there are some whose molecular functions are related to the endomembrane system: endoplasmic reticulum (ER), Golgi apparatus, and lysosomes. These proteins involved in vesicle production and trafficking inside the cells are particularly relevant due to possible roles in drug resistance. Vesicles formed inside the cells could act as drug containers, which would decrease the free drug concentration inside cells. Main cellular structures available to act as drug containers are lysosomes and storage vesicles. Lysosomes are especially interesting due to the function they play during catabolism of biomolecules. Lysosomes contain a large number of different enzymes such as hydrolases that digest proteins, nucleic acids, lipids and other biomolecules. These enzymes could limit the bioavailability by drug degradation. Lysosomal drug sequestration of hydrophobic weak base drugs (Duvvuri and Krise 2005) and consequently lysosomal drug storage has been recently described by Zhitomirsky and Assaraf. Lysosomal drug storage converges into an increase of the number and size of lysosomes inside cells. Further, drug transporters from

the ABC superfamily were found localized on lysosomes membrane and involved in the active transport of drugs into the lysosome (Zhitomirsky and Assaraf 2016). In the same way, another drug transporter known as ATP7B was defined as necessary for copper-dependent lysosomal exocytosis (Peña, Coblenz et al. 2015). All these recent findings indicate lysosomes are potential mediators of drug resistance. Among the proteins found significantly up-regulated in DLD-1 5-FU resistant subline, 11 are associated with lysosome an exosome formation and whose relevance in 5-FU resistance is summarised in Table 3.18 below.

Protein Name	Main Function	Role in Cancer	Reference
Cysteine proteinase legumain (LGMN)	Exopeptidase activity	Poor prognosis in CRC	(Dall and Brandstetter 2013) and (Haugen, Boye et al. 2015)
EH domain–binding protein 1–like 1 (EHBP1L1)	Late endosome and lysosomes formation	Unknown	(Zhen, Chunlei et al. 2014) and (Nakajo, Yoshimura et al. 2016)
Lysosomal α –glucosidase (GAA)	Hydrolysis of glycogen in lysosomes	GAA inhibitors decrease CRC risk	(Nakajo, Yoshimura et al. 2016)
Lysosomal-associated membrane proteins (LAMP1, LAMP2)	Constitute 50% of the lysosomal membrane	LAMPs downregulation inhibit proliferation in prostate cancer	(Eskelinen 2006) and (Okato, Goto et al. 2016).
Protein Rab-2B (RAB2B)	Modulation of Golgi complex and exocytosis	Unknown	(Ostrowski, Carmo et al. 2010) and (Aizawa and Fukuda 2015)
Sec24D	Transport to the Golgi complex	Unknown	(Tang, Kausalya et al. 1999)
VPS16	Fusion of lysosomes with endosomes	Unknown	(Wartosch, Günesdogan et al. 2015)
Components of the lysosome-related organelles complex 1 (BLOC-1)	Synthesis of melanosomes	Cisplatin resistance	(Chen, Leapman et al. 2009) and (Chen, Valencia et al. 2006)
HID1 protein	Vesicle trafficking in secretory cell lines	Unknown	(Wang, Zhan et al. 2011)
Mucins (MUC5AC and MUC2)	Protection and survival of epithelial cells	Carcinogenesis in CRC, MUC5AC inhibition repress migration in CRC	(Kufe 2009), (Truant, Bruyneel et al. 2003) and (Zhu, Long et al. 2016)
Transmembrane emp24 domain-containing protein 4 (TMED4)	Endoplasmic reticulum modulation under stress conditions	Unknown	(Hwang, Boswell et al. 2008)
Synaptotagmin-like protein 2 (SYTL2)	Exocytosis processes	Biomarker in metastatic breast cancer	Sung *et al.,* 2016 (Sung, Han et al. 2016)

Table 3.18: Summary table showing significantly up-regulated proteins in DLD-1 5-FU associated with lysosome an exosome formation.

3.4.3.3.1.5 Cellular membrane transporters and cell membrane organization (5)

An important significantly up-regulated protein (but not included in the 10% of most altered proteins group) was CD44. CD44 is a transmembrane receptor protein found significantly overexpressed in DLD-1 5-FU resistant subline and it has been related to poor prognosis and aggressiveness by EGFR modulation in breast cancer (Bellerby, Smith et al. 2016). Additionally, CD44 is known to be a cell surface biomarker of CSCs**.** Tumour cells with CSCs properties have potential to proliferate through self-renewal and they are able to survive chemotherapy (Bonneau, Rouzier et al. 2015). CD44 acts as a receptor for hyaluronic acid, which activates intracellular survival pathways and it is involved in proliferation, differentiation, and motility. Overexpression of CD44 in DLD-1 5-FU was validated by WB and similar results to SILAC approach were obtained (see section 3.3.10). CD44 has been associated with chemoresistance in colorectal and ovarian cancer. It is known that in addition to its role as CSCs biomarker and hyaluronic acid receptor involved in stress response, CD44 may act as protector of drug transporters such as P-glycoprotein from ubiquitination (Hiraga, Ito et al. 2013, PYLVÄS-EEROLA, Liakka et al. 2016, Xia and Xu 2016). Finally, CD117, also known as KIT, is another surface marker of embryonic stem cells that was found notably overexpressed in DLD-1 5-FU cell line but it has not been associated with 5-FU resistance.

One more protein significantly up-regulated in DLD-1 5-FU and involved in cell membrane organizations was galectin-3 (Mac-2-BP). Mac-2-BP is a protein implicated in modulating cell–cell and cell–matrix interactions and participates in multiple extracellular functions like cell adhesion, migration, invasion, angiogenesis, immune functions, apoptosis, endocytosis and it has been found elevated in the serum of patients with cancer. So, it has been discussed as a biomarker of cancer progression (Bresalier, Mazurek et al. 1998, Marchetti, Tinari et al. 2002, Iacovazzi, Notarnicola et al. 2010). Furthermore, Mac-2-BP has been considered as CSCs surface marker like CD44, previously described. Experiments *in vitro* evidence how subpopulations of DLD-1 with high levels of Mac-2-BP on its surface are more resistance to chemotherapeutic treatments like 5-FU, leucovorin, OXA and IRI (Ilmer, Mazurek et al. 2016). These evidence

of a crucial role of Mac-2 BP in CRC resistance are complemented by discoveries using 196 CRC patients where LGALS3BP overexpression in tumour tissue was defined as unique and independent prognostic factor of poor survival (Piccolo, Tinari et al. 2015). Finally, one last protein found significantly up-regulated and with high interaction with Mac-2-BP protein was the integrin α-3 (ITGA3). ITGA3 was found up-regulated in DLD-1 5-FU. ITGA3 promotes cell invasion and contributes to matrix degradation processes and invadopodia formation process (Mueller, Ghersi et al. 1999, Fukushi, Makagiansar et al. 2004)**.** Invadopodia promotes metastasis and may contribute to tumoural cell migration to distant sites of the body where chemotherapy agents show a lower effect (Stoletov and Lewis 2015)**.** But no role of ITGA3 in CRC resistance has been described until now.

Finally, fascin (FSCN1) is another interesting finding in DLD-1 5-FU. Main role of FSCN1 protein is to mediate in filopodia formation and distribution of actin filamentous fibres that play their crucial role during cell motility, cell-cell interaction and reorganization of the cytoskeleton (Yamashiro, Yamakita et al. 1998, Chen, Yang et al. 2011)**.** Up-regulation of *FSCN1* gene has been reported previously in resistant gastric cell lines to 5-FU. The paper was published in 2014 and the methodology followed to develop resistant sublines *in vitro* was by the culture of gastric cancer cells for more than ten months in a medium containing 5-FU, so using a similar methodology to the protocol used in this thesis study. The current proteomics study findings complement the previous study of FSCN1 at the gene level under 5-FU conditions. In summary, use of overexpression of FSCN1 should be studied as a predictive biomarker for 5-FU resistance in cancer (Maeda, Ando et al. 2014).

3.4.3.3.2 KM 12 5-FU

The complexity of the protein network model for KM 12 5-FU was the highest in contrast with the rest of resistant sublines models developed. This fact can be consequence of different initial genomic background between CRC cell lines. Additionally, new changes in proteins expression occurred during establishment of CRC sublines can affect proteins involved in DNA repair process such as PARP2 (see section 3.4.3.3.2.2 below) and alterations in these proteins can

affect to the DNA repair process, causing further alterations in additional proteins and molecular pathways. The main problem was that significantly altered proteins selected by 5th percentile in KM 12 5-FU sample were too many to be shown in a single network of protein interaction. Additionally, the number of interactions between these proteins was higher than in remaining resistant models. So, percentile was decreased to 2.5th percentile criteria to develop a new protein network model of the 5% of most altered proteins which are discussed below.

3.4.3.3.2.1 Apoptotic process (1)

It is known that stress-induced cell death occurs as consequence of DNA damage and cytotoxic stress that happens during cell lines drug exposure. Stress-induced signals converge upon the mitochondria via regulation of BCL2 family proteins. After BCL2 proteins activation, mitochondrial outer membrane permeabilization triggers the release of intramembrane space proteins including cytochrome c (CYCS), which permits assembly of a large multiprotein complex referred to as the apoptosome (Gupta, Cuffe et al. 2010). Significant down-regulation of CYCS in DLD-1 5-FU may be affecting stress-induced cell death that occurs as consequence of 5-FU treatment through DNA damage. Inhibition of CYCS in resistant cell lines would avoid the apoptosome assembly and it would decrease apoptotic processes (Deegan, Saveljeva et al. 2014)**.** Cytochrome c-type heme lyase (HCCS) is a protein that links covalently the heme group to CYCS which was found significantly down-regulated in KM 12 5-FU too (Babbitt, San Francisco et al. 2014).

Another important and significantly down-regulated protein that may be taking part in the development of resistance to 5-FU in KM 12 subline was the telomerase Cajal body protein 1 (WRAP53). WRAP53 mRNA regulates p53 protein at the post-transcriptional level during DNA damage. Under chemotherapy conditions, the transcription of p53 is increased by WRAP53 overexpression and this fact induces apoptosis of cells with DNA damage (Mahmoudi, Henriksson et al. 2016). In absence of WRAP53 or during down-regulation of WRAP53, p53 levels could be decreased and tumour cells would proliferate with DNA damage, increasing tumour size and tumour heterogeneity.

3.4.3.3.2.2 DNA repair process (2)

No significantly up-regulated protein involved in DNA repair was found in KM 12 5-FU and the unique significantly down-regulated protein was the poly [ADP-ribose] polymerase 2 (PARP2). PARP2 is involved in the base excision repair (BER) pathway (Schreiber, Amé et al. 2002), previous publications have shown that PARP2 is a protein which joins to DNA damage sites in cells to facilitate DNA repair process (Riccio, Cingolani et al. 2015). Additionally, recent studies with PARP2-deficient model organisms and cell lines, show sensitivity to several DNA damage agents. Hence, PARP inhibitors are now considered as a new treatment in cancer therapy (Murai, Shar-yin et al. 2012). According to the new data obtained here, it may be considered that a review of PARP proteins and their potential role as mediators of resistance to 5-FU should be done.

3.4.3.3.2.3 Drug and small molecules metabolism (3)

KM 12 5-FU showed a high number of altered proteins involved in drugs and small molecules metabolism. However, there is no clear evidence to link these up-regulated proteins to mechanisms of drug resistance in cancer. These significantly up-regulated proteins are summarised in the table below.

Protein Name	Main Function	Reference
Glycogen phosphorylase (PYGM)	Carbohydrate metabolism	(Nogales-Gadea, Mormeneo et al. 2010)
Cytosolic 5'-nucleotidase 3A (NT5C3A	CMP and m7GMP metabolism	(Amici, Ciccioli et al. 2005)
Guanine nucleotide-binding protein G (i) subunit α-2 (GNAI2)	Mediators of transmembrane signalling systems	(Cho and Kehrl 2007)
Subunit β type-10 of the proteasome (PSMB10)	Mediates cleaving of peptides with Arg, Phe, Tyr, Leu, and Glu	(Rouette, Trofimov et al. 2016)
Heat shock protein 105 kDa (HSPH1)	Prevents aggregation of denatured proteins	(Shorter 2011)

Table 3.19: Summary table with most significantly altered proteins seen in KM 12 5-FU related to drug and small molecules metabolism.

3.4.3.3.2.4 Intracellular protein transport (4)

Most of the significantly up-regulated proteins found in KM-12 5-FU belong to the intracellular protein transport group. One of these up-regulated proteins was the stromal interaction molecule 1 (STIM1), previously discussed in more detail in section 3.4.3.2.

Endoplasmic reticulum metallopeptidase 1 (ERMP1) is other significantly up-regulated protein in KM 12 5-FU. ERMP1 is required for the organization of somatic cells and normal ovarian histogenesis, but no implications in cancer are known (Garcia-Rudaz, Luna et al. 2007).

Charged multivesicular body protein 2a (CHMP2A) that is involved in multivesicular bodies' formation (MVBs) was found significantly up-regulated in

KM 12 5-FU too. CHMP2A is required for a normal function of endosomal sorting complex required for transport (ESCRT) of proteins. ESCRT proteins are involved in cellular functions related to membrane fission events such as: releasing of cytokines, mitosis, late anaphase processes (Guizetti, Schermelleh et al. 2011) and membrane fission activities through its interaction with VPS4 protein, which was found increased in all resistant sublines except HT 29 5-FU (Obita, Saksena et al. 2007) (Vietri, Schink et al. 2015). Increasing of MVBs activity is being one of the main aims in cancer resistance fight, as it has been found evidence of MDR development in prostate cancer by increasing of MVBs and other extracellular vesicles (Soekmadji and Nelson 2015)**.** However, no evidence of MVBs activity in CRC resistance has been established yet.

Importin-7 (IPO7) (RanBP7) is a significantly up-regulated protein of KM 12 5-FU. Previous studies of IPO7 show overexpression of IPO7 as a common feature in CRC cells. IPO7 main role is to transport nuclear receptors responsible for the nuclear import of histone H1 and ribosomal proteins. High mRNA levels of IPO7 show a positive correlation with high proliferation rate in colorectal tumour tissue, although the mechanism behind this IPO7 expression to mediate cell proliferation is still unknown (Li, Gyselman et al. 2000). Contrary to previous publications that found IPO7 repressed by p53 in the CRC cell line HCT116 (Golomb, Bublik et al. 2012), these proteomics results of KM 12 5-FU show higher levels of both IPO7 and p53 in the KM 12 5-FU resistant subline than in the sensitive parent cell line KM 12.

3.4.3.3.2.5 Cellular membrane transporters and cell membrane organization (5)

KM 12 5-FU analysis showed up-regulation in some proteins involved in cell membrane organisation and cell membrane transporters. Galectin-3-binding protein (LGALS3BP) is a protein that increases cell adhesion, promoting tumour cell aggregation that increases cancer progression and metastasis in the human melanoma cell line A375 (Sasaki, Brakebusch et al. 1998, Tinari, Kuwabara et al. 2001). While very little is known about how cell adhesion may contribute to drug resistance, cell adhesion is being one of the main issues of study under cellular biology and biomedical engineering fields (Khalili and Ahmad 2015).

Ephrin-B1 (EFNB1) is other significantly up-regulated protein that enhances cell adhesion via cell-cell signalling that has not been related to CRC yet. Although, it is known that inhibition of EFNB1 *in vitro* decreases tumour growth in head and neck squamous cell carcinomas (Vermeer, Colbert et al. 2013).

In KM 12 5-FU, one of the most relevant significantly up-regulated proteins is the proto-oncogene tyrosine-protein kinase Src (SRC). Up-regulation of SRC can occur by mutations as consequence of DNA mutations affecting cytoplasmic kinase domains that constitutively active signalling involved in cell adhesion, cell cycle progression, apoptosis, migration, and transformation. SRC is also activated at the sites of cell-cell contact adherences junctions and phosphorylates substrates such as β-catenin (CTNNB1), delta-catenin (CTNND1), and plakoglobin (JUP) and SRC mediates phosphorylation of both STAT1 and STAT3 by epidermal growth factor (EGF), leading to increased DNA binding activity of these TFs (Vasilenko, Butylin et al. 2000)**.** STAT1 was found significantly up-regulated in KM 12 5-FU, hence the value of this SRC-STAT1 hypothesis acquires more relevance. STAT1 is a transcription factor that has been suggested as an anti-tumour target to avoid drug resistance. In the CRC cell line Colon26L5-Vec resistant doxorubicin, the inhibition of STAT1 returns the sensitive phenotype (Malilas, Koh et al. 2013)**.** In the same way, a study using Stat1−/− mice showed that overexpression of STAT1 enhances a cell environment that promotes cell survival under genotoxic stress (Wang, Patsis et al. 2015).

Phospholipid scramblase 1 (PLSCR1) was also found significantly up-regulated in KM 12 5-FU. PLSCR1 plays an important role during apoptosis by recognition of damaged cells by the reticuloendothelial system. Inhibition of PLSCR1 protein by antiphospholipid scramblase 1 antibody has shown to have an anti-proliferative effect in CRC cell lines *in vitro* (Chen, Chen et al. 2014). Additionally, PLSCR1 is thought to be involved in tumour proliferation because overexpression of PLSCR1 has been observed under EGF stimulation pathways (Sun, Nanjundan et al. 2002). However, PLSCR1 as a mediator of drug resistance has not been described yet.

3.4.3.3.3 HT 29 5-FU

HT 29 5-FU was one of the resistant sublines that showed the lowest resistant fold change (3.5-fold) with only seven significantly up-regulated proteins.

3.4.3.3.3.1 Apoptotic process (1)

Only the transcription factor GATA-6 (GATA6) was found significantly up-regulated in HT 29 5-FU. Previous studies using HT 29 cell line show that overexpression of GATA6 is involved in proliferation process (Gao, Sedgwick et al. 1998) and mediates radiotherapy resistance *in vitro* (Cai, Shen et al. 2014).

3.4.3.3.3.2 DNA repair process (2), Drug and small molecule metabolism (3) and Intracellular protein transport (4)

No significantly up-regulated proteins were found involved neither in DNA process nor in drug and small molecules metabolism in HT 29 5-FU. In contrast to all remaining resistant sublines, HT 29 5-FU was the unique resistant subline that did not show any significantly up-regulated protein involved in intracellular protein transport.

Phosphoglucomutase-1 (PGM1) enzyme is a significantly down-regulated protein which catalyses the breakdown and synthesis of glucose (Bae, Kim et al. 2014)**.** PGM1 activity may be decreased as result of constant exposure to drugs that decrease cell survival and cell proliferation. Tumour cells could be decreasing their metabolism and glycolysis pathways as consequence of a constant interaction with chemotherapy. Effects of 5-FU in glycolysis and glucose metabolism have been studied in A549 cell line (Zhao, Ren et al. 2014). So, the low fold change in the resistant sublines HT 29 5-FU may be explained as a resistance establishment step process where cells show a lower metabolic rate before they are available to develop a better consistent resistance that may be established after long time drug exposure. In the same way, previous studies with MCF-7 breast cancer cell lines showed that decreasing of glycolysis pathways can drive into an increasing of mitochondrial respiration that declines anti-proliferative effects of drugs such as carboplatin, OXA, 5-FU, camptothecin, doxorubicin, paclitaxel, docetaxel, and hydrogen peroxide (Leung, Kim et al. 2014).

Another significantly down-regulated protein is the dihydropyrimidinase-related protein 2 (DPYSL2) which has a role in neuronal polarity and axon growth. Although DPYSL2 has not been related to cancer, alterations in DPYSL2 expression are involved in development of Alzheimer's disease (Natalia Silva, Furuya et al. 2013).

3'(2')-5'-bisphosphate nucleotidase 1 (BPNT1) enzyme metabolises conversion of both PAPS to APS and PAP to AMP. Apart from KM 12 5-FU, BPNT1 protein was found significantly down-regulated in the resistant subline HT 29 5-FU and it will be discussed in more detail below in the Chapter 7, section 7.3.1.4.

Vacuolar protein sorting-associated protein 45 (VPS45) plays a role in vesicle-mediated protein trafficking from the Golgi stack through the trans-Golgi network (Rajasekariah, Eyre et al. 1999)**.** Apart from HT 29 5-FU was found significantly down-regulated in the resistant subline DLD-1 5-FU and it has been discussed previously in section 3.4.3.2.4.

Finally, a last significantly down-regulated protein was the ADP-ribosylation factor-like protein 3 (ARL3) is a small GTP-binding protein involved in transporting of lipid proteins and cilia signalling but its relevance in cancer is unknown (Fansa and Wittinghofer 2016).

3.4.3.3.3.3 Cellular membrane transporters and cell membrane organization (5)

Three significantly up-regulated proteins involved in membrane transport were found in HT 29 5-FU. One of these proteins was the BET1 homolog (BET1) protein. BET1 mediates vesicle transport along the cytoplasm from the endoplasmic reticulum (ER) to the Golgi apparatus, taking part in the fusion activity of transport vesicles to the Golgi apparatus membrane (Petrosyan 2015) (Wlodkowic, Skommer et al. 2009). Inhibition of transporting activity of vesicles from ER to Golgi apparatus has been previously used as a strategy to reverse fludarabine resistance phenotype in resistant chronic lymphocytic leukaemia (CLL) cells *in vitro*. The mechanism behind this loss of resistance resides in that the blocking of protein trafficking caused by brefeldin A treatment leads to

activation of caspases and increases sequestration of the survival factors APRIL and VEGF (Carew, Nawrocki et al. 2006).

A second significantly up-regulated protein found in HT 29 5-FU was the transferrin receptor protein 1 (TFRC). TFRC mediates iron uptake via endosomes internalization after ligand binding to the transferrin receptor that activates endocytosis of endosomes (Rothenberger, Iacopetta et al. 1987). In CRC cells levels of TFRC are related with proliferation rate of tumour cells (Okazaki, Matsunaga et al. 2010) and it has been considered as enhancer of platinum drugs delivery (Daniels, Delgado et al. 2006), especially for OXA (Suzuki, Takizawa et al. 2008). This new potential role for TFRC as a mediator of resistance discovered during our proteomics study, it is proposed as a point of disagreement. It looks clear that use of liposomes for platinum drugs delivery is having success in animal models, where drugs are maintained inside interstitial space during a long time (Maruyama 2011).

Finally, the third protein significantly up-regulated included in membrane transport group and unique of HT 29 5-FU subline was the ferritin heavy chain (FTH1). FTH1 is another protein related to the previously discussed protein FTRC. After iron uptake mediated by FTRC, the protein FTH1 with ferroxidase activity mediates iron homeostasis and stores iron molecules in vesicles within cells (Wu, Polack et al. 1999). Although nothing is known about FTH1 role in 5-FU and cancer resistance, the present proteomics analysis suggests that an increase in iron uptake activity could be associated with resistance to 5-FU.

3.4.3.4 Significantly altered proteins seen in DLD-1 5-FU, HT 29 5-FU, and KM 12 5-FU resistant sublines

RICTOR, FAM83B, TEP1, and GLCE proteins were quantified and showed a high light/heavy ratio in DLD-1 5-FU, HT 29 5-FU, and KM 12 5-FU resistant sublines during proteomics quantification. However, these proteins were not quantified in any of the six parent control samples. This lack of quantification in any of the six control samples may be due to the limit of quantification (LOQ) by the mass spectrometer. LOQ is one of the main challenges in proteomics quantification. A mass spectrometer requires a minimum quantity of peptides concentration to be reliable to detect, identify and quantify a protein. If the cell

sample does not achieve this minimum concentration of the protein to be identified by the mass spectrometer, the protein may not be detected by this technique. So, a further analysis of the protein by other technique as WB should be carried out to confirm these results.

The protein FAM83B was discovered in 2012, this protein is an oncogene that acts at EGFR signalling pathway. FAM83B expression levels were associated with specific cancer subtypes, with increasing of tumour size and with patients survival decrease. FAM83B may act by EGFR direct activation or by the mediation of RAS/MAPK and PI3K/AKT/TOR signalling cascades in breast cancer cell lines and mice models (Cipriano, Graham et al. 2012, Lee, Meier et al. 2012, Cipriano, Miskimen et al. 2014). Overexpression of FAM83B was significantly associated with estrogen receptor– (ER-) and progesterone receptor–negative (PR-negative) breast tumours and poor outcome. All evidence about FAM83 over the last years have increased the interest of the science community on this new oncogene that has been found up-regulated in the three different resistant sublines to 5-FU developed *in vitro*.

Glucuronyl C5-Epimerase (GLCE) (HSepi) is an enzyme that mediates heparan sulfate (HS) and heparin biosynthesis by catalysing the epimerization of D-glucuronic acid (GlcA) to L-iduronic acid (IdoA) at polymer level. HS is a negatively charged linear polysaccharide derived from proteoglycan (HSPG) in which two or three HS chains are attached to the cell surface or extracellular matrix proteins to mediate the selective binding and cellular internalisation of circulating soluble and insoluble extracellular ligands including growth factors and viral proteins. HS participates in multiple biological processes as tissue development, coagulation, angiogenesis and tumour metastasis. Other minor forms of membrane HSPG include ß-glycan and the V-3 isoform of CD44 present on keratinocytes and activated monocytes (Qin, Ke et al. 2015).

Telomerase-Associated Protein 1 (TEP1) is a component of the ribonucleoprotein complex responsible for telomerase activity which catalyses the addition of new telomerase on the chromosome ends. To find this protein up-regulated in all 5-FU resistant subsamples acquires a crucial importance due to its role during cell proliferation. The main role of telomerase is to maintain

telomere homeostasis and to protect telomeres damage (Olovnikov 1996). Telomerase is essential to let cells outgrowth and to maintain genomic integrity of telomeres (Gillis, Schuller et al. 2008). In humans, a high presence of telomerase occurs in telomeres from cells that need to maintain its proliferation activated after fetal development. Proliferating cells that keep its division and with a high presence of telomerase are stem cells, germ cells, hair follicles, activated lymphocytes. In other cells such as epithelial cells, fibroblasts, endothelial cells and in the majority of healthy tissues, telomerase is presented at low levels with a low expression. While 80-90% of metastatic tumour cells show a very high expression of telomerase. Each time a cell is divided, it has been estimated that a cell loses around 150-200 base pairs per cell division before cell senescence and before cells death by apoptosis. This number was established in cell culture experiments using breast cancer cell lines (Jafri, Ansari et al. 2016). High levels of telomerase in resistant cell lines may explain the fact that resistant sublines show a bigger size than its respective sensitive parent cell line. A similar study about the effect that high passaging produces in DLD-1 colorectal cell lines *in vitro*, showed that long-term cultivation promotes telomere elongation and overexpression of *MDR1* and *MRP* genes (Kuranaga, Shinomiya et al. 2001). In CRC, a high presence of telomerase has been described as a possible biomarker of resistance to radiotherapy (Shin, Foot et al. 2012, Bertorelle, Rampazzo et al. 2014).

Additionally, its expression is related to vault components MVP, TEP1 and vPARP and their correlation to other MDR proteins in ovarian cancer. Vaults are ribonucleoprotein particles found in the cytoplasm of eucaryotic cells. The 13 MDa particles are composed of multiple copies of three proteins: a Mr 100 000 major vault protein (MVP) and two minor vault proteins of Mr 193 000 (vault poly-(ADP-ribose) polymerase) and Mr 240 000 (telomerase-associated protein 1), as well as small untranslated RNA molecules of approximately 100 bases. Although the existence of vaults was first reported in the mid-1980s, no function has yet been attributed to this organelle. The notion that vaults might play a role in drug resistance was suggested by the molecular identification of the lung resistance-related (LRP) protein as the human MVP. Expression profiles of vault components MVP, TEP1, and vPARP and their correlation to other MDR

proteins in ovarian cancer (Mossink, van Zon et al. 2003, Szaflarski, Sujka-Kordowska et al. 2013). MVP was found up-regulated in KM 12 5-FU and KM 12 OXA resistant sublines.

3.4.4 Discussion of WB validation results for CD44 and UMPS in 5-FU

In order to validate the findings of the quantitative proteomics methodology, 2 proteins whose expressions were identified as being up-regulated in the 5-FU resistant sublines, were further investigated using immunodetection techniques.

3.4.4.1 CD44 in resistant sublines to 5-FU

CD44 was studied due to it has recently been discovered for its potential role as CSCs biomarker and it was found significantly up-regulated in DLD-1 5-FU resistant subline but not in DLD-1 parent samples (Fig. 3.31a). WB results obtained in DLD-1 5-FU, DLD-1 P=9, DLD-1 P=65 and DLD-1 SILAC P=9, indicate that the difference in bar graphs distribution between the WB results and the SILAC approach results is not great for DLD-1 Set. Unique differences are due to certain additional adjustments as the measurement and using the sample DLD-1 SILAC to estimate the relative abundance of CD44 protein in different samples. Additionally, using different experimental approaches, measures of SILAC samples to calculate the relative expression ratio and statistics analysis may increase differences between both results. However, in both cases (WB bar graph and SILAC bar graph) the general trend and profile of samples are maintained. In this way, in both experiments, CD44 relative expression in DLD-1 set of samples, was found from the highest to the lowest levels in the following order DLD-1 5-FU, DLD-1 P=65, and DLD-1 P=9. In both cases, a significantly up-regulation was found for CD44 in DLD-1 5-FU resistant subline. In KM 12 set of samples, WB results obtained in KM 12 5-FU, KM 12 P=9, KM 12 P=55, and KM 12 SILAC P=9, indicate that the small differences in bar graphs distribution between the KM 12 WB results and the KM 12 SILAC approach results, is due to experimental technique differences (Fig. 3.31b). However, no significant differences in CD44 expression were found in KM 12 resistant subline. Finally, WB results obtained in HT 29 5-FU, HT 29 P=9, HT 29 P=57, and HT 29 SILAC P=9, indicate similarity in bar graphs distribution between the WB results and the SILAC approach results (Fig. 3.31c). A clear

high expression of CD44 was found in HT 29 5-FU, following by HT 29 P=9 in both experiments. Whilst, HT 29 P=65 showed the lowest expression of CD44 in both cases too.

3.4.4.2 UMPS DLD-1

As it has been described above, in the section 3.4.3.3.1.3, levels between UMPS isoforms are important for the development of resistance to 5-FU in CRC. From initial mass spectrometry results, a significantly down-regulation in UMPS has been found in the resistant subline DLD-1 5-FU. However, initial WB results obtained do not show a significantly down-regulation in UMPS enzyme levels. Contrary to expectations, in DLD-1 5-FU sample a high expression of a second isoform of the enzyme UMPS was found (Fig. 3.32a). A further analysis was done by estimation of the relative expression ratio between the two isoforms of the enzyme UMPS found. Interestingly, as it has been described in previous publications the resistant subline DLD-1 5-FU showed the most similar levels between the two isoforms of UMPS (Fig 3.32c). So, it may be confirmed that data obtained from microarray hybridization and analysis of microarray data on the ALEXA splicing microarray platform by M. Griffith *et al.*, and new relative ratio abundance of UMPS isoform A / UMPS isoform B found during the present thesis are similar (Fig. 3.32c,d). The unique difference was that SILAC-approach did not show the same trend than WB and microarray data previously described.

So, to understand the absence of any conceptual or visual similarity between WB results and SILAC approach results, a review of SILAC-ratio data obtained for UMPS was done.

For WB study of UMPS in DLD-1 5-FU resistant subline, the GTX 114872 UMPS antibody was used. The UMPS recombinant antibody encompasses a sequence within the centre region of human UMPS. However, the exact sequence is proprietary of GenteTex Antibodies. According to the observed target size in WB results (Fig. 3.32a), it can be confirmed that the two isoforms detected are the Isoform A: Length: 480; Mass (Da):52,22 and the Isoform B: Length:302; Mass (Da):33,05. The difference between Isoform A and Isoform B

is that Isoform B misses the 1-178 regions. However, antibody binding is not occurring to encompass this missing region as it is binding to the centre region.

In conclusion, it is crucial to know both the amino acid sequence that it is used by the Orbitrap Analyser to quantify the proteins and the amino acid sequence recognized by the antibody during WB. This issue may cause failures in results similar during the comparison between WB and mass spectrometry results and it needs to be avoided by a properly antibody selection during WB validation.

3.4.5 Conclusion

Development of 5-FU resistant sublines was carried out by continuous drug exposure. Differences in resistance fold change may be because the initial parent cell lines have different genomic background and cellular sensitivity to 5-FU effects may be different for each cell line. Additionally, establishment of resistant sublines is a long process (more than 10 months), so during this period of time, new randomly and different mutations appear in parent cell lines and these can have different roles in 5-FU response. Hence, final outcome in resistance fold change is the result of multiple cellular responses to 5-FU. All this genetic variability and different protein expressions, contribute to the development of different resistant phenotypes with different grades of resistance fold change.

These differences explain why DLD-1 5-FU showed a 130.2 fold change whilst KM 12 5-FU and HT 29 5-FU showed fold change of 3.2 and 3.5, respectively. A further validation of resistant sublines establishment methodology was based on the development of mice xenograft models. *In vivo* results showed resistance maintained suggesting DLD-1 subline as a 5-FU resistant model.

Validation of proteomics as a technique for identifying alterations in protein expression was carried out using Western Blotting for 2 proteins with identified altered expression profiles, CD44 and UMPS. Results from WB were in line with the initial results obtained by SILAC approach. The SILAC proteomic quantification approach is a robust and widely accepted method to quantify significant differences between two or more biological samples. This issue is confirmed as the SILAC-approach and analysis led to quantification of a similar

number of proteins (3500-4000) in the three cell lines (DLD-1, KM 12, HT 29) studied (Fig. 3.22).

DLD-1 5-FU xenograft mice models developed (see Fig. 3.18) will be used to further validate by WB and immunohistochemistry (IHC) the observations obtained from *in vitro* studies. Tumour-derived cell lines may not completely recapitulate tumour microenvironment, hence *in vivo* models are important to employ to study processes such as angiogenesis and hypoxia. The role of myeloid cells and cell surface receptors in acquired resistance to anti-Vascular Endothelial Growth Factor (VEGF) therapy has been recently discovered (see Chapter 3, section 3.4.3.2.1) (Rosa, Monteleone et al. 2014). Hence, up-regulated proteins involved in myeloid differentiation process such as NFAT5, MYADM and cell surface receptors such as CD44, SARG involved in proliferation and differentiation of intestinal colon cells, are some of the most interesting candidate altered proteins for further studies as targeted protein to avoid acquired resistance to 5-FU in CRC.

- Chapter four -

Identification of new mechanisms of resistance to IRI

4 Identification of new mechanisms of resistance to IRI

4.1 Introduction

The prodrug IRI, 7-Ethyl-10-[4-(1-piperidino)-1-piperidino] carbonyloxy camptothecin (CPT-11), is a derivative of camptothecin. It is a cytotoxic quinoline alkaloid that acts as Topo I inhibitor (Liu, Desai et al. 2000).

Topo I enzyme catalyses the relaxation of superhelical DNA. This is possible through cycles of transient single strand cleavage and its religation in the DNA duplex. Topo I cleaves and reseals the phosphodiester backbone of DNA in a repetitive process. The Topo I-DNA complex makes possible the passage of the single DNA and double DNA through the nicked DNA (Shao, Cao et al. 1999).

4.1.1 Mechanisms of action of IRI

IRI has S-phase-specific cytotoxicity because interacts with cellular Topo I–DNA complexes (Xu and Villalona-Calero 2002). The active form of IRI is SN-38) binds to Topo I-DNA complex and prevents religation of cleaved DNA complex. Once the SN-38-Topo I-DNA complex has been formed and collides with the advancing replication fork, the failure of the replication process happens and the formation of a double-strand DNA break occurs (Liu, Desai et al. 2000). This is the final and critical damage that causes the arresting of proteins of the replication fork in G2, which is arrested and delayed by DNA damage signalling during S-phase checkpoint, leading to apoptosis (Liu, Desai et al. 2000). Under high IRI concentration, cells that are not in S-phase may also die from IRI toxicity. This kind of anti-proliferative effect by high concentrations appears to be related to the damage at a transcriptional level, which converges into the activation of genes involved in apoptosis (Liu, Desai et al. 2000).

4.1.2 Known mechanisms of resistance to IRI

Metabolism of IRI is a complex process that involves the action of a large number of enzymes such as Carboxylesterase (CE), Topo I, Protein kinase ataxia telangiectasia mutated (ATM) (Rasheed and Rubin 2003), Serine/threonine protein kinase (ATR), DNA-dependent protein kinase (DNA-PK). Alterations in regulation of these proteins and changes at expression level

in the Mitogen-Activated Protein Kinase (MAPK) (p38) or in the nuclear factor kappa B (NF-κB) may lead to resistance development to IRI. All roles of these factors in IRI resistance are known and are explained in detail below (Rasheed and Rubin 2003).

4.1.2.1 Mechanisms of resistance to IRI related to carboxylesterase

IRI is activated through its hydrolysis to SN-38, by CE. CE is a member of the carboxylesterase family which contains enzymes that take part in the hydrolysis or transesterification of various xenobiotics and drugs (Sanghani, Quinney et al. 2003). Therefore a variation in CE expression can affect the IRI metabolism process. IRI resistance and low chemosensitivity to the drug are related to low CE expression *in vitro* (Guichard, Terret et al. 1999) and in the same way, *CE* gene expression is directly related to the inter-individual variation in therapeutic outcome of CRC patients when they are treated with IRI (Sanghani, Quinney et al. 2003).

4.1.2.2 Mechanisms of resistance to IRI related to DNA damage

There are some alterations in terms of DNA repairing effects that can lead to resistance to IRI. ATM, ATR, and DNA-PK activation show the highest activity during DNA damage detection and DNA repairing processes (Reinhardt, Aslanian et al. 2007). ATM is a protein kinase which is activated primarily by double-strand breaks (DSBs), while the chromatin binding protein kinase ATR is activated in response to persistent single-stranded DNA that is generated by DNA damage and by blocking proteins of the replication fork (Schwab 2008). The ATM/ATR kinases also activate by phosphorylation the checkpoint Chk1/Chk2 kinases, which consecutively can play critical roles acting like messengers during cell cycle checkpoints (Schwab 2008). Subsequently, they regulate the cell cycle control, DNA repair systems and cell survival (Reinhardt, Aslanian et al. 2007, Schwab 2008).

4.1.2.3 Mechanisms of resistance to IRI related to p38α

Related to SN-38, it has been shown that p38α phosphorylation is increased in SN-38 resistant clones derived from HCT 116 and SW480 CRC cell lines, suggesting that p38α activation might represent a general resistance

mechanism (Paillas, Boissière et al. 2011). This data was surprising because it was assumed that p38α activity induced the expression of pro-apoptotic proteins and acted as a tumour suppressor (Grossi, Peserico et al. 2014). Now, a recent publication showed similar results suggesting that MAPK p38α could act through two different pathways with completely different consequences in CRC. One of these pathways regulates the suppression effect of colitis-associated tumour initiation (Fig. 4.1). Contrary, p38α stimulates proliferation and survival of transformed epithelial tumour cells, contributing to tumour burden (van Houdt, de Bruijn et al. 2010, Gupta, del Barco Barrantes et al. 2014).

The protumoural activity of p38α in CRC could be due to the capacity of p38α to stimulate CRC cell survival by enhancing DNA repair in response to chemotherapy and the autophagy pathway. Evidence for involvement in autophagy comes from a study which demonstrated that p38α mediates autophagy and cell death inhibition in CRC cells suggesting that p38α activation is essential for their survival (Fig. 4.1) (Paillas, Causse et al. 2012). These authors showed that the activation of the autophagy process by p38α was mediated by *GABARAP* gene activation. GABARAP is a gamma-aminobutyric acid A receptor that takes part in vacuoles and autophagosomes formation. Under low levels of p38α activity, the *GABARAP* gene is upregulated and cell death by autophagy occurs. So, the use of p38α inhibitors can cause cell death by autophagy (Fig. 4.1) (Comes, Matrone et al. 2007).

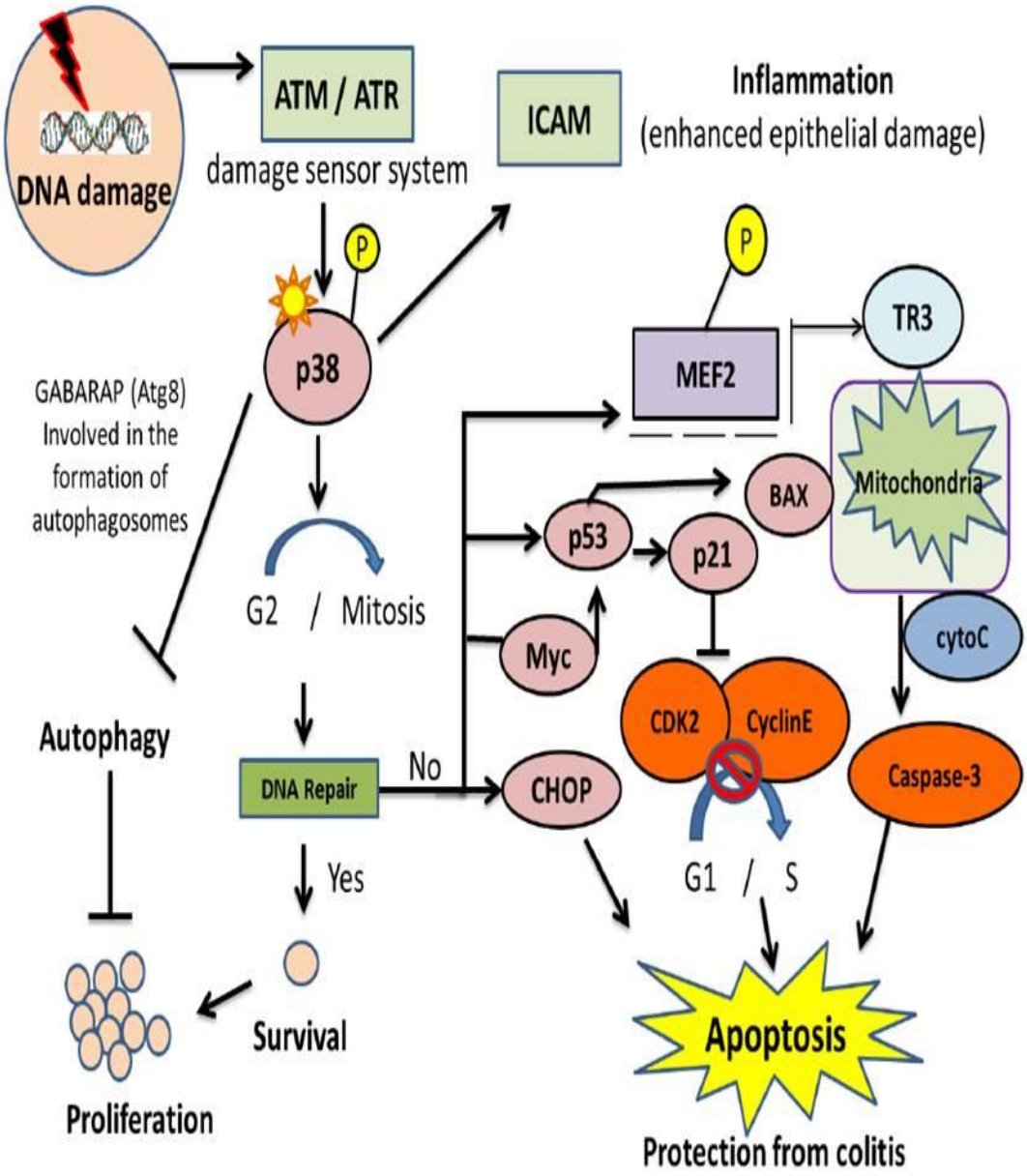

Figure 4.1: Schematic diagram of p38 role in proliferation and apoptosis in CRC. Non-tumoural cells with DNA damage activate DNA repair system, but if it is not possible to repair DNA, p38 activates some TFs such as p53, p21, Myc, etc which arrest the cell cycle at the G1/S phase by blocking of CDK2 and CyclinE interaction. Alterations and overexpression in p38 protein can deregulate this pro-apoptotic mechanism, increasing number of cells with DNA damage that are more likely to develop new malignant and resistant phenotypes.

4.1.2.4 Mechanisms of resistance to IRI related to Topoisomerase I

Another crucial factor in IRI mechanism of action is Topo I. This enzyme is the natural target of Topo I inhibitors like IRI, so it is believed that the cellular levels of Topo I could be proportional to cellular sensitivity to IRI. It has been observed that in CRC resistant cell lines that have been exposed continuously to IRI treatment, the expression of Topo I was reduced in contrast to the IRI-sensitive parent cell line (Husain, Mohler et al. 1994). There is evidence that CRC cell lines express higher levels of Topo I than normal colon mucosa in xenografts (Giovanella, Stehlin et al. 1989). Additionally, Topo I overexpression has been suggested as a predictor for high sensitivity to the drug (Xu and Villalona-Calero 2002). However, detailed knowledge about regulation of Topo I is needed, because the level of Topo I in cells depends on multiple molecular mechanisms that regulate the expression of the enzyme. Some studies in CRC tumours demonstrated that upregulation of Topo I mRNA increases Topo I in cell lines at the protein level (Husain, Mohler et al. 1994). Nevertheless, a clear relation between sensitivity to IRI and pre-treatment tumoural Topo I expression has not been established.

Otherwise, studies in colon, breast and leukaemia cell lines have demonstrated that IRI can down-regulate Topo I through an ubiquitin/26S proteasome-dependent system. The 26S proteasome is a complex protein formed by 31 different subunits (Voges, Zwickl et al. 1999). This molecular machinery catalyses proteins degradation and it has been found activated as consequence of the formation of the Topo I-DNA and IRI complex (Voges, Zwickl et al. 1999, Desai, Li et al. 2001). Moreover, it is known that most of tumour cell lines show defects at some point during the degradation pathway of Topo I. In peripheral blood mononuclear cells of patients who have been previously treated with IRI, it has been found reduction of Topo I (Liu, Desai et al. 2000). As a result, it should be studied if the Topo I reduction can be used as a mechanism of resistance by normal cells against IRI therapy.

4.1.2.5 Mechanisms of resistance to IRI related to NF-κB

Finally, treatment with IRI can stimulate proliferation. This proliferative process is initiated by activation of NF-κB. This protein complex is a ubiquitous

transcription factor that controls the DNA transcription by regulation of a large number of genes involved in inflammation and immune response (Veiby and Read 2004). During first stages of protumoural cells development, NF-κB acts like a suppressor factor of the apoptotic cascade. It acts on the apoptotic cascade that can be suppressed by gene activation such as oncogenic *Ras*, tumour necrosis factor-α (TNF-α) and chemotherapy drugs as IRI. After this, the transcriptional factor activated can regulate chemoresistance by changes around the tumour area (Liu, Desai et al. 2000, Veiby and Read 2004).

4.1.3 Aims & Objectives for IRI

The main aims and objectives of this study were focused on developing new resistant sublines to IRI which could be used to explore novel mechanisms of resistance in CRC. This was achieved by the following objectives:

1) Establish and characterise IRI resistant sublines for DLD-1 in terms of sensitivity to IRI *in vitro*.

2) Identify novel mechanisms of IRI resistance using a proteomic approach.

4.2 Material & Methods

All general material and methods used were carried out as it has been previously described in Chapter 2 and Chapter 3.

4.3 Results

4.3.1 Establishment of DLD-1 drug resistant cell line to IRI

An IRI resistant subline was established from DLD-1 by episodic exposure to IRI over a period of ten months (Fig. 4.2). The DLD-1 resistant IRI subline was maintained and growth in a drug-free medium over a month, keeping stability in IRI resistant phenotype. A significant increase of 1.7-fold change was found in DLD-1 IRI subline. Unfortunately, it was not possible to establish IRI-resistant sublines for KM 12 and HT 29 cell lines over the treatment period due to the high anti-proliferative effect of the drug in these two cell lines.

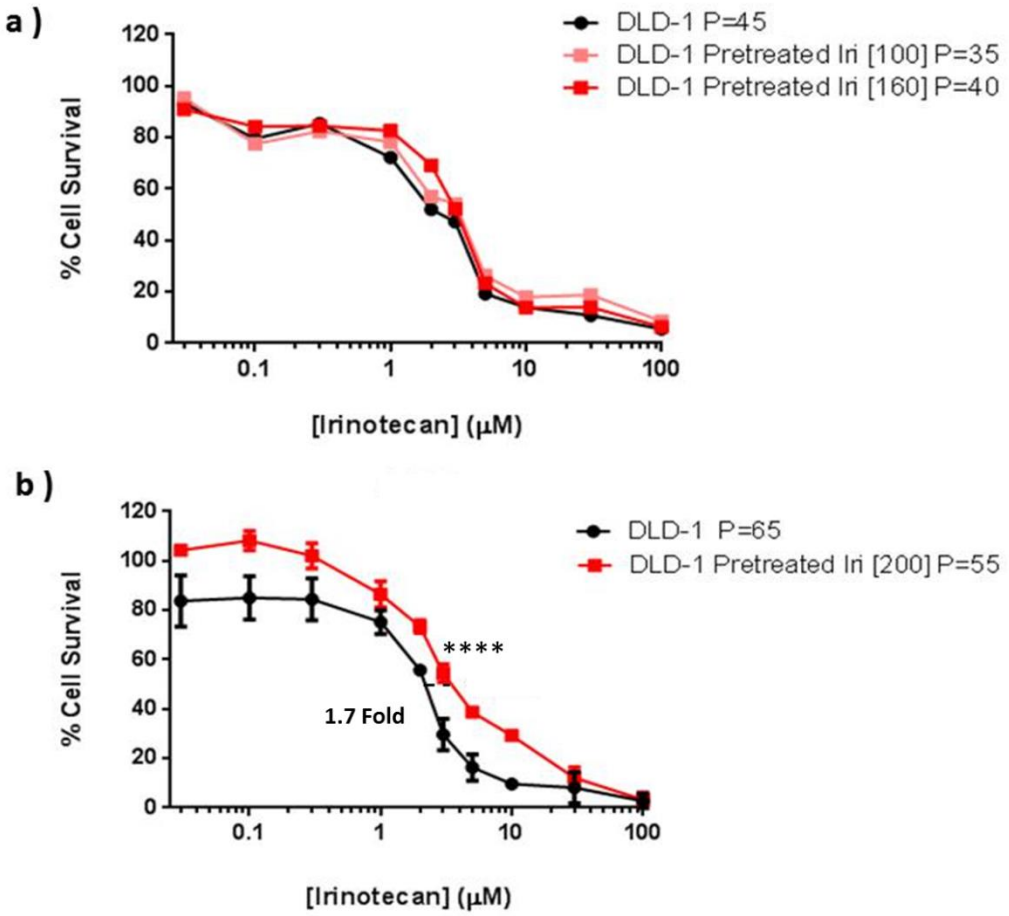

Figure 4.2: Chemosensitivity curve profiles for DLD-1. (a) Three independent chemosensitivity curve profiles for DLD-1 parent and pretreated DLD-1 IRI cell line during establishment of DLD1 IRI resistant subline. (b) DLD-1 no pretreated cell lines and DLD-1 IRI P=55, were exposed to IRI [0.03-100 µM] doses during 96 h. MTT assays were performed in three independent experiments. Graphs show the cell survival of DLD-1 pretreated and non-pretreated cell lines against different IRI concentrations. A significant difference of 1.7-fold change in IC_{50} was found between DLD-1 parent cell line and DLD-1 IRI resistant subline (**** $p \leq 0.0001$). Error bars showing standard deviations between replicates are displayed too.

4.3.2 Characterisation of cell growth for DLD-1 IRI resistant subline

To confirm results obtained by MTT and to test if the number of passage of the flask could have some effect on the MTT assay, a growth curve analysis was done for DLD-1 IRI resistant subline. Growth rate and capacity to proliferate was measured for resistant subline and parent cell line (Fig. 4.3). Growth curves

were done using an initial concentration of $1x10^4$ cells/ml. No significant differences in growth rate were found in DLD-1 IRI resistant subline.

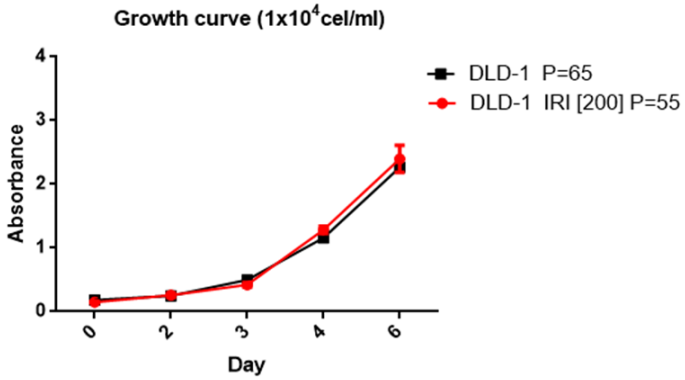

Figure 4.3: MTT Growth curve profiles for DLD-1 parent cell line and DLD-1 IRI resistant subline. No significant difference ($p>0.05$) was found in growth curve profiles between parent and resistant subline.

4.3.3 Identification of proteome changes in DLD-1 resistant subline to IRI using mass spectrometry by SILAC approach

Results for DLD-1 IRI were obtained as it has been previously described for 5-FU (see Chapter 3, section 3.3.6). Lowest Mascot score used in each sample were established by Mascot software for a 95 % confidence rate and these Mascot score are summarized in table 4.1.

Cell Line	DLD-1 P=9	DLD-1 P=65	DLD-1 IRI
Mascot Score	>31	>30	>31

Table 4.1: Lowest Mascot scores used during analysis of DLD-1 samples.

Total number of proteins quantified in DLD-1 parent samples and DLD-1 IRI resistant subline are shown in a Venn diagram below (Fig. 4.4). Total number of commonly quantified proteins is shown within circles intersections. Complete protein lists are enclosed in a soft copy which is attached in a CD along with this thesis.

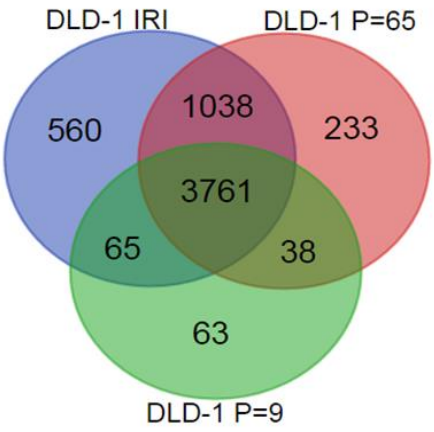

Figure 4.4: Venn diagram of multi SILAC dataset in DLD-1 IRI. Middle cells with the number of unique proteins commonly quantified in DLD-1 long and low generation controls and DLD-1 IRI resistant subline are shown.

4.3.4 Protein quantification and results of the MS analysis

4.3.4.1 Raw data normalization and transformation

Initially, after Log_2 transformation of the normalized SILAC-ratio data, frequency distributions of commonly quantified proteins of parent cell lines (DLD-1 P=9, DLD-1 P=65) and DLD-1 IRI were plotting in figure 4.5. Distribution of Log_2 SILAC-ratio proteins in DLD-1 IRI overlays by little both parent cell lines distributions. This difference in data distribution may be presumably caused by IRI effects, which increases number of altered proteins in DLD-1 IRI treated cell line.

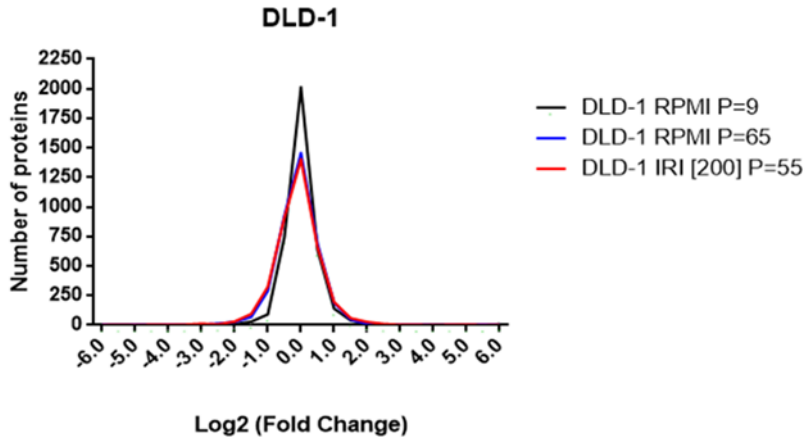

Figure 4.5: A histogram overlaid fold change distribution of multi SILAC data set in DLD-1 IRI showing fold change distribution of proteins commonly quantified.

Resistant cell lines to IRI	Significant Up-regulated Proteins	Significant Down-regulated Proteins	Percentage of Significantly Altered proteins
DLD-1	51	74	3.32%

Table 4.2: Significantly up-regulated (Fold change ≥ 2) and down-regulated (Fold change ≤ 2) proteins in DLD-1 resistant subline to IRI.

4.3.4.2 "R" LIMMA analysis

DLD-1 IRI multi SILAC dataset was analysed by LIMMA as it has been described in Chapter 3, section 3.2.5.7. Proteins fold change between DLD-1 IRI and DLD-1 parent cell lines were summarised in a Volcano plot below. The data for all proteins are plotted as Log_2 fold change versus the $-Log_{10}$ of the adjusted p-value (Fig. 4.6).

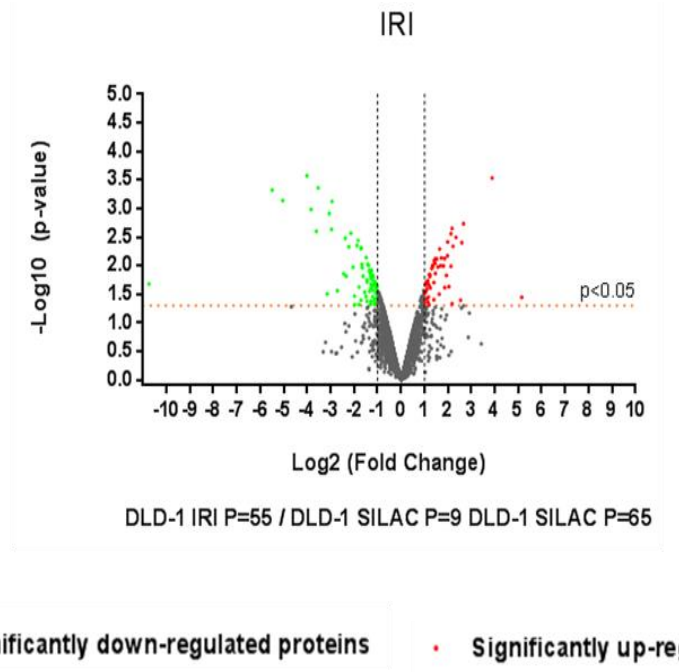

Figure 4.6: Volcano plots showing the distribution of significantly altered proteins following LIMMA modelling in DLD-1 IRI. Criteria for significance are a 2-fold change for the DLD-1 IRI subline compared to the parent data, with p<0.05. Key: Red-Upregulated, Green – Downregulated proteins, Grey-Unaltered and non-significant proteins.

Log_2 fold changes and their respective p-value were calculated using LIMMA. Proteins of each sample were ordered from the highest to the lowest according to normalized Log_2 ratio data from SILAC results before cluster analysis.

4.3.4.3 Cluster analysis

The ordered list of proteins was divided into three groups of proteins as it has been described in Chapter 3, section 3.2.5.7.

Initial results containing all probable proteins status among DLD-1 IRI and DLD-1 parent cell lines are shown in Table 4.3. Proteins unaltered in parent cell lines but also up-regulated or down-regulated in DLD-1 IRI subline were used to build the cluster analysis.

Cluster analysis for DLD-1 IRI resistant subline showed similar results to those observed during “R” LIMMA analysis (see Fig. 4.6). The highest number of proteins remain unaltered in both parent cells lines, whilst DLD-1 IRI shows a high symmetry in (a) up- and (b) down-regulated proteins fold change dispersion. Detailed results are summarized in Table 4.4 and Table 4.5.

Status in Parent cell line with Low Passage	Status in Parent cell line with High Passage	Status in IRI Resistant Subline	Status Sum-up	Number of proteins in Set DLD-1
D	D	D	DDD	34
D	D	N	DDN	23
D	D	U	DDU	2
D	N	D	DND	8
D	N	N	DNN	109
D	N	U	DNU	6
D	U	D	DUD	2
D	U	N	DUN	3
D	U	U	DUU	5
N	D	D	NDD	55
N	D	N	NDN	74
N	D	U	NDU	2
N	**N**	**D**	**NND**	**84**
N	**N**	**N**	**NNN**	**2983**
N	**N**	**U**	**NNU**	**71**
N	U	D	NUD	1
N	U	N	NUN	59
N	U	U	NUU	51
U	D	D	UDD	1
U	D	N	UDN	0
U	D	U	UDU	1
U	N	D	UND	3
U	N	N	UNN	98
U	N	U	UNU	18
U	U	D	UUD	4
U	U	N	UUN	31
U	U	U	UUU	33
			TOTAL	**3761**

Table 4.3: Thresholds for protein status in DLD-1 IRI multi SILAC dataset of were established using a 5th percentile criteria. From the column of "Status Sum-up" in the table, only the proteins which remain as unaltered (N, brown) in both parent cell lines and with an altered status (D green or U red) in DLD-1 IRI resistant subline were considered to be studied as altered proteins involved in IRI drug-resistance.

a)

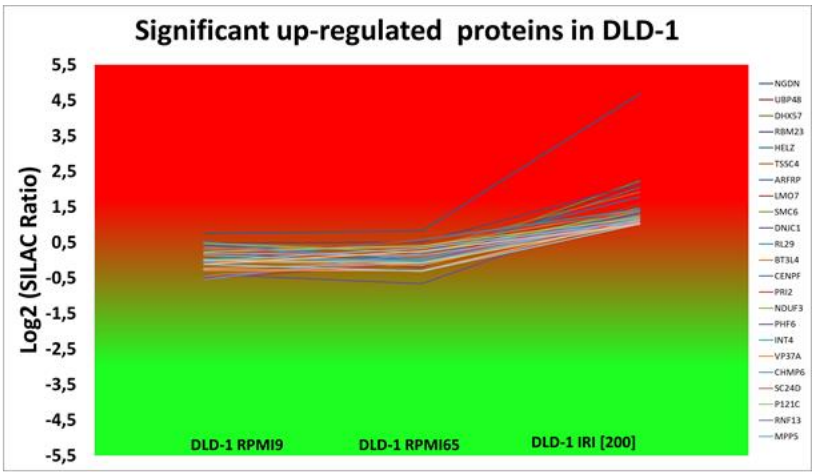

b)

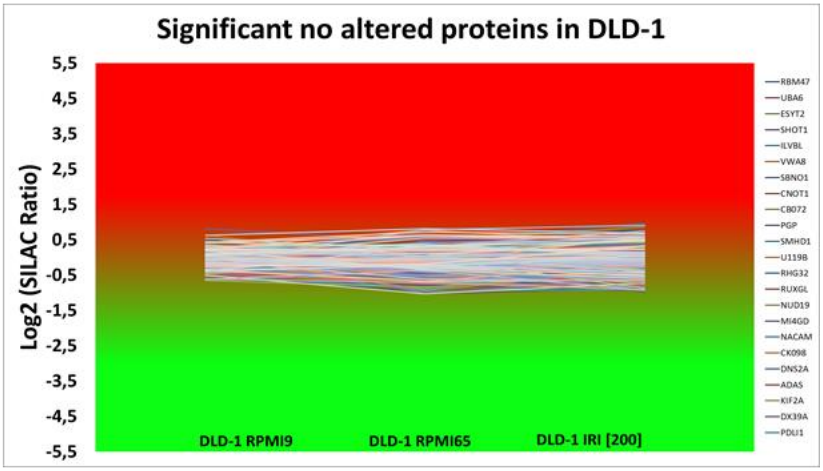

c)

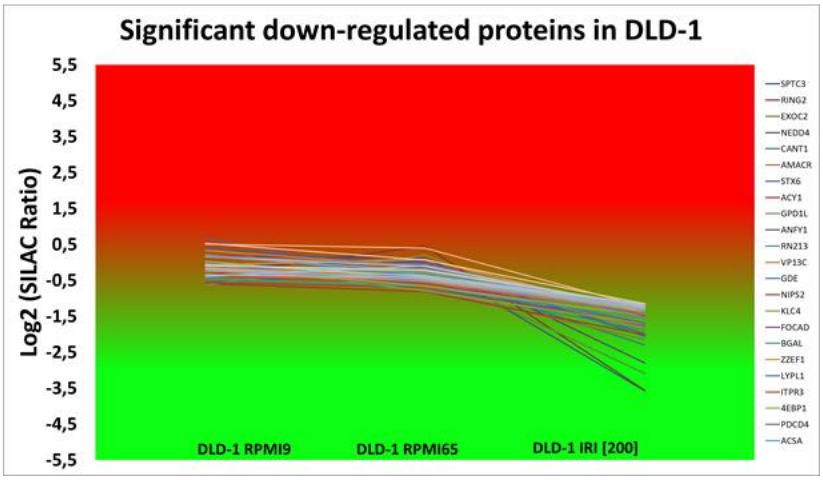

Figure 4.7: Cluster analysis of DLD-1 IRI. Proteins were classified using a 5^{th} percentile criteria for significantly (a) up-regulated proteins; (b) unaltered proteins; (c) down-regulated proteins in sensitive parent cell lines DLD-1 P=9, DLD-1 P=65 and DLD-1 IRI resistant subline.

N	Protein name	AC. number	MW [kDa]	SC %	PSMs	Unique Peptides	Score Mascot	Normalized Log2 Ratio: L/H	p-value
1	NGDN	Q8NEJ9	35.9	24.1	17	4	135	4.67	0.000
2	USP48	Q86UV5	119.0	6.0	7	4	47	2.25	0.005
3	DHX57	Q6P158	155.5	7.7	28	5	307	2.23	0.007
4	RBM23	Q86U06	48.7	20.5	34	4	373	2.14	0.005
5	HELZ	P42694	218.8	6.8	24	7	56	2.04	0.010
6	TSSC4	Q9Y5U2	34.3	9.4	13	3	94	1.92	0.008
7	FSCN1	Q16658	54.5	58.4	306	24	4586	1.87	0.058
8	ARFRP1	Q13795	22.6	15.4	3	2	113	1.78	0.009
9	LMO7	Q8WWI1	192.6	32.6	302	38	4419	1.56	0.008
10	RIOK1	Q9BRS2	65.5	25.7	24	9	299	1.54	0.111
11	SMC6	Q96SB8	126.2	9.0	18	6	140	1.48	0.008
12	Hsp40	Q96KC8	63.8	22.7	33	9	449	1.46	0.004
13	RPL29	P47914	17.7	9.4	33	1	913	1.44	0.043
14	ESRP2	Q9H6T0	78.4	25.3	53	10	536	1.42	0.060
15	BTF3L4	Q96K17	17.3	37.3	79	6	647	1.40	0.022
16	PHRF1	Q9P1Y6	178.6	4.9	26	5	217	1.40	0.089
17	IGFBP2	P18065	34.8	42.8	40	8	533	1.39	0.141
18	CENPF	P49454	367.5	13.0	50	25	446	1.39	0.049
19	BOD1L1	Q8NFC6	330.3	4.7	39	7	451	1.37	0.079
20	NFKB2	Q00653	96.7	35.2	123	21	1188	1.37	0.062
21	Hsp40	O75190	36.1	23.3	25	6	430	1.37	0.055
22	DNA	P49643	58.8	14.1	31	4	164	1.36	0.045
23	NDUFAF3	Q9BU61	20.3	44.6	39	5	624	1.35	0.030
24	PHF6	Q8IWS0	41.3	17.8	23	4	279	1.34	0.010
25	TIMM8B	Q9Y5J9	9.3	33.7	12	2	235	1.33	0.067
26	TENM3	Q9P273	300.8	1.6	7	2	97	1.33	0.168
27	TRAPPC12	Q8WVT3	79.3	10.9	13	4	101	1.31	0.143
28	MRPL52	Q86TS9	13.7	42.3	32	2	365	1.28	0.081
29	INTS4	Q96HW7	108.1	6.1	10	3	72	1.27	0.011
30	VPS37A	Q8NEZ2	44.3	14.1	13	3	222	1.24	0.011
31	RAD51	Q06609	36.9	18.6	27	4	393	1.24	0.161
32	AAMP	Q13685	46.7	29.7	58	7	729	1.24	0.094
33	CHMP6	Q96FZ7	23.5	19.4	20	3	221	1.22	0.040
34	SEC24D	O94855	112.9	17.8	42	11	492	1.22	0.014
35	CHD1	O14646	196.6	15.6	82	16	748	1.20	0.090
36	POM121C	A8CG34	125.0	13.5	48	8	595	1.19	0.039
37	CIZ1	Q9ULV3	100.0	21.8	46	10	535	1.19	0.113
38	BCAR1	P56945	93.3	26.3	106	13	1126	1.19	0.069
39	RNF13	O43567	42.8	11.8	13	2	133	1.17	0.039
40	DNTTIP2	Q5QJE6	84.4	31.7	130	16	1309	1.16	0.143
41	MPP5	Q8N3R9	77.2	22.5	43	9	538	1.16	0.021
42	LIMD1	Q9UGP4	72.1	33.7	39	9	379	1.15	0.268
43	SPAST	Q9UBP0	67.2	19.5	34	8	760	1.15	0.215
44	RHBDD1	Q8TEB9	35.8	11.1	11	2	431	1.13	0.008

45	ARHGAP5	Q13017	172.4	17.7	65	15	462	1.13	0.099
46	TWISTNB	Q3B726	37.4	12.1	16	3	293	1.13	0.155
47	TIMMDC1	Q9NPL8	32.2	23.2	26	5	205	1.13	0.225
48	TIMM23	O14925	21.9	45.9	28	5	277	1.12	0.128
49	WDR73	Q6P4I2	41.7	14.6	12	3	74	1.12	0.148
50	ZNF428	Q96B54	20.5	23.9	18	3	408	1.11	0.104
51	SFSWAP	Q12872	104.8	8.7	22	5	389	1.10	0.190
52	UHRF1	Q96T88	89.8	40.5	115	22	1218	1.10	0.114
53	CHMP2A	O43633	25.1	11.7	21	3	713	1.09	0.337
54	EHD4	Q9H223	61.1	57.1	195	23	2995	1.08	0.049
55	SSU72	Q9NP77	22.6	42.3	46	8	624	1.08	0.099
56	NOP16	Q9Y3C1	21.2	32.6	62	5	543	1.08	0.152
57	KLK6	Q92876	26.8	30.3	29	4	293	1.08	0.058
58	PPWD1	Q96BP3	73.5	26.9	43	11	395	1.07	0.053
59	IL6ST	P40189	103.5	11.1	32	6	339	1.07	0.014
60	C1orf122	Q6ZSJ8	11.5	46.4	8	3	133	1.06	0.074
61	RRS1	Q15050	41.2	32.1	86	13	921	1.05	0.214
62	MRPL24	Q96A35	24.9	17.6	14	3	318	1.04	0.020
63	BAIAP2L1	Q9UHR4	56.8	46.8	97	15	903	1.04	0.036
64	GATA6	Q92908	60.0	23.4	25	8	544	1.04	0.361
65	TNFRSF10A	O00220	50.1	13.7	26	4	457	1.04	0.069
66	WDR74	Q6RFH5	42.4	42.1	71	11	1189	1.03	0.118
67	NFRKB	Q6P4R8	138.9	8.6	21	6	189	1.03	0.099
68	ERBIN	Q96RT1	158.2	26.6	110	22	1053	1.02	0.084
69	MDC1	Q14676	226.5	33.7	222	32	2509	1.02	0.267
70	Hsp70	P48723	51.9	11.9	15	5	95	1.01	0.015
71	DHPS	P49366	40.9	34.1	34	8	369	1.01	0.046

Table 4.4: Results of high SILAC-ratios for single SILAC DLD-1 IRI experiment. p-value from multi SILAC dataset analysed by LIMMA is included.

N	Protein name	AC. number	MW [kDa]	SC %	PSMs	Unique Peptides	Score Mascot	Normalized Log2 Ratio: L/H	p-value
1	SPTLC3	Q9NUV7	62.0	6.5	4	2	52	-3.58	0.000
2	RNF2	Q99496	37.6	22.3	43	3	371	-3.56	0.003
3	EXOC2	Q96KP1	104.0	6.8	9	4	108	-3.09	0.001
4	NEDD4	P46934	149.0	11.4	33	8	257	-2.80	0.001
5	CANT1	Q8WVQ1	44.8	36.7	24	8	499	-2.30	0.004
6	AMACR	Q9UHK6	42.4	29.3	42	7	555	-2.14	0.034
7	STX6	O43752	29.2	47.8	39	7	338	-2.06	0.005
8	ACY1	Q03154	45.9	24.0	28	6	241	-2.02	0.013
9	GPD1L	Q8N335	38.4	17.4	15	5	407	-1.99	0.024
10	ANKFY1	Q9P2R3	128.3	26.1	124	18	1739	-1.99	0.004

11	DPYSL3	Q14195	61.9	49.6	247	16	3926	-1.95	0.055
12	RNF213	Q63HN8	591.0	4.1	37	13	248	-1.89	0.029
13	VPS13C	Q709C8	422.1	5.3	34	13	293	-1.82	0.010
14	AGL	P35573	174.7	18.2	78	18	978	-1.77	0.019
15	GBAS	O75323	33.7	19.9	32	4	201	-1.74	0.019
16	PSPH	P78330	25.0	36.0	55	6	929	-1.73	0.094
17	KLC4	Q9NSK0	68.6	17.3	36	4	505	-1.73	0.048
18	NIPSNAP3A	Q9UFN0	28.4	9.3	5	2	43	-1.72	0.074
19	FOCAD	Q5VW36	199.9	1.3	8	2	110	-1.69	0.048
20	MIF	P14174	12.5	36.5	304	4	4559	-1.68	0.091
21	GLB1	P16278	76.0	21.7	61	11	1127	-1.58	0.028
22	MRPL17	Q9NRX2	20.0	23.4	19	4	158	-1.57	0.068
23	ZZEF1	O43149	330.9	2.9	10	6	185	-1.55	0.011
24	LYPLAL1	Q5VWZ2	26.3	30.0	39	5	203	-1.53	0.017
25	URB1	O60287	254.2	7.8	54	12	222	-1.52	0.137
26	ITPR3	Q14573	303.9	13.0	77	19	659	-1.51	0.026
27	NGLY1	Q96IV0	74.3	17.3	20	6	108	-1.51	0.122
28	EIF4EBP1	Q13541	12.6	38.1	19	3	141	-1.49	0.046
29	PDCD4	Q53EL6	51.7	27.3	45	9	634	-1.49	0.012
30	TLN2	Q9Y4G6	271.4	8.1	76	6	980	-1.49	0.083
31	RAB3GAP2	Q9H2M9	155.9	8.7	46	9	520	-1.46	0.117
32	PFN2	P35080	15.0	36.4	83	5	1493	-1.44	0.085
33	MCU	Q8NE86	39.8	24.8	55	7	202	-1.44	0.165
34	BLMH	Q13867	52.5	18.5	23	5	300	-1.42	0.138
35	PDK3	Q15120	46.9	8.1	11	2	78	-1.42	0.168
36	ACSS2	Q9NR19	78.5	4.1	10	2	62	-1.42	0.028
37	SLC7A1	P30825	67.6	6.8	16	3	328	-1.41	0.103
38	WASH1	A8K0Z3	50.3	10.5	30	2	451	-1.41	0.010
39	PRKDC	P78527	468.8	35.4	1309	129	18704	-1.41	0.030
40	HUWE1	Q7Z6Z7	481.6	20.6	390	52	5509	-1.41	0.038
41	PTER	Q96BW5	39.0	41.8	72	10	700	-1.40	0.156
42	ALDH5A1	P51649	57.2	20.7	58	8	1194	-1.40	0.091
43	DOPEY2	Q9Y3R5	258.1	0.6	11	1	213	-1.40	0.088
44	IGF2R	P11717	274.2	29.3	304	48	3216	-1.36	0.111
45	FDFT1	P37268	48.1	41.7	74	13	966	-1.35	0.040
46	NADP	O75874	46.6	57.2	557	20	7653	-1.35	0.196
47	LSS	P48449	83.3	23.0	83	13	1058	-1.35	0.204
48	SLC26A6	Q9BXS9	82.9	4.5	7	2	147	-1.34	0.165
49	PSMC5	P62195	45.6	54.4	482	20	8289	-1.33	0.169
50	DHCR7	Q9UBM7	54.5	11.4	20	4	500	-1.33	0.104
51	LCLAT1	Q6UWP7	48.9	7.5	14	2	106	-1.32	0.012
52	NAGA	P17050	46.5	15.8	35	5	561	-1.31	0.021
53	MGST3	O14880	16.5	34.2	121	4	768	-1.31	0.139
54	PAFAH1B3	Q15102	25.7	42.9	71	6	686	-1.31	0.025
55	LRBA	P50851	318.9	13.8	130	28	1384	-1.30	0.029

56	ARL6IP5	O75915	21.6	20.2	88	4	1846	-1.29	0.207
57	DYNC1H1	Q14204	532.1	41.2	1624	156	20175	-1.28	0.044
58	MPP7	Q5T2T1	65.5	23.4	33	8	159	-1.28	0.015
59	DHRS1	Q96LJ7	33.9	14.7	11	2	96	-1.28	0.024
60	MBOAT7	Q96N66	52.7	8.7	32	3	759	-1.27	0.114
61	EXOC4	Q96A65	110.4	12.8	43	8	734	-1.27	0.037
62	THYN1	Q9P016	25.7	14.2	12	2	202	-1.26	0.064
63	FLOT2	Q14254	47.0	34.1	62	11	975	-1.26	0.137
64	EHBP1	Q8NDI1	139.9	7.4	19	5	308	-1.25	0.005
65	OSBPL8	Q9BZF1	101.1	18.6	36	10	245	-1.25	0.034
66	ABCD3	P28288	75.4	30.0	185	14	1994	-1.25	0.099
67	ABHD14B	Q96IU4	22.3	34.8	97	5	901	-1.22	0.141
68	RAB1A	P62820	22.7	60.0	252	3	4211	-1.22	0.202
69	CASP6	P55212	33.3	24.2	35	5	221	-1.21	0.097
70	COX2	P00403	25.5	20.7	61	4	519	-1.20	0.022
71	SCCPDH	Q8NBX0	47.1	25.4	34	8	295	-1.20	0.145
72	NUP205	Q92621	227.8	10.7	77	14	473	-1.20	0.024
73	SACM1L	Q9NTJ5	66.9	22.1	87	11	631	-1.19	0.055
74	ADH5	P11766	39.7	25.1	150	10	2009	-1.19	0.086
75	NIPSNAP1	Q9BPW8	33.3	27.5	103	6	916	-1.19	0.046
76	STT3B	Q8TCJ2	93.6	9.4	66	8	849	-1.18	0.115
77	CMAS	Q8NFW8	48.3	43.5	156	13	2368	-1.17	0.329
78	MTOR	P42345	288.7	6.5	34	10	238	-1.17	0.091
79	G6PC3	Q9BUM1	38.7	6.1	6	1	193	-1.17	0.043
80	CRAT	P43155	70.8	16.6	42	7	416	-1.16	0.310
81	MYO6	Q9UM54	149.6	39.2	462	43	5907	-1.15	0.018
82	EXD2	Q9NVH0	70.3	10.6	17	4	258	-1.15	0.096
83	RAB3GAP1	Q15042	110.5	19.0	86	13	857	-1.14	0.363
84	UGGT1	Q9NYU2	177.1	40.8	426	38	6704	-1.14	0.279

Table 4.5: Results of low SILAC-ratios for single SILAC DLD-1 IRI experiment. p-value from multi SILAC dataset analysed by LIMMA is included.

4.3.4.4 Bioinformatics analysis of proteins significantly changed due to resistance

Only proteins classified in the altered group using the 5th percentile cluster analysis and with a significant p-value ($p<0.05$) obtained from LIMMA analysis were selected to develop a protein network model. Initially, STRING analysis was applied to identify relationships between proteins significantly altered in resistant sublines, based on molecular functions identified by GO and pathway analysis for selected proteins using EnrichNet (Fig. 4.8).

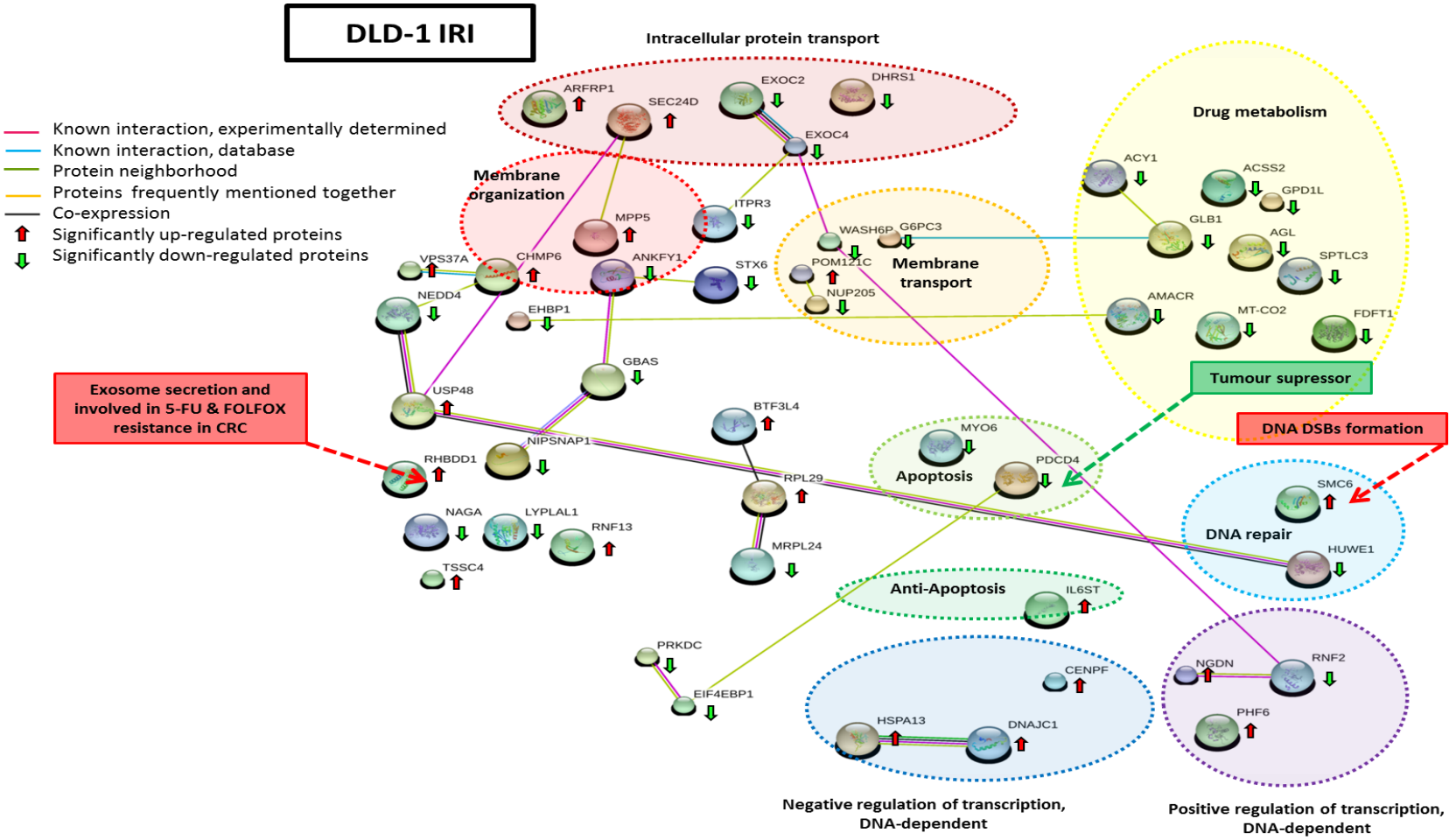

Figure 4.8: The figure shows a proteomic network model for DLD-1 IRI. Significantly altered proteins obtained by modification on EnrichNet and GO from the initial bubble map obtained in STRING. Proteins were classified into different biological processes groups represented with a circle. Dotted arrows indicate the most relevant altered proteins and its main function as mediator of drug resistance. Key: Green arrow: significantly down-regulated protein; Red arrow: significantly up-regulated proteins.

4.3.4.5 Verification of experimental fold changes using housekeeping-control proteins

As it has been explained in Chapter 3, section 3.3.9, seven housekeeping control proteins were used to validate fold changes findings in DLD-1 IRI. Results for these seven housekeeping proteins are summarized in Table 4.6.

N	Protein name	Gene name	Abundance Ratio: L / H			Normalized Log2 Ratio: L / H			Log2 Fold-change	Significant differences p-value
			DLD-1 RPMI P=9	DLD-1 RPMI P=65	DLD-1 IRI [200] P=55	DLD-1 RPMI P=9	DLD-1 RPMI P=65	DLD-1 IRI [200] P=55	DLD-1 IRI	DLD-1 IRI
1	Peptidyl-prolyl cis-trans isomerase A	PPIA	1.09	1.63	1.92	-0.30	-0.44	-0.52	-0.15	0.61
2	ADP-ribosylation factor 3	ARF3	1.31	1.72	1.92	-0.03	-0.36	-0.51	-0.32	0.36
3	Hypoxia up-regulated protein 1	HYOU1	1.31	1.31	2.00	-0.03	-0.75	-0.46	-0.07	0.88
4	ATP synthase subunit d, mitochondrial	ATP5H	1.58	2.07	2.82	0.24	-0.09	0.03	-0.04	0.90
5	Osteoclast-stimulating factor 1	OSTF1	1.44	1.96	2.49	0.11	-0.18	-0.15	-0.11	0.73
6	Heme oxygenase 2	HMOX2	1.00	1.61	2.13	-0.42	-0.46	-0.37	0.07	0.81
7	Cytoskeleton-associated protein 5	CKAP5	1.12	1.73	1.94	-0.26	-0.35	-0.51	-0.21	0.49

Table 4.6: Control proteins that are unaltered by IRI effects and which were used to evaluate the success of SILAC approach and statistical analysis applied to DLD-1 IRI resistant subline. Log_2 fold change of all control proteins were found close to zero in the unique IRI resistant sublines when they were compared to its respective parent-control cell lines. A Log_2 fold proximal to 0, means that levels of the proteins quantified were similar in light and heavy samples.

4.4 Discussion

Development of resistant sublines from KM 12 and HT 29 parent cell lines was not possible. Failure during establishment of resistant sublines may be due to the high anti-proliferative effect that the drug had on KM 12 and HT 29 cell lines, which were more sensitive than DLD-1 during long-term (10 months) drug exposure times. Proteomics quantification results for DLD-1 IRI resistant subline were also similar in productiveness to the three previous results in 5-FU resistant sublines with a total of 3761 proteins quantified. From histograms, volcano plots and cluster analysis obtained, it was observed that DLD-1 IRI resistant subline was the subline with the lowest fold change (1.7-fold) according to MTT assay (Fig. 4.2b) and with the lowest number of significantly altered proteins (Fig. 4.6).

A summary table containing proteins altered in DLD-1 IRI resistant subline is shown below. Most relevant up-regulated proteins were classified based on the specific literature background of the protein in two groups:

1) Altered proteins by direct effect of IRI exposure as proteins involved in apoptotic mechanism and stress regulation.

2) Altered proteins by indirect effect of IRI exposure as proteins related to DNA repair, drug transport, drug metabolism, exocytosis and vesicle formation.

	Indirect effect of IRI	**Direct effect of IRI**
DLD-1 IRI	SMC6, ARFRP1, SEC24D, CHMP6, VPS37A, RHBDD1	**-**

Table 4.7: Up-regulated proteins identified in 5-FU resistant sublines.

4.4.1 Mechanisms of resistance to IRI identified by proteomics: Significantly altered proteins in DLD-1 IRI

Among the three resistant sublines of DLD-1, DLD-1 IRI was the resistant subline with the lowest number of significantly up-regulated proteins. Additionally, DLD-1 IRI resistant subline showed the lowest fold change

resistant phenotype in comparison with DLD-1 parent cell line. Among 5% of the most significantly up-regulated proteins none was involved in drug metabolism and just one was found in anti-apoptotic proteins. Drug metabolism and avoiding of apoptotic pathways are essential steps during drug resistance metabolism in CRC. So, lack of up-regulated proteins belonging in these processes may be related to the lack of success during DLD-1 resistance development to IRI.

4.4.1.1 Apoptotic process (1)

One noteworthy significantly down-regulated protein was the programmed cell death protein 4 (PDCD4). PDCD4 is a tumour suppressor that acts promoting apoptotic pathways. Decreasing of PDCD4 activity has been associated with resistance development in glioblastoma (Liwak, Jordan et al. 2013). PDCD4 decreases tumour progression through cell cycle and cell proliferation regulation in CRC cells by down-regulation of MAP4K1 transcription. A direct consequence of MAP4K1 inhibition is blocking of c-Jun activation. Although it is clear that PDCD4 shows translational inhibition of target mRNAs, which suppress tumourigenesis. However, the mechanisms behind this process are still unknown (Allgayer 2010).

Recent results from 2015 show that increasing of PDCD4 levels in CRC cells increases 5-FU sensitivity by negative regulation of ABC transporters and negative regulation of surface stem cell markers as CD44 expression (Wu, Li et al. 2015). Therefore, a decreasing of PDCD4 expression could increase the ABC transporters and stem cell markers levels, driving cells to develop a resistant phenotype to drugs like IRI. Additionally, down-regulation of PDCD4 drives in a decrease of paclitaxel toxicity in different human cancer cells (Xu, Dephoure et al. 2015).

4.4.1.2 DNA repair process (2)

Only the structural maintenance of chromosomes protein 6 (SMC6) was found significantly up-regulated in DNA repair process of DLD-1 IRI. SMC6 with SMC5 together form a complex that mediates during formation of DNA double-strand

breaks by homologous recombination, a high expression of the SMC5 protein was found also in DLD-1 IRI. The SMC6-SMC5 complex is required for telomere maintenance during cell division (De Piccoli, Cortes-Ledesma et al. 2006, Räschle, Smeenk et al. 2015). Nevertheless, no evidence of SMC5-SMC6 protein expression has been related yet with chemotherapy resistance in cancer. Due to its role as a mediator of sister-chromatid recombination for DNA repair and maintenance of telomeres, the SMC5-SMC6 complex may be part of a mechanism of resistance to drugs and the inhibition of SMC5-SMC6 complex during chemotherapy treatment should be studied.

4.4.1.3 Drug and small molecules metabolism (3)

DLD-1 IRI did not show any significantly up-regulated protein involved in drug metabolism among the 10% of most altered protein. This issue may be related to the fact that the final resistant fold change of DLD-1 IRI was the lowest (1.7 fold change). So, maybe the lack of altered proteins involved in drug metabolism may partially explain the lack of success during DLD-1 IRI establishment process.

4.4.1.4 Intracellular protein transport (4)

One significantly up-regulated protein was the ADP-ribosylation factor-related protein 1 (ARFRP1) that takes part in protein transport and lysosome vesicles formation (Vitale, Horiba et al. 1998).

A second significantly up-regulated protein of DLD-1 IRI was the transport protein SEC24D that promotes the transport of secretory vesicles and vacuolar proteins from the endoplasmic reticulum to the Golgi complex (Tang, Kausalya et al. 1999).

Finally, charged multivesicular body protein 6 (CHMP6) and vacuolar protein sorting-associated protein 37A (VPS37A) were also found significantly up-regulated and their role is to mediate invagination and scission of the endosomes and lysosomes in experiments with the yeast *Saccharomyces cerevisiae* (Hurley and Hanson 2010). Up-regulation of SEC24D, CHMP6, VPS37A proteins together, increase transport of cell vesicles. Increasing of

vesicle transport has been described as a mechanism of drug resistance. It is based on the idea that cells may decrease drug levels inside the cells by collecting drug molecules within lysosomes and other vesicles that will be delivery to the extracellular space (Zhitomirsky and Assaraf 2016).

4.4.1.5 Cellular membrane transporters and cell membrane organization (5)

The unique significantly up-regulated protein related with transcellular membrane transport was the Rhomboid-related protein 4 (RHBDD1). RHBDD1 has two main functions that may contribute to drug resistance developing. RHBDD1 inhibits the pro-apoptotic pathways in Human embryonic kidney cells 293 (HEK 293T) (Wang, Guan et al. 2008), increasing exosome secretion that may increase both 5-FU and FOLFOX resistance in CRC (Bigagli, Luceri et al. 2016).

4.4.2 Conclusion

Among the three parent cell lines used, only DLD-1 developed a low acquired resistance to IRI. Hence, IRI was the drug with the highest anti-proliferative effect of all CRC cell lines studied (see Chapter 2, section 2.4.2.2). Initial IRI-toxicity panel matches with the results of the establishment of resistant sublines, which only were successful with DLD-1 IRI development. Most of the significantly altered proteins seen in DLD-1 IRI sublines were more related to consequences of IRI effects than to cellular mechanisms of resistance to the drug. It would be interesting to study if hydroxylation of IRI (CPT-11) by carboxylesterase (CE) to the active metabolite SN-38 (see Chapter 4, section 4.1.2.1) may be a limiting factor during development of resistant sublines to this drug. Protein expression levels of CE in parent and resistant sublines were not quantified during our proteomics study. The measurement of CE protein expression can be done by real-time PCR platforms, WB and immunostaining. It would be interesting to know if different expression levels of CE among all CRC cell lines studied are affecting the development of acquired resistance process, as under low levels of CE conditions IRI would not be activated and cells would not be affected by its anti-proliferative effect.

- Chapter five -

Identification of new mechanisms of resistance to OXA

5 Identification of new mechanisms of resistance to OXA

5.1 Introduction

OXA (1,2-diaminocyclohexane-oxalate platinum) is the only member of the family of platinum analogues that shows activity against CRC (Rabik and Dolan 2007). OXA has an oxalate ligand and a diaminocyclohexane ligand (DACH) that has replaced the amine group from cisplatin (André, Boni et al. 2004, Alcindor and Beauger 2011). Structural differences between the two molecules explain differences in OXA and cisplatin activity. The hydrogen bond formation between Pt-amine-hydrogens and surrounding bases of the DNA are different for cisplatin and OXA (Chaney, Ramachandran et al. 2009). Those differences in hydrogen binding patterns result in DNA conformational differences that allow selective recognition of OXA or cisplatin by different proteins that can play a role in toxicity and resistance of these drugs.

5.1.1 Mechanisms of action of OXA

The pathways of action of OXA are far from being fully known (Martinez-Cardús, Martinez-Balibrea et al. 2009). DNA is the natural target of OXA and of the rest of platinum-based drugs. The DACH-Pt complex is critical for a high cytotoxicity and a high binding to cellular DNA by OXA (Woynarowski, Chapman et al. 1998). DACH-Pt reacts with the sulfhydryl and amino groups of proteins, DNA and RNA. Although OXA binds with all four DNA nucleobases, it predominantly forms adducts with adenine and guanine (Woynarowski, Chapman et al. 1998, Kerr, Shoeib et al. 2008). DNA lesions and arrest of both DNA and RNA synthesis lead to a switching on of the damage sensor system of the cell. The activation of the DNA repair mechanism system converges in the activation of ATM and ATR proteins that results in the stabilization and activation of p53 that can subsequently activate genes involved in apoptosis pathways (Schwab 2008, Muller and Vousden 2013). OXA shows synergism when it is used together with other cytotoxic drugs as 5-FU, however additional in-depth studies are required to know more about these effects (Alcindor and Beauger 2011).

5.1.2 Known mechanisms of resistance to OXA

5.1.2.1 Mechanisms of resistance to OXA related to membrane transporters

There are multiple processes that may play a role in OXA resistance. The main mechanisms of resistance to OXA are related to membrane transporters that mediate the efflux of platinum agents out from the cell (Alcindor and Beauger 2011). The main group of proteins that can act as transporter for cisplatin agents are the copper transporters, especially ATP7a and ATP7b (Komatsu, Sumizawa et al. 2000, Martinez-Cardús, Martinez-Balibrea et al. 2009, Martinez-Balibrea, Martínez-Cardús et al. 2009). In the case of ATP7a, high levels of this copper transporter have been found in cisplatin-resistant ovarian carcinoma cell lines after be treated with cisplatin and OXA (Samimi, Safaei et al. 2004). Further, an association between high levels of ATP7b transporter and a poor prognosis in CRC patients under OXA treatment has been found (Martinez-Balibrea, Martínez-Cardús et al. 2009).

5.1.2.2 Mechanisms of resistance to OXA related to glutathione

Other mechanisms associated with resistance to cisplatin drugs are related to intracellular glutathione (GSH) levels (Balendiran, Dabur et al. 2004). GSH is increased in cisplatin resistant ovarian cancer cell lines (Rabik and Dolan 2007). The increase of intracellular GSH in A2780 ovarian carcinoma cell line is caused by γ-glutamyl transpeptidase activity (El-Akawi, Abu-Hadid et al. 1996). γ-glutamyl transpeptidase is a cell surface enzyme that catalyses the transfer of the gamma-glutamyl moiety of GSH to an acceptor that may be an amino acid, a peptide or water (Yang, Faustino et al. 2000). The correlation between high levels of GSH and cisplatin resistance is due to that some membrane transporters require GSH as cofactor for substrate transporting, so an increase in GSH levels can make easier the transport of cisplatin drugs (Kuo 2009).

5.1.2.3 Mechanisms of resistance to OXA related to mitochondrial apoptotic pathway

Finally, a recent study found that defects in the mitochondrial apoptotic pathway could contribute to resistance to OXA in CRC (Gourdier, Crabbe et al. 2004). This is because one of OXA's mechanisms of action is via Bax/Bak dependent mitochondrial apoptosis (Gourdier, Del Rio et al. 2002). Bax/Bak are pro-apoptotic proteins that are activated by cell stress or DNA damage (Yang, Faustino et al. 2000). These proteins mediate the permeabilization of the mitochondria, an essential process for apoptosis. A mutation in *Bax* gene has been demonstrated to enable resistance in the HCT 116-R2 CRC cell line (Gourdier, Del Rio et al. 2002, Gourdier, Crabbe et al. 2004).

5.1.3 Aims & Objectives for OXA

Main aims and objectives of the investigation were focused on developing new resistant sublines to OXA to identify novel mechanisms of resistance in CRC, and use as experimental models for evaluation of novel therapies which may overcome drug resistance and will be carried out as follows:

1) Select suitable cell lines for development OXA resistant sublines from a CRC cell line panel.

2) Establish resistant sublines.

3) Cell growth characterisation of DLD-1 OXA and KM 12 OXA

6) Study of MDR mechanisms from KM 12 OXA by MTT.

7) Identify novel mechanisms of OXA resistance using a proteomic approach.

5.2 Material & Methods

All general material and methods used were carried out as it has been previously described in Chapter 2 and Chapter 3.

5.3 Results

5.3.1 Establishment of DLD-1 drug resistant cell lines to OXA

OXA resistant sublines were established from DLD-1 and KM 12 parent cell lines by episodic exposure to OXA over a period of ten months. Evolve of DLD-1 parent cell lines to DLD-1 OXA is shown by the interval between four successive different passages of DLD-1 parent cell line under OXA exposure conditions (Fig. 5.1a). The DLD-1 OXA resistant subline was maintained and growth in a drug-free medium during a month, keeping stability in OXA resistant phenotype. Regarding HT 29 parent cell line, it was not possible establishment of its resistant subline as OXA cytotoxic effects on this cell line were too high during long-term drug exposure process.

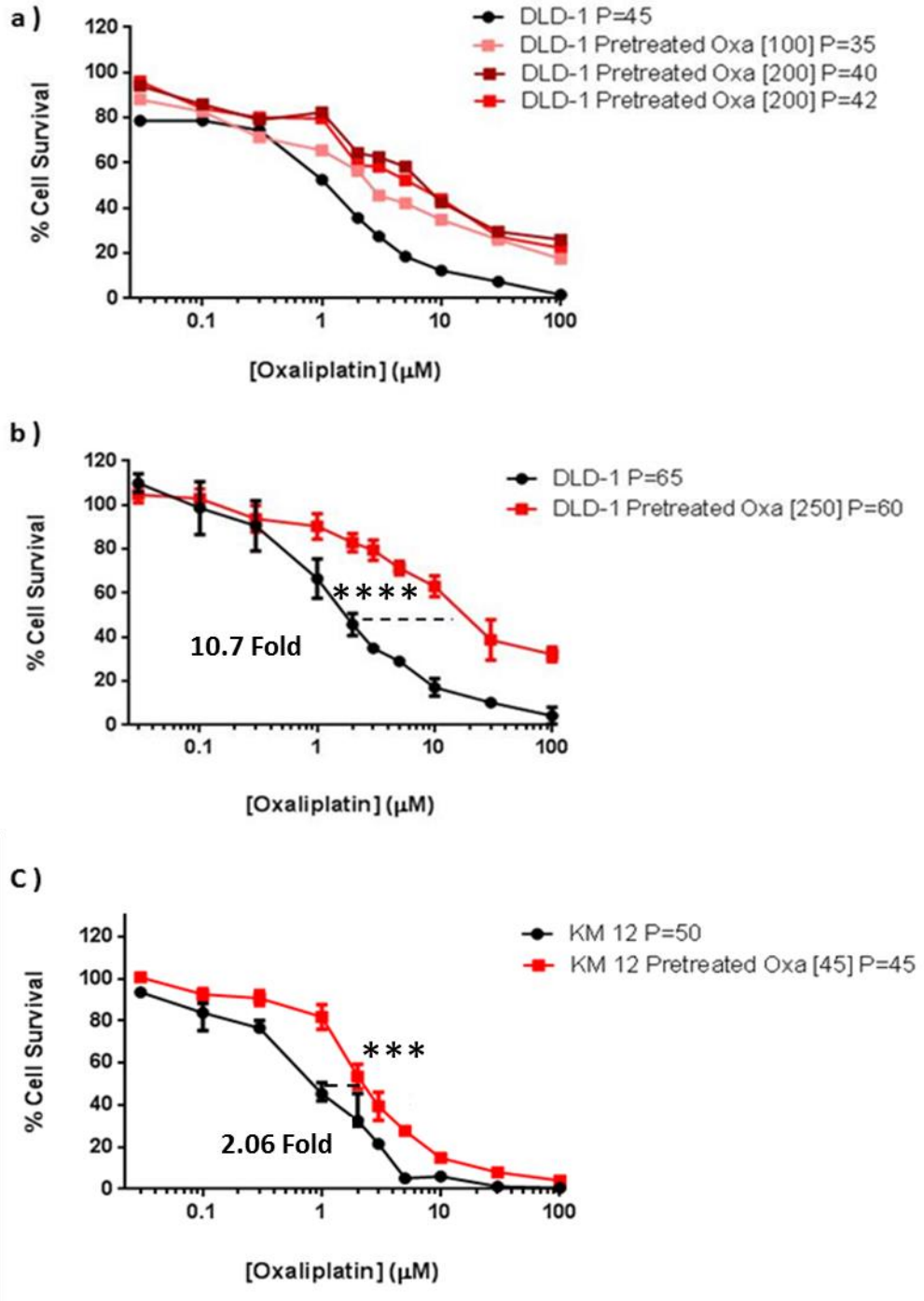

Figure 5.1: Chemosensitivity curve profiles of OXA resistant sublines. Three independent chemosensitivity curve profiles for (a) DLD-1 parent and DLD-1 pretreated with OXA during establishment of DLD-1 OXA resistant subline. (b) DLD-1 no pretreated cell line and DLD-1 OXA P=60. (c) KM 12 no pretreated cell line and KM 12 OXA P=30. All cell lines were exposed to OXA [0.03-100 µM] concentration during

96 h. MTT assays were performed in three independent experiments (mean ± SEM). Graphs show the cell survival of DLD-1 OXA and non-pretreated cell lines against different OXA concentrations. The difference in IC_{50} among DLD-1 non-pretreated parent cell line and DLD-1 OXA was 10.7-fold change (**** $p \leq 0.0001$). The difference in IC_{50} among KM 12 non-pretreated parent cell line and KM 12 OXA was 2.06-fold change and significant (*** $p \leq 0.001$). Error bars showing standard deviations between replicates are displayed too.

5.3.2 Characterisation of cell growth for DLD-1 and KM 12 resistant sublines to OXA

To confirm results obtained by MTT and to test if the number of passage of the flask could have some effect on the MTT assay, a growth curve analysis was done for the two resistant sublines to OXA established. Growth rate and capacity to proliferate was measured for OXA resistant sublines (Fig. 5.2). Growth curves were done using an initial concentration of $1x10^4$ cells/ml.

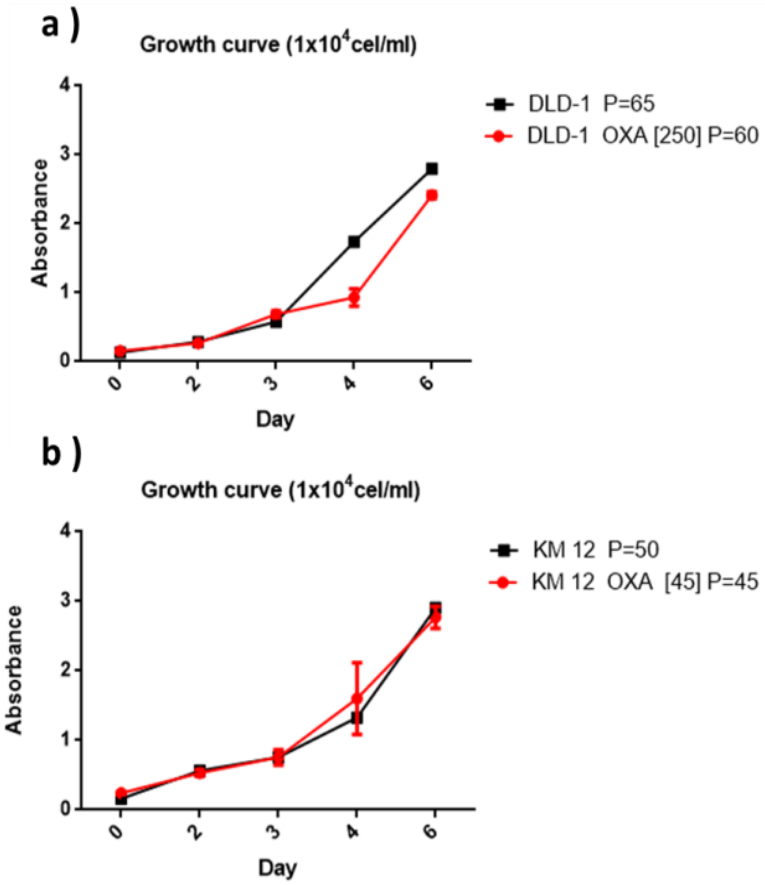

Figure 5.2: MTT Growth curve profiles. (a) DLD-1 parent cell line and DLD-1 OXA resistant subline, and (b) KM 12 parent cell lines and KM 12 OXA resistant subline. No significant differences ($p>0.05$) were found in growth curve profiles between parent and resistant sublines.

5.3.3 Evaluation of cross-resistance in the KM 12 OXA subline by MTT

MDR was studied following same methodology previously described for DLD-1 5-FU (see Chapter 3, section 3.3.3). So, to support with new knowledge related to cross-resistance mechanisms in OXA chemotherapy, a further study of collateral loss of sensitivity to eight chemotherapy agents used in CRC was carried out using the resistant sublines KM12 OXA (Fig. 5.3).

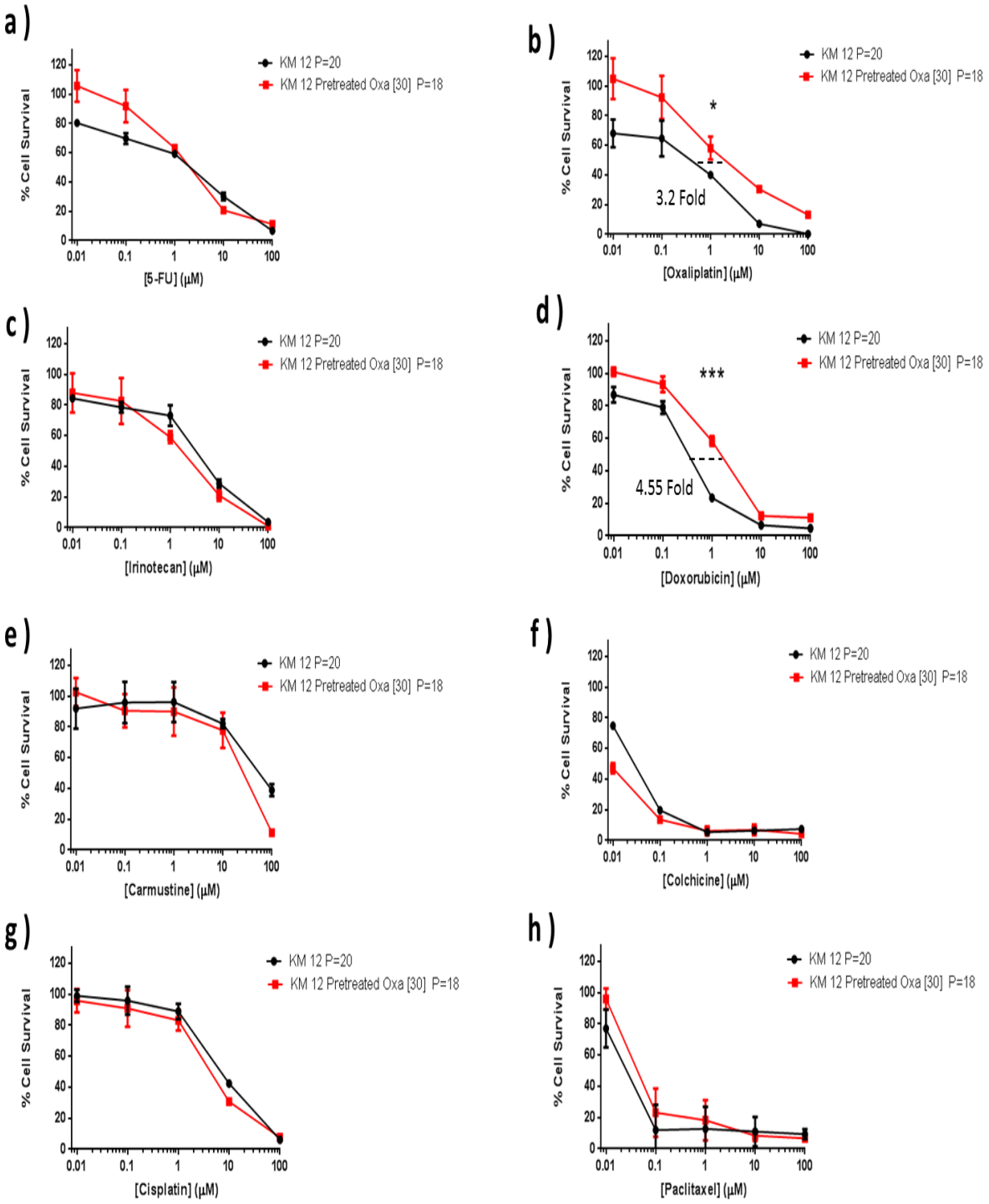

Figure 5.3: Cross-resistance profile conferred by KM 12 OXA and KM 12 parent cell line. The 96 h cytotoxicity assays were performed with eight different drugs: (a) 5-FU, (b) OXA, (c) IRI, (d) doxorubicin, (e) carmustine, (f) colchicine, (g) cisplatin and (h) paclitaxel. Curves are representative of separate experiments in triplicate. Relative resistance values were obtained by dividing the IC_{50} value of the resistant KM 12 OXA resistant subline by the IC_{50} value of the KM 12 parent cell line. (*$p \leq 0.05$; ** $p \leq 0.01$; *** $p \leq 0.001$; **** $p \leq 0.0001$).

5.3.4 Identification of proteome changes in DLD-1 and KM 12 resistant sublines to OXA using mass spectrometry by SILAC approach

Results for OXA resistant sublines were carried out as it has been previously described for 5-FU in Chapter 3, section 3.3.6. Lowest Mascot score used in each sample were established by Mascot software for a 95 % confidence rate and these Mascot score are summarized in table 5.1.

Cell Line	DLD-1 P=9	DLD-1 P=65	DLD-1 OXA	KM 12 P=9	KM 12 P=55	KM 12 OXA
Mascot Score	>31	>30	>30	>28	>28	>28

Table 5.1: Lowest Mascot scores used during analysis of OXA resistant sublines.

Multi SILAC datasets of OXA resistant sublines were similar and is shown in two Venn diagrams below. The total number of commonly quantified proteins is shown within circles intersections. Complete protein lists are enclosed in a soft copy which is attached in a CD along with this thesis.

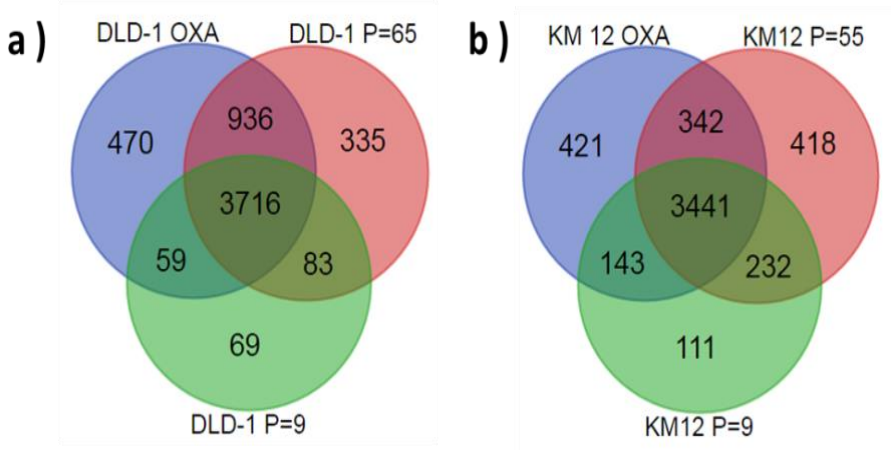

Figure 5.4: Venn diagrams of multi SILAC datasets in OXA. (a) DLD-1 and (b) KM 12 parent cell lines with a high and a low number of passages and their respective drug-resistant sublines to OXA. These commonly up-regulated and down-regulated proteins presented at the intersection of Venn diagrams are discussed in detail further in section 5.4.2.1.

5.3.5 Protein quantification and results of the MS analysis

SILAC labelling method was used to determine changes in protein expression from parent cell lines and their resistant OXA subline.

5.3.5.1 Raw data normalization

Initially, after Log_2 transformation of the normalized SILAC-ratio data, a histogram frequency distribution of Log_2 SILAC-ratio data figure for common proteins quantified in each set of parent cell lines (two parent cell lines with high and low number of passages and sensitive to 5-FU) and its respective resistant subline established *in vitro* was carried out and they are shown below (Fig. 5.5). Histogram relevance lies in the number of high Log_2 SILAC-ratio proteins value for each sample, which should show lower values of Log_2 SILAC-ratio in proteins of parent cell lines than in resistant sublines that show an increase in Log_2 SILAC-ratio caused by drug effects. These trends are observed in the two histogram views (Fig. 5.5) and they are useful to validate that the experimental procedure is replicable as it was expected.

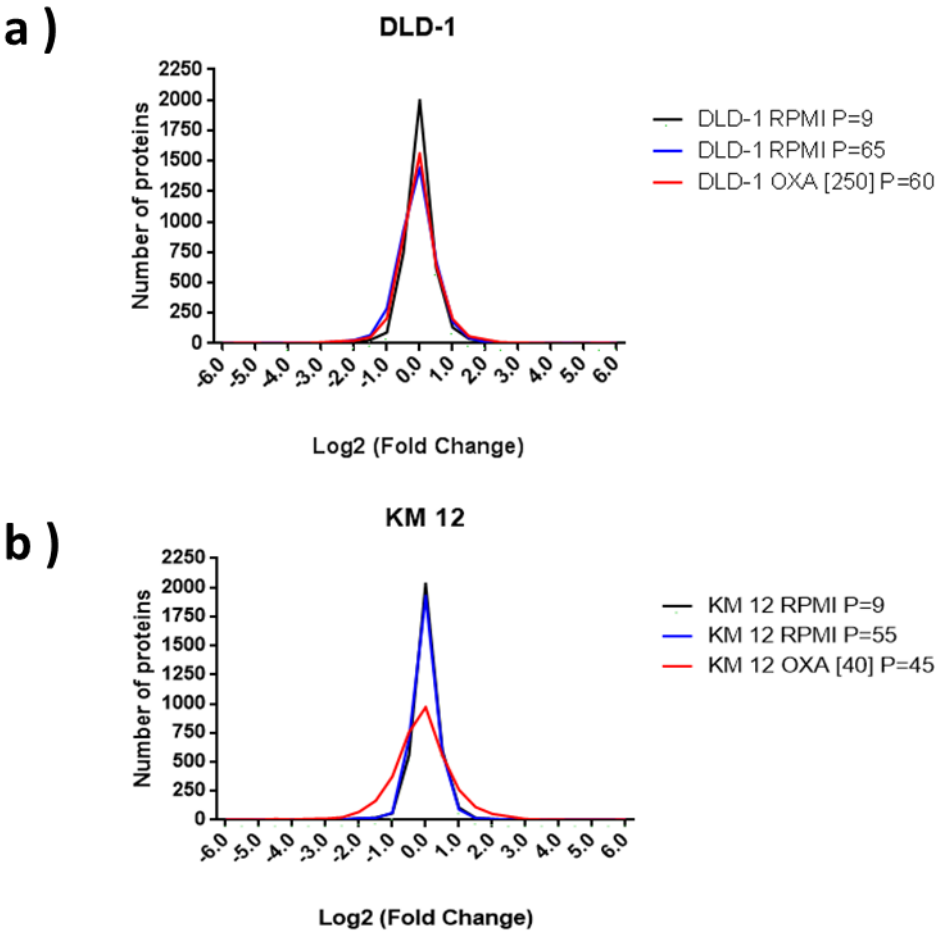

Figure 5.5: A histogram view of overlaid fold change distributions of multi SILAC datasets in OXA. (a) DLD-1 and (b) KM 12 resistant sublines to OXA compared with their respective parent and sensitive cell lines after Log_2-transformation and normalization of experimental data ratios (L/H).

Resistant cell lines to OXA	Significant Up-regulated Proteins	Significant Down-regulated Proteins	Percentage of Significantly Altered proteins
DLD-1	153	109	7.05%
KM 12	270	453	21.01%

Table 5.2: Significantly up-regulated (Fold change ≥ 2) and down-regulated (Fold change ≤ 2) proteins in resistant cell lines to OXA.

5.3.5.2 "R" LIMMA analysis

OXA multi SILAC datasets were analysed by LIMMA. A fold change and its associated p-value were calculated for each protein according to their significant different ratio expressions between the OXA resistant sublines and its two related parent-control cell lines with a high and a low number of passages. This information was summarised in a Volcano plot of LIMMA-modelled proteomics data. The data for all proteins are plotted as Log_2 fold change versus the $-Log_{10}$ of the adjusted p-value (Fig. 5.6).

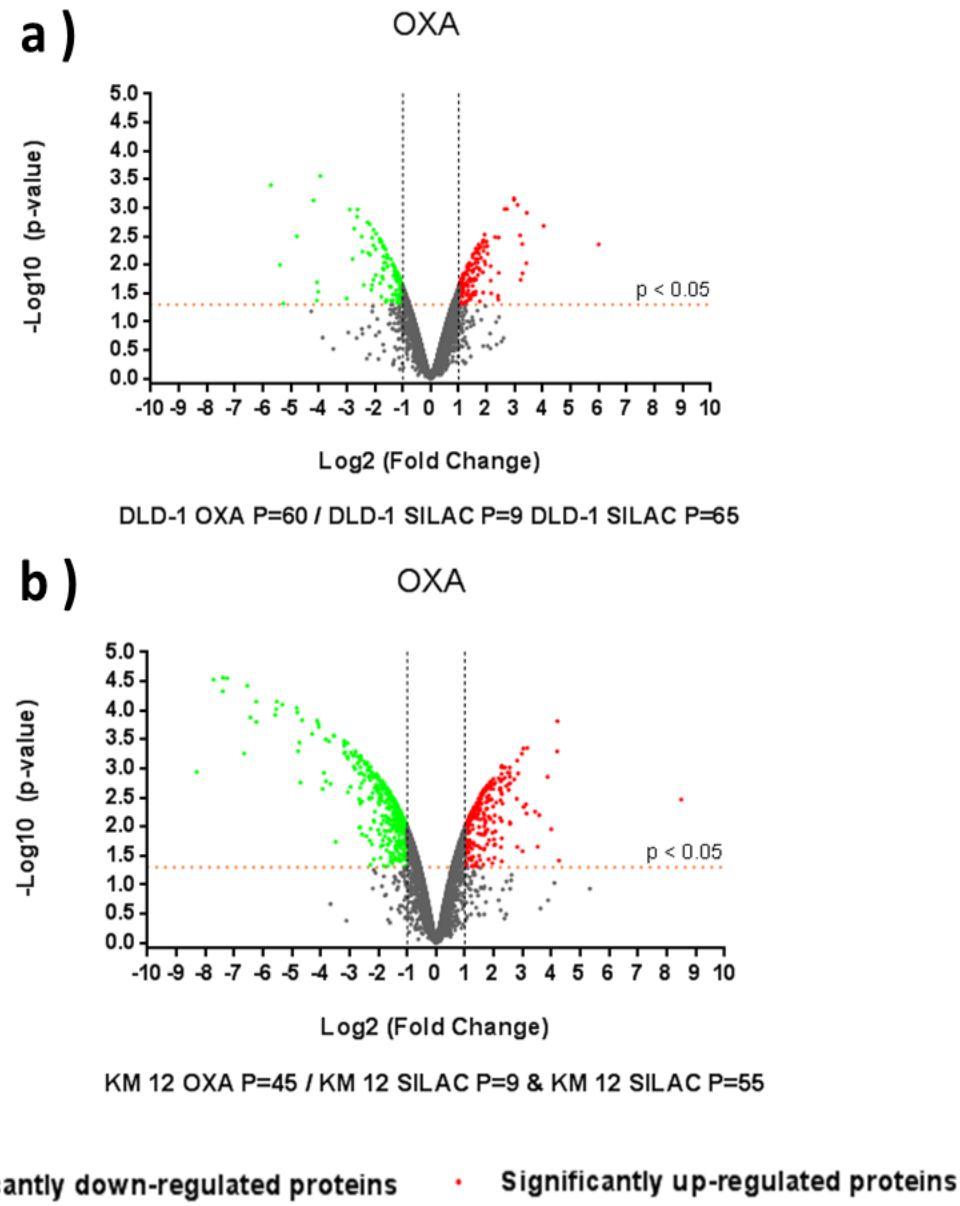

Figure 5.6: Volcano plots showing the distribution of significantly down- and up-regulated proteins following LIMMA modelling in OXA sublines. Criteria for significance are a 2-fold change for the (a) DLD-1 5-FU and (b) KM 12 5-FU sublines compared to the parent data, with $p<0.05$. Key: Red-Upregulated, Green – Downregulated proteins, Grey-Unaltered and non-significant proteins.

Log_2 fold changes and their respective p-value were calculated using LIMMA. Proteins of each sample were ordered from the highest to the lowest according to normalised Log_2 ratio data from SILAC results.

5.3.5.3 Cluster analysis

The ordered list of proteins was divided into three groups of proteins using a 5th percentile threshold of the total population as it has been previously described in Chapter 3, section 3.3.7.3. The most significantly altered proteins in OXA resistant sublines but which remain as unaltered in both parent samples under 5th percentile criteria were used to build up a cluster analysis (Fig. 5.7 and Fig. 5.8). Significance was obtained from LIMMA analysis p-value. Finally, lists of the most significant high and low SILAC-ratios of proteins quantified in DLD-1 OXA and KM 12 OXA resistant sublines were done (Table 5.4-5.7).

Status in Parent cell line with Low Passage	Status in Parent cell line with High Passage	Status in OXA Resistant Subline	Status Sum-up	Number of proteins in Set DLD-1	Number of proteins in Set KM 12
D	D	D	DDD	21	4
D	D	N	DDN	32	34
D	D	U	DDU	3	4
D	N	D	DND	12	8
D	N	N	DNN	101	105
D	N	U	DNU	10	9
D	U	D	DUD	3	2
D	U	N	DUN	7	7
D	U	U	DUU	1	3
N	D	D	NDD	34	9
N	D	N	NDN	96	100
N	D	U	NDU	2	11
N	**N**	**D**	**NND**	**109**	**130**
N	**N**	**N**	**NNN**	**2900**	**2633**
N	**N**	**U**	**NNU**	**89**	**102**
N	U	D	NUD	2	5
N	U	N	NUN	69	86
N	U	U	NUU	39	17
U	D	D	UDD	2	1
U	D	N	UDN	0	9
U	D	U	UDU	0	4
U	N	D	UND	6	10
U	N	N	UNN	101	83
U	N	U	UNU	12	13
U	U	D	UUD	1	7
U	U	N	UUN	34	36
U	U	U	UUU	30	9
			TOTAL	3716	3441

Table 5.3: Thresholds for protein status in DLD-1 and KM 12 multi SILAC datasets were established using a 5th percentile criteria. From the column of "Status Sum-up" in the table, only the proteins which remain as unaltered (brown) in both parent cell lines and with an altered status (green or red) in the resistant sublines were considered to be studied as altered proteins involved in drug-resistance.

Cluster analysis results for DLD-1 OXA are shown in Figure 5.7. Detailed results for significantly altered proteins in DLD-1 OXA resistant subline are summarized in Tables 5.4 and 5.5. Log_2 SILAC results for DLD-1 OXA / DLD-1 SILAC P=9 ratio and p-values from R analysis of resistant and control cell lines are included.

Cluster analysis for DLD-1 OXA resistant subline showed similar results to those observed during “R” LIMMA analysis (see Fig. 5.6a). The highest number of proteins remain unaltered in both parent cells lines, whilst DLD-1 OXA shows a high symmetry in (a) up- and (b) down-regulated proteins fold change dispersion.

a)

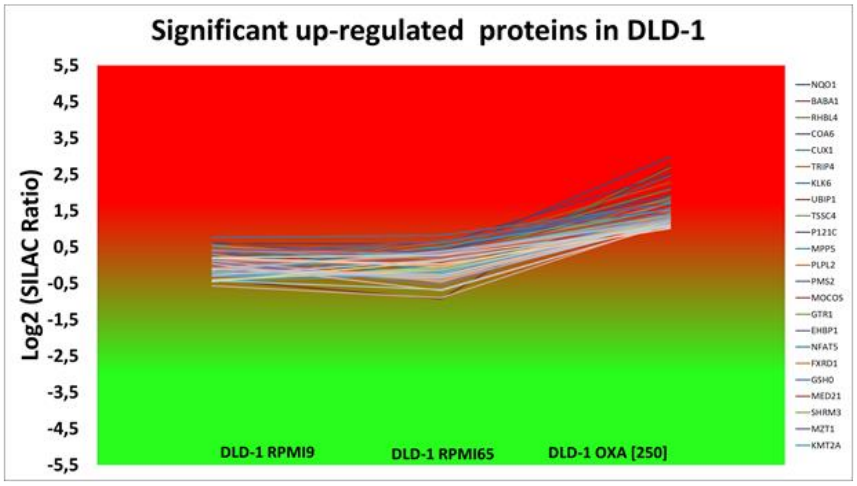

b)

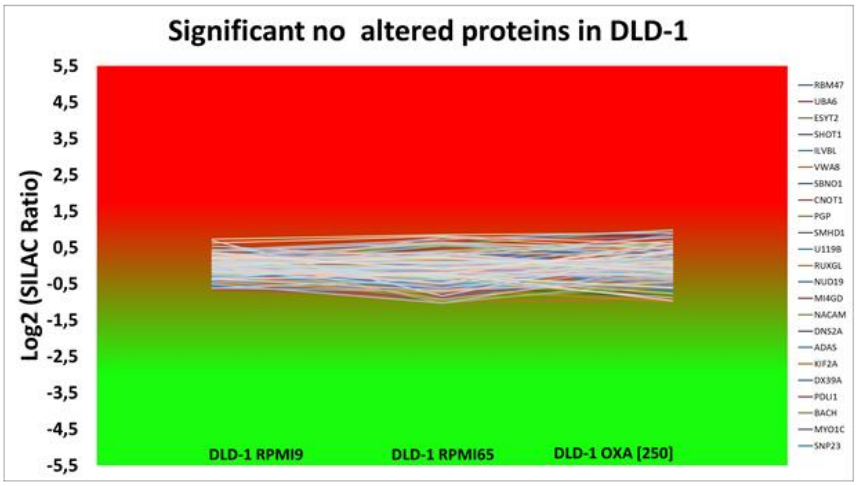

c)

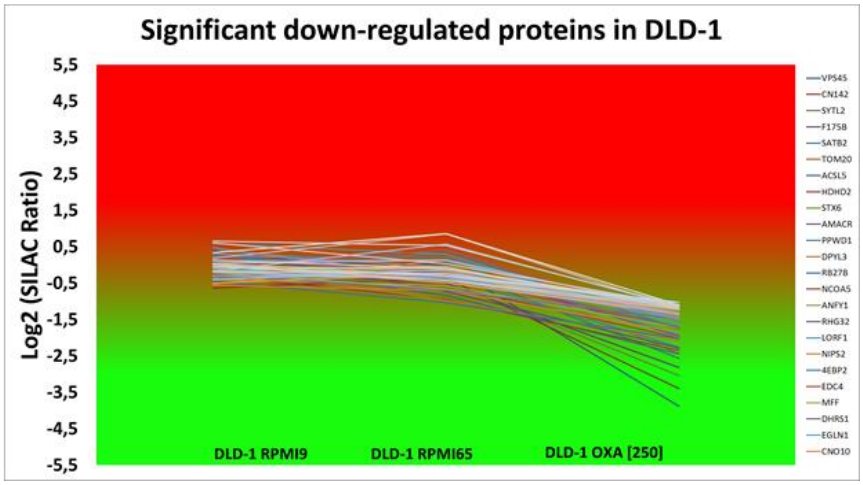

Figure 5.7: Cluster analysis of DLD-1 OXA. Proteins were classified using 5th percentile threshold for significantly (a) up-regulated proteins; (b) unaltered proteins; (c) down-regulated proteins in sensitive parent cell lines DLD-1 P=9, DLD-1 P=65 and in DLD-1 OXA resistant subline.

N	Protein name	AC. number	MW [kDa]	SC %	PSMs	Unique Peptides	Score Mascot	Normalized Log2 Ratio: L/H	p-value
1	NQO1	P15559	30.8	36.5	467	12	7156	2.98	0.001
2	BABAM1	Q9NWV8	36.5	17.6	14	4	55	2.77	0.001
3	RHBDD1	Q8TEB9	35.8	11.1	7	2	254	2.68	0.001
4	COA6	Q5JTJ3	14.1	32.0	9	3	45	2.51	0.003
5	CUX1	P39880	164.1	12.6	44	4	170	2.47	0.003
6	TRIP4	Q15650	66.1	27.4	36	8	316	2.28	0.004
7	KLK6	Q92876	26.8	41.8	70	6	908	2.14	0.006
8	UBP1	Q9NZI7	60.5	9.6	13	2	343	2.12	0.004
9	TSSC4	Q9Y5U2	34.3	13.4	19	4	76	2.09	0.005
10	POM121C	A8CG34	125.0	10.5	23	6	309	1.93	0.006
11	MPP5	Q8N3R9	77.2	23.0	51	9	813	1.89	0.004
12	PNPLA2	Q96AD5	55.3	12.5	38	4	554	1.86	0.009
13	LOC107984056	P54278	95.7	3.8	9	2	131	1.85	0.006
14	MOCOS	Q96EN8	98.1	18.1	43	9	309	1.85	0.019
15	SLC2A1	P11166	54.0	17.5	376	12	5632	1.84	0.008
16	FSCN1	Q16658	54.5	57.2	307	22	5241	1.79	0.064
17	EHBP1	Q8NDI1	139.9	14.4	46	10	735	1.79	0.010
18	NFAT5	O94916	165.7	12.5	37	11	1300	1.78	0.017
19	FOXRED1	Q96CU9	53.8	18.9	17	6	191	1.78	0.034
20	GCLM	P48507	30.7	36.1	76	7	1379	1.76	0.014
21	MED21	Q13503	15.6	13.9	9	1	201	1.76	0.033
22	SHROOM3	Q8TF72	216.7	23.6	126	25	1164	1.74	0.012
23	MZT1	Q08AG7	8.5	32.9	6	2	76	1.73	0.006
24	KMT2A	Q03164	431.5	1.9	8	4	33	1.72	0.031
25	OS9	Q13438	75.5	7.9	12	3	45	1.69	0.015
26	ZNF638	Q14966	220.5	18.1	94	21	1162	1.68	0.066
27	NGDN	Q8NEJ9	35.9	19.7	20	3	165	1.68	0.033
28	GOLPH3	Q9H4A6	33.8	36.2	66	5	1682	1.60	0.010
29	MYADM	Q96S97	35.3	12.1	39	3	1015	1.57	0.011
30	Hsp40	O75190	36.1	23.0	34	6	558	1.56	0.031
31	CPTP	Q5TA50	24.4	16.4	6	2	115	1.53	0.032
32	C1orf122	Q6ZSJ8	11.5	33.6	4	2	69	1.52	0.030
33	TNFRSF1A	Q9NXR7	43.5	18.0	12	4	86	1.49	0.012
34	TERF2IP	Q9NYB0	44.2	34.8	48	8	1039	1.47	0.020
35	INPP4A	Q96PE3	109.9	11.2	25	6	338	1.44	0.006
36	LASP1	Q14847	29.7	41.4	282	8	1700	1.43	0.020
37	C1orf116	Q9BW04	63.9	35.6	99	12	1235	1.42	0.005
38	Hsp70	P48723	51.9	8.5	9	3	80	1.42	0.006
39	ZYX	Q15942	61.2	30.1	86	10	684	1.41	0.022
40	NOL3	O60936	22.6	60.6	58	7	848	1.41	0.013
41	PSMG2	Q969U7	29.4	11.0	18	3	145	1.40	0.101
42	NUDT4	Q9NZJ9	20.3	60.6	52	6	567	1.38	0.017

43	OCLN	Q16625	59.1	27.0	97	10	1094	1.38	0.018
44	TJP3	O95049	101.3	13.6	50	8	508	1.37	0.005
45	SPCS2	Q15005	25.0	17.3	46	5	563	1.34	0.018
46	STK39	Q9UEW8	59.4	32.3	50	7	853	1.32	0.064
47	TDP2	O95551	40.9	22.9	29	5	685	1.32	0.056
48	G6PD	P11413	59.2	80.6	1626	36	19800	1.32	0.005
49	GCLC	P48506	72.7	46.5	178	23	1895	1.32	0.028
50	APOBEC3B	Q9UH17	45.9	31.2	87	9	878	1.31	0.009
51	TNFRSF10A	O00220	50.1	13.7	28	4	434	1.30	0.028
52	PARD6B	Q9BYG5	41.2	28.2	53	8	269	1.27	0.007
53	ANXA6	P08133	75.8	62.3	486	34	7421	1.26	0.026
54	BAIAP2	Q9UQB8	60.8	44.2	134	16	2339	1.26	0.036
55	IGF2BP3	O00425	63.7	33.5	142	12	2359	1.25	0.015
56	SEC24D	O94855	112.9	24.61	79	14	777	1.24	0.013
57	STIM1	Q13586	77.4	40.73	167	18	3519	1.24	0.010
58	TBC1D17	Q9HA65	72.7	5.556	4	3	117	1.23	0.007
59	SMG9	Q9H0W8	57.6	12.88	14	4	152	1.23	0.103
60	CHTF18	Q8WVB6	107.3	18.77	57	11	348	1.20	0.062
61	CORO7	P57737	100.5	18.59	37	8	455	1.19	0.021
62	EPS8L3	Q8TE67	66.8	26.14	90	11	809	1.19	0.048
63	KRT80	Q6KB66	50.5	35.62	222	11	3782	1.18	0.005
64	PTPN1	P18031	49.9	30.11	135	11	2621	1.18	0.010
65	FHL2	Q14192	32.2	58.42	171	15	3061	1.17	0.028
66	TENM3	Q9P273	300.8	7.929	26	11	285	1.17	0.213
67	ALKBH5	Q6P6C2	44.2	17.51	16	4	90	1.16	0.212
68	AGRN	O00468	217.1	9.386	40	12	614	1.14	0.093
69	ITGA3	P26006	116.5	17.41	99	12	1505	1.12	0.006
70	CPNE1	Q99829	59	23.84	156	9	2187	1.12	0.011
71	LIMCH1	Q9UPQ0	121.8	28.9	110	23	2217	1.12	0.012
72	RNF213	Q63HN8	591	18.76	229	63	1885	1.12	0.034
73	CD81	P60033	25.8	25	135	3	2472	1.11	0.065
74	LPCAT2	Q7L5N7	60.2	26.47	63	9	684	1.11	0.079
75	TAP1	Q03518	87.2	20.67	90	9	1954	1.11	0.033
76	UBE2R2	Q712K3	27.1	18.91	7	2	34	1.10	0.163
77	NXT1	Q9UKK6	15.8	25.71	22	3	543	1.09	0.172
78	CPPED1	Q9BRF8	35.5	48.09	96	9	2079	1.07	0.031
79	FECH	P22830	47.8	30.73	46	9	402	1.07	0.073
80	PIK3C2A	O00443	190.6	14.12	69	17	680	1.07	0.063
81	XRCC4	Q13426	38.3	27.68	32	6	908	1.07	0.257
82	NDUFS5	O43920	12.5	41.5	14	4	192	1.06	0.068
83	STAU1	O95793	63.1	47.8	280	25	3323	1.06	0.141

84	MTHFD2	P13995	37.9	52.6	156	11	2010	1.05	0.042
85	ERBIN	Q96RT1	158.2	30.3	100	24	801	1.04	0.080
86	ESF1	Q9H501	98.7	10.2	58	7	769	1.02	0.200
87	STAT2	P52630	97.9	9.8	26	5	201	1.02	0.104
88	PYGO2	Q9BRQ0	41.2	9.1	11	2	330	1.01	0.103
89	OSBPL3	Q9H4L5	101.2	22.2	50	14	766	1.00	0.037

Table 5.4: Results of high SILAC-ratios for single SILAC DLD-1 OXA experiment. p-value from multi SILAC dataset analysed by LIMMA is included.

N	Protein name	AC. number	MW [kDa]	SC %	PSMs	Unique Peptides	Score Mascot	Normalized Log2 Ratio: L/H	p-value
1	VPS45	Q9NRW7	65.0	17.2	58	7	620	-3.89	0.000
2	GON7	Q9BXV9	10.9	18.0	5	1	39	-3.40	0.001
3	SYTL2	Q9HCH5	104.9	7.6	14	4	87	-3.04	0.001
4	FAM175B	Q15018	46.9	10.4	13	3	110	-2.82	0.008
5	SATB2	Q9UPW6	82.5	14.7	56	7	706	-2.57	0.002
6	TOMM20	Q15388	16.3	31.0	19	3	227	-2.45	0.001
7	ACSL5	Q9ULC5	75.9	43.0	85	19	923	-2.44	0.018
8	HDHD2	Q9H0R4	28.5	20.8	27	4	200	-2.35	0.016
9	STX6	O43752	29.2	23.1	21	4	199	-2.31	0.003
10	AMACR	Q9UHK6	42.4	33.2	29	7	313	-2.29	0.028
11	PPWD1	Q96BP3	73.5	21.7	30	8	412	-2.26	0.006
12	DPYSL3	Q14195	61.9	50.2	278	15	4484	-2.09	0.042
13	RAB27B	O00194	24.6	31.2	64	5	780	-2.03	0.033
14	NCOA5	Q9HCD5	65.5	35.1	94	10	504	-2.01	0.012
15	ANKFY1	Q9P2R3	128.3	24.6	122	17	1444	-1.99	0.003
16	ARHGAP32	A7KAX9	230.4	10.7	56	11	1079	-1.96	0.003
17	L1RE1	Q9UN81	40.0	7.1	18	2	335	-1.92	0.002
18	GBAS	O75323	33.7	19.9	29	4	126	-1.86	0.014
19	USP4	Q13107	108.5	7.4	23	4	127	-1.79	0.050
20	EIF4EBP2	Q13542	12.9	25.8	15	1	184	-1.77	0.005
21	EDC4	Q6P2E9	151.6	21.8	77	17	812	-1.75	0.008
22	MFF	Q9GZY8	38.4	20.5	18	4	173	-1.73	0.014
23	DHRS1	Q96LJ7	33.9	8.6	10	1	122	-1.71	0.009
24	EGLN1	Q9GZT9	46.0	12.0	4	3	44	-1.66	0.003
25	EPM2AIP1	Q7L775	70.3	13.2	14	5	79	-1.64	0.067
26	CMAS	Q8NFW8	48.3	43.5	153	13	2527	-1.62	0.121
27	ACOT11	Q8WXI4	68.4	14.3	13	5	55	-1.56	0.063
28	CNOT10	Q9H9A5	82.3	18.7	20	9	129	-1.55	0.034
29	SORL1	Q92673	248.3	2.5	8	4	76	-1.55	0.004
30	TLN2	Q9Y4G6	271.4	6.3	94	4	1196	-1.54	0.075

31	CUL4B	Q13620	103.9	25.6	149	14	1370	-1.53	0.088
32	ARFGAP1	Q8N6T3	44.6	20.0	27	5	500	-1.51	0.012
33	DLGAP5	Q15398	95.1	11.3	16	6	215	-1.51	0.041
34	TAGLN2	P37802	22.4	72.4	269	12	5529	-1.50	0.044
35	MTR	Q99707	140.4	10.6	39	9	482	-1.50	0.055
36	YTHDF1	Q9BYJ9	60.8	14.3	33	3	334	-1.49	0.005
37	TRAF2	Q12933	55.8	6.0	2	2	32	-1.48	0.023
38	STAT1	P42224	87.3	37.9	333	21	5080	-1.48	0.016
39	ALDH5A1	P51649	57.2	18.3	38	6	984	-1.47	0.074
40	SLC7A1	P30825	67.6	6.8	19	3	279	-1.47	0.087
41	SLC26A6	Q9BXS9	82.9	4.5	9	2	75	-1.47	0.113
42	STT3B	Q8TCJ2	93.6	9.1	87	7	1183	-1.44	0.061
43	CTSC	P53634	51.8	19.0	57	6	579	-1.42	0.011
44	BLMH	Q13867	52.5	29.0	37	8	358	-1.40	0.143
45	FANCD2	Q9BXW9	164.0	1.8	15	2	302	-1.37	0.012
46	KDELC2	Q7Z4H8	58.5	22.1	21	7	140	-1.37	0.068
47	NIPSNAP3A	Q9UFN0	28.4	15.0	15	2	63	-1.37	0.136
48	RAB8B	Q92930	23.6	29.5	71	1	616	-1.37	0.043
49	ATP2B1	P20020	138.7	23.4	176	14	2986	-1.37	0.026
50	MRPL17	Q9NRX2	20.0	18.9	24	4	315	-1.36	0.101
51	CSE1L	P55060	110.3	32.5	388	25	5659	-1.35	0.039
52	TRIM24	O15164	116.8	8.1	23	5	280	-1.33	0.023
53	DNPEP	Q9ULA0	52.4	47.8	151	17	1367	-1.32	0.014
54	RPS9	P46781	22.6	29.9	134	9	1075	-1.31	0.127
55	ABCD3	P28288	75.4	34.6	248	17	2887	-1.31	0.080
56	HSD17B11	Q8NBQ5	32.9	49.33	74	10	567	-1.31	0.121
57	COX20	Q5RI15	13.3	22.03	18	2	391	-1.29	0.068
58	HSD17B7	P56937	38.2	3.519	11	1	235	-1.29	0.053
59	OXR1	Q8N573	97.9	15.79	35	7	708	-1.28	0.050
60	SH3BGRL2	Q9UJC5	12.3	56.07	61	4	748	-1.28	0.178
61	MDN1	Q9NU22	632.4	2.77	36	10	146	-1.25	0.054
62	ATPAF2	Q8N5M1	32.8	21.11	19	4	127	-1.25	0.027
63	CIRBP	Q14011	18.6	26.74	18	3	401	-1.23	0.027
64	ELMO2	Q96JJ3	82.6	12.22	25	5	267	-1.23	0.070
65	NDUFA4	O00483	9.4	27.16	24	2	362	-1.22	0.136
66	LYPLAL1	Q5VWZ2	26.3	29.96	48	5	153	-1.22	0.038
67	NPTN	Q9Y639	44.4	7.035	15	2	134	-1.21	0.045
68	PRKDC	P78527	468.8	35.56	1582	126	23795	-1.21	0.050
69	HMGCS1	Q01581	57.3	49.62	269	17	4377	-1.21	0.011
70	SDCBP	O00560	32.4	52.68	127	7	1579	-1.20	0.059

71	MESDC2	Q14696	26.1	18.38	33	3	194	-1.20	0.170
72	AK3	Q9UIJ7	25.6	35.24	81	8	1381	-1.20	0.297
73	CHDH	Q8NE62	65.3	8.923	16	3	76	-1.19	0.018
74	FKBP5	Q13451	51.2	35.45	163	13	2191	-1.19	0.111
75	LONP2	Q86WA8	94.6	16.78	29	9	124	-1.19	0.182
76	OSGEP	Q9NPF4	36.4	34.63	13	6	44	-1.18	0.017
77	GNPDA1	P46926	32.6	47.06	59	4	893	-1.17	0.098
78	PATJ	Q8NI35	196.2	20.6	103	19	1584	-1.15	0.042
79	NNT	Q13423	113.8	23.3	163	16	1878	-1.14	0.150
80	PIN1	Q13526	18.2	43.56	78	5	1296	-1.14	0.047
81	ACOT13	Q9NPJ3	15.0	37.9	29	4	309	-1.14	0.109
82	MIF	P14174	12.5	36.52	322	4	5042	-1.14	0.351
83	HSD17B4	P51659	79.6	46.2	528	25	10523	-1.14	0.050
84	TBCE	Q15813	59.3	33.4	63	11	802	-1.13	0.206
85	PKN1	Q16512	103.9	13.1	17	8	52	-1.13	0.019
86	NUP210	Q8TEM1	205.0	14.9	131	16	1466	-1.13	0.092
87	FABP5	Q01469	15.2	65.2	576	12	10680	-1.12	0.056
88	SLC12A2	P55011	131.4	29.9	342	25	4255	-1.11	0.005
89	PSPC1	Q8WXF1	58.7	34.8	125	11	1965	-1.11	0.153
90	PEX3	P56589	42.1	25.7	30	5	308	-1.11	0.025
91	NOA1	Q8NC60	78.4	14.3	11	6	32	-1.10	0.012
92	SLC12A9	Q9BXP2	96.0	3.2	7	2	102	-1.10	0.033
93	CPOX	P36551	50.1	44.1	404	21	4526	-1.10	0.076
94	TBC1D9B	Q66K14	140.4	6.8	20	6	164	-1.09	0.057
95	CPT2	P23786	73.7	34.0	79	14	714	-1.09	0.362
96	THNSL1	Q8IYQ7	83.0	22.9	37	11	785	-1.09	0.052
97	MYO5C	Q9NQX4	202.7	1.5	13	2	100	-1.08	0.080
98	TRMT10C	Q7L0Y3	47.3	39.0	132	13	1002	-1.08	0.104
99	LSS	P48449	83.3	24.7	101	14	1681	-1.08	0.425
100	RPL9	P32969	21.9	62.5	274	11	3582	-1.07	0.144
101	FAM136A	Q96C01	15.6	42.8	41	5	547	-1.07	0.311
102	MOGS	Q13724	91.9	33.1	235	19	3441	-1.04	0.066
103	NADK2	Q4G0N4	49.4	12.9	18	3	169	-1.04	0.136
104	SCCPDH	Q8NBX0	47.1	24.5	22	7	281	-1.03	0.248
105	NAGA	P17050	46.5	21.2	19	6	268	-1.03	0.047
106	FAM162A	Q96A26	17.3	24.68	55	4	638	-1.03	0.156
107	VPS13C	Q709C8	422.1	7.4	64	18	387	-1.03	0.101
108	SEPT8	Q92599	55.7	25.1	92	7	700	-1.02	0.347
109	GSTO1	P78417	27.5	45.2	125	12	1234	-1.01	0.227

Table 5.5: Results of low SILAC-ratios for single SILAC DLD-1 OXA experiment. p-value from multi SILAC dataset analysed by LIMMA is included.

Cluster analysis results for KM 12 OXA are shown in Figure 5.8. Detailed results for significantly altered proteins in KM 12 OXA resistant subline are summarized in Tables 5.6 and 5.7. Log_2 SILAC results for DLD-1 OXA / DLD-1 SILAC P=9 ratio and p-values from R-LIMMA analysis of resistant and control cell lines are included.

Cluster analysis for KM 12 OXA resistant subline showed similar results to those observed during “R” LIMMA analysis (see Fig. 5.6b). The highest number of proteins remain unaltered in both parent cells lines, whilst KM 12 OXA shows a higher number of down-regulated proteins than up-regulated proteins altered.

a)

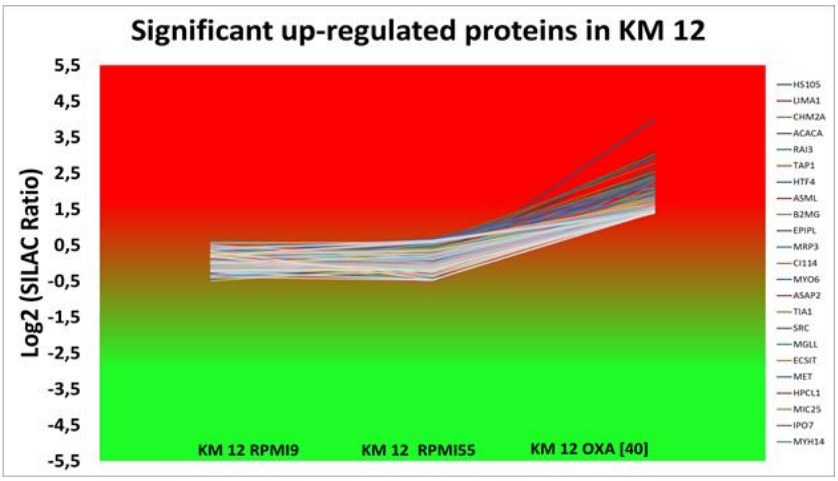

b)

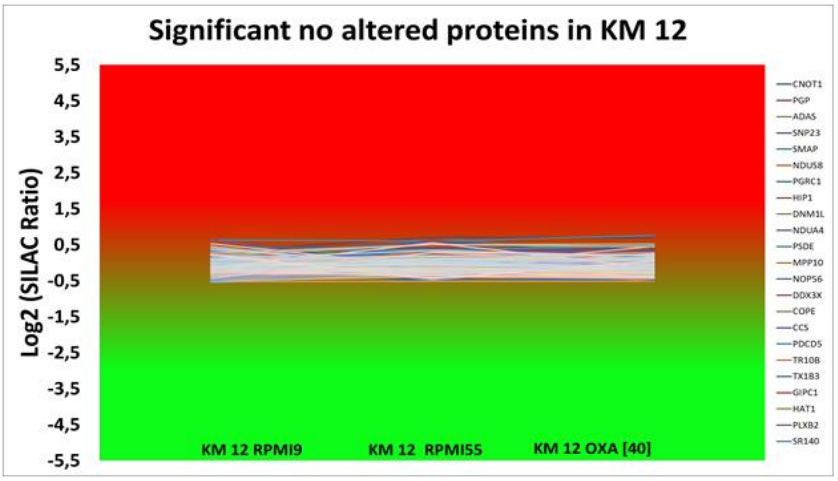

c)

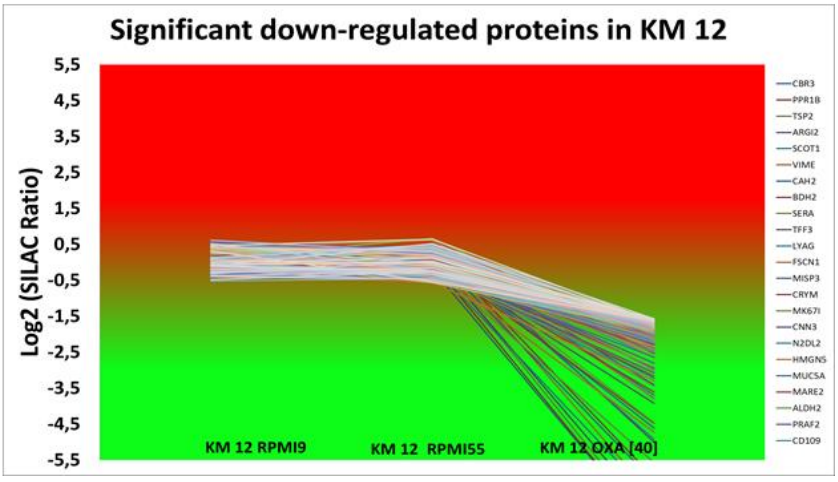

Figure 5.8: Cluster analysis of KM 12 OXA. Proteins were classified using 5th percentile threshold for significantly (a) up-regulated proteins; (b) unaltered proteins; (c) down-regulated proteins in sensitive parent cell KM 12 with 9 passages, in sensitive parent cell KM 12 with 55 passages and in KM 12 OXA resistant subline.

N	Protein name	AC. number	MW [kDa]	SC %	PSMs	Unique Peptides	Score Mascot	Normalized Log2 Ratio: L/H	p-value
1	Hsp110	Q92598	96.8	48.1	384	33	6285	4.00	0.032
2	LIMA1	Q9UHB6	85.2	31.8	133	18	2041	3.08	0.048
3	CHMP2A	O43633	25.1	11.7	25	3	1006	3.03	0.052
4	ACACA	Q13085	265.4	31.3	204	47	2179	2.96	0.050
5	GPRC5A	Q8NFJ5	40.2	21.0	87	5	893	2.91	0.052
6	TAP1	Q03518	87.2	16.6	40	6	762	2.78	0.065
7	TCF12	Q99081	72.9	5.1	4	2	80	2.65	0.066
8	ASMTL	O95671	68.8	22.4	26	9	324	2.55	0.052
9	B2M	P61769	13.7	27.7	47	3	327	2.54	0.052
10	EPPK1	P58107	555.3	54.7	669	62	9270	2.47	0.052
11	ABCC3	O15438	169.2	9.4	25	8	202	2.45	0.052
12	SPOUT1	Q5T280	42.0	9.8	27	2	253	2.41	0.062
13	MYO6	Q9UM54	149.6	30.8	172	30	2407	2.41	0.052
14	ASAP2	O43150	111.6	17.1	32	9	453	2.41	0.052
15	TIA1	P31483	42.9	16.8	38	3	365	2.40	0.064
16	SRC	P12931	59.8	34.0	57	9	875	2.35	0.052
17	MGLL	Q99685	33.2	12.9	18	2	264	2.34	0.052
18	ECSIT	Q9BQ95	49.1	21.1	25	4	318	2.33	0.052
19	MET	P08581	155.4	18.8	68	16	1226	2.32	0.052
20	HPCAL1	P37235	22.3	31.1	38	5	472	2.31	0.052
21	CHCHD6	Q9BRQ6	26.4	17.9	22	2	164	2.30	0.052
22	IPO7	O95373	119.4	22.6	185	20	1997	2.28	0.052
23	MYH14	Q7Z406	227.7	41.1	650	62	11857	2.26	0.052
24	DAG1	Q14118	97.4	6.7	10	3	76	2.18	0.082
25	FAM96B	Q9Y3D0	17.7	57.1	46	6	527	2.16	0.066
26	TMEM43	Q9BTV4	44.8	43.8	54	10	629	2.12	0.052
27	CDK4	P11802	33.7	18.5	35	3	242	2.10	0.055
28	KPNA1	P52294	60.2	20.4	41	5	452	2.06	0.127
29	RAC1	O96013	64.0	22.2	45	5	307	2.04	0.063
30	SLC9A3R1	O14745	38.8	42.5	134	9	1544	2.02	0.052
31	HTATIP2	Q9BUP3	27.0	25.6	38	5	264	2.02	0.052
32	ACAD9	Q9H845	68.7	21.7	58	9	966	2.01	0.052
33	WDR55	Q9H6Y2	42.0	41.0	65	10	558	1.99	0.052
34	CD59	P13987	14.2	19.5	20	3	144	1.97	0.052
35	GNS	P15586	62.0	23.4	37	7	421	1.97	0.084
36	CLPTM1L	Q96KA5	62.2	7.2	28	2	78	1.96	0.074
37	PARP4	Q9UKK3	192.5	16.5	74	16	719	1.94	0.052
38	GNAI2	P04899	40.4	39.7	92	8	790	1.93	0.055
39	BAIAP2	Q9UQB8	60.8	42.2	84	15	1157	1.93	0.073
40	ENDOD1	O94919	55.0	25.6	46	7	509	1.92	0.057
41	STAT1	P42224	87.3	37.2	208	21	3560	1.91	0.052
42	NSDHL	Q15738	41.9	44.2	66	12	1044	1.90	0.053
43	GEMIN5	Q8TEQ6	168.5	20.6	109	17	1494	1.89	0.052
44	NDUFS6	O75380	13.7	29.0	15	2	206	1.89	0.062

45	RNMT	O43148	54.8	20.8	39	7	576	1.89	0.073
46	TP53	P04637	43.6	30.8	63	5	806	1.88	0.064
47	AHNAK	Q09666	628.7	72.4	3013	256	31662	1.86	0.054
48	LIG3	P49916	112.8	18.1	56	13	581	1.84	0.052
49	RAP2C	Q9Y3L5	20.7	43.2	21	2	270	1.84	0.054
50	REPIN1	Q9BWE0	63.5	2.6	6	1	143	1.83	0.052
51	APLP2	Q06481	86.9	8.8	24	4	285	1.83	0.059
52	SH3KBP1	Q96B97	73.1	25.7	69	9	1060	1.82	0.052
53	ARHGAP18	Q8N392	74.9	19.6	41	8	530	1.81	0.055
54	ST14	Q9Y5Y6	94.7	17.0	59	9	631	1.80	0.069
55	ERMP1	Q7Z2K6	100.2	16.9	48	9	283	1.79	0.059
56	IVD	P26440	46.3	27.0	69	6	1141	1.78	0.059
57	STIM1	Q13586	77.4	23.8	37	9	619	1.76	0.057
58	CLN6	Q9NWW5	35.9	11.3	26	3	391	1.72	0.052
59	NUP153	P49790	153.8	29.0	95	19	1027	1.69	0.059
60	MRE11	P49959	80.5	30.4	93	17	733	1.69	0.055
61	ACOT13	Q9NPJ3	15.0	30.7	24	3	326	1.69	0.091
62	ITGB5	P18084	88.0	23.8	50	10	475	1.69	0.063
63	CETN2	P41208	19.7	44.2	17	4	537	1.68	0.058
64	IDE	P14735	117.9	18.5	58	12	291	1.68	0.074
65	USP14	P54578	56.0	46.8	207	16	2918	1.68	0.052
66	NPC2	P61916	16.6	25.8	50	2	293	1.67	0.064
67	ASL	P04424	51.6	22.2	50	9	333	1.62	0.062
68	PPP1R13L	Q8WUF5	89.0	23.6	50	11	329	1.61	0.052
69	UFD1L	Q92890	34.5	28.7	27	5	422	1.61	0.052
70	METAP2	P50579	52.9	38.1	76	12	1066	1.61	0.052
71	CHRAC1	Q9NRG0	14.7	51.1	29	4	683	1.59	0.055
72	PTK2	Q05397	119.2	24.7	63	14	526	1.59	0.061
73	CNDP2	Q96KP4	52.8	44.8	134	15	1283	1.58	0.052
74	AGK	Q53H12	47.1	21.3	38	5	518	1.58	0.059
75	UBA2	Q9UBT2	71.2	44.5	169	22	2640	1.57	0.052
76	TFAM	Q00059	29.1	15.9	31	4	440	1.54	0.088
77	REXO2	Q9Y3B8	26.8	30.4	18	7	66	1.54	0.059
78	FAM49B	Q9NUQ9	36.7	40.7	164	10	3076	1.53	0.052
79	FAM129B	Q96TA1	84.1	49.9	394	22	4044	1.52	0.052
80	CEP131	Q9UPN4	122.1	6.6	10	4	108	1.50	0.090
81	AAGAB	Q6PD74	34.6	22.5	25	4	296	1.50	0.052
82	PDCD6	O75340	21.9	37.7	74	5	1144	1.49	0.055
83	FAM21A	Q641Q2	147.1	19.0	42	5	581	1.49	0.075
84	ABCF2	Q9UG63	71.2	18.0	68	9	583	1.49	0.075
85	VAPA	Q9P0L0	27.9	20.1	91	4	1021	1.48	0.054
86	SRPRA	P08240	69.8	26.0	69	11	971	1.48	0.063
87	RTN4	Q9NQC3	129.9	10.4	131	6	1358	1.48	0.062
88	ABCF1	Q8NE71	95.9	17.8	51	10	1143	1.48	0.168

89	USP8	P40818	127.4	9.7	35	7	334	1.47	0.167
90	ABHD12	Q8N2K0	45.1	42.5	77	10	538	1.47	0.084
91	ABLIM1	O14639	87.6	21.6	41	9	305	1.46	0.061
92	NUDT3	O95989	19.5	29.7	20	3	132	1.46	0.118
93	RAD50	Q92878	153.8	19.0	93	16	1124	1.46	0.091
94	SYAP1	Q96A49	39.9	37.8	79	12	1200	1.46	0.052
95	CNPY3	Q9BT09	30.7	13.3	33	2	318	1.45	0.063
96	ADAM10	O14672	84.1	20.3	66	10	1061	1.44	0.052
97	CUTA	O60888	19.1	40.8	65	5	780	1.43	0.060
98	ARHGAP35	Q9NRY4	170.4	19.1	59	16	439	1.42	0.074
99	Hsp70	P0DMV9	70.0	52.4	1009	22	14270	1.42	0.054
100	RALB	P11234	23.4	33.5	87	3	1322	1.42	0.108
101	TXLNG	Q9NUQ3	60.5	22.2	25	6	207	1.40	0.178
102	EMD	P50402	29.0	34.3	68	8	1075	1.39	0.052

Table 5.6: Results of high SILAC-ratios for single SILAC KM 12 OXA experiment. p-value from multi SILAC dataset analysed by LIMMA is included.

N	Protein name	AC. number	MW [kDa]	SC %	PSMs	Unique Peptides	Score Mascot	Normalized Log2 Ratio: L/H	p-value
1	CBR3	O75828	30.8	30.7	85	3	1459	-7.54	0.000
2	PPP1R1B	Q9UD71	22.9	54.9	57	6	656	-7.54	0.000
3	THBS2	P35442	129.9	5.9	32	4	401	-7.40	0.000
4	ARG2	P78540	38.6	23.7	11	4	212	-7.05	0.000
5	OXCT1	P55809	56.1	36.3	99	13	2050	-6.61	0.000
6	VIM	P08670	53.6	27.3	36	8	306	-6.54	0.001
7	CA2	P00918	29.2	43.5	80	8	777	-6.10	0.000
8	BDH2	Q9BUT1	26.7	24.9	14	4	314	-6.00	0.000
9	PHGDH	O43175	56.6	43.5	419	21	6051	-5.57	0.000
10	TFF3	Q07654	8.6	22.5	9	1	97	-5.00	0.000
11	GAA	P10253	105.3	15.1	20	8	276	-4.93	0.000
12	FSCN1	Q16658	54.5	46.5	152	16	1974	-4.73	0.000
13	MISP3	Q96FF7	24.0	34.7	9	4	102	-4.61	0.000
14	CRYM	Q14894	33.8	10.8	10	2	166	-4.48	0.000
15	NIFK	Q9BYG3	34.2	25.6	26	6	555	-4.47	0.000
16	CNN3	Q15417	36.4	25.5	22	6	76	-3.93	0.000

17	ULBP2	Q9BZM5	27.4	13.0	6	2	80	-3.79	0.002
18	HMGN5	P82970	31.5	21.6	31	4	578	-3.77	0.000
19	MUC5AC	P98088	585.2	11.1	71	21	746	-3.70	0.000
20	MAPRE2	Q15555	37.0	17.7	21	4	94	-3.61	0.000
21	ALDH2	P05091	56.3	49.9	237	19	4557	-3.44	0.000
22	PRAF2	O60831	19.2	16.9	20	3	218	-3.42	0.000
23	CD109	Q6YHK3	161.6	14.6	45	12	750	-3.30	0.001
24	PPOX	P50336	50.7	18.9	15	5	89	-3.29	0.001
25	S100A14	Q9HCY8	11.7	77.9	66	5	843	-3.22	0.000
26	MTX3	Q5HYI7	35.1	5.8	2	1	79	-3.17	0.001
27	PLIN2	Q99541	48.0	9.8	4	2	59	-3.08	0.001
28	FUT8	Q9BYC5	66.5	5.0	4	2	30	-3.07	0.001
29	ASB9	Q96DX5	31.8	6.5	13	1	68	-3.01	0.003
30	CKAP4	Q07065	66.0	40.2	127	16	2846	-3.00	0.000
31	PTER	Q96BW5	39.0	10.0	8	3	67	-2.96	0.001
32	ALCAM	Q13740	65.1	33.1	105	13	1567	-2.92	0.001
33	RIDA	P52758	14.5	45.3	25	4	479	-2.92	0.001
34	SOD2	P04179	24.7	42.8	152	6	1942	-2.81	0.001
35	TESC	Q96BS2	24.7	18.2	23	3	202	-2.65	0.004
36	TRIM2	Q9C040	81.5	16.5	25	6	221	-2.65	0.001
37	BLMH	Q13867	52.5	25.3	19	6	290	-2.64	0.002
38	IQGAP2	Q13576	180.5	15.9	38	11	365	-2.55	0.001
39	PAPOLA	P51003	82.8	13.0	24	5	131	-2.52	0.001
40	METTL26	Q96S19	22.6	7.4	2	1	33	-2.52	0.001
41	DECR1	Q16698	36.0	34.3	109	8	1116	-2.50	0.001
42	TRIOBP	Q9H2D6	261.2	2.5	6	4	77	-2.48	0.001
43	C1orf35	Q9BU76	29.4	10.3	4	2	29	-2.46	0.002
44	APOO	Q9BUR5	22.3	17.7	22	2	349	-2.44	0.001
45	OAT	P04181	48.5	63.8	300	19	4539	-2.44	0.001
46	LACTB	P83111	60.7	5.5	7	2	222	-2.39	0.001
47	AGR2	O95994	20.0	57.1	382	8	7254	-2.36	0.001
48	BPNT1	O95861	33.4	29.5	87	7	1756	-2.35	0.001
49	COQ5	Q5HYK3	37.1	17.1	18	3	212	-2.30	0.006
50	DPYSL2	Q16555	62.3	68.9	414	29	7557	-2.30	0.001
51	ACADM	P11310	46.6	34.0	55	9	789	-2.27	0.001
52	MVD	P53602	43.4	34.3	53	6	497	-2.27	0.002
53	RAP1GDS1	P52306	66.3	17.1	48	6	881	-2.23	0.003
54	DDT	P30046	12.7	50.0	211	7	2052	-2.21	0.002
55	TAMM41	Q96BW9	51.0	19.5	44	6	586	-2.18	0.002
56	ALDH6A1	Q02252	57.8	15.0	24	4	88	-2.18	0.004
57	ACADS	P16219	44.3	28.6	37	6	766	-2.18	0.011
58	HCCS	P53701	30.6	20.5	13	4	93	-2.16	0.001
59	PACSIN3	Q9UKS6	48.5	14.4	7	4	180	-2.16	0.001
60	MPC2	O95563	14.3	22.8	15	2	81	-2.12	0.008

61	S100P	P25815	10.4	49.5	49	4	899	-2.10	0.002
62	ABHD6	Q9BV23	38.3	8.3	10	2	82	-2.09	0.002
63	KIF2C	Q99661	81.3	28.6	52	12	649	-2.08	0.002
64	SLC25A11	Q02978	34.0	27.1	42	6	873	-2.07	0.001
65	PHLDA1	Q8WV24	45.0	2.2	3	1	30	-2.07	0.003
66	GPHN	Q9NQX3	79.7	9.8	16	4	160	-2.05	0.002
67	FABP5	Q01469	15.2	71.1	454	14	6909	-2.05	0.003
68	PARP2	Q9UGN5	66.2	4.5	16	2	164	-2.04	0.003
69	ATP1B1	P05026	35.0	30.4	111	8	1420	-2.02	0.001
70	LYN	P07948	58.5	10.5	38	3	142	-2.02	0.001
71	SLC16A1	P53985	53.9	4.0	6	1	42	-2.00	0.001
72	MYO1E	Q12965	127.0	8.5	14	6	156	-2.00	0.001
73	LONP1	P36776	106.4	36.4	291	26	4044	-1.99	0.001
74	MIA2	Q96PC5	159.7	1.0	4	1	40	-1.96	0.001
75	MGST3	O14880	16.5	15.8	55	2	184	-1.96	0.014
76	SLK	Q9H2G2	142.6	15.4	60	12	441	-1.94	0.003
77	CORO7	P57737	100.5	19.4	51	8	578	-1.93	0.012
78	CYCS	P99999	11.7	56.2	59	7	341	-1.93	0.002
79	SLC25A4	P12235	33.0	37.2	139	2	2153	-1.92	0.003
80	VDAC3	Q9Y277	30.6	50.5	223	10	3029	-1.91	0.002
81	PLEK2	Q9NYT0	39.9	30.3	38	5	244	-1.90	0.020
82	KIF20A	O95235	100.2	10.7	13	5	265	-1.88	0.002
83	HMGCS2	P54868	56.6	42.3	209	11	3218	-1.88	0.004
84	GLOD4	Q9HC38	34.8	50.2	133	10	2362	-1.88	0.003
85	PGM1	P36871	61.4	44.1	98	17	1512	-1.87	0.002
86	HAX1	O00165	31.6	32.3	16	5	53	-1.87	0.003
87	GEMIN2	O14893	31.6	7.1	5	2	115	-1.86	0.001
88	MYO1D	O94832	116.1	16.6	66	10	400	-1.85	0.002
89	NUCB2	P80303	50.2	21.0	30	6	85	-1.85	0.002
90	S100A16	Q96FQ6	11.8	29.1	19	2	491	-1.85	0.002
91	PRPSAP2	O60256	40.9	39.6	97	8	806	-1.82	0.007
92	ACO2	Q99798	85.4	38.1	308	22	4323	-1.82	0.003
93	PYGL	P06737	97.1	41.9	319	23	3192	-1.81	0.001
94	VDAC1	P21796	30.8	69.6	501	17	9879	-1.80	0.002
95	STOM	P27105	31.7	11.1	6	2	29	-1.80	0.004
96	UROD	P06132	40.8	26.2	38	7	606	-1.79	0.003
97	PEPD	P12955	54.5	29.8	106	13	1588	-1.79	0.004
98	PYCR2	Q96C36	33.6	36.9	81	8	1582	-1.78	0.003
99	PDE6D	O43924	17.4	20.7	10	2	44	-1.78	0.007
100	GLUL	P15104	42.0	10.2	7	2	86	-1.76	0.002

101	USP13	Q92995	97.3	4.4	13	1	160	-1.76	0.003
102	PRDX2	P32119	21.9	66.7	316	14	3613	-1.76	0.003
103	MTFR1	Q15390	37.0	3.6	2	1	35	-1.76	0.003
104	DNA	P11388	174.3	29.1	290	27	3751	-1.76	0.003
105	S100A6	P06703	10.2	16.67	10	2	123	-1.73	0.003
106	SFN	P31947	27.8	48.8	265	8	2975	-1.73	0.008
107	PBK	Q96KB5	36.1	30.7	48	6	697	-1.71	0.007
108	PAPSS2	O95340	69.5	35.7	94	13	1437	-1.71	0.002
109	MVK	Q03426	42.4	18.2	25	3	183	-1.71	0.021
110	LBR	Q14739	70.7	13.3	77	4	858	-1.70	0.002
111	PFKFB2	O60825	58.4	11.7	10	4	248	-1.68	0.009
112	SRSF4	Q08170	56.6	10.9	23	4	328	-1.68	0.012
113	TERF2IP	Q9NYB0	44.2	15.5	32	3	541	-1.67	0.004
114	COPS7A	Q9UBW8	30.3	9.5	11	2	224	-1.67	0.004
115	HACL1	Q9UJ83	63.7	14.7	20	4	368	-1.65	0.003
116	HSP90AA1	P07900	84.6	60.8	2582	37	41847	-1.65	0.006
117	DOCK6	Q96HP0	229.4	3.3	12	4	89	-1.65	0.001
118	ALDH1B1	P30837	57.2	42.7	215	15	3440	-1.63	0.003
119	GTPBP3	Q969Y2	52.0	12.8	7	3	147	-1.63	0.008
120	HSD17B11	Q8NBQ5	32.9	29.0	29	6	410	-1.63	0.043
121	ANP32E	Q9BTT0	30.7	23.1	70	4	1544	-1.62	0.004
122	ATP2B1	P20020	138.7	21.1	106	17	1523	-1.61	0.002
123	HEATR3	Q7Z4Q2	74.5	10.7	35	6	276	-1.61	0.007
124	DDI2	Q5TDH0	44.5	41.6	41	9	450	-1.60	0.004
125	GOT1	P17174	46.2	50.6	373	12	5053	-1.60	0.004
126	ACSL1	P33121	77.9	27.1	61	12	469	-1.59	0.003
127	ABCB10	Q9NRK6	79.1	1.2	7	1	127	-1.58	0.009
128	LUC7L	Q9NQ29	43.7	18.9	120	4	692	-1.58	0.003
129	ISG15	P05161	17.9	26.1	40	3	694	-1.58	0.006
130	KRI1	Q8N9T8	82.5	8.1	33	4	350	-1.57	0.015

Table 5.7: Results of low SILAC-ratios for single SILAC KM 12 OXA experiment. p-value from multi SILAC dataset analysed by LIMMA is included.

5.3.5.4 Bioinformatics analysis of proteins significantly changed due to resistance

Only proteins classified in the altered group using the 5th percentile cluster analysis and with a significant p-value ($p<0.05$) obtained from LIMMA analysis were selected to develop protein network models by STRING (Protein-Protein Interaction Network) which will be discussed in the section 5.4.2.2. Finally, significantly altered proteins discussed were used to build up the Venn diagrams that show common significantly up-regulated and significantly down-regulated protein in resistant sublines to OXA. These commonly up-regulated and down-regulated proteins presented at the intersection of the Venn diagrams will be discussed in detail further in section 5.4.2.1.

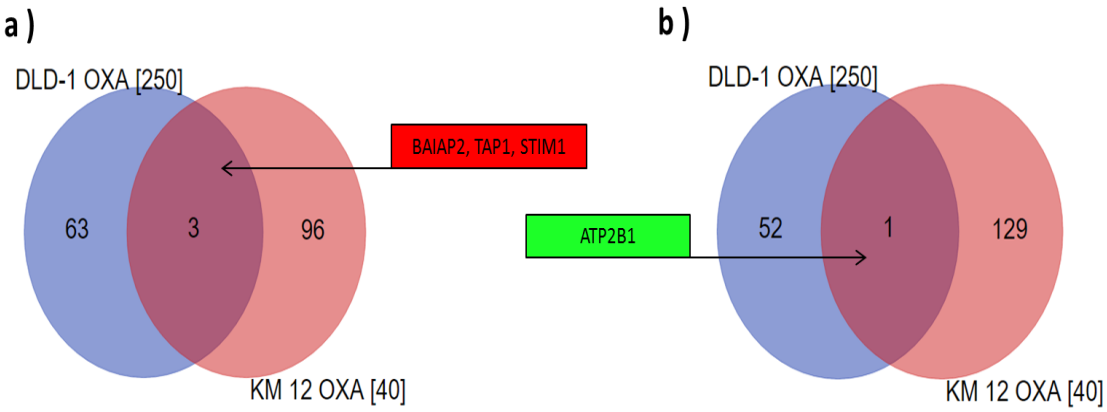

Figure 5.9: Venn diagrams of OXA resistant sublines. Common significantly (a) up-regulated; (b) down-regulated proteins using 5th percentile threshold in two different resistant CRC sublines to OXA.

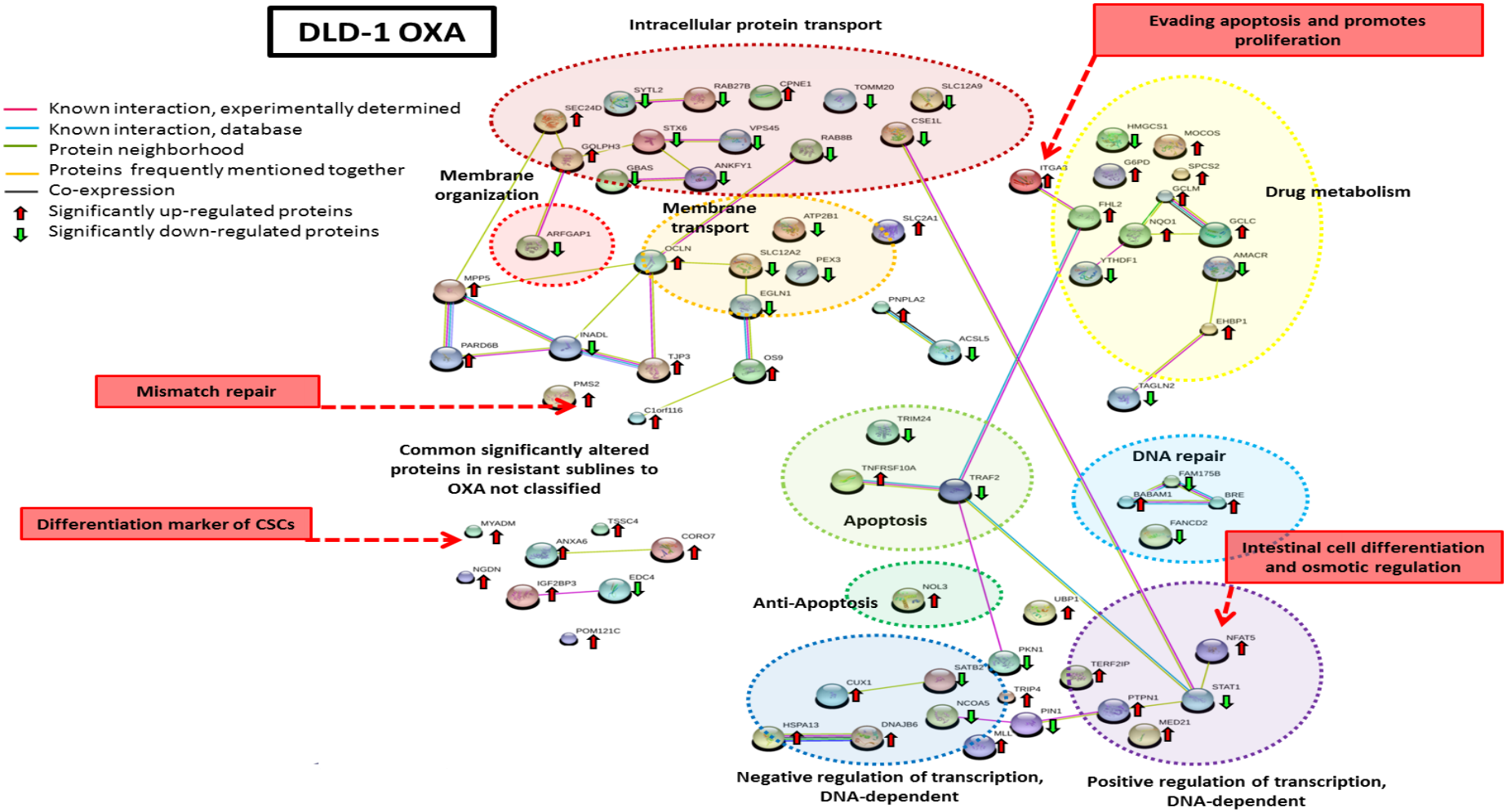

Figure 5.10: The figure shows a proteomic network model for DLD-1 OXA. Significantly altered proteins obtained by modification on EnrichNet and GO from the initial bubble map obtained in STRING. Proteins were classified into different biological processes groups represented with a circle. Dotted arrows indicate the most relevant altered proteins and its main function as mediator of drug resistance. Key: Green arrow: significantly down-regulated protein; Red arrow: significantly up-regulated protein.

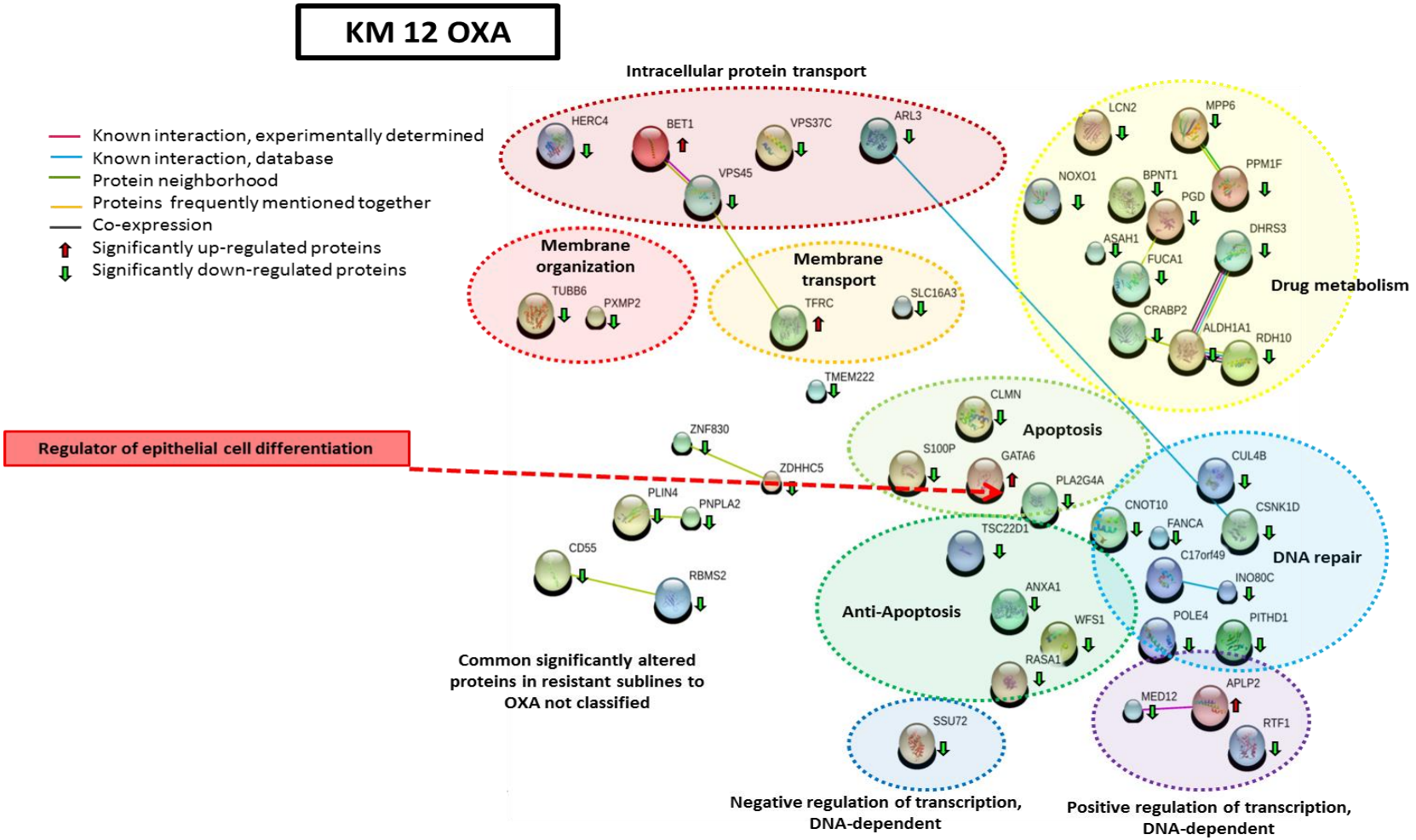

Figure 5.11: The figure shows a proteomic network model for KM 12 OXA significantly altered proteins obtained by modification on EnrichNet and GO from the initial bubble map obtained in STRING. Proteins were classified into different biological processes groups represented with a circle. Dotted arrows indicate the most relevant altered proteins and its main function as mediator of drug resistance. Key: Green arrow: significantly down-regulated protein; Red arrow: significantly up-regulated protein.

5.3.5.5 Verification of experimental fold changes using housekeeping-control proteins

N	Protein name	Gene name	Abundance Ratio: L / H						Normalized Log2 Ratio: L / H						Log2 Fold-change		Significant differences p-value	
			DLD-1 RPMI P=9	DLD-1 RPMI P=65	DLD-1 OXA [250] P=60	KM 12 RPMI P=9	KM 12 RPMI P=55	KM 12 OXA [40] P=45	DLD-1 RPMI P=9	DLD-1 RPMI P=65	DLD-1 OXA [250] P=60	KM 12 RPMI P=9	KM 12 RPMI P=55	KM 12 OXA [40] P=45	DLD-1 OXA	KM 12 OXA	DLD-1 OXA	KM 12 OXA
1	Brain-specific angiogenesis inhibitor 1-associated protein 2	BAIAP2	1.23	2.85	5.56	1.31	2.34	7.07	-0.12	0.36	1.26	-0.05	0.48	1.93	1.14	1.71	0.04	0.01
2	Antigen peptide transporter 1	TAP1	0.98	2.41	5.01	2.07	1.49	12.72	-0.45	0.12	1.11	0.60	-0.17	2.78	1.27	2.56	0.03	0.01
3	Stromal interaction molecule 1	STIM1	1.28	1.79	5.51	1.79	2.02	6.28	-0.07	-0.31	1.24	0.40	0.27	1.76	1.43	1.42	0.01	0.00
4	Plasma membrane calcium-transporting ATPase 1	ATP2B1	1.25	1.66	0.90	1.83	2.07	0.61	-0.11	-0.42	-1.37	0.43	0.31	-1.61	-1.10	-1.98	0.03	0.00

Table 5.8: Commonly significantly altered proteins in two resistant sublines to OXA and which were used to identify new mechanisms of resistance involved in resistance to OXA. Key: Red: up-regulated, Green: down-regulated proteins.

N	Protein name	Gene name	Abundance Ratio: L / H						Normalized Log2 Ratio: L / H						Log2 Fold-change		Significant differences p-value	
			DLD-1 RPMI P=9	DLD-1 RPMI P=65	DLD-1 OXA [250] P=60	KM 12 RPMI P=9	KM 12 RPMI P=55	KM 12 OXA [40] P=45	DLD-1 RPMI P=9	DLD-1 RPMI P=65	DLD-1 OXA [250] P=60	KM 12 RPMI P=9	KM 12 RPMI P=55	KM 12 OXA [40] P=45	DLD-1 OXA [250] P=60	KM 12 OXA [40] P=45	DLD-1 OXA [250] P=60	KM 12 OXA [40] P=45
1	Peptidyl-prolyl cis-trans isomerase A	PPIA	1.09	1.63	1.52	1.23	1.43	1.81	-0.30	-0.44	-0.62	-0.15	-0.23	-0.04	-0.25	0.15	0.41	0.45
2	ADP-ribosylation factor 3	ARF3	1.31	1.72	1.92	1.34	1.45	2.05	-0.03	-0.36	-0.27	-0.02	-0.21	0.14	-0.08	0.25	0.81	0.29
3	Hypoxia up-regulated protein 1	HYOU1	1.31	1.31	2.90	1.43	1.85	1.48	-0.03	-0.75	0.32	0.07	0.14	-0.33	0.71	-0.44	0.18	0.10
4	ATP synthase subunit d, mitochondrial	ATP5H	1.58	2.07	2.36	1.36	2.07	1.44	0.24	-0.09	0.02	-0.01	0.30	-0.37	-0.05	-0.52	0.88	0.11
5	Osteoclast-stimulating factor 1	OSTF1	1.44	1.96	2.33	1.28	1.29	1.30	0.11	-0.18	0.01	-0.10	-0.38	-0.52	0.04	0.28	0.89	0.30
6	Heme oxygenase 2	HMOX2	1.00	1.61	2.08	1.40	1.94	1.98	-0.42	-0.46	-0.16	0.04	0.22	0.09	0.28	-0.03	0.36	0.87
7	Cytoskeleton-associated protein 5	CKAP5	1.12	1.73	2.73	1.38	1.34	2.03	-0.26	-0.35	0.23	0.01	-0.32	0.13	0.54	0.28	0.12	0.32

Table 5.9: Control proteins that are unaltered by drug effects and which were used to evaluate the success of SILAC approach and statistical analysis applied to OXA resistant sublines. Log_2 fold change of all control proteins were found close to zero in both OXA resistant sublines when they were compared to its respective parent-control cell lines. A Log_2 fold change proximaly to 0, means that levels of the proteins quantified were similar in light and heavy samples.

5.4 Discussion

5.4.1 Evaluation of cross-resistance in the KM 12 OXA resistant subline

To shed some light on the cross-resistance problem in CRC patients, a study of cross-resistance mechanisms using KM 12 resistant subline to OXA was done. Initially, two cross-resistance MTT screenings were done using KM 12 resistant subline to OXA (Fig. 5.3).

Due to a significant cross-resistant effect observed for KM 12 OXA [30] resistant subline to doxorubicin, the OXA and doxorubicin combinational therapy should be avoided (Fig. 5.3d),

Researcher partnerships could create data platforms using CRC cell lines and cross-resistance studies *in vitro* and *in vivo*, that may help to understand the cross-resistance process. Establishment of cross-resistance guides of successful combinational therapies would avoid cross-resistance problems and it will promote working on personalized combinational therapies based on the presence of specific mechanisms of resistance in each patient.

5.4.2 Mechanisms of resistance to OXA identified by proteomics

5.4.2.1 Significantly altered proteins seen in more than one OXA resistant subline

The total number of commonly quantified proteins in parent cell lines, DLD-1 OXA and KM 12 OXA samples were 3716 and 3441 respectively, a similar number of the quantified proteins in all 5-FU resistant samples (see Chapter 3, section 3.3.7.1).

From histograms, volcano plots and cluster analysis obtained from parent cell lines and resistant sublines analysis, it was observed that the OXA resistant subline with the highest number of significantly altered proteins was KM 12, followed by DLD-1, as it was observed for resistant cell lines to 5-FU.

Four significantly altered proteins were found in both resistant sublines to OXA and they are discussed below. Due to the low number of commonly altered proteins in OXA resistant sublines, a deeper study of uniquely altered proteins

in each particular resistant subline to OXA was done and discussed in section 5.4.2.2.

5.4.2.1.1 Up-regulated proteins of DLD-1 OXA and KM 12 OXA (3)

STIM1 is one of the three common significantly up-regulated proteins of DLD-1 OXA and KM 12 OXA, that was also found in KM 12 5-FU resistant subline. STIM1 is a protein that regulates store-operated Ca2+ entry (SOCE) in the endoplasmic reticulum via its EF-hand domain. High levels of STIM1 protein have been observed in metastatic CRC patients. STIM1 overexpression has been associated with tumour size and tumour invasion features using tissue microarray (TMA) technology in tissue samples from CRC patients at different stages of disease (Wang, Sun et al. 2015). Interestingly, use of STIM1 overexpression has been suggested as an indicator of the transaction between colon and rectum adenocarcinomas too. The same study showed a direct correlation between STIM1 expression and a poor outcome in CRC patients (Wong and Chang 2015). New results found in this thesis with previous findings of STIM1 suggest that an in-depth study of STIM1 overexpression as a predictive biomarker involved in MDR to 5-FU and OXA should be carried out.

A second significantly up-regulated protein in DLD-1 OXA and KM 12 OXA was the brain-specific angiogenesis inhibitor 1-associated protein 2 (BAIAP2). BAIAP2 mediates the interaction of membrane-bound small G-proteins with their effector proteins. The main role BAIAP2 occurs during filipodia formation that is required for neurite growth (Oda, Shiratsuchi et al. 1999), although its role in cancer is completely unknown.

The third significantly up-regulated protein presented in DLD-1 OXA and KM 12 OXA resistant sublines was the antigen peptide transporter 1 (TAP1). TAP1 is a transporter used by cells to remove antigens and xenobiotics molecules that cause damaging to cells. TAP1 transports harmful particles from the cytoplasm to the endoplasmic reticulum to be associated with MHC class I molecules (Ritz, Momburg et al. 2001). TAP1 can be considered as a drug transporter from the ATP-binding cassette (ABC) transporters family (ter Beek, Guskov et al. 2014). Role of TAP1 in resistance is known and it causes drug resistance to

gemcitabine in pancreatic ductal adenocarcinoma (Xu, Li et al. 2013) and mitoxantrone resistance in lung cancer cell lines (Boonstra, Timmer-Bosscha et al. 2004). In CRC, the expression of TAP1 seems to have a crucial role during early steps of carcinogenesis (Andersen, Vogel et al. 2015). However, its contribution to CRC resistance is completely unknown.

5.4.2.1.2 Down-regulated proteins of DLD-1 OXA and KM 12 OXA (1)

The unique significantly down-regulated protein commonly found in DLD-1 OXA and KM 12 OXA was the plasma membrane calcium-transporting ATPase 1 protein (ATP2B1). ATP2B1 catalyses the hydrolysis of ATP coupled with calcium efflux from cells to the extracellular space. Nothing is known about ATP2B1 activity in CRC, however, it has been observed that platinum compounds disturb calcium homeostasis within cells and downregulation of PMCA1 appears to be one of the first consequences (Piccolini, Bottone et al. 2013).

5.4.2.2 Significantly altered proteins unique to one of the OXA resistant sublines

A summary table containing unique proteins altered in OXA resistant sublines derived from DLD-1 and KM 12 is shown below. Most relevant up-regulated proteins were classified based on the specific literature background of the protein in two groups:

1) Altered proteins by direct effect of OXA exposure related to apoptotic pathways and stress proteins.

2) Altered proteins by indirect effect of OXA exposure such as proteins involved in DNA repair, drug transport, drug metabolism, exocytosis, and vesicle formation.

	Indirect effect of OXA	Direct effect of OXA
DLD-1 OXA	NOL3, FLH2, BABAM1, NQO1, G6PD, PARD6B, TJP3, OCLN, SEC24D, SLC2A1	BRISC, BRE, TNFRSF10A, FAM175B, PMS2
KM 12 OXA	BET1, TFRC	GATA6

Table 5.10: Up-regulated proteins identified in OXA resistant sublines

Detailed discussion of uniquely altered proteins showed in Table 5.10 is shown below.

5.4.2.2.1 DLD-1 OXA

5.4.2.2.1.1 Apoptotic process (1)

Tumour necrosis factor receptor superfamily member 10A (TNFRSF10A) was found significantly up-regulated in DLD-1 OXA resistant subline. TNFRSF10A is the receptor of APO-2 ligand protein, the main function of TNFRSF10A is to mediate the extrinsic apoptotic signalling pathway via death domain receptors (Walczak, Degli-Esposti et al. 1997)**.** Contrary, high levels of nucleolar protein 3 (NOL3) were found in DLD-1 OXA too. NOL3 inhibits extrinsic apoptotic pathways (Gustafsson, Tsai et al. 2004)**.** Once tumour cells have been treated with an anticancer agent like OXA, cancer cells evolve and develop resistance to chemotherapy sometimes through disruption of the extrinsic apoptotic pathways. So, alterations of extrinsic apoptotic pathways may be a consequence of a direct drug effect that promotes apoptosis in treated cells, but also may product of an extrinsic apoptotic pathway evolution that acts as a mechanism of resistance like NOL3 up-regulation that inhibits cell death (Fulda and Debatin 2006).

Four and a half LIM domains protein 2 (FHL2) mediates transcriptional regulation through various signalling pathways. Overexpression of FLH2 decreases forkhead box protein O1 (FOXO1)-induced apoptosis by inhibition of

FOXO1 transcriptional process in prostate cancer cells (Yang, Hou et al. 2005). Inhibition of FOXO1 transcription occurs when FLH2 interacts with the amino terminus by DNA binding of FOXO1, blocking the interaction of FOXO1 with transcriptional coactivators (Puigserver, Rhee et al. 2003). Although FHL2 was significantly up-regulated in DLD-1 OXA, FOXO1 was not detected during protein quantification. So, it cannot be confirmed that FLH2 is promoting resistance to OXA by inhibition of FOXO1-induced apoptosis.

5.4.2.2.1.2 DNA repair process (2)

BRISC and BRE are two members of the BRCA1-A complex that were found significantly up-regulated in DLD-1 OXA resistant subline. BRCA1-A recognizes double-strand breaks (DSBs) that occur during DNA damage. DSBs are recognized by BRCA1-A through a specific recognition of Lys-63-linked ubiquitinated histones H2A and H2AX at DNA damage sites. Additionally, BABM1 is necessary during mitotic spindle assembly and microtubule attachment to kinetochores mediating its role by deubiquitinating of NUMA1, a protein that keeps nuclear matrix structure during non-mitotic phases (Wang, Hurov et al. 2009). BRE is essential for DNA DSBs repair by helping BRCA1-A complex to localize DNA damage sites, avoiding premature senescence and cell death (Shi, Tang et al. 2016). The role of the complex BRCA1-A is crucial during DNA repair after DNA damage that occurs during chemotherapy treatments. DLD-1 OXA resistant subline shows high levels of BABAM1 can control cell cycle checkpoint and maintenance of genomic stability that is affected during DLD-1 cell line exposition to OXA (Kim and Chen 2008). Additionally, BRE and BRISC up-regulation in DLD-1 OXA cell line enable DNA repair after OXA damage, promoting cell proliferation in adverse conditions as occurs during chemotherapy treatments. A significantly down-regulated protein of DLD-1 OXA subline that is related with DNA repair process is the BRISC complex subunit Abro1 (FAM175B). FAM175B interacts with NUMA1 independently of BRISC complex. FAM175B promotes deubiquitination of p53/TP53, preventing p53/TP53 degradation and increasing apoptosis response of p53/TP53 in response to DNA damage. A down-regulation of FAM175B in DLD-1 OXA lets p53/TP53 degradation that will decrease

p53/TP53 response to DNA damage, keeping tumoural cells alive in culture medium with OXA (Zhang, Cao et al. 2014).

PMS2 was found significantly up-regulated in DLD-1 OXA and DLD-1 5-FU resistant sublines. This mismatch repair endonuclease protein forms part of the post-replicative DNA mismatch repair system (MMR) and it has been previously described in Chapter 3 (section 3.4.3.3.1). Although no evidence of OXA resistance by PMS2 overexpression has been found yet. Losing and inhibition of PMS2 increases p53-deficient cells apoptosis by losing of tumoural cell ability to arrest at the G2/M upon cisplatin treatment in mice primary fibroblasts. So, PMS2 inhibition increases the cytotoxic effect caused by cisplatin, doxorubicin, etoposide, docetaxel, and 5-FU. In conclusion, PMS2 may be studied as a complementary strategy to improve chemotherapy treatments (Fedier, Ruefenacht et al. 2002).

5.4.2.2.1.3 Drug and small molecules metabolism (3)

A significantly up-regulation of enzymes involved in redox homeostasis was observed in DLD-1 OXA resistant subline. One of the most significantly up-regulated proteins was NAD(P)H dehydrogenase [quinone] 1 (NQO1). NQO1 is a very effective protector of cells by its antioxidant activity by decreasing cytology damage associated with oxidative stress induced by cytotoxic drugs. NQO1 is involved in detoxification pathways that occur during drug treatments. NQO1 polymorphisms and NQO1 overexpression have been proposed as a resistance marker to OXA and 5-FU treatments in breast and gastric cancer patients (Geng, Chen et al. 2014, Yang, Zhang et al. 2014). This antioxidant effect of NQO1 is inherent in its catalytic mechanism: the obligatory two-electron reduction of a broad array of quinones to their corresponding hydroquinones by using either NADPH or NADH as the hydride donor (Bianchet, Faig et al. 2004). Use of NQO1 has shown good results in cancer patients under a cisplatin treatment. Particularly, NQO1 shows a protective effect of renal failure nephrons in patients under a cisplatin chemotherapy (Gang, Kim et al. 2013). In breast, colorectal and cervical cancers, the high-level expression of NQO1 was found to be associated with the late clinical stage of the disease, poor differentiation and lymph node metastasis (Ma, Kong et al.

2014, Yang, Zhang et al. 2014) Interestingly under stress conditions like exposure to drugs, NQO1 acts as protector of p53 protein. In 2001, Asher *et al.,* described NQO1 overexpression as the main mechanism of p53 degradation inhibition in HCT 116 CRC cell lines (Asher, Lotem et al. 2001). NQO1 kidnaps p53 protein by a physical direct binding that protects p53 from 20S proteasomes degradation (Asher, Tsvetkov et al. 2005)**.** In DLD-1 resistant subline to OXA, both p53 and NQO1 proteins were found significantly up-regulated. So, a possible mechanism of resistance could be behind the up-regulation of both proteins. The overexpression of p53 has been previously described as biomarker of poor prognosis in lymphoma cancer patients, oesophageal squamous cell carcinoma (ESCC) in advanced stages of cancer (Fu, Shao et al. 2013, Yao, Qin et al. 2014). Up-regulation of p53 has been described as a mediator of cisplatin resistance in non-small cell lung cancer (Tung, Lin et al. 2015). Overexpression of p53 mediates resistance to cisplatin compounds by Nrf2 protein. Nrf2 is a key transcription factor for genes coding for antioxidants, detoxification enzymes, and MDR. Although Nrf2 was not detected in any of DLD-1 study samples, an up-regulated protein by Nrf2 was found overexpressed in DLD-1 OXA resistant cell line. This protein is the apoptosis regulator Bcl-2 protein that participates in apoptosis suppression and it has been related to drug resistance (Niture and Jaiswal 2012).

Together with NQO1, GCLM and GCLC are other two redox homeostasis significantly up-regulated enzymes also observed in DLD-1 OXA resistant subline. GCLM and GCLC are two enzymes that metabolise the synthesis of glutathione from L-cysteine and L-glutamate. Glutathione maintains redox homeostasis that occurs during drug treatments. Different studies have shown that high levels of glutathione are presented in the IGROVCDDP cisplatin-resistant ovarian cell line. This cisplatin-resistant cell line shows also an increased expression of the DNA repair gene *BRCA1* that has been previously associated with cisplatin resistance (Stordal and Davey 2009). In the same way, BRISC and BRE components of BRCA1 have been found significantly up-regulated in DLD-1 OXA resistant subline too (Stordal, Hamon et al. 2012). Due to the high similarity of cisplatin and OXA drugs, may be possible that up-

regulation of the biosynthesis of glutathione and up-regulation of BRCA1 DNA repair system are taking part in a common mechanism of resistance to OXA in DLD-1. In breast cancer patients with poor prognosis, new studies suggest a new potential role of glutathione as a biomarker of cancer resistance (Gamcsik, Kasibhatla et al. 2012). High levels of glutathione have been found in the resistant human leukaemia cell line K562 too. K562 showed also overexpression of Glucose-6-phosphate 1-dehydrogenase (G6PD). G6PD is an enzyme that provides a reducing power of (NADPH) and pentose phosphates for fatty acid and nucleic acid synthesis (Tsukamoto, Chen et al. 1998). G6PD was found also significantly up-regulated in DLD-1 OXA. So, up-regulation of glutathione biosynthesis and up-regulation of G6PD may be a consequence of a similar mechanism of resistance in K562 resistant cell lines to cisplatin and DLD-1 OXA.

5.4.2.2.1.4 Intracellular protein transport (4)

In DLD-1 OXA cell line, one of the most interesting significantly up-regulated proteins due to its multifactorial role was the transcription factor p65. p65 is the most abundant component of the NF-kappa-B transcription factor. The NF-kappa-B-p65 complex is involved in invasin-mediated activation of IL-8 expression (Duckett, Perkins et al. 1993)**.** Although NFκB-p65 function in CRC is not understood, it looks clear that high expression of NFκB-p65 in CRC patients is a common issue that plays an important role in colorectal tumourigenesis (Rezapour, Bahrami et al. 2016). Finally, it has been observed that the use of ursolic acid in CRC cell lines used *in vitro* and *in vivo*, enhance the cytotoxicity effect of OXA and this synergistic process occurs by inhibition of p65 phosphorylation (Shan, Xuan et al. 2016).

A second significantly up-regulated protein in DLD-1 OXA and involved in intracellular protein transport was the transport protein Sec24D. Sec24D is a transporter protein that promotes transport of vesicles from the endoplasmic reticulum to the Golgi complex and its role as a mechanism of chemoresistance in CRC has been described in the Chapter 4, section 4.4.1.4 (Tang, Kausalya et al. 1999).

Other significantly up-regulated protein in DLD-1 OXA was the Golgi phosphoprotein 3 (GOLPH3). GOLPH3 is a protein involved in the anterograde transport of vesicles from Golgi membrane to plasma membrane, mediating in vesicle secretion process. GOLPH3 is involved in the modulation of mTOR signalling. GOLPH3 has been described in resistance of rapamycin (Scott, Kabbarah et al. 2009) in non-small cell lung cancer and colon adenocarcinomas. Furthermore, overexpression of GOLPH3 in CRC patients has shown to be a poor prognosis marker (Zhou, Wang et al. 2016).

5.4.2.2.1.5 Cellular membrane transporters and cell membrane organization (5)

Among all proteins involved in cell membrane organisation, there are four significantly up-regulated proteins that may be taking part of the same resistance pathway in DLD-1 OXA. These four proteins were the partitioning defective 6 homolog β (PARD6B), the MAGUK p55 subfamily member 5 (MPP5), the tight junction protein ZO-3 (TJP3) and the occluding protein (OCLN). All these proteins mediate polarization processes and they increase tight junctions of epithelial cells (Hurd, Gao et al. 2003, Aho, Lupo et al. 2009). Additionally, MPP5 was found significantly up-regulated in DLD-1 IRI resistant subline (Tobioka, Isomura et al. 2002)**.** It would be interesting to study the importance of tight junctions in colorectal cells as an able mechanism of resistance against OXA. There is no evidence of mechanisms of resistance development through increasing of tight junctions. However, some researchers have previously proposed as consequence of up-regulation findings in groups of genes related to cell-cell contact through tight junctions which may favor tumour survival. Finally, transmembrane proteins have been proposed to be more likely to remodel the tumour microenvironment increasing drug resistance (Morin 2003).

A singular and important up-regulated protein quantified in DLD-1 OXA resistant subline was the solute carrier family 2, facilitated glucose transporter member 1 (SLC2A1) (GLUT1) protein. GLUT protein family consists of 12 members. Overexpression of glucose transporters has been broadly studied during the fight against cancer resistance. High levels of the GLUT protein family have

been found in patients with poor prognosis in all type of cancers (Szablewski 2013). The role of GLUT1 is to transport glucose into the cells to be used as an energy source during cell proliferation and other cellular processes (Young, Lewis et al. 2011). An increase in glucose transport is also required for high cell proliferation rates of tumoural cells that express the EGFR (Weihua, Tsan et al. 2008). Specifically, in CRC GLUT1 overexpression has been related to 5-FU resistance *in vitro* and *in vivo*. Use of GLUT1 inhibitors such as WZB117 reverse resistant phenotype to 5-FU in CRC (Liu, Fang et al. 2014). Furthermore, in CRC patient levels of GLUT proteins are used as indicators to select preoperative chemo-radiotherapy (CRT) treatments (Saigusa, Toiyama et al. 2012). Overexpression of GLUT1 transporter is being studied as anticancer therapy to prevent increasing of tumour cells proliferation that leads to drug resistance (Calvo, Figueroa et al. 2010). Down-regulation of GLUT1 has been demonstrated to overcome the sensitive phenotype of cisplatin and daunorubicin in resistant cell lines of head and CRC respectively (Cao, Fang et al. 2007, Brophy, Sheehan et al. 2009, Wang, Li et al. 2013) However, the mechanism behind these results is unknown and it is not proposed to be by GLUT1 direct transport of neither cisplatin nor OXA.

5.4.2.2.2 KM 12 OXA

KM 12 OXA was one of the resistant cell lines with lowest resistance fold-change. Most of the significantly altered proteins using 5^{th} percentile threshold were found down-regulated. This issue complicates the identification of target proteins to be used as resistant biomarkers and to avoid drug resistance.

5.4.2.2.2.1 Apoptotic process (1)

Only the transcription factor GATA-6 (GATA6) protein was found significantly up-regulated and involved in apoptotic processes of KM 12 OXA. Additionally, a significant up-regulation of GATA6 was also found in HT 29 5-FU resistant subline. GATA6 is a specific protein that regulates intestinal and gastric epithelial cell differentiation. Overexpression of GATA6 has been identified in undifferentiated and proliferating HT 29 cell line (Gao, Sedgwick et al. 1998). Another study with HT 29 and HT 55 showed that levels of GATA6 increase

after radiotherapy exposure and that the effect of irradiation may be increased after inhibition of GATA6, suggesting a key role of GATA6 in cell survival to radiotherapy (Cai, Shen et al. 2014).

5.4.2.2.2.2 DNA repair process (2) and Drug and small molecules metabolism (3)

No up-regulated proteins were found involved neither in DNA repair process nor in drug and small molecules metabolism in KM 12 OXA resistant subline.

5.4.2.2.2.3 Intracellular protein transport (4)

The unique significantly up-regulated protein involved in intracellular protein transport of KM 12 OXA was BET1 homolog (BET1). BET1 was also found significantly up-regulated in HT 29 5-FU. BET1 is a protein that mediates vesicle transport along the cytoplasm from the endoplasmic reticulum (ER) to the Golgi apparatus, playing its key role during vesicle fusion to the Golgi apparatus membrane. So, the activity of vesicles transport from ER to the Golgi apparatus may be involved in resistance development to OXA in KM 12 cell line (Petrosyan 2015)**.** Inhibition of transporting activity of vesicles from ER to Golgi apparatus has been previously used as a strategy to reverse fludarabine resistance phenotype in resistant chronic lymphocytic leukemia (CLL) cells *in vitro*. The mechanism behind this overcome resistance resides in blocking protein trafficking by brefeldin A treatment leads to activation of caspases and increases sequestration of the survival factors APRIL and VEGF (Carew, Nawrocki et al. 2006).

5.4.2.2.2.4 Cellular membrane transporters and cell membrane organization (5)

Only transferrin receptor protein 1 (TFRC) was found significantly up-regulated in cell membrane transport and cellular membrane organization group. TFRC was found significantly up-regulated in HT 29 5-FU too. TFRC is involved in iron uptake via endosomes internalization after ligand binding to the transferrin receptor that activates endocytosis of endosomes (Rothenberger, Iacopetta et al. 1987)**.** In CRC cells levels of TFRC are related with proliferation rate of tumour cells (Okazaki, Matsunaga et al. 2010) and it has been considered

TFRC as enhancer of platinum drugs delivery (Daniels, Delgado et al. 2006), especially for OXA (Suzuki, Takizawa et al. 2008). Additionally, use of liposomes for platinum drugs delivery is having success in animal models, where drugs are maintained inside interstitial space during a long time (Maruyama 2011). Finally, it has been observed in a human cervical cancer cell line resistant to OXA that resistance it was mediated by TFRC expression and maintained in xenograft animal models (Chen, Kuo et al. 2016). However, the mechanism behind TFRC overexpression to mediate OXA resistance is completely unknown. Thus, keeping in mind these previous publications about TFRC overexpression and the new findings presented, TFRC may be involved in endosome encapsulation of OXA decreasing free OXA inside cells and reducing cytotoxic effects of the drug.

5.4.3 Conclusion

The development of OXA resistant sublines was carried out by continuous drug exposure. From the three initial parent cell lines, only HT 29 cell line was not able to develop a resistant phenotype. Differences in resistance fold change between DLD-1 OXA (10.7) and KM 12 OXA (2.06) may be because initial parent cell lines have different genomic background and cellular sensitivity to OXA effects. A similar number of proteins (3500-4000) in both set of resistant sublines (DLD-1, KM 12) were quantified (Fig. 5.5).

The main difference between DLD-1 OXA and KM 12 OXA resistant sublines was the large amount of down-regulated proteins seen in KM 12 OXA. According to resistance fold change results, DLD-1 OXA showed a higher resistance fold change. However, DLD-1 OXA showed fewer altered proteins than KM 12 OXA too. These proteomic results suggest that the type of altered proteins and their potential roles as a mediator of drug resistance are more relevant than the number of altered proteins that may not be directly related with cell survival under drug effects. Among the most significant up-regulated proteins in DLD-1 OXA, PMS2 involved in DNA mismatch repair system may be studied as future targeted protein to avoid acquired resistance in CRC (Fedier, Ruefenacht et al. 2002). Among up-regulated proteins in KM 12 OXA,

GATA6 involved in intestinal epithelial cell differentiation process is known by its role during radiotherapy resistance (Cai, Shen et al. 2014) and its inhibition may be studied as target therapy during acquired resistance to OXA too.

In summary, heterogeneity between both OXA resistant sublines was found and some potential mechanisms of resistance were identified by proteomics. All these different changes in protein expression of DLD-1 OXA and KM 12 OXA resistant sublines act together to increase survival of cells by being more resistant to OXA effects. This may explain difficulties in developing new drugs to avoid mechanisms of resistance against tumour cells able to develop multiple mechanisms of resistance that affect a large range of biological processe.

- Chapter six -

Identification of new MDR mechanisms in CRC

6 Identification of new MDR mechanisms in CRC

6.1 Introduction

In addition to utilising the data to identify drug-specific mechanisms of resistance, results can also be used to identify potential mechanisms of MDR. However the analytical metrics used for investigating a single drug are not necessarily appropriate for studying 2 or more compounds as explained below. DLD-1 resistant sublines were used to find commonly altered proteins. These commonly altered proteins might not be so significantly relevant as commonly altered proteins found in different resistant sublines to the same drug. This is due to few limitations regarding the quantitative proteomics and SILAC approach and it is explained below.

During protein fold change calculation, SILAC ratios from both parent sensitive cell lines were used as a reference control to be compared to the resistant subline. SILAC ratios from parent cell lines are product of three independent readings in the mass spectrometer. It is important to keep in mind that the resistant subline fold change is calculated with these same control SILAC ratios. Therefore, a standard deviation of a specific protein in SILAC parent cell lines will affect to the protein fold change estimation in all resistant cell lines compared to these controls. Consequently, fold changes of proteins found commonly altered in resistant sublines derived from the same original cell line (e.g., DLD-1 5-FU and DLD-1 OXA) have been calculated using the same two parent-control cell lines (e.g., DLD-1 P=9, DLD-1 P=65). Using the same two controls to estimate fold change of a protein in resistant sublines, the probability to find a similar fold change for the same protein is increased. However, fold changes of proteins found commonly altered in different resistant sublines derived from different parent cell lines (e.g., DLD-1 5-FU and KM 12 5-FU) have been calculated using different parent-control cell lines (e.g., DLD-1 P=9, DLD-1 P=65 and KM 12 P=9, KM 12 P=55, respectively). So, their fold changes were calculated based on their respective controls, which are independent of each specific cell line.

All previous results showed in this thesis have been discussed under a high level of statistical significance. To be discussed all previously proteins have satisfied two requirements: 1) they are presented in the 10% group of the most altered proteins of each resistant subline and 2) differences in protein expression between resistant subline and its parent cell lines are significant in fold change terms. All these results previously described support the hypothesis of the existence of specific proteins that play individual roles to mediate resistance to drugs among different CRC cell lines. Although proteins discussed in Chapters 3-5 showed a high significance change at the expression level, most of these altered proteins have not shown any connection between different resistant sublines. These proteins have been described individually and they have not been grouped into a common cellular pathway that may explain the CRC resistance in global terms. To identify altered proteins associated with a common cellular pathway presented in different resistant sublines, the whole list of proteins was studied, independently of 5^{th} criteria. So, the fold-change difference between each resistant subline with its control parent cell lines was the unique factor analysed. This new and extended study that included also proteins with high significant fold change and not only proteins included in the 10% of the most altered proteins, enable to extend the chance to identify new common pathways altered in more than one resistant subline. Hence, the aims of this chapter are to establish analytical metrics for identifying MDR candidates and to use this info to identify and investigate potential new mechanisms of cross-resistance.

6.2 Results

6.2.1 Overall strategy

An overall strategy flow chart followed during identification of proteins involved in MDR is shown below.

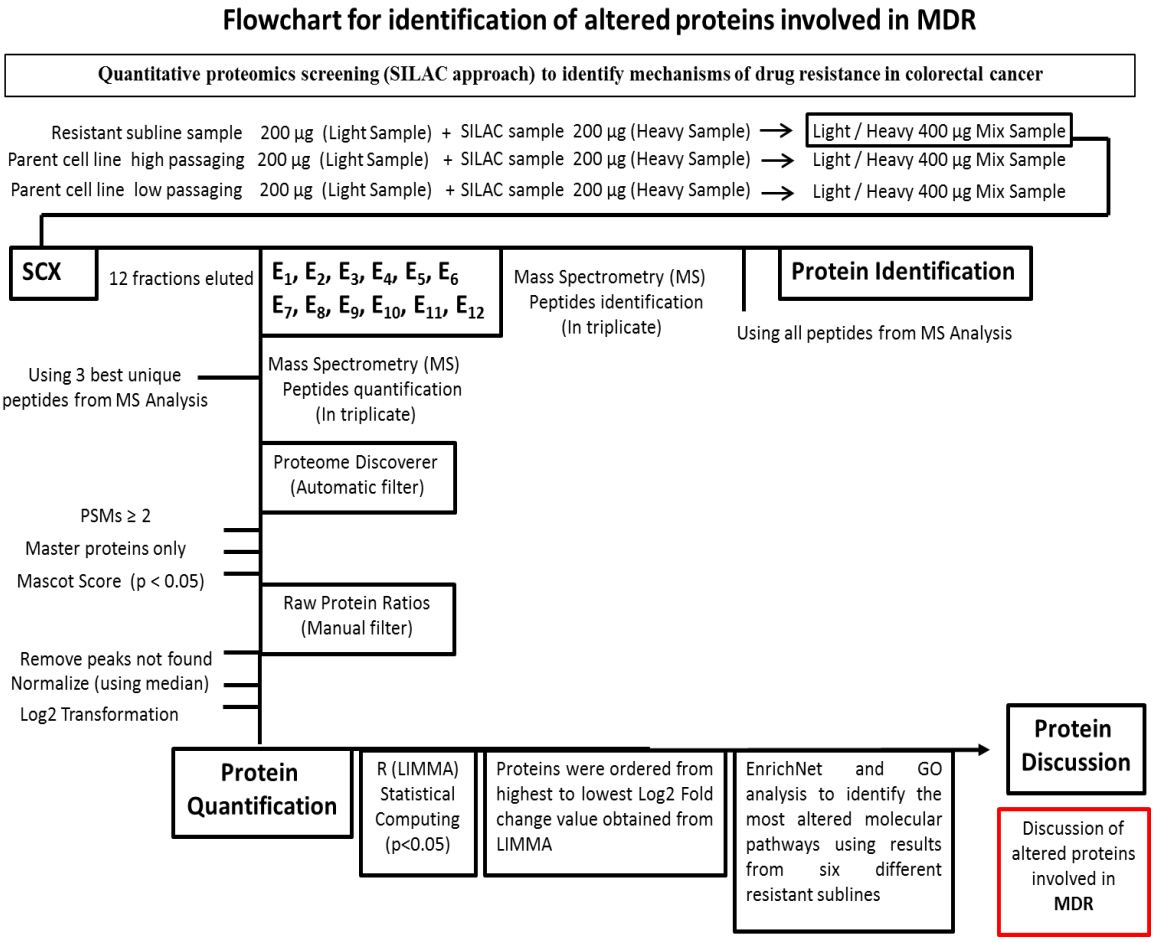

Figure 6.1: Flowchart describing quantitative screening analysis used to identify altered proteins in MDR by SILAC approach. Initially, 200 µg of light sample and 200 µg of heavy sample were mixed to get 400 µg (Light/Heavy) sample. L/H sample was separated in 12 L/H subsamples by SCX using 12 different EB. Each eluted subsample was analysed by MS in triplicate and all identified peptides were used for protein identification. From all peptides detected during MS analysis, only the three best peptides were used for peptides quantification in triplicate. After protein quantification three filters were applied: 1) Only proteins quantified from unique peptides with 2 or more PSMs were used 2) Only master proteins were considered 3) Mascot score applied for $p<0.05$. Proteins only quantified in heavy or light sample were removed. Finally, after LIMMA analysis, proteins with highest Log_2 fold change were used to identify the most commonly altered molecular pathways between the six different resistant sublines established using EnrichNet and GO analysis.

A new study with EnrichNet and GO was carried out using the Log_2 fold change results obtained from LIMMA analysis.

6.2.2 Overall view of altered proteins in MDR

The most abundant and altered biological processes identified in resistant sublines were related to endosome compartments and multivesicular bodies (MVBs) formation. Alteration of the vacuolar protein sorting-associated protein 4 (VSP4) was the most relevant. VPS4 is a mediator of cellular stress response found up-regulated in resistant sublines but not in parent cell lines. Additionally, the proto-oncogene SRC was found up-regulated in four resistant sublines too. So, a model containing these most relevant up-regulated proteins found in at least two resistant sublines was developed and a summary of these up-regulated protein data is included in table 6.1. Additionally, CD63 was found up-regulated in HT 29 5-FU and it was included in the model due to its known role as marker of MVB-derived vesicles and during endosome biogenesis (Ostrowski, Carmo et al. 2010). Furthermore, CD63 was included in the model as it has been described previously its interaction with Timp1 protein developing anoikis resistance in melanoma and Timp1 protein was found significantly up-regulated in KM 12 5-FU and KM 12 OXA resistant sublines (Toricelli, Melo et al. 2013).

Proteins VPS4, CD63, TIMP1 and SRC, shown in Table 6.1 were found up-regulated among resistant sublines and are discussed in detail in section 6.3.1. Following validation of VPS4 expression in sensitive and resistant cell lines, evidence for involvement was investigated by studying expression of VPS4 and CD63 following treatment of parent cells with 5-FU. A WB study of VPS4 using the three parent cell lines DLD-1, KM 12 and HT 29 after three passages under 5-FU exposure were done, to check if drug exposure increases VPS4 levels as it was predicted in the model.

N	Protein name	Gene name	Abundance Ratio: L / H												Normalized Log2 Ratio: L/H											
			DLD-1 RPMI P=9	DLD-1 RPMI P=65	DLD-1 5-FU [250] P=70	DLD-1 OXA [250] P=60	DLD-1 IRI [200] P=55	KM 12 RPMI P=9	KM 12 RPMI P=55	KM 12 5-FU [60] P=50	KM 12 OXA [40] P=45	HT 29 RPMI P=9	HT 29 RPMI P=57	HT 29 5-FU [60] P=48	DLD-1 RPMI P=9	DLD-1 RPMI P=65	DLD-1 5-FU [250] P=70	DLD-1 OXA [250] P=60	DLD-1 IRI [200] P=55	KM 12 RPMI P=9	KM 12 RPMI P=55	KM 12 5-FU [60] P=50	KM 12 OXA [40] P=45	HT 29 RPMI P=9	HT 29 RPMI P=57	HT 29 5-FU [60] P=48
1	Proto-oncogene tyrosine-protein kinase Src	SRC	0.61	2.75	3.99	9.25	9.37	1.37	1.31	13.14	9.49	1.20	1.01	2.60	-1.13	0.31	0.70	1.99	1.77	0.00	-0.35	3.03	2.35	0.40	-0.14	0.80
2	Vacuolar protein sorting-associated protein 4	VPS4	1.22	2.24	3.34	2.93	3.55	1.44	1.89	3.12	2.59	0.65	0.84	0.93	-0.14	0.02	0.45	0.33	0.36	0.08	0.17	0.95	0.48	-0.49	-0.42	-0.69
3	Major vault protein	MVP	0.51	0.56	2.60	2.77	1.73	1.10	0.89	19.99	17.65	1.38	1.04	2.37	-1.40	-1.99	0.08	0.25	-0.67	-0.31	-0.91	3.63	3.25	0.60	-0.10	0.66
4	Metalloproteinase inhibitor 1	TIMP1	#	1.53	3.01	2.55	6.60	1.67	3.19	5.33	8.20	1.08	3.25	4.78	#	-0.54	0.30	0.14	1.26	0.29	0.93	1.72	2.14	0.24	1.54	1.68
5	Syntenin-1	SDCBP	1.87	1.75	4.69	1.01	4.72	1.78	2.42	4.32	3.45	0.35	2.14	1.37	0.48	-0.34	0.94	-1.20	0.78	0.39	0.53	1.42	0.89	-1.40	0.94	-0.13
6	CD63 antigen	CD63	#	2.00	8.89	#	90.63	#	#	9.67	16.19	1.10	0.82	3.00	#	-0.14	1.86	#	5.04	#	#	2.58	3.12	0.26	-0.45	1.00
7	Telomerase protein component 1	TEP1	#	#	9.42	#	#	#	#	2.51	#	#	#	5.95	#	#	1.94	#	#	#	#	0.64	#	#	#	1.99
8	Laminin subunit alpha-5	LAMA5	#	#	11.14	#	#	1.83	#	6.59	7.24	2.15	1.02	2.20	#	#	2.19	#	#	0.43	#	2.03	1.96	1.24	-0.14	0.55

N	Protein name	Gene name	Log2 Fold change						Significant differences p.value					
			DLD-1 5-FU	DLD-1 OXA	DLD-1 IRI	KM 12 5-FU	KM 12 OXA	HT 29 5-FU	DLD-1 5-FU	DLD-1 OXA	DLD-1 IRI	KM 12 5-FU	KM 12 OXA	HT 29 5-FU
1	Proto-oncogene tyrosine-protein kinase Src	SRC	1.11	2.40	2.17	3.20	2.53	0.67	0.21	0.04	0.05	0.00	0.00	0.18
2	Vacuolar protein sorting-associated protein 4	VPS4	0.51	0.40	0.43	0.82	0.36	0.06	0.14	0.22	0.20	0.02	0.14	0.89
3	Major vault protein	MVP	1.78	1.94	1.03	4.25	3.86	0.42	0.01	0.01	0.06	0.00	0.00	0.42
4	Metalloproteinase inhibitor 1	TIMP1	#	#	#	1.11	1.53	0.88	#	#	#	0.05	0.02	0.24
5	Syntenin-1	SDCBP	0.86	-1.27	0.71	0.96	0.43	0.11	0.14	0.06	0.21	0.01	0.10	0.93
6	CD63 antigen	CD63	#	#	#	#	#	1.09	#	#	#	#	#	0.09
7	Telomerase protein component 1	TEP1	#	#	#	#	#	#	#	#	#	#	#	#
8	Laminin subunit alpha-5	LAMA5	#	#	#	#	#	0.00	#	#	#	#	#	0.99

Table 6.1: Most commonly altered proteins in six resistant sublines to 5-FU, OXA, IRI. Key: Red – Up-regulated proteins. # unquantified protein

6.2.2.1 WB validation of the proteomics findings for VPS4 expression in sensitive and resistant sublines

The MDR model proposed is based on the idea that VPS4 regulates lysosome homeostasis that is altered under drug treatments, where cells are growing in metabolic stress conditions. Additionally, it is known that VPS4 is involved in late steps of the endosomal MVBs pathways, which have been discussed to play resistance to multiple drugs as it will be discussed below section 6.3.1. To confirm if increasing of VPS4 levels occurs during drug treatments, initially, new parent cell lines DLD-1, KM 12 and HT 29 were cultured under 5-FU conditions during three passages using IC_{50} of the drug for each cell line. Secondly, WB analysis was done to compare if levels of VPS4 had increased in the three cell lines after drug exposure and these results are shown below (Fig. 6.6). Furthermore, and immunocytofluorescence microscopy study was done for CD63 in DLD-1 5-FU to confirm results obtained from mass spectrometry. In order to validate proteomics results, expression of VPS4 (Fig. 6.2) was further analysed using WB. Validation of quantitative proteomics results was necessary to support the initial outcomes from SILAC-approach and LIMMA analysis.

6.2.2.1.1 VPS4 in resistant sublines to 5-FU

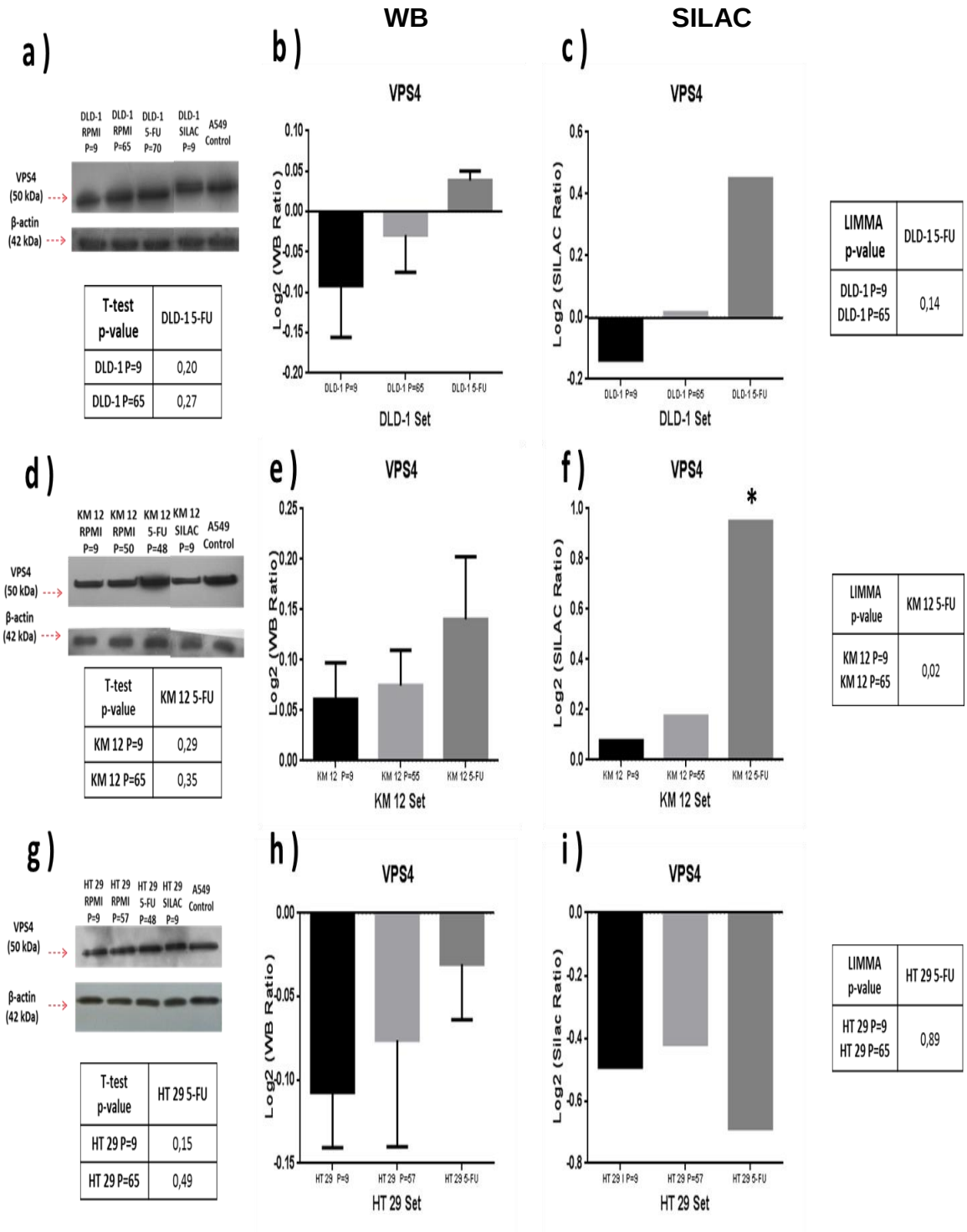

Figure 6.2: WB of VPS4 in 5-FU sublines. On the left side, (a) (d) (g) WB results for VPS4 and ß-actin in parent cell lines and 5-FU resistant sublines. In the middle and right side, bar graph comparisons between WB results and SILAC-approach results for 5-FU resistant sublines are shown. (*p≤0.05)

VPS4 Western blot analysis of DLD-1 parent and 5-FU resistant subline showed a single band of 50 kDa molecular weight, which was slightly most intense in DLD-1 5-FU resistant subline sample. Band intensities were adjusted relative to ß-actin, which was analysed as a house-keeping protein. After correction for cross-experiment variations, the ratios for VPS4, closely matched the SILAC data (Fig. 6.2b,c). Similar results were obtained for VPS4 Western blot analysis of KM 12 parent and resistant sublines which showed the most intense single band of 50 kDa molecular weight in KM 12 5-FU and matched between WB results with previous SILAC data (Fig. 6.2e,f). However, no differences were found in intensity bands for VPS4 in HT 29 resistant and sensitive sublines to 5-FU (Fig. 6.2h,i). MDA-MB 231 cell line was used as positive control for VPS4 during immunoblotting. Bar graphs were obtained from SILAC approach with Log_2 (SILAC-ratios) data for each sample and tables show p-values obtained from SILAC approach by LIMMA statistics analysis. Data are presented as mean; an asterisk represents significant differences ($p \leq 0.05$).

6.2.2.1.2 VPS4 in OXA resistant sublines

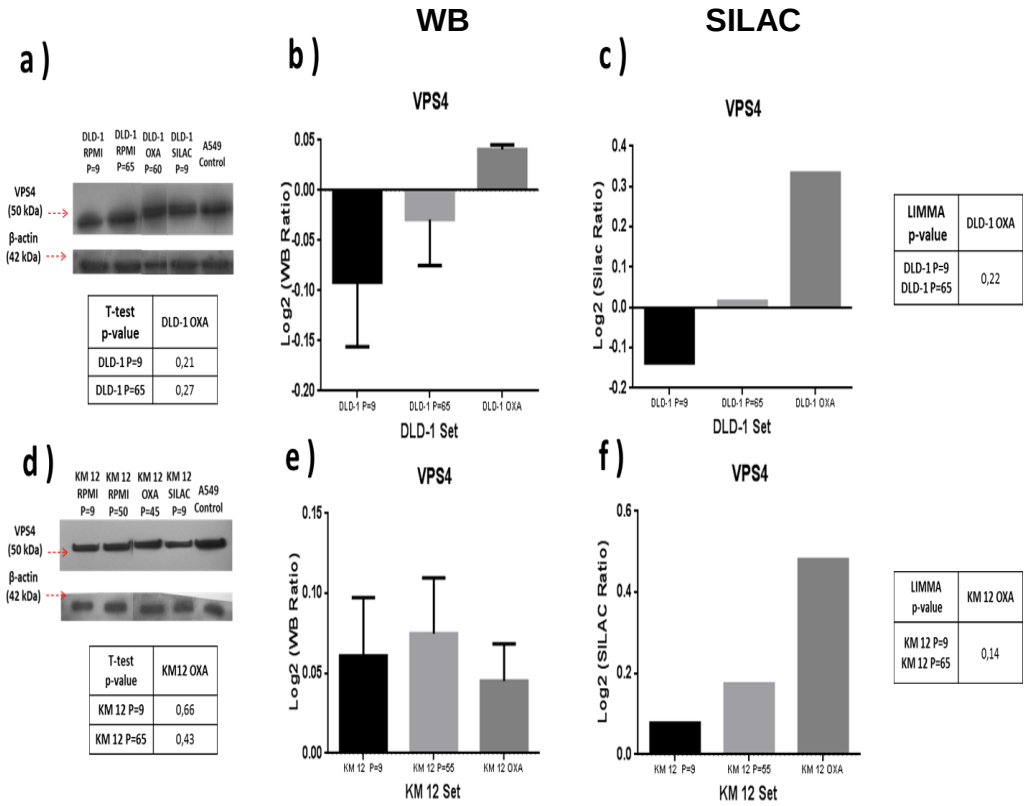

Figure 6.3: WB of VPS4 in OXA sublines. On the left side, (a) (d) WB results for VPS4 and ß-actin in parent cell lines and OXA resistant sublines. In the middle and right side, bar graph comparisons between WB results and SILAC-approach results for OXA resistant sublines are shown.

VPS4 Western blot analysis of DLD-1 parent and OXA resistant subline showed a single band of 50 kDa molecular weight, which was slightly most intense in DLD-1 5-FU resistant subline sample. Band intensities were adjusted relative to ß-actin, which was analysed as a house-keeping protein (Fig. 6.3a). After correction for cross-experiment variations, the ratios for VPS4, closely matched the SILAC data (Fig. 6.3b,c). For VPS4 Western blot analysis of KM 12 parent and resistant sublines, a single band of 50 kDa molecular weight and similar intensity was found in all samples in KM 12 OXA, which showed a poor matched with previous results from SILAC approach (Fig. 6.3e,f). MDA-MB 231 cell line was used as positive control for VPS4 during immunoblotting. Bar graphs were obtained from SILAC approach with Log_2 (SILAC-ratios) data for each sample and tables showing p-values obtained from SILAC approach by

LIMMA statistics analysis. Data are presented as mean; an asterisk represents significant differences (P≤0.05).

6.2.2.1.3 VPS4 in resistant sublines to IRI

VPS4 Western blot analysis of DLD-1 parent and IRI resistant subline showed a single band of 50 kDa molecular weight, which showed a similar intensity in all samples. Band intensities were adjusted relative to ß-actin, which was analysed as a house-keeping protein (Fig. 6.4a). Once cross-experiment variations were corrected, the ratios for VPS4, closely matched the SILAC data (Fig. 6.4b,c). MDA-MB 231 cell line was used as positive control for VPS4 during immunoblotting. Bar graphs were obtained from SILAC approach with Log_2 (SILAC-ratios) data for each sample and tables showing p-values obtained from SILAC approach by LIMMA statistics analysis. Data are presented as mean; an asterisk represents significant differences (P≤0.05).

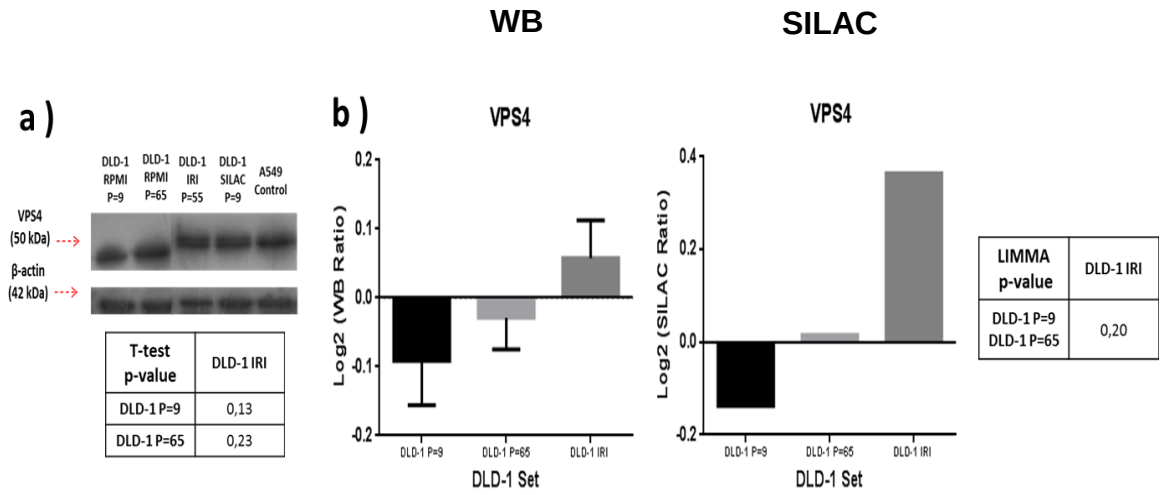

Figure 6.4: WB of VPS4 in DLD-1 IRI subline. On the left side, (a) WB results for VPS4 and ß-actin in DLD-1 parent cell lines and DLD-1 IRI resistant subline. (b) (c) Comparisons between WB results and SILAC-approach results for DLD-1 IRI resistant subline. Matched between WB and SILAC results is observed in all samples.

6.2.2.2 ICF validation of VPS4 results identified by proteomics in DLD-1 5-FU resistant subline

After validation of VPS4 levels by WB in all samples, an additional ICF assay was done for VPS4 in DLD-1 5-FU and DLD-1 parent cell line.

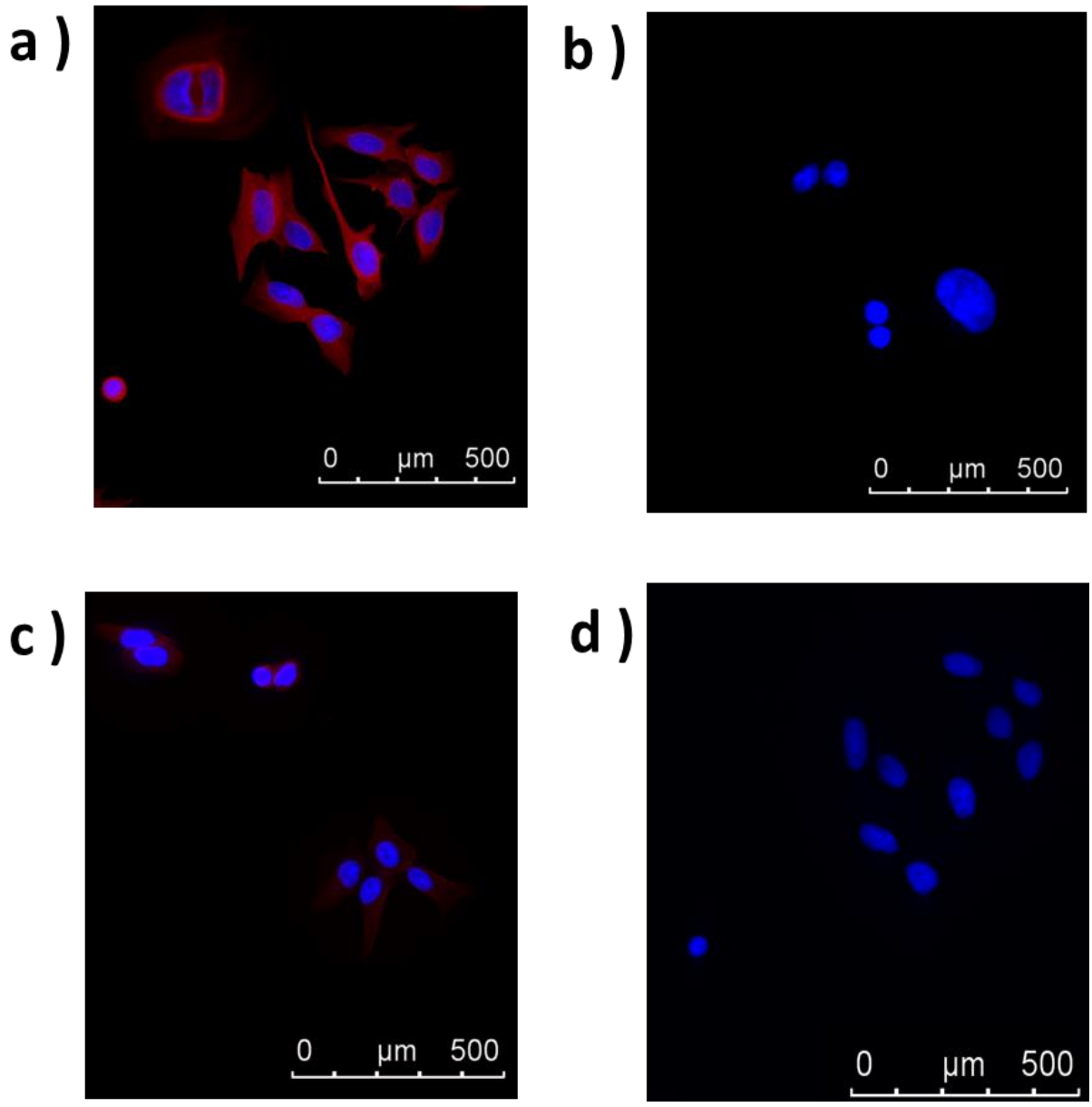

Figure 6.5: Subcellular localization of VPS4. Labelling of VPS4 in (a) DLD-1 5-FU resistant subline and (c) DLD-1 high generation control. Negative controls for (b) DLD-1 5-FU and (d) DLD-1 high generation control. Cells were defrosted and grown during 24 h in 6-well plates, fixed and analysed by fluorescence microscopy. For each well, $1x10^4$ cells/ml were seeded and observed under microscope at 40x magnification.

From results is clearly observed that labelling of VPS4 protein in DLD-1 5-FU resistant sublines was higher than in DLD-1 parent cell lines, confirming results previously obtained by both SILAC-approach and WB results (Fig. 6.2). Additionally, differences in size were observed, DLD-1 5-FU size was higher

than DLD-1 parent cell line and it was previously shown in Figure 3.14 in Chapter 3, section 3.3.1. Some of these differences in cell size, were observed between cells can be due to different cell cycle step between different cells and different depths of field during picture acquisition too.

6.2.2.2.1 VPS4 levels are unaltered during short-term exposure to 5-FU

According to previous results of VPS4 in resistant sublines, a model was developed. Model was based on the idea that VPS4 level is increased during drug exposure. Hence, after five passages of parent cell lines under 5-FU exposure during three generations, the expression of VPS4 protein was analysed. A single band of 50 kDa molecular weight was found in all samples and after intensities were adjusted relative to ß-actin, VPS4 expression was shown in bar graphs below.

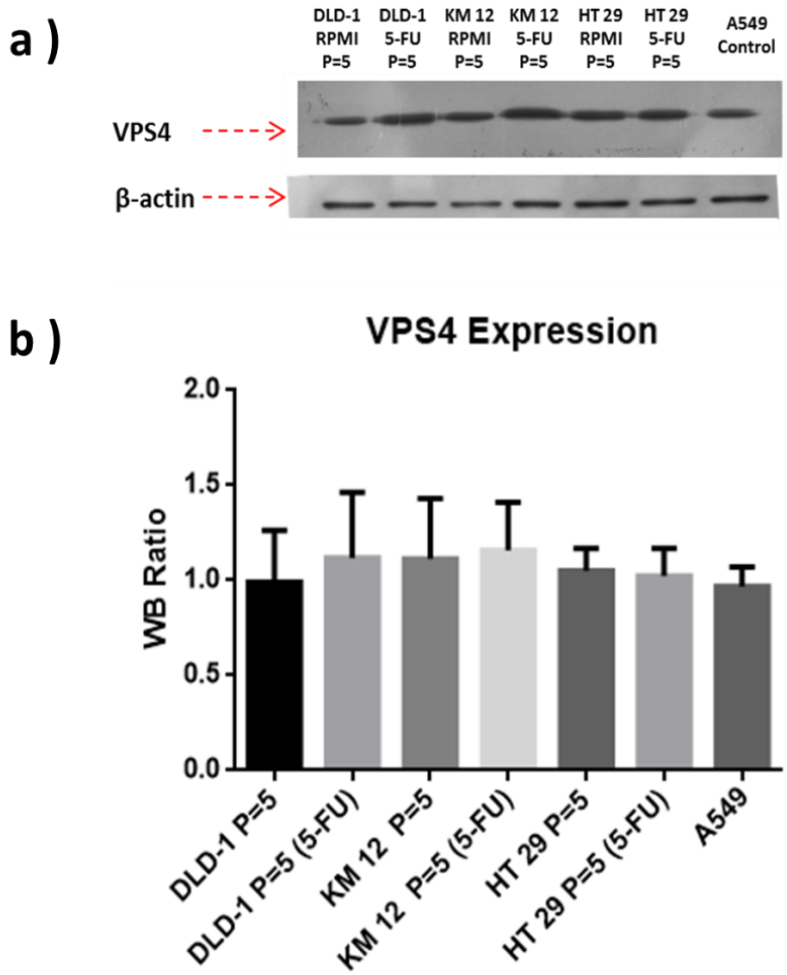

Figure 6.6: VPS4 levels after 5-FU short-term exposure. (a) WB results for VPS4 and ß-actin in DLD-1, KM 12 and HT 29 parent cell lines and parent cell lines grown during five passages under 5-FU exposure conditions. (b) Bar graphs showing comparisons between WB results for parent cell lines grown in normal RPMI media and parent cell lines grown in media with 5-FU during three passages. No significant differences were found among any of the all 7 samples analysed.

No significant changes were found in VPS4 expression after five passages of 5-FU exposure. Hence, overexpression of VPS4 observed in resistant sublines during SILAC experiments can be the result of other molecular processes alteration or the result of drug effects during long-term exposure.

6.2.2.3 CD63 expression patterns are similar to VPS4

CD63 protein has been described as mediator of resistance in melanoma. Additionally, CD63 was found overexpressed in HT 29 5-FU resistant cell line but it was not quantified in the remaining samples during mass spectrometry analysis. Due to its important interaction with MVBs and VPS4 protein previously studied, an ICF study of CD63 was done in DLD-1 parent cell line and DLD-1 5-FU resistant subline.

Labelling of CD63 was almost exclusively for DLD-1 5-FU resistant subline, and DLD-1 parent cell line did not show labelling. An additional graph bar was done containing the percentage of cells with high and low levels of CD63 expression (Fig. 6.8). Disperse internal vesicles (endosomes, MVBs) were observed under microscope within DLD-1 5-FU resistant subline but absent in DLD-1 parent cell line. These vesicles could be acting as drug storage bodies to decrease cytotoxic effect of free 5-FU inside the cells (Fig. 6.7).

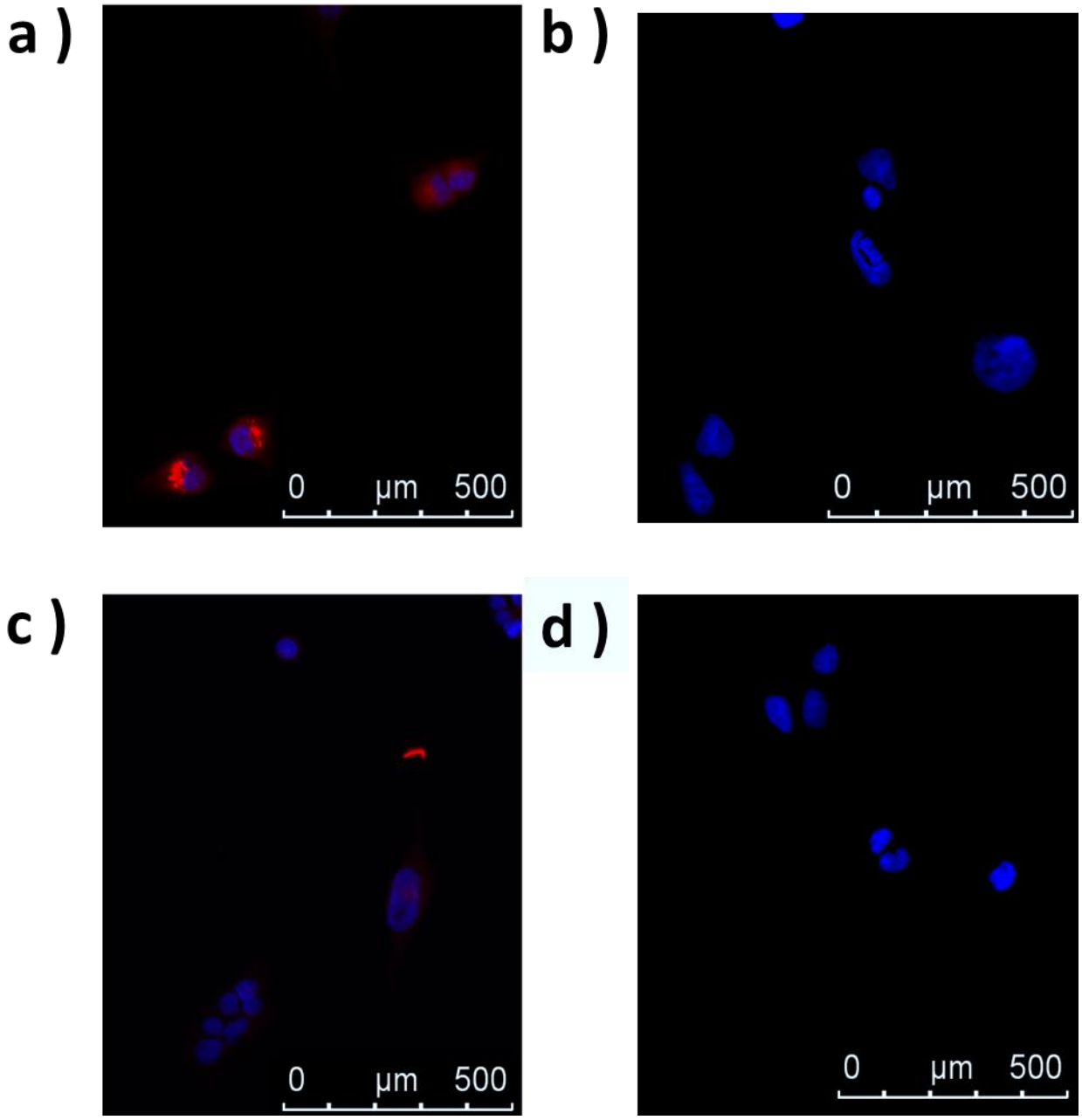

Figure 6.7: Subcellular localization of CD63 in (a) DLD-1 5-FU resistant subline and in (c) DLD-1 high generation control. Negative control of CD63 in (b) DLD-1 5-FU resistant subline and (d) DLD-1 high generation control. Cells were defrosted, growth during 24 h in 6-well plates, fixed and analysed by fluorescence microscopy. For each well, $1x10^4$ cells/ml were seeded and observed under microscope at 40x magnification. Internal vesicles containing CD63 expression were observed in (a) DLD-1 5-FU resistant sublines but not in (c) DLD-1 parent cell lines.

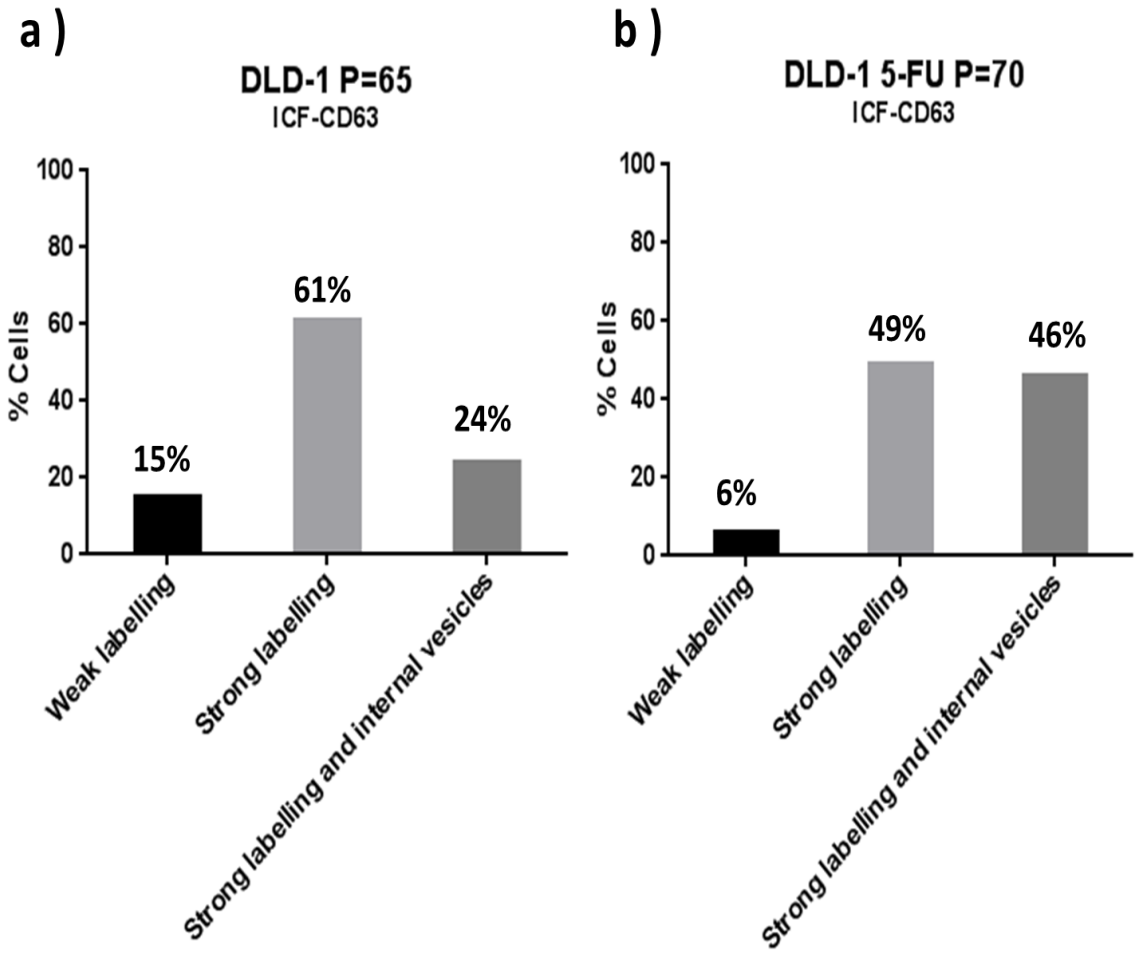

Figure 6.8: Bar graph showing percentage of cells with strong and weak CD63 labelling. DLD-1 5-FU subline showed an increase in 22% of cells with internal vesicles (endosome/MVBs) which were observed under microscope at 40x magnification.

6.2.3 DLD-1 resistant sublines to identify MDR mechanisms

Two Venn diagrams showing commonly altered (a) up-regulated (b) down-regulated proteins found in three different DLD-1 resistant sublines were done. These results may be affected by the limitation during quantification of SILAC-ratio as same two control samples were used to calculate the fold change of the three DLD-1 resistant sublines during quantification data. However, it cannot be ruled out that some of these altered proteins may be playing an important role in MDR resistance.

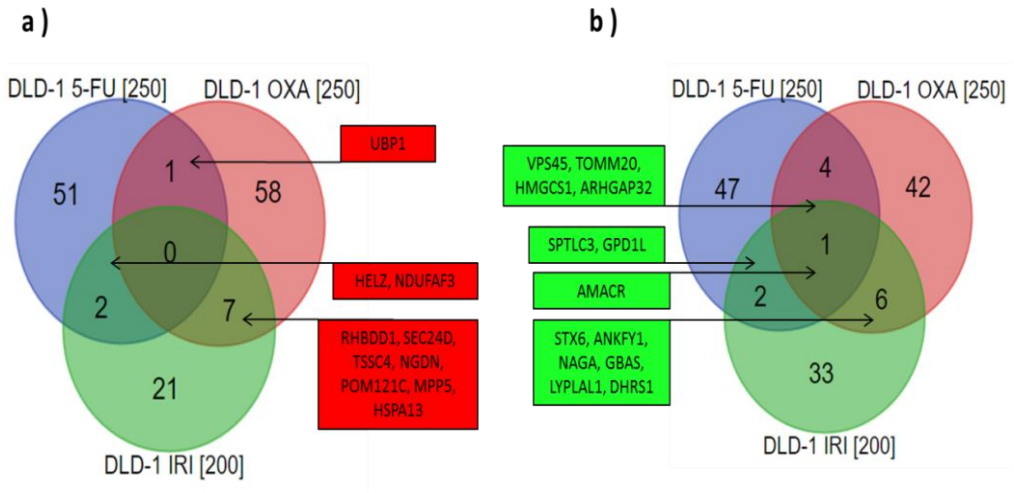

Figure 6.9: Common significantly (a) up-regulated and (b) down-regulated proteins using 5th percentile threshold in DLD-1 resistant sublines to 5-FU, OXA, and IRI.

6.3 Discussion

6.3.1 Discussion of MDR model established

From altered proteins identified across the 3 drug types, the vacuolar protein sorting-associated protein 4 (VPS4) is of most interest. It is known that VPS4 promotes autophagy and tolerance of specific proteins and receptors during the metabolic stress in cancer cells. Cellular stress is a normal cellular response during drugs exposure and it is mediated by different proteins. Drugs cause stress at different biological processes within cells. Main effects of drugs over cells depend on the mechanism of action of the specific drug. Additionally, there are some additional alterations such as lysosome alterations or metabolic changes that normally are caused by homeostasis imbalance inside cells. These issues occur when cells are unable to remain in equilibrium between the internal and external microenvironment. Four of the common altered proteins shown in Table 6.1 were used to develop a protein network model based on VPS4 expression to explain MDR problem in established resistant sublines. Model is shown and explained in detail below.

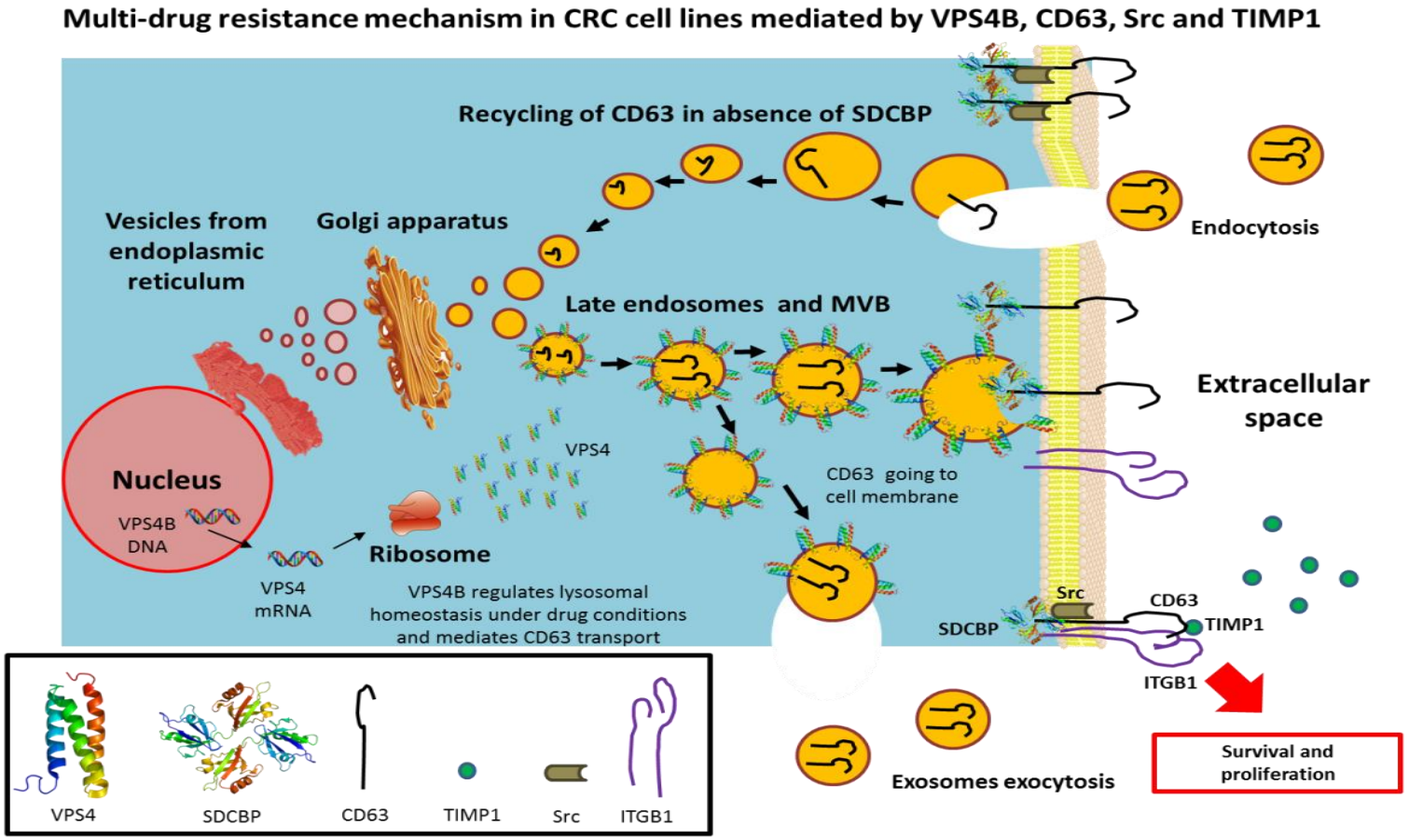

Figure 6.10: MDR model proposed for MDR in CRC. Under drug stress conditions VPS4 involved in MVBs and endosome formation is up-regulated. High levels of VPS4 and high late endosome activity would increase CD63 releasing. CD63can act as cell surface receptor for TIMP1. SRC and SDCBP are known proteins that under TIMP1 conditions play crucial role in cancer survival and proliferation. Additionally, high levels of SDCBP increase binding to the cytoplasmic tail of CD63 at the plasma membrane.

The main role of VPS4 is to regulate lysosome homeostasis that is altered under drug treatments, which increase metabolic stress conditions (Li, Zhang et al. 2011). Additionally, VPS4 is involved in late steps of the endosomal MVBs pathway and it may promote autophagy and tolerance of specific proteins and receptors during the metabolic stress in cancer cells (Adell, Vogel et al. 2014). VPS4 recognizes membrane-associated ESCRT-III assemblies and catalyses their disassembly, possibly in combination with membrane fission. VPS4 redistributes the ESCRT-III components to the cytoplasm for further rounds of MVB sorting (Herlevsen, Oxford et al. 2007). The main complex of MVB is formed by three proteins: namely major vault protein (MVP), v-PARP, and TEP1. In connection with this matter, present thesis shows up-regulation of MVP in all resistant sublines. Also, TEP1 was found up-regulated in all resistant cell lines to 5-FU, confirming a possible up-regulation of VPS4 protein. The function of drug transporter by vault proteins was published in 2003 and it is discussed to be involved in drug transport (Mossink, van Zon et al. 2003).

Recent studies show that VPS4 overexpression promotes autophagy and cell proliferation during *in vitro* starvation increasing tumour growth and poor prognosis in human hepatocellular carcinoma. Whilst, regarding CRC, overexpression of VP4S has been found in intestinal epithelial cells with a high presence of apoptotic markers in patients with Crohn's disease and colorectal HT 29 cell line (Zhang, Wang et al. 2015)**.** With respect to drug resistance in cancer, VPS4 overexpression was linked to anthracycline resistance in patients with primary breast cancers and it is associated with poor prognosis. This mechanism of resistance to anthracycline is mediated by cytosolic retention of the drug anthracycline in lysosomes (Li, Zhang et al. 2011)**.**

VPS4 overexpression observed by SILAC approach was validated by WB in all DLD-1 resistant sublines. Initial WB results for VPS4 expression obtained indicate that differences in bar graphs distribution between all resistant sublines studied by WB correlated with previous results from SILAC approach (Fig. 6.4b,c). Unique differences observed may be due to the use of different experimental approaches and statistics analysis that may increase differences between both results. However, the general trend and profile of samples are

maintained between SILAC and WB results, confirming validity of SILAC approach. Unique difference was observed in KM 12 5-FU that showed up-regulation of VPS4 only under SILAC approach (Fig. 6.2e,f). Hence, after validation by WB of VPS4 results obtained during SILAC approach, next step was to confirm that VPS4 overexpression is a direct consequence of drug exposure. After five passages of parent cell lines DLD-1, KM 12 and HT 29 under 5-FU conditions levels of VPS4 were measured by WB (Fig. 6.6) to verify if drug treatments may increase levels of VPS4 as was shown in the MDR model developed. However, no significant alterations in VPS4 levels were found for any parent cell lines after five passages under 5-FU exposure. No difference seen in terms of expression for the parent line experiment with 5-FU may be due to the short-term of drug exposure. Establishment of resistant sublines is a long-term experiment which requires genomic changes that will lead into an adaptation process, which will lead into proteome changes by cell line evolution.

Apart from the previous role of VPS4 regulating homeostasis under abnormal metabolic conditions, VPS4 is required for the exosomal release of syntenin-1 (SDCBP) and the melanoma 1 antigen (CD63) proteins (Scott, Gaspar et al. 2005, Baietti, Zhang et al. 2012, Colombo, Moita et al. 2013, Jackson 2016). Both SDCBP and CD63 proteins showed high levels of expression in most of the resistant sublines established. So, a high level of VPS4 might be required by tumour cells to increase releasing of CD63 and SDCBP proteins. SDCBP is a protein that binds to the cytoplasmic tail of CD63 at the plasma membrane and it is, therefore, part of the tetraspanin-enriched microdomains. Overexpression of SDCBP can limit internalisation of CD63, suggesting a role for SDCBP as inhibitor of CD63 endocytosis, increasing membrane levels of CD63 (Latysheva, Muratov et al. 2006).

The other protein released by VPS4 was CD63. CD63 is a molecule encoded by the *CD63* gene on human chromosome 12q13. CD63 was found overexpressed in all resistant cell lines with the exception of DLD-1 OXA, where it was not quantified. CD63 is associated with the membrane of intracellular vesicles and it may be expressed on the cell surface. CD63 is a protein of the tetraspanin family also known as transmembrane 4 superfamily. Tetraspanin

proteins participate in numerous physiological processes like cell adhesion, motility, and proliferation. Localization and expression of CD63 are mediated by the enzyme dolichyl-diphosphooligosaccharide-protein glycosyltransferase subunit 2 (RPN2) that mediates CD63 glycosylation in breast cancer cell lines (Tominaga, Hagiwara et al. 2014). However, no significant changes in expression of RPN2 were found in resistant sublines during proteomics analysis. CD63 may be variably glycosylated and it shows three main N-linked glycosylation sites, two sites relate to internalization or intracellular localization and another site of glycosylation (hCD63N172A) responsible for CD63 cell surface localization. The molecular weight of CD63 has been identified in WB to be 32, 35 and 50kDa depending on the glycosylation. A previous study of CD63 overexpression at mRNA level has been linked high levels of CD63 mRNA to metastasis and invasiveness in ovarian cancer (Zhijun, Shulan et al. 2006).

An interesting role has been described for CD63 as a metastatic marker which acts as a signal transduction factor in exosomes (Ji, Greening et al. 2013). After these findings, CD63 has been considered also as endosome late endocytic compartments marker and exosome differentiation marker (Ostrowski, Carmo et al. 2010, Andreu and Yáñez-Mó 2014). CD63 show multiple roles in cancer development. CD63 plays a role in melanoma cell growth regulation and it is overexpressed in breast cancer cell lines resistant to doxorubicin (Turton, Judah et al. 2001). Moreover, CD63 mRNA expression is positive in most of the breast cancer patients according to Huang *et al.* (Tominaga, Hagiwara et al. 2014).

However, the role of CD63 in CRC is still unknown and the only data available in CRC is that CD63 and α3-Integrin show different expression in human colon carcinoma cells with high and low metastatic properties (Sordat, Decraene et al. 2002). Additionally, alterations in expression of CD63 have been observed to occur in apoptotic peripheral blood leukocytes (PBL) of CRC patients after 5-FU drug administration. Although results of 5-FU effect on CD63 are contraries, it is clear that there exist a direct effect of the drug on the CD63 protein. However, the mechanisms behind the effects that 5-FU and other drugs have on CD63 are unknown (Kimhi, Drucker et al. 2004).

To validate SILAC results for CD63 overexpression, ICF of CD63 in DLD-1 5-FU subline was carried out. CD63 was found overexpressed in the resistant subline but not in DLD-1 sensitive cell line. Additionally, an increase of 22% in number of cells with internal vesicles (endosome/MVBs) was observed.

The hypothesis of overexpression of CD63 as a potential mechanism of MDR was reinforced by the finding of some up-regulated proteins related with CD63 activity and which are discussed below.

First protein related to CD63 activity is the proto-oncogene tyrosine-protein kinase Src (SRC) (Iizuka, Kudo et al. 2011). It has been observed that CD63 promotes osteogenesis in osteosarcoma cell lines via SRC pathways. SRC has been described to be one of the proto-oncogenes with more relevance during chemotherapy resistance development, including resistance to 5-FU in CRC (Ahn, Lee et al. 2015). During the proteomics study, SRC was found overexpressed in all resistant cell lines but not in parent cell lines. This fact, together with its interaction with CD63 suggests a common mechanism of resistance involving CD63 and SRC proteins.

A second protein that is also known for its interaction with CD63 is the laminin subunit α-5 (LAMA5). LAMA5 is a ligand that interacts with the α3ß1/CD63 complex and it was found overexpressed in DLD-1 5-FU, KM 12 5-FU, KM 12 OXA and KM 12 5-FU resistant sublines, but also in HT 29 P=9. So, it cannot be deducted it LAMA5 is playing a role in the new mechanism of resistance discussed (Sordat, Decraene et al. 2002).

A last known protein that interacts with CD63 is the metalloproteinase inhibitor 1 (TIMP1). CD63 acts as the surface cellular receptor of the growth factor TIMP1. TIMP1 regulates cell differentiation, migration and activates cellular signalling cascades via CD63 and ITGB1. In melanoma CD63 and TIMP1 interaction has been related with anoikis resistance by PI3-K signalling pathway (Toricelli, Melo et al. 2013). Multiple activities of TIMP1 have been described in different kind of cancers. TIMP1 has been associated with poor prognosis in breast cancer patients and it has been considered as predictive biomarker for fulvestrant resistance in breast cancer (Bjerre, Vinther et al. 2013). In CRC patients with

liver metastases, patients with high levels of TIMP1 showed poor response to palliative 5-FU treatment. (Gentner, Wein et al. 2009)**.** These results have been complemented by recent studies about the role of TIMP1 in CRC progression, where TIMP1 is described as a marker of poor prognosis and metastasis mediated by MAPK pathway (Song, Xu et al. 2016). A similar situation has been found in human neural stem cells (hNSCs) with overexpression of TIMP1. These hNSCs cells showed a high capacity of migration during intracranial glioma development. This increasing of migration and proliferation was mediated by interaction of CD63 and TIMP1 that modulates cell spreading and the rearrangement of the cytoskeleton of hNSCs cells (Lee, Kim et al. 2014). TIMP1 was found also up-regulated in all five resistant sublines to 5-FU, OXA, and IRI.

6.3.2 DLD-1 resistant sublines to identify MDR mechanisms

Cancer is the result of an imbalance in protein expression levels and it is not just the product of a single protein overexpression. In the same way, drug-resistance occurs through changes at protein expression level that can have a little or high impact depending on other related proteins. Hence, a small alteration in a single protein expression would be enough to carry forward drug-resistance since other related proteins would foster the resistance process. Each cancer cell line shows diverse genomics and proteomics profiles and the unique common characteristic among different cancer cell lines is that they exist because, after an alteration in apoptosis and proliferation balance, the cell division process has been stronger than apoptosis. Disruption of the apoptotic and anti-apoptotic balance is a consequence of heterogeneous and constant evolution by a huge fund of mutations, where different proteins increase and decrease their levels influenced by other proteins expression. In summary, at the end of the tumorigenic process, proliferation pathways are predominant over the pro-apoptotic via. Therefore, both cancer and drug-resistance development would depend primarily on the expression level of a protein under a specific proteome and cellular microenvironment context. Hence, resistance phenotype development may happen through a complex proteome unbalance and not due to a single protein expression threshold exceeded. Based on this approach,

where a specific balance between proteins would be presented in more than one resistant subline, a MDR model in CRC cell lines was developed.

6.3.2.1 Common significantly up-regulated proteins found in at least two of the resistant DLD-1 sublines

Proteins significantly up-regulated in more than two resistant DLD-1 sublines were summarised in Table 6.2 below.

Protein name	Main function	DLD-1 5-FU	DLD-1 OXA	DLD-1 IRI
UBP1	Transcription factor of Cytochrome P450	Up-regulated	Up-regulated	Unaltered
HELZ	Helicase during mRNA metabolism	Up-regulated	Unaltered	Up-regulated
NDUFAF3	Mitochondrial respiratory chain	Up-regulated	Unaltered	Up-regulated
RHBDD1, SEC24D, and MPP5	Transport of vesicles to the Golgi complex	Unaltered	Up-regulated	Up-regulated

Table 6.2: Commonly up-regulated proteins quantified in more than two resistant DLD-1 sublines.

Only the upstream-binding protein 1 (UBP1) was found simultaneously as significantly up-regulated in the DLD-1 5-FU and DLD-1 OXA samples. UBP1 is a transcriptional activation factor that acts on different genes promotors such as CYP11A1 and TFCP2 (Miller and Auchus 2010). However, CYP11A1 was not found during proteomics analysis and TFCP2 was quantified but it did not show any change at expression level in resistant sublines.

Between DLD-1 5-FU and DLD-1 IRI resistant sublines proteins, two proteins were found significantly up-regulated. The probable helicase with zinc finger domain (HELZ) and the NADH dehydrogenase [ubiquinone] 1 α-subcomplex assembly factor 3 (NDUFAF3). HELZ acts as helicase during mRNA metabolism and its induced expression in thymus and brain cell lines is associated with growth inhibition (Nagai, Yabe et al. 2003). In relation to NDUFAF3, is involved in mitochondrial respiratory chain (Saada, Vogel et al. 2009).

Among DLD-1 OXA and DLD-1 IRI, seven different proteins were found significantly up-regulated. RHBDD1, SEC24D and MPP5 which have been previously described in Chapter 4, section 4.4.1, and four new up-regulated proteins not previously described: 1) Protein TSSC4 that is a candidate tumour-suppressing subchromosomal transferable fragment candidate protein (Zaitoun and Khatib 2008). 2) Neuroguidin (NGDN) involved in the translational repression of cytoplasmic polyadenylation and its up-regulation in myeloid leukaemia cells has been associated with poor response to vincristine (VCR), etoposide (VP-16), and epirubicin (EPI) drugs (Chen, Lü et al. 2015). 3) Nuclear envelope pore membrane protein POM 121C and 4) Heat shock 70 kDa protein 13 (HSPA13) which has peptide-independent ATPase activity.

6.3.2.2 Common significantly down-regulated proteins found in at least two of the resistant DLD-1 sublines

Proteins significantly down-regulated in more than two resistant DLD-1 sublines were summarised in Table 6.3 below.

Protein name	Main function	DLD-1 5-FU	DLD-1 OXA	DLD-1 IRI
AMACR	Lipids metabolism	Down-regulated	Down -regulated	Down -regulated
VPS45	Chapter 3, in section 3.4.3.2.3	Down-regulated	Down -regulated	Unaltered
TOMM20	Transport of mitochondrially synthesised pre-proteins	Down-regulated	Down -regulated	Unaltered
HMGCS1	Limiting enzyme during cholesterol formation	Down-regulated	Down -regulated	Unaltered
ARHGAP32	Rho-regulated signalling pathways	Down-regulated	Down -regulated	Unaltered
GPD1L	Chapter 3, in section 3.4.3.2.3	Down-regulated	Unaltered	Down-regulated
STX6, ANKFY1, NAGA, GBAS, LYPLAL, DHRS1	Chapter 6, in section 6.3.2.2	Unaltered	Down-regulated	Down-regulated

Table 6.3: Commonly down-regulated proteins quantified in more than two resistant DLD-1 sublines.

The protein α-methylacyl-CoA racemase (AMACR) was the unique significantly down-regulated protein that was commonly found in the three DLD-1 sublines resistant to the three different drugs 5-FU, OXA and IRI. AMACR is involved in the biosynthesis of bile acid and lipids metabolism. Additionally, AMACR may play a role in cancer drug resistance through increasing the expression of enzymes such as cyclooxygenase-2 (COX-2) (Nakamura, Komiya et al. 2002).

Between common significantly down-regulated proteins found, just four proteins were found in samples DLD-1 5-FU and DLD-1 OXA. One of these proteins was VPS45, previously described in Chapter 3, in section 3.4.3.2.3. Remaining three proteins are described below.

Mitochondrial import receptor subunit TOM20 homolog (TOMM20) that mediates transport of mitochondrially synthesised pre-proteins from the cytoplasm (Yano, Terada et al. 2003)**.** Interestingly, in Korean CRC patients, it has been found a correlation between the genetic variation of the gene *TOMM20* and CRC susceptibility (Lee, Park et al. 2016). Second protein was the Hydroxymethylglutaryl-CoA synthase, cytoplasmic (HMGCS1) whose main activity is to produce HMG-CoA a molecule that acts as limiting enzyme during cholesterol formation (Gillespie and Hardie 1992)**.** Third protein was the Rho GTPase-activating protein 32 (ARHGAP32). This protein may promote cell growth regulation through Rho-regulated signalling pathways, especially during the development of neurons (Nakamura, Komiya et al. 2002).

Two significantly down-regulated proteins were found in DLD-1 5-FU and DLD-1 IRI. One was the protein GPD1L, which has been previously described in Chapter 3, section 3.4.3.2.3. The second protein was the serine palmitoyltransferase 3 (SPTLC3) that is involved in sphingolipids biosynthetic process and it has an unknown role in cancer.

Finally, six proteins were found down-regulated among DLD-1 OXA and DLD-1 IRI samples:

1) Syntaxin-6 (STX6) involved in intracellular transport of vesicles to mediate endocytic recycling (Simonsen, Gaullier et al. 1999). 2) Rabankyrin-5 (ANKFY1) also implicated in vesicle transporting and early endosomes

formation. Overexpression of Rabankyrin-5 has been link with the increase of the uptake process of solutes from the extracellular space (Schnatwinkel, Christoforidis et al. 2004)**.** So, maybe down-regulation of Rabankyrin-5 may decrease this drug uptake from extracellular space into the cells and concentration of drug inside cells would decrease. 3) α-N-acetylgalactosaminidase (NAGA) also involved in the metabolism of glycolipids and with an unknown role in cancer. 4) Protein NipSnap homolog 2 (GBAS) that metabolises oxidative phosphorylation process (Martherus, Sluiter et al. 2010). 5) Lysophospholipase-like protein 1 (LYPLAL) with lysophospholipase activity. 6) Dehydrogenase/reductase SDR family member 1 (DHRS1) with oxidoreductase as its main molecular function.

The use of resistant sublines from same original parent cell line by SILAC approach helps gather information about cell line evolution under different types of drugs. However, this information about altered proteins in different resistant sublines has the problem of using the same controls during proteomic SILAC ratios calculation. Hence, expression of the proteins in SILAC control samples will affect fold change estimation in different resistant sublines from the same parent cell line, increasing false discoveries. False discoveries would be consequence of a low or high protein during quantification of the SILAC heavy sample.

Studies of different resistant sublines from different origin, leads into an overall view of the MDR process that can be used to collect data in the MDR model. Results presented in this model show a crucial role of CD63 in CRC resistance that has never been described before in DLD-1 5-FU resistant subline. An increase of CD63 may be caused by increase in VPS4 under drug stress conditions which promote releasing of CD63 protein and exosomes. So, it is proposed a new pathway involving VPS4 up-regulation as long-term drug response. Consequently, VPS4 function as a mediator for CD63 exosomal release and by TIMP1 binding, may together regulate cell-cell signalling processes and drug resistance responses in CRC.

- Chapter seven -

General discussion

&

Future objectives

7 General Discussion & Future Objectives

Despite therapeutic advances, CRC still has a 5-year relative survival rate of 45% (stage II-III), with the development of acquired resistance to treatment with anticancer drugs a major problem (Kufe, Pollock et al. 2003). There is a paucity of molecules which can be utilised as predictive biomarkers for drug response. Biomarkers have been discovered in CRC as a predictor of resistance to anti-EGFR therapy, such as KRAS and PIK3CA mutations that now are part of routine testing in clinical practice (Zhang, Zheng et al. 2015). However, there are no biomarkers for predicting resistance to chemotherapeutic agents. Discovery of new mechanisms of resistance and predictive biomarkers would improve treatments and help decrease unnecessary toxicity and therapy and in addition these mechanisms could be investigated as therapeutic targets for modulation of acquired drug resistance. Tumours present molecular heterogeneity that must be considered when developing therapeutic strategies for a particular patient. Predictive biomarkers of drug response based on DNA sequences or RNA characterisation are not always easy to translate into the clinic. This is due to mutations identified from mRNA transcription strategies which in many cases show a low correlation with the amount of protein expressed (Seo and Lee 2004). Hence, the present thesis proposes both a new screening strategy based on proteomics using drug resistant CRC cell lines and a consequently multidrug model developed *in vitro* from CRC cell lines.

Thus, an initial chemosensitivity panel of eight CRC cell lines was investigated to select three cell lines for the establishment of resistant sublines. Based on the best correlations between drug doses and cell survival DLD-1, KM 12 and HT 29 were analysed. Development of CRC resistant sublines *in vitro* by continuous increasing of drug exposure is a complex process whose success depends on multiple factors. The main two factors that lead to success or failure of resistant subline establishment are: the respective genetic background of the cell line used and the nature of the drugs used and its mechanism of action. For the three drugs used to establish resistant sublines, 5-FU showed the lowest chemotoxicity and consequently, three different resistant sublines were established to this drug (DLD-1 5-FU, KM 12 5-FU, HT 29 5-FU). Two different

resistant sublines were developed for OXA (DLD-1 OXA, KM 12 OXA) and finally one resistant subline was developed with resistance to IRI (DLD-1 IRI). Mice xenograft models were developed using DLD-1 5-FU and relative sensitivity to 5-FU was seen to be maintained *in vivo* matching the results observed *in vitro* for DLD-1 5-FU and DLD-1 parent cell lines.

The results described above support the hypothesis of the existence of different genetic backgrounds in CRC cell lines (Woerner, Yuan et al. 2010). Taking into account some available background from online sources such as ATCC, CLDB, ICLAC and ColonAtlas about the eight CRC cell lines used, microsatellite instability (MSI) information has been discussed as the most relevant (Sinicrope and Sargent 2012). It is known that the MSI is considered in CRC as the main source of hypermutable phenotype caused by the loss of DNA mismatch repair activity. Both DLD-1 and KM 12 have an MSI state that will drive somatic mutations, increasing development of resistant sublines (Ahmed, Eide et al. 2013). However, HT 29 presents as a microsatellite stable (MSS) state, decreasing its potential to mutate and evolve to a resistant phenotype. Due to the lack of information available about cell line background, future experiments should be done to confirm the initial staging of these cell lines, as well as the cell line origin and treatments used in patient from were obtained. Next step was to identify what mechanisms of resistance are involved in the resistance of CRC established sublines.

Identification of new mechanisms of resistance by a SILAC approach has been a useful technique to quantify differences in relative protein abundance between sensitive and resistant cell lines. As a metabolic labelling approach, the best advantage of SILAC over chemical-labelling methods is that samples can be mixed in an early stage during the sample processing, decreasing experimental errors (Lau, Suh et al. 2014).

In terms of robustness, the SILAC approach has shown a high sensitivity, able to detect a high number of significant changes in protein expression using a small amount of sample. In comparison with other proteomics techniques such as WB, with the same amount of sample (around 100 µg of proteins lysate), the SILAC approach using an Orbitrap Analyser is able to produce quantification

results on average for ~3500 proteins, while WB with the same amount of sample shows results for ~ 4-5 proteins. Due to the large quantity of results obtained by this methodology, data must be ordered from the highest level of significance that corresponds to a low level of noise under normal operating conditions. On the other hand, WB is based on the labelling of a single specific protein and the main noise occurs due to human errors during manual work in the laboratory.

Reproducibility was similar under both proteomics techniques used with consistency from SILAC and WB results, which correlated for most of the validated proteins.

Thus it can be considered that the SILAC-approach is an available technique to be used as a screening method to compare proteome expression between similar biological samples and a further analysis by WB may be used as validation technique to confirm the most relevant results obtained by mass spectrometry during initial screening.

The latest trends in SILAC and proteomics studies are focused on super-SILAC methodology development. The main goal of super-SILAC is to achieve metabolic labelling in tissues and model organisms for its application to the study of clinical samples, and not just in cell culture. Hence, initial studies with Super-SILAC are based on stable-isotope labelling of organoids derived from human carcinoma tissues (Shenoy and Geiger 2015). This Super-SILAC mix achieves superior quantification accuracy compared with single cell line labelling from SILAC (Geiger, Wisniewski et al. 2011).

Giving the complexity and heterogeneity of the tumoural cells, identification of what proteomic changes enable cells to develop resistant phenotypes is a highly challenging task. Proteome analysis complexity resides in the high number of proteins that are differently expressed among different tumoural cells. Hence, the challenge is to identify specific proteins involved in mechanisms of resistance. Subsequently, six resistant sublines were established *in vitro* and were analysed by SILAC approach.

An average of 3500 proteins were quantified for each sample and analysed by two different methods (R-LIMMA analysis and Cluster analysis) after median normalization and Log_2 transformation of raw SILAC-ratio data. Lack of consensus about the best hypothesis test methodology for SILAC data measuring led to Nguyen *et al*., to compare the most used hypothesis test methodologies in SILAC data measurement (Nguyen, Wood et al. 2012). In their paper from 2012, the superiority of applying permutation test over t-test, z-test, robust z-test and Wilcoxon signed-rank test to analyse SILAC proteomics results was demonstrated. Permutation testing has been broadly used in microarray gene analysis, network analysis and biomarker discovery (Al-Shahrour, Díaz-Uriarte et al. 2004, Goeman and Bühlmann 2007, Walther and Mann 2011).

A common response from treated resistant sublines was a trend of upregulation of proteomes from CRC cell lines. In all cases, the number of altered proteins was higher in resistant cells than in both parent control cell lines, independently of the number of passages. This can be explained through the drug effect on cell lines that after a long exposure may develop new genomic alterations, DNA damage, mutations and chromosome alterations caused by the chemotherapy. These alterations increase the variance of changes in protein expression of resistant sublines that were higher than in the non-treated cells. During comparison of control samples, no significant differences were found. However, the overlay for altered proteins was always higher in the long generation control. This is due to the changes in protein expression which occur during long-term cell culture passaging. Some passaging effects on the expression profile of efflux proteins and proliferation rates have been described (Hughes, Marshall et al. 2007, Siissalo, Laitinen et al. 2007).

Chemotherapy resistance is a multifactorial process that depends on different variables like cell and tumour genetic variability and different genetic alterations. Tumour resistance is the main weakness of chemotherapy and this resistance may be acquired or intrinsic if it presents before drug treatment. Resistance limits the efficacy of chemotherapy agents and it is thought to be responsible for 90% of treatment failure in metastatic cancer patients (Longley and Johnston

2005). Although intrinsic resistance has been a global problem during chemotherapy resistance history, developing more efficient new chemotherapy treatments based on personal therapy have been a factor in the increasing acquired resistance problem in CRC treatment (Gottesman 2002)**.** Currently, specific treatments which are having success in clinical trials, such as Gefitinib and Erlotinib, are based on attacking target proteins to avoid resistance development problem. Gefitinib and Erlotinib are reversible inhibitors of tyrosine kinase activity of EGFR by blocking the ATP binding site (Chen, Solimando et al. 2013). Gefitinib and Erlotinib have shown a better prognosis during CRC treatment in patients that have tumours with overexpression of EGFR (Dienstmann, De Dosso et al. 2012). These results highlight that it is crucial to identify new genetic alterations and tumour proteome changes in each patient. The new knowledge about CRC heterogeneity is leading the development of new personalized therapies which are more effective against specific tumoural cells and with fewer side effects. Identification of altered protein expression among the resistant sublines has been used to establish different CRC resistant models based on the up-regulated and down-regulated proteins quantified that may be used to identify new proteins to be targeted for CRC therapy.

Depending on the mechanism of action of the compound used, there are considerable differences in proteins altered during the establishment of resistant sublines. Cytotoxicity from compounds such as 5-FU that targets specific enzymes e.g. thymidylate synthase, to block synthesis of the pyrimidine thymidine avoiding DNA replication, may be avoided by different alterations of protein expression. These proteins can be involved in avoiding apoptotic pathways, DNA repair and metabolic pathways including 5-FU metabolism and 5-FU transport. This broad range of proteins enables tumour cells to develop different altered protein networks with resistance activity. The data presented here show eleven common altered proteins with a potential role for the development of resistance to 5-FU. These proteins were MYADM, DDAH2, SARG (up-regulated) and SLC3A2, TAMM41, GPD1L, VPS45, RAP1GDS1, NCDN, BPNT1 (down-regulated).

Secondly, platinum compounds like OXA that binds covalently with macromolecules may block different processes such as DNA synthesis and transcription, being cell-cycle nonspecific compounds. This wide range of available targets makes survival of tumour cells harder. This occurs because cancer cells must develop multiple and different genomic and proteomic changes to cover the damage caused by different biological cellular processes. The presence of a high number of up-regulated proteins involved in multiple metabolisms pathways of resistant sublines to OXA may be a consequence of OXA disturbance within cells. The commonly altered proteins found in resistant sublines to OXA were BAIAP2, TAP1, STIM1 (up-regulated) and ATP2B1 (down-regulated).

Finally, there are more recent drugs like IRI that target crucial proteins which are required for cell survival such as topoisomerase I. IRI causes both lethal double-stranded breaks in DNA and inhibition of DNA replication, activating apoptotic pathways. This serious and direct mechanism of action that may activate pro-apoptotic pathways is the hardest mechanism of action to be avoided by tumour cells. So, the development of resistant sublines to IRI was the most difficult with only one cell line (DLD-1) successfully developed. Additionally, the fold change of this unique resistant cell line established (DLD-1 IRI) was the lowest among all resistant sublines established to the three drugs and this can be due to the high chemotoxicity of this compound.

The majority of the mechanisms of drug resistance identified in this thesis are mechanisms acquired by overexpression and down-regulation of proteins involved in apoptotic process (NOL3, TAOK1, PAWR, WRAP53, CYCS, GATA6, FHL2, PDCD4), DNA repair process (JUND, MMR, PARP2, BRCA1, PMS2, SMCs), drug and small molecules metabolism (DDAH2, TAMM41, GPD1L, BPNT1), and intracellular protein transport and cell membrane organization (MYADM, SAGR, APLP2, NCDN, BAIAP2, TAP1, STIM1, ATP2B1, CD44, LGALS3BP).

Among the significantly altered proteins quantified in resistant sublines, this thesis highlights results for commonly significantly altered proteins that were identified in more than one resistant subline. Based on these results new potential biomarkers of drug response in CRC to 5-FU and OXA are suggested for the first time. New mechanisms of CRC resistance suggested in this thesis include resistance to 5-FU by both up-regulation of MYADM, SARG, APLP2 and down-regulation of SLC3A2, TAMM41, GPD1L, VPS45, RAP1GDS1, NCDN, BPNT1. For OXA new mechanisms of resistance in CRC involve both up-regulation of BAIAP2, TAP1, STIM1 and down-regulation of ATP2B1. For validation in further studies, these proteins will be evaluated retrospectively in tumour biopsies from CRC patients to assess their value as predictive biomarkers for drug resistance or potential therapeutic targets.

In considering MDR, commonly and not significant up-regulated proteins were used to design a MDR network model. The model is based on VPS4 as a mediator of drug resistance by regulation of lysosome homeostasis that is altered under drug effects (Li, Zhang et al. 2011). This mechanism of resistance can be related to the MVBs pathway, promoting autophagy (Adell, Vogel et al. 2014). Additionally, these results were complemented by ICF studies of CD63 expression in DLD-1 5-FU resistant subline which showed an increase in internal vesicles in resistant sublines. These internal vesicles might be acting as storage compartments for cytotoxic compounds, decreasing drug concentrations within the cells, and these studies warrant further investigation.

In conclusion, in this study we have developed six resistant sublines to 5-FU, OXA and IRI, the three most common drugs used in CRC patients and analysed these proteomically using a SILAC-approach with Orbitrap Fusion™ Tribrid™ Mass Spectrometry analysis. Significantly altered proteins have been identified as either upregulated or downregulated in one or more of the resistant sublines, and thus the findings here provide a strong platform for further work to validate these proteins as either new biomarkers for drug resistance, or as potential targets for therapeutic intervention to modulate acquired drug resistance in CRC.

7.1 Future perspectives

One of the main findings of this thesis is identification of proteins which either as biomarkers or therapeutic targets may be used to overcome the problem of acquired resistance in CRC patients. Extensive data collected in this study gives a good starting point to explore the drug resistance problem in CRC. It can be seen from the heterogeneity observed and generated with just 3 cell lines that development of additional resistant sublines derived from different parent cell lines would be useful to identify new commonly altered proteins. Some specific proteins have been identified, e.g. VPS4 for MDR and CD44, UMPS, CD63 for 5-FU and these can be studied through further experimental investigations using established models. Proteomics characterisation of resistant sublines leads to the identification of common proteins and molecular pathways that are relevant in drug resistance of different samples. Hence, alteration of these common proteins might be associated with a poor drug-response. Therefore, after validation of results obtained *in vitro* and after the validation of some proteins results here presented as potential biomarkers *in vivo* a more heterogeneous range of CRC cell types predict tumour response to the different drugs will be investigated. Up-regulation and down-regulation of these same proteins *in vivo* and in biopsy of the tumour tissue or a sample of cells from the CRC patient can be used to study the potential role in resistance to a specific drug, or multiple drugs.

Matching proteomic profiles from tumours and drug-response outcomes would reduce the resistance problem in the clinic, decreasing the risk of recurrence and resistance development. Characterisation of tumours based on proteomics and genomics features will be able to shed some light on the selection of the correct chemotherapy treatment. For example, proteins altered and involved in MDR must be represented in CRC tumours from CRC patients to be validated as good target candidates. Additionally, the use of xenograft models derived from cancer cells of CRC patients may complement these studies and offer a choice to recapitulate tumour characterisation under different drug conditions before using the drug in the patient. In addition to the use of altered proteins as

new biomarkers of drug-response, these altered proteins can be used as target molecules for chemo/immunotherapies.

After selection of the best proteins to be targeted as responsible for the partial phenotype of resistance, current drugs and inhibitors could be used to reverse the resistance phenotype *in vitro*. In cases established drugs are not available to target the specific proteins, new small molecules and novel drug combinations may be developed. Once, results *in vitro* have shown success with the drug, studies *in vivo* and xenograft models should be done before moving to clinical trials.

This knowledge will allow researchers to develop new treatments for cancer and with technological advances such as new mass spectrometry analysers with even greater sensitivity; this will also allow further proteomic investigation of these drug resistant cell lines. This should allow lead even more information on the proteome to be obtained and improve the chances of a strong identification.

- Chapter eight -

References

8 References

"CRUK (2014a). Colorectal cancer 2016.".

(2016). "Colon Cancer Treatment Protocols: Treatment Protocols." Retrieved Web. 1 Mar. 2016.

Adamsen, B. L., K. L. Kravik and P. M. De Angelis (2011). "DNA damage signaling in response to 5-fluorouracil in three eolorectal cancer cell lines with different mismatch repair and TP53 status." International journal of oncology **39**(3): 673.

Adell, M. A. Y., G. F. Vogel, M. Pakdel, M. Müller, H. Lindner, M. W. Hess and D. Teis (2014). "Coordinated binding of Vps4 to ESCRT-III drives membrane neck constriction during MVB vesicle formation." J Cell Biol **205**(1): 33-49.

Ahmed, D., P. Eide, I. Eilertsen, S. Danielsen, M. Eknæs, M. Hektoen, G. Lind and R. Lothe (2013). "Epigenetic and genetic features of 24 colon cancer cell lines." Oncogenesis **2**(9): e71.

Ahn, J.-Y., J.-S. Lee, H.-Y. Min and H.-Y. Lee (2015). "Acquired resistance to 5-fluorouracil via HSP90/Src-mediated increase in thymidylate synthase expression in colon cancer." Oncotarget **6**(32): 32622.

Aho, S., J. Lupo, P. A. Coly, A. Sabine, M. Castellazzi, P. Morand, A. Sergeant, E. Manet, V. Boyer and H. Gruffat (2009). "Characterization of the ubinuclein protein as a new member of the nuclear and adhesion complex components (NACos)." Biology of the Cell **101**(6): 319-334.

Aizawa, M. and M. Fukuda (2015). "Small GTPase Rab2B and its specific binding protein Golgi-associated Rab2B interactor-like 4 (GARI-L4) regulate Golgi morphology." Journal of Biological Chemistry **290**(36): 22250-22261.

Al-Shahrour, F., R. Díaz-Uriarte and J. Dopazo (2004). "FatiGO: a web tool for finding significant associations of Gene Ontology terms with groups of genes." Bioinformatics **20**(4): 578-580.

Alcindor, T. and N. Beauger (2011). "Oxaliplatin: a review in the era of molecularly targeted therapy." Current Oncology **18**(1): 18-25.

Allgayer, H. (2010). "Pdcd4, a colon cancer prognostic that is regulated by a microRNA." Critical reviews in oncology/hematology **73**(3): 185-191.

Amici, A., K. Ciccioli, V. Naponelli, N. Raffaelli and G. Magni (2005). "Evidence for essential catalytic determinants for human erythrocyte pyrimidine 5'-nucleotidase." Cellular and molecular life sciences **62**(14): 1613-1620.

An, Q., P. Robins, T. Lindahl and D. E. Barnes (2007). "5-Fluorouracil incorporated into DNA is excised by the Smug1 DNA glycosylase to reduce drug cytotoxicity." Cancer research **67**(3): 940-945.

Andersen, V., L. K. Vogel, T. I. Kopp, M. Sæbø, A. W. Nonboe, J. Hamfjord, E. H. Kure and U. Vogel (2015). "High ABCC2 and low ABCG2 gene expression are early events in the colorectal adenoma-carcinoma sequence." PloS one **10**(3): e0119255.

André, T., C. Boni, L. Mounedji-Boudiaf, M. Navarro, J. Tabernero, T. Hickish, C. Topham, M. Zaninelli, P. Clingan and J. Bridgewater (2004). "Oxaliplatin, fluorouracil, and leucovorin as adjuvant treatment for colon cancer." New England Journal of Medicine **350**(23): 2343-2351.

Andreu, Z. and M. Yáñez-Mó (2014). "Tetraspanins in extracellular vesicle formation and function." Frontiers in immunology **5**: 442.

Aranda, J. F., N. Reglero-Real, B. Marcos-Ramiro, A. Ruiz-Sáenz, L. Fernández-Martín, M. Bernabé-Rubio, L. Kremer, A. J. Ridley, I. Correas and M. A. Alonso (2013). "MYADM controls endothelial barrier function through ERM-dependent regulation of ICAM-1 expression." Molecular biology of the cell **24**(4): 483-494.

Arvidsson, Y., E. Andersson, A. Bergström, M. K. Andersson, G. Altiparmak, A.-C. Illerskog, H. Ahlman, D. Lamazhapova and O. Nilsson (2008). "Amyloid precursor-like protein 1 is differentially upregulated in neuroendocrine tumours of the gastrointestinal tract." Endocrine-related cancer **15**(2): 569-581.

Asher, G., J. Lotem, B. Cohen, L. Sachs and Y. Shaul (2001). "Regulation of p53 stability and p53-dependent apoptosis by NADH quinone oxidoreductase 1." Proceedings of the National Academy of Sciences **98**(3): 1188-1193.

Asher, G., P. Tsvetkov, C. Kahana and Y. Shaul (2005). "A mechanism of ubiquitin-independent proteasomal degradation of the tumor suppressors p53 and p73." Genes & development **19**(3): 316-321.

Ashton, D., C. Beddell, B. Green and R. Oliver (1994). "Rapid validation of molecular structures of biological samples by electrospray-mass spectrometry." FEBS letters **342**(1): 1-6.

Babbitt, S. E., B. San Francisco, E. C. Bretsnyder and R. G. Kranz (2014). "Conserved residues of the human mitochondrial holocytochrome c synthase mediate interactions with heme." Biochemistry **53**(32): 5261-5271.

Bäckdahl, L., M. Herberth, G. Wilson, P. Tate, L. S. Campos, R. Cortese, F. Eckhardt and S. Beck (2009). "Gene body methylation of the dimethylarginine dimethylamino-hydrolase 2 (Ddah2) gene is an epigenetic biomarker for neural stem cell differentiation." Epigenetics **4**(4): 248-254.

Bae, E., H. E. Kim, E. Koh and K.-S. Kim (2014). "Phosphoglucomutase1 is necessary for sustained cell growth under repetitive glucose depletion." FEBS letters **588**(17): 3074-3080.

Baietti, M. F., Z. Zhang, E. Mortier, A. Melchior, G. Degeest, A. Geeraerts, Y. Ivarsson, F. Depoortere, C. Coomans and E. Vermeiren (2012). "Syndecan-syntenin-ALIX regulates the biogenesis of exosomes." Nature cell biology **14**(7): 677-685.

Baker, E. K. and A. El-Osta (2003). "The rise of DNA methylation and the importance of chromatin on multidrug resistance in cancer." Experimental cell research **290**(2): 177-194.

Baldwin, A. S. (2001). "Control of oncogenesis and cancer therapy resistance by the transcription factor NF-κB." The Journal of clinical investigation **107**(3): 241-246.

Balendiran, G. K., R. Dabur and D. Fraser (2004). "The role of glutathione in cancer." Cell biochemistry and function **22**(6): 343-352.

Bandrés, E., R. Zárate, N. Ramirez, A. Abajo, N. Bitarte and J. Garíia-Foncillas (2007). "Pharmacogenomics in colorectal cancer: the first step for individualized-therapy." World journal of gastroenterology: WJG **13**(44): 5888-5901.

Banuelos, C. A., J. P. Banáth, S. H. MacPhail, J. Zhao, T. Reitsema and P. L. Olive (2007). "Radiosensitization by the histone deacetylase inhibitor PCI-24781." Clinical Cancer Research **13**(22): 6816-6826.

Barderas, R., M. Mendes, S. Torres, R. A. Bartolomé, M. López-Lucendo, R. Villar-Vázquez, A. Peláez-García, E. Fuente, F. Bonilla and J. I. Casal (2013). "In-depth characterization of the secretome of colorectal cancer metastatic cells identifies key proteins in cell adhesion, migration, and invasion." Molecular & Cellular Proteomics **12**(6): 1602-1620.

Bauer, K. M., P. A. Lambert and A. B. Hummon (2012). "Comparative label-free LC-MS/MS analysis of colorectal adenocarcinoma and metastatic cells treated with 5-fluorouracil." Proteomics **12**(12): 1928-1937.

Bellerby, R., C. Smith, S. Kyme, J. Gee, U. Günthert, A. Green, E. Rakha, P. Barrett-Lee and S. Hiscox (2016). "Overexpression of specific cD44 isoforms is associated with aggressive cell Features in acquired endocrine resistance." Frontiers in Oncology **6**.

Benhattar , J., J.-P. Cerottini, G. M. Emilia SARAGA and J.-C. GIVEL (1996). "p53 mutations as a possible predictor of response to chemotherapy in metastatic colorectal carcinomas." Int. J. Cancer (Pred. Oncol.) **69**: 190-192.

Berger, I. and Y. Shaul (1991). "Structure and function of human jun-D." Oncogene **6**(4): 561-566.

Bertorelle, R., E. Rampazzo, S. Pucciarelli, D. Nitti and A. De Rossi (2014). "Telomeres, telomerase and colorectal cancer." World J Gastroenterol **20**(8): 1940-1950.

Bianchet, M. A., M. Faig and L. M. Amzel (2004). "Structure and mechanism of NAD [P] H: quinone acceptor oxidoreductases (NQO)." Methods in enzymology **382**: 144-174.

Bigagli, E., C. Luceri, D. Guasti and L. Cinci (2016). "Exosomes secreted from human colon cancer cells influence the adhesion of neighboring metastatic cells: Role of microRNA-210." Cancer biology & therapy **17**(10): 1062-1069.

Biondi, M., S. Fusco, A. L. Lewis and P. A. Netti (2013). "Investigation of the mechanisms governing doxorubicin and irinotecan release from drug-eluting beads: mathematical modeling and experimental verification." Journal of Materials Science: Materials in Medicine **24**(10): 2359.

Bjerre, C., L. Vinther, K. C. Belling, S. Ø. Würtz, R. Yadav, U. Lademann, O. Rigina, K. N. Do, H. J. Ditzel and A. E. Lykkesfeldt (2013). "TIMP1 overexpression mediates resistance of MCF-7 human breast cancer cells to fulvestrant and down-regulates progesterone receptor expression." Tumor Biology **34**(6): 3839-3851.

Bombuwala, K., T. Kinstle, V. Popik, S. O. Uppal, J. B. Olesen, J. Viña and C. A. Heckman (2006). "Colchitaxel, a coupled compound made from microtubule inhibitors colchicine and paclitaxel." Beilstein journal of organic chemistry **2**(1): 13.

Bonneau, C., R. Rouzier, C. Geyl, A. Cortez, M. Castela, R. Lis, E. Daraï and C. Touboul (2015). "Predictive markers of chemoresistance in advanced stages epithelial ovarian carcinoma." Gynecologic oncology **136**(1): 112-120.

Boonstra, R., H. Timmer-Bosscha, J. van Echten-Arends, D. van der Kolk, A. Van Den Berg, B. De Jong, K. Tew, S. Poppema and E. De Vries (2004). "Mitoxantrone resistance in a small cell lung cancer cell line is associated with ABCA2 upregulation." British journal of cancer **90**(12): 2411-2417.

Bradford, M. M. (1976). "A rapid and sensitive method for the quantitation of microgram quantities of protein utilizing the principle of protein-dye binding." Anal Biochem **72**(1-2): 248-254.

Braig, M., S. Lee, C. Loddenkemper, C. Rudolph, A. H. Peters, B. Schlegelberger, H. Stein, B. Dörken, T. Jenuwein and C. A. Schmitt (2005). "Oncogene-induced senescence as an initial barrier in lymphoma development." Nature **436**(7051): 660-665.

Breen, L., M. Heenan, V. Amberger-Murphy and M. Clynes (2007). "Investigation of the role of p53 in chemotherapy resistance of lung cancer cell lines." Anticancer research **27**(3A): 1361-1364.

Bresalier, R. S., N. Mazurek, L. R. Sternberg, J. C. Byrd, C. K. Yunker, P. Nangia-Makker and A. Raz (1998). "Metastasis of human colon cancer is altered by modifying expression of the β-galactoside-binding protein galectin 3." Gastroenterology **115**(2): 287-296.

Brophy, S., K. M. Sheehan, D. A. McNamara, J. Deasy, D. J. Bouchier-Hayes and E. W. Kay (2009). "GLUT-1 expression and response to chemoradiotherapy in rectal cancer." International journal of cancer **125**(12): 2778-2782.

Brunelle, J. L. and R. Green (2014). "One-dimensional SDS-polyacrylamide gel electrophoresis (1D SDS-PAGE)." Methods in enzymology **541**: 151.

Brusniak, M.-Y., B. Bodenmiller, D. Campbell, K. Cooke, J. Eddes, A. Garbutt, H. Lau, S. Letarte, L. N. Mueller and V. Sharma (2008). "Corra: Computational framework and tools for LC-MS discovery and targeted mass spectrometry-based proteomics." BMC bioinformatics **9**(1): 542.

Cai, B., Y. Miao, Y. Liu, X. Xu, S. Guan, J. Wu and Y. Liu (2013). "Nuclear Multidrug-Resistance Related Protein 1 Contributes to Multidrug-Resistance of Mucoepidermoid Carcinoma Mainly via Regulating Multidrug-Resistance Protein 1: A Human Mucoepidermoid Carcinoma Cells Model and Spearman's Rank Correlation Analysis." PloS one **8**(8): e69611.

Cai, W.-s., F. Shen, J.-l. Li, Z. Feng, Y.-c. Wang, H.-q. Xiao and B. Xu (2014). "Activated protease receptor-2 induces GATA6 expression to promote survival in irradiated colon cancer cells." Archives of biochemistry and biophysics **555**: 28-32.

Calvo, M. B., A. Figueroa, E. G. Pulido, R. G. Campelo and L. A. Aparicio (2010). "Potential role of sugar transporters in cancer and their relationship with anticancer therapy." International journal of endocrinology **2010**.

Camilloni, C., A. B. Sahakyan, M. J. Holliday, N. G. Isern, F. Zhang, E. Z. Eisenmesser and M. Vendruscolo (2014). "Cyclophilin A catalyzes proline isomerization by an electrostatic handle mechanism." Proceedings of the National Academy of Sciences **111**(28): 10203-10208.

Cao, X., L. Fang, S. Gibbs, Y. Huang, Z. Dai, P. Wen, X. Zheng, W. Sadee and D. Sun (2007). "Glucose uptake inhibitor sensitizes cancer cells to daunorubicin and overcomes drug resistance in hypoxia." Cancer chemotherapy and pharmacology **59**(4): 495-505.

Carew, J. S., S. T. Nawrocki, Y. V. Krupnik, K. Dunner, D. J. McConkey, M. J. Keating and P. Huang (2006). "Targeting endoplasmic reticulum protein transport: a novel strategy to kill malignant B cells and overcome fludarabine resistance in CLL." Blood **107**(1): 222-231.

Chaney, S. G., S. Ramachandran, S. Sharma, N. V. Dokholyan, B. Temple, D. Bhattacharyya, Y. Wu and S. Campbell (2009). Differences in conformation and conformational dynamics between cisplatin and oxaliplatin DNA adducts. Platinum and Other Heavy Metal Compounds in Cancer Chemotherapy, Springer**:** 157-169.

Chang-Liu, C.-M. and G. E. Woloschak (1997). "Effect of passage number on cellular response to DNA-damaging agents: cell survival and gene expression." Cancer letters **113**(1): 77-86.

Chen, A., J. Solimando, Dominic and J. A. Waddell (2013). "Gefitinib, Fluorouracil, Oxaliplatin, and Leucovorin (IFOX) Regimen for Colorectal Cancer." Hospital pharmacy **48**(11): 905-911.

Chen, C. Y., J. S. Chen, Y. P. Chou, Y. B. Kuo, C. W. Fan and E. C. Chan (2014). "Antibody Against N-terminal Domain of Phospholipid Scramblase 1 Induces Apoptosis in Colorectal Cancer Cells Through the Intrinsic Apoptotic Pathway." Chemical biology & drug design **84**(1): 36-43.

Chen, K., S. Lü, H. Cheng, G. Tang, M. Liu, H. Zhou and J. Wang (2015). "High expression of neuroguidin increases the sensitivity of acute myeloid leukemia cells to chemotherapeutic drugs." Journal of hematology & oncology **8**(1): 11.

Chen, K. G., R. D. Leapman, G. Zhang, B. Lai, J. C. Valencia, C. O. Cardarelli, W. D. Vieira, V. J. Hearing and M. M. Gottesman (2009). "Influence of melanosome dynamics on melanoma drug sensitivity." Journal of the National Cancer Institute.

Chen, K. G., J. C. Valencia, B. Lai, G. Zhang, J. K. Paterson, F. Rouzaud, W. Berens, S. M. Wincovitch, S. H. Garfield and R. D. Leapman (2006). "Melanosomal sequestration of cytotoxic drugs contributes to the intractability of malignant melanomas." Proceedings of the National Academy of Sciences **103**(26): 9903-9907.

Chen, L., S. Yang, J. Jakoncic, J. J. Zhang and X.-Y. Huang (2011). "Migrastatin analogues target fascin to block tumour metastasis." Nature **476**(7359): 240-240.

Chen, S., C. Kuo, H. Pan, T. Tsou, S. Yeh and J. Chang (2016). "Desferal regulates hCtr1 and transferrin receptor expression through Sp1 and exhibits synergistic cytotoxicity with platinum drugs in oxaliplatin-resistant human cervical cancer cells in vitro and in vivo."

Cho, H. and J. H. Kehrl (2007). "Localization of Giα proteins in the centrosomes and at the midbody: implication for their role in cell division." The Journal of cell biology **178**(2): 245-255.

Cho, W. C. (2016). Application of proteomics in non-small-cell lung cancer, Taylor & Francis.

Choudhari, S. K., M. Chaudhary, S. Bagde, A. R. Gadbail and V. Joshi (2013). "Nitric oxide and cancer: a review." World journal of surgical oncology **11**(1): 118.

Chu, E., S. Zinn, D. Boarman and C. J. Allegra (1990). "Interaction of γ interferon and 5-fluorouracil in the H630 human colon carcinoma cell line." Cancer research **50**(18): 5834-5840.

Chu, X.-Y., H. Suzuki, K. Ueda, Y. Kato, S.-I. Akiyama and Y. Sugiyama (1999). "Active efflux of CPT-11 and its metabolites in human KB-derived cell lines." Journal of Pharmacology and Experimental Therapeutics **288**(2): 735-741.

Ciechanover, A. (1998). "The ubiquitin–proteasome pathway: on protein death and cell life." The EMBO journal **17**(24): 7151-7160.

Cipriano, R., J. Graham, K. L. Miskimen, B. L. Bryson, R. C. Bruntz, S. A. Scott, H. A. Brown, G. R. Stark and M. W. Jackson (2012). "FAM83B mediates EGFR-and RAS-driven oncogenic transformation." The Journal of clinical investigation **122**(9): 3197-3210.

Cipriano, R., K. L. Miskimen, B. L. Bryson, C. R. Foy, C. A. Bartel and M. W. Jackson (2014). "Conserved oncogenic behavior of the FAM83 family regulates MAPK signaling in human cancer." Molecular Cancer Research **12**(8): 1156-1165.

Cohen, A. A., N. Geva-Zatorsky, E. Eden, M. Frenkel-Morgenstern, I. Issaeva, A. Sigal, R. Milo, C. Cohen-Saidon, Y. Liron and Z. Kam (2008). "Dynamic proteomics of individual cancer cells in response to a drug." science **322**(5907): 1511-1516.

Coley, H. M. (2004). "Development of drug-resistant models." Methods Mol Med **88**: 267-273.

Coley, H. M. (2008). "Mechanisms and strategies to overcome chemotherapy resistance in metastatic breast cancer." Cancer treatment reviews **34**(4): 378-390.

Collins, F. S. and A. D. Barker (2007). "Mapping the cancer genome." Scientific American **296**(3): 50-57.

Collins, F. S. and M. K. Mansoura (2001). "The human genome project." Cancer **91**(S1): 221-225.

Colombo, M., C. Moita, G. van Niel, J. Kowal, J. Vigneron, P. Benaroch, N. Manel, L. F. Moita, C. Théry and G. Raposo (2013). "Analysis of ESCRT functions in exosome biogenesis, composition and secretion highlights the heterogeneity of extracellular vesicles." J Cell Sci **126**(24): 5553-5565.

Comes, F., A. Matrone, P. Lastella, B. Nico, F. Susca, R. Bagnulo, G. Ingravallo, S. Modica, G. L. Sasso and A. Moschetta (2007). "A novel cell type-specific role of p38α in the control of autophagy and cell death in colorectal cancer cells." Cell Death & Differentiation **14**(4): 693-702.

Consortium, G. P. (2012). "An integrated map of genetic variation from 1,092 human genomes." Nature **491**(7422): 56-65.

Consortium, I. H. G. S. (2004). "Finishing the euchromatic sequence of the human genome." Nature **431**(7011): 931-945.

Cortés, F., S. Mateos, N. Pastor and I. Domínguez (2004). "Toward a comprehensive model for induced endoreduplication." Life sciences **76**(2): 121-135.

Corti, A., M. Franzini, A. Paolicchi and A. Pompella (2010). "Gamma-glutamyltransferase of cancer cells at the crossroads of tumor progression, drug resistance and drug targeting." Anticancer research **30**(4): 1169-1181.

Coward, J. and A. Harding (2007). "Size does matter: why polyploid tumor cells are critical drug targets in the war on cancer." Molecular mechanisms of cellular stress responses in cancer and their therapeutic implications: 88.

Cruz, I. N., H. M. Coley, H. B. Kramer, T. K. Madhuri, N. A. Safuwan, A. R. Angelino and M. Yang (2017). "Proteomics Analysis of Ovarian Cancer Cell Lines and Tissues Reveals Drug Resistance-associated Proteins." Cancer Genomics-Proteomics **14**(1): 35-51.

Cui, W., L. Yu, H. He, Y. Chu, J. Gao, B. Wan, L. Tang and S. Zhao (2001). "Cloning of human myeloid-associated differentiation marker (MYADM) gene whose expression was up-regulated in NB4 cells induced by all-trans retinoic acid." Molecular biology reports **28**(3): 123-138.

Dall, E. and H. Brandstetter (2013). "Mechanistic and structural studies on legumain explain its zymogenicity, distinct activation pathways, and regulation." Proceedings of the National Academy of Sciences **110**(27): 10940-10945.

Danenberg, P. V. (1977). "Thymidylate synthetase - a target enzyme in cancer chemotherapy." Biochim Biophys Acta **473**(2): 73-92.

Daniels, T. R., T. Delgado, G. Helguera and M. L. Penichet (2006). "The transferrin receptor part II: targeted delivery of therapeutic agents into cancer cells." Clinical immunology **121**(2): 159-176.

De Las Rivas, J. and C. Fontanillo (2010). "Protein–protein interactions essentials: key concepts to building and analyzing interactome networks." PLoS Comput Biol **6**(6): e1000807.

De Piccoli, G., F. Cortes-Ledesma, G. Ira, J. Torres-Rosell, S. Uhle, S. Farmer, J.-Y. Hwang, F. Machin, A. Ceschia and A. McAleenan (2006). "Smc5–Smc6 mediate DNA double-strand-break repair by promoting sister-chromatid recombination." Nature cell biology **8**(9): 1032-1034.

De Wit, N., J. Rijntjes, J. Diepstra, T. Van Kuppevelt, U. Weidle, D. Ruiter and G. van Muijen (2005). "Analysis of differential gene expression in human melanocytic tumour lesions by custom made oligonucleotide arrays." British journal of cancer **92**(12): 2249-2261.

Deegan, S., S. Saveljeva, S. E. Logue, K. Pakos-Zebrucka, S. Gupta, P. Vandenabeele, M. J. Bertrand and A. Samali (2014). "Deficiency in the mitochondrial apoptotic pathway reveals the toxic potential of autophagy under ER stress conditions." Autophagy **10**(11): 1921-1936.

Desai, S. D., T.-K. Li, A. Rodriguez-Bauman, E. H. Rubin and L. F. Liu (2001). "Ubiquitin/26S proteasome-mediated degradation of topoisomerase I as a resistance mechanism to camptothecin in tumor cells." Cancer research **61**(15): 5926-5932.

Diaz-Rubio, E., T. Evans, J. Tabernero, J. Cassidy, J. Sastre, M. Eatock, D. Bisset, P. Regueiro and J. Baselga (2002). "Capecitabine (Xeloda®) in combination with oxaliplatin: a phase I, dose-escalation study in patients with advanced or metastatic solid tumors." Annals of oncology **13**(4): 558-565.

Dienstmann, R., S. De Dosso, E. Felip and J. Tabernero (2012). "Drug development to overcome resistance to EGFR inhibitors in lung and colorectal cancer." Molecular oncology **6**(1): 15-26.

Drabovich, A. P., M. P. Pavlou, A. Dimitromanolakis and E. P. Diamandis (2012). "Quantitative analysis of energy metabolic pathways in MCF-7 breast cancer cells by selected reaction monitoring assay." Molecular & Cellular Proteomics **11**(8): 422-434.

Duckett, C. S., N. D. Perkins, T. F. Kowalik, R. M. Schmid, E. S. Huang, A. S. Baldwin and G. J. Nabel (1993). "Dimerization of NF-KB2 with RelA (p65) regulates DNA binding, transcriptional activation, and inhibition by an I kappa B-alpha (MAD-3)." Molecular and cellular biology **13**(3): 1315-1322.

Duvvuri, M. and J. P. Krise (2005). "Intracellular drug sequestration events associated with the emergence of multidrug resistance: a mechanistic review." Front Biosci **10**(2): 1499-1509.

Efferth, T. and M. Volm (2005). "Pharmacogenetics for individualized cancer chemotherapy." Pharmacology & therapeutics **107**(2): 155-176.

El-Akawi, Z., M. Abu-Hadid, R. Perez, J. Glavy, J. Zdanowicz, P. Creaven and L. Pendyala (1996). "Altered glutathione metabolism in oxaliplatin resistant ovarian carcinoma cells." Cancer letters **105**(1): 5-14.

Erenpreisa, J., K. Salmina, A. Huna, T. R. Jackson, A. Vazquez-Martin and M. S. Cragg (2015). "The “virgin birth”, polyploidy, and the origin of cancer." Oncoscience **2**(1): 3.

Eskelinen, E.-L. (2006). "Roles of LAMP-1 and LAMP-2 in lysosome biogenesis and autophagy." Molecular aspects of medicine **27**(5): 495-502.

Fanali, C., D. Lucchetti, M. Farina, M. Corbi, V. Cufino, A. Cittadini and A. Sgambato (2014). "Cancer stem cells in colorectal cancer from pathogenesis to therapy: controversies and perspectives." World J Gastroenterol **20**(4): 923-942.

Fansa, E. K. and A. Wittinghofer (2016). "Sorting of lipidated cargo by the Arl2/Arl3 system." Small GTPases **7**(4): 222-230.

Fedier, A., U. Ruefenacht, V. Schwarz, U. Haller and D. Fink (2002). "Increased sensitivity of p53-deficient cells to anticancer agents due to loss of Pms2." British journal of cancer **87**(9): 1027-1033.

Fentiman, I. (2012). "Gamma-glutamyl transferase: risk and prognosis of cancer." The British Journal of Cancer **106**(9): 1467.

Ferguson, R. E., H. P. Carroll, A. Harris, E. R. Maher, P. J. Selby and R. E. Banks (2005). "Housekeeping proteins: a preliminary study illustrating some limitations as useful references in protein expression studies." Proteomics **5**(2): 566-571.

Ferlay, J., I. Soerjomataram, R. Dikshit, S. Eser, C. Mathers, M. Rebelo, D. M. Parkin, D. Forman and F. Bray (2015). "Cancer incidence and mortality worldwide: sources, methods and major patterns in GLOBOCAN 2012." Int J Cancer **136**(5): E359-386.

Fodde, R., R. Smits and H. Clevers (2001). "APC, signal transduction and genetic instability in colorectal cancer." Nature Reviews Cancer **1**(1): 55-67.

Forsthoefel, A. M., M. M. O. Peña, Y. Y. Xing, Z. Rafique and F. G. Berger (2004). "Structural determinants for the intracellular degradation of human thymidylate synthase." Biochemistry **43**(7): 1972-1979.

Francke, F., R. J. Ward, L. Jenkins, E. Kellett, D. Richter, G. Milligan and D. Bächner (2006). "Interaction of neurochondrin with the melanin-concentrating hormone receptor 1 interferes with G protein-coupled signal transduction but not agonist-mediated internalization." Journal of Biological Chemistry **281**(43): 32496-32507.

Fu, D., J. A. Calvo and L. D. Samson (2012). "Balancing repair and tolerance of DNA damage caused by alkylating agents." Nat Rev Cancer **12**(2): 104-120.

Fu, H.-L., L. Shao, Q. Wang, T. Jia, M. Li and D.-P. Yang (2013). "A systematic review of p53 as a biomarker of survival in patients with osteosarcoma." Tumor Biology **34**(6): 3817-3821.

Fu, Y., G. Yang, F. Zhu, C. Peng, W. Li, H. Li, H.-G. Kim, A. M. Bode and Z. Dong (2014). "Antioxidants decrease the apoptotic effect of 5-Fu in colon cancer by regulating Src-dependent caspase-7 phosphorylation." Cell death & disease **5**(1): e983.

Fuertes, M. A., C. Alonso and J. M. Pérez (2003). "Biochemical modulation of cisplatin mechanisms of action: enhancement of antitumor activity and circumvention of drug resistance." Chemical reviews **103**(3): 645-662.

Fukushi, J.-i., I. T. Makagiansar and W. B. Stallcup (2004). "NG2 proteoglycan promotes endothelial cell motility and angiogenesis via engagement of galectin-3 and α3β1 integrin." Molecular biology of the cell **15**(8): 3580-3590.

Fulda, S. and K. Debatin (2006). "Extrinsic versus intrinsic apoptosis pathways in anticancer chemotherapy." Oncogene **25**(34): 4798-4811.

Furukawa, T., H. Kohno, R. Tokunaga and S. Taketani (1995). "Nitric oxide-mediated inactivation of mammalian ferrochelatase in vivo and in vitro: possible involvement of the iron-sulphur cluster of the enzyme." Biochemical Journal **310**(2): 533-538.

Gamcsik, M. P., M. S. Kasibhatla, S. D. Teeter and O. M. Colvin (2012). "Glutathione levels in human tumors." Biomarkers **17**(8): 671-691.

Gang, G.-T., Y.-H. Kim, J.-R. Noh, K.-S. Kim, J.-Y. Jung, M. Shong, J. H. Hwang and C.-H. Lee (2013). "Protective role of NAD (P) H: quinone oxidoreductase 1 (NQO1) in cisplatin-induced nephrotoxicity." Toxicology letters **221**(3): 165-175.

Gao, X., T. Sedgwick, Y.-B. Shi and T. Evans (1998). "Distinct functions are implicated for the GATA-4,-5, and-6 transcription factors in the regulation of intestine epithelial cell differentiation." Molecular and Cellular Biology **18**(5): 2901-2911.

Garcia-Rudaz, C., F. Luna, V. Tapia, B. Kerr, L. Colgin, F. Galimi, G. A. Dissen, N. D. Rawlings and S. R. Ojeda (2007). "Fxna, a novel gene differentially expressed in the rat ovary at the time of folliculogenesis, is required for normal ovarian histogenesis." Development **134**(5): 945-957.

Geiger, T., J. R. Wisniewski, J. Cox, S. Zanivan, M. Kruger, Y. Ishihama and M. Mann (2011). "Use of stable isotope labeling by amino acids in cell culture as a spike-in standard in quantitative proteomics." Nature protocols **6**(2): 147-157.

Geng, R., Z. Chen, X. Zhao, L. Qiu, X. Liu, R. Liu, W. Guo, G. He, J. Li and X. Zhu (2014). "Oxidative stress-related genetic polymorphisms are associated with the prognosis of metastatic gastric cancer patients treated with epirubicin, oxaliplatin and 5-fluorouracil combination chemotherapy." PloS one **9**(12): e116027.

Gentner, B., A. Wein, R. S. Croner, I. Zeittraeger, R. M. Wirtz, F. Roedel, A. Dimmler, L. Dorlaque, W. Hohenberger and E. G. Hahn (2009). "Differences in the gene expression profile of matrix metalloproteinases (MMPs) and their inhibitors (TIMPs) in primary colorectal tumors and their synchronous liver metastases." Anticancer research **29**(1): 67-74.

Ghosh, D., H. Yu, X. F. Tan, T. K. Lim, R. M. Zubaidah, H. T. Tan, M. C. Chung and Q. Lin (2011). "Identification of key players for colorectal cancer metastasis by iTRAQ quantitative proteomics profiling of isogenic SW480 and SW620 cell lines." Journal of proteome research **10**(10): 4373-4387.

Ghoshal, K. and S. T. Jacob (1994). "Specific inhibition of pre-ribosomal RNA processing in extracts from the lymphosarcoma cells treated with 5-fluorouracil." Cancer Res **54**(3): 632-636.

Gibson, S. L., L. Narayanan, D. C. Hegan, A. B. Buermeyer, R. M. Liskay and P. M. Glazer (2006). "Overexpression of the DNA mismatch repair factor, PMS2, confers hypermutability and DNA damage tolerance." Cancer letters **244**(2): 195-202.

Gillespie, J. G. and D. G. Hardie (1992). "Phosphorylation and inactivation of HMG-CoA reductase at the AMP-activated protein kinase site in response to fructose treatment of isolated rat hepatocytes." FEBS letters **306**(1): 59-62.

Gillis, A. J., A. P. Schuller and E. Skordalakes (2008). "Structure of the Tribolium castaneum telomerase catalytic subunit TERT." Nature **455**(7213): 633-637.

Ginés, A., S. Bystrup, V. R. de Porras, C. Guardia, E. Musulén, A. Martínez-Cardús, J. L. Manzano, L. Layos, A. Abad and E. Martínez-Balibrea (2015). "PKM2 subcellular localization is involved in oxaliplatin resistance acquisition in HT29 human colorectal cancer cell lines." PLoS One **10**(5): e0123830.

Giovanella, B. C., J. S. Stehlin, M. E. Wall, M. C. Wani, A. W. Nicholas, L. F. Liu, R. Silber and M. Potmesil (1989). "DNA topoisomerase I--targeted chemotherapy of human colon cancer in xenografts." Science **246**(4933): 1046-1048.

Goeman, J. J. and P. Bühlmann (2007). "Analyzing gene expression data in terms of gene sets: methodological issues." Bioinformatics **23**(8): 980-987.

Golomb, L., D. R. Bublik, S. Wilder, R. Nevo, V. Kiss, K. Grabusic, S. Volarevic and M. Oren (2012). "Importin 7 and exportin 1 link c-Myc and p53 to regulation of ribosomal biogenesis." Molecular cell **45**(2): 222-232.

Gottesman, M. M. (2002). "Mechanisms of cancer drug resistance." Annual review of medicine **53**(1): 615-627.

Gottesman, M. M. and I. Pastan (1993). "Biochemistry of multidrug resistance mediated by the multidrug transporter." Annual review of biochemistry **62**(1): 385-427.

Gourdier, I., L. Crabbe, K. Andreau, B. Pau and G. Kroemer (2004). "Oxaliplatin-induced mitochondrial apoptotic response of colon carcinoma cells does not require nuclear DNA." Oncogene **23**(45): 7449-7457.

Gourdier, I., M. Del Rio, L. Crabbé, L. Candeil, V. Copois, M. Ychou, C. Auffray, P. Martineau, N. Mechti and Y. Pommier (2002). "Drug specific resistance to oxaliplatin is associated with apoptosis defect in a cellular model of colon carcinoma." FEBS letters **529**(2-3): 232-236.

Grady, W. M. (2004). "Genomic instability and colon cancer." Cancer and Metastasis Reviews **23**(1-2): 11-27.

Greenman, C., P. Stephens, R. Smith, G. L. Dalgliesh, C. Hunter, G. Bignell, H. Davies, J. Teague, A. Butler and C. Stevens (2007). "Patterns of somatic mutation in human cancer genomes." Nature **446**(7132): 153-158.

Griffith, M., J. Mwenifumbo, P. Cheung, J. Paul, T. Pugh, M. Tang, S. Chittaranjan, R. Morin, J. Asano and A. Ally (2013). "Novel mRNA isoforms and mutations of uridine monophosphate synthetase and 5-fluorouracil resistance in colorectal cancer." The pharmacogenomics journal **13**(2): 148-158.

Grossi, V., A. Peserico, T. Tezil and C. Simone (2014). "p38α MAPK pathway: A key factor in colorectal cancer therapy and chemoresistance." World J Gastroenterol **20**(29): 9744-9758.

Group, F. C. (2012). "Feasibility of preoperative chemotherapy for locally advanced, operable colon cancer: the pilot phase of a randomised controlled trial." The Lancet Oncology **13**(11): 1152-1160.

Guan, H., P. Zhao, Z. Dai, X. Liu and X. Wang (2016). "SH3GL1 inhibition reverses multidrug resistance in colorectal cancer cells by downregulation of MDR1/P-glycoprotein via EGFR/ERK/AP-1 pathway." Tumor Biology **37**(9): 12153-12160.

Guichard, S., C. Terret, I. Hennebelle, I. Lochon, P. Chevreau, E. Fretigny, J. Selves, E. Chatelut, R. Bugat and R. Canal (1999). "CPT-11 converting carboxylesterase and topoisomerase I activities in tumour and normal colon and liver tissues." British journal of cancer **80**(3-4): 364.

Guizetti, J., L. Schermelleh, J. Mäntler, S. Maar, I. Poser, H. Leonhardt, T. Müller-Reichert and D. W. Gerlich (2011). "Cortical constriction during abscission involves helices of ESCRT-III–dependent filaments." Science **331**(6024): 1616-1620.

Guo, X., E. Goessl, G. JIN, E. S. COLLIE-DUGUID, J. CASSIDY, W. WANG and V. O'BRIEN (2008). "Cell cycle perturbation and acquired 5-fluorouracil chemoresistance." Anticancer research **28**(1A): 9-14.

Gupta, J., I. del Barco Barrantes, A. Igea, S. Sakellariou, I. S. Pateras, V. G. Gorgoulis and A. R. Nebreda (2014). "Dual function of p38α MAPK in colon cancer: suppression of colitis-associated tumor initiation but requirement for cancer cell survival." Cancer Cell **25**(4): 484-500.

Gupta, S., L. Cuffe, E. Szegezdi, S. E. Logue, C. Neary, S. Healy and A. Samali (2010). "Mechanisms of ER stress-mediated mitochondrial membrane permeabilization." International journal of cell biology **2010**.

Gustafsson, Å. B., J. G. Tsai, S. E. Logue, M. T. Crow and R. A. Gottlieb (2004). "Apoptosis repressor with caspase recruitment domain protects against cell death by interfering with Bax activation." Journal of Biological Chemistry **279**(20): 21233-21238.

Hammond, W. A., A. Swaika and K. Mody (2016). "Pharmacologic resistance in colorectal cancer: a review." Therapeutic advances in medical oncology **8**(1): 57-84.

Hanahan, D. and R. A. Weinberg (2000). "The hallmarks of cancer." Cell **100**(1): 57-70.

Hanahan, D. and R. A. Weinberg (2011). "Hallmarks of cancer: the next generation." Cell **144**(5): 646-674.

Hasegawa, K., S. Wakino, T. Tanaka, M. Kimoto, S. Tatematsu, T. Kanda, K. Yoshioka, K. Homma, N. Sugano and M. Kurabayashi (2006). "Dimethylarginine dimethylaminohydrolase 2

increases vascular endothelial growth factor expression through Sp1 transcription factor in endothelial cells." Arteriosclerosis, thrombosis, and vascular biology **26**(7): 1488-1494.

Hasegawa, N., K. Mizutani, T. Suzuki, T. Deguchi and Y. Nozawa (2006). "A comparative study of protein profiling by proteomic analysis in camptothecin-resistant PC3 and camptothecin-sensitive LNCaP human prostate cancer cells." Urologia internationalis **77**(4): 347-354.

Haugen, M. H., K. Boye, J. M. Nesland, S. J. Pettersen, E. V. Egeland, T. Tamhane, K. Brix, G. M. Maelandsmo and K. Flatmark (2015). "High expression of the cysteine proteinase legumain in colorectal cancer–Implications for therapeutic targeting." European journal of cancer **51**(1): 9-17.

Hediger, M. A., M. F. Romero, J.-B. Peng, A. Rolfs, H. Takanaga and E. A. Bruford (2004). "The ABCs of solute carriers: physiological, pathological and therapeutic implications of human membrane transport proteins." Pflügers Archiv **447**(5): 465-468.

Heinrich, J. C., S. Donakonda, V. J. Haupt, P. Lennig, Y. Zhang and M. Schroeder (2016). "New HSP27 inhibitors efficiently suppress drug resistance development in cancer cells." Oncotarget **7**(42): 68156-68169.

Herlevsen, M., G. Oxford, C. R. Owens, M. Conaway and D. Theodorescu (2007). "Depletion of major vault protein increases doxorubicin sensitivity and nuclear accumulation and disrupts its sequestration in lysosomes." Molecular Cancer Therapeutics **6**(6): 1804-1813.

Hervouet, E., M. Cheray, F. M. Vallette and P.-F. Cartron (2013). "DNA methylation and apoptosis resistance in cancer cells." Cells **2**(3): 545-573.

Hiraga, T., S. Ito and H. Nakamura (2013). "Cancer stem–like cell marker CD44 promotes bone metastases by enhancing tumorigenicity, cell motility, and hyaluronan production." Cancer research **73**(13): 4112-4122.

Hoff, P. M., R. Ansari, G. Batist, J. Cox, W. Kocha, M. Kuperminc, J. Maroun, D. Walde, C. Weaver and E. Harrison (2001). "Comparison of oral capecitabine versus intravenous fluorouracil plus leucovorin as first-line treatment in 605 patients with metastatic colorectal cancer: results of a randomized phase III study." Journal of Clinical Oncology **19**(8): 2282-2292.

Hopkins, S. and P. A. Gallay (2015). "The role of immunophilins in viral infection." Biochimica et Biophysica Acta (BBA)-General Subjects **1850**(10): 2103-2110.

Hosokawa, M., M. Saito, A. Nakano, S. Iwashita, A. Ishizaka, K. Ueda and S. Iwakawa (2015). "Acquired resistance to decitabine and cross-resistance to gemcitabine during the long-term treatment of human HCT116 colorectal cancer cells with decitabine." Oncology letters **10**(2): 761-767.

Housman, G., S. Byler, S. Heerboth, K. Lapinska, M. Longacre, N. Snyder and S. Sarkar (2014). "Drug resistance in cancer: an overview." Cancers **6**(3): 1769-1792.

Huang, V., J. Zheng, Z. Qi, J. Wang, R. F. Place, J. Yu, H. Li and L.-C. Li (2013). "Ago1 Interacts with RNA polymerase II and binds to the promoters of actively transcribed genes in human cancer cells." PLoS Genet **9**(9): e1003821.

Hudson, T. J., W. Anderson, A. Aretz, A. D. Barker, C. Bell, R. R. Bernabé, M. Bhan, F. Calvo, I. Eerola and D. S. Gerhard (2010). "International network of cancer genome projects." Nature **464**(7291): 993-998.

Hughes, P., D. Marshall, Y. Reid, H. Parkes and C. Gelber (2007). "The costs of using unauthenticated, over-passaged cell lines: how much more data do we need?" Biotechniques **43**(5): 575.

Hulme, A. T., S. L. Price and D. A. Tocher (2005). "A new polymorph of 5-fluorouracil found following computational crystal structure predictions." Journal of the American Chemical Society **127**(4): 1116-1117.

Hurd, T. W., L. Gao, M. H. Roh, I. G. Macara and B. Margolis (2003). "Direct interaction of two polarity complexes implicated in epithelial tight junction assembly." Nature cell biology **5**(2): 137-142.

Hurley, J. H. and P. I. Hanson (2010). "Membrane budding and scission by the ESCRT machinery: it's all in the neck." Nature reviews Molecular cell biology **11**(8): 556-566.

Husain, I., J. L. Mohler, H. F. Seigler and J. M. Besterman (1994). "Elevation of topoisomerase I messenger RNA, protein, and catalytic activity in human tumors: demonstration of tumor-type specificity and implications for cancer chemotherapy." Cancer research **54**(2): 539-546.

Hwang, G.-W., Y. Murai, T. Takahashi and A. Naganuma (2014). "The protein transportation pathway from Golgi to vacuoles via endosomes plays a role in enhancement of methylmercury toxicity." Scientific reports **4**: 5888.

Hwang, I. T., Y. M. Chung, J. J. Kim, J. S. Chung, B. S. Kim, H. J. Kim, J. S. Kim and Y. Do Yoo (2007). "Drug resistance to 5-FU linked to reactive oxygen species modulator 1." Biochemical and biophysical research communications **359**(2): 304-310.

Hwang, S. O., S. A. Boswell, J.-S. Seo and S. W. Lee (2008). "Novel oxidative stress-responsive gene ERS25 functions as a regulator of the heat-shock and cell death response." Journal of Biological Chemistry **283**(19): 13063-13069.

Iacovazzi, P. A., M. Notarnicola, M. G. Caruso, V. Guerra, S. Frisullo, D. F. Altomare and M. Correale (2010). "Serum levels of galectin-3 and its ligand 90k/mac-2bp in colorectal cancer patients." Immunopharmacology and immunotoxicology **32**(1): 160-164.

Iizuka, S., Y. Kudo, M. Yoshida, T. Tsunematsu, Y. Yoshiko, T. Uchida, I. Ogawa, M. Miyauchi and T. Takata (2011). "Ameloblastin regulates osteogenic differentiation by inhibiting Src kinase via cross talk between integrin β1 and CD63." Molecular and cellular biology **31**(4): 783-792.

Ilmer, M., N. Mazurek, J. C. Byrd, K. Ramirez, M. Hafley, E. Alt, J. Vykoukal and R. S. Bresalier (2016). "Cell surface galectin-3 defines a subset of chemoresistant gastrointestinal tumor-initiating cancer cells with heightened stem cell characteristics." Cell Death & Disease **7**(8): e2337.

Ismaili, N. (2011). "Treatment of colorectal liver metastases." World J Surg Oncol **9**: 154.

Jackson, C. E. (2016). "Mechanisms of Extracellular Vesicle Biogenesis."

Jafri, M. A., S. A. Ansari, M. H. Alqahtani and J. W. Shay (2016). "Roles of telomeres and telomerase in cancer, and advances in telomerase-targeted therapies." Genome medicine **8**(1): 69.

Jalilian, I., C. Heu, H. Cheng, H. Freittag, M. Desouza, J. R. Stehn, N. S. Bryce, R. M. Whan, E. C. Hardeman and T. Fath (2015). "Cell elasticity is regulated by the tropomyosin isoform composition of the actin cytoskeleton." PloS one **10**(5): e0126214.

Jankova, L., C. Chan, C. L. Fung, X. Song, S. Y. Kwun, M. J. Cowley, W. Kaplan, O. F. Dent, E. L. Bokey and P. H. Chapuis (2011). "Proteomic comparison of colorectal tumours and non-neoplastic mucosa from paired patient samples using iTRAQ mass spectrometry." Molecular Biosystems **7**(11): 2997-3005.

Ji, H., D. W. Greening, T. W. Barnes, J. W. Lim, B. J. Tauro, A. Rai, R. Xu, C. Adda, S. Mathivanan and W. Zhao (2013). "Proteome profiling of exosomes derived from human primary and

metastatic colorectal cancer cells reveal differential expression of key metastatic factors and signal transduction components." Proteomics **13**(10-11): 1672-1686.

Johnstone, R. W., A. A. Ruefli and S. W. Lowe (2002). "Apoptosis: a link between cancer genetics and chemotherapy." Cell **108**(2): 153-164.

Jung, J.-J., H.-C. Jeung, J. O. Lee, T. S. Kim, H. C. Chung and S. Y. Rha (2007). "Putative chemosensitivity predictive genes in colorectal cancer cell lines for anticancer agents." Oncology reports **18**(3): 593-599.

Kahn, R. A. and A. G. Gilman (1986). "The Protein Cofactor Necessary for Adp-Ribosylation of Gs by Cholera-Toxin Is Itself a Gtp Binding-Protein." Journal of Biological Chemistry **261**(17): 7906-7911.

Kaller, M., S.-T. Liffers, S. Oeljeklaus, K. Kuhlmann, S. Röh, R. Hoffmann, B. Warscheid and H. Hermeking (2011). "Genome-wide characterization of miR-34a induced changes in protein and mRNA expression by a combined pulsed SILAC and microarray analysis." Molecular & Cellular Proteomics **10**(8): M111. 010462.

Kammers, K., R. N. Cole, C. Tiengwe and I. Ruczinski (2015). "Detecting significant changes in protein abundance." EuPA open proteomics **7**: 11-19.

Kerr, S. L., T. Shoeib and B. L. Sharp (2008). "A study of oxaliplatin–nucleobase interactions using ion trap electrospray mass spectrometry." Analytical and bioanalytical chemistry **391**(6): 2339-2348.

Khalili, A. A. and M. R. Ahmad (2015). "A review of cell adhesion studies for biomedical and biological applications." International journal of molecular sciences **16**(8): 18149-18184.

Kikuchi, A., K. Kaibuchi, Y. Hori, H. Nonaka, T. Sakoda, M. Kawamura, T. Mizuno and Y. Takai (1992). "Molecular cloning of the human cDNA for a stimulatory GDP/GTP exchange protein for c-Ki-ras p21 and smg p21." Oncogene **7**(2): 289-293.

Kim, H.-J., D. Lin, M. Li and D. C. Liebler (2015). "Quantitative profiling of protein tyrosine kinases in human cancer cell lines by multiplexed parallel reaction monitoring assays." Molecular & Cellular Proteomics: mcp. O115. 051813.

Kim, H. and J. Chen (2008). "New players in the BRCA1-mediated DNA damage responsive pathway." Molecules and cells **25**(4): 457.

Kim, M. S., J. E. Oh, Y. R. Kim, S. W. Park, M. R. Kang, S. S. Kim, C. H. Ahn, N. J. Yoo and S. H. Lee (2010). "Somatic mutations and losses of expression of microRNA regulation-related genes AGO2 and TNRC6A in gastric and colorectal cancers." The Journal of pathology **221**(2): 139-146.

Kimhi, O., L. Drucker, A. Neumann, H. Shapiro, J. Shapira, S. Yarkoni, M. Lahav, J. Radnay and M. Lishner (2004). "Fluorouracil induces apoptosis and surface molecule modulation of peripheral blood leukocytes." Clinical & Laboratory Haematology **26**(5): 327-333.

Kline, C. L. B. and R. B. Irby (2011). "The pro-apoptotic protein Prostate Apoptosis Response Protein-4 (Par-4) can be activated in colon cancer cells by treatment with Src inhibitor and 5-FU." Apoptosis **16**(12): 1285.

Klingbiel, D., Z. Saridaki, A. Roth, F. Bosman, M. Delorenzi and S. Tejpar (2015). "Prognosis of stage II and III colon cancer treated with adjuvant 5-fluorouracil or FOLFIRI in relation to microsatellite status: results of the PETACC-3 trial." Annals of Oncology **26**(1): 126-132.

Komatsu, M., T. Sumizawa, M. Mutoh, Z.-S. Chen, K. Terada, T. Furukawa, X.-L. Yang, H. Gao, N. Miura and T. Sugiyama (2000). "Copper-transporting P-type adenosine triphosphatase (ATP7B) is associated with cisplatin resistance." Cancer research **60**(5): 1312-1316.

Kramer, R., T. Weber, B. Morse, R. Arceci, R. Staniunas, G. Steele and I. Summerhayes (1993). "Constitutive expression of multidrug resistance in human colorectal tumours and cell lines." British journal of cancer **67**(5): 959-968.

Kreso, A., C. A. O'Brien, P. van Galen, O. I. Gan, F. Notta, A. M. Brown, K. Ng, J. Ma, E. Wienholds and C. Dunant (2013). "Variable clonal repopulation dynamics influence chemotherapy response in colorectal cancer." Science **339**(6119): 543-548.

Kufe, D. W. (2009). "Mucins in cancer: function, prognosis and therapy." Nature Reviews Cancer **9**(12): 874-885.

Kufe, D. W., R. E. Pollock, R. R. Weichselbaum, R. C. Bast, T. S. Gansler, J. F. Holland and E. Frei (2003). "Holland-Frei cancer medicine."

Kugimiya, N., A. Nishimoto, T. Hosoyama, K. Ueno, T. Enoki, T. S. Li and K. Hamano (2015). "The c-MYC-ABCB5 axis plays a pivotal role in 5-fluorouracil resistance in human colon cancer cells." Journal of cellular and molecular medicine **19**(7): 1569-1581.

Kumar, P., D.-M. Zhang, K. Degenhardt and Z.-S. Chen (2012). "Autophagy and transporter-based multi-drug resistance." Cells **1**(3): 558-575.

Kuo, M. T. (2009). "Redox regulation of multidrug resistance in cancer chemotherapy: molecular mechanisms and therapeutic opportunities." Antioxidants & redox signaling **11**(1): 99-133.

Kuranaga, N., N. Shinomiya and H. Mochizuki (2001). "Long-term cultivation of colorectal carcinoma cells with anti-cancer drugs induces drug resistance and telomere elongation: an in vitro study." BMC cancer **1**(1): 10.

Kweekel, D., H. Gelderblom and H.-J. Guchelaar (2005). "Pharmacology of oxaliplatin and the use of pharmacogenomics to individualize therapy." Cancer treatment reviews **31**(2): 90-105.

Lachner, M., R. J. O'Sullivan and T. Jenuwein (2003). "An epigenetic road map for histone lysine methylation." Journal of cell science **116**(11): 2117-2124.

Lacy, A. M., J. C. Garcia-Valdecasas, S. Delgado, A. Castells, P. Taura, J. M. Pique and J. Visa (2002). "Laparoscopy-assisted colectomy versus open colectomy for treatment of non-metastatic colon cancer: a randomised trial." Lancet **359**(9325): 2224-2229.

Latysheva, N., G. Muratov, S. Rajesh, M. Padgett, N. A. Hotchin, M. Overduin and F. Berditchevski (2006). "Syntenin-1 is a new component of tetraspanin-enriched microdomains: mechanisms and consequences of the interaction of syntenin-1 with CD63." Molecular and cellular biology **26**(20): 7707-7718.

Lau, H.-T., H. W. Suh, M. Golkowski and S.-E. Ong (2014). "Comparing SILAC-and stable isotope dimethyl-labeling approaches for quantitative proteomics." Journal of proteome research **13**(9): 4164-4174.

Lee, A.-R., J. Park, K. J. Jung, S. H. Jee and S. Kim-Yoon (2016). "genetic variation rs7930 in the mir-4273-5p target site is associated with a risk of colorectal cancer." OncoTargets and therapy **9**: 6885.

Lee, S.-Y., R. Meier, S. Furuta, M. E. Lenburg, P. A. Kenny, R. Xu and M. J. Bissell (2012). "FAM83A confers EGFR-TKI resistance in breast cancer cells and in mice." The Journal of clinical investigation **122**(9): 3211-3220.

Lee, S. Y., J. M. Kim, S. Y. Cho, H. S. Kim, H. S. Shin, J. Y. Jeon, R. Kausar, S. Y. Jeong, Y. S. Lee and M. A. Lee (2014). "TIMP-1 modulates chemotaxis of human neural stem cells through CD63 and integrin signalling." Biochemical Journal **459**(3): 565-576.

Lengauer, C., K. W. Kinzler and B. Vogelstein (1998). "Genetic instabilities in human cancers." Nature **396**(6712): 643-649.

Leung, E. Y., J. E. Kim, M. Askarian-Amiri, W. R. Joseph, M. J. McKeage and B. C. Baguley (2014). "Hormone resistance in two MCF-7 breast cancer cell lines is associated with reduced mTOR signaling, decreased glycolysis, and increased sensitivity to cytotoxic drugs." Frontiers in oncology **4**: 221.

Leyva, J. A., M. A. Bianchet and L. M. Amzel (2003). "Understanding ATP synthesis: structure and mechanism of the F1-ATPase (Review)." Molecular membrane biology **20**(1): 27-33.

Li, J., N. Hou, A. Faried, S. Tsutsumi and H. Kuwano (2010). "Inhibition of autophagy augments 5-fluorouracil chemotherapy in human colon cancer in vitro and in vivo model." European Journal of Cancer **46**(10): 1900-1909.

Li, Q. and Y. Shu (2014). "Role of solute carriers in response to anticancer drugs." Molecular and cellular therapies **2**(1): 1.

Li, S.-R., V. G. Gyselman, S. Dorudi and S. A. Bustin (2000). "Elevated levels of RanBP7 mRNA in colorectal carcinoma are associated with increased proliferation and are similar to the transcription pattern of the proto-oncogene c-myc." Biochemical and biophysical research communications **271**(2): 537-543.

Li, S., J. Finley, Z.-J. Liu, S.-H. Qiu, H. Chen, C.-H. Luan, M. Carson, J. Tsao, D. Johnson and G. Lin (2002). "Crystal structure of the cytoskeleton-associated protein glycine-rich (CAP-Gly) domain." Journal of Biological Chemistry **277**(50): 48596-48601.

Li, X.-L., J. Zhou, Z.-R. Chen and W.-J. Chng (2015). "p53 mutations in colorectal cancer-molecular pathogenesis and pharmacological reactivation." World J Gastroenterol **21**(1): 84-93.

Li, Y., Q. Zhang, R. Tian, Q. Wang, J. J. Zhao, J. D. Iglehart, Z. C. Wang and A. L. Richardson (2011). "Lysosomal transmembrane protein LAPTM4B promotes autophagy and tolerance to metabolic stress in cancer cells." Cancer research **71**(24): 7481-7489.

Liu, L. and J. Ruan (2013). Network-based pathway enrichment analysis. Bioinformatics and Biomedicine (BIBM), 2013 IEEE International Conference on, IEEE.

Liu, L. and W. Xu (2013). "The Role of Nitric Oxide in Cancer Cell DNA Repair, Hypoxia Adaptation and Drug Resistance." Single Cell Biol **2**(103): 2.

Liu, L. F., S. D. Desai, T. K. LI, Y. Mao, M. Sun and S. P. SIM (2000). "Mechanism of action of camptothecin." Annals of the New York Academy of Sciences **922**(1): 1-10.

Liu, W., Y. Fang, X.-T. Wang, J. Liu, X. Dan and L.-L. Sun (2014). "Overcoming 5-Fu resistance of colon cells through inhibition of Glut1 by the specific inhibitor WZB117." Asian Pac J Cancer Prev **15**(17): 7037-7041.

Liu, Y.-Y., V. Gupta, G. A. Patwardhan, K. Bhinge, Y. Zhao, J. Bao, H. Mehendale, M. C. Cabot, Y.-T. Li and S. M. Jazwinski (2010). "Glucosylceramide synthase upregulates MDR1 expression in the regulation of cancer drug resistance through cSrc and β-catenin signaling." Molecular cancer **9**(1): 1.

Liu, Y.-y., T.-y. Han, A. E. Giuliano and M. C. CABOT (2001). "Ceramide glycosylation potentiates cellular multidrug resistance." The FASEB Journal **15**(3): 719-730.

Liu, Y.-Y. and Y.-T. Li (2013). "Ceramide glycosylation catalyzed by glucosylceramide synthase and cancer drug resistance." Advances in cancer research **117**: 59.

Liwak, U., L. E. Jordan, S. D. Von-Holt, P. Singh, J. Hanson, I. A. Lorimer, F. Roncaroli and M. Holcik (2013). "Loss of PDCD4 contributes to enhanced chemoresistance in Glioblastoma multiforme through de-repression of Bcl-xL translation." Oncotarget **4**(9): 1365-1372.

Lliakis, G. (1991). "The role of DNA double strand breaks in lonizing radiation-induced killing of eukaryotic cells." Bioessays **13**(12): 641-648.

Longey, D. (2003). "5-fluorouracil—mechanisms of action and clinical strategies. ." Nature Reviews Cancer **3**: 330-338.

Longley, D. and P. Johnston (2005). "Molecular mechanisms of drug resistance." The Journal of pathology **205**(2): 275-292.

López-Rodríguez, C., J. Aramburu, L. Jin, A. S. Rakeman, M. Michino and A. Rao (2001). "Bridging the NFAT and NF-κB families: NFAT5 dimerization regulates cytokine gene transcription in response to osmotic stress." Immunity **15**(1): 47-58.

Loupakis, F., A. Ruzzo, C. Cremolini, B. Vincenzi, L. Salvatore, D. Santini, G. Masi, I. Stasi, E. Canestrari and E. Rulli (2009). "KRAS codon 61, 146 and BRAF mutations predict resistance to cetuximab plus irinotecan in KRAS codon 12 and 13 wild-type metastatic colorectal cancer." British journal of cancer **101**(4): 715-721.

Lu, H., C. Sun, T. Zhou, B. Zhou, E. Guo, W. Shan, M. Xia, K. Li, D. Weng and L. Meng (2016). "HSP27 Knockdown Increases Cytoplasmic p21 and Cisplatin Sensitivity in Ovarian Carcinoma Cells." Oncology Research Featuring Preclinical and Clinical Cancer Therapeutics **23**(3): 119-128.

Lu, S.-Z. and D. D. Harrison-Findik (2013). "Autophagy and cancer." World J Biol Chem **4**(3): 64-70.

Ly, T., Y. Ahmad, A. Shlien, D. Soroka, A. Mills, M. J. Emanuele, M. R. Stratton and A. I. Lamond (2014). "A proteomic chronology of gene expression through the cell cycle in human myeloid leukemia cells." Elife **3**: e01630.

Ma, Y., J. Kong, G. Yan, X. Ren, D. Jin, T. Jin, L. Lin and Z. Lin (2014). "NQO1 overexpression is associated with poor prognosis in squamous cell carcinoma of the uterine cervix." BMC cancer **14**(1): 414.

Maeda, O., T. Ando, N. Ohmiya, K. Ishiguro, O. Watanabe, R. Miyahara, Y. Hibi, T. Nagai, K. Yamada and H. Goto (2014). "Alteration of gene expression and DNA methylation in drug-resistant gastric cancer." Oncology reports **31**(4): 1883-1890.

Mahalingam, D., E. Szegezdi, M. Keane, S. de Jong and A. Samali (2009). "TRAIL receptor signalling and modulation: Are we on the right TRAIL?" Cancer treatment reviews **35**(3): 280-288.

Mahmoudi, S., S. Henriksson, M. Corcoran, C. Méndez-Vidal, K. G. Wiman and M. Farnebo (2016). "Wrap53, a Natural p53 Antisense Transcript Required for p53 Induction upon DNA Damage." Molecular Cell **64**(5): 1009.

Maliepaard, M., M. A. van Gastelen, A. Tohgo, F. H. Hausheer, R. C. van Waardenburg, L. A. de Jong, D. Pluim, J. H. Beijnen and J. H. Schellens (2001). "Circumvention of breast cancer resistance protein (BCRP)-mediated resistance to camptothecins in vitro using non-substrate drugs or the BCRP inhibitor GF120918." Clinical Cancer Research **7**(4): 935-941.

Malilas, W., S. S. Koh, S. Kim, R. Srisuttee, I.-R. Cho, J. Moon, H.-S. Yoo, S. Oh, R. N. Johnston and Y.-H. Chung (2013). "Cancer upregulated gene 2, a novel oncogene, enhances migration and drug resistance of colon cancer cells via STAT1 activation." International journal of oncology **43**(4): 1111-1116.

Marchetti, A., N. Tinari, F. Buttitta, A. Chella, C. A. Angeletti, R. Sacco, F. Mucilli, A. Ullrich and S. Iacobelli (2002). "Expression of 90K (Mac-2 BP) correlates with distant metastasis and predicts survival in stage I non-small cell lung cancer patients." Cancer research **62**(9): 2535-2539.

Margolin, A. A., S.-E. Ong, M. Schenone, R. Gould, S. L. Schreiber, S. A. Carr and T. R. Golub (2009). "Empirical Bayes analysis of quantitative proteomics experiments." PLoS One **4**(10): e7454.

Marks, P. A., R. A. Rifkind, V. M. Richon, R. Breslow, T. Miller and W. K. Kelly (2001). "Histone deacetylases and cancer: causes and therapies." Nature Reviews Cancer **1**(3): 194-202.

Martherus, R. S. R. M., W. Sluiter, E. D. J. Timmer, S. J. V. VanHerle, H. J. M. Smeets and T. A. Y. Ayoubi (2010). "Functional annotation of heart enriched mitochondrial genes GBAS and CHCHD10 through guilt by association." Biochemical and Biophysical Research Communications **402**(2): 203-208.

Martinez-Cardús, A., E. Martinez-Balibrea, E. Bandrés, R. Malumbres, A. Ginés, J. L. Manzano, M. Taron, J. Garcia-Foncillas and A. Abad (2009). "Pharmacogenomic approach for the identification of novel determinants of acquired resistance to oxaliplatin in colorectal cancer." Molecular cancer therapeutics **8**(1): 194-202.

Martinez-Balibrea, E., A. Martínez-Cardús, E. Musulén, A. Ginés, J. L. Manzano, E. Aranda, C. Plasencia, N. Neamati and A. Abad (2009). "Increased levels of copper efflux transporter ATP7B are associated with poor outcome in colorectal cancer patients receiving oxaliplatin-based chemotherapy." International Journal of Cancer **124**(12): 2905-2910.

Maruyama, K. (2011). "Intracellular targeting delivery of liposomal drugs to solid tumors based on EPR effects." Advanced drug delivery reviews **63**(3): 161-169.

Mathivanan, S., M. Ahmed, N. G. Ahn, H. Alexandre, R. Amanchy, P. C. Andrews, J. S. Bader, B. M. Balgley, M. Bantscheff and K. L. Bennett (2008). "Human Proteinpedia enables sharing of human protein data." Nature biotechnology **26**(2): 164-167.

Mathonnet, M., A. Perraud, N. Christou, H. Akil, C. Melin, S. Battu, M. O. Jauberteau and Y. Denizot (2014). "Hallmarks in colorectal cancer: angiogenesis and cancer stem-like cells." World J Gastroenterol **20**(15): 4189-4196.

Matsunaga, A., Y. Ishii, M. Tsuruta, K. Okabayashi, H. Hasegawa and Y. Kitagawa (2014). "Inhibition of heat shock protein 27 phosphorylation promotes sensitivity to 5‐fluorouracil in colorectal cancer cells." Oncology letters **8**(6): 2496-2500.

McLeod, H. L. and W. E. Evans (2001). "Pharmacogenomics: unlocking the human genome for better drug therapy." Annual review of pharmacology and toxicology **41**(1): 101-121.

Mechetner, E., A. Kyshtoobayeva, S. Zonis, H. Kim, R. Stroup, R. Garcia, R. J. Parker and J. P. Fruehauf (1998). "Levels of multidrug resistance (MDR1) P-glycoprotein expression by human breast cancer correlate with in vitro resistance to taxol and doxorubicin." Clinical Cancer Research **4**(2): 389-398.

Medico, E., M. Russo, G. Picco, C. Cancelliere, E. Valtorta, G. Corti, M. Buscarino, C. Isella, S. Lamba and B. Martinoglio (2015). "The molecular landscape of colorectal cancer cell lines unveils clinically actionable kinase targets." Nature communications **6**: 7002.

Mhaidat, N. M., M. Bouklihacene and R. F. Thorne (2014). "5‐Fluorouracil‐induced apoptosis in colorectal cancer cells is caspase‐9‐dependent and mediated by activation of protein kinase C‐δ." Oncology letters **8**(2): 699-704.

Milano, G., M. Etienne, V. Pierrefite, M. Barberi-Heyob, R. Deporte-Fety and N. Renée (1999). "Dihydropyrimidine dehydrogenase deficiency and fluorouracil-related toxicity." British journal of cancer **79**(3-4): 627.

Miller, W. L. and R. J. Auchus (2010). "The molecular biology, biochemistry, and physiology of human steroidogenesis and its disorders." Endocrine reviews **32**(1): 81-151.

Mondal, T., D. Pal, M. Bhadra and U. Bhadra (2016). "Argonaute-1 Machinery Silent Cancer Noises." Can surg **1**(102): 28-30.

Moore, N., J. Houghton and S. Lyle (2011). "Slow-cycling therapy-resistant cancer cells." Stem cells and development **21**(10): 1822-1830.

Morin, P. J. (2003). "Drug resistance and the microenvironment: nature and nurture." Drug Resistance Updates **6**(4): 169-172.

Mossink, M. H., A. van Zon, R. J. Scheper, P. Sonneveld and E. A. Wiemer (2003). "Vaults: a ribonucleoprotein particle involved in drug resistance?" Oncogene **22**(47): 7458-7467.

Mueller, S. C., G. Ghersi, S. K. Akiyama, Q.-X. A. Sang, L. Howard, M. Pineiro-Sanchez, H. Nakahara, Y. Yeh and W.-T. Chen (1999). "A novel protease-docking function of integrin at invadopodia." Journal of Biological Chemistry **274**(35): 24947-24952.

Muhale, F. A., B. A. Wetmore, R. S. Thomas and H. L. McLeod (2011). "Systems pharmacology assessment of the 5-fluorouracil pathway." Pharmacogenomics **12**(3): 341-350.

Muller, P. A. and K. H. Vousden (2013). "p53 mutations in cancer." Nature cell biology **15**(1): 2-8.

Murai, J., N. H. Shar-yin, B. B. Das, A. Renaud, Y. Zhang, J. H. Doroshow, J. Ji, S. Takeda and Y. Pommier (2012). "Trapping of PARP1 and PARP2 by clinical PARP inhibitors." Cancer research **72**(21): 5588-5599.

Nagai, H., A. Yabe, N. Mine, I. Mikami, H. Fujiwara, Y. Terada, A. Hirano, M. Tsuneizumi, T. Yokota and M. Emi (2003). "Down-regulation in human cancers of DRHC, a novel helicase-like gene from 17q25. 1 that inhibits cell growth." Cancer letters **193**(1): 41-47.

Nakajo, A., S.-i. Yoshimura, H. Togawa, M. Kunii, T. Iwano, A. Izumi, Y. Noguchi, A. Watanabe, A. Goto and T. Sato (2016). "EHBP1L1 coordinates Rab8 and Bin1 to regulate apical-directed transport in polarized epithelial cells." J Cell Biol **212**(3): 297-306.

Nakamura, T., M. Komiya, K. Sone, E. Hirose, N. Gotoh, H. Morii, Y. Ohta and N. Mori (2002). "Grit, a GTPase-activating protein for the Rho family, regulates neurite extension through association with the TrkA receptor and N-Shc and CrkL/Crk adapter molecules." Molecular and cellular biology **22**(24): 8721-8734.

Nakanishi, T. and D. D. Ross (2012). "Breast cancer resistance protein (BCRP/ABCG2): its role in multidrug resistance and regulation of its gene expression." Chinese journal of cancer **31**(2): 73.

Nakase, I., N. B. Kobayashi, T. Takatani-Nakase and T. Yoshida (2015). "Active macropinocytosis induction by stimulation of epidermal growth factor receptor and oncogenic Ras expression potentiates cellular uptake efficacy of exosomes." Scientific reports **5**: 10300.

Natalia Silva, P., T. K. Furuya, I. Sampaio Braga, L. T. Rasmussen, R. W. de Labio, P. H. Bertolucci, E. S. Chen, G. Turecki, N. Mechawar and S. L. Payao (2013). "CNP and DPYSL2 mRNA expression and promoter methylation levels in brain of Alzheimer's disease patients." Journal of Alzheimer's Disease **33**(2): 349-355.

Nelson, M. R., D. Wegmann, M. G. Ehm, D. Kessner, P. S. Jean, C. Verzilli, J. Shen, Z. Tang, S.-A. Bacanu and D. Fraser (2012). "An abundance of rare functional variants in 202 drug target genes sequenced in 14,002 people." Science **337**(6090): 100-104.

Nguyen, C. T., D. J. Weisenberger, M. Velicescu, F. A. Gonzales, J. C. Lin, G. Liang and P. A. Jones (2002). "Histone H3-lysine 9 methylation is associated with aberrant gene silencing in cancer cells and is rapidly reversed by 5-aza-2'-deoxycytidine." Cancer research **62**(22): 6456-6461.

Nguyen, H. D., I. Wood and M. M. Hill (2012). "A robust permutation test for quantitative SILAC proteomics experiments." Journal of Integrated OMICS **2**(2): 80-93.

Nilsen, T. W. and B. R. Graveley (2010). "Expansion of the eukaryotic proteome by alternative splicing." Nature **463**(7280): 457-463.

Niture, S. K. and A. K. Jaiswal (2012). "Nrf2 protein up-regulates antiapoptotic protein Bcl-2 and prevents cellular apoptosis." Journal of Biological Chemistry **287**(13): 9873-9886.

Nogales-Gadea, G., E. Mormeneo, I. García-Consuegra, J. C. Rubio, A. Orozco, J. Arenas, M. A. Martín, A. Lucia, A. M. Gomez-Foix and R. Martí (2010). "Expression of glycogen phosphorylase isoforms in cultured muscle from patients with McArdle's disease carrying the p. R771PfsX33 PYGM mutation." PLoS One **5**(10): e13164.

Nordlinger, B., H. Sorbye, B. Glimelius, G. J. Poston, P. M. Schlag, P. Rougier, W. O. Bechstein, J. N. Primrose, E. T. Walpole, M. Finch-Jones, D. Jaeck, D. Mirza, R. W. Parks, L. Collette, M. Praet, U. Bethe, E. Van Cutsem, W. Scheithauer, T. Gruenberger, E. G.-I. T. C. Group, U. K. Cancer Research, O. Arbeitsgruppe Lebermetastasen und-tumoren in der Chirurgischen Arbeitsgemeinschaft, G. Australasian Gastro-Intestinal Trials and D. Federation Francophone de Cancerologie (2008). "Perioperative chemotherapy with FOLFOX4 and surgery versus surgery alone for resectable liver metastases from colorectal cancer (EORTC Intergroup trial 40983): a randomised controlled trial." Lancet **371**(9617): 1007-1016.

O'Farrell, P. H. (1975). "High resolution two-dimensional electrophoresis of proteins." J Biol Chem **250**(10): 4007-4021.

Obita, T., S. Saksena, S. Ghazi-Tabatabai, D. J. Gill, O. Perisic, S. D. Emr and R. L. Williams (2007). "Structural basis for selective recognition of ESCRT-III by the AAA ATPase Vps4." Nature **449**(7163): 735-739.

Oda, K., T. Shiratsuchi, H. Nishimori, J. Inazawa, H. Yoshikawa, Y. Taketani, Y. Nakamura and T. Tokino (1999). "Identification of BAIAP2 (BAI-associated protein 2), a novel human homologue of hamster IRSp53, whose SH3 domain interacts with the cytoplasmic domain of BAI1." Cytogenetic and Genome Research **84**(1-2): 75-82.

Oh, Y. S., E. J. Na and M. C. Gye (2016). "Effects of bilateral vasectomy on the interleukin 1 system in mouse epididymis." American Journal of Reproductive Immunology **76**(3): 235-242.

Okato, A., Y. Goto, A. Kurozumi, M. Kato, S. Kojima, R. Matsushita, M. Yonemori, K. Miyamoto, T. Ichikawa and N. Seki (2016). "Direct regulation of LAMP1 by tumor-suppressive microRNA-320a in prostate cancer." International journal of oncology **49**(1): 111-122.

Okazaki, F., N. Matsunaga, H. Okazaki, N. Utoguchi, R. Suzuki, K. Maruyama, S. Koyanagi and S. Ohdo (2010). "Circadian rhythm of transferrin receptor 1 gene expression controlled by c-Myc in colon cancer–bearing mice." Cancer research **70**(15): 6238-6246.

Olive, P. L. (1998). "The role of DNA single- and double-strand breaks in cell killing by ionizing radiation." Radiat Res **150**(5 Suppl): S42-51.

Olovnikov, A. M. (1996). "Telomeres, telomerase, and aging: origin of the theory." Experimental gerontology **31**(4): 443-448.

Ong, S.-E. and M. Mann (2006). "A practical recipe for stable isotope labeling by amino acids in cell culture (SILAC)." Nature protocols **1**(6): 2650-2660.

Ostrowski, M., N. B. Carmo, S. Krumeich, I. Fanget, G. Raposo, A. Savina, C. F. Moita, K. Schauer, A. N. Hume and R. P. Freitas (2010). "Rab27a and Rab27b control different steps of the exosome secretion pathway." Nature cell biology **12**(1): 19-30.

Paillas, S., F. Boissière, F. Bibeau, A. Denouel, C. Mollevi, A. Causse, V. Denis, N. Vezzio-Vié, L. Marzi and C. Cortijo (2011). "Targeting the p38 MAPK pathway inhibits irinotecan resistance in colon adenocarcinoma." Cancer research **71**(3): 1041-1049.

Paillas, S., A. Causse, L. Marzi, P. De Medina, M. Poirot, V. Denis, N. Vezzio-Vie, L. Espert, H. Arzouk and A. Coquelle (2012). "MAPK14/p38α confers irinotecan resistance to TP53-defective cells by inducing survival autophagy." Autophagy **8**(7): 1098-1112.

Palaniappan, A., K. Ramar and S. Ramalingam (2016). "Computational Identification of Novel Stage-Specific Biomarkers in Colorectal Cancer Progression." PloS one **11**(5): e0156665.

Pandey, P., B. Sliker, H. L. Peters, A. Tuli, J. Herskovitz, K. Smits, A. Purohit, R. K. Singh, J. Dong and S. K. Batra (2016). "Amyloid precursor protein and amyloid precursor-like protein 2 in cancer." Oncotarget **7**(15): 19430.

Park, C., K.-h. Yoon, Y.-J. Lee, Y.-K. Kim, Y.-C. Choi, J.-H. Shin, J.-H. Cho and R. Park (2002). "5-FU Induces Apoptosis of Fas (+), HepG2 Cells Via Activation of Fas-mediated Caspase and Mitochondria Dysfunction." Cancer Res Treat **34**: 128-138.

Paschall, A. V., D. Yang, C. Lu, P. S. Redd, J. H. Choi, C. M. Heaton, J. R. Lee, A. Nayak-Kapoor and K. Liu (2016). "CD133+CD24lo defines a 5-Fluorouracil-resistant colon cancer stem cell-like phenotype." Oncotarget **7**(48): 78698-78712.

Peña, K., J. Coblenz and K. Kiselyov (2015). "Brief exposure to copper activates lysosomal exocytosis." Cell calcium **57**(4): 257-262.

Peng, X., F. M. Gong, M. Ren, P. Ai, S. Wu, J. Tang and X. Hu (2016). "Proteomic analysis of docetaxel resistance in human nasopharyngeal carcinoma cells using the two-dimensional gel electrophoresis method." Anti-Cancer Drugs **27**(8): 748-755.

Pentheroudakis, G. and C. Twelves (2002). "Capecitabine (Xeloda®): From the Laboratory to the Patient's Home." Clinical colorectal cancer **2**(1): 16-23.

Perez-Herrero, E. and A. Fernandez-Medarde (2015). "Advanced targeted therapies in cancer: Drug nanocarriers, the future of chemotherapy." Eur J Pharm Biopharm **93**: 52-79.

Peters, G., H. Backus, S. Freemantle, B. Van Triest, G. Codacci-Pisanelli, C. Van der Wilt, K. Smid, J. Lunec, A. Calvert and S. Marsh (2002). "Induction of thymidylate synthase as a 5-fluorouracil resistance mechanism." Biochimica et Biophysica Acta (BBA)-Molecular Basis of Disease **1587**(2): 194-205.

Peters, H. L., Y. Yan and J. C. Solheim (2013). "APLP2 regulates the expression of MHC class I molecules on irradiated Ewing's sarcoma cells." Oncoimmunology **2**(10): e26293.

Petitjean, A., E. Mathe, S. Kato, C. Ishioka, S. V. Tavtigian, P. Hainaut and M. Olivier (2007). "Impact of mutant p53 functional properties on TP53 mutation patterns and tumor phenotype:

lessons from recent developments in the IARC TP53 database." Human mutation **28**(6): 622-629.

Petrosyan, A. (2015). "Onco-Golgi: is fragmentation a gate to cancer progression?" Biochemistry & molecular biology journal **1**(1).

Pettigrew, M., P. Kavan, L. Surprenant and H. Lim (2016). "Comparative net cost impact of the utilization of panitumumab versus cetuximab for the treatment of patients with metastatic colorectal cancer in Canada." Journal of medical economics **19**(2): 145-157.

Piccolini, V. M., M. G. Bottone, G. Bottiroli, S. A. De Pascali, F. P. Fanizzi and G. Bernocchi (2013). "Platinum drugs and neurotoxicity: effects on intracellular calcium homeostasis." Cell biology and toxicology **29**(5): 339-353.

Piccolo, E., N. Tinari, D. D'Addario, C. Rossi, V. Iacobelli, R. La Sorda, R. Lattanzio, M. D'Egidio, A. Di Risio and M. Piantelli (2015). "Prognostic relevance of LGALS3BP in human colorectal carcinoma." Journal of translational medicine **13**(1): 248.

Pino, M. S. and D. C. Chung (2010). "The chromosomal instability pathway in colon cancer." Gastroenterology **138**(6): 2059-2072.

Porro, A., C. Chrochemore, F. Cambuli, N. Iraci, A. Contestabile and G. Perini (2010). "Nitric oxide control of MYCN expression and multi drug resistance genes in tumours of neural origin." Current pharmaceutical design **16**(4): 431-439.

Pratt, J. M., D. H. Robertson, S. J. Gaskell, I. Riba-Garcia, S. J. Hubbard, K. Sidhu, S. G. Oliver, P. Butler, A. Hayes and J. Petty (2002). "Stable isotope labelling in vivo as an aid to protein identification in peptide mass fingerprinting." Proteomics **2**(2): 157.

Pronsato, L., A. La Colla, A. C. Ronda, L. Milanesi, R. Boland and A. Vasconsuelo (2013). "High passage numbers induce resistance to apoptosis in C2C12 muscle cells." Biocell **37**(1): 1-9.

Puigserver, P., J. Rhee, J. Donovan, C. J. Walkey, J. C. Yoon, F. Oriente, Y. Kitamura, J. Altomonte, H. Dong and D. Accili (2003). "Insulin-regulated hepatic gluconeogenesis through FOXO1–PGC-1α interaction." Nature **423**(6939): 550-555.

PYLVÄS-EEROLA, M., A. Liakka, U. Puistola, J. Koivunen and P. Karihtala (2016). "Cancer Stem Cell Properties as Factors Predictive of Chemoresistance in Neoadjuvantly-treated Patients with Ovarian Cancer." Anticancer Research **36**(7): 3425-3431.

Qin, Y., J. Ke, X. Gu, J. Fang, W. Wang, Q. Cong, J. Li, J. Tan, J. S. Brunzelle and C. Zhang (2015). "Structural and functional study of D-glucuronyl C5-epimerase." Journal of Biological Chemistry **290**(8): 4620-4630.

Rabik, C. A. and M. E. Dolan (2007). "Molecular mechanisms of resistance and toxicity associated with platinating agents." Cancer treatment reviews **33**(1): 9-23.

Rajasekariah, P., H. J. Eyre, K. K. Stanley, R. S. Walls and G. R. Sutherland (1999). "Molecular cloning and characterization of a cDNA encoding the human leucocyte vacuolar protein sorting (hlVps45)." The international journal of biochemistry & cell biology **31**(6): 683-694.

Raman, M., S. Earnest, K. Zhang, Y. Zhao and M. H. Cobb (2007). "TAO kinases mediate activation of p38 in response to DNA damage." The EMBO journal **26**(8): 2005-2014.

Rando, T. A. (2006). "Stem cells, ageing and the quest for immortality." Nature **441**(7097): 1080-1086.

Räschle, M., G. Smeenk, R. K. Hansen, T. Temu, Y. Oka, M. Y. Hein, N. Nagaraj, D. T. Long, J. C. Walter and K. Hofmann (2015). "Proteomics reveals dynamic assembly of repair complexes during bypass of DNA cross-links." Science **348**(6234): 1253671.

Rasheed, Z. A. and E. H. Rubin (2003). "Mechanisms of resistance to topoisomerase I-targeting drugs." Oncogene **22**(47): 7296-7304.

Rauniyar, N. (2015). "Parallel Reaction Monitoring: A Targeted Experiment Performed Using High Resolution and High Mass Accuracy Mass Spectrometry." International journal of molecular sciences **16**(12): 28566-28581.

Reinhardt, H. C., A. S. Aslanian, J. A. Lees and M. B. Yaffe (2007). "p53-deficient cells rely on ATM-and ATR-mediated checkpoint signaling through the p38MAPK/MK2 pathway for survival after DNA damage." Cancer cell **11**(2): 175-189.

Rezapour, S., T. Bahrami, S. Hashemzadeh, M. A. Estiar, M. Nemati, R. Ravanbakhsh, M. Feizi, H. S. Kafil, N. Pouladi and M. Ghojazadeh (2016). "STC1 and NF-κB p65 (Rel A) is Constitutively Activated in Colorectal Cancer." Clinical laboratory **62**(3): 463-469.

Riccio, A. A., G. Cingolani and J. M. Pascal (2015). "PARP-2 domain requirements for DNA damage-dependent activation and localization to sites of DNA damage." Nucleic acids research: gkv1376.

Rich, J. N. and S. Bao (2007). "Chemotherapy and cancer stem cells." Cell stem cell **1**(4): 353-355.

Ritchie, M. E., B. Phipson, D. Wu, Y. Hu, C. W. Law, W. Shi and G. K. Smyth (2015). "limma powers differential expression analyses for RNA-sequencing and microarray studies." Nucleic acids research: gkv007.

Ritz, U., F. Momburg, H.-P. Pircher, D. Strand, C. Huber and B. Seliger (2001). "Identification of sequences in the human peptide transporter subunit TAP1 required for transporter associated with antigen processing (TAP) function." International immunology **13**(1): 31-41.

Rodriguez-Bigas MA, L. E., Crane CH. (2003). Surgical Management of Colorectal Cancer.

Roodman, G. D. (1999). "Cell biology of the osteoclast." Experimental hematology **27**(8): 1229-1241.

Rosa, R., F. Monteleone, N. Zambrano and R. Bianco (2014). "In vitro and in vivo models for analysis of resistance to anticancer molecular therapies." Current medicinal chemistry **21**(14): 1595-1606.

Rothenberger, S., B. J. Iacopetta and L. C. Kühn (1987). "Endocytosis of the transferrin receptor requires the cytoplasmic domain but not its phosphorylation site." Cell **49**(3): 423-431.

Rouette, A., A. Trofimov, D. Haberl, G. Boucher, V.-P. Lavallée, G. D'Angelo, J. Hébert, G. Sauvageau, S. Lemieux and C. Perreault (2016). "Expression of immunoproteasome genes is regulated by cell-intrinsic and–extrinsic factors in human cancers." Scientific Reports **6**.

Ryter, S. W., S. M. Cloonan and A. M. Choi (2013). "Autophagy: a critical regulator of cellular metabolism and homeostasis." Molecules and cells **36**(1): 7-16.

Saada, A., R. O. Vogel, S. J. Hoefs, M. A. van den Brand, H. J. Wessels, P. H. Willems, H. Venselaar, A. Shaag, F. Barghuti and O. Reish (2009). "Mutations in NDUFAF3 (C3ORF60), encoding an NDUFAF4 (C6ORF66)-interacting complex I assembly protein, cause fatal neonatal mitochondrial disease." The American Journal of Human Genetics **84**(6): 718-727.

Sadanandam, A., C. A. Lyssiotis, K. Homicsko, E. A. Collisson, W. J. Gibb, S. Wullschleger, L. C. G. Ostos, W. A. Lannon, C. Grotzinger and M. Del Rio (2013). "A colorectal cancer classification system that associates cellular phenotype and responses to therapy." Nature medicine **19**(5): 619-625.

Sahlberg, S. H., D. Spiegelberg, B. Glimelius, B. Stenerlöw and M. Nestor (2014). "Evaluation of cancer stem cell markers CD133, CD44, CD24: association with AKT isoforms and radiation resistance in colon cancer cells." PloS one **9**(4): e94621.

Saigusa, S., Y. Toiyama, K. Tanaka, Y. Okugawa, H. Fujikawa, K. Matsushita, K. Uchida, Y. Inoue and M. Kusunoki (2012). "Prognostic significance of glucose transporter-1 (GLUT1) gene expression in rectal cancer after preoperative chemoradiotherapy." Surgery today **42**(5): 460-469.

Samimi, G., R. Safaei, K. Katano, A. K. Holzer, M. Rochdi, M. Tomioka, M. Goodman and S. B. Howell (2004). "Increased expression of the copper efflux transporter ATP7A mediates resistance to cisplatin, carboplatin, and oxaliplatin in ovarian cancer cells." Clinical Cancer Research **10**(14): 4661-4669.

Sanghani, S. P., S. K. Quinney, T. B. Fredenburg, Z. Sun, W. I. Davis, D. J. Murry, O. W. Cummings, D. E. Seitz and W. F. Bosron (2003). "Carboxylesterases expressed in human colon tumor tissue and their role in CPT-11 hydrolysis." Clinical Cancer Research **9**(13): 4983-4991.

Sasaki, T., C. Brakebusch, J. Engel and R. Timpl (1998). "Mac-2 binding protein is a cell-adhesive protein of the extracellular matrix which self-assembles into ring-like structures and binds β1 integrins, collagens and fibronectin." The EMBO journal **17**(6): 1606-1613.

Scherf, U., D. T. Ross, M. Waltham, L. H. Smith, J. K. Lee, L. Tanabe, K. W. Kohn, W. C. Reinhold, T. G. Myers and D. T. Andrews (2000). "A gene expression database for the molecular pharmacology of cancer." Nature genetics **24**(3): 236-244.

Schnatwinkel, C., S. Christoforidis, M. R. Lindsay, S. Uttenweiler-Joseph, M. Wilm, R. G. Parton and M. Zerial (2004). "The Rab5 effector Rabankyrin-5 regulates and coordinates different endocytic mechanisms." PLoS Biol **2**(9): e261.

Schrag, D., L. D. Cramer, P. B. Bach and C. B. Begg (2001). "Age and adjuvant chemotherapy use after surgery for stage III colon cancer." Journal of the National Cancer Institute **93**(11): 850-857.

Schreiber, V., J.-C. Amé, P. Dollé, I. Schultz, B. Rinaldi, V. Fraulob, J. Ménissier-de Murcia and G. de Murcia (2002). "Poly (ADP-ribose) polymerase-2 (PARP-2) is required for efficient base excision DNA repair in association with PARP-1 and XRCC1." Journal of Biological Chemistry **277**(25): 23028-23036.

Schumacher, U., N. Nehmann, E. Adam, D. Mukthar, I. N. Slotki, H. P. Horny, M. J. Flens, B. Schlegelberger and D. Steinemann (2012). "MDR-1-overexpression in HT 29 colon cancer cells grown in SCID mice." Acta Histochem **114**(6): 594-602.

Schwab, M. (2008). Encyclopedia of cancer, Springer Science & Business Media.

Scott, A., J. Gaspar, M. D. Stuchell-Brereton, S. L. Alam, J. J. Skalicky and W. I. Sundquist (2005). "Structure and ESCRT-III protein interactions of the MIT domain of human VPS4A." Proceedings of the National Academy of Sciences of the United States of America **102**(39): 13813-13818.

Scott, K. L., O. Kabbarah, M.-C. Liang, E. Ivanova, V. Anagnostou, J. Wu, S. Dhakal, M. Wu, S. Chen and T. Feinberg (2009). "GOLPH3 modulates mTOR signalling and rapamycin sensitivity in cancer." Nature **459**(7250): 1085-1090.

Scotto, K. W. (2003). "Transcriptional regulation of ABC drug transporters." Oncogene **22**(47): 7496-7511.

Seligson, D. B., S. Horvath, T. Shi, H. Yu, S. Tze, M. Grunstein and S. K. Kurdistani (2005). "Global histone modification patterns predict risk of prostate cancer recurrence." Nature **435**(7046): 1262-1266.

Semenza, G. L. (2002). "Signal transduction to hypoxia-inducible factor 1." Biochemical pharmacology **64**(5): 993-998.

Semple, T. U., L. A. Quinn, L. K. Woods and G. E. Moore (1978). "Tumor and lymphoid cell lines from a patient with carcinoma of the colon for a cytotoxicity model." Cancer Res **38**(5): 1345-1355.

Seo, J. and K.-J. Lee (2004). "Post-translational modifications and their biological functions: proteomic analysis and systematic approaches." Journal of biochemistry and molecular biology **37**(1): 35-44.

Shah, M. A. and G. K. Schwartz (2001). "Cell cycle-mediated drug resistance an emerging concept in cancer therapy." Clinical Cancer Research **7**(8): 2168-2181.

Shan, J., Y. Xuan, Q. Zhang, C. Zhu, Z. Liu and S. Zhang (2016). "Ursolic acid synergistically enhances the therapeutic effects of oxaliplatin in colorectal cancer." Protein & Cell **7**(8): 571-585.

Shao, R. G., C. X. Cao, H. Zhang, K. W. Kohn, M. S. Wold and Y. Pommier (1999). "Replication-mediated DNA damage by camptothecin induces phosphorylation of RPA by DNA-dependent protein kinase and dissociates RPA: DNA-PK complexes." The EMBO journal **18**(5): 1397-1406.

Shenoy, A. and T. Geiger (2015). "Super-SILAC: current trends and future perspectives." Expert review of proteomics **12**(1): 13-19.

Shental-Bechor, D. and Y. Levy (2008). "Effect of glycosylation on protein folding: a close look at thermodynamic stabilization." Proceedings of the National Academy of Sciences **105**(24): 8256-8261.

Shi, Q., S. Hui, A.-H. Zhang, X. Hong-Ying, Y. Guang-Li, H. Ying and W. Xi-Jun (2014). "Natural alkaloids: basic aspects, biological roles, and future perspectives." Chinese journal of natural medicines **12**(6): 401-406.

Shi, Q. and G. Jackowski (1998). "One-dimensional polyacrylamide gel electrophoresis." Gel electrophoresis of proteins: A practical approach, 3rd ed. Oxford University Press, Oxford: 1-52.

Shi, W., M. K. Tang, Y. Yao, C. Tang, Y. L. Chui and K. K. H. Lee (2016). "BRE plays an essential role in preventing replicative and DNA damage-induced premature senescence." Scientific reports **6**.

Shin, J.-S., T. Foot, A. Hong, M. Zhang, T. Lum, M. J. Solomon and C. S. Lee (2012). "Telomerase expression as a predictive marker of radiotherapy response in rectal cancer: in vitro and in vivo study." Pathology **44**(3): 209-215.

Shin, Y.-K., B. C. Yoo, H. J. Chang, E. Jeon, S.-H. Hong, M.-S. Jung, S.-J. Lim and J.-G. Park (2005). "Down-regulation of mitochondrial F1F0-ATP synthase in human colon cancer cells with induced 5-fluorouracil resistance." Cancer research **65**(8): 3162-3170.

Shiozawa, T., S. Iyama, S. Toshima, A. Sakata, S. Usui, Y. Minami, Y. Sato, N. Hizawa and M. Noguchi (2016). "Dimethylarginine dimethylaminohydrolase 2 promotes tumor angiogenesis in lung adenocarcinoma." Virchows Archiv **468**(2): 179-190.

Shorter, J. (2011). "The mammalian disaggregase machinery: Hsp110 synergizes with Hsp70 and Hsp40 to catalyze protein disaggregation and reactivation in a cell-free system." PloS one **6**(10): e26319.

Shtanko, O., R. A. Nikitina, C. Z. Altuntas, A. A. Chepurnov and R. A. Davey (2014). "Crimean-Congo hemorrhagic fever virus entry into host cells occurs through the multivesicular body and requires ESCRT regulators." PLoS Pathog **10**(9): e1004390.

Siissalo, S., L. Laitinen, M. Koljonen, K.-S. Vellonen, H. Kortejärvi, A. Urtti, J. Hirvonen and A. M. Kaukonen (2007). "Effect of cell differentiation and passage number on the expression of efflux proteins in wild type and vinblastine-induced Caco-2 cell lines." European Journal of Pharmaceutics and Biopharmaceutics **67**(2): 548-554.

Simonsen, A., J.-M. Gaullier, A. D'Arrigo and H. Stenmark (1999). "The Rab5 effector EEA1 interacts directly with syntaxin-6." Journal of Biological Chemistry **274**(41): 28857-28860.

Sinicrope, F. A. and D. J. Sargent (2012). "Molecular pathways: microsatellite instability in colorectal cancer: prognostic, predictive, and therapeutic implications." Clinical cancer research **18**(6): 1506-1512.

Sjöblom, T., S. Jones, L. D. Wood, D. W. Parsons, J. Lin, T. D. Barber, D. Mandelker, R. J. Leary, J. Ptak and N. Silliman (2006). "The consensus coding sequences of human breast and colorectal cancers." science **314**(5797): 268-274.

Soekmadji, C. and C. C. Nelson (2015). "The emerging role of extracellular vesicle-mediated drug resistance in cancers: implications in advanced prostate cancer." BioMed research international **2015**.

Song, G., S. Xu, H. Zhang, Y. Wang, C. Xiao, T. Jiang, L. Wu, T. Zhang, X. Sun and L. Zhong (2016). "TIMP1 is a prognostic marker for the progression and metastasis of colon cancer through FAK-PI3K/AKT and MAPK pathway." Journal of Experimental & Clinical Cancer Research **35**(1): 148.

Sordat, I., C. Decraene, T. Silvestre, O. Petermann, C. Auffray, G. Piétu and B. Sordat (2002). "Complementary DNA arrays identify CD63 tetraspanin and α3 integrin chain as differentially expressed in low and high metastatic human colon carcinoma cells." Laboratory investigation **82**(12): 1715-1724.

Spiegelberg, B. D., J.-P. Xiong, J. J. Smith, R. F. Gu and J. D. York (1999). "Cloning and characterization of a mammalian lithium-sensitive bisphosphate 3'-nucleotidase inhibited by inositol 1, 4-bisphosphate." Journal of Biological Chemistry **274**(19): 13619-13628.

Srivastava, M., P. Khurana and R. Sugadev (2012). "Lung cancer signature biomarkers: tissue specific semantic similarity based clustering of digital differential display (DDD) data." BMC research notes **5**(1): 617.

Stebbing, J., H. Zhang, Y. Xu, A. Grothey, P. Ajuh, N. Angelopoulos and G. Giamas (2015). "Characterization of the tyrosine kinase-regulated proteome in breast cancer by combined use of RNA interference (RNAi) and stable isotope labeling with amino acids in cell culture (SILAC) quantitative proteomics." Molecular & Cellular Proteomics **14**(9): 2479-2492.

Steketee, K., A. C. Ziel-van der Made, H. A. van der Korput, A. B. Houtsmuller and J. Trapman (2004). "A bioinformatics-based functional analysis shows that the specifically androgen-regulated gene SARG contains an active direct repeat androgen response element in the first intron." Journal of molecular endocrinology **33**(2): 477-491.

Stocker, R. and M. A. Perrella (2006). "Heme oxygenase-1." Circulation **114**(20): 2178-2189.

Stoletov, K. and J. D. Lewis (2015). Invadopodia: a new therapeutic target to block cancer metastasis, Taylor & Francis.

Stordal, B. and R. Davey (2009). "A systematic review of genes involved in the inverse resistance relationship between cisplatin and paclitaxel chemotherapy: role of BRCA1." Current cancer drug targets **9**(3): 354-365.

Stordal, B., M. Hamon, V. McEneaney, S. Roche, J.-P. Gillet, J. J. O'Leary, M. Gottesman and M. Clynes (2012). "Resistance to paclitaxel in a cisplatin-resistant ovarian cancer cell line is mediated by P-glycoprotein." PloS one **7**(7): e40717.

Stumpf, M. P., T. Thorne, E. de Silva, R. Stewart, H. J. An, M. Lappe and C. Wiuf (2008). "Estimating the size of the human interactome." Proceedings of the National Academy of Sciences **105**(19): 6959-6964.

Sui, X., N. Kong, X. Wang, Y. Fang, X. Hu, Y. Xu, W. Chen, K. Wang, D. Li and W. Jin (2014). "JNK confers 5-fluorouracil resistance in p53-deficient and mutant p53-expressing colon cancer cells by inducing survival autophagy." Scientific reports **4**.

Sun, J., M. Nanjundan, L. J. Pike, T. Wiedmer and P. J. Sims (2002). "Plasma membrane phospholipid scramblase 1 is enriched in lipid rafts and interacts with the epidermal growth factor receptor." Biochemistry **41**(20): 6338-6345.

Sung, H. Y., J. Han, W. Ju and J.-H. Ahn (2016). "Synaptotagmin-like protein 2 gene promotes the metastatic potential in ovarian cancer." Oncology reports **36**(1): 535-541.

Suzuki, R., T. Takizawa, Y. Kuwata, M. Mutoh, N. Ishiguro, N. Utoguchi, A. Shinohara, M. Eriguchi, H. Yanagie and K. Maruyama (2008). "Effective anti-tumor activity of oxaliplatin encapsulated in transferrin–PEG-liposome." International journal of pharmaceutics **346**(1): 143-150.

Swan, E., A. Maxwell and A. McKnight (2015). "Distinct methylation patterns in genes that affect mitochondrial function are associated with kidney disease in blood-derived DNA from individuals with Type 1 diabetes." Diabetic Medicine **32**(8): 1110-1115.

Szablewski, L. (2013). "Expression of glucose transporters in cancers." Biochimica et Biophysica Acta (BBA)-Reviews on Cancer **1835**(2): 164-169.

Szaflarski, W., P. Sujka-Kordowska, B. Pula, K. Jaszczyńska-Nowinka, M. Andrzejewska, P. Zawierucha, P. Dziegiel, M. Nowicki, P. Ivanov and M. Zabel (2013). "Expression profiles of vault components MVP, TEP1 and vPARP and their correlation to other multidrug resistance proteins in ovarian cancer." Int J Oncol **43**(2): 513-520.

Tajima, A., M. T. Hess, B. L. Cabrera, R. D. Kolodner and J. M. Carethers (2004). "The mismatch repair complex hMutSα recognizes 5-fluorouracil-modified DNA: Implications for chemosensitivity and resistance." Gastroenterology **127**(6): 1678-1684.

Tang, B. L., J. Kausalya, D. Y. Low, M. L. Lock and W. Hong (1999). "A family of mammalian proteins homologous to yeast Sec24p." Biochemical and biophysical research communications **258**(3): 679-684.

ter Beek, J., A. Guskov and D. J. Slotboom (2014). "Structural diversity of ABC transporters." The Journal of general physiology: jgp. 201411164.

Tinari, N., I. Kuwabara, M. E. Huflejt, P. F. Shen, S. Iacobelli and F. T. Liu (2001). "Glycoprotein 90K/MAC-2BP interacts with galectin-1 and mediates galectin-1–induced cell aggregation." International journal of cancer **91**(2): 167-172.

Ting, L., M. J. Cowley, S. L. Hoon, M. Guilhaus, M. J. Raftery and R. Cavicchioli (2009). "Normalization and statistical analysis of quantitative proteomics data generated by metabolic labeling." Molecular & Cellular Proteomics **8**(10): 2227-2242.

Tiwari, M. (2012). "Antimetabolites: established cancer therapy." J Cancer Res Ther **8**(4): 510-519.

Tobioka, H., H. Isomura, Y. Kokai and N. Sawada (2002). "Polarized distribution of carcinoembryonic antigen is associated with a tight junction molecule in human colorectal adenocarcinoma." The Journal of pathology **198**(2): 207-212.

Todaro, M., M. Perez Alea, A. Scopelliti, J. P. Medema and G. Stassi (2008). "IL-4-mediated drug resistance in colon cancer stem cells." Cell Cycle **7**(3): 309-313.

Tominaga, N., K. Hagiwara, N. Kosaka, K. Honma, H. Nakagama and T. Ochiya (2014). "RPN2-mediated glycosylation of tetraspanin CD63 regulates breast cancer cell malignancy." Molecular cancer **13**(1): 134.

Toricelli, M., F. H. Melo, G. B. Peres, D. C. Silva and M. G. Jasiulionis (2013). "Timp1 interacts with beta-1 integrin and CD63 along melanoma genesis and confers anoikis resistance by activating PI3-K signaling pathway independently of Akt phosphorylation." Molecular cancer **12**(1): 22.

Tóth, C., J. Meinrath, E. Herpel, J. Derix, J. Fries, R. Buettner, P. Schirmacher and S. Heikaus (2016). "Expression of the apoptosis repressor with caspase recruitment domain (ARC) in liver metastasis of colorectal cancer and its correlation with DNA mismatch repair proteins and p53." Journal of cancer research and clinical oncology **142**(5): 927-935.

Truant, S., E. Bruyneel, V. Gouyer, O. De Wever, F. R. Pruvot, M. Mareel and G. Huet (2003). "Requirement of both mucins and proteoglycans in cell-cell dissociation and invasiveness of colon carcinoma HT-29 cells." International journal of cancer **104**(6): 683-694.

Tsui, I. F., R. Chari, T. P. Buys and W. L. Lam (2007). "Public databases and software for the pathway analysis of cancer genomes." Cancer informatics **3**.

Tsukamoto, N., J. Chen and A. Yoshida (1998). "Enhanced expressions of glucose-6-phosphate dehydrogenase and cytosolic aldehyde dehydrogenase and elevation of reduced glutathione level in cyclophosphamide-resistant human leukemia cells." Blood Cells, Molecules, and Diseases **24**(2): 231-238.

Tung, M.-C., P.-L. Lin, Y.-C. Wang, T.-Y. He, M.-C. Lee, S.-D. Yeh, C.-Y. Chen and H. Lee (2015). "Mutant p53 confers chemoresistance in non-small cell lung cancer by upregulating Nrf2." Oncotarget **6**(39): 41692.

Turton, N. J., D. J. Judah, J. Riley, R. Davies, D. Lipson, J. A. Styles, A. G. Smith and T. W. Gant (2001). "Gene expression and amplification in breast carcinoma cells with intrinsic and acquired doxorubicin resistance." Oncogene **20**(11): 1300.

Twomey, J. D., S.-R. Kim, L. Zhao, W. P. Bozza and B. Zhang (2015). "Spatial dynamics of TRAIL death receptors in cancer cells." Drug Resistance Updates **19**: 13-21.

Tyers, M. and M. Mann (2003). "From genomics to proteomics." Nature **422**(6928): 193-197.

Uhlén, M., L. Fagerberg, B. M. Hallström, C. Lindskog, P. Oksvold, A. Mardinoglu, Å. Sivertsson, C. Kampf, E. Sjöstedt and A. Asplund (2015). "Tissue-based map of the human proteome." Science **347**(6220): 1260419.

Valdivia, C. R., K. Ueda, M. J. Ackerman and J. C. Makielski (2009). "GPD1L links redox state to cardiac excitability by PKC-dependent phosphorylation of the sodium channel SCN5A." American Journal of Physiology-Heart and Circulatory Physiology **297**(4): H1446-H1452.

Van Cutsem, E., P. Hoff, P. Harper, R. Bukowski, D. Cunningham, P. Dufour, U. Graeven, J. Lokich, S. Madajewicz and J. Maroun (2004). "Oral capecitabine vs intravenous 5-fluorouracil and leucovorin: integrated efficacy data and novel analyses from two large, randomised, phase III trials." British journal of cancer **90**(6): 1190-1197.

Van Cutsem, E., C. Twelves, J. Cassidy, D. Allman, E. Bajetta, M. Boyer, R. Bugat, M. Findlay, S. Frings and M. Jahn (2001). "Oral capecitabine compared with intravenous fluorouracil plus leucovorin in patients with metastatic colorectal cancer: results of a large phase III study." Journal of Clinical Oncology **19**(21): 4097-4106.

van der Meij, W., A. J. Rombouts, H. Rutten, A. J. Bremers and J. H. de Wilt (2016). "Treatment of Locally Recurrent Rectal Carcinoma in Previously (Chemo)Irradiated Patients: A Review." Dis Colon Rectum **59**(2): 148-156.

van Gijn, W., C. A. Marijnen, I. D. Nagtegaal, E. M. Kranenbarg, H. Putter, T. Wiggers, H. J. Rutten, L. Pahlman, B. Glimelius, C. J. van de Velde and G. Dutch Colorectal Cancer (2011). "Preoperative radiotherapy combined with total mesorectal excision for resectable rectal cancer: 12-year follow-up of the multicentre, randomised controlled TME trial." Lancet Oncol **12**(6): 575-582.

Van Hoof, D., M. W. Pinkse, D. Ward-Van Oostwaard, C. L. Mummery, A. J. Heck and J. Krijgsveld (2007). "An experimental correction for arginine-to-proline conversion artifacts in SILAC-based quantitative proteomics." Nature methods **4**(9): 677-678.

van Houdt, W. J., M. T. de Bruijn, B. L. Emmink, D. Raats, F. J. Hoogwater, I. H. Rinkes and O. Kranenburg (2010). "Oncogenic K-ras activates p38 to maintain colorectal cancer cell proliferation during MEK inhibition." Analytical Cellular Pathology **32**(4): 245-257.

van Meerloo, J., G. J. Kaspers and J. Cloos (2011). "Cell sensitivity assays: the MTT assay." Cancer cell culture: methods and protocols: 237-245.

Vasilenko, K., P. Butylin, A. Arnautov and N. Nikol'skiĭ (2000). "The role of SRC kinase in activation of transcription factor STAT1." Tsitologiia **43**(11): 1031-1037.

Vasudevan, D. and D. D. Thomas (2014). "Insights into the diverse effects of nitric oxide on tumor biology." Vitam Horm **96**: 265-298.

Veiby, O. P. and M. A. Read (2004). "Chemoresistance: Impact of Nuclear Factor (NF)-κB Inhibition by Small Interfering RNA Commentary re J. Guo et al., Enhanced Chemosensitivity to Irinotecan by RNA Interference-Mediated Down-Regulation of the NF-κB p65 Subunit. Clin Cancer Res 2004; 10: 3333–3341." Clinical cancer research **10**(10): 3262-3264.

Vermeer, P. D., P. L. Colbert, B. G. Wieking, D. W. Vermeer and J. H. Lee (2013). "Targeting ERBB receptors shifts their partners and triggers persistent ERK signaling through a novel ERBB/EFNB1 complex." Cancer research **73**(18): 5787-5797.

Vidal, S., V. Rodriguez-Bravo, M. Galsky, C. Cordon-Cardo and J. Domingo-Domenech (2014). "Targeting cancer stem cells to suppress acquired chemotherapy resistance." Oncogene **33**(36): 4451-4463.

Vietri, M., K. O. Schink, C. Campsteijn, C. S. Wegner, S. W. Schultz, L. Christ, S. B. Thoresen, A. Brech, C. Raiborg and H. Stenmark (2015). "Spastin and ESCRT-III coordinate mitotic spindle disassembly and nuclear envelope sealing." Nature **522**(7555): 231-235.

Violette, S., L. Poulain, E. Dussaulx, D. Pepin, A. M. Faussat, J. Chambaz, J. M. Lacorte, C. Staedel and T. Lesuffleur (2002). "Resistance of colon cancer cells to long-term 5-fluorouracil exposure is correlated to the relative level of Bcl-2 and Bcl-XL in addition to Bax and p53 status." International Journal of Cancer **98**(4): 498-504.

Vitale, N., K. Horiba, V. J. Ferrans, J. Moss and M. Vaughan (1998). "Localization of ADP-ribosylation factor domain protein 1 (ARD1) in lysosomes and Golgi apparatus." Proceedings of the National Academy of Sciences **95**(15): 8613-8618.

Voges, D., P. Zwickl and W. Baumeister (1999). "The 26S proteasome: a molecular machine designed for controlled proteolysis." Annual review of biochemistry **68**(1): 1015-1068.

Von Mering, C., M. Huynen, D. Jaeggi, S. Schmidt, P. Bork and B. Snel (2003). "STRING: a database of predicted functional associations between proteins." Nucleic acids research **31**(1): 258-261.

Waanders, L. F., S. Hanke and M. Mann (2007). "Top-down quantitation and characterization of SILAC-labeled proteins." Journal of the American Society for Mass Spectrometry **18**(11): 2058-2064.

Walczak, H., M. A. Degli-Esposti, R. S. Johnson, P. J. Smolak, J. Y. Waugh, N. Boiani, M. S. Timour, M. J. Gerhart, K. A. Schooley and C. A. Smith (1997). "TRAIL-R2: a novel apoptosis-mediating receptor for TRAIL." The EMBO journal **16**(17): 5386-5397.

Walther, D. M. and M. Mann (2011). "Accurate quantification of more than 4000 mouse tissue proteins reveals minimal proteome changes during aging." Molecular & Cellular Proteomics **10**(2): M110. 004523.

Wang, B., K. Hurov, K. Hofmann and S. J. Elledge (2009). "NBA1, a new player in the Brca1 A complex, is required for DNA damage resistance and checkpoint control." Genes & development **23**(6): 729-739.

Wang, H., C. Huang, L. Zhao, H. Zhang, J. M. Yang, P. Luo, B.-X. Zhan, Q. Pan, J. Li and B.-L. Wang (2016). "Histone deacetylase inhibitors regulate P-gp expression in colorectal cancer via transcriptional activation and mRNA stabilization." Oncotarget **7**(31): 49848-49858.

Wang, J.-Y., J. Sun, M.-Y. Huang, Y.-S. Wang, M.-F. Hou, Y. Sun, H. He, N. Krishna, S.-J. Chiu and S. Lin (2015). "STIM1 overexpression promotes colorectal cancer progression, cell motility and COX-2 expression." Oncogene **34**(33): 4358-4367.

Wang, L., Y. Zhan, E. Song, Y. Yu, Y. Jiu, W. Du, J. Lu, P. Liu, P. Xu and T. Xu (2011). "HID-1 is a peripheral membrane protein primarily associated with the medial-and trans-Golgi apparatus." Protein & cell **2**(1): 74-85.

Wang, S., C. Patsis and A. E. Koromilas (2015). "Stat1 stimulates cap-independent mRNA translation to inhibit cell proliferation and promote survival in response to antitumor drugs." Proceedings of the National Academy of Sciences **112**(17): E2149-E2155.

Wang, W., H. L. McLeod, J. Cassidy and E. S. Collie-Duguid (2007). "Mechanisms of acquired chemoresistance to 5-fluorouracil and tomudex: thymidylate synthase dependent and independent networks." Cancer chemotherapy and pharmacology **59**(6): 839-845.

Wang, Y.-D., S.-J. Li and J.-X. Liao (2013). "Inhibition of glucose transporter 1 (GLUT1) chemosensitized head and neck cancer cells to cisplatin." Technology in cancer research & treatment **12**(6): 525-535.

Wang, Y., X. Guan, K. Fok, S. Li, X. Zhang, S. Miao, S. Zong, S. Koide, H. Chan and L. Wang (2008). "A novel member of the Rhomboid family, RHBDD1, regulates BIK-mediated apoptosis." Cellular and molecular life sciences **65**(23): 3822-3829.

Wartosch, L., U. Günesdogan, S. C. Graham and J. P. Luzio (2015). "Recruitment of VPS33A to HOPS by VPS16 is required for lysosome fusion with endosomes and autophagosomes." Traffic **16**(7): 727-742.

Watson, E. C. (1964). "5-Fluouracil in the Treatment of Disseminated Colon and Rectal Carcinoma." N Z Med J **63**: 583-586.

Weihua, Z., R. Tsan, W.-C. Huang, Q. Wu, C.-H. Chiu, I. J. Fidler and M.-C. Hung (2008). "Survival of cancer cells is maintained by EGFR independent of its kinase activity." Cancer cell **13**(5): 385-393.

White, C. I., M. A. Jansen, K. McGregor, K. J. Mylonas, R. V. Richardson, A. Thomson, C. M. Moran, J. R. Seckl, B. R. Walker and K. E. Chapman (2015). "Cardiomyocyte and vascular smooth muscle-independent 11β-hydroxysteroid dehydrogenase 1 amplifies infarct expansion, hypertrophy, and the development of heart failure after myocardial infarction in male mice." Endocrinology **157**(1): 346-357.

White, E. (2008). Role of the metabolic stress responses of apoptosis and autophagy in tumor suppression. Oncogenes Meet Metabolism, Springer**:** 23-34.

Wilhelm, M., J. Schlegl, H. Hahne, A. M. Gholami, M. Lieberenz, M. M. Savitski, E. Ziegler, L. Butzmann, S. Gessulat and H. Marx (2014). "Mass-spectrometry-based draft of the human proteome." Nature **509**(7502): 582-587.

Wlodkowic, D., J. Skommer, D. McGuinness, C. Hillier and Z. Darzynkiewicz (2009). "ER–Golgi network—A future target for anti-cancer therapy." Leukemia research **33**(11): 1440-1447.

Woerner, S. M., Y. P. Yuan, A. Benner, S. Korff, M. von Knebel Doeberitz and P. Bork (2010). "SelTarbase, a database of human mononucleotide-microsatellite mutations and their potential impact to tumorigenesis and immunology." Nucleic acids research **38**(suppl 1): D682-D689.

Wong, C., V. Wong, C. Chan, B. Ma, E. P. Hui, M. Wong, M. Lam, T. Au, W. Chan and W. Cheuk (2008). "Identification of 5-fluorouracil response proteins in colorectal carcinoma cell line SW480 by two-dimensional electrophoresis and MALDI-TOF mass spectrometry." Oncology reports **20**(1): 89.

Wong, H. S.-C. and W.-C. Chang (2015). "Correlation of clinical features and genetic profiles of stromal interaction molecule 1 (STIM1) in colorectal cancers." Oncotarget **6**(39): 42169.

Woynarowski, J. M., W. G. Chapman, C. Napier, M. C. Herzig and P. Juniewicz (1998). "Sequence-and region-specificity of oxaliplatin adducts in naked and cellular DNA." Molecular pharmacology **54**(5): 770-777.

Wu, K.-J., A. Polack and R. Dalla-Favera (1999). "Coordinated regulation of iron-controlling genes, H-ferritin and IRP2, by c-MYC." Science **283**(5402): 676-679.

Wu, L., S. Li, R. Peng, S. Gong, L. Xu and F. Zou (2015). "Drug resistance of colon cancer cells to 5-fluorouracil mediated by microRNA-21." Zhonghua yi xue yi chuan xue za zhi= Zhonghua yixue yichuanxue zazhi= Chinese journal of medical genetics **32**(5): 620-624.

Xia, P. and X.-Y. Xu (2016). "Prognostic significance of CD44 in human colon cancer and gastric cancer: Evidence from bioinformatic analyses." Oncotarget **7**(29): 45538-45546.

Xu, H., N. Dephoure, H. Sun, H. Zhang, F. Fan, J. Liu, X. Ning, S. Dai, B. Liu and M. Gao (2015). "Proteomic profiling of paclitaxel treated cells identifies a novel mechanism of drug resistance mediated by PDCD4." Journal of proteome research **14**(6): 2480-2491.

Xu, M., L. Li, Z. Liu, Z. Jiao, P. Xu, X. Kong, H. Huang and Y. Zhang (2013). "ABCB2 (TAP1) as the downstream target of SHH signaling enhances pancreatic ductal adenocarcinoma drug resistance." Cancer letters **333**(2): 152-158.

Xu, Y. and M. Villalona-Calero (2002). "Irinotecan: mechanisms of tumor resistance and novel strategies for modulating its activity." Annals of oncology **13**(12): 1841-1851.

Yamashiro, S., Y. Yamakita, S. Ono and F. Matsumura (1998). "Fascin, an actin-bundling protein, induces membrane protrusions and increases cell motility of epithelial cells." Molecular biology of the cell **9**(5): 993-1006.

Yang, G., Z. Xu, W. Lu, X. Li, C. Sun, J. Guo, P. Xue and F. Guan (2015). "Quantitative analysis of differential proteome expression in bladder cancer vs. normal bladder cells using SILAC method." PloS one **10**(7): e0134727.

Yang, Y., H. Hou, E. M. Haller, S. V. Nicosia and W. Bai (2005). "Suppression of FOXO1 activity by FHL2 through SIRT1-mediated deacetylation." The EMBO journal **24**(5): 1021-1032.

Yang, Y., Y. Zhang, Q. Wu, X. Cui, Z. Lin, S. Liu and L. Chen (2014). "Clinical implications of high NQO1 expression in breast cancers." Journal of Experimental & Clinical Cancer Research **33**(1): 14.

Yang, Z., P. J. Faustino, P. A. Andrews, R. Monastra, A. A. Rasmussen, C. D. Ellison and K. J. Cullen (2000). "Decreased cisplatin/DNA adduct formation is associated with cisplatin resistance in human head and neck cancer cell lines." Cancer chemotherapy and pharmacology **46**(4): 255-262.

Yano, M., K. Terada and M. Mori (2003). "AIP is a mitochondrial import mediator that binds to both import receptor Tom20 and preproteins." The Journal of cell biology **163**(1): 45-56.

Yao, W., X. Qin, B. Qi, J. Lu, L. Guo, F. Liu, S. Liu and B. Zhao (2014). "Association of p53 expression with prognosis in patients with esophageal squamous cell carcinoma." International journal of clinical and experimental pathology **7**(10): 7158.

Yarmush, M. L. and A. Jayaraman (2002). "Advances in proteomic technologies." Annual review of biomedical engineering **4**(1): 349-373.

Young, C. D., A. S. Lewis, M. C. Rudolph, M. D. Ruehle, M. R. Jackman, U. J. Yun, O. Ilkun, R. Pereira, E. D. Abel and S. M. Anderson (2011). "Modulation of glucose transporter 1 (GLUT1) expression levels alters mouse mammary tumor cell growth in vitro and in vivo." PloS one **6**(8): e23205.

Zahreddine, H. and K. Borden (2013). "Mechanisms and insights into drug resistance in cancer." Front Pharmacol **4**(28.10): 3389.

Zaitoun, I. and H. Khatib (2008). "Comparative genomic imprinting and expression analysis of six cattle genes1." Journal of animal science **86**(1): 25.

Zeng, X., P. Yang, B. Chen, X. Jin, Y. Liu, X. Zhao and S. Liang (2013). "Quantitative secretome analysis reveals the interactions between epithelia and tumor cells by in vitro modulating colon cancer microenvironment." Journal of proteomics **89**: 51-70.

Zhang, D., L. Wang, L. Yan, X. Miao, C. Gong, M. Xiao, R. Ni and Q. Tang (2015). "Vacuolar protein sorting 4B regulates apoptosis of intestinal epithelial cells via p38 MAPK in Crohn's disease." Experimental and molecular pathology **98**(1): 55-64.

Zhang, F., M. Kumano, E. Beraldi, L. Fazli, C. Du, S. Moore, P. Sorensen, A. Zoubeidi and M. E. Gleave (2014). "Clusterin facilitates stress-induced lipidation of LC3 and autophagosome biogenesis to enhance cancer cell survival." Nature communications **5**.

Zhang, H., Y. Xu, P. Papanastasopoulos, J. Stebbing and G. Giamas (2014). "Broader implications of SILAC-based proteomics for dissecting signaling dynamics in cancer." Expert review of proteomics **11**(6): 713-731.

Zhang, J., M. Cao, J. Dong, C. Li, W. Xu, Y. Zhan, X. Wang, M. Yu, C. Ge and Z. Ge (2014). "ABRO1 suppresses tumourigenesis and regulates the DNA damage response by stabilizing p53." Nature communications **5**.

Zhang, J., J. Zheng, Y. Yang, J. Lu, J. Gao, T. Lu, J. Sun, H. Jiang, Y. Zhu and Y. Zheng (2015). "Molecular spectrum of KRAS, NRAS, BRAF and PIK3CA mutations in Chinese colorectal cancer patients: analysis of 1,110 cases." Scientific reports **5**: 18678.

Zhang, N., Y. Yin, S.-J. Xu and W.-S. Chen (2008). "5-Fluorouracil: mechanisms of resistance and reversal strategies." Molecules **13**(8): 1551-1569.

Zhao, J.-g., K.-m. Ren and J. Tang (2014). "Overcoming 5-Fu resistance in human non-small cell lung cancer cells by the combination of 5-Fu and cisplatin through the inhibition of glucose metabolism." Tumor Biology **35**(12): 12305-12315.

Zhao, S., R. Li, X. Cai, W. Chen, Q. Li, T. Xing, W. Zhu, Y. E. Chen, R. Zeng and Y. Deng (2013). "The application of SILAC mouse in human body fluid proteomics analysis reveals protein patterns associated with IgA nephropathy." Evidence-Based Complementary and Alternative Medicine **2013**.

Zhen, Y., G. Chunlei, S. Wenzhi, Z. Shuangtao, L. Na, W. Rongrong, L. Xiaohe, N. Haiying, L. Dehong and J. Shan (2014). "Clinicopathologic significance of legumain overexpression in cancer: a systematic review and meta-analysis." Scientific reports **5**: 16599-16599.

Zhijun, X., Z. Shulan and Z. Zhuo (2006). "Expression and significance of the protein and mRNA of metastasis suppressor gene ME491/CD63 and integrin alpha5 in ovarian cancer tissues." European journal of gynaecological oncology **28**(3): 179-183.

Zhitomirsky, B. and Y. G. Assaraf (2016). "Lysosomes as mediators of drug resistance in cancer." Drug Resistance Updates **24**: 23-33.

Zhou, B., G. Wang, S. Gao, Y. Chen, C. Jin, Z. Wang, Y. Yang, Z. Ma, W. Zhang and X. Feng (2016). "Expression of GOLPH3 protein in colon cancer tissues and its association with the prognosis of patients." Oncology Letters **12**(5): 3936-3940.

Zhou, J. and Y. Yin (2016). "Strategies for large-scale targeted metabolomics quantification by liquid chromatography-mass spectrometry." Analyst **141**(23): 6362-6373.

Zhu, X., X. Long, X. Luo, Z. Song, S. Li and H. Wang (2016). "Abrogation of MUC5AC Expression Contributes to the Apoptosis and Cell Cycle Arrest of Colon Cancer Cells." Cancer Biotherapy and Radiopharmaceuticals **31**(7): 261-267.